UNIVERSITY OF CALIFORNIA,
IRVINE

Huntington's disease astrocyte and brain-microvascular endothelial cell dysregulation

DISSERTATION

submitted in partial satisfaction of the requirements
for the degree of

DOCTOR OF PHILOSOPHY

in Biomedical Sciences

by

Andrea Marina Reyes-Ortiz

Dissertation Committee:
Professor Leslie M. Thompson, Chair
Professor Mathew Blurton-Jones
Professor Peter J. Donovan
Professor Suzanne B. Sandmeyer

2021

DEDICATION

To my loving grandparents and heroes: Dr. William Evans Neville, Artis Jane Neville, Jose Reyes-Ortiz, and Luisiana Reyes-Ortiz. Each of them strived for improving the lives of their families and those around them. They all inspired an aspect of this dissertation and, in their own ways, paved this journey for me. I am forever grateful for everything I learned from them.

To my parents for their unconditional love and support that made this journey possible.

TABLE OF CONTENTS

LIST OF FIGURES

LIST OF TABLES

LIST OF ABBREVIATIONS

AMPA	Alpha-amino-3-hydroxy-5-methyl-4-isoxazolepropionic acid
ATP	Adenosine triphosphate
BBB	Blood-brain barrier
BDNF	Brain-derived neurotrophic factor
CNS	Central nervous system
DEG	Differentially expressed gene
DNA	Deoxyribonucleic acid
ECM	Extracellular matrix
ESC	Embryonic stem cell
GABA	Gamma-aminobutyric acid
GDNF	Glial cell line-derived neurotrophic factor
GRIA1	Glutamate Ionotropic Receptor AMPA Type Subunit 1 (RNA)
GluR1	Glutamate Receptor 1 (protein)
HD	Huntington's disease
HTT	Huntingtin (protein or gene)
HTTKD	Huntingtin knockdown
iAstros	iPSC-derived astrocytes
iBMECs	iPSC-derived brain microvascular endothelial cells
IPA	Ingenuity Pathway Analysis
iPSCs	Induced pluripotent stem cells
KD	Knockdown
LPS	Lipopolysaccharide
MCAO	Middle cerebral artery occlusion
mHTT	Mutant Huntingtin
MSN	Medium spiny neuron
NMDA	N-methyl-D-aspartate
NSC	Neural stem cell
NT	Non-transgenic
NVU	Neurovascular unit
RNA	Ribonucleic acid
SNP	Single nucleotide polymorphisms
TCA	Tricarboxylic acid
TJ	Tight junction
WT	Wild type

ACKNOWLEDGEMENTS

I would like to acknowledge my committee members, Dr. Mathew Blurton-Jones, Dr. Peter Donovan, and Dr. Suzanne Sandmeyer for their extremely helpful discussions and input that were imperative to the completion of this dissertation as well as their support.

I would like to thank my advisor, Dr. Leslie Thompson. Not only is she a brilliant scientist but an incredibly inspiring patient advocate and leader, but she is also a great mentor. It has been an honor to be in her lab and be mentored by her. Her support and encouragement to pursue new things in the lab and my career were essential to my personal and scientific growth during this journey. I cannot thank her enough for everything she has provided me.

Thank you to Dr. Ryan Lim for his mentorship and friendship during these past six years. Since the first day of my rotation in the Thompson lab, he showed me what a great PhD scientist looked like and helped to guide me through my own unique route of success. He soon became a great friend that I was able to celebrate with (and complain to) through all the ups and downs of my PhD, he has always been there for me.

Thank you also to Dr. Sarah Hernandez, my unofficial mentor in lab (and life). An incredibly inspiring HD researcher and even greater friend. Day by day, she taught me how to be a thorough and rigorous scientist. If there is something I am going to miss most, it would be the quiet early mornings diligently working next to her in bay 6 with a warm chai or coffee in hand. From sharing recipes to organizing HD-CARE fundraisers then to sharing bottles of wine, it has been such a pleasure being your friend and learning from you.

This work would not have been possible without the help of several Thompson Lab members. Many thanks to Dr. Ryan Lim, for spearheading the iBMEC work and guiding each aspect of the astrocyte work. Thanks to Dr. Jenny Wu, for her bioinformatic and statistical guidance as well as friendship. Thank you to Keona Wang for her technical assistance with astrocyte differentiations, FACS, and doing everything to help make the stem cell lab function. Many thanks to Corey Schulz for his hard work on stem cell culturing and astrocyte differentiations that was critical to the start of this project. Thank you to Ricardo Miramontes for his technical assistance in quality control analysis of many astrocyte differentiation time points. Thanks to Chris Quan for his diligent work on the iBMEC project. Thank you to Dr. Lisa Salazar for the generation of the CD09iHD109n1 HTT KD line and helpful discussions on data. Many thanks to Jack Reidling for his scientific guidance, especially on mouse-related work as well as Alice Lau for guidance on with nuclei isolations and diligent mouse work. Thank you to Niki Geller for her meticulous and beautiful Western blots. I would like to acknowledge Mara Burns, who has been an absolute pleasure to mentor for the beginning of her graduate career. I am so excited to be handing off a project that I started in lab to such a talented new graduate student and friend. Can't wait to hear how she brings astrocyte research to new heights! Thank you also to Yuna for being the glue to makes the Thompson lab function behind the scenes.

I would like to acknowledge the OG Gross Hall girls: Dr. Lisa Salazar, Dr. Sarah Hernandez, Dr. Charlie Smith-Geater, Dr. Isabella Sanchez, Jennifer Stocksdale, and Keona Wang. To the long nights and weekends that we spent in the large and small hoods of the TC room, we commiserated together when the contamination got the best of us, got fake Starbucks when the caffeine was needed, had aliquoting parties before massive differentiations, then celebrated together when those massive harvests were completed. And at some point, you guys all babysat my astrocytes or cat (or both). For that, I thank you all.

To the Thompson lab fellow and past graduate students, technicians, and project scientists not listed above, especially Dr. Gianna Fote, Dr. Isabella Sanchez, and Dr. Eva Morozko for their friendship and commiseration. I am grateful to have been able to work so closely with such talented scientists and great people.

To my collaborators and their labs. Dr. Wayne Poon and Dr. Edsel Abud for their work on defining the astrocyte differentiation used in this dissertation. Dr. Vivek Swarup and lab for their collaboration on the R6/2 snRNA-seq project. Dr. Dritan Agalliu, Dr. David Housman, Dr. Ernest Fraenkel, and Dr. Clive Svendsen labs for their collaboration on the HD iBMEC project.

I would also like to acknowledge my undergraduate labs at UC Santa Cruz, in particular Dr. David Haussler's Wet Lab. They opened my eyes to research and helped excel me to where I am today.

Thanks to the UCI Biological Chemistry department, including Dr. Peter Kaiser and Dr. Kyoko Yokomori as well as Barbara Shainberg for their support.

I would like to thank Elsevier for permission to include Chapter 1 of my dissertation, which was originally published in *Cell Reports.* Financial support was provided by the University of California, Irvine, National Institutes of Health, UCI School of Medicine.

Thank my best friends: Ginger Berryman, Amanda Knapp, and Sarah Bernardini for their continued friendship and support during this journey. To my friends from my CMB cohort that helped me get through these years and the friends I gained from the UCI Women's Club Volleyball team that pushed me through the last years. All these friendships helped me complete this dissertation and I am grateful for the experiences I shared with them.

I could not have completed this PhD without the love and support of my fiancé, Jory Hollander. All the many late nights that turned into early mornings, he stayed up next to me while I analyzed data or worked on presentations and grants – he has always been there for me. The stability of love and laughter he provided during this rollercoaster was how I was able to get through. I love that during this time, we were able to rekindle both of our first loves, volleyball, and find new ones together, like coaching. From all the stages of life we have gone through together during more than a decade, this recent one has been the best; I can't wait to see where the future takes us. I would also like to Jory's family, in particular his mother, Sally, for her warmth and kindness as I completed this work.

Most importantly, thank you to my family. My parents for their unconditional support and encouragement. The nurturing and loving attitude they bestowed on me will live on through my work and life. They never hesitated to provide whatever I needed to achieve my goals – I only hope that one day I can be the parents you were to me. Thank you to my mom for teaching me strength, empathy, and love in heart and spirit. Thank you to my dad for teaching me how to climb mountains (physically and mentally) at a young age and the determination to strive for efficiency in all parts of life. Thank you to my sister and role model, Talia, for her unwavering confidence in me and fun-loving attitude in all things in life; you taught me to push myself out of my comfort zone and to cherish all the moments. Thank you to my grandparents for their endless love. Their pride in my achievements drove me to want to work even harder for those "two more points." Together they all have been an immeasurable part of this journey. I know, because of them, I can achieve anything I put my heart and mind to.

Finally, I would like to thank Huntington's disease patients and their families for their invaluable contribution to the work in this dissertation.

CURRICULUM VITAE

Andrea Marina Reyes-Ortiz

EDUCATION

2015 – 2021	University of California, Irvine Doctor of Philosophy in Biomedical Sciences Advisor: Leslie M. Thompson, Ph.D. Department of Biological Chemistry, School of Medicine
2015 – 2018	University of California, Irvine Master of Science in Biomedical Sciences Advisor: Leslie M. Thompson, Ph.D. Department of Biological Chemistry, School of Medicine
2010 – 2014	University of California, Santa Cruz Bachelor of Science in Bioengineering, Biomolecular Concentration Minor in Bioinformatics Jack Baskin School of Engineering

RESEARCH EXPERIENCE

Huntington's Disease Astrocyte and Brain-Microvascular Endothelial Cell Dysregulation
PhD Thesis Project, Thompson Lab
University of California, Irvine
January 2016 – October 27th, 2021
Mentor: Leslie M. Thompson

Derivation of CD271-Positive Melanocytic Lineage Populations from Human Embryonic Stem Cells
Graduate School Rotation, Boiko Lab
University of California, Irvine
July 2015 – December 2015

Characterizing Orangutan Induced Pluripotent Stem Cell Lines
HHMI Research Technician, Haussler Lab
University of California, Santa Cruz
December 2014 – April 2015

Examining Nuclear Lamina Mutations for Maturation of Human iPSC-Derived Neural Cells
Undergraduate Summer Research, Lowry Lab
University of California, Los Angeles
June 2014-September 2014

Reprogramming of Primate Fibroblasts into Induced Pluripotent Stem Cells
Undergraduate Thesis Research, Haussler Lab
University of California, Santa Cruz
September 2013 – December 2014

Marine Microecology Lab
Undergraduate Research, Zehr Lab
University of California, Santa Cruz
June 2012 – September 2013

AWARDS

2020	Outstanding Predoctoral Scholar: UCI Institute for Memory Impairments and Neurological Disorders Symposium
2020	First Place Business Pitch Competition: UCI Business Concepts for STEM Scientists Certificate Course
2020	Coach of the Year Nominee: UCI Club Sports
2019–2020	NIH-R01 Diversity Supplement Fellowship
2019	Stanley Behrens Research Excellence Award: UCI School of Medicine
2019	Gordon Research Seminar Honorable Mention Poster Award
2018	Shark Tank Competition Winner: UCI T32 Training Grant Retreat
2018	Howard Hughes Medical Institute Gilliam Graduate Fellowship Finalist
2017	Elevator Pitch Competition Winner: UCI T32 Training Grant Retreat
2017	Carl Storm Underrepresented Minority Fellowship
2017–2019	NIH/NINDS-National Research Service Award: T32 Trainee for Stem Cells and Translational Medicine in Neurological Disorders
2016	UCI School of Medicine Travel Award
2016	Huntington's Disease Community, Advocacy, Research, and Education (HD-CARE) Everest Award
2015–2017	University of California Bridge to the Doctorate Fellowship
2015	NIH Initiative for Maximizing Student Development (IMSD) Fellowship
2015	UCI Diversity Recruitment Fellowship
2015	UCI Graduate Opportunity Fellowship
2013	Society for the Advancement of Chicanos/Hispanics and Native Americans in Science (SACNAS) Travel Award Scholarship
2012, 2014	UCSC Jack Baskin School of Engineering Dean's Honors
2012–2014	University of California's Leadership Excellence through Advanced Degrees (UC LEADs) Undergraduate Research Fellowship
2012	NSF-California Alliance for Minority Participation (CAMP) Summer Undergraduate Research Fellowship
2010	Mushroom Mardi Gras Scholarship Recipient
2009–2010	Live Oak High School Associated Student Body President

ACADEMIC SERVICE

2020–Present	Mentor to Mara S. Burns Graduate Student: PhD Neurobiology and Behavior Department University of California, Irvine
2019	Tech Trek Co-leader, American Association of University Women
2018–2019	Mentor to Corey J. Schulz Undergraduate Intern: B.S. Molecular and Biotechnology, Biology CIRM Bridges to Stem Cell Research Scholar

2016–2020	STEM Volunteer and Science Fair Judge, Irvine Unified School District
2013–2014	Biomedical Engineering Society Secretary University of California, Santa Cruz

COMMUNITY SERVICE

2016–Present	Volunteer, Huntington's Disease Community, Advocacy, Research, and Education (HD-CARE)
2017–2019	Huntington's Disease Society for America Team Hope Walk
2018	Co-chair, HD-CARE Fundraising Gala
2010	Volunteer, Resource Area for Teaching (RAFT)

PROFESSIONAL DEVELOPMENT & LEADERSHIP

2021	Genentech gRED Portfolio Strategy and Planning Co-op/Intern
2021	Project Management Foundations Certificate
2021	Management Beyond the Classroom Certificate, UCI
2020	Business Concepts for STEM Scientist Certificate, UCI
2020	Data Science Math Skills Certificate, Duke University
2020	Scientific Writing and Publishing Certificate, Nature Masterclass
2019	Scientific Communication Certificate, Activate to Captivate
2019	Mentoring Excellence Program Certificate, UCI
2017–2019	Trainee, NINDS/NIH-National Research Service Award: T32 Trainee for Stem Cells and Translational Medicine in Neurological Disorders
2015	Fellow, NIH Initiative for Maximizing Student Development (IMSD)
2013–2014	Secretary, UCSC Biomedical Engineering Society
2012–2014	Fellow, University of California's Leadership Excellence through Advanced Degrees (UC LEADs)
2012	Fellow, NSF California Alliance for Minority Participation (CAMP)
2010–2013	NCAA Athlete, UCSC Women's Varsity Volleyball Team

PUBLICATIONS

Reyes-Ortiz AM, Wu J, Abud EM, Geller NR, Wu J, Miramontes R, Wang KQ, Schulz C, Lau A, Michael N, Miyoshi E, Reidling JC, Blurton-Jones M, Swarup V, Poon WW, Lim RG, Thompson LM. "Dysregulated synaptogenesis and actin transcriptional states in Huntington's disease iPSC-derived and mouse astrocytes." *Cell Reports (Submitted).*

Lim RG, Al-Dalahmah O, Wu J, Gold M, Tang G, Reidling JC, Adam M, Miramontes R, Reyes-Ortiz AM, Khan F, Ofori K, Lau A, Miyoshi E, Michael N, Geller NR, Schulte-Bisping M, Vonsattel JP, Davidson S, Menon V, Swarup V, Fraenkel E, Goldman JE, Thompson LM. "Single-nuclei RNAseq analysis of HD mouse model and human brain reveals impaired oligodendrocyte maturation and potential causal regulators." *Nature Communications (In revision).*

Hernandez SJ, Fote GM, Reyes-Ortiz AM, Steffan JS, Thompson LM. "Cooperation of cell adhesion and autophagy in the brain: functional roles in development and neurodegenerative disease." Dec 2021. *Matrix Biology Plus* 12, 1-27.

Fote GM, Geller NR, Reyes-Ortiz AM, Thompson LM, Steffan JS, Grill JD. "A scoping review of dietary factors conferring risk or protection for cognitive decline in APOE ε4 carriers." Nov 2021. *The Journal of Nutrition, Health & Aging*.

Field AR, Jacobs FMJ, Fiddes IT, Phillips AP, Reyes-Ortiz AM, LaMontagne E, Whitehead L, Meng V, Rosenkrantz JL, Olsen M, Hauessler M, Katzman S, Salama S, Haussler D. "Structurally Conserved Primate LncRNAs Are Transiently Expressed during Human Cortical Differentiation and Influence Cell-Type-Specific Genes." Feb 2019. *Stem Cell Reports* 12, 245-257.

Lim RG, Quan C, Reyes-Ortiz AM, Lutz SE, Kedaigle AJ, Gipson TA, Wu J, Vatine GD, Stocksdale J, Casale MS, Svendsen CN, Fraenkel E, Housman DE, Agalliu D, Thompson LM. "Huntington's Disease iPSC-Derived Brain Microvascular Endothelial Cells Reveal WNT-Mediated Angiogenic and Blood-Brain Barrier Deficits." May 2017. *Cell Reports* 19, 1365-1377

RESEARCH PRESENTATIONS

Astrocyte cell states in Huntington's disease mouse and patient iPSC models

November 2020	UCI Biological Chemistry Department Research in Progress Seminar, Oral presentation
July 2020	Cold Spring Harbor Laboratory: Glia in Health and Disease Meeting, Poster

Evaluating the contribution of astrocytes to Huntington's disease pathogenesis

February 2020	UCI Institute for Memory Impairments and Neurological Disorders (REMIND) Emerging Scientists Symposium, Poster
October 2019	UCI School of Medicine Grad Day, Poster
June 2019	Gordon Research Conference CAG Triplet Repeat Disorders, Poster
June 2019	Gordon Research Seminar CAG Triplet Repeat Disorders, Oral presentation and Poster
May 2019	UCI Biological Chemistry Department Research in Progress Seminar, Oral presentation
February 2019	UCI Institute for Memory Impairments and Neurological Disorders (REMIND) Emerging Scientists Symposium, Poster
October 2018	UCI School of Medicine Grad Day, Poster
August 2018	Hereditary Disease Foundation (HDF) Symposium, Poster
July 2018	Cold Spring Harbor Laboratory: Glia in Health and Disease Meeting, Poster
April 2018	UCI Biological Chemistry Department Research in Progress Seminar, Oral presentation

Transcriptomic and functional analysis of Huntington's disease neurovascular unit

April 2018	UCI Biological Chemistry Department Research in Progress Seminar, Oral presentation
June 2017	UCI Biological Chemistry Department Second Year Symposium, Oral presentation

Blood-brain barrier and neurovascular unit deficits in Huntington's disease induced pluripotent stem cell-derived cells

March 2018	UCI Institute for Memory Impairments and Neurological Disorders (REMIND) Symposium, Poster

September 2017	UCI School of Medicine Grad Day, Poster
June 2017	Gordon Research Conference CAG Triplet Repeat Disorders, Poster
June 2017	Gordon Research Seminar CAG Triplet Repeat Disorders, Poster
February 2017	UCI Institute for Memory Impairments and Neurological Disorders (REMIND) Emerging Scientists Symposium, Poster

Transcriptomic and functional analysis of HD iPSC-derived brain microvascular endothelial cells reveals angiogenic and BBB deficits

June 2017	Gordon Research Conference CAG Triplet Repeat Disorders, Oral presentation

Antisense oligonucleotide-mediated knockdown of HTT to rescue blood-brain barrier deficits in Huntington's disease iPSC-derived brain endothelial cells

June 2016	UCI Cell and Molecular Biosciences Program Spring Symposium, Oral presentation
March 2016	UCI Cell and Molecular Biosciences Program Winter Symposium, Oral presentation

Derivation of CD271-positive melanocytic lineage populations from human embryonic stem cells

December 2015	UCI Cell and Molecular Biosciences Program Fall Symposium, Oral presentation

Examining the role of nuclear lamina in the maturation of human iPSC-derived neural progenitor cells and neurons

August 2014	UCLA Summer Programs for Undergraduate Research Symposium, Poster

Reprogramming of Primate Fibroblasts for Integration-Free Induced Pluripotent Stem Cell Lines

February 2015	Genome 10K Meeting, Poster
October 2014	Society for the Advancement of Chicanos/Hispanics and Native Americans in Science (SACNAS) National Conference, Poster
April 2014	Launch! A Celebration of the UCSC Student Experience, Poster
March 2014	University of California's Leadership Excellence through Advanced Degrees (UC LEADs) Statewide Symposium, Poster

Design of Molecular Chemistries to Evaluate Synechococcus Iron Limitation in the Monterey Bay

October 2013	Society for the Advancement of Chicanos/Hispanics and Native Americans in Science (SACNAS) National Conference, Poster
August 2013	UCSC Summer Undergraduate Research Symposium, Poster

Examining the Relationship of Ammonia-Oxidizing Archaea to Ammonia and Phytoplankton in Monterey Bay Using Autonomous Instrumentation

March 2013	University of California's Leadership Excellence through Advanced Degrees (UC LEADs) Statewide Symposium, Poster
October 2012	Annual Biomedical Research Conference for Minority Students (ABRCMS) National Conference, Poster
August 2012	UCSC Summer Undergraduate Research Symposium, Poster

ABSTRACT OF THE DISSERTATION

Huntington's disease astrocyte and brain-microvascular endothelial cell dysregulation

by

Andrea Marina Reyes-Ortiz

Doctor of Philosophy in Biomedical Sciences

University of California, Irvine, 2021

Professor Leslie M. Thompson, Chair

Huntington's disease (HD) is a devastating inherited neurodegenerative disease caused by a CAG repeat expansion in the Huntingtin (*HTT*) gene. The HD disease-causing mutation affects numerous cellular processes, contributing to overall dysregulated cellular homeostasis in the central nervous system, particularly in the striatum and cortex of the brain. While HD is predominately characterized by the loss of neurons, other non-neuronal cell types have been demonstrated to be significantly affected by mutant *HTT*; however, characterization of non-cell autonomous effects caused by *HTT* CAG repeat expansion in non-neuronal cell types was largely lacking prior to initiating this dissertation. Here, I describe my investigation into the cell-autonomous affects caused by mutant *HTT* through patient induced pluripotent stem cell (iPSC) modeling of two critical cellular regulators of brain homeostasis—brain microvascular endothelial cells (BMECs) and astrocytes. Assessing the dysregulation of HD BMECs and astrocytes provides a clearer understanding of disease pathogenesis and can provide additional knowledge to aid in the development of effective therapeutic interventions needed for HD patients.

This dissertation describes several transcriptomic analyses to provide mechanistic insights into pathways that underlie dysregulated HD iPSCs-derived BMECs (iBMECs) and iPSC-derived astrocytes (iAstros). First, bulk RNA-sequencing (RNA-seq) demonstrated aberrant WNT activation in HD iBMECs that when inhibited pharmacologically, prevented angiogenic deficits

and improved paracellular barrier function in iBMECs. Secondly, single-nuclei RNA-seq highlighted inhibited synaptogenesis and glutamate receptor signaling states in both HD iAstros and HD mouse model astrocytes as well as a novel activated actin cytoskeletal signaling cell state unique in HD human astrocytes. HD iBMEC and HD astrocyte studies demonstrated dysfunctional properties that may be due to aberrant developmental trajectories. These data further support the hypothesis that mutant *HTT* induces dysregulated non-neuronal cell types that promote dysfunctional properties unique to each cell type, contributing to HD pathogenesis. Together, my analyses provide novel insights into molecular mechanisms that contribute to disease pathogenesis, and this knowledge can be used to inform future therapeutic investigations for HD.

INTRODUCTION

1.1 Huntington's Disease

Huntington's disease (HD) is a devastating, autosomal-dominant neurodegenerative disease characterized by movement abnormalities, psychiatric disturbances, and behavioral changes (Ross & Tabrizi, 2011). HD is considered the most common monogenic neurological disorder in the developed world (Kay et al., 2018), affecting nearly 14 in 100,000 individuals in Western populations (G. P. Bates et al., 2015; McColgan & Tabrizi, 2018).

1.1.1 Huntington's Disease Pathogenesis

The genetic cause of HD is a CAG repeat expansion in the first exon of the *huntingtin* (*HTT*) gene, which encodes a polyglutamine (polyQ) repeat expansion in the HTT protein (The Huntington's Disease Collaborative Research Group, 1993). When the *HTT* CAG repeat is expanded to 40 or above repeats, HD is fully penetrant, typically striking patients in the prime of life between 35 and 50 years of age. Relatively rare occurrences of juvenile-onset HD (~10% of cases) can occur when expanded to over 60 CAGs, with symptoms typically developing before 20 years of age (Cronin et al., 2019; Nance & Myers, 2001; Zuccato et al., 2010). CAG repeat length is generally anti-correlated with age of onset but only accounts for around 50% of age of onset variance, suggesting a role for additional genetic or environmental factors in HD age of onset. Single-nucleotide polymorphisms (SNPs) in HD patients have been discovered using genome-wide association studies that correlate with either a delayed or accelerated clinical onset (GeM-HD Consortium, 2015, 2019; The U.S.–Venezuela Collaborative Research Project & Wexler, 2004). Nevertheless, chronic mutant HTT expression induces a spectrum of defects in cellular and molecular processes.

The polyQ expansion of mutant HTT alters the protein structure of this large 348kDa protein. Expanded polyQ tracts induce protein misfolding, hypothetically through polyQ's

tendency to collapse into hydrogen bond-stabilized, compact coiled structures (Crick et al., 2006; Punihaole et al., 2017; H. Wang et al., 2006; Wen et al., 2017); this leads to mutant HTT protein aggregation, which may lead to proteasome-dependent cellular dysregulation (Bence et al., 2001). Proteolytic cleavage induced by caspases and proteases results in the accumulation of HTT fragments (Lunkes et al., 2002; Wellington et al., 2000). Proteolytic cleavage (Gafni et al., 2004; Lunkes et al., 2002; Ratovitski et al., 2007; Wellington et al., 2000) and incomplete splicing (Sathasivam et al., 2013) are two mechanisms that can produce an extremely toxic N-terminal fragment containing the N17 domain of mutant HTT's polyQ tract (G. Bates, 2003). Protein oligomerization and aggregation are common pathological occurrences in neurological disorders with protein misfolding, such as the production of beta-amyloid and aggregation of alpha-synuclein in Alzheimer's disease (AD) and Parkinson's disease (PD), respectively (Hipp et al., 2014; Kurtishi et al., 2019; Ross & Poirier, 2004). CAG repeat expansion is linked to at least 9 other neurological, like spinocerebellar ataxia type 1 (SCA1) and X-linked spinal and bulbar muscular atrophy (SBMA) (Adegbuyiro et al., 2017; Fan et al., 2014; la Spada et al., 1994).

HTT is ubiquitously expressed in all cell types in the body and a broad range of cellular processes predominantly in the brain are impacted by chronic mutant HTT expression (Bates et al., 2015; Ross & Tabrizi, 2011). There is a growing awareness that other peripheral tissues may also be affected (e.g., liver, cardiac and other muscle); however, the most overt effects are observed neuropathologically in striatum and cortex. Wildtype HTT is predominantly expressed in the cytoplasm of cells but can shuttle in and out of the nucleus. With expression of an expanded repeat within HTT, there is a progressive accumulation of the mutant protein in the nucleus. Within the nucleus, mutant HTT can interact with and bind transcription factors, chromatin, and DNA; accordingly, mutant HTT-induced transcriptional dysregulation is an early event in HD pathogenesis (G. P. Bates et al., 2015; Tabrizi et al., 2019) although the mechanisms are still being elucidated. While the function of normal HTT is still not fully understood, it is believed to serve as a scaffolding protein. HTT has been demonstrated to mediate brain-derived neurotrophic

factor (BDNF) trafficking along microtubules (Gauthier et al., 2004); therefore, dysfunction in this process may contribute to regional vulnerability from the loss of neurotrophic support from cortex to striatum. HTT also appears to function as a scaffold for selective autophagy through HTT's interaction with key autophagic proteins (Cha, 2007; Steffan et al., 2000). mutant HTT triggers autophagic dysregulation at several disease stages, contributing to alterations in protein degradation (Ochaba et al., 2014). Together with transcriptional and functional alterations, mutant HTT is believed to induce loss of normal HTT functions and gain of toxic functions (G. P. Bates et al., 2015; Tabrizi et al., 2019).

The central nervous system (CNS) has the highest expression level of HTT in the body, and mutant HTT appears to have the most significant effect on neurons (Bates et al., 2015). Specifically, GABAergic medium spiny neurons (MSNs), located within the striatal region of the brain, are the most sensitive to mutant HTT expression and exhibit the most overt HD neuropathology, together with cortical atrophy. My laboratory and others have demonstrated major cell-autonomous impairments in non-neuronal cell types—from glia (Benraiss et al., 2021; Garcia et al., 2019; Juopperi et al., 2012; Osipovitch et al., 2019) to the blood-brain barrier endothelium (Lim et al., 2017)—suggesting that chronic expression of mutant HTT may induce intrinsic deficits within each cell type.

As there are no effective disease-modifying treatments, ultimately HD is a fatal diagnosis, with a mean survival rate of about 20 years (Ross & Tabrizi, 2011; Tabrizi et al., 2019). Therapies aimed at decreasing overall levels of either wildtype HTT or expanded mutant HTT in patients have been ongoing areas of clinical research since the discovery of the disease-causing protein in 1993 (The Huntington's Disease Collaborative Research Group, 1993). However, homozygous HTT knockout in mice results in embryonic lethality and HTT knockdown during embryogenesis induce impairments in striatal and cortical development that led to death shortly after birth (Duyao et al., 1995; Nasir et al., 1995; White et al., 1997); this evidence indicates the importance of HTT in mammalian development and the delicate nature of this potential therapeutic intervention.

Additional therapies targeting disease age of onset modifiers and cellular replacement are also active areas of research. More basic research on mechanisms involved in HD pathogenesis can help to uncover additional therapeutic targets.

1.1.2 Modeling Huntington's Disease

The monogenic nature of HD provides the ability to study disease *in vivo* and *in vitro*. Animal models are classically utilized for investigating the molecular mechanisms involved in HD pathogenesis and the assessment of potential therapeutic interventions *in vivo*; however, with the generation of induced pluripotent stem cell (iPSC) reprogramming (Takahashi & Yamanaka, 2006; Yamanaka et al., 2007) HD researchers have begun modeling the disease *in vitro* over the past decade using patient-derived cells (e.g. HD iPSC Consortium, 2013, 2017).

1.1.2.1 Huntington's Disease Mouse Models

Since the discovery of the disease-causing mutation, transgenic, full-length, and knock-in mouse models have been used to model the pathophysiology HD *in vivo*. The R6/2 mouse model, created through the transgenic overexpression of the first exon of human *HTT* containing around 115 to 150CAG repeats, is the most extensively characterized and utilized HD mouse model. R6/2 recapitulates many aspects of HD symptomology, including severe progressive neurological deficits, involuntary movements, and impaired motor function (Mangiarini et al., 1996). Although there is brain volume loss, there is minimal neurodegeneration visualized in the R6/2 model, which is often the case for mouse models for other neurodegenerative diseases (Dawson et al., 2018). The R6/2 mouse model is rapidly progressing; as early as 7 weeks of age, mutant HTT aggregates are visualized in the nuclei of R6/2 neurons, similar to that observed neuropathologically in human HD post-mortem tissue. By 8 to 12 weeks, R6/2 mice are severely impaired with premature death at approximately 13 to 16 weeks (J. Y. Li et al., 2005). Another transgenic fragment mouse model

is R6/1 in which the *HTT* exon one transgene is inserted into an alternative integration site and displays slightly slower pathogenesis with a decline in motor function around 13 to 20 weeks. N171-82Q is an N-terminal transgenic model expressing the first 171 amino acids of human *HTT* (J. Y. Li et al., 2005). zQ175 and *HdhQ150* are knock-in mouse models of murine Htt at the endogenous locus. BACHD and YAC128 are commonly used full-length transgenic models of human *HTT* (Farshim & Bates, 2018). These HD mouse models and others not listed here recapitulate various aspects of the human disease, allowing HD researchers the ability to study mechanisms underlying HD pathogenesis (Crook & Housman, 2013).

1.1.2.2 Huntington's Disease iPSC Modeling

Since iPSCs were discovered, they have been utilized extensively to model diseases *in vitro*. iPSCs provide a nearly unlimited source of pluripotent cells that can differentiate into every cell in the adult body. They are generated through the reprogramming of somatic cells, like fibroblasts, via the genetic insertion of various combinations of pluripotency transcription factors including: octamer-binding transcription factor 4/POU domain class 5 transcription factor 1 (OCT4/POU5F1), SRY-box 2 (SOX2), MYC proto-oncogene (c-MYC), Krueppel-like factor 4 (KLF4), homeobox protein NANOG, and/or RNA-binding protein (LIN28) (HD iPSC Consortium, 2013; Takahashi & Yamanaka, 2006; Yamanaka et al., 2007). These reprogrammed cells mimic the pluripotency of embryonic stem cells (ESCs). iPSCs are coaxed into specific developmental lineages through the influence of specific growth mediums containing defined growth factors that have been described to regulate their development *in vivo*. iPSCs allow researchers to study the development of diseases in their endogenous forms *in vitro*, without the artificial overexpression of disease-causing mutations for example (Rivetti di Val Cervo et al., 2021). This is especially important since mouse models often do not fully recapitulate aspects of disease pathogenesis in humans—even for a monogenic disease—and there are significant challenges associated with

gaining adequate human material from neurogenerative diseases like HD, and tissues obtained are end stage with significant tissue loss.

The history of HD iPSC modeling began with modeling the most vulnerable cell type, neuronal cells, but more recently, researchers have begun using iPSCs to model alternative neural and non-neural cells for HD. For example, the HD iPSC consortium labs, which includes my lab, have utilized HD patient-derived iPSCs (HD iPSC Consortium, 2013) with a variety of CAG lengths to describe phenotypes from NSCs (HD iPSC Consortium, 2017), MSN-enriched cultures (Smith-Geater et al., 2020), and brain microvascular endothelial cells (Lim et al., 2017). A large portion of my dissertation furthers our elucidation into HD iPSC-derived phenotypes by modeling HD astrocytes *in vitro*.

1.2 Astrocytes

Astrocytes are the beautiful star-shaped cells within the CNS, containing processes that branch outward from the soma. Their morphology can range in number and length of processes depending on age, species, and spatial location in the brain. Astrocytes have been classified into two major subtypes, although their degree of heterogeneity is just beginning to be explored (Batiuk et al., 2020; Hu et al., 2016). *Protoplasmic astrocytes* have many short, highly branched processes that end in characteristic endfeet, which wrap around blood vessels or ensheath thousands of synapses (Bushong et al., 2002; Khakh & Sofroniew, 2015; Miller & Raff, 1984). Protoplasmic astrocytes are confined to the gray matter, while fibrous astrocytes often run parallel to white matter tracts. *Fibrous astrocytes* are more elongated with less numerous but longer processes. Fibrous astrocytes can be involved in the repair of damaged tissue by helping to form a glial scar through astrocytic proliferation around the injury site (Sofroniew & Vinters, 2010). The morphological variations of astrocytes and their widespread numbers throughout regions of the

CNS suggest potential functional heterogeneity in astrocyte subtypes, an area of astrocyte biology actively being studied.

Protein marker expression can vary across different astrocyte subtypes and across species. Glial fibrillary acidic protein (GFAP) has been the most widely used astrocyte marker for the past several decades. This intermediate filament protein is abundantly expressed across the CNS and highly expressed throughout astrocyte processes to their endfeet. For these reasons, GFAP has traditionally been considered an ideal marker to detect astrocyte morphology; however, GFAP has some drawbacks as an astrocyte-specific marker. GFAP can be upregulated in many disease states, such as reactive astrogliosis. Additionally, ependymal cells have been demonstrated to express GFAP during development. Finally, GFAP is primarily expressed by white matter astrocytes *in vivo*, making it difficult to detect gray matter astrocytes if other markers are not utilized. Double staining with additional astrocyte markers, such as aldehyde dehydrogenase 1 family member L1 (ALDH1L1), is highly recommended. Other markers that are important players in astrocyte functions, such as excitatory amino acid transporter 1 (EAAT1) and excitatory amino acid transporter 2 (EAAT2), are also recommended astrocyte markers, although their protein levels have been demonstrated to be dysregulated in diseased states including HD. This lack of clearly defined astrocyte markers for each stage, region, and even species aids in the complication of studying astrocytes.

1.2.1 Astrocyte Functions

Astrocytes are the major glial cell type in the CNS, where they have numerous functions regulating the homeostasis of the brain. Derived from the late Greek word for glue, γλία*,* astroglia were originally thought to primarily provide structural support for neurons. Increasing evidence has shed light on a wide array of astrocytic functions critical for multiple facets of CNS homeostasis.

1.2.1.1 Neuronal Regulation

Astrocytes have roles in neurotrophic support, synaptogenesis, neuronal maturation, and neuronal maintenance. Astrocyte processes envelop nearly all synapses to form the tripartite synapse where they situate their endfeet between pre-synaptic and post-synaptic neurons (Sofroniew & Vinters, 2010). Here astrocytes release a range of molecules that regulate the formation and maturation of synapses. Synapse formation establishes neural circuitry and, therefore, all essential functions of the nervous system.

Many astrocyte-secreted factors are critical to synapse formation and maturation in the developing brain. Thrombospondins are astrocyte-secreted extracellular matrix (ECM) proteins involved in the development of neuronal spines, or the protrusions that receive neuronal input from an axon at the synapse (Barres, 2008; Dowell et al., 2009; Ullian et al., 2004). More specifically, thrombospondins induce clustering of presynaptic and postsynaptic proteins, synapsin and PSD-95, respectively. Tumor necrosis factor alpha (TNFα) turns immature and silent synapses into functional synapses through the recruitment of α-Amino-3-hydroxy-5-methyl-4-isoxazolepropionic acid (AMPA) receptors to the synaptic surface. Glypicans (GPC4 and GPC6) are a family of astrocyte-secreted molecules that play a role in synapse assembly (Clarke & Barres, 2013). Hevin/secreted protein acidic and rich in cysteine (SPARC) is another group of astrocyte-secreted proteins that regulate synapse formation are for excitatory synapses (Clarke & Barres, 2013; Kucukdereli et al., 2011). Together, this formation of active neuronal synapses through the influence of astrocyte-secreted factors is called synaptogenesis.

Astrocytes are the sole provider of cholesterol for the adult human brain. Cholesterol is a critical molecule in neuronal synaptogenesis, increasing presynaptic function nearly 100-fold. Cholesterol is a major component of synaptic vesicles, where it controls the formation, shape, and release of synaptic vesicles (Mauch et al., 2001). Within the brain, astrocytes also have the highest production capacity of the most important cholesterol transport protein, apolipoprotein E

(APOE) (Björkhem & Meaney, 2004; Garcia-Segura & Melcangi, 2006). The astrocytic synthesis and regulation of cholesterol is vital to healthy brain function.

In addition to synaptogenesis regulation, astrocytes are critical for the active elimination of synapses through synaptic pruning (together with microglia) throughout development (Chung et al., 2013). Synaptic pruning is a fundamental neural developmental step that occurs postnatally in humans. Overproduction of synaptic contacts from birth to early childhood requires synaptic elimination into adulthood. Synaptic pruning enhances neuronal transmission through the elimination of ineffective synapses. This process is vital for the establishment and maturation of brain circuitry (Chechik et al., 1999). Deficits in synaptic pruning can lead to excessive synaptic connections, which has been linked to neuropsychiatric disorders, such as autism spectrum disorder and bipolar disorder (Eltokhi et al., 2020; Tang et al., 2014; X. Wang et al., 2018). In mammalian astrocytes, the engulfment of synaptic connections through phagocytosis is regulated through MER proto-oncogene tyrosine kinase (MERTK) and multiple EGF-like domains 10 (MEGF10)-dependent pathways (Chung et al., 2013). Astrocytes can also release signals that induce synaptic expression of complement C1q, which tags synapses for elimination by microglia (Barres, 2008; Stevens et al., 2007).

Inter-astrocytic communication of calcium signaling is a function of astrocytes that is thought to help control blood flow for coupling to neuronal energy demand (Khakh & Sofroniew, 2015; Zhao et al., 2015). Gap junctions connect adjacent astrocytes through connexin proteins, allowing calcium waves to propagate. This signaling, lasting tens of seconds, is slow in comparison to neuronal action potentials that take just milliseconds. Calcium signaling induces the release of molecules, like prostanoids and arachidonic acid, that signal vasoconstriction or vasodilation based on the current metabolic environment, to couple blood flow to neuronal energy demand (Attwell et al., 2010; Biesecker & Srienc, 2015). Calcium signaling can also be triggered by neurotransmitters, like glutamate, and induce the release of transmitters, like glutamine, from astrocytes (Sofroniew & Vinters, 2010). In addition to calcium signaling, potassium and sodium

ions released by neuronal activity flow into astrocytes via ion channels occurs for buffering purposes (Allaman et al., 2011); this process can evoke inward currents within astrocytes but is not capable of propagating action potentials (Sofroniew & Vinters, 2010). Astrocyte endfeet are comprised of high densities of the water channel aquaporin 4 (AQP4) and the ATP-sensitive potassium channel (Kir4.1) where they buffer the osmotic imbalance created by neuronal activity (Larsen et al., 2014). Overall, astrocytes regulate the movement of ions and toxic metabolites from synapses as well as deliver nutrients (Barres, 2008).

Astrocytes are centrally located between neurons and the vasculature where they uptake, metabolize, and secrete transmitters critical for neuronal signaling. Astrocytes terminate the action of neurotransmitters, like glutamate (also referred to as glutamic acid) and gamma-aminobutyric acid (GABA), through uptake at the tripartite synapse. There are no enzymes that can degrade glutamate extracellularly therefore, once released by neurons, intracellular uptake of glutamate is required for its removal (Zhou & Danbolt, 2014). Astrocytes take up this excitatory neurotransmitter through transporters (EAAT1/GLT1 and EAAT2/GLAST) with the help of transmembrane glutamate receptors (GRIA1 and GRIA2) that form ligand-gated ion channels (Schousboe et al., 2015). Within the cytosol of astrocytes, glutamate is then degraded into the neuro-inactive state, glutamine, via glutamine synthetase (GLUL or GS) in an ATP-dependent manner (Schousboe et al., 2015). Glutamine is released from astrocytes via glutamine transporters (SNAT1 and 3, LATs, and ASCs), then taken up by neurons at the tri-partite synapse (Leke & Schousboe, 2016). Neurons convert glutamine to glutamate via phosphate-activated glutaminase (PAG), followed by the efflux of glutamate from glutamatergic neurons to complete one round of the glutamate-glutamine cycle (Schousboe et al., 2015). Glutamate originates from the tricarboxylic acid (TCA) cycle, which involves a series of enzymatic reactions in the mitochondria beginning with acetyl coenzyme A then eventually leads to α-ketoglutarate (αKG)'s reversible conversion by glutamate dehydrogenase (GDH) into glutamate (Plaitakis et al., 2017). Glutamate can be further catalyzed to GABA via glutamate decarboxylase (GAD) in the cytosol

for the GABAergic neuronal efflux of this inhibitory neurotransmitter (Schousboe et al., 2015).. Upon the dyshomeostasis of this cycle, alterations of the fine balance of glutamate or GABA at the tripartite synapse can be detrimental to brain homeostasis and ultimately lead to neuronal degeneration via excitotoxicity or to other clinical manifestations, like depression (Sanacora et al., 2012).

Astrocytes exhibit high glycolytic rates to produce enough lactate for the high energy demand of neurons. As the primary CNS storage site for glycogen, the stored form of glucose, astrocytes can sustain neuronal activity during hypoglycemia and phases of high neuronal activity through lactate transfer to neurons or other neighboring cells via astrocytic gap junctions (Sofroniew & Vinters, 2010). This process begins with the supply of glucose from the blood through the brain endothelium to astrocytes via glucose transporters (GLUT1). Glucose is then converted into pyruvate in a series of enzymatic reactions, called glycolysis, and then converted to lactate via lactate dehydrogenase isoenzyme A (LDHA). Finally, lactate is effluxed out of the cell by monocarboxylate transported (MCT) 1 or 4 to be influxed into neurons via MCT2. Within neuronal mitochondria, lactate is converted back to pyruvate via lactate dehydrogenase isoenzyme B (LDHB) to be used for oxidative phosphorylation, the main provider of energy for neuronal activity (Hall et al., 2012; Newington et al., 2013).

1.2.1.2 The Neurovascular Unit

Astrocytes maintain direct interactions with the brain endothelium to regulate the neurovascular unit (NVU). The NVU is the functional unit in charge of controlling the complex relationship between cellular and extracellular components to regulate blood-brain barrier (BBB) function and cerebral blood flow. The BBB is the highly selective barrier that supplies the brain with oxygen and essential nutrients, as well as mediates the efflux of waste products. The NVU is primarily comprised of brain endothelial cells (BECs), astrocytes, pericytes, and neurons. BECs are the

core element of the BBB restricting paracellular and transcellular molecular movement, but astrocytes are a critical component to NVU structure and function.

Tight and adherens junctions are cell-cell adhesion structures that play an important role in how BECs regulate the BBB. Tight junctions (TJs) are the primary and most apical structure restricting BBB paracellular permeability (Sandoval & Witt, 2008). TJs made up of transmembrane proteins, occludin (OCLN), and the Claudin family (CLDN3, CLDN5, CLDN12), as well as TJ-associated proteins, Zonula occluden/tight junction proteins 1-3 (ZO1-3 or TJ1-3), and junction adhesion molecules (JAM-A, JAM-B, JAM-C), that act as scaffolds linking TJs to the actin cytoskeleton (Abbott et al., 2006). BEC adherens junctions, involving proteins like platelet endothelial cell adhesion molecule 1 (PECAM1) and vascular endothelial (VE)-cadherin also aid in restricting paracellular permeability of the BBB. Together, TJs and adherens junctions separate the luminal and abluminal sides of the plasma membrane, forming a zipper-like seal between neighboring BECs (Sandoval & Witt, 2008). The restriction of paracellular permeability by a healthy complex of TJs and adherens junctions allows only for the transport of water-soluble agents between the blood and the brain.

Transcellular movement through BECs is how many molecules pass between the blood and brain. Bi-directional BEC transport proteins, such as glucose transporter 1 (GLUT1) and large neutral amino acids transporter small subunit 1 (LAT1), are required to shuttle non-lipid soluble nutrients between the brain and blood, like glucose and amino acids, respectively. Nucleoside and organic ion transporters are also present on BECs. Transcytosis is required for the transcellular movement of large molecules across the BBB. Transcytosis can be either absorptive, in the case of albumin or other plasma proteins, or receptor-mediated, for molecules like insulin and transferrin. Energy from ATP is required for efflux against a concentration gradient via transcytosis receptors ATP-dependent translocase (MDR1), also called p-glycoprotein (P-gp). Additionally, sodium-dependent glutamate transporters (EAAT1-3) efflux glutamate against a concentration gradient out of the brain. Dysregulation of tight junction proteins and transcellular

movement contribute to BBB permeability and has been described in neurodegenerative diseases (Sweeney et al., 2018).

Astrocytes are fundamental for establishing and maintaining BBB and neuronal functions through soluble and physical communications at the NVU (Abbott et al., 2006). The perivascular endfeet of astrocyte processes are comprised of highly specialized structures covering nearly 100% of the abluminal surface of the endothelium, allowing for the release of barrier-inducing factors and ions required for brain homeostasis (Abbott et al., 1992, 2006; Villaseñor et al., 2019). During embryonic development, astrocyte progenitors are fundamental for the release of the chemoattractant vascular endothelial growth factor-A (VEGF-A) to guide the development of new blood vessels, termed angiogenesis (Abbott et al., 2006; Iadecola, 2017). Astrocyte-secreted SHH is a critical molecule for barrier induction as it upregulates TJ proteins OCLN and CLND5 to seal the barrier during development. Throughout BBB maturation, astrocyte-secreted angiopoietin proteins (ANG1 and ANG2) upregulate and enhance TJ subcellular distribution. ANG2 and APOE from astrocytes also play roles in post-translationally modifying OCLN for further BBB maturation. Transforming growth factor beta (TGFβ), basic fibroblast growth factor (bFGF), and glial-derived neurotrophic factor (GDNF) are other astrocytes-secreted factors that support the formation of barrier properties (Abbott et al., 2006). Without astrocyte regulation of the BBB, the NVU can develop abnormalities, such as increased permeability or aberrant angiogenesis.

Astrocytes play a critical role in depositing extracellular matrix (ECM) proteins for cellular scaffolding of neurons and NVU's basal lamina. Astrocyte-secreted ECM molecules, like the glycoprotein tenascin cytotactin (TNC), help to control cell migration and proliferation, as well as neuronal homeostasis (Jones & Bouvier, 2014). At the NVU, BECs are anchored to the basal lamina via integrin proteins (ITGs) (Zhao et al., 2015). Integrins are transmembrane proteins that interact with ECM proteins, like laminins, collagens, and perlecans. ECM ligands can directly affect intracellular signaling via ITGs, and therefore another way in which astrocytes influence external cellular processes (Wiese et al., 2012).

1.2.2 Astrocyte Development

Astrocytes are believed to develop in a stepwise progression starting from a neural stem cell (NSC) pool in the ventricular zone of the brain. This differentiation process begins during embryogenesis at around 16-18 weeks post-conception in human gestation or E17 in rodents (S. Liddelow & Barres, 2015; Rowitch & Kriegstein, 2010). NSCs first differentiate into neuroepithelial cells then to radial glial stages where they are fated to become either neurons, astrocytes, oligodendrocytes, or ependymal cells.

Fate specification from neural stem cells to astrocytes is poorly understood; however, studies suggest several transcription factors and epigenetic mechanisms aid in astrogliogenesis, the development of astrocytes. Nuclear factor I-A (NFIA) was identified to be a necessary transcription factor for early astrogliogenesis (Deneen et al., 2006; Tiwari et al., 2018). NFIA targets DNA methylation of astrocyte-specific gene promoters by displacing DNA methyltransferase 1 (DNMT1) (Stolt et al., 2003). Sonic hedgehog (SHH) is a major developmental regulator believed to regulate the expression of SRY-box transcription factor 9 (SOX9), a transcription factor recently shown to regulate early astrogliogenesis by regulating NFIA induction (Kang et al., 2012). NOTCH plays an intermediate step in astrocyte development by inducing the expression of NFIA in neural progenitor cells (NPCs) (Molofsky & Deneen, 2015). NFIA potentiates activation of signal transducer and activator of transcription 3 (STAT3), which in turn activates GFAP expression. STAT3-mediated astrogliogenesis is also promoted by bone morphogenetic protein 2 (BMP2) signaling through the STAT3-SMAD3-p300 complex, which binds to astrocyte-specific gene promoters. Recently, activating transcription factor 3 (ATF3) and NFIA have been implicated in activating early astrocyte genes, while Runt-related family transcription factor 2 (RUNX2) activates late-stage astrocyte genes for the differentiation of mouse astrocytes *in vitro* (Tiwari et al., 2018). Additionally, polycomb group proteins restrict the propensity of NPCs to differentiate into neurons by repressing pro-neuronal genes (Hirabayashi

et al., 2009), while high-mobility group nucleoside binding family proteins promote astrocyte differentiation (Nagao et al., 2014). Expression of SOX9, NFIA, and NFIB is sufficient to convert mouse fibroblasts into astrocyte-like cells with ~20% efficiency (Caiazzo et al., 2015); however, the conversion efficiency was only ~2% in human fibroblasts, suggesting these transcription factors may play a less significant role in human astrogliogenesis. Nonetheless, the genetic and epigenetic regulation of astrogliogenesis steps are critical, and alterations in astrocyte maturation may disrupt the functions of mature astrocytes essential for brain homeostasis.

The migration of astrocyte precursor cells to their destination distributed across all areas of the CNS also plays a role in their maturation. Astrocyte precursors are believed to utilize radial glia processes to migrate out of the ventricular zone; however, the processes regulating this are poorly defined *in vivo* (Molofsky & Deneen, 2015). At this point, astrocytes begin to express mature and functionally relevant markers, such as ALDH1L1, ALDOC, EAAT1, and AQP4 (Molofsky & Deneen, 2015; Zhang et al., 2016). Finally, astrocytes undergo a process of gliogenesis where astrocytic morphology becomes more complex, arborization and length of processes increase, and specific astrocytic functions are acquired. Astrocyte maturation is completed after about 15 years postnatal in humans or around 10 weeks in mice (S. Liddelow & Barres, 2015; Rowitch & Kriegstein, 2010).

The lack of complete understanding of the mechanisms controlling astrocyte development and the wide window of astrocyte maturation has brought significant challenges to astrocyte researchers. For those utilizing pluripotent stem cells to study human astrocytes, differentiation protocols are long and laborious—requiring more than 100 days *in vitro* to generate functional, morphologically, and molecularly mature pluripotent stem cell-derived astrocytes (Krencik et al., 2011; Roybon et al., 2013) and often require cellular enrichment techniques, like fluorescence-activated cell sorting (FACS), for selection of purer astrocytic cultures. Fetal bovine serum can be supplemented in differentiation mediums to speed up astrocyte differentiations, but this has been demonstrated to induce long-term reactive astrogliosis-like phenotypes *in vitro* (Perriot et al.,

2018; Zhang et al., 2016). Overall, these challenges in modeling astrocytes *in vitro* make it even more essential to cross-validate findings in multiple models.

1.2.3 Human-Mouse Astrocyte Differences

Compared to rodents, humans have greater development of astrocyte networks both in numbers—from about 20% of the rodent CNS to more than 40% of the human CNS—and complexity, exhibiting significantly more multi-branched processes (Khakh & Sofroniew, 2015; Oberheim et al., 2009). A single mouse astrocyte can envelop about 120,000 synapses, while a human astrocyte might connect from 270,000 to 2 million synapses (De Luca et al., 2020). Not only is there an increased percentage of astrocytes and numbers of connections to neurons in the human brain, but the ratio of astrocytes to neurons is also increased compared to rodents—1.4 astrocytes to 1 neuron in humans compared to 1 astrocyte to 3 neurons in rodents (Sofroniew & Vinters, 2010). The increased ratio of astrocytes to neurons and their connections in higher order organisms indicates a potential role in the evolution of brain complexity. In a comprehensive transcriptomic-wide comparison of mouse and human astrocytes, Dr. Ben Barres's laboratory identified over 600 significantly enriched human astrocyte genes that were not similarly expressed in mouse astrocytes (Zhang et al., 2016). The difference in the ability of adult human and mouse astrocytes to respond to extracellular glutamate is one example that suggests adult human astrocytes may have evolved an improved capability to respond to synaptic activity (Oberheim et al., 2009; Sun et al., 2013). Additionally, there is significant expression of a human-specific calcium-permeable ion channel on the endoplasmic reticulum, RYR3, and increased astrocytic propagation of calcium transients between human and mouse astrocytes (Zhang et al., 2016; Zhao et al., 2015). Interestingly, thrombospondins are among the few genes highly upregulated in the human brain compared to non-human primates, suggesting how astrocytes may play a role in the enhanced brain plasticity of humans (Christopherson et al., 2005; Risher & Eroglu, 2012).

On the other hand, human astrocytes are more susceptible to oxidative stress than mouse astrocytes, which may be explained by differences in mitochondrial and detoxification pathways (J. Li et al., 2021). This evidence leads researchers to propose that human astrocytes have an even more significant role in regulating CNS homeostasis in humans than previously appreciated, making it critical to focus efforts on an in-depth investigation of human astrocytic dysfunction in neurodegeneration.

1.2.4 Reactive Astrogliosis

Under pathological conditions, astrocytes can become reactive, transitioning to different cellular states. This response, classified as reactive astrogliosis, causes modulation of complex cytokine and transmitter signaling between astrocytes and other NVU cells. In general, reactive astrocytes have specific characteristics that can include increased proliferation, hypertrophic morphology changes, increased secretion of proinflammatory and proangiogenic cytokines, and GFAP overexpression (S. A. Liddelow et al., 2017; S. A. Liddelow & Barres, 2017; Obermeier et al., 2013; Pekny et al., 2014; Sofroniew & Vinters, 2010). Depending on the cellular state, reactive astrogliosis may induce harmful or protective properties, triggering reversible changes in gene expression that cause molecular and functional alterations to themselves and neighboring cells (Pekny et al., 2014).

Reactive astrocytes have been classically defined by the increased expression of the intermediate filament proteins—primarily GFAP, but also vimentin (VIM) and nestin (NES). Correlated with these astrogliosis-induced changes in cytoskeletal structure proteins, morphological changes in reactive astrocytes are a common occurrence. Examples of such reactive astrocytic morphology changes are increased hypertrophy, or cellular swelling, and remodeling of processes. Additionally, increased astrocyte proliferation has been linked to a reactive state. This can be a bit confusing as these markers are highly expressed in progenitor

cells that are proliferating during CNS development. Together with increased proliferative state and lack of clear markers for reactive astrogliosis states specific to the human CNS, there is a critical need for defining human reactive astrocyte states with greater depth.

The relevance of these astrocytic cellular states in the context of CNS function has been the topic of investigation. In a 2012 publication, Dr. Zamanian and colleagues from the Barres laboratory began defining transcriptional profiles for endotoxin lipopolysaccharide (LPS) neuroinflammatory-induced A1 model and middle cerebral artery occlusion (MCAO) injury-induced A2 model in mice using microarray technology (Zamanian et al., 2012). Zamanian et al identified ECM/adhesion and immune response as the most enriched Gene Ontology (GO) categories for both A1 and A2 astrocytes (Zamanian et al., 2012). A 2017 publication defines the induction and properties of "neurotoxic" A1 astrocytes in mice under neuroinflammatory conditions (S. A. Liddelow et al., 2017). Liddelow et al demonstrated that A1 astrocytes have decreased phagocytic capacity, inhibited synapse formation and neurite outgrowth upon co-culture with neurons, and potentially results in secretion of a toxic factor promoting cell death (S. A. Liddelow et al., 2017). In this mouse study, IL-1α, TNF, and C1q secreted from activated microglia were necessary and sufficient to induce these reactive astrocytes (S. A. Liddelow et al., 2017), but alternative mechanisms for astrogliosis induction have been described (Sofroniew & Vinters, 2010). On the other hand, "neuroprotective" A2 reactive astrocytes can secrete increased levels of synaptogenesis-related proteins, like thrombospondins, to help repair damaged tissue; however, this can lead to unwanted synapse formation, which is associated with disorders such as epilepsy or neuropathic pain (Boroujerdi et al., 2009; Clarke & Barres, 2013; Zamanian et al., 2012). Another publication from the Barres laboratory in 2018 has indicated that A1 astrogliosis increases with age in mouse astrocytes and was particularly increased in the aged striatum compared to the cortex or hippocampus (Clarke et al., 2018), which has direct relevance to basal ganglia diseases like HD. While astrogliosis and A1 astrocytes have been observed in HD post-mortem human tissue (S. A. Liddelow et al., 2017), the molecular signatures, functional

consequences of astrocyte dysregulation, and their impact on neighboring cell types in the CNS are largely unknown in the context of HD.

1.2.5 Astrocytes in Huntington's Disease

Since astrocytes make up nearly half of all cells in the human brain, every CNS disease is associated with some form of astrocyte dysregulation, and HD is no exception (Barres, 2008). HD astrocytes have been described to exhibit morphological changes and dysfunctional phenotypes involving nearly every astrocytic function—from neuronal homeostasis to metabolic regulation.

1.2.5.1 Astrocyte Phenotypes in Huntington's Disease

HD astrocytes have molecular and morphological changes described that correlate with reactive phenotypes. The most common HD pathology of mutant HTT aggregation occurs within astrocytes from HD patient brains (Faideau et al., 2010; Myers et al., 1991; Sapp et al., 2001; Singhrao et al., 1998). GFAP immunoreactivity in striatal astrocytes is observed in early HD and increases with each grade of HD, concluding with severe fibrillary astrogliosis occurring by HD grade 4 (Faideau et al., 2010). Additionally, mutant Htt nuclear inclusions in striatal R6/2 mouse model S100β-positive astrocytes correlate with disease severity, peaking to approximately 50% in symptomatic (8-12 week) R6/2 mice (Shin et al., 2005; Tong et al., 2014). Accumulation of mutant Htt in astrocytes appears later in disease pathogenesis and to a lesser degree than in neurons, which may be explained by evidence that glia are more capable of clearing misfolded Htt (Bradford et al., 2009; Shin et al., 2005). In monolayer cell culture, mutant HTT aggregates were visualized in rat primary cortical astrocytes expressing N-terminal HTT, which could influence neuronal dysfunction (L. Wang et al., 2012b). Aggregates were also observed in mutant HTT expressing iPSC-derived monkey astrocytes, which were reduced by HTT knockdown,

supporting that mutant HTT can drive aggregation in astrocytes in a cell-autonomous manner. Similar astrogliosis pathology has been described in mouse models of HD to varying degrees (Khakh et al., 2017). Evidence of pathological phenotypes in astrocytes illustrate that neurons are not the only brain cell type significantly affected by mutant HTT.

An assessment of snRNA-seq on HD astrocytes from post-mortem patient cortical tissue identified heterogeneous cell states in HD human astrocytes for the first time (Al-Dalahmah et al., 2020). Upregulation of metallothionein and heatshock genes were highlighted in addition to the loss of astrocyte gene expression (Al-Dalahmah et al., 2020); however, gaps remain in understanding disease development of HD astrocytes and the extent of cell-autonomous effects.

Cell-autonomous changes in HD astrocytes have been documented in HD, and lead to altered astrocytic morphology and GFAP expression that suggest a reactive astrogliosis state. Lentiviral-mediated expression of mutant Htt in striatal mouse astrocytes induces increased GFAP expression and hypertrophic morphology (Faideau et al., 2010). The first human pluripotent stem cell-derived astrocyte phenotypes documented in HD revealed increased vacuolation in 109CAG astrocytes that suggested dysregulated autophagic response (Juopperi et al., 2012b) and an increased evoked inflammatory phenotype in astrocytes with 43 CAGs that contributed to VEGFA-induced endothelial proliferation (H. Y. Hsiao et al., 2015). More recently, HD patient-derived ESCs containing adult-onset repeat lengths (40CAG, 46CAG, 48CAG) were differentiated into astrocytes that exhibited morphological alterations, including decreased branching of processes and increased process length, as well as dysregulation of ECM and synapse-related genes (Osipovitch et al., 2019). Contrary to the Faideau et al study, Osipovitch et al described a decrease in GFAP expression in HD patient-derived astrocytes (Osipovitch et al., 2019); however, in relation to the modeling this paper utilized, decreased GFAP can be explained by impaired astrocytic differentiation efficiency. Additionally, HD iPSC-derived astrocytes with juvenile CAG repeat lengths (77CAG and 109CAG) have also been described to provide less support for functional neuronal maturation and contribute to glutamate-induced toxicity in iPSC-derived

striatal neurons (Garcia et al., 2019). Together, these cell-autonomous HD astrocyte changes suggest mutant HTT expression in astrocytes alone induces astrocytic dysfunction, contributing the HD pathogenesis.

Genetic age of onset modifiers for HD (GeM-HD Consortium, 2015, 2019) have been demonstrated to reside within genes that are highly expressed in human astrocytes compared to other brain cell types, such as myotubularin related protein 10 (MTMR10) and Fanconi-associated nuclease 1 (FAN1) (www.brainrnaseq.org; Zhang et al., 2016). Additional investigations are needed to highlight the greater importance of astrocytes in this influence on HD pathogenesis.

1.2.5.2 Huntington's Disease Astrocytic Functional Changes

Several studies have highlighted how HD astrocytic dysfunction contributes to neuronal dyshomeostasis. One of the earliest molecular phenotypes described in HD is the loss of GLT1/EAAT1/SLC1A2 (Faideau et al., 2010; Khakh et al., 2017), a protein responsible for nearly 90% of glutamate uptake in the mammalian brain and highly expressed in astrocytes (Lehre et al., 1995; Rothstein et al., 1994, 1996; Sattler & Rothstein, 2006). Mutant HTT-expressing mouse astrocytes have significantly decreased GLT1 transcript and protein expression. In several studies, this GLT1 downregulation is progressive and correlates with decreased glutamate uptake in mutant HTT-expressing glia, which increases neuronal toxicity when co-cultured with neurons (Bradford et al., 2009, 2010; Faideau et al., 2010; Shin et al., 2005). GLT1 overexpression has demonstrated therapeutic potential *in vivo* by rescuing GFAP activation and hypertrophic morphology in mutant Htt-expressing striatal mouse astrocytes (Faideau et al., 2010). A publication characterizing the metabolome and proteome of an HD mouse model highlighted key proteome changes related to energy metabolism, synapse function, and neurotransmitter homeostasis, further confirming impaired astrocytic glutamine release in HD models (Skotte et al., 2018). More recently, HD iPSC-derived astrocytes with juvenile CAG repeat lengths (77CAG

and 109CAG) contributed to glutamate-induced toxicity in iPSC-derived striatal neurons (Garcia et al., 2019). Several of these studies investigating mutant HTT response in HD astrocytes alone suggest glutamate dysregulation as a cell-autonomous affect (Bradford et al., 2009, 2010; Faideau et al., 2010; Garcia et al., 2019; Shin et al., 2005), but this functional alteration has yet to be validated in human astrocytes containing adult-onset repeat lengths.

Dysregulated ion signaling is another phenotype described in HD astrocytes that may have significant implications in brain homeostasis. Several studies have highlighted decreased expression and function of the potassium ion channel, Kir4.1, in R6/2 HD mouse model astrocytes. Consequently, the R6/2 striatum displays increased extracellular levels of potassium ions, which contributes to striatal neuron excitability (Tong et al., 2014; Vagner et al., 2016). This phenotype was preventable by viral delivery of Kir4.1 to astrocytes *in vivo*, which attenuated an HD motor deficit and prolonged survival in R6/2 mice (Tong et al., 2014). Altered calcium signaling has also been reported in HD mouse models and may be dependent on GLT1 expression, implicating dysregulation of HD astrocytes (Jiang et al., 2016; Lee et al., 2013). Spontaneous calcium signals are reduced in the R6/2 mouse model and are likely due to glutamate spillover (Khakh et al., 2017). Additionally, astrocyte-specific expression of Kir4.1 rescued calcium signaling alterations (Jiang et al., 2016). Similarly, AAV-mediated expression of Kir4.1 targeting GFAP-expressing astrocytes in one-year-old, symptomatic zQ175 mice improved spontaneous synaptic activity and motor behavior (Vagner et al., 2016). In a 2019 study, mature astrocytes derived from HD adult-onset repeat length iPSCs exhibited significant electrophysiological impairments of potassium currents, as well as lengthened spontaneous calcium waves and reduced neuronal support upon co-culture with MSN-enriched neuronal cultures (Garcia et al., 2019). HD astrocytic functional impairments in glutamate uptake and electrophysiology were also revealed in iPSC-derived astrocytes from an HD transgenic monkey model, demonstrating a cell-autonomous dysfunction in HD astrocytes (Cho et al., 2019). Suppressed processing and secretion of mature BDNF in primary cortical rat astrocytes containing mutant HTT is another

astrocytic dysfunction and is believed to induce decreased neurite outgrowth upon co-culture with primary cortical neurons (L. Wang et al., 2012a). The study also showed the formation of aggregates in the mutant HTT-expressing primary rat cortical astrocytes (L. Wang et al., 2012a). Taken together, HD astrocyte dysfunction of glutamate, ion, and other trophic signaling pathways can have significant consequences on neuronal homeostasis in HD.

Metabolic changes in HD striatal astrocytes arise and may underlie region-specific neuronal susceptibility in the *HdhQ(150/150)* mouse model of HD (Polyzos et al., 2019). When glucose levels in the striatum decrease with disease pathogenesis, astrocytes shift from glycolysis to non-glycolytic intermediates, particularly fatty acid oxidation as a fuel source to compensate (Polyzos et al., 2019). Consequently, this switch increases reactive oxygen species, which contributes to neurotoxicity (Polyzos et al., 2019).

Several studies have indicated dysregulation of cholesterol metabolism, another important astrocyte-secreted molecule contributing to neuronal homeostasis (Gray, 2019). Gene and protein expression of cholesterol intermediates and related enzymes have been described in HD patients (del Toro et al., 2010; Valenza et al., 2005) and mouse models (Benraiss et al., 2021; Shankaran et al., 2017; Trushina et al., 2006; Valenza et al., 2007, 2010) as either significantly upregulated (del Toro et al., 2010; Trushina et al., 2006) or downregulated (Shankaran et al., 2017; Valenza et al., 2005, 2007, 2010) depending on the study; this inconsistency may be due to the varying disease stages, animal model, polyQ repeat length, mutant HTT version (full-length vs truncated), timing assessed, or the relationship between autophagic mechanisms controlling protein homeostasis at each stage of HD (Gray, 2019). To add to these findings, a recent study demonstrated inhibited cholesterol signaling in astrocytes from truncated mutant HTT mouse and human PSC-derived models but not in full-length mutant HTT models (Benraiss et al., 2021). The complexity of HD cholesterol signaling dysregulation demonstrates the need for further elucidation into complex astrocytic mechanisms with thoughtful consideration of methodology and models.

At the NVU, evidence suggests HD astrocytes mediate changes in vasculature. HD mouse and human astrocytes produce increased levels of the angiogenesis factor VEGF-A (H. Hsiao et al., 2015). When primary mouse endothelial cells were treated with R6/2 astrocyte conditioned media, endothelial cells increased their proliferation (H. Hsiao et al., 2015). Conditioned medium from R6/2 primary astrocytes also induced vascular reactivity by reducing pericyte survival (H. Hsiao et al., 2015). This mechanism is believed to be due to increased inhibitor of nuclear factor-κB kinase (IKK) complex-mediated activation of proinflammatory cytokines, IL-1β and TNFα (H. Hsiao et al., 2015; H. Y. Hsiao et al., 2013). In short, mutant HTT-induced astrocyte reactivity can have broad effects on multiple cell types at the NVU.

1.2.5.3 Therapeutic Potential of Astrocytes for Huntington's Disease

Glia have been a topic of therapeutic intervention for HD for over a decade. Reduction of mutant HTT in astrocytes within the conditional BACHD mouse model improved neuropathology, electrophysiology, and motor function, demonstrating the role astrocytes play in such HD phenotypes (Wood et al., 2019). An interesting study by Benraiss and colleagues utilized human glial chimeric mice to explore this topic further. Neonatal R6/2 striatal glia were replaced with wildtype glia to slow disease progression, as indicated through improved cognitive and motor functions as well as rescued hyperexcitability of striatal neurons (Benraiss et al., 2016). Conversely, implantation of HD ESC-derived glial progenitors into the striatum impaired motor learning (Benraiss et al., 2016).

In another study, *ex vivo* glial cell-line derived neurotrophic factor (GDNF) prevented neuronal loss and improved motor function in the N171-82Q HD transgenic mouse model. Mouse neural progenitor cells (NPCs) were used as delivery vehicles for the growth factor. These GDNF-secreting NPCs differentiated into GFAP-positive astrocytes *in vitro* and *in vivo*. Due to the potential prion-like mechanism of mutant HTT cellular transfer (Masnata et al., 2019) and the

inherent nature of astrocytes to be more resistant to mutant HTT aggregation (Bradford et al., 2009; Shin et al., 2005), glial modulation or replacement might be a promising therapeutic avenue to investigate for HD.

Astrocytes have also been assessed for *in vivo* cellular conversion therapy for HD and other neurodegenerative diseases (Y. Wang et al., 2021). The co-expression of two neural transcription factors, neuronal differentiation 1 (NeuroD1) and distal-less homeobox 2 (Dlx2), by adeno-associated virus (AAV)-2/5 targeting GFAP-positive cells was sufficient to convert striatal astrocytes into neurons with 80% efficiency in R6/2 and YAC128 HD mice (Wu et al., 2020). More than 50% of the newly converted were dopamine- and cAMP-regulated neuronal phosphoprotein (DARPP32)-positive medium spiny neurons, demonstrating the replacement opportunity for this degenerating cell type in HD (Wu et al., 2020). These astrocyte-converted neurons show synaptic events and significantly improved the motor function and lifespan of R6/2 mice (Wu et al., 2020). Together, their findings suggest *in vivo* astrocyte-to-neuron conversion holds therapeutic promise as a disease-modifying therapy for HD.

In summary, these studies highlight the contribution of astrocytes to HD pathogenesis and their potential therapeutic potential for restoring brain dyshomeostasis.

1.3 Overview of the Dissertation

Huntington's disease (HD) is a devastating neurodegenerative disease caused by a CAG repeat expansion within the coding region of the *Huntingtin* gene (*HTT*) and results in expansion of a repeated glutamine track within the Huntingtin protein. This mutation affects numerous cellular processes, contributing to overall dysregulated cellular homeostasis in the central nervous system (CNS), particularly in neurons of the striatum and cortex. This dissertation describes the cumulative research I performed as a doctoral candidate elucidating Huntington's disease pathogenesis in non-neuronal brain cell types—astrocytes and brain microvascular endothelial

cells (BMECs). Utilizing patient stem cell modeling, mouse models, and transcriptomic analyses, I have uncovered dysregulated signatures of astrocytes and BBB cells with predicted dysfunctions that are likely to contribute to HD pathogenesis.

In Chapters 1 and 2, I contributed to studies investigating BBB deficits in HD. Chapter 2 includes a published study from our lab on which I was a co-author . In this study, HD iPSCs-derived BMECs (iBMECs) were utilized to model the blood-brain barrier (BBB) of HD. We demonstrated HD cell-autonomous neurovascular unit deficits that included dysfunctional angiogenic and barrier properties *in vitro*. Transcriptomic analysis provided mechanistic insights into pathways that underlie HD iBMEC dysfunction, including defects in WNT signaling. Next, WNT activation was validated in BECs HD post-mortem tissue, corroborating this mechanism in patient tissue. Furthermore, inhibition of WNT in iBMECs rescued the functional angiogenic deficits observed, suggesting a mechanism for reduced disease burden. Finally, this study also discussed the implications of BBB penetration of drugs for HD.

Chapter 2 describes follow-up iBMEC studies not published in Chapter 1. These included my exploration into how modulation of WNT and HTT in HD iBMECs affects BBB properties. To further investigate WNT-mediated alterations in the HD BBB, I performed alternative angiogenesis and paracellular transport assays on WNT-inhibited HD and unaffected control iBMECs. Additionally, I assessed barrier properties following HTT knockdown in HD iBMECs to observe HTT's effect on a critical BBB function. Together, these studies further demonstrated the utility of the iPSC-derived BMEC model in studying HD BBB properties.

Chapter 3 dives into the HD astrocyte dysregulation I identified using mouse and human iPSC modeling. Single-nuclei RNA-sequencing (snRNA-seq) analysis was employed to reveal HD astrocytic cell states that could not be described with traditional bulk RNA-sequencing methods. HD astrocyte cell states across the R6/2 mouse model and iPSC-derived astrocytes (iAstros) were enriched in genes that indicated altered astrocyte functions: inhibited synaptogenesis, activated actin associated signaling, and cell states that suggest impaired

maturation. Several key genes from the data were validated at the protein level. Moreover, the deficits in astrocyte maturation showed predicted regulatory roles for astrogenesis transcription factors SOX9, NFIA, and ATF3. These data support my hypothesis that mutant HTT induces dysregulated astrocyte cell states that may induce dysfunctional astrocytic properties, contributing to HD pathogenesis.

In the last chapter, the implications of my findings are discussed, including potential future work to mechanistically understand the regulators of HD astrocyte pathogenesis and their functional significance. Studies investigating the functional consequences of HD astrocyte transcriptional alterations in glutamate receptor signaling and actin dynamics and cytoskeletal signaling would provide evidence into how these cell-autonomous alterations in HD astrocytes affect the cells around them. This may include co-culturing of various iPSC-derived cell types found in the brain (e.g., striatal neurons, iBMECs, and microglia) to investigate how HD astrocytes directly induce alterations in those cells or even how those dysregulated cell types in HD may bring out alternative non-cell-autonomous dysfunctions in HD astrocytes. HD iAstro aging either through increased time in culture *in vitro* or implantation into mice for *in* vivo maturation may also reveal additional HD astrocyte phenotypes. Studies focusing on the use of isogenic iPSC lines could provide a clearer picture of HD iAstro dysregulation without the patient variability that can contribute to outcomes of iPSC modeling. Finally, investigations into the molecular mechanisms influencing HD astrocyte dysregulation and dysfunction would greatly benefit the field. I hypothesize that perturbation of astrogliogenesis transcription factors may rescue the developmental deficits in HD astrocytes, but alternative regulatory mechanisms may also be at play. Studies utilizing Chromatin Immunoprecipitation sequencing (ChIP-seq) can help to provide insights into gene regulatory events controlling HD astrocyte dysregulation. By targeting these predicted upstream regulators, we may be able to reverse HD astrocyte dysfunction and their destruction to neighboring cell types, to help provide a more holistic therapeutic intervention that HD patients deserve.

1.4 References

Abbott, N. J., Revest, P. A., & Romerso, I. A. (1992). Astrocyte-endothelial interaction: physiology and pathology. *Neuropathology and Applied Neurobiology*, *18*, 424–433. https://doi.org/10.1111/j.1365-2990.1992.tb00808.x.

Abbott, N. J., Rönnbäck, L., & Hansson, E. (2006). Astrocyte–endothelial interactions at the blood–brain barrier. *Nature Reviews Neuroscience*, *7*(1), 41–53. https://doi.org/10.1038/nrn1824

Adegbuyiro, A., Sedighi, F., Pilkington Iv, A. W., Groover, S., & Legleiter, J. (2017). Proteins containing expanded polyglutamine tracts and neurodegenerative disease. *Biochemistry*, *56*(9), 1199–1217. https://doi.org/10.1021/acs.biochem.6b00936

Al-Dalahmah, O., Sosunov, A. A., Shaik, A., Ofori, K., Liu, Y., Vonsattel, J. P., Adorjan, I., Menon, V., & Goldman, J. E. (2020). Single-nucleus RNA-seq identifies Huntington disease astrocyte states. *Acta Neuropathologica Communications*, *8*(1). https://doi.org/10.1186/s40478-020-0880-6

Allaman, I., Bélanger, M., & Magistretti, P. J. (2011). Astrocyte–neuron metabolic relationships: for better and for worse. *Trends in Neurosciences*, *34*(2), 76–87. https://doi.org/10.1016/j.tins.2010.12.001

Attwell, D., Buchan, A. M., Charpak, S., Lauritzen, M., Macvicar, B. A., & Newman, E. A. (2010). Glial and neuronal control of brain blood flow. *Nature*, *468*, 232–243. https://doi.org/10.1038/nature09613

Barres, B. A. (2008). The Mystery and Magic of Glia: A Perspective on Their Roles in Health and Disease. *Neuron*, *60*(3), 430–440. https://doi.org/10.1016/j.neuron.2008.10.013

Bates, G. (2003). Huntingtin aggregation and toxicity in Huntington's disease. *The Lancet*, *361*, 1642–1644. https://doi.org/10.1016/S0140-6736(03)13304-1

Bates, G. P., Dorsey, R., Gusella, J. F., Hayden, M. R., Kay, C., Leavitt, B. R., Nance, M., Ross, C. a., Scahill, R. I., Wetzel, R., Wild, E. J., & Tabrizi, S. J. (2015). Huntington disease. *Nature Reviews Disease Primers*, *April*, 15005. https://doi.org/10.1038/nrdp.2015.5

Batiuk, M. Y., Martirosyan, A., Wahis, J., de Vin, F., Marneffe, C., Kusserow, C., Koeppen, J., Viana, J. F., Oliveira, J. F., Voet, T., Ponting, C. P., Belgard, T. G., & Holt, M. G. (2020). Identification of region-specific astrocyte subtypes at single cell resolution. *Nature Communications*, *11*(1). https://doi.org/10.1038/s41467-019-14198-8

Bence, N. F., Sampat, R. M., & Kopito, R. R. (2001). Impairment of the Ubiquitin-Proteasome System by Protein Aggregation. *Science*, *292*, 1552–1555. https://doi.org/10.1126/science.292.5521.1552.

Benraiss, A., Mariani, J. N., Osipovitch, M., Cornwell, A., Windrem, M. S., Villanueva, C. B., Chandler-Militello, D., & Goldman, S. A. (2021). Cell-intrinsic glial pathology is conserved across human and murine models of Huntington's disease. *Cell Reports*, *36*. https://doi.org/10.1016/j.celrep.2021.109308ll

Benraiss, A., Wang, S., Herrlinger, S., Li, X., Chandler-militello, D., Mauceri, J., Burm, H. B., Toner, M., Osipovitch, M., Xu, Q. J., Ding, F., Wang, F., Kang, N., Kang, J., Curtin, P. C., Brunner, D., Windrem, M. S., Munoz-sanjuan, I., & Goldman, S. A. (2016). Human glia can both induce and rescue aspects of disease phenotype in Huntington disease. *Nature Communications*, *7*, 1–13. https://doi.org/10.1038/ncomms11758

Biesecker, K. R., & Srienc, A. I. (2015). The Functional Role of Astrocyte Calcium Signaling in Cortical Blood Flow Regulation. *The Journal of Neuroscience*, *35*(3), 868–870. https://doi.org/10.1523/JNEUROSCI.4422-14.2015

Björkhem, I., & Meaney, S. (2004). Brain Cholesterol: Long Secret Life Behind a Barrier. *Arterioscler Thromb Vasc Biol.*, *24*, 806–815. https://doi.org/10.1161/01.ATV.0000120374.59826.1b

Boroujerdi, A., Kee, H., Su, Y., Kim, D., Figueroa, K. W., Mo, J., & Luo, Z. D. (2009). Injury discharges regulate calcium channel alpha-2-delta-1 subunit upregulation in the dorsal horn that contributes to initiation of neuropathic pain. *Pain*, *139*(2), 358–366. https://doi.org/10.1016/j.pain.2008.05.004

Bradford, J., Shin, J., Roberts, M., Wang, C., Li, X., & Li, S. (2009). Expression of mutant huntingtin in mouse brain astrocytes causes age-dependent neurological symptoms. *Proceedings of the National Academy of Sciences*, *106*(52), 22480–22485.

Bradford, J., Shin, J.-Y., Roberts, M., Wang, C.-E., Sheng, G., Li, S., & Li, X.-J. (2010). Mutant Huntingtin in Glial Cells Exacerbates Neurological Symptoms of Huntington Disease Mice. *Journal of Biological Chemistry*, *285*(14), 10653–10661. https://doi.org/10.1074/jbc.M109.083287

Bushong, E. A., Martone, M. E., Jones, Y. Z., & Ellisman, M. H. (2002). Protoplasmic Astrocytes in CA1 Stratum Radiatum Occupy Separate Anatomical Domains. *The Journal of Neuroscience*, *22*(1), 183–192. https://doi.org/10.1523/JNEUROSCI.22-01-00183.2002.

Caiazzo, M., Giannelli, S., Valente, P., Lignani, G., Carissimo, A., Sessa, A., Colasante, G., Bartolomeo, R., Massimino, L., Ferroni, S., Settembre, C., Benfenati, F., & Broccoli, V. (2015). Direct Conversion of Fibroblasts into Functional Astrocytes by Defined Transcription Factors. *Stem Cell Reports*, *4*(1), 25–36. https://doi.org/10.1016/j.stemcr.2014.12.002

Cha, J.-H. J. (2007). Transcriptional signatures in Huntington's disease. *Progress in Neurobiology*, *83*, 228–248. https://doi.org/10.1016/j.pneurobio.2007.03.004

Chechik, G., Meilijson, I., & Ruppin, E. (1999). Neuronal Regulation: A Mechanism for Synaptic Pruning During Brain Maturation. *Neural Computation*, *11*, 2061–2080. https://doi.org/10.1162/089976699300016089.

Cho, I. K., Yang, B., Forest, C., Qian, L., & Chan, A. W. S. (2019). Amelioration of Huntington's disease phenotype in astrocytes derived from iPSC-derived neural progenitor cells of Huntington's disease monkeys. *PLoS ONE*, *14*(3). https://doi.org/10.1371/journal.pone.0214156

Christopherson, K. S., Ullian, E. M., Stokes, C. C. A., Mullowney, C. E., Hell, J. W., Agah, A., Lawler, J., Mosher, D. F., Bornstein, P., & Barres, B. A. (2005). Thrombospondins Are Astrocyte-Secreted Proteins that Promote CNS Synaptogenesis. *Cell*, *120*, 421–433. https://doi.org/10.1016/j.cell.2004.12.020

Chung, W. S., Clarke, L. E., Wang, G. X., Stafford, B. K., Sher, A., Chakraborty, C., Joung, J., Foo, L. C., Thompson, A., Chen, C., Smith, S. J., & Barres, B. A. (2013). Astrocytes mediate synapse elimination through MEGF10 and MERTK pathways. *Nature*, *504*(7480), 394–400. https://doi.org/10.1038/nature12776

Clarke, L. E., & Barres, B. A. (2013). Emerging roles of astrocytes in neural circuit development. *Nature Reviews Neuroscience*, *14*(May), 311–321. https://doi.org/10.1038/nrn3484

Clarke, L. E., Liddelow, S. A., Chakraborty, C., Münch, A. E., Heiman, M., & Barres, B. A. (2018). Normal aging induces A1-like astrocyte reactivity. *Proceedings of the National Academy of Sciences*, *115*(8), E1896–E1905. https://doi.org/10.1073/pnas.1800165115

Crick, S. L., Jayaraman, M., Frieden, C., Wetzel, R., & Pappu, R. V. (2006). Fluorescence correlation spectroscopy shows that monomeric polyglutamine molecules form collapsed structures in aqueous solutions. *Proceedings of the National Academy of Sciences*, *103*(45), 16764–16769. https://doi.org/10.1073/pnas.0608175103

Cronin, T., Rosser, A., & Massey, T. (2019). Clinical Presentation and Features of Juvenile-Onset Huntington's Disease: A Systematic Review. In *Journal of Huntington's Disease* (Vol. 8, Issue 2, pp. 171–179). IOS Press. https://doi.org/10.3233/JHD-180339

Crook, Z. R., & Housman, D. E. (2013). Surveying the landscape of huntington's disease mechanisms, measurements, and medicines. *Journal of Huntington's Disease*, *2*(4), 405–436. https://doi.org/10.3233/JHD-130072

Dawson, T. M., Golde, T. E., & Lagier-Tourenne, C. (2018). Animal models of neurodegenerative diseases. In *Nature Neuroscience* (Vol. 21, Issue 10, pp. 1370–1379). Nature Publishing Group. https://doi.org/10.1038/s41593-018-0236-8

De Luca, C., Colangelo, A. M., Virtuoso, A., Alberghina, L., & Papa, M. (2020). Neurons, Glia, Extracellular Matrix and Neurovascular Unit: A Systems Biology Approach to the Complexity of Synaptic Plasticity in Health and Disease. *International Journal of Molecular Sciences*, *21*, 1–25. https://doi.org/10.3390/ijms21041539

del Toro, D., Xifró, X., Pol, A., Humbert, S., Saudou, F., Canals, J. M., & Alberch, J. (2010). Altered cholesterol homeostasis contributes to enhanced excitotoxicity in Huntington's disease. *Journal of Neurochemistry*, *115*(1), 153–167. https://doi.org/10.1111/j.1471-4159.2010.06912.x

Deneen, B., Ho, R., Lukaszewicz, A., Hochstim, C. J., Gronostajski, R. M., & Anderson, D. J. (2006). The Transcription Factor NFIA Controls the Onset of Gliogenesis in the Developing Spinal Cord. *Neuron*, *52*, 953–968. https://doi.org/10.1016/j.neuron.2006.11.019

Dowell, J. A., Johnson, J. A., & Li, L. (2009). Identification of Astrocyte Secreted Proteins with a Combination of Shotgun Proteomics and Bioinformatics. *Journal of Proteome Research*, *8*, 4135–4143. https://doi.org/10.1021/pr900248y

Duyao, M. P., Auerbach, A. B., Ryan, A., Persichetti, F., Barnes, G. T., McNeil, S. M., Ge, P., Vonsattel, J. P., Gusella, J. F., Joyner, A. L., & MacDonald, M. E. (1995). Inactivation of the Mouse Huntington's Disease Gene Homolog Hdh. *Science*, *269*(5222), 407–410. https://doi.org/10.1126/science.7618107

Eltokhi, A., Janmaat, I. E., Genedi, M., Haarman, B. C. M., & Sommer, I. E. C. (2020). Dysregulation of synaptic pruning as a possible link between intestinal microbiota dysbiosis and neuropsychiatric disorders. *Journal of Neuroscience Research*, *September 2019*, 1–35. https://doi.org/10.1002/jnr.24616

Faideau, M., Kim, J., Cormier, K., Gilmore, R., Welch, M., Auregan, G., Dufour, N., Guillermier, M., Ferrante, R. J., Brouillet, E., Hantraye, P., & De, N. (2010). In vivo expression of polyglutamine-expanded huntingtin by mouse striatal astrocytes impairs glutamate transport: a correlation with Huntington's disease subjects. *Human Molecular Genetics*, *19*(15), 3053–3067. https://doi.org/10.1093/hmg/ddq212

Fan, H.-C., Ho, L.-I., Chi, C.-S., Chen, S.-J., Peng, G.-S., Chan, T.-M., Lin, S.-Z., & Harn, H.-J. (2014). Polyglutamine (PolyQ) Diseases: Genetics to Treatments. *Cell Transplantation*, *23*, 441–458. https://doi.org/10.3727/096368914X678454

Farshim, P. P., & Bates, G. P. (2018). *Mouse Models of Huntington's Disease* (Vol. 1780). https://doi.org/10.1007/978-1-4939-7825-0

Gafni, J., Hermel, E., Young, J. E., Wellington, C. L., Hayden, M. R., & Ellerby, L. M. (2004). Inhibition of Calpain Cleavage of Huntingtin Reduces Toxicity: Accumulation of Calpain/Caspase Fragments in the Nucleus. *The Journal of Biochemistry*, *279*(19), 20211–20220. https://doi.org/10.1074/jbc.M401267200

Garcia, V. J., Rushton, D. J., Tom, C. M., Allen, N. D., Kemp, P. J., Svendsen, C. N., & Mattis, V. B. (2019). Huntington's Disease Patient-Derived Astrocytes Display Electrophysiological Impairments and Reduced Neuronal Support. *Frontiers in Neuroscience*, *13*(June), 1–14. https://doi.org/10.3389/fnins.2019.00669

Garcia-Segura, L. M., & Melcangi, R. C. (2006). Steroids and Glial Cell Function. *Glia*, *498*(July), 485–498. https://doi.org/10.1002/glia

Gauthier, L. R., Charrin, B. C., Borrell-Pagès, M., Dompierre, J. P., Rangone, H., Cordelières, F. P., de Mey, J., Macdonald, M. E., Lessmann, V., Humbert, S., & Saudou, F. (2004). Huntingtin Controls Neurotrophic Support and Survival of Neurons by Enhancing BDNF Vesicular Transport along Microtubules. *Cell*, *118*, 127–138. https://doi.org/10.1016/j.cell.2004.06.018

GeM-HD Consortium. (2015). Identification of Genetic Factors that Modify Clinical Onset of Huntington's Disease. *Cell*, *162*(3), 516–526. https://doi.org/10.1016/j.cell.2015.07.003

GeM-HD Consortium. (2019). CAG Repeat Not Polyglutamine Length Determines Timing of Huntington's Disease Onset. *Cell*, *178*, 887–900. https://doi.org/10.1016/j.cell.2019.06.036

Gray, M. (2019). Neuroglia in Neurodegenerative Diseases: Astrocytes in Huntington's Disease. *Advances in Experimental Medicine and Biology*, *1175*, 355–381. https://doi.org/10.1007/978-981-13-9913-8_14

Hall, C. N., Klein-flu, M. C., Howarth, C., & Attwell, D. (2012). Oxidative Phosphorylation, Not Glycolysis, Powers Presynaptic and Postsynaptic Mechanisms Underlying Brain Information Processing. *The Journal of Neuroscience*, *32*(26), 8940–8951. https://doi.org/10.1523/JNEUROSCI.0026-12.2012

HD iPSC Consortium. (2013). Induced Pluripotent Stem Cells from Patients with Huntington's Disease Show CAG Repeat Expansion Associated Phenotypes. *Cell Stem Cell*, *11*(2), 264–278. https://doi.org/10.1016/j.stem.2012.04.027.Induced

HD iPSC Consortium. (2017). Developmental alterations in Huntington's disease neural cells and pharmacological rescue in cells and mice. *Nature Neuroscience*, *20*(5), 648–660. https://doi.org/10.1038/nn.4532

Hipp, M. S., Park, S. H., & Hartl, U. U. (2014). Proteostasis impairment in protein-misfolding and -aggregation diseases. In *Trends in Cell Biology* (Vol. 24, Issue 9, pp. 506–514). Elsevier Ltd. https://doi.org/10.1016/j.tcb.2014.05.003

Hirabayashi, Y., Suzki, N., Tsuboi, M., Endo, T. A., Toyoda, T., Shinga, J., Koseki, H., Vidal, M., & Gotoh, Y. (2009). Polycomb Limits the Neurogenic Competence of Neural Precursor Cells to Promote Astrogenic Fate Transition. *Neuron*, *63*(5), 600–613. https://doi.org/10.1016/j.neuron.2009.08.021

Hsiao, H., Chen, Y., Huang, C., Chen, C., Hsu, Y., Chen, H., Chiu, F., Kuo, H., Chang, C., & Chern, Y. (2015). Aberrant Astrocytes Impair Vascular Reactivity in Huntington Disease. *Annals of Neurology*, *78*(2), 178–192. https://doi.org/10.1002/ana.24428

Hsiao, H. Y., Chen, Y. C., Chen, H. M., Tu, P. H., & Chern, Y. (2013). A critical role of astrocyte-mediated nuclear factor-κB-dependent inflammation in huntington's disease. *Human Molecular Genetics*, *22*(9), 1826–1842. https://doi.org/10.1093/hmg/ddt036

Hsiao, H. Y., Chen, Y. C., Huang, C. H., Chen, C. C., Hsu, Y. H., Chen, H. M., Chiu, F. L., Kuo, H. C., Chang, C., & Chern, Y. (2015). Aberrant astrocytes impair vascular reactivity in Huntington disease. *Annals of Neurology*, *78*(2), 178–192. https://doi.org/10.1002/ana.24428

https://www.brainrnaseq.org/. (n.d.). *Brain RNA-Seq*. Https://Www.Brainrnaseq.Org/. Retrieved August 31, 2021, from https://www.brainrnaseq.org/

Hu, X., Yuan, Y., Wang, D., & Su, Z. (2016). Heterogeneous astrocytes: Active players in CNS. In *Brain Research Bulletin* (Vol. 125, pp. 1–18). Elsevier Inc. https://doi.org/10.1016/j.brainresbull.2016.03.017

Iadecola, C. (2017). The Neurovascular Unit Coming of Age: A Journey through Neurovascular Coupling in Health and Disease. *Neuron*, *96*(1), 17–42. https://doi.org/10.1016/j.neuron.2017.07.030

Jiang, R., Diaz-Castro, B., Looger, L. L., & Khakh, B. S. (2016). Dysfunctional Calcium and Glutamate Signaling in Striatal Astrocytes from Huntington's Disease Model Mice. *Journal of Neuroscience*, *36*(12), 3453–3470. https://doi.org/10.1523/JNEUROSCI.3693-15.2016

Jones, E. V, & Bouvier, D. S. (2014). Astrocyte-Secreted Matricellular Proteins in CNS Remodelling during Development and Disease. *Neural Plasticity*, *2014*, 1–12. https://doi.org/10.1155/2014/321209

Juopperi, T. A., Kim, W. R., Chiang, C., Yu, H., Margolis, R. L., Ross, C. A., Ming, G., & Song, H. (2012a). Astrocytes generated from patient induced pluripotent stem cells recapitulate features of Huntington's disease patient cells. *Molecular Brain*, *5*(17), 1–14.

Juopperi, T. A., Kim, W. R., Chiang, C., Yu, H., Margolis, R. L., Ross, C. A., Ming, G., & Song, H. (2012b). Astrocytes generated from patient induced pluripotent stem cells recapitulate features of Huntington's disease patient cells. *Molecular Brain*, *5*(17), 1–14.

Kang, P., Lee, H. K., Glasgow, S. M., Finley, M., Donti, T., Gaber, Z. B., Graham, B. H., Foster, A. E., Novitch, B. G., Gronostajski, R. M., & Deneen, B. (2012). Sox9 and NFIA Coordinate a Transcriptional Regulatory Cascade during the Initiation of Gliogenesis. *Neuron*, *74*(1), 79–94. https://doi.org/10.1016/j.neuron.2012.01.024

Kay, C., Collins, J. A., Wright, G. E. B., Baine, F., Miedzybrodzka, Z., Aminkeng, F., Semaka, A. J., Mcdonald, C., Davidson, M., Madore, S. J., Gordon, E. S., Gerry, N. P., Squitieri, F., Tishkoff, S., Greenberg, J. L., Krause, A., & Hayden, M. R. (2018). The molecular epidemiology of Huntington disease is related to intermediate allele frequency and haplotype in the general population. *Am J Med Genet.*, *May 2017*, 1–12. https://doi.org/10.1002/ajmg.b.32618

Khakh, B. S., Beaumont, V., Cachope, R., Munoz-Sanjuan, I., Goldman, S. A., & Grantyn, R. (2017). Unravelling and Exploiting Astrocyte Dysfunction in Huntington's Disease. *Trends in Neurosciences*, *40*(7), 422–437. https://doi.org/10.1016/j.tins.2017.05.002

Khakh, B. S., & Sofroniew, M. V. (2015). Diversity of astrocyte functions and phenotypes in neural circuits. *Nature Neuroscience*, *18*(7), 942–952. https://doi.org/10.1038/nn.4043

Krencik, R., Weick, J. P., Liu, Y., Zhang, Z., & Zhang, S. (2011). Specification of transplantable astroglial subtypes from human pluripotent stem cells. *Nature Biotechnology*, *29*(6), 528–534. https://doi.org/10.1038/nbt.1877

Kucukdereli, H., Allen, N. J., Lee, A. T., Feng, A., Ozlu, M. I., Conatser, L. M., Chakraborty, C., Workman, G., Weaver, M., Sage, E. H., Barres, B. A., & Eroglu, C. (2011). Control of excitatory CNS synaptogenesis by astrocyte-secreted proteins Hevin and SPARC. *Proceedings of the National Academy of Sciences*, *108*(32), E440–E449. https://doi.org/10.1073/pnas.1104977108/

Kurtishi, A., Rosen, B., Patil, K. S., Alves, G. W., & Møller, S. G. (2019). Cellular Proteostasis in Neurodegeneration. *Molecular Neurobiology*, *56*(5), 3676–3689. https://doi.org/10.1007/s12035-018-1334-z

la Spada, A. R., Paulson, H. L., & Fischbeck, K. H. (1994). Trinucleotide Repeat Expansion in Neurologcal Disease. *Neurological Progress*, 814–822. https://doi.org/10.1002/ana.410360604

Larsen, B. R., Assentoft, M., Cotrina, M. L., Hua, S. Z., Nedergaard, M., Kaila, K., Voipio, J., & Macaulay, N. (2014). Contributions of the Na+/K+ ATPase, NKCC1, and Kir4.1 Hippocampal K+ Clearance and Volume Responses. *Glia*, *62*, 608–622. https://doi.org/10.1002/glia.22629

Lee, W., Reyes, R. C., Gottipati, M. K., Lewis, K., Lesort, M., Parpura, V., & Gray, M. (2013). Enhanced Ca2+-dependent glutamate release from astrocytes of the BACHD Huntington's disease mouse model. *Neurobiology of Disease*, *58*, 192–199. https://doi.org/10.1016/j.nbd.2013.06.002

Lehre, K. P., Levy, L. M., Ottersen, O. P., Storm-Mathisen, J., & Danbolt, N. C. (1995). Differential Expression of Two Glial Glutamate Transporters in the Rat Brain: Quantitative and Immunocytochemical Observations. *The Journal of Neuroscience*, *15*(3), 1835–1853. https://doi.org/10.1523/JNEUROSCI.15-03-01835.1995

Leke, R., & Schousboe, A. (2016). *The Glutamine Transporters and Their Role in the Glutamate/GABA-Glutamine Cycle* (Advances i). Springer International Publishing Switzerland 2016. https://doi.org/10.1007/978-3-319-45096-4

Li, J., Pan, L., Pembroke, W. G., Rexach, J. E., Godoy, M. I., Condro, M. C., Alvarado, A. G., Harteni, M., Chen, Y., Stiles, L., Chen, A. Y., Wanner, I. B., Yang, X., Goldman, S. A., Geschwind, D. H., Kornblum, H. I., & Zhang, Y. (2021). Conservation and divergence of vulnerability and responses to stressors between human and mouse astrocytes. *Nature Communications*, *12*, 1–20. https://doi.org/10.1038/s41467-021-24232-3

Li, J. Y., Popovic, N., & Brundin, P. (2005). The Use of the R6 Transgenic Mouse Models of Huntington's Disease in Attempts to Develop Novel Therapeutic Strategies. *NeuroRx*, *2*(July), 447–464. https://doi.org/10.1602/neurorx.2.3.447.

Liddelow, S. A., & Barres, B. A. (2017). Reactive Astrocytes: Production, Function, and Therapeutic Potential. *Immunity*, *46*(6), 957–967. https://doi.org/10.1016/j.immuni.2017.06.006

Liddelow, S. A., Guttenplan, K. A., Clarke, L. E., Bennett, F. C., Bohlen, C. J., Schirmer, L., Bennett, M. L., Münch, A. E., Chung, W., Peterson, T. C., & Wilton, D. K. (2017). Neurotoxic reactive astrocytes are induced by activated microglia. *Nature*, *541*(7638), 481–487. https://doi.org/10.1038/nature21029

Liddelow, S., & Barres, B. (2015). SnapShot: Astrocytes in Health and Disease. *Cell*, *162*(5), 1170-1170.e1. https://doi.org/10.1016/j.cell.2015.08.029

Lim, R. G., Quan, C., Reyes-Ortiz, A. M., Lutz, S. E., Kedaigle, A. J., Gipson, T. A., Wu, J., Vatine, G. D., Stocksdale, J., Casale, M. S., Svendsen, C. N., Fraenkel, E., Housman, D. E., Agalliu, D., & Thompson, L. M. (2017). Huntington's Disease iPSC-Derived Brain Microvascular Endothelial Cells Reveal WNT-Mediated Angiogenic and Blood-Brain Barrier Deficits. *Cell Reports*, *19*(7), 1365–1377. https://doi.org/10.1016/j.celrep.2017.04.021

Lunkes, A., Lindenberg, K. S., Ben-Haïem, L., Weber, C., Devys, D., Landwehrmeyer, G. B., Mandel, J.-L., & Trottier, Y. (2002). Proteases Acting on Mutant Huntingtin Generate Cleaved Products that Differentially Build Up Cytoplasmic and Nuclear Inclusions. *Molecular Cell*, *10*(8), 259–269. https://doi.org/10.1016/s1097-2765(02)00602-0

Mangiarini, L., Sathasivam, K., Seller, M., Cozens, B., Harper, A., Hetherington, C., Lawton, M., Trottier, Y., Lehrach, H., Davies, S. W., & Bates, G. P. (1996). Exon 1 of the HD Gene with an Expanded CAG Repeat Is Sufficient to Cause a Progressive Neurological Phenotype in Transgenic Mice. *Cell*, *87*, 493–506. http://ac.els-cdn.com/S0092867400813690/1-s2.0-S0092867400813690-main.pdf?_tid=7db7695e-7afe-11e7-94f8-00000aacb35d&acdnat=1502062090_1e45eb383db00141a08e5daa67072892

Masnata, M., Sciacca, G., Maxan, A., Bousset, L., Denis, H. L., Lauruol, F., David, L., Pierre, M. Saint, Kordower, J. H., Melki, R., Alpaugh, M., & Cicchetti, F. (2019). Demonstration of prion-like properties of mutant huntingtin fibrils in both in vitro and in vivo paradigms. *Acta Neuropathologica*. https://doi.org/10.1007/s00401-019-01973-6

Mauch, D. H., Nägler, K., Schumacher, S., Göritz, C., Müller, E.-C., Otto, A., & Pfrieger, F. W. (2001). CNS Synaptogenesis Promoted by Glia-Derived Cholesterol. *Science*, *294*, 1354–1357.

McColgan, P., & Tabrizi, S. J. (2018). Huntington's disease: a clinical review. In *European Journal of Neurology* (Vol. 25, Issue 1, pp. 24–34). Blackwell Publishing Ltd. https://doi.org/10.1111/ene.13413

Miller, R. H., & Raff, M. C. (1984). Fibrous and protoplasmic astrocytes are biochemically and developmentally distinct. *The Journal of Neuroscience*, *4*(2), 585–592. https://doi.org/10.1523/JNEUROSCI.04-02-00585.1984.

Molofsky, A. V., & Deneen, B. (2015). Astrocyte Development: A Guide for the Perplexed. *Glia*, *63*, 1320–1329. https://doi.org/10.1002/glia.22836

Myers, R. H., Vonsattel, J. P., Paskevich, P. A., Kiely, D. K., Stevens, T. J., Cupples, L. A., Jr, E. P. R., & Bird, E. D. (1991). Decreased neuronal and increased oligodendroglial densities in Huntington's disease caudate nucleus. *Journal of Neuropathology and Experimental Neurology*, *50*(6), 729–742. https://doi.org/10.1097/00005072-199111000-00005.

Nagao, M., Lanjakornsiripan, D., Itoh, Y., Kishi, Y., Ogata, T., & Gotoh, Y. (2014). HMGN Family Proteins Promote Astrocyte Differentiation of Neural Precursor Cells. *Stem Cells*, *21*(11), 1–20. https://doi.org/10.1002/stem.1787

Nance, M. A., & Myers, R. H. (2001). Juvenile onset Huntington's disease — clinical and research perspectives. *Ment Retard Dev Disabil Res Rev.*, *7*, 153–157.

Nasir, J., Floresco, S. B., O, J. R., Diewert, V. M., Richman, J. M., Zeisler, J., Anita Borowski, I., Marth, J. D., Phillips, A. G., & Hayden, M. R. (1995). Targeted Disruption of the Huntington's Disease Gene Results in Embryonic Lethality and Behavioral and Morphological Changes in Heterozygotes. In *Cell* (Vol. 81). https://doi.org/10.1016/0092-8674(95)90542-1

Newington, J. T., Harris, R. A., & Cumming, R. C. (2013). Reevaluating Metabolism in Alzheimer's Disease from the Perspective of the Astrocyte-Neuron Lactate Shuttle Model. *Journal of Neurodegenerative Diseases*, *2013*, 1–13. https://doi.org/10.1155/2013/234572

Oberheim, N. A., Takano, T., Han, X., He, W., Lin, J. H. C., Wang, F., Xu, Q., Wyatt, J. D., Pilcher, W., Ojemann, J. G., Ransom, B. R., Goldman, S. A., & Nedergaard, M. (2009). Uniquely Hominid Features of Adult Human Astrocytes. *Journal of Neuroscience*, *29*(10), 3276–3287. https://doi.org/10.1523/JNEUROSCI.4707-08.2009

Obermeier, B., Daneman, R., & Ransohoff, R. M. (2013). Development, maintenance and disruption of the blood-brain barrier. *Nature Medicine*, *19*(12), 1584–1596. https://doi.org/10.1038/nm.3407

Ochaba, J., Lukacsovich, T., Csikos, G., Zheng, S., Margulis, J., Salazar, L., Mao, K., Lau, A. L., Yeung, S. Y., Humbert, S., Saudou, F., Klionsky, D. J., Finkbeiner, S., Zeitlin, S. O., Marsh, L., Housman, D. E., Thompso, L. M., & Steffan, J. S. (2014). Potential function for the Huntingtin protein as a scaffold for selective autophagy. *Proceedings of the National Academy of Sciences*, *111*(47), 16889–16894. https://doi.org/10.1073/pnas.1420103111

Osipovitch, M., Martinez, A. A., Mariani, J. N., Cornwell, A., Dhaliwal, S., Zou, L., Chandler-Militello, D., Wang, S., Li, X., Benraiss, S.-J., Agate, R., Lampp, A., Benraiss, A., Windrem, M. S., & Goldman, S. A. (2019). Human ESC-Derived Chimeric Mouse Models of Huntington's Disease Reveal Cell-Intrinsic Defects in Glial Progenitor Cell Differentiation. *Cell Stem Cell*, *24*(1), 107–122. https://doi.org/10.1016/j.stem.2018.11.010

Pekny, M., Wilhelmsson, U., & Pekna, M. (2014). The dual role of astrocyte activation and reactive gliosis. *Neuroscience Letters*, *565*, 30–38. https://doi.org/10.1016/j.neulet.2013.12.071

Perriot, S., Mathias, A., Perriard, G., Canales, M., Jonkmans, N., Merienne, N., Meunier, C., El Kassar, L., Perrier, A. L., Laplaud, D.-A., Schluep, M., Déglon, N., & Du Pasquier, R. (2018). Human Induced Pluripotent Stem Cell-Derived Astrocytes Are Differentially Activated by Multiple Sclerosis-Associated Cytokines. *Stem Cell Reports*, *11*, 1199–1210. https://doi.org/10.1016/j.stemcr.2018.09.015

Plaitakis, A., Kalef-Ezra, E., Kotzamani, D., Zaganas, I., & Spanaki, C. (2017). The glutamate dehydrogenase pathway and its roles in cell and tissue biology in health and disease. *Biology*, *6*(1). https://doi.org/10.3390/biology6010011

Polyzos, A. A., Lee, D. Y., Datta, R., Hauser, M., Budworth, H., Holt, A., Mihalik, S., Goldschmidt, P., Frankel, K., Trego, K., Bennett, M. J., Vockley, J., Xu, K., Gratton, E., & McMurray, C. T. (2019). Metabolic Reprogramming in Astrocytes Distinguishes Region-Specific Neuronal Susceptibility in Huntington Mice. *Cell Metabolism*, *29*, 1258–1273. https://doi.org/10.1016/j.cmet.2019.03.004

Punihaole, D., Jakubek, R. S., Workman, R. J., Marbella, L. E., Campbell, P., Madura, D., & Asher, S. A. (2017). Monomeric Polyglutamine Structures That Evolve into Fibrils. *The Journal of Physical Chemistry*, *121*, 5953–5967. https://doi.org/10.1021/acs.jpcb.7b04060

Ratovitski, T., Nakamura, M., D'ambola, J., Chighladze, E., Liang, Y., Wang, W., Graham, R., Hayden, M. R., Borchelt, D. R., Hirschhorn, R. R., & Ross, C. A. (2007). N-Terminal

Proteolysis of Full-Length Mutant Huntingtin in an Inducible PC12 Cell Model of Huntington's Disease. *Cell Cycle*, *6*(23), 2970–2981. https://doi.org/10.4161/cc.6.23.4992

Risher, W. C., & Eroglu, C. (2012). Thrombospondins as key regulators of synaptogenesis in the central nervous system. *Matrix Biology*, *31*(3), 170–177. https://doi.org/10.1016/j.matbio.2012.01.004

Rivetti di Val Cervo, P., Besusso, D., Conforti, P., & Cattaneo, E. (2021). hiPSCs for predictive modelling of neurodegenerative diseases: dreaming the possible. *Nature Reviews Neurology*, *17*(6), 381–392. https://doi.org/10.1038/s41582-021-00465-0

Ross, C. A., & Poirier, M. A. (2004). Protein aggregation and neurodegenerative disease. *Nature Medicine*, *10*(Suppl), S10–S17. https://doi.org/10.1038/nm1066

Ross, C. A., & Tabrizi, S. J. (2011). Huntington's disease: from molecular pathogenesis to clinical treatment. *The Lancet Neurology*, *10*(1), 83–98. https://doi.org/10.1016/S1474-4422(10)70245-3

Rothstein, J. D., Dykes-Hoberg, M., Pardo, C. A., Bristol, L., Jin, L., Kuncl, R. W., Kanai, Y., Hediger, M. A., Wang, Y., Schielke, J. P., & Welty, D. (1996). Knockout of Glutamate Transporters Reveals a Major Role for Astroglial Transport in Excitotoxicity and Clearance of Glutamate. *Neuron*, *16*, 675–686. https://doi.org/10.1016/s0896-6273(00)80086-0

Rothstein, J. D., Martin, L., Levey, A. I., Dykes-Hoberg, M., Jin, L., Wu, D., Nash, N., & Kuncl, R. W. (1994). Localization of Neuronal and Glial Glutamate Transporters. *Neuron*, *13*, 713–725. https://doi.org/10.1016/0896-6273(94)90038-8

Rowitch, D. H., & Kriegstein, A. R. (2010). Developmental genetics of vertebrate glial-cell specification. *Nature*, *468*(7321), 214–222. https://doi.org/10.1038/nature09611

Roybon, L., Lamas, N. J., Garcia-diaz, A., Yang, E. J., Sattler, R., Jackson-lewis, V., Kim, Y. A., Kachel, C. A., Rothstein, J. D., Przedborski, S., & Wichterle, H. (2013). Human Stem Cell-Derived Spinal Cord Astrocytes with Defined Mature or Reactive Phenotypes. *Cell Reports*, *4*(5), 1035–1048. https://doi.org/10.1016/j.celrep.2013.06.021

Sanacora, G., Treccani, G., & Popoli, M. (2012). Towards a glutamate hypothesis of depression An emerging frontier of neuropsychopharmacology for mood disorders. *Neuropharmacology*, *62*(1), 63–77. https://doi.org/10.1016/j.neuropharm.2011.07.036

Sandoval, K. E., & Witt, K. A. (2008). Blood-brain barrier tight junction permeability and ischemic stroke. *Neurobiology of Disease*, *32*(2), 200–219. https://doi.org/10.1016/j.nbd.2008.08.005

Sapp, E., Kegel, K. B., Aronin, N., Hashikawa, T., Uchiyama, Y., Tohyama, K., Bhide, P. G., Vonsattel, J. P., & Difiglia, M. (2001). Early and progressive accumulation of reactive microglia in the Huntington disease brain. *Journal of Neuropathology and Experimental Neurology*, *60*(2), 161–172. https://doi.org/10.1093/jnen/60.2.161

Sathasivam, K., Neueder, A., Gipson, T. A., Landles, C., Benjamin, A. C., Bondulich, M. K., Smith, D. L., Faull, R. L. M., Roos, R. A. C., Howland, D., Detloff, P. J., Housman, D. E., & Bates, G. P. (2013). Aberrant splicing of HTT generates the pathogenic exon 1 protein in

Huntington disease. *Proceedings of the National Academy of Sciences*, *110*(6), 2366–2370. https://doi.org/10.1073/pnas.1221891110

Sattler, R., & Rothstein, J. D. (2006). Regulation and Dysregulation of Glutamate Transporters. *Handbook of Experimental Pharmacology*, *175*, 277–303. https://doi.org/10.1007/3-540-29784-7_14

Schousboe, A., Scafidi, S., Bak, L. K., Waagepetersen, H. S., & Mckenna, M. C. (2015). Glutamate Metabolism in the Brain Focusing on Astrocytes. *Advances in Neurobiology*, *11*, 13–30. https://doi.org/10.1007/978-3-319-08894-5

Shankaran, M., di Paolo, E., Leoni, V., Caccia, C., Ferrari Bardile, C., Mohammed, H., di Donato, S., Kwak, S., Marchionini, D., Turner, S., Cattaneo, E., & Valenza, M. (2017). Early and brain region-specific decrease of de novo cholesterol biosynthesis in Huntington's disease: A cross-validation study in Q175 knock-in mice. *Neurobiology of Disease*, *98*, 66–76. https://doi.org/10.1016/j.nbd.2016.11.013

Shin, J., Fang, Z., Yu, Z., Wang, C., Li, S., & Li, X. (2005). Expression of mutant huntingtin in glial cells contributes to neuronal excitotoxicity. *Journal of Cell Biology*, *171*(6), 1001–1012. https://doi.org/10.1083/jcb.200508072

Singhrao, S. K., Thomas, P., Wood, J. D., Macmillan, J. C., Neal, J. W., Harper, P. S., & Jones, A. L. (1998). Huntingtin Protein Colocalizes with Lesions of Neurodegenerative Diseases: An Investigation in Huntington's , Alzheimer's , and Pick's Diseases. *Experimental Neurology*, *222*(150), 213–222. https://doi.org/10.1006/exnr.1998.6778

Skotte, N. H., Andersen, J. V, Santos, A., Nørremølle, A., Waagepetersen, H. S., Nielsen Correspondence, M. L., Aldana, B. I., Willert, C. W., & Nielsen, M. L. (2018). Integrative Characterization of the R6/2 Mouse Model of Huntington's Disease Reveals Dysfunctional Astrocyte Metabolism. *Cell Reports*, *23*(7), 2211–2224. https://doi.org/10.1016/j.celrep.2018.04.052

Smith-Geater, C., Hernandez, S. J., Lim, R. G., Adam, M., Wu, J., Stocksdale, J. T., Wassie, B. T., Gold, M. P., Wang, K. Q., Miramontes, R., Kopan, L., Orellana, I., Joy, S., Kemp, P. J., Allen, N. D., Fraenkel, E., & Thompson, L. M. (2020). Aberrant Development Corrected in Adult-Onset Huntington's Disease iPSC-Derived Neuronal Cultures via WNT Signaling Modulation. *Stem Cell Reports*, *14*, 406–419. https://doi.org/10.1016/j.stemcr.2020.01.015

Sofroniew, M. v, & Vinters, H. v. (2010). Astrocytes: biology and pathology. *Acta. Neuropathol.*, *119*, 7–35. https://doi.org/10.1007/s00401-009-0619-8

Steffan, J. S., Kazantsev, A., Spasic-boskovic, O., Greenwald, M., Zhu, Y., Gohler, H., Wanker, E. E., Bates, G. P., Housman, D. E., & Thompson, L. M. (2000). The Huntington's disease protein interacts with p53 and CREB-binding protein and represses transcription. *Proceedings of the National Academy of Sciences*, *97*(12), 6763–6768. https://doi.org/10.1073/pnas.100110097

Stevens, B., Allen, N. J., Vazquez, L. E., Howell, G. R., Christopherson, K. S., Nouri, N., Micheva, K. D., Mehalow, A. K., Huberman, A. D., Stafford, B., Sher, A., Litke, A. M., Lambris, J. D., Smith, S. J., John, S. W. M., & Barres, B. A. (2007). The Classical

Complement Cascade Mediates CNS Synapse Elimination. *Cell*, *131*, 1164–1178. https://doi.org/10.1016/j.cell.2007.10.036

Stolt, C. C., Lommes, P., Sock, E., Chaboissier, M., Schedl, A., & Wegner, M. (2003). The Sox9 transcription factor determines glial fate choice in the developing spinal cord. *Genes and Development*, *17*, 1677–1689. https://doi.org/10.1101/gad.259003.)

Sun, W., McConnell, E., Pare, J.-F., Xu, Q., Chen, M., Peng, W., Lovatt, D., Han, X., Smith, Y., & Nedergaard, M. (2013). Glutamate-Dependent Neuroglial Calcium Signaling Differs Between Young and Adult Brain. *Science*, *339*(6116), 197–200. https://doi.org/10.1126/science.1226740.Glutamate-Dependent

Sweeney, M. D., Sagare, A. P., & Zlokovic, B. V. (2018). Blood–brain barrier breakdown in Alzheimer disease and other neurodegenerative disorders. *Nature Publishing Group*, *14*(3), 133–150. https://doi.org/10.1038/nrneurol.2017.188

Tabrizi, S. J., Ghosh, R., & Leavitt, B. R. (2019). Review Huntingtin Lowering Strategies for Disease Modification in Huntingtons Disease. *Neuron*, *101*(5), 801–819. https://doi.org/10.1016/j.neuron.2019.01.039

Takahashi, K., & Yamanaka, S. (2006). Induction of Pluripotent Stem Cells from Mouse Embryonic and Adult Fibroblast Cultures by Defined Factors. *Cell*, *126*(4), 663–676. https://doi.org/10.1016/j.cell.2006.07.024

Tang, G., Gudsnuk, K., Kuo, S., Cotrina, M. L., Rosoklija, G., Sosunov, A., Sonders, M. S., Kanter, E., Castagna, C., Yamamoto, A., Yue, Z., Arancio, O., Peterson, B. S., Champagne, F., Dwork, A. J., Goldman, J., & Sulzer, D. (2014). Loss of mTOR-Dependent Macroautophagy Causes Autistic-like Synaptic Pruning Deficits. *Neuron*, *83*(5), 1131–1143. https://doi.org/10.1016/j.neuron.2014.07.040

The Huntington's Disease Collaborative Research Group. (1993). *A Novel Gene Containing a Trinucleotide That Is Expanded and Unstable on Huntington's Disease Chromosomes*. *72*, 971–983.

The U.S.–Venezuela Collaborative Research Project, & Wexler, N. S. (2004). Venezuelan kindreds reveal that genetic and environmental factors modulate Huntington's disease age of onset. *Proceedings of the National Academy of Sciences*, *101*(10), 3498–3503. https://doi.org/10.1073/pnas.0308679101

Tiwari, N., Pataskar, A., Péron, S., Thakurela, S., Sahu, S. K., Figueres-Oñate, M., Marichal, N., López-Mascaraque, L., Tiwari, V. K., & Berninger, B. (2018). Stage-Specific Transcription Factors Drive Astrogliogenesis by Remodeling Gene Regulatory Article Stage-Specific Transcription Factors Drive Astrogliogenesis by Remodeling Gene Regulatory Landscapes. *Cell Stem Cell*, *23*, 557–571. https://doi.org/10.1016/j.stem.2018.09.008

Tong, X., Ao, Y., Faas, G. C., Nwaobi, S. E., Xu, J., Haustein, M. D., Anderson, M. A., Mody, I., Olsen, M. L., Sofroniew, M. v, & Khakh, B. S. (2014). Astrocyte Kir4.1 ion channel deficits contribute to neuronal dysfunction in Huntington's disease model mice. *Nature Neuroscience*, *17*(5), 694–703. https://doi.org/10.1038/nn.3691

Trushina, E., Deep Singh, R., Dyer, R. B., Cao, S., Shah, V. H., Parton, R. G., Pagano, R. E., & Mcmurray, C. T. (2006). Mutant huntingtin inhibits clathrin-independent endocytosis and causes accumulation of cholesterol in vitro and in vivo. *Human Molecular Genetics*, *15*(24), 3578–3591. https://doi.org/10.1093/hmg/ddl434

Ullian, E. M., Christopherson, K. S., & Barres, B. A. (2004). Role for Glia in Synaptogenesis. *Glia*, *216*(April), 209–216. https://doi.org/10.1002/glia.20082

Vagner, T., Dvorzhak, A., Wójtowicz, A. M., Harms, C., & Grantyn, R. (2016). Systemic application of AAV vectors targeting GFAP-expressing astrocytes in Z-Q175-KI Huntington's disease mice. *Molecular and Cellular Neuroscience*, *77*, 76–86. https://doi.org/10.1016/j.mcn.2016.10.007

Valenza, M., Leoni, V., Karasinska, J. M., Petricca, L., Fan, J., Carroll, J., Pouladi, M. A., Fossale, E., Nguyen, H. P., Riess, O., Macdonald, M., Wellington, C., Didonato, S., Hayden, M., & Cattaneo, E. (2010). Cholesterol Defect Is Marked across Multiple Rodent Models of Huntington's Disease and Is Manifest in Astrocytes. *The Journal of Neuroscience*, *30*(32), 10844–10850. https://doi.org/10.1523/JNEUROSCI.0917-10.2010

Valenza, M., Leoni, V., Tarditi, A., Mariotti, C., Björkhem, I., di Donato, S., & Cattaneo, E. (2007). Progressive dysfunction of the cholesterol biosynthesis pathway in the R6/2 mouse model of Huntington's disease. *Neurobiology of Disease*, *28*(1), 133–142. https://doi.org/10.1016/j.nbd.2007.07.004

Valenza, M., Rigamonti, D., Goffredo, D., Zuccato, C., Fenu, ‡ Simone, Jamot, L., Strand, A., Tarditi, A., Woodman, B., Racchi, M., Mariotti, C., Donato, S. di, Corsini, A., Bates, G., Pruss, R., Olson, J. M., Sipione, S., Tartari, M., & Cattaneo, E. (2005). Dysfunction of the Cholesterol Biosynthetic Pathway in Huntington's Disease. *Neurobiology of Disease*, *25*(43), 9932–9939. https://doi.org/10.1523/JNEUROSCI.3355-05.2005

Villaseñor, R., Lampe, J., Schwaninger, M., & Collin, L. (2019). Intracellular transport and regulation of transcytosis across the blood-brain barrier. *Cellular and Molecular Life Sciences*, *76*(6), 1081–1092. https://doi.org/10.1007/s00018-018-2982-x

Wang, H., Lim, P. J., Yin, C., Rieckher, M., Vogel, B. E., & Monteiro, M. J. (2006). Suppression of polyglutamine-induced toxicity in cell and animal models of Huntington's disease by ubiquilin. *Human Molecular Genetics*, *15*(6), 1025–1041. https://doi.org/10.1093/hmg/ddl017

Wang, L., Lin, F., Wang, J., Wu, J., Han, R., Zhu, L., Difiglia, M., & Qin, Z. (2012a). Expression of mutant N-terminal huntingtin fragment (htt552-100Q) in astrocytes suppresses the secretion of BDNF. *Brain Research*, *1449*, 69–82. https://doi.org/10.1016/j.brainres.2012.01.077

Wang, L., Lin, F., Wang, J., Wu, J., Han, R., Zhu, L., Difiglia, M., & Qin, Z. (2012b). Expression of mutant N-terminal huntingtin fragment (htt552-100Q) in astrocytes suppresses the secretion of BDNF. *Brain Research*, *1449*, 69–82. https://doi.org/10.1016/j.brainres.2012.01.077

Wang, X., Christian, K. M., Song, H., & Ming, G. (2018). Synaptic dysfunction in complex psychiatric disorders: from genetics to mechanisms. *Genome Medicine*, *10*(9), 9–11. https://doi.org/10.1186/s13073-018-0518-5

Wang, Y., Zhang, X., Chen, F., Song, N., & Xie, J. (2021). In vivo Direct Conversion of Astrocytes to Neurons Maybe a Potential Alternative Strategy for Neurodegenerative Diseases. In *Frontiers in Aging Neuroscience* (Vol. 13). Frontiers Media S.A. https://doi.org/10.3389/fnagi.2021.689276

Wellington, C. L., Singaraja, R., Ellerby, L., Savill, J., Roy, S., Leavitt, B., Cattaneo, E., Hackam, A., Sharp, A., Thornberry, N., Nicholson, D. W., Bredesen, D. E., & Hayden, M. R. (2000). Inhibiting caspase cleavage of huntingtin reduces toxicity and aggregate formation in neuronal and nonneuronal cells. *Journal of Biological Chemistry*, *275*(26), 19831–19838. https://doi.org/10.1074/jbc.M001475200

Wen, J., Scoles, D. R., & Facelli, J. C. (2017). Molecular dynamics analysis of the aggregation propensity of polyglutamine segments. *PLoS ONE*, 10–14. https://doi.org/10.1371/journal.pone.0178333

White, J. K., Auerbach, W., Duyao, M. P., Vonsattel, J.-P., Gusella, J. F., Joyner, A. L., & Macdonald, M. E. (1997). Huntingtin is required for neurogenesis and is not impaired by the Huntington's disease CAG expansion. *Nature Genetics*, *17*(December), 404–410. https://doi.org/10.1038/ng1297-404

Wiese, S., Karus, M., & Faissner, A. (2012). Astrocytes as a source for extracellular matrix molecules and cytokines. *Frontiers in Pharmacology*, *3*(June), 1–13. https://doi.org/10.3389/fphar.2012.00120

Wood, T. E., Barry, J., Yang, Z., Cepeda, C., Levine, M. S., & Gray, M. (2019). Mutant huntingtin reduction in astrocytes slows disease progression in the BACHD conditional Huntington's disease mouse model. *Human Molecular Genetics*, *28*(3), 487–500. https://doi.org/10.1093/hmg/ddy363

Wu, Z., Parry, M., Hou, X. Y., Liu, M. H., Wang, H., Cain, R., Pei, Z. F., Chen, Y. C., Guo, Z. Y., Abhijeet, S., & Chen, G. (2020). Gene therapy conversion of striatal astrocytes into GABAergic neurons in mouse models of Huntington's disease. *Nature Communications*, *11*(1). https://doi.org/10.1038/s41467-020-14855-3

Yamanaka, S., Takahashi, K., Tanabe, K., Ohnuki, M., Narita, M., Ichisaka, T., & Tomoda, K. (2007). Induction of pluripotent stem cells from adult human fibroblasts by defined factors. *Cell*, *131*(5), 861–872. https://doi.org/10.1016/j.cell.2007.11.019

Zamanian, J. L., Xu, L., Foo, L. C., Nouri, N., Zhou, L., Giffard, R. G., & Barres, B. A. (2012). Genomic Analysis of Reactive Astrogliosis. *Journal of Neuroscience*, *32*(18), 6391–6410. https://doi.org/10.1523/JNEUROSCI.6221-11.2012

Zhang, Y., Sloan, S. A., Clarke, L. E., Grant, G. A., Gephart, M. G. H., Barres, B. A., Zhang, Y., Sloan, S. A., Clarke, L. E., Caneda, C., Plaza, C. A., & Blumenthal, P. D. (2016). Purification and Characterization of Progenitor and Mature Human Astrocytes Reveals Transcriptional and Functional Differences with Mouse. *Neuron*, *89*(1), 37–53. https://doi.org/10.1016/j.neuron.2015.11.013

Zhao, Z., Nelson, A. R., Betsholtz, C., & Zlokovic, B. v. (2015). Establishment and Dysfunction of the Blood-Brain Barrier. *Cell*, *163*(5), 1064–1078. https://doi.org/10.1016/j.cell.2015.10.067

Zhou, Y., & Danbolt, N. C. (2014). Glutamate as a neurotransmitter in the healthy brain. In *Journal of Neural Transmission* (Vol. 121, Issue 8, pp. 799–817). https://doi.org/10.1007/s00702-014-1180-8

Zuccato, C., Valenza, M., & Cattaneo, E. (2010). Molecular Mechanisms and Potential Therapeutical Targets in Huntington's Disease. *Physiol Rev*, *90*, 905–981. https://doi.org/10.1152/physrev.00041.2009.

CHAPTER I

Huntington's disease iPSC-derived brain microvascular endothelial cells reveal WNT-mediated angiogenic and blood-brain barrier deficits

Ryan G. Lim, Chris Quan, Andrea M. Reyes-Ortiz, Sarah E. Lutz, Amanda J. Kedaigle, Theresa A. Gipson, Jie Wu, Gad D. Vatine, Jennifer Stocksdale, Malcolm S. Casale, Clive N. Svendsen, Ernest Fraenkel, David E. Housman, Dritan Agalliu*, and Leslie M. Thompson*

CHAPTER I

Huntington's Disease iPSC-Derived Brain Microvascular Endothelial Cells Reveal WNT-Mediated Angiogenic and Blood-Brain Barrier Deficits

2.1 Summary of Chapter 1

Brain microvascular endothelial cells (BMECs) are an essential component of the blood-brain barrier (BBB) that shields the brain against toxins and immune cells. While BBB dysfunction exists in neurological disorders, including Huntington's disease (HD), it is not known if BMECs themselves are functionally compromised to promote BBB dysfunction. Further, the underlying mechanisms of BBB dysfunction remain elusive given limitations with mouse models and post-mortem tissue to identify primary deficits. We undertook a transcriptome and functional analysis of human induced pluripotent stem cell (iPSC)-derived BMECs (iBMEC) from HD patients or unaffected controls. We demonstrate that HD iBMECs have intrinsic abnormalities in angiogenesis and barrier properties, as well as in signaling pathways governing these processes. Thus, our findings provide an iPSC-derived BBB model for a neurodegenerative disease and demonstrate autonomous neurovascular deficits that may underlie HD pathology with implications for therapeutics and drug delivery. My role on this project included experimental planning, iBMEC differentiations, immunocytochemistry, microscopy, and analysis necessary for assessing iBMEC proliferation, transwell migration, and protein analysis. **This work has been published in Cell Reports.** Lim et al., 2017 May 16; 19(7): 1365–1377. doi: 10.1016/j.celrep.2017.04.021.

2.2 Introduction

Huntington's disease (HD) is a devastating neurodegenerative disorder caused by a CAG repeat expansion in the *Huntingtin (HTT)* gene (The Huntington's Disease Collaborative Research Group, 1993) encoding an expanded polyglutamine (polyQ) track in the Huntingtin (HTT) protein. A broad range of cellular functions are impacted by mutant HTT (mHTT) expression (Munoz-

Sanjuan and Bates, 2011; Ross and Tabrizi, 2011). Symptoms include progressive cognitive, psychiatric and motor impairment, and degeneration of striatal neurons and atrophy of cortical neurons are hallmark neuropathological features (Walker, 2007).

Impairment of the neurovascular unit (NVU) and blood-brain barrier (BBB) has emerged as a feature of various neurodegenerative diseases, including HD (Drouin-Ouellet et al., 2015; Hua et al., 2014; Lin et al., 2013). The NVU is composed of both neuronal and non-neuronal cells (astrocytes) that regulate central nervous system (CNS) homeostasis through interactions with blood vessels (brain microvascular endothelial cells, BMECs, pericytes). BMECs are the main component of the NVU that restricts paracellular and transcellular entry into the CNS via tight junctions (TJs), a limited number of caveolae, and selective transporters (**Figure 2.1A**) (Zhao et al., 2015). Chronic mHTT expression alters the neurovasculature by increasing cerebral blood volume, small vessel density, and BBB permeability in rodent models of HD and patient tissue (Drouin-Ouellet et al., 2015; Franciosi et al., 2012; Hsiao et al., 2015; Hua et al., 2014; Lin et al., 2013). These changes were initially thought to originate from neuronal deficits leading to secondary effects on the NVU; however, recent studies have highlighted a dependency on HD astrocytes for BBB pathology (Hsiao et al., 2015). Yet, it is not known whether BMECs manifest cell-autonomous deficits induced by mHTT expression, thereby potentially contributing to observed HD pathology, or if BBB dysfunction is secondary to neurodegeneration.

The development of iPSCs (Takahashi et al., 2007; Yu et al., 2007) and efficient protocols to generate BMECs (Lippmann et al., 2014) provide an opportunity to investigate the primary effects of neurodegenerative disease mutations on BMECs and their contribution to disease pathogenesis. To address whether BMECs have intrinsic deficits in HD, we generated human iPSC-derived BMECs (iBMECs) from either unaffected or HD subjects and performed functional assays and RNA-sequencing. Through transcriptome analysis, we identify a set of novel BMEC genes that could impact normal and diseased BBB function. This analysis, coupled with assays that measure angiogenesis and barrier function, suggest that HD iBMECs have increased

angiogenic potential and impaired barrier function through defects in signaling pathways governing these processes. The transcriptome analysis suggests that mutant HTT protein regulates epigenetic marks that control changes in BMEC-specific gene expression, including those crucial for angiogenesis and barrier formation. Moreover, it suggests a potential mechanism that links mHTT with BBB dysfunction in HD, which is validated through a targeted intervention to ameliorate the angiogenic deficit. This HD iBMEC model represents an important resource to evaluate therapeutics that might restore normal BBB function and to assess drug delivery to the CNS.

2.3 Results

2.3.1 Generation and Transcriptome Analysis of Unaffected Control Human iPSC-Derived BMECs

To define the transcriptome and functional characteristics of healthy iBMEC, iPSCs from unaffected individuals were differentiated into BMECs as described (Lippmann et al., 2014). There were two control iPSC lines from unaffected individuals having 33 or 28 CAG repeats in the *HTT* gene (CS83iCTR33n1, designated 33Qn1 [33Q] and CS14iCTR28n6, designated 28Qn6 [28Q]) that were differentiated (HD iPSC Consortium, 2017; Tables S1 and S2). Each line expressed markers of human BMECs including PECAM1 (CD31) and GLUT1 (SLC2A1) and formed linear TJ strands characterized by co-localization of CLAUDIN-5 (CLDN5), OCCLUDIN (OCLN), and TIGHT JUNCTION PROTEIN 1 (TJP1 [ZO1]) (**Figure 2.1B**). Flow cytometry analysis of the fraction of $CD31^+$ and $GLUT1^+$ double positive cells after differentiation and subculture showed that greater than 90% of the cell population were BMECs (**Figure 2.1C**). Functionally, iBMECs exhibited a high transendothelial electrical resistance (TEER) over several days, characteristic of normal BMECs (**Figure 2.1D**). TEER values peaked between 48 and 72 hr post-subculture, but remained higher than $300\Omega \times cm^2$ for over 120 hr (**Figure 2.1D**). In contrast,

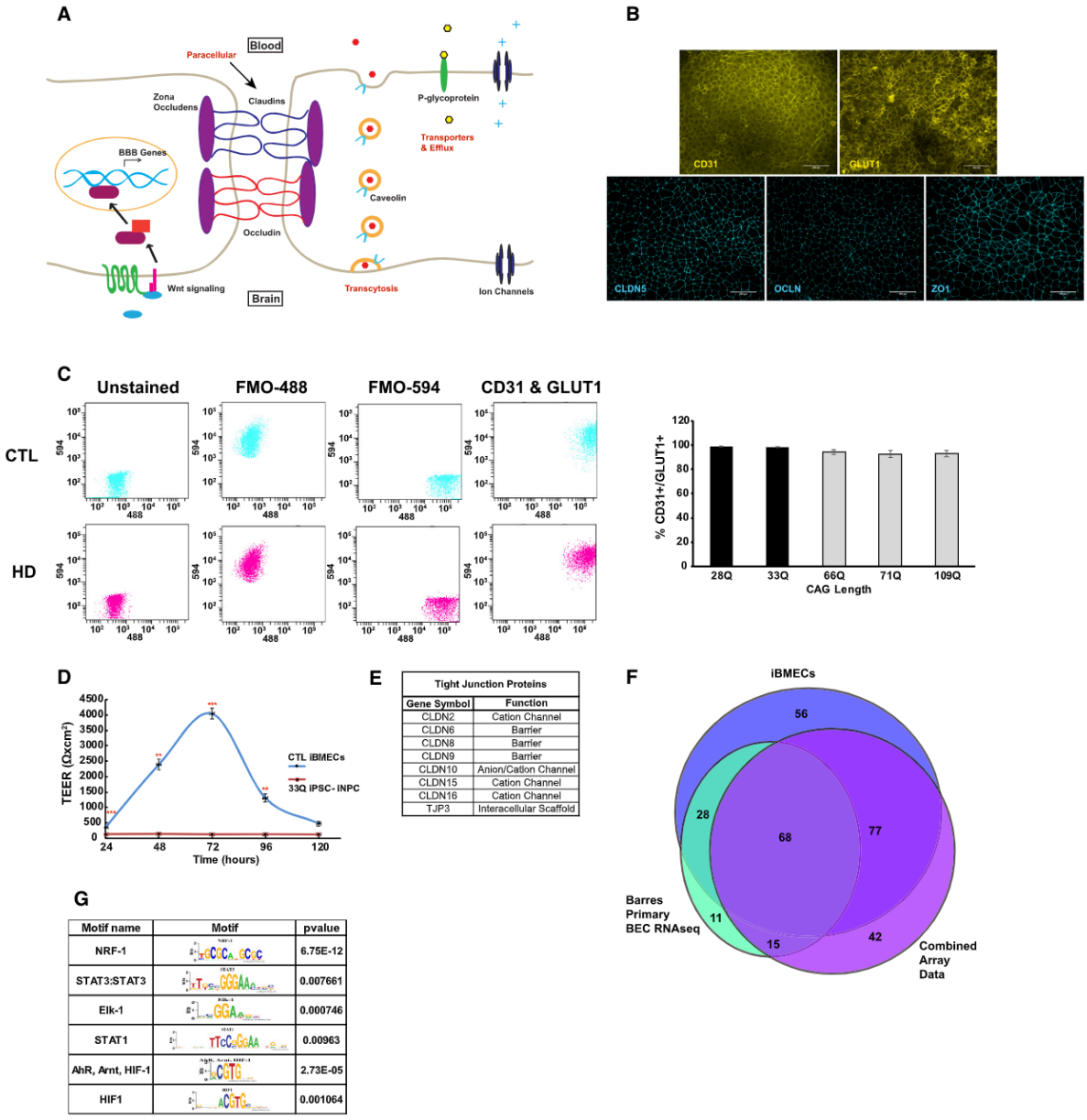

Figure 2.1. iBMECs from Healthy Control Patients Stain for BBB Markers, Show Functional Barrier Properties, and Provide Insight into Novel Regulators of BBB Genes. (A) Diagram of the human BBB. Paracellular transport is prevented by TJs formed by CLAUDINS (CLDN; blue), OCCLUDIN (OCLN; red), and ZONA OCCLUDENS (ZO; purple oval). The low levels of transcytosis are controlled by a small number of caveolae expressing CAVEOLIN-1 (orange circles and light blue). Lastly, the transport and efflux of molecules are regulated by solute carriers, ATP-binding cassette genes, and other ion channels. (B) Representative images for control iBMEC stained for PECAM-1 (CD31) (28Q), GLUT-1 (SLC2A1) (33Q), CLDN-5 (28Q), OCLN (33Q), and ZO-1 (33Q). The scale bars represent 100 µm. (C) Flow cytometry quantification of % $CD31^+$ (594) and $GLUT1^+$ (488) double positive control and HD cells. The bar graph shows greater than 90% pure populations of iBMECs and no statistical difference between each sample using a one-way ANOVA [n = 3 (28Q), 5 (33Q), 7 (66Q), 5 (71Q), and 7 (109Q), independent experiments/differentiations with a minimum of two technical replicates). The dot plot is shown for 33Q and 66Q iBMECs unstained, FMO, and fully stained cells. (D) Scatterplot of TEER values from control iBMECs (blue, 33Q and 28Q) and control iNPCs (red, 33Q) lines over 120 hr. The TEER values for the iBMECs are shown as average between two control iPSC lines (28Q and 33Q) and one iNPC control line over three

continued from previous page; individual readings taken from triplicate wells. There was no statistical difference in TEER values between two control iBMEC samples, but a significant difference was seen between two control iBMECs with the iNPCs [(n) = 14 (33Q BMEC), 16 (28Q BMEC), 3 (NPCs, adjusted p values = 1.94×10^{-4} (24 hr), 1.44×10^{-3} (48 hr), 2.74×10^{-4} (72 hr), and 9.37×10^{-3} (96 h), n.s. (120 hr) independent experiments/differentiations per sample; ANOVA with Bonferroni post hoc correction]. (E) List of uniquely expressed CLDNs found in RNA-seq data from control iBMECs. (F) A Venn diagram of shared SLC- and ABC- transporters between control iBMECs data and previously published BMEC transcriptomic data. (G) Selected results from motif analysis on all SLC- and ABC- transporter genes expressed in control iBMECs. p values represent the likelihood of finding the calculated enrichment of that motif in random sequences with similar GC content. See also Tables S1–S5. # (*p < 0.05; **p < 0.01; and ***p < 0.001). For all of the error bars (mean ± SEM).

iPSC-derived neural precursor cells (iNPCs) from the same patient (33Q) showed no TEER over 120 hr (**Figure 2.1D**) (n = 3, 33Q-iNPC adjusted p values = 1.94×10^{-4} [24 hr], 1.44×10^{-3} [48 hr], 2.74×10^{-4} [72 hr], and 9.37×10^{-3} [96 hr], n.s. [120 hr], two-way ANOVA and Bonferroni post hoc correction].

iBMECs were analyzed for expression of BBB-specific genes by comparing their transcriptome (RNA-sequencing [seq]) to existing gene expression data collected from either primary human BMECs isolated by laser capture microdissection and purification or two immortalized BMEC lines (hCMEC/D3 and HBEC-5i) (datasets are listed in Table S3 and described in Huntley et al., 2014; Zhang et al., 2014). Due to difficulties in comparing RNA-seq and microarray data across studies (SEQC/MAQC-III Consortium, 2014), we focused on a binary approach by comparing whether a BBB-specific gene was present or absent.

The control iBMEC data were mined for genes essential for BBB function, including junctional, caveolar, and transporter proteins. CLDNs are the principal constituents of TJs that form a paracellular barrier. Although CLDN-3 and −5 are the main TJs, we found additional *CLDN* genes (e.g., *CLDN*-1, −4, −7, −11, −12, −18, −19, −20, and −23) expressed in our dataset. Some *CLDN* genes (e.g., *CLDN*-2, −6, −8, −9, −10, −15, and −16) and ZO-3 were uniquely expressed in iBMECs (**Figure 2.1E**), whereas OCLN and all three JAM proteins (F11R, JAM-2, and −3) were expressed in all datasets (**Figure 2.1E**). A second key constituent of the BBB is transporter proteins, including solute carrier transporters (SLC) and active efflux

transporters. Profiling of 359 human SLC and 49 ATP-binding cassette (ABC) genes showed that 286 transporter-encoding genes were unique to human BMECs and 59 non-unique genes were expressed 2-fold higher in BMECs than cortex (Geier et al., 2013). Our RNA-seq data identified 173 genes that overlapped with 241 previously identified genes of the combined SLC and ABC families and revealed an additional 56 novel SLC and ABC genes (**Figure 2.1F**; **Table S4**). These findings (173 of the 241 transporter genes) showed a high statistical significance of overlap ($p <$ of 0.000), validating the use of iBMECs as a model.

To identify potentially novel upstream transcription factors that regulate SLC and ABC genes, we used transcription factor motif analysis (**Figure 2.1G**; **Table S5).** THEME software was used to identify enriched upstream regions of every motif in the TRANSFAC and SELEX databases (Jolma et al., 2013; Wingender et al., 1996). The top motif identified the transcription factor NRF-1 ($p = 6.75 \times 10^{-12}$), that regulates not only mitochondrial biogenesis, but also HIF1α during hypoxia (Wang et al., 2016). The HIF-1 motif, where HIF-1α binds in hypoxic conditions to upregulate pro-angiogenic genes (Forsythe et al., 1996), was also highly enriched (**Figure 2.1G**). Finally, ELK-1 and STAT-3 DNA binding motifs were enriched suggesting that these transcription factors may function in cooperation with HIF-1α in iBMECs to promote angiogenesis (Chamorro-Jorganes et al., 2016; Cheranov et al., 2008). Thus, pro-angiogenic transcription factors function upstream of BBB-specific genes to coordinate angiogenesis and barrier maturation in iBMECs.

2.3.2 HD iBMECs Have Functional Deficits in Angiogenesis and Barrier Properties

We next differentiated HD patient-derived iPSCs into iBMECs as above to determine whether the presence of mHTT confers impairment in BMEC function. There were four human HD iPSC lines with expanded repeats of 60Q, 66Q, 71Q, and 109Q (CS21iHD60n8, CS04iHD66n4, CS81iHD71n3, and CS09iHD109n1; Seong et al., 2010), representative of early onset HD, that were differentiated into iBMECs (Lippmann et al., 2014). No statistically significant differences in

the percentage of HD iBMECs ($CD31^+/GLUT1^+$ cells; >90% pure populations; **Figure 2.1C**) compared to control iBMECs were observed after differentiation. HTT protein levels were similar between control and highly expanded repeat lines (HD iPSC Consortium, 2012; Mattis et al., 2015).

We first performed a wound-healing assay to assess the angiogenic potential of iBMECs by measuring the distance that cells travel toward a wound area. HD iBMECs showed increased migration into the wound over a 6 hr time period compared to control lines (**Figures 2.2A** and **2.2B**) [adjusted p value = (66Q 4.69×10^{-4}), (71Q 9.02×10^{-3}); one-way ANOVA and Bonferroni post hoc correction]. To determine whether this effect was due to either increased migration or altered proliferation, we quantified the number of proliferating iBMECs in both control and HD lines and migration across a Transwell system with increasing doses of VEGF in the bottom chamber. There was no significant difference in the number of proliferating iBMECs between any of the HD or control lines, but there was a marked increase in HD iBMEC migration in the Transwell migration assay (**Figures 2.2C** and **2.2D**). Although each iBMEC line (control or HD) showed a dose-dependent response to VEGF, HD iBMECs had increased migration compared to control iBMECs even in the absence of VEGF (**Figure 2.2C**) [adjusted p value = (66Q 2.22×10^{-2}, 3.22×10^{-2}, and 7.15×10^{-3}), (71Q 2.83×10^{-2}, 2.31×10^{-2}, and 3.21×10^{-2}), and (109Q 9.06×10^{-3}, 4.67×10^{-4}, and 8.85×10^{-5}; two-way ANOVA and Bonferroni post hoc correction]. There was no significant difference in the number of apoptotic or dead cells among any of the control or HD iBMECs with the exception of the highly expanded 109Q line, which has a higher susceptibility to cell death (**Figures 2.2E** and **2.2F**) (adjusted p value = 109Q 1.99×10^{-2} and 5.26×10^{-4}, ANOVA and Bonferroni post hoc). These findings demonstrate that HD iBMECs have increased angiogenesis compared to control iBMECs.

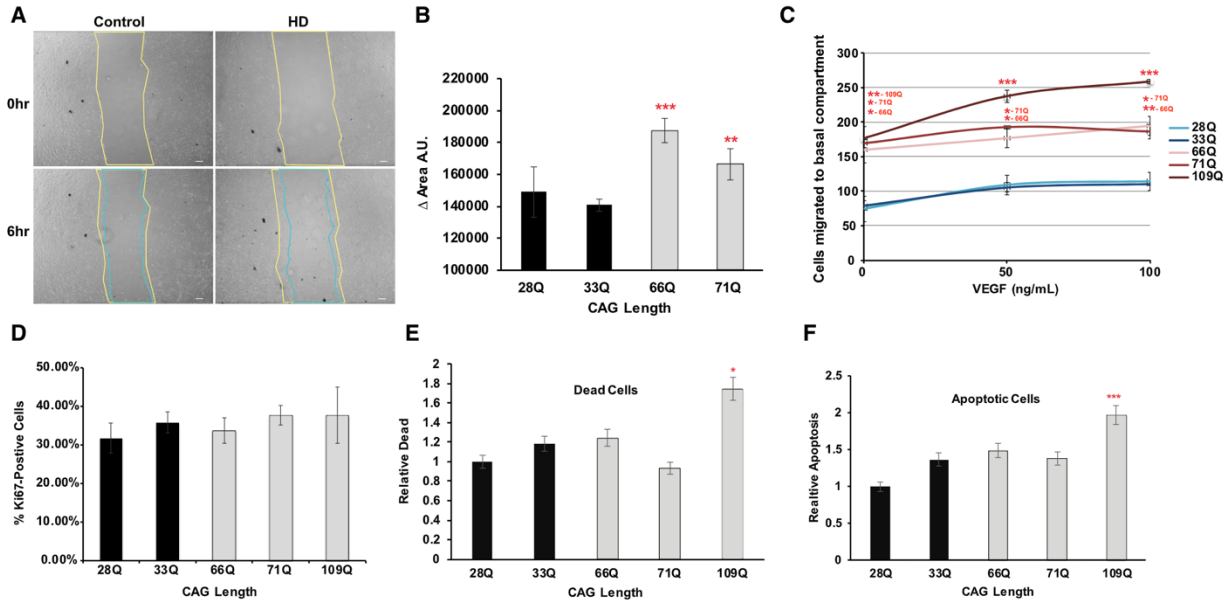

Figure 2.2. HD iBMECs Show Increased Migration. (A) Wound-healing assay shows HD iBMECs have increased migration into wound. The images are 0 and 6 hr time points. The scale bars represent 200 μm. (B) Plot shows change in area over time [(n) = 4 (all lines) independent experiments/differentiations; adjusted p value = (66Q 4.69 × 10−4) and (71Q 9.02 × 10−3) with ANOVA and Bonferroni post hoc correction]. The lines used were 28Q, 33Q, 66Q, and 71Q. (C) Transwell migration assay showing increased migration after 24 hr of HD compared to control iBMECs treated with 0, 50, or 100 ng/mL VEGF [(n = 3 (28Q), 3 (33Q), 3 (66Q), 2 (71Q), and 3 (109Q) independent experiment/differentiations with five images counted per growth replicate; adjusted p value = (66Q 2.22 × 10−2, 3.22 × 10−2, and 7.15 × 10−3), (71Q 2.83 × 10−2, 2.31 × 10−2, and 3.21 × 10−2), and (109Q 9.06 × 10−3, 4.67 × 10−4, and 8.85 × 10−5); two-way ANOVA and Bonferroni post hoc correction]. (D) Quantification of proliferating cells in HD and control iBMECs by % Ki67 positive shows no statistical difference (n = 3 independent experiments/differentiations with five images counted per two growth replicates each; one-way ANOVA). (E and F) Quantification of relative number of dead (E) and apoptotic (F) cells in HD and control iBMECs by flow cytometry. Only 109Q HD iBMECs have a significant increase in the number of apoptotic and dead cells [(n = 10 (28Q), 8 (33Q), 11 (66Q), 9 (71Q), and 8 (109Q) independent experiment/differentiations comparing controls to each individual HD line (adjusted p value = 109Q 1.99 × 10−2 and 5.26 × 10−4); one-way ANOVA and Bonferroni post hoc correction]. # (*p < 0.05; **p < 0.01; and ***p < 0.001). For all of the error bars (mean ± SEM).

We next examined whether HD iBMECs displayed altered TJs and paracellular barrier function. iBMECs did not show any abnormalities in OCLN localization at cell junctions in control or HD lines (**Figure 2.3A**); however, CLDN5 was localized both at junctions and intracellularly in HD (66Q, 71Q, and 109Q), but not control (28Q and 33Q) iBMECs (**Figure 2.3A**) [p value = (7.76 × 10^{-3}); Student's t test]. Protein levels for either CLDN5 or OCLN were unchanged (**Figure 2.3B**;

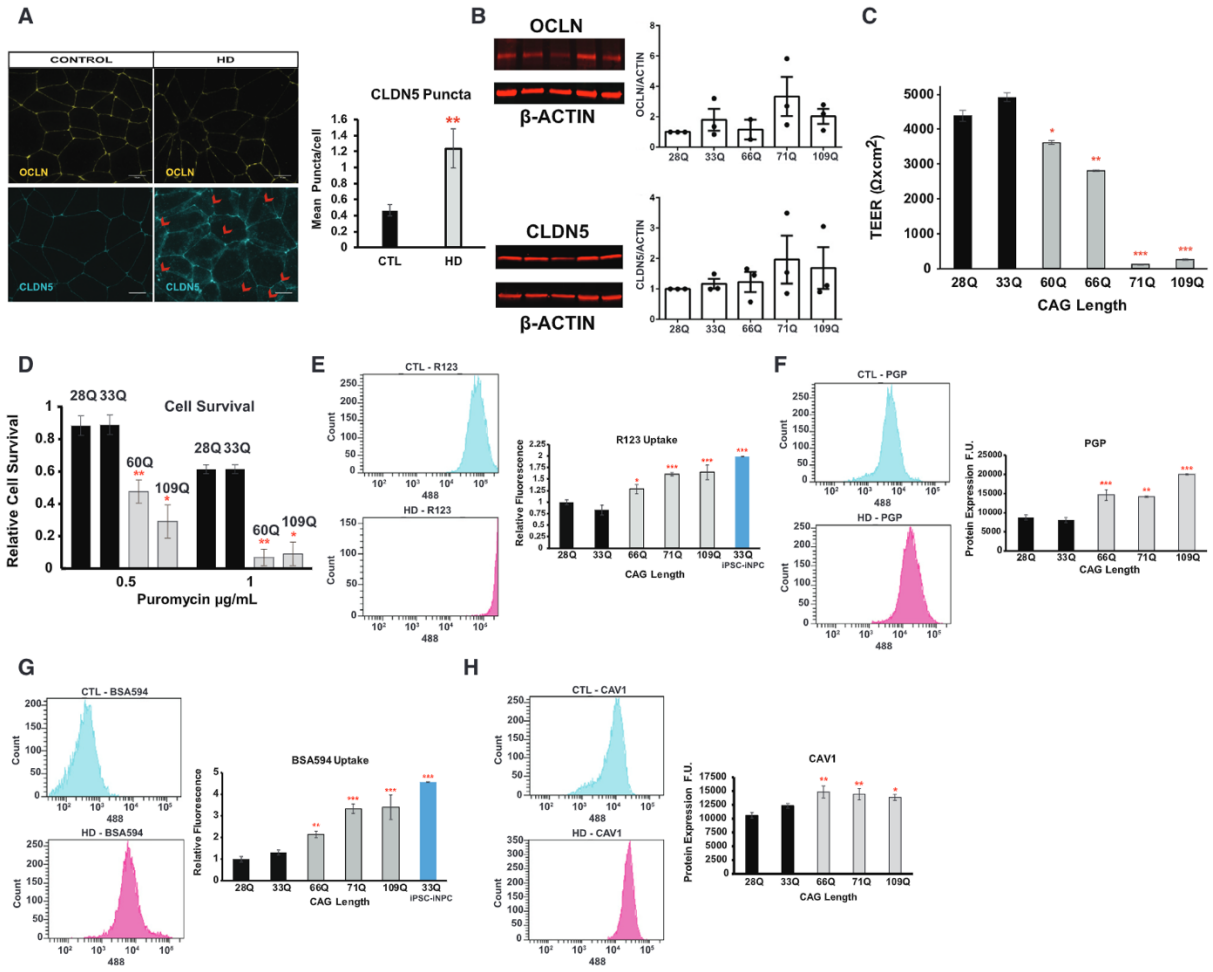

Figure 2.3. HD iBMECs Have Abnormal BBB Function. (A) Representative immunofluorescence micrographs for CLDN5 (33Q and 109Q) and OCLN (33Q and 71Q) in control and HD iBMECs (red arrows mark larger puncta). The scale bars represent 10 µm. The bar graph shows relative CLDN5 intracellular puncta per cell. There is an increase in intracellular CLDN5 protein inside HD cells, [(33Q n = 6), (28Q n = 3), (66Q n = 3), (71Q n = 6), and (109Q n = 3); p value = 7.76 × 10−3, Student's t test]. There were at least three images at 100× per experiment that were used. (B) Western blots with bar graph quantitation of CLDN5 and OCLN levels with the LICOR system. The quantitation was normalized to β-ACTIN, and the bar graph values are shown relative to 28Q line. No difference between any lines was found (ANOVA and Dunnett's multiple comparison test). (C) A bar graph of TEER values for control (black) and HD (gray) lines at 72 hr post subculture. The TEER is decreased in all HD iBMECs. The resistance values from each triplicate measurement/well were averaged in each experiment containing three replicate wells per condition/sample [n and adjusted p value; (n) = 14 (33Q) and 16 (28Q), (60Q n = 20 and 4 × 10−2), (66Q n = 11 and 1 × 10−3), (71Q n = 8 and 1 × 10−6), and (109Q n = 16 and 1 × 10−9); ANOVA with Bonferroni correction]. (D) Histograms and bar graphs of the puromycin survival assay. The bar graph values are relative to untreated for each cell line (n = 3 independent experiments/differentiations with triplicate wells for each condition and five images per well were counted comparing controls to each individual HD line [adjusted p value (60Q 9 × 10−3 and 1.05 × 10−3) and (109Q 1 × 10−2 and 1.08 × 10−2; ANOVA and Bonferroni post hoc correction]. (E) Flow cytometry quantification of Rhodamine 123 efflux/uptake in control and HD iBMECs. For the R123 uptake assay, controls were compared to each individual HD line and a positive control iNPC [n and adjusted p value; (n) = 8 (33Q) and 17 (28Q), (66Q n = 13 and 1.23 × 10−2), (71Q n = 5 and 4.5 × 10−4), (109Q n = 10 and 1.96 × 10−6), and (33Q-iNPCs n = 3 and 5.59 × 10−7); ANOVA and Bonferroni post hoc correction]. (F) Histograms shown for 33Q and 109Q and flow cytometry

continued from previous page; quantification of PGP protein levels showing an increase in HD iBMECs compared to controls [n and adjusted p value; (n) = 4 (33Q) and 8 (28Q), (66Q n = 6 and 4.59 × 10−5), (71Q n = 3 and 1.77 × 10−3), and (109Q n = 3 and 2.89 × 10−6); ANOVA and Bonferroni post hoc correction]. The histograms are shown for 28Q and 109Q. (G) Flow cytometry quantification of CAV1 protein levels showing an increase in HD iBMECs [n and adjusted p value; (n) = 4 (33Q) and 11 (28Q), (66Q n = 8 and 4 × 10−3), (71Q n = 11 and 5 × 10−3), and (109Q n = 9 and 3 × 10−2); one-way ANOVA and Bonferroni post hoc correction]. The histograms are shown for 28Q and 66Q. There is reduced MDR1 function in HD iBMECs (R123) and less cell survival due to decreased efflux of puromycin. (H) Histograms and bar graph of the albumin uptake assay show increased uptake of albumin-A594 in HD iBMECs and positive control 33Q iNPCs compared to control iBMECs [n and adjusted p values; (n) = 12 (33Q) and 17 (28Q), (66Q n = 13 and 3.04 × 10−3), (71Q n = 5 and 9.18 × 10−6), (109Q n = 10 and 1.01 × 10−8), and (33Q-iNPCs n = 3 and 1.59 × 10−9); by one-way ANOVA and Bonferroni post hoc]. The histogram is shown for 28Q and 109Q. # (*p < 0.05; **p < 0.01; and ***p < 0.001). For all of the error bars (mean ± SEM). See also Figure S2.

ANOVA with Dunnett's multiple comparison test). To examine BBB function, TEER measurements were performed on HD and control iBMECs over 96 hr. There was a significant decrease in maximal TEER values in HD iBMECs at 72 hr compared to control lines particularly in those with expanded repeats above 70Qs (e.g., 71Q and 109Q) (**Figure 2.3C**) [adjusted p value = (60Q 4 × 10^{-2}), (66Q 1 × 10^{-3}), (71Q 1 × 10^{-6}), and (109Q 1 × 10^{-9}); ANOVA with Bonferroni post hoc correction]. Thus, some TJ proteins and paracellular barrier function are altered in HD iBMECs.

A major function of the BBB is to prevent influx of harmful molecules into the brain (Zhao et al., 2015). Altered MDR1 (ABCB1 or P-GLYCOPROTEIN) transporter function has been reported in HD (Kao et al., 2015), prompting us to examine whether this transporter might be impaired in HD iBMECs. We performed a puromycin survival assay that relies on the ability of BMECs to extrude puromycin and survive via MDR1 for 48 hr (Perrière et al., 2005). HD iBMECs were unable to survive the antibiotic treatment, even at low levels of puromycin, compared to control lines (**Figure 2.3D**) [adjusted p value = (60Q 9 × 10^{-3} and 1.05 × 10^{-3}) and (109Q 1 × 10^{-2} and 1.08 × 10^{-2}); two-way ANOVA with Bonferroni post hoc correction]. The poor survival rate correlated with increased polyQ length, suggesting that MDR1 has either low expression or aberrant function (**Figure 2.3D**). As an independent assay for MDR1 function, we used flow

cytometry to quantify the uptake of Rhodamine 123 (R123), a dye transported by MDR1 (Miller et al., 1997). We also tested an iNPC line from the same 33Q iPSC, since these cells do not express the MDR1 gene and will take up the dye. An increase in R123 uptake was observed in all HD samples, and the 33Q iNPC cells, compared to control iBMECs (**Figure 2.3E**) [adjusted p value = (66Q 1.23×10^{-2}), (71Q 4.5×10^{-4}), (109Q 1.96×10^{-6}), and (33Q-iNPC 5.58×10^{-7}); one-way ANOVA with Bonferroni post hoc correction], verifying that efflux function is reduced in HD iBMECs. Additionally, treatment with the MDR1 inhibitor Cyclosporine A for 1 hr prior to R123 exposure, inhibited the ability of both control and HD iBMECs to efflux R123 (**Figure S2**). We quantified MDR1 protein levels by flow cytometry to determine if it was reduced, but surprisingly we found increased MDR1 levels in all HD lines (**Figure 2.3F**) [adjusted p value: 33Q (n = 4) and 28Q (n = 8), 66Q (n = 6 and 4.59×10^{-5}), 71Q (n = 3 and 1.77×10^{-3}), and 109Q (n = 3 and 2.89×10^{-6}); one-way ANOVA and Bonferroni post hoc correction]. These findings demonstrate altered MDR1 function in iBMECs carrying mHTT.

2.3.3 Endothelial Transcytosis Is Impaired in HD iBMECs

mHTT aggregates are primarily concentrated in endocytotic vesicles within CNS blood vessels of HD mice and patients (Drouin-Ouellet et al., 2015). Increased fluorescently labeled albumin, which enters the CNS by CAVEOLIN-1-mediated transcytosis, is also found within the CNS of R6/2 mice after intravenous injection (Drouin-Ouellet et al., 2015). We examined endothelial endocytosis in control or HD iBMECs and 33Q iNPCs by measuring the amount of fluorescently labeled albumin inside cells after a 1 hr treatment by flow cytometry. Each HD iBMEC line and the iNPCs had increased albumin uptake compared to control iBMECs (**Figure 2.3G**) [adjusted p value = (66Q 3.04×10^{-3}), (71Q 9.18×10^{-6}), (109Q 1.01×10^{-8}), and (33Q-iNPC 1.59×10^{-9}); ANOVA with Bonferroni post hoc correction], suggesting a higher rate of endocytosis. CAV-1 was also expressed at higher levels in HD iBMECs compared to controls by flow cytometry (**Figure**

2.3H) [adjusted p value = (66Q 4 × 10^{-3}), (71Q 5 × 10^{-3}), (109Q 3 × 10^{-2}); one-way ANOVA with Bonferroni post hoc correction], suggesting an impaired transcytotic barrier in HD iBMECs.

2.3.4 The Transcriptome of HD iBMECs Reveals Altered Angiogenic and Barrier Gene Networks

The data above suggest that there are intrinsic deficits arising in mHTT-expressing iBMECs. To determine whether mHTT impacts BMEC gene expression leading to functional deficits, RNA-seq was carried out on the HD iBMEC lines. Unsupervised exploratory analysis (PCA) was used to examine differences between HD and control cells (**Figure 2.4A**). Although the highest variance is seen across all patient samples in principle component (PC) #1, there is clear separation between control and HD samples across PC #2. A list of differentially expressed genes (DEGs) between control and HD iBMECs was generated using DEseq2 and Partek Flow (Table S6). We then used the tissue specific expression analysis (TSEA) tool (Xu et al., 2014) to explore tissue specificity, which revealed that DEGs were mainly comprised of genes expressed in blood vessels (FDR = 1.048 × 10^{-21} and 8.268 × 10^{-9}, Fisher's exact test with Benjamini-Hochberg correction) (**Figure S1A).**

To identify specific pathways and regulators that control neurovascular function in HD, Ingenuity Pathway Analysis (IPA) was conducted on the DEGs. WNT/β-catenin, pro-angiogenic, and leukocyte extravasation signaling, as well as cell junction or caveolar-mediated transcytosis proteins, essential for BMEC barrier function, were altered (**Figure 2.4B**). To determine changes in transcription factor activity that might contribute to altered gene expression and pathway activity, upstream regulator analysis (IPA) and motif analysis were performed on HD iBMECs. WNT (WNT3A), SHH (GLI2), Angiopoietin/Tie2 (ANGPT2), and TGFβ1 signaling were predicted to be activated (**Figure 2.4C**). Motif analysis on DEGs either expressed only, or upregulated, in HD iBMECs, revealed that many DEGs were regulated by either HIF-1α or ELK-1 (Table S7). This analysis supports the pro-angiogenesis phenotype of HD iBMECs (**Figures 2.2A–2.2C**). To

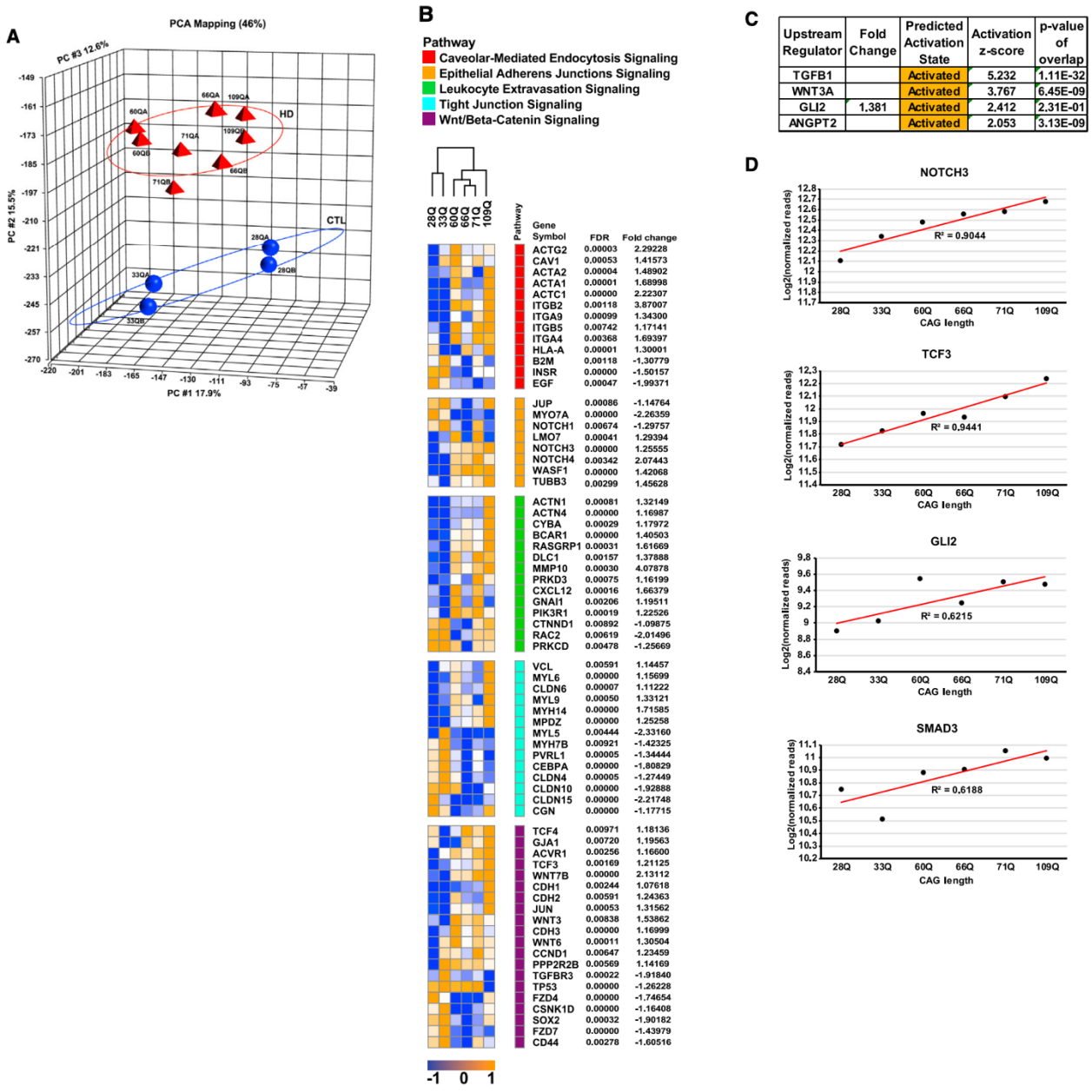

Figure 2.4. Exploratory, Pathway, and Motif Analysis of Transcriptomic Data from Control and HD iBMECs Reveals mHTT Dysregulation of BBB Genes and Related Pathways. (A) PCA of log2 normalized count data on global expression demonstrates grouping within individual control or HD samples and separation between both groups along PC#2. (B) Hierarchical clustering of DEGs in signaling pathways regulating BBB function using log2 normalized count data. The heatmap shows expression values normalized to row min (blue) and max (orange), with genes grouped by pathways indicated by the color bar. The FDR and fold change are displayed for each gene. (C) IPA upstream regulator analysis showing transcriptional regulators predicted to be activated by calculation of activation Z scores. The p value was calculated by Fisher's exact test from expected and observed genes overlapping with our DEG list and all genes regulated by each transcription factor. (D) Scatterplots of log2 normalized count data for NOTCH3, TCF3, GLI2, and SMAD3, plotted by increasing CAG length, with best fit line and R2 values displayed. See also Tables S6 and S7.

determine if there is any correlation between the length of the CAG-repeat with the predicted activation of the above pathways/regulators, we plotted the log2 normalized read count data for each gene (downstream targets or critical pathway members) and found a high correlation between CAG length and DEGs expression/activation (**Figure 2.4D**).

To further uncover potential mechanisms contributing to transcriptional dysregulation in HD iBMECs, we conducted GO analysis, using Cytoscape (Shannon et al., 2003) and EnrichR (Kuleshov et al., 2016). Biological process enrichment revealed that genes promoting vascular sprouting and remodeling were altered in HD iBMECs (**Figures 2.5A** and **2.5B**). The majority of DEGs in the HD iBMECs correspond to either cell adhesion proteins, signaling receptors, or endothelial barrier regulators (**Figures S1B** and **S1C**). Within the parent category of signaling, components of the WNT/β-catenin pathway that regulate CNS angiogenesis and BBB maturation (Zhao et al., 2015) were upregulated in HD iBMECs including ligands (*WNT-3*, *−4*, *−6*, *−7B*, and *−10A*), effectors (*TCF3* and *TCF4*), and downstream targets (*AXIN2* and *APDCC1*) (**Figures 2.4B** and **2.5B**). Other pro-angiogenic genes, such as *NOTCH-3*, *−4*, α_V-*INTEGRIN*, and *SMAD3* (Mancuso et al., 2008), were also upregulated (**Figures 2.4B** and **2.5B**). Surprisingly, *ROBO-1* and *−2* that downregulate VEGFR2 at the beginning of EC differentiation (Mancuso et al., 2008) were upregulated (**Figures 2.4B** and **2.5B**). Collectively, these data indicate that HD iBMECs are starting to mature by expressing the correct gene sets required for maturation (e.g., *ROBO-1* and *2*); however, there is a delay compared to their control counterparts.

Enrichr analysis was used to identify possible epigenomic modifications associated with altered gene expression in HD iBMECs. SUZ12, a member of the polycomb repressive complex 2 (PRC2), had the highest adjusted p value of all transcription factors, suggesting a role for this complex in silencing endothelial genes in HD iBMECs (**Figure 2.5C**) similar to neuronal genes in HD neurons (Seong et al., 2010). This analysis also implicates WNT signaling (TCF3), suggesting that the TCF3/β-CATENIN complex may cooperate with PRC2 to dysregulate HD iBMEC genes

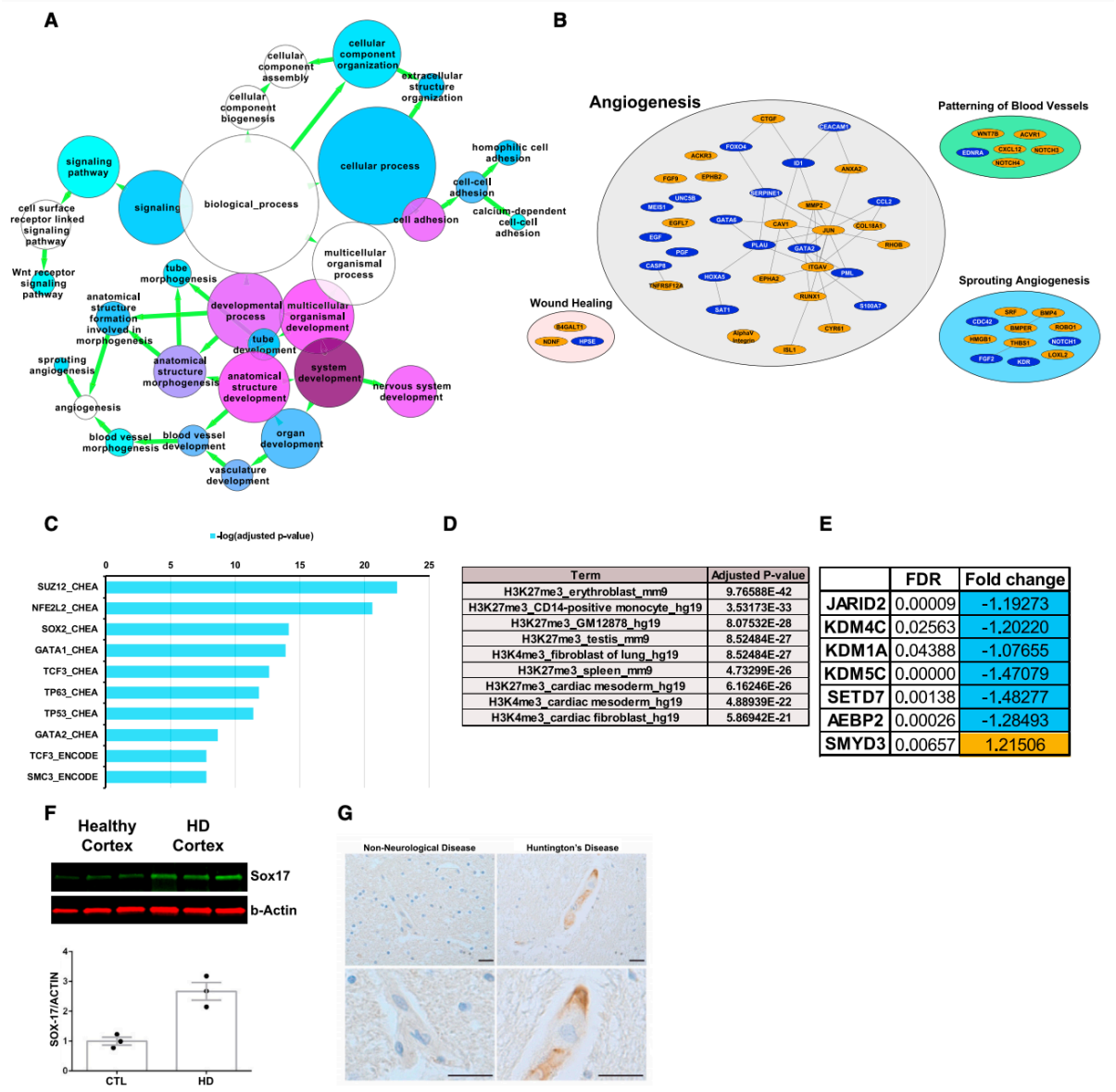

Term	Adjusted P-value
H3K27me3_erythroblast_mm9	9.76588E-42
H3K27me3_CD14-positive monocyte_hg19	3.53173E-33
H3K27me3_GM12878_hg19	8.07532E-28
H3K27me3_testis_mm9	8.52484E-27
H3K4me3_fibroblast of lung_hg19	8.52484E-27
H3K27me3_spleen_mm9	4.73299E-26
H3K27me3_cardiac mesoderm_hg19	6.16246E-26
H3K4me3_cardiac mesoderm_hg19	4.88939E-22
H3K4me3_cardiac fibroblast_hg19	5.86942E-21

	FDR	Fold change
JARID2	0.00009	-1.19273
KDM4C	0.02563	-1.20220
KDM1A	0.04388	-1.07655
KDM5C	0.00000	-1.47079
SETD7	0.00138	-1.48277
AEBP2	0.00026	-1.28493
SMYD3	0.00657	1.21506

Figure 2.5. HD iBMECs and Patient Tissue Show Enrichment for Angiogenesis, WNT, and PRC2 Signaling and Histone Methylation (A) Network mapping of BiNGO biological process analysis showing enrichment for genes that regulate WNT signaling, angiogenesis, and vascular development. Node size = number of genes and node color = decreasing FDR blue to purple. All enrichment nodes have an adjusted p value < 0.05. Adjusted p values were calculated based on overrepresentation of categories over a background sample using a hypergeometric test and adjusted using a Benjamini-Hochberg FDR. (B) Gene network showing differentially expressed genes that are involved in angiogenesis and have a direct protein-protein interaction connection (edges). The orange denotes genes upregulated and blue downregulated in HD. (C) Combined ChEA and ENCODE analysis to determine transcription factors that regulate the DEGs. Adjusted p value by Fisher's exact test and Benjamini-Hochberg correction log (adjusted p value). (D) Enrichment analysis of ENCODE histone modifications relevant to DEGs. Adjusted p value by Fisher's exact test and Benjamini-Hochberg correction. (E) PRC2 genes/effectors and histone methyltransferases that are dysregulated in HD iBMECs. (F) Western blotting in human HD cortical tissue for the WNT/β-catenin transcriptional target SOX17. SOX17 is 2.5-fold higher in HD patient samples ($p < 0.01$, Student's t test). (G) Immunohistochemistry for SOX17 in control or HD human cortex. The SOX17 (brown) is expressed in blood vessels (hematoxylin, blue). The scale bars represent 20 μm. See also Table S8 and Figure S1. # (*$p < 0.05$; **$p < 0.01$; and ***$p < 0.001$). For all of the error bars (mean ± SEM).

(**Figure 2.5C**). Consistent with the above findings, ENCODE genome-wide histone modification analysis identified H3K27me3 and H3K4me3 as marks present at regulatory sites on DEGs altered in HD iBMECs (**Figure 2.5D**). Since several genes of the PRC2 complex and effectors of histone methylation are downregulated in both HD iBMECs (**Figure 2.5E**) and neurons, mHTT may promote dysfunction of multiple cell types at the epigenomic level.

2.3.5 WNT/β-Catenin Pathway Is Activated in Human HD Brain Tissue and Its Inhibition Rescues Angiogenic Deficit In Vitro

To validate some of the transcriptome findings from HD iBMECs in human patient tissue, we performed immunohistochemistry and western blotting on human cortical tissue obtained at autopsy from patients with early-grade HD and age-matched non-neurological disease controls (New York Brain Bank; Table S8). Since WNT signaling is activated in HD iBMECs (**Figures 2.4B, 2.5B,** and **2.5C**), we examined expression levels of SOX17, a transcriptional target of WNT/β-catenin signaling in both mouse and human BMECs (Lengfeld et al., 2017). SOX17 was expressed in blood vessels in HD cortex and was 2.5-fold higher in HD brain compared to unaffected tissue ($p < 0.01$, two-way Student's t test) (**Figures 2.5F** and **2.5G**).

To test whether our transcriptome analysis can identify underlying mechanisms contributing to altered iBMEC function, we performed the wound healing assay in the presence of a small molecule WNT inhibitor, XAV939. Treatment of 33Q iBMECs with 20 μM XAV939 had no effect on their ability to migrate; however, XAV939 significantly reduced the migration of each HD iBMEC line compared to vehicle treated cells, comparable to the control 33Q line [adjusted p value = (33Qv66Q 4×10^{-2}), (33Qv71Q 2×10^{-6}), (33Qv109Q 5×10^{-5}), (66Qv66Q-XAV 5×10^{-3}), (71Qv71Q-XAV 1×10^{-4}), and (109Qv109Q-XAV 2×10^{-3}); two-way ANOVA with Bonferroni post hoc correction] (**Figure 2.6A**). These data demonstrate that inhibition of aberrant WNT signaling in HD iBMECs rescues some of the angiogenic defects and provides validation that aberrant WNT signaling contributes to intrinsic deficits of HD iBMECs. Thus, the transcriptome data provide

predictive information about underlying pathogenic mechanisms that cause intrinsic functional deficits in BMECs and potential targets for therapeutic intervention in HD.

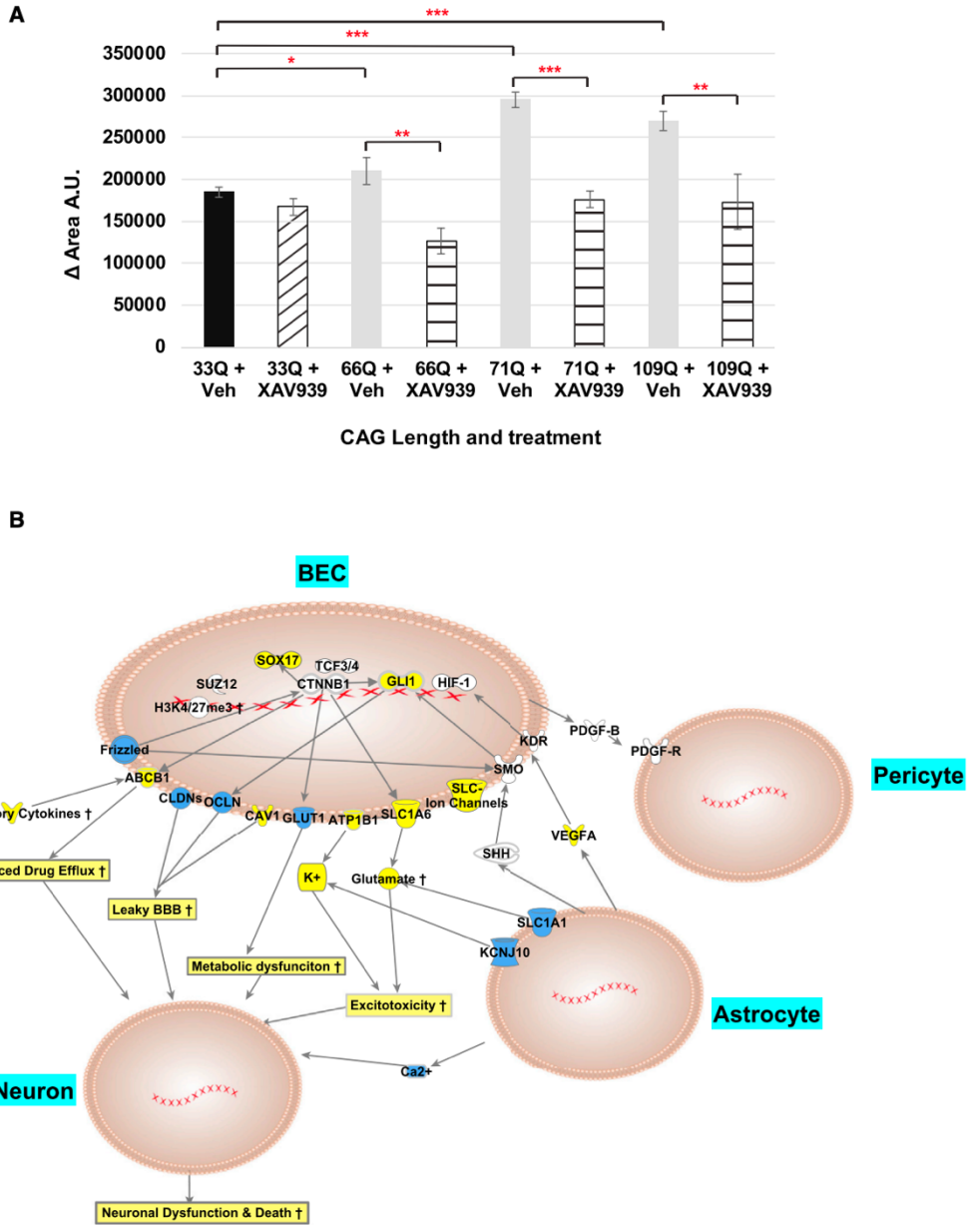

Figure 2.6. WNT Inhibition Restores Angiogenic Deficits in HD iBMECs and Model of NVU Impairment in HD. (A) Wound-healing assay shows HD iBMECs treated with 20 μM XAV939 have decreased migration into the wound. The plot shows change in area overtime. [(n) = 3 (all lines) independent experiments/differentiations and adjusted p value; (33Qv66Q 4.43 × 10−2), (33Qv71Q 2.27 × 10−6), (33Qv109Q 5.31 × 10−5), (66Qv66Q-XAV 5.70 × 10−3), (71Qv71Q-XAV 1.34 × 10−4), and (109Qv109Q-XAV 2.96 × 10−3); two-way ANOVA and bonferroni post hoc]. (B) Model of EC barrier dysfunction in HD. Schematic diagram of NVU in HD and selected genes (yellow denotes genes upregulated and blue downregulated in HD) that are changed in HD iBMECs and HD astrocytes. These genes may contribute to neuronal dysfunction and death. # (*p < 0.05; **p < 0.01; and ***p < 0.001). For all of the error bars (mean ± SEM).

2.4 Discussion

With the advent of iPSC technology and development of disease relevant models through differentiation of patient cells into cells of the NVU, we have the capability to determine cell-specific contributions to disease pathogenesis. Using iPSCs to generate iBMECs from HD and unaffected control subjects, we identified transcriptional and functional differences in human HD iBMECs that demonstrate primary intrinsic deficits in signaling pathways critical for CNS angiogenesis and BBB function.

Studies suggest that constituents of the NVU are altered in neurodegenerative diseases and may contribute to pathogenesis in cell-intrinsic or extrinsic ways including BBB dysfunction (Zhao et al., 2015). Classically, it was assumed that there was no overt BBB leakage in HD; however, recent data indicate vascular abnormalities and BBB dysfunction (Drouin-Ouellet et al., 2015; Hsiao et al., 2015). Our transcriptomic analysis of the HD versus unaffected control iBMECs provides insights into the networks uniquely altered that may underlie specific BBB functions. For instance, WNT signaling that contributes to development of the cerebrovascular network and BBB is altered in HD iBMECs. The increase in WNT target gene (SOX17) in a small cohort of early grade human HD cortical brain tissue and rescue of angiogenic deficits in iBMECs by WNT inhibition are consistent with dysregulation of WNT signaling in the endothelium. Thus, mHTT affects WNT/β-catenin signaling activity and as a consequence inhibits proper BMEC differentiation and maturation. Dysfunctional WNT/β-catenin signaling has also been implicated in BBB breakdown in Alzheimer's disease (Liu et al., 2014; Riise et al., 2015). Our findings consolidate the role of WNT signaling as a key target leading to BBB dysfunction in neurodegenerative diseases.

Since several dysregulated pathways (WNT, NOTCH, and TGFβ signaling) in HD iBMECs control angiogenesis and barrier-genesis, this provides a potential mechanism to explain vascular defects found in HD patients and mouse models. Prior studies have attributed BBB deficits to

increased astrocyte-mediated VEGF signaling (Hsiao et al., 2015); however, our data suggest that BMEC-intrinsic activation of pro-angiogenic signals likely makes blood vessels more permeable, leading to neurovascular dysfunction in HD. The delay in barrier formation may be due to high levels of mHTT that uncouples angiogenesis with proper expression of BBB-forming genes, leaving new small vessels that increase in density as the disease progresses with defective barrier properties unable to protect the CNS. This is consistent with our findings of aberrant paracellular, transcellular, or transporter barrier function in HD iBMECs. Pathway analysis of the RNA-seq data showed that a significant number of affected genes regulate both clathrin- and caveolin-mediated endocytosis, which could lead to abnormal endo/transcytosis. These include FABP4, DYNAMIN, and FILAMIN, which initiate vesicle formation and scission, F-actin, several integrin subunits, and receptors that activate endocytosis (transferrin and low density lipoprotein receptors) (**Figure 2.4B**). CAV-1-dependent endocytosis is normally downregulated in mature BMECs (Zhao et al., 2015). The presence of higher levels of transcytosis proteins (CAV-1) suggests that HD iBMECs have not undergone full maturation, but instead retain a more non-CNS endothelial phenotype. Although MDR1 is increased in expression, the transporter is non-functional. A recent study also showed increased MDR1 expression in both human HD post-mortem tissue and the R6/2 mouse model of HD; however, there was increased functional activity of the transporter in the HD mice (Kao et al., 2015). These differences suggest the need to examine transporter function in human CNS and the consequences for HD pathogenesis in greater detail.

We previously identified a specific pattern of H3K4me3 occupancy that marked genes dysregulated in HD neuronal cells in both a mouse model of HD (Vashishtha et al., 2013) and cortex of HD patients (Dong et al., 2015). Specific patterns of H3K4me3 and H3K27me3 occupancy are also observed in HD iPSC-derived neurons (HD iPSC Consortium, 2017), suggesting that these histone modifications are ubiquitously disrupted in multiple CNS cell types during HD progression. Therefore, epigenomic modulators may improve the function of multiple

cells in the HD brain. Moreover, our proof of concept studies targeting WNT signaling in HD iBMECs suggest additional therapeutic targets that could be used in combination with those targeting neuronal deficits.

From a clinical perspective, therapeutic drug delivery into the brain necessitates an understanding of the state of BBB function in neurodegenerative diseases in order to develop effective treatments. The network data and functional outcomes reflecting these deficits in the HD iBMECs can help to identify the most critical targets for therapeutic intervention and be a tool for investigating fundamental biological and disease processes in the NVU that affect the human cerebral vascular network. In a complementary study (Vatine et al., 2017), a similar approach was used to generate iBMECs from Allan-Herndon-Dudley syndrome patients and identify the underlying cause of pathology, which had not been elucidated using animal models. The authors find that reduced TH availability to neural cells underlies the disease phenotype. The use of iBMECs to identify disease mechanisms for two separate neurological disorders provides confidence in the use of iPSC-derived BMEC models to understand human disease. Finally, the iBMEC model may be used to assess the CNS penetration of drugs under consideration for CNS drug discovery programs and guide future treatments for HD and other neurological disorder patients.

2.5 Experimental Procedures

2.5.1 Generation and Characterization of Human Non-integrating iPSCs Using Episomal Plasmids

HD and non-disease repeat iPSCs were generated and characterized as described (Mattis et al., 2015) (and in Supplemental Information).

2.5.2 Maintenance and Differentiation of Human iPSC-Derived BMECs and iNPCs

There were seven iPSC lines that were maintained on matrigel (BD Biosciences) with mTESR (Stemcell Technologies). These cells were differentiated into BMECs as described (Lippmann et al., 2014) and in Supplemental Information. Control 33Q iPSC were differentiated into iNPCs as described (Ebert et al., 2013).

2.5.3 Immunofluorescence

Cells were stained as described (Lippmann et al., 2014) and in Supplemental Information. A list of antibodies and their use can be found in Supplemental Experimental Procedures (Table S9).

2.5.4 Wound Healing, Migration, and Proliferation Assays

Wound healing: following differentiation, iBMECs were plated in collagen/fibronectin-coated 12-well plates. After 24 hr, the cells reached 100% confluence and the initial scratch/wound was made. BMECs were either untreated, treated with DMSO (vehicle), or 20 μM XAV939. There were two images/well that were taken on an EVOS microscope at time 0 and 6 hr and six wells were used for each experiment/differentiation.

Transwell migration: BMECs were plated in collagen IV/fibronectin-coated Transwells with 3.0 μM pores. After 24 hr, cells were treated with VEGF (50 or 100 ng/mL) or vehicle. At 24 hr after VEGF treatment, the upper chamber of the Transwell was cleared of cells using a cotton swab, the bottom well was fixed with 4% PFA. The Transwell membrane was cut out and mounted on a glass slide with DAPI. There were five DAPI images that were taken per well and three wells were used for each experiment/differentiation.

Proliferation: At 48 hr after subculture, iBMECs were fixed and stained for Ki67. There were five images that were taken per chamber and two chambers were used for each

experiment/differentiation. ImageJ software was used to quantify the area of the wound, the number of migrating cells, or Ki67 positive cells.

2.5.5 Transendothelial Electrical Resistance

TEER measurements were performed using an EVOM2 voltohmmeter (World Precision Instruments). The resistance value ($\Omega x cm^2$) of an empty filter coated with collagen/fibronectin was subtracted from each measurement.

2.5.6 RNA-Seq and DE Statistics

Total RNA was isolated from cells. RNA with quality scores >9 were used for the RNA-seq library generation. Paired-end reads were trimmed using a base quality score threshold of >20 and aligned to hg19. Counts per gene were quantified and analyzed with the R package DESeq2, or Partek Flow, to identify differentially expressed genes. See Supplemental Experimental Procedures and Table S6.

2.5.7 Exploratory, Pathway, and Motif Analysis of DEGs

Spearman's ranked correlation was used for hierarchical clustering, and log2 transformed global expression values were used for PCA. QIAGEN's IPA (http://www.qiagen.com/ingenuity) and EnrichR (Kuleshov et al., 2016) were used for pathway, network, and upstream regulator analysis. Cytoscape was used to visualize GO analysis networks from BiNGO, Enrichment Map, and ClueGO (Bindea et al., 2009; Maere et al., 2005; Merico et al., 2010; Shannon et al., 2003). THEME software was used for motif analysis. Also see Supplemental Experimental Procedures for more detail.

2.5.8 Flow Cytometry, Efflux, and Transporter Assays

For uptake assays, cells were treated with either 10 μM rhodamine 123 (Life Technologies) or 10 mM Albumin-Alexa594 (Life Technologies) and incubated for 1 hr at 37°C. Cells were dissociated into a single cell suspension, fixed using 4% PFA, and analyzed for molecule uptake by flow cytometry. Puromycin efflux was measured based on cell death after 48 hr treatment with either 0.5 or 1 μM puromycin. Flow cytometry was also used for protein quantification and to determine the fraction of $CD31^+/GLUT1^+$ by dissociating cells 48 hr after subculture, fixing, and staining with primary and secondary antibodies. Apoptotic and dead cells were quantified by flow cytometry as described in Life Technologies CellEvent Caspase-3/7 Green Flow Cytometry Assay Kit.

2.5.9 Human Tissue

Fresh frozen human cortical tissue was obtained from the New York Brain Bank at Columbia University from three healthy controls and three individuals with early HD (Table S8). Paraffin-embedded brain tissues from HD patients and non-neurological disease controls were obtained from the tissue bank at CUMC (D.A.; IRB protocol #AAAQ7343).

2.5.10 Western Blotting and Immunohistochemistry

Cell pellets from three independent experiments were lysed and western analysis performed with the LICOR quantitative fluorescence system as described (Lengfeld et al., 2017), with antibodies against human CLDN-5, OCLN, β-ACTIN (Invitrogen), and SOX17 (Abcam). Paraffin-embedded brain tissues were used to assess SOX17 expression as described (Lengfeld et al., 2017).

2.5.11 Author Contributions

Conceptualization, R.G.L., D.A., and L.M.T.; Methodology, R.G.L., C.Q., S.E.L., D.A., and L.M.T.; Formal Analysis, R.G.L., T.A.G., A.J.K., and J.W.; Investigation, R.G.L., C.Q., A.M.R.-O., T.A.G., A.J.K., J.S., and S.E.L.; Resources, C.N.S.; Visualization, R.G.L., Writing - Original Draft, R.G.L., D.A., and L.M.T.; Writing - Review and Editing, C.Q., G.D.V., T.A.G., A.J.K., C.N.S., M.S.C., E.F., and D.E.H.; and Supervision, C.N.S., M.S.C., E.F., and D.E.H.

2.5.12 Acknowledgements

We thank Dr. Sara Winokur for editorial assistance, Alice Lau for technical assistance, and Drs. Jean Paul Vonsattel and Etty Cortes at the New York Brain Bank for providing human HD cortical tissue. Support for this work was provided by the American Heart Association 12PRE10410000 and CIRM TG2-01152; NIH NRSA 5F31NS090859-02 fellowships (R.G.L.); NIH NS078370 (L.M.T. and C.N.S.), NIH NS089076 (E.F., L.M.T., and D.E.H.), NIH NS089076 (E.F.), NIH HL116995-01 (D.A. and S.E.L.), NIH MH109987 (D.A.), NeuroLINCS Center U54 NS091046 (L.M.T., C.N.S., and E.F.); and the NIH Biotechnology Training Program Fellowship T32GM008334 (A.J.K.). Additional support was provided by The Leducq Foundation (FDNLEDQ 15CVD 02) (D.A.), a gift from John Castle to the CUMC Neurology, Stroke Division (D.A.), and CIRM Bridges Program TB1-01182 (C.Q.). Computing resources were funded by the National Science Foundation under Award No. DB1-0821391. This work was made possible through access to the Genomic High Throughput Facility Shared Resource of the Cancer Center Support Grant (CA-62203) at the University of California, Irvine.

2.5.13 Accession Numbers

The accession number for the RNA-seq reported in this paper is GEO: GSE97100. Any additional data that support the findings of this study are available from the corresponding author upon reasonable request.

2.5.14 Supplemental information links

Document S1. Supplemental Experimental Procedures, Figures S1 and S2, and Tables S1–S5 and S7–S9

Table S6. Full Differentially Expressed Gene List at 0.05 FDR, Related to Figure 4

Table S10. Table of Statistical Methodology, Related to Supplemental Experimental Procedures

2.6 References

Bindea G, Mlecnik B, Hackl H, Charoentong P, Tosolini M, Kirilovsky A, Fridman WH, Pagès F, Trajanoski Z, Galon J. ClueGO: a Cytoscape plug-in to decipher functionally grouped gene ontology and pathway annotation networks. *Bioinformatics.* 2009;25:1091–1093.

Chamorro-Jorganes A, Lee MY, Araldi E, Landskroner-Eiger S, Fernández-Fuertes M, Sahraei M, Quiles Del Rey M, van Solingen C, Yu J, Fernández-Hernando C, et al. VEGF-induced expression of miR-17–92 cluster in endothelial cells is mediated by ERK/ELK1 activation and regulates angiogenesis. *Circ Res.* 2016;118:38–47.

Cheranov SY, Karpurapu M, Wang D, Zhang B, Venema RC, Rao GN. An essential role for SRC-activated STAT-3 in 14,15-EET-induced VEGF expression and angiogenesis. *Blood.* 2008;111:5581–5591.

Dong X, Tsuji J, Labadorf A, Roussos P, Chen JF, Myers RH, Akbarian S, Weng Z. The role of H3K4me3 in transcriptional regulation is altered in Huntington's disease. *PLoS ONE.* 2015;10:e0144398.

Drouin-Ouellet J, Sawiak SJ, Cisbani G, Lagacé M, Kuan WL, Saint-Pierre M, Dury RJ, Alata W, St-Amour I, Mason SL, et al. Cerebrovascular and blood-brain barrier impairments in Huntington's disease: Potential implications for its pathophysiology. *Ann Neurol.* 2015;78:160–177.

Ebert AD, Shelley BC, Hurley AM, Onorati M, Castiglioni V, Patitucci TN, Svendsen SP, Mattis VB, McGivern JV, Schwab AJ, et al. EZ spheres: a stable and expandable culture system for the generation of pre-rosette multipotent stem cells from human ESCs and iPSCs. *Stem Cell Res (Amst)* 2013;10:417–427.

Forsythe JA, Jiang BH, Iyer NV, Agani F, Leung SW, Koos RD, Semenza GL. Activation of vascular endothelial growth factor gene transcription by hypoxia-inducible factor 1. *Mol Cell Biol.* 1996;16:4604–4613.

Franciosi S, Ryu JK, Shim Y, Hill A, Connolly C, Hayden MR, McLarnon JG, Leavitt BR. Age-dependent neurovascular abnormalities and altered microglial morphology in the YAC128 mouse model of Huntington disease. *Neurobiol Dis.* 2012;45:438–449.

Geier EG, Chen EC, Webb A, Papp AC, Yee SW, Sadee W, Giacomini KM. Profiling solute carrier transporters in the human blood-brain barrier. *Clin Pharmacol Ther.* 2013;94:636–639.

HD iPSC Consortium. Induced pluripotent stem cells from patients with Huntington's disease show CAG-repeat-expansion-associated phenotypes. *Cell Stem Cell.* 2012;11:264–278.

HD iPSC Consortium. Developmental alterations in Huntington's disease neural cells and pharmacological rescue in cells and mice. *Nat Neurosci.* 2017;20:648–660.

Hsiao HY, Chen YC, Huang CH, Chen CC, Hsu YH, Chen HM, Chiu FL, Kuo HC, Chang C, Chern Y. Aberrant astrocytes impair vascular reactivity in Huntington disease. *Ann Neurol.* 2015;78:178–192.

Hua J, Unschuld PG, Margolis RL, van Zijl PC, Ross CA. Elevated arteriolar cerebral blood volume in prodromal Huntington's disease. *Mov Disord.* 2014;29(Suppl 3):396–401.

Huntley MA, Bien-Ly N, Daneman R, Watts RJ. Dissecting gene expression at the blood-brain barrier. *Front Neurosci.* 2014;8:355.

Jolma A, Yan J, Whitington T, Toivonen J, Nitta KR, Rastas P, Morgunova E, Enge M, Taipale M, Wei G, et al. DNA-binding specificities of human transcription factors. *Cell.* 2013;152:327–339.

Kao YH, Chern Y, Yang HT, Chen HM, Lin CJ. Regulation of P-glycoprotein expression in brain capillaries in Huntington's disease and its impact on brain availability of antipsychotic agents risperidone and paliperidone. *J Cereb Blood Flow Metab.* 2015;36:1412–1423.

Kuleshov MV, Jones MR, Rouillard AD, Fernandez NF, Duan Q, Wang Z, Koplev S, Jenkins SL, Jagodnik KM, Lachmann A, et al. Enrichr: a comprehensive gene set enrichment analysis web server 2016 update. *Nucleic Acids Res.* 2016;44(W1):W90–97.

Lengfeld JE, Lutz SE, Smith JR, Diaconu C, Scott C, Kofman SB, Choi C, Walsh CM, Raine CS, Agalliu I, Agalliu D. Endothelial Wnt/β-catenin signaling reduces immune cell infiltration in multiple sclerosis. *Proc Natl Acad Sci USA.* 2017;114:E1168–E1177.

Lin CY, Hsu YH, Lin MH, Yang TH, Chen HM, Chen YC, Hsiao HY, Chen CC, Chern Y, Chang C. Neurovascular abnormalities in humans and mice with Huntington's disease. *Exp Neurol.* 2013;250:20–30.

Lippmann ES, Al-Ahmad A, Azarin SM, Palecek SP, Shusta EV. A retinoic acid-enhanced, multicellular human blood-brain barrier model derived from stem cell sources. *Sci Rep.* 2014;4:4160.

Liu L, Wan W, Xia S, Kalionis B, Li Y. Dysfunctional Wnt/β-catenin signaling contributes to blood-brain barrier breakdown in Alzheimer's disease. *Neurochem Int.* 2014;75:19–25.

Maere S, Heymans K, Kuiper M. BiNGO: a Cytoscape plugin to assess overrepresentation of gene ontology categories in biological networks. *Bioinformatics.* 2005;21:3448–3449.

Mancuso MR, Kuhnert F, Kuo CJ. Developmental angiogenesis of the central nervous system. *Lymphat Res Biol.* 2008;6:173–180.

Mattis VB, Tom C, Akimov S, Saeedian J, Østergaard ME, Southwell AL, Doty CN, Ornelas L, Sahabian A, Lenaeus L, et al. HD iPSC-derived neural progenitors accumulate in culture and are susceptible to BDNF withdrawal due to glutamate toxicity. *Hum Mol Genet.* 2015;24:3257–3271.

Merico D, Isserlin R, Stueker O, Emili A, Bader GD. Enrichment map: a network-based method for gene-set enrichment visualization and interpretation. *PLoS ONE.* 2010;5:e13984.

Miller DW, Batrakova EV, Waltner TO, Yu Alakhov V, Kabanov AV. Interactions of pluronic block copolymers with brain microvessel endothelial cells: evidence of two potential pathways for drug absorption. *Bioconjug Chem.* 1997;8:649–657.

Munoz-Sanjuan I, Bates GP. The importance of integrating basic and clinical research toward the development of new therapies for Huntington disease. *J Clin Invest.* 2011;121:476–483.

Perrière N, Demeuse P, Garcia E, Regina A, Debray M, Andreux JP, Couvreur P, Scherrmann JM, Temsamani J, Couraud PO, et al. Puromycin-based purification of rat brain capillary endothelial cell cultures. Effect on the expression of blood-brain barrier-specific properties. *J Neurochem.* 2005;93:279–289.

Riise J, Plath N, Pakkenberg B, Parachikova A. Aberrant Wnt signaling pathway in medial temporal lobe structures of Alzheimer's disease. *J Neural Transm (Vienna)* 2015;122:1303–1318.

Ross CA, Tabrizi SJ. Huntington's disease: from molecular pathogenesis to clinical treatment. *Lancet Neurol.* 2011;10:83–98.

Seong IS, Woda JM, Song JJ, Lloret A, Abeyrathne PD, Woo CJ, Gregory G, Lee JM, Wheeler VC, Walz T, et al. Huntingtin facilitates polycomb repressive complex 2. *Hum Mol Genet.* 2010;19:573–583.

SEQC/MAQC-III Consortium. A comprehensive assessment of RNA-seq accuracy, reproducibility and information content by the Sequencing Quality Control Consortium. *Nat Biotechnol.* 2014;32:903–914.

Shannon P, Markiel A, Ozier O, Baliga NS, Wang JT, Ramage D, Amin N, Schwikowski B, Ideker T. Cytoscape: a software environment for integrated models of biomolecular interaction networks. *Genome Res.* 2003;13:2498–2504.

Takahashi K, Tanabe K, Ohnuki M, Narita M, Ichisaka T, Tomoda K, Yamanaka S. Induction of pluripotent stem cells from adult human fibroblasts by defined factors. *Cell.* 2007;131:861–872.

The Huntington's Disease Collaborative Research Group. A novel gene containing a trinucleotide repeat that is expanded and unstable on Huntington's disease chromosomes. *Cell.* 1993;72:971–983.

Vashishtha M, Ng CW, Yildirim F, Gipson TA, Kratter IH, Bodai L, Song W, Lau A, Labadorf A, Vogel-Ciernia A, et al. Targeting H3K4 trimethylation in Huntington disease. *Proc Natl Acad Sci USA.* 2013;110:E3027–E3036.

Vatine GD, Al-Ahmad A, Barriga BK, Svendsen S, Salim A, Garcia L, Garcia VJ, Ho R, Yucer N, Qian T, et al. Modeling psychomotor retardation using iPSCs from MCT8-deficient patients indicates a prominent role for the blood-brain barrier. *Cell Stem Cell.* 2017;20.

Walker FO. Huntington's disease. *Semin Neurol.* 2007;27:143–150.

Wang D, Zhang J, Lu Y, Luo Q, Zhu L. Nuclear respiratory factor-1 (NRF-1) regulated hypoxia-inducible factor-1α (HIF-1α) under hypoxia in HEK293T. *IUBMB Life.* 2016;68:748–755.

Wingender E, Dietze P, Karas H, Knüppel R. TRANSFAC: a database on transcription factors and their DNA binding sites. *Nucleic Acids Res.* 1996;24:238–241.

Xu X, Wells AB, O'Brien DR, Nehorai A, Dougherty JD. Cell type-specific expression analysis to identify putative cellular mechanisms for neurogenetic disorders. *J Neurosci.* 2014;34:1420–1431.

Yu J, Vodyanik MA, Smuga-Otto K, Antosiewicz-Bourget J, Frane JL, Tian S, Nie J, Jonsdottir GA, Ruotti V, Stewart R, et al. Induced pluripotent stem cell lines derived from human somatic cells. *Science.* 2007;318:1917–1920.

Zhang Y, Chen K, Sloan SA, Bennett ML, Scholze AR, O'Keeffe S, Phatnani HP, Guarnieri P, Caneda C, Ruderisch N, et al. An RNA-sequencing transcriptome and splicing database of glia, neurons, and vascular cells of the cerebral cortex. *J Neurosci.* 2014;34:11929–11947.

Zhao Z, Nelson AR, Betsholtz C, Zlokovic BV. Establishment and dysfunction of the blood-brain barrier. *Cell.* 2015;163:1064–1078.

CHAPTER II

Assessing blood-brain barrier functions following perturbations in Huntington's disease brain microvascular endothelial cells

CHAPTER II

Assessing blood-brain barrier functions following perturbations in Huntington's disease brain microvascular endothelial cells

3.1 Summary of Chapter 2

Brain microvascular endothelial cells (BMECs) are the cellular component of the blood-brain barrier (BBB) controlling the movement of substances between the brain and blood. Impairments in the Huntington's disease (HD) BBB have been described in mouse models and human tissue (Drouin-Ouellet et al., 2015; Hsiao et al., 2015). Our lab has identified cell intrinsic impairments to HD induced pluripotent stem cell (iPSC)-derived BMECs (iBMECs) that implicated WNT activation as a key feature of dysfunctional HD iBMECs (Lim et al., 2017). I further assessed the functional effect of WNT signaling modulation and knockdown of the disease-causing HTT protein in HD iBMECs. Unaffected control and HD iBMECs were either treated with a WNT inhibitor XAV939 or with a miRNA-targeting *HTT* for knockdown. These iBMECs underwent functional assessment of barrier properties, which included paracellular barrier function by transendothelial electrical resistance (TEER) measurements, and angiogenic migration assessment by a high throughput woundhealing assay (Lim et al., 2017). WNT inhibition improved angiogenic migration but also increased paracellular barrier permeability in HD iBMECs. Additionally, HTT knockdown slightly improved paracellular barrier integrity. This project stemmed from a continuation of the work described in Lim et al., 2017 and in Chapter 1 of this dissertation. My role on this project included experimental design, data analysis, statistical analysis, interpretation and execution of all cell culture, qPCR, paracellular functional assessments, and angiogenic migration assessments through time-lapse imaging

3.2 Introduction

The blood-brain barrier (BBB) is a key homeostatic site formed by brain endothelial cells and maintained by the neurovascular unit to control transport between the peripheral organs and the brain. BBB disruption can lead to alterations in the cerebral vasculature, which could exacerbate neuronal dysfunction and be involved in the causing neurodegeneration. It is critical to examine the role mHTT plays in the loss of BBB integrity to better understand the molecular mechanisms controlling HD pathogenesis and how BBB deficits contribute to progressive neurodegeneration.

Research in HD mouse and post-mortem patient tissue demonstrated impairments of the neurovascular unit and the BBB (Drouin-Ouellet et al., 2015; Hsiao et al., 2015), and recently, similar impairments have been described in iPSC-based models of BBB cells (Lim et al., 2017). HD patient-specific induced pluripotent stem cell (iPSC) lines recapitulate several HD phenotypes *in vitro*, including changes in transcription, intracellular signaling and transport, endocytic recycling, and synaptic dysfunction (HD iPSC Consortium, 2013, 2017; Lim et al., 2017; Mattis et al., 2015; Smith-Geater et al., 2020). These HD iPSC lines can be successfully differentiated into brain microvascular endothelial cells (iBMECs) using a rapid protocol (Lippmann et al., 2012, 2014). As described in Lim et al., 2017 and in Chapter 1 of this dissertation, HD iBMECs derived from HD patient iPSCs show transcriptional alterations in genes involved in BBB development, including WNT signaling activation, and exhibit loss of BBB function in paracellular and transcellular permeability as well as aberrant angiogenesis (**Figure1.2-1.5** and Lim et al., 2017). Since HD-iPSCs provide a unique model system to investigate BBB deficits in HD *in vitro*, this chapter aimed to test whether WNT inhibition or HTT knockdown could prevent or reverse cell-autonomous HD-associated BBB deficits of paracellular permeability and angiogenesis in HD iBMECs. This project includes pilot experiments to gain a greater understanding of HD and the BBB for the development of novel HD therapeutics.

3.3 Results

3.3.1 WNT Inhibition for Perturbation of BBB Function

Our lab previously demonstrated that WNT inhibition by XAV939 rescued aberrant angiogenesis in HD iBMECs (described in Chapter 1 of this dissertation **Figure 1.6A**; Lim et al., 2017). To assess a higher throughput angiogenic migration assay for the prospect of future high throughput drug screens, I utilized the Incucyte Scratch WoundMaker Tool and Analysis Software. This system was used to generate consistent "wounds" across a monolayer of HD (HD71n3 and HD109n1) and unaffected control (CTR33n1) iBMECs within wells of a 96-well plate. The analysis software allowed for label-free detection of cellular migration into the wound area at specified time intervals for the entire time-course of the experiment without the need to remove the cells from a 37°C incubator. First, I was able to replicate the increased angiogenic phenotype in HD iBMECs (**Figure 2.1A** and **Figure 1.2B**) under the conditions previously described (Lim et al., 2017). Next, I utilized this assay to test various concentrations of XAV939 on HD and unaffected control iBMECs (**Figure 2.1B-D**). The small molecule WNT inhibitor **XAV939** acts on a component of the β-catenin destruction complex, Axin, by inhibiting its ubiquitination by Tankyrase (TNKS) to stabilize the β-catenin destruction complex and inhibit downstream activation of WNT signaling. Similar to our previously published data (**Figure 1.6A** and Lim et al., 2017), XAV939 decreased the rate in which HD109n1 iBMECs migrated into the wound area, with 10 μM XAV939 having the slowest rate of migration. WNT inhibition appeared to have minimal effect on CTR33n1 and HD71n3 under the experimental conditions tested, suggesting XAV939 may be most effective on juvenile CAG expanded repeat lengths, where dysfunctional and molecular dysregulation (including WNT activation) are more severe. This data demonstrates the potential of this angiogenic functional assay to further assess perturbations in a high-throughput manner.

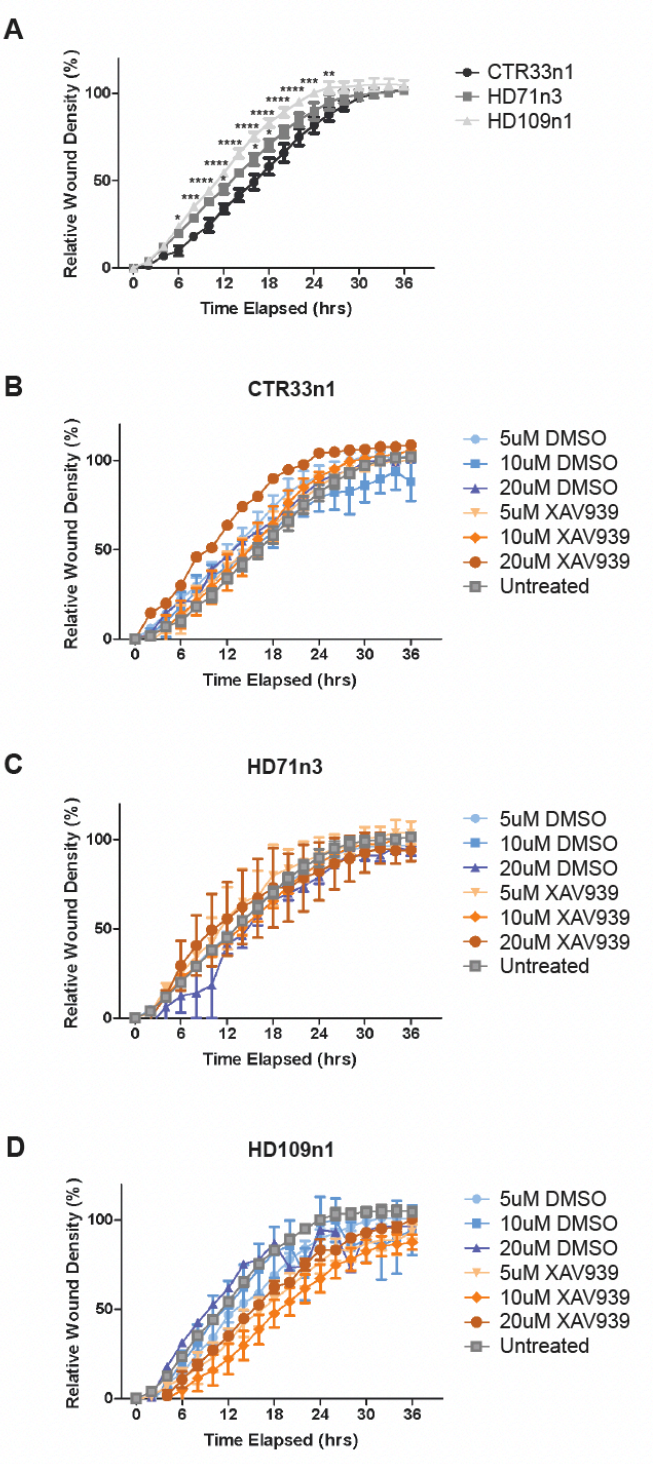

Figure 3.1. Time-lapse Angiogenesis Migration Assay Following WNT Inhibition in HD and Control iBMECs. (A) HD iBMECs demonstrate significantly increased angiogenic migration compared to control iBMECs. 2-way ANOVA *p<0.05, **p<0.01, ***p<0.001 ****p<0.0001. N=1 biological/differentiation replicate, n=5 technical replicates, mean +/- standard error mean. **(B-D)** CTR33n1 (B), HD71n3 (C), and HD109n1 (D) treated with WNT inhibitor, XAV939, or vehicle, DMSO at varying concentrations does not significantly alter angiogenic migration. N=1 biological/differentiation replicate, n=1-5 technical replicates, mean +/- standard error mean.

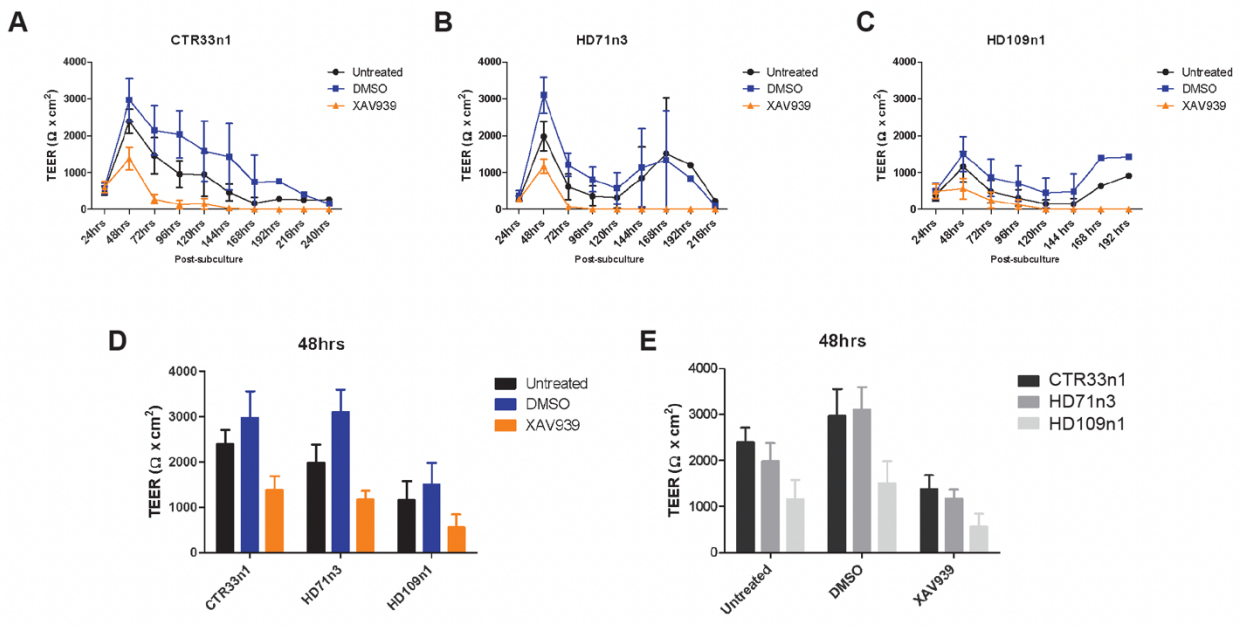

Figure 3.2. Paracellular Barrier Function Following WNT Inhibition in HD and Control iBMECs. (A-C) Transendothelial electrical resistance (TEER) measurements across iBMECs with and without WNT inhibition (XAV939, 20uM) or vehicle control treatment in CTR33n1 (A), HD71n3 (B), and HD109n1 (C). **(D-E)** TEER measurement 48hrs organized by cell line (D) or by treatment conditions (E). 20uM XAV939 was used. (N=4 biological/differentiation replicates for 24hrs-120hrs, n=3 technical replicates per biological replicate, mean +/- standard error mean).

To assess the effect of WNT inhibition on another critical BMEC function, paracellular barrier function, I treated HD and unaffected iBMECs with 20 μM XAV939 24 hours post subculture then measured TEER. WNT inhibition appeared to exacerbate paracellular permeability, although this observation was not statistically significant (**Figure 2.2A-C**). For iBMECs differentiated from unaffected control CTR33n1 iPSCs, TEER values 48 hours post subculture (24 hours post XAV939 treatment) decreased by nearly half when compared to the vehicle control of DMSO (**Figure 2.2**). This effect was also demonstrated in the HD iBMECs derived from HD71n3 and HD109n1 iPSCs. TEER values were nearly undetectable by 48 hours post XAV939 treatment at 72 hours post-subculture for all iBMECs (**Figure 2.2A-C**) while cellular survival was not significantly affected, demonstrating a lack of paracellular barrier function and not a loss of a monolayer. Interestingly, the DMSO vehicle-treated iBMECs displayed overall

slightly increased TEER values compared to untreated iBMECs, with TEER values detectable for more than 144 hours post-subculture in DMSO-treated wells (**Figure 2.2A-C**). Overall, WNT inhibition did not rescue paracellular barrier deficit in HD iBMECs under the conditions assessed; rather it appeared to exacerbate the deficit.

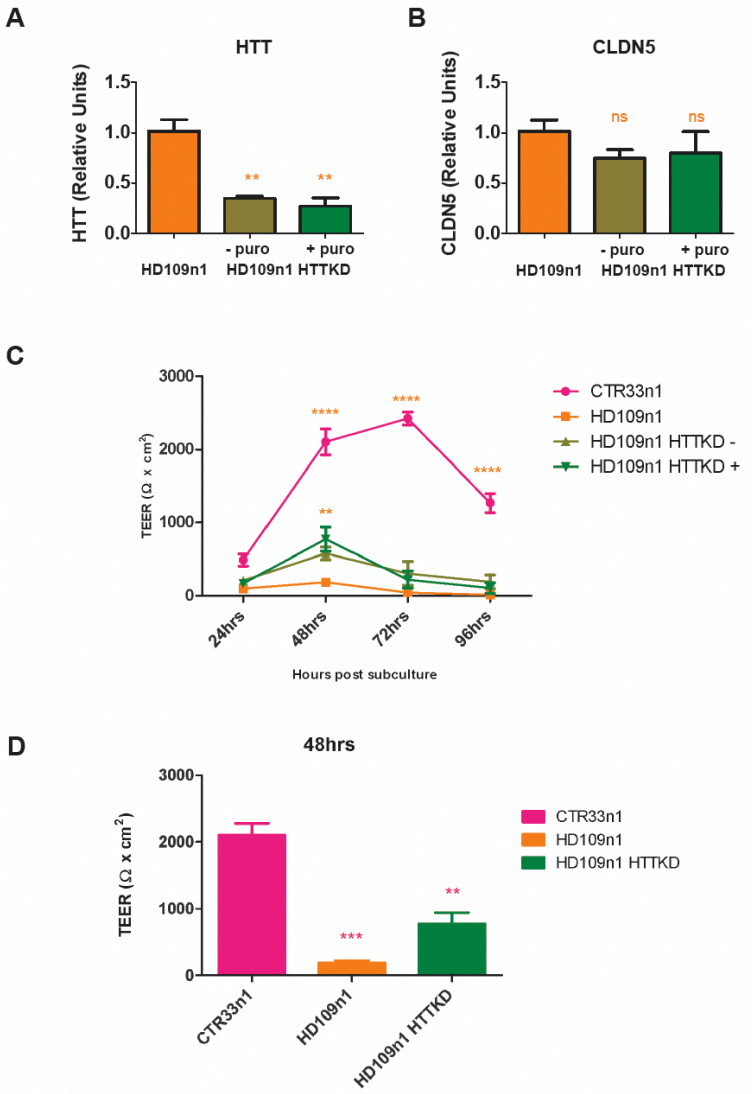

Figure 3.3. HTT Knockdown in HD iBMECs Improves Barrier Deficit. (A) qPCR data demonstrating significant *HTT* knockdown. 1-way ANOVA **p<0.01. **(B)** HTT knockdown does not significantly alter the expression of a transcript that encodes a tight junction protein, *CLDN5*. 1-way ANOVA not significant (ns) p>0.05. **(C)** Transendothelial electrical resistance (TEER) following HTT knockdown in iBMECs. (-) indicates no puromycin antibiotic was used during iBMEC differentiation, while (+) indicates puromycin was used during the iBMEC differentiation. 2-way ANOVA **p<0.01, ****p<0.0001. **(D)** TEER data at 48 hours demonstrates significant improvement of paracellular transport in HD iBMECs with HTT knockdown. 1-way ANOVA **p<0.01, ***p<0.001. N=1 biological/differentiation replicate, n=3 technical replicates for all experiments, mean +/- standard error mean.

3.3.2 HTT Knockdown Perturbation on Barrier Function

Reduction of the disease-causing protein has been a primary strategy of therapeutic intervention for HD. I assessed how HTT reduction would affect blood-brain barrier paracellular function in HD iBMECs differentiated from HD109n1 iPSCs that underwent HTT knockdown (HTTKD). I first monitored knockdown by qPCR and showed ~60% knockdown of HTT in HD iBMECs that were cultured with and without puromycin in the differentiation medium (**Figure 2.3A**). I also assessed how HTT knockdown affected RNA expression of a tight junction protein *Claudin-5 (CLDN5)* by qPCR but did not see a significant effect (**Figure 2.3B**). Regardless of the lack of change in *CLDN5* expression, I still observed a slight, but significant rescue of paracellular permeability in HD109n1 HTT KD iBMECs (**Figure 2.3C**). The sustained knockdown of *HTT* was controlled by puromycin; however, puromycin was demonstrated to produce a significant decrease in cell survival of HD iBMECs (**Figure 1.3D** and Lim et al., 2017). For this reason, I assessed treatment of puromycin on paracellular function using TEER as a readout. Under these conditions, I did not see a significant effect of puromycin on *HTT* expression (**Figure 2.3A**), *CLDN5* expression (**Figure 2.3B**), or TEER measurements (**Figure 2.3C**) compared to HD109n1 HTT KD iBMECs not cultured with puromycin in the differentiation medium, therefore the puromycin was not contributing to the rescue of paracellular function or cell death. Together, this data demonstrated a significant effect of a reduction of *HTT* on improving paracellular function in HD iBMECs.

3.4 Discussion

This study confirmed that the dysfunctional phenotypes in HD iBMECs are modifiable. Here I tested WNT inhibition and *HTT* knockdown to evaluate whether they could rescue specific phenotypes. **In this study,** BBB function was not significantly affected following XAV939 treatment in HD iBMECs; however, there was a minor improvement in angiogenic migration and

minor exacerbation of paracellular barrier permeability. Conversely, HTT knockdown induced a significant increase in paracellular barrier function (as measured by TEER) in HD109n1 HTTKD iBMECs compared to control HD109n1 iBMECs. Since tight junctions play a key role in preventing BBB paracellular transport by restricting movement of substances between endothelial cells (Zhao et al., 2015), I hypothesized that an upregulation of these molecules would increase TEER values. However, decreasing *HTT*, which provided benefit to barrier function, and expression of a tight junction molecule (*CLDN5*) were not correlated upon HTT knockdown in HD iBMECs. Additional exploration into protein levels of CLDN5 or other tight junction-associated proteins would further inform potential mechanisms controlling the improved HD iBMEC barrier function.

Upon further investigation after completing my assessment of HTT knockdown in HD iBMECs, we noticed a contracted CAG repeat in the HD109n1 HTTKD iPSC line to approximately 73 CAG repeats and that the repeat in these lines was highly unstable. Therefore, a potential explanation for the improved barrier function in the HD109n1 HTTKD iBMECs may simply be due to the lower CAG repeat length. Therefore, the resulting comparison was of a contracted HD109n1 HTTKD line (73 CAG) to a parental HD109n1 line with ~126 CAG repeats. This means any improvement in barrier function may have been due to either HTT knockdown or to the shorter CAG repeat length present in the HD109n1 HTTKD line. It is not entirely clear if the contraction was sufficient for rescue as alleles of this size also cause severe barrier deficits. Nonetheless, if the contraction of CAG repeat length to 73 repeats is the reason for increased TEER measurements, it would validate the CAG repeat length-dependent change in TEER observed in **Figure 1.3C** and in Lim et al., 2017. Future studies can utilize new KD lines generated with matched CAG repeat lengths.

Another interesting finding from this study was the improvement of paracellular barrier function with dimethylsulfoxide (DMSO) treatment in iBMECs. DMSO is a polar, organic solvent with membrane-penetrating properties often used as a vehicle to solubilize compounds, like small-molecule inhibitors (e.g. XAV939), at high concentrations (Capriotti & Capriotti, 2012).

Interestingly, DMSO alone has been demonstrated to induce changes in gene expression, differentiation, and epigenetic changes even at low concentrations (Tunçer et al., 2018). This may explain the potential increase in TEER measurements following treatment with DMSO alone in control and HD iBMECs. Additional investigation into this phenotype is necessary.

My data validates the BBB deficits previously observed in HD iBMECs described in Chapter 1 of this thesis and in Lim et al., 2017. I also provided a proof-of-concept study for utilizing the Incucyte woundhealing angiogenic migration assay for future higher-throughput drug screening experimentation; however, further investigation is necessary to confirm the significance of these results and the effect of BBB integrity upon modulation of HTT or WNT signaling, as well as other perturbations. Together, these would provide additional mechanistic understanding of BBB breakdown observed in HD iBMECs and how to target this therapeutically.

3.5 Experimental Procedures

3.5.1 Pluripotent Stem Cell Culture and iBMEC Differentiation

Human iPSCs reprogrammed from control (CTR33n1) and HD (HD71n3 and HD109n1) patient fibroblasts as previously described (HD iPSC Consortium, 2013, 2017; Lim et al., 2017; Smith-Geater et al., 2020) were maintained between passages 17-35 on ESC-qualified matrigel (BD Biosciences) in stem cell culture medium mTeSR1 (Stem Cell Technologies). See **Table 3.1** for additional details on iPSC lines used. For iBMEC differentiation (Lippmann et al., 2012, 2014), cells were passaged onto matrigel in mTeSR1 medium for 2-3 days of expansion and then switched to unconditioned medium (UM) lacking bFGF for 6 days. Endothelial cell (EC) medium, consisting of human endothelial serum-free medium (hESFM; Life Technologies) supplemented with 20 ng/mL bFGF (R&D Systems), 1% platelet-poor plasma-derived bovine serum (Biomedical Technologies, Inc.), and 10 μM RA (Sigma-Aldrich), was then added for an additional two days. Cells were then dissociated with Versene (Life Technologies) and plated onto 6-well tissue culture polystyrene plates or 1.12 cm^2 transwell-clear permeable inserts (0.4 mm pore size) coated with a mixture of collagen IV (400 mg/mL; Sigma-Aldrich) and fibronectin (100 mg/mL; Sigma-Aldrich) in water. Culture plates and inserts were incubated with the coating for 4-24 hours at 37°C. Resultant, purified iPSC-derived iBMECs were then grown in EC medium for three days without RA. iBMECs were either untreated, treated with DMSO (vehicle), or 5-20 μM XAV939 (Sigma-Aldrich, X3004) 24 hours following subculture. For HTT knockdown experiments, iPSCs were maintained in 200-300 ng/mL puromycin (Invitrogen) and the same concentration was added to UM and EC medium unless otherwise noted.

3.5.2 Generation of HTT Knockdown Line

The HD109n1 HTT knockdown (HD109n1 HTTKD) iPSC line was generated by Dr. Lisa Salazar at University of California, Irvine. Guide RNAs (GAGCCACATTAACCGGCCCT and

GTCCCCTCCACCCCACAGTG) targeting the AAVS1 Safe Harbor locus were independently cloned into the pX334 Cas9 nickase expression vector from Feng Zhang (Addgene plasmid # 42333; Cong et al., 2013). *HTT*-targeting miRNA (mi2.1) was provided by Beverly Davidson (Harper et al., 2005) and cloned into the AAVS1 SA-2A-puro-pA donor vector (from Rudolf Jaenisch, Addgene plasmid # 22075; Hockemeyer et al., 2009). One million HD109n1 iPSCs were transfected with 1.25 µg of each CRISPR plasmid together with 2.50 µg of donor plasmid using Nucleofector Solution Kit 1 (Lonza) with program B-016. Puromycin was added to the cultures 2 days after transfection. Colonies derived from single cells were expanded for screening and a single clone was used for the studies described here. Correct targeting was determined by PCR amplification across the 5' junction as described by Mali et al., 2013 using a forward primer within the endogenous AAVS1 locus (CTGCCGTCTCTCTCCTGAGT) and reverse primer within the insert (GTGGGCTTGTACTCGGTCAT). Genomic integrity was confirmed by aCGH analysis (Cell Line Genetics) and pluripotency validated by immunofluorescence staining for established markers including OCT4, Nanog, TRA1-81, and SOX2.

3.5.3 RNA Transcript Analysis

Total RNA was extracted from cell lysates using a QIAshredder homogenization column (Qiagen) and RNeasy Mini Kit (Qiagen) according to the manufacturer's instructions. RNA was quantified using a NanoDrop ND-2000. Oligo(dT)-primed cDNA synthesis was performed on 1ug of total RNA using the SuperScript III First-Strand Synthesis System for RT-PCR (Life Technologies). qPCR was conducted using 1 µL of cDNA and a SYBR Green I Mastermix (Bio-Rad) in a 384-well format on a ViiA 7 real-time PCR system (Applied Biosystems 4309155). Primers for qPCR were designed by Origene and ordered through Eurofins MWG Operon:

Table 3.5.1. qPCR Primers for Assessing HTT Knockdown in iBMECs

Gene	Forward Sequence	Reverse Sequence
HTT	CTCTGGTGTCAGATACTGCTGC	CTCCTCTTCTCCAGACATCTGG
CLDN5	ATGTGGCAGGTGACCGCCTTC	CGAGTCGTACACTTTGCACTGC
RPLP0	TGGTCATCCAGCAGGTGTTCGA	ACAGACACTGGCAACATTGCGG

Relative expression was quantified between samples using the comparative cycle threshold (C_t) method. For each sample, HTT expression or CLDN5 expression was normalized to Ribosomal Protein, Large P0 (RPLP0) as the housekeeper gene, and expression in the knockdown line was further normalized to the parental HD109n1 line. Data was plotted as fold change with standard error mean plotted as error bars. N=1, n=3 technical replicates per reaction. Statistical analysis of differences in gene expression was performed using an unpaired, two-tailed t-test in GraphPad Prism 8.

3.5.4 Transendothelial Electrical Resistance (TEER)

TEER was measured using an EVOM^2 Epithelial Voltohmmeter with STX2 electrodes (World Precision Instruments) and approximately every 24 hours thereafter as necessary. Raw TEER values were adjusted by subtracting TEER measured across an empty transwell and multiplied by filter surface area to yield TEER ($\Omega x cm^2$) imparted by the iBMECs. Each filter was measured three times. TEER measurements were taken at room temperature (22-24°C) and analyzed in GraphPad Prism 8.

3.5.5 Woundhealing Angiogenesis Assay and Incucyte Imaging

iBMECs were subcultured onto 96-well plate pre-coated with a mixture of collagen IV (400 mg/mL; Sigma-Aldrich) and fibronectin (100 mg/mL; Sigma-Aldrich) in water. Culture plates were incubated with the coating for 4-24 hours at 37°C. 24 hours following subculture, Incucyte Scratch WoundMaker Tool (Sartorius) was used to generate wounds within wells. One 20X image per well

was taken by IncuCyte Live Cell Analysis System (Sartorius) every 2 hours in 37°C incubator. Incucyte Scratch WoundMaker Analysis S3 software was used to create mask settings that were applied to a batch of images for analysis of migration into wound area. Wells with inconsistent (too large or too small) wounds were eliminated from analysis; 1-5 replicate wells per condition were used for analysis and analyzed in GraphPad Prism 8.

3.6 References

Capriotti, K., & Capriotti, J. A. (2012). Dimethyl Sulfoxide History, Chemistry, and Clinical Utility in Dermatology. *J. Clin. Aesthet. Dermatol.*, *5*(9), 24–26.

Cong, L., Ran, F. A., Cox, D., Lin, S., Barretto, R., Habib, N., Hsu, P. D., Wu, X., Jiang, W., Marraffini, L. A., & Zhang, F. (2013). Multiplex genome engineering using CRISPR/Cas systems. *Science*, *339*(6121), 819–823. https://doi.org/10.1126/science.1231143

Drouin-Ouellet, J., Sawiak, S. J., Cisbani, G., Lagacé, M., Kuan, W.-L., Saint-Pierre, M., Dury, R. J., Alata, W., St-Amour, I., Mason, S. L., Calon, F., Lacroix, S., Gowland, P. a., Francis, S. T., Barker, R. a., & Cicchetti, F. (2015). Cerebrovascular and blood-brain barrier impairments in Huntington's disease: Potential implications for its pathophysiology. *Annals of Neurology*, 1–17. https://doi.org/10.1002/ana.24406

Harper, S. Q., Staber, P. D., He, X., Eliason, S. L., Martins, I. H., Mao, Q., Yang, L., Kotin, R. M., Paulson, H. L., & Davidson, B. L. (2005). RNA interference improves motor and neuropathological abnormalities in a Huntington's disease mouse model. *Proceedings of the National Academy of Sciences*, *102*(5820). https://doi.org/10.1073pnas.0501507102

HD iPSC Consortium. (2013). Induced Pluripotent Stem Cells from Patients with Huntington's Disease Show CAG Repeat Expansion Associated Phenotypes. *Cell Stem Cell*, *11*(2), 264–278. https://doi.org/10.1016/j.stem.2012.04.027.Induced

HD iPSC Consortium. (2017). Developmental alterations in Huntington's disease neural cells and pharmacological rescue in cells and mice. *Nature Neuroscience*, *20*(5), 648–660. https://doi.org/10.1038/nn.4532

Hockemeyer, D., Soldner, F., Beard, C., Gao, Q., Mitalipova, M., Dekelver, R. C., Katibah, G. E., Amora, R., Boydston, E. A., Zeitler, B., Meng, X., Miller, J. C., Zhang, L., Rebar, E. J., Gregory, P. D., Urnov, F. D., & Jaenisch, R. (2009). Efficient targeting of expressed and silent genes in human ESCs and iPSCs using zinc-finger nucleases. *Nature Biotechnology*, *27*(9), 851–857. https://doi.org/10.1038/nbt.1562

Hsiao, H. Y., Chen, Y. C., Huang, C. H., Chen, C. C., Hsu, Y. H., Chen, H. M., Chiu, F. L., Kuo, H. C., Chang, C., & Chern, Y. (2015). Aberrant astrocytes impair vascular reactivity in Huntington disease. *Annals of Neurology*, *78*(2), 178–192. https://doi.org/10.1002/ana.24428

Lim, R. G., Quan, C., Reyes-Ortiz, A. M., Lutz, S. E., Kedaigle, A. J., Gipson, T. A., Wu, J., Vatine, G. D., Stocksdale, J., Casale, M. S., Svendsen, C. N., Fraenkel, E., Housman, D. E., Agalliu, D., & Thompson, L. M. (2017). Huntington's Disease iPSC-Derived Brain Microvascular Endothelial Cells Reveal WNT-Mediated Angiogenic and Blood-Brain Barrier Deficits. *Cell Reports*, *19*(7), 1365–1377. https://doi.org/10.1016/j.celrep.2017.04.021

Lippmann, E. S., Al-ahmad, A., Azarin, S. M., Palecek, S. P., & Shusta, E. v. (2014). A retinoic acid-enhanced, multicellular human blood-brain barrier model derived from stem cell sources. *Scientific Reports*, *4*(4160), 1–10. https://doi.org/10.1038/srep04160

Lippmann, E. S., Azarin, S. M., Kay, J. E., Nessler, R. A., Wilson, H. K., Al-Ahmad, A., Palecek, S. P., & Shusta, E. v. (2012). Derivation of blood-brain barrier endothelial cells from human pluripotent stem cells. *Nature Biotechnology*, *30*(8), 783–791. https://doi.org/10.1038/nbt.2247

Mali, P., Yang, L., Esvelt, K. M., Aach, J., Guell, M., DiCarlo, J. E., Norville, J. E., & Church, G. M. (2013). RNA-guided human genome engineering via Cas9. *Science*, *339*(6121), 823–826. https://doi.org/10.1126/science.1232033

Mattis, V. B., Tom, C., Akimov, S., Saeedian, J., Østergaard, M. E., Southwell, A. L., Doty, C. N., Ornelas, L., Sahabian, A., Lenaeus, L., Mandefro, B., Sareen, D., Arjomand, J., Hayden, M. R., Ross, C. A., & Svendsen, C. N. (2015). HD iPSC-derived neural progenitors accumulate in culture and are susceptible to BDNF withdrawal due to glutamate toxicity. *Human Molecular Genetics*, *24*(11), 3257–3271. https://doi.org/10.1093/hmg/ddv080

Smith-Geater, C., Hernandez, S. J., Lim, R. G., Adam, M., Wu, J., Stocksdale, J. T., Wassie, B. T., Gold, M. P., Wang, K. Q., Miramontes, R., Kopan, L., Orellana, I., Joy, S., Kemp, P. J., Allen, N. D., Fraenkel, E., & Thompson, L. M. (2020). Aberrant Development Corrected in Adult-Onset Huntington's Disease iPSC-Derived Neuronal Cultures via WNT Signaling Modulation. *Stem Cell Reports*, *14*, 406–419. https://doi.org/10.1016/j.stemcr.2020.01.015

Tunçer, S., Gurbanov, R., Sheraj, I., Solel, E., Esenturk, O., & Banerjee, S. (2018). Low dose dimethyl sulfoxide driven gross molecular changes have the potential to interfere with various cellular processes. *Scientific Reports*, *8*(1). https://doi.org/10.1038/s41598-018-33234-z

Zhao, Z., Nelson, A. R., Betsholtz, C., & Zlokovic, B. v. (2015). Establishment and Dysfunction of the Blood-Brain Barrier. *Cell*, *163*(5), 1064–1078. https://doi.org/10.1016/j.cell.2015.10.067

CHAPTER III

Dysregulated synaptogenesis and actin transcriptional states in Huntington's disease iPSC-derived and mouse astrocytes

Andrea M. Reyes-Ortiz, Edsel M. Abud, Jie Wu, Nicolette R. Geller, Ricardo Miramontes, Keona Q. Wang, Corey Schulz, Alice Lau, Neethu Michael, Emily Miyoshi, Jack C. Reidling, Mathew Blurton-Jones, Vivek Swarup, Wayne W. Poon, Ryan G. Lim*, Leslie M. Thompson*

CHAPTER III

Dysregulated synaptogenesis and actin transcriptional states in Huntington's disease iPSC-derived and mouse astrocytes

4.1 Summary of Chapter 3

Huntington's disease (HD) is a devastating neurodegenerative disease caused by an expanded CAG repeat within the *Huntingtin* (*HTT*) gene with dysregulated cellular homeostasis in the central nervous system, particularly in the striatum and cortex. Astrocytes establish and maintain neuronal functions through the secretion of soluble factors and physical interactions with other neurovascular unit cell types. Under pathological conditions, astrocytes can become reactive, causing cell state transitions that affect brain function. To investigate transitions between cellular states in unaffected and HD astrocytes at high resolution, single-nuclei RNA-sequencing (snRNA-seq) was performed on human HD patient induced pluripotent stem cell (iPSC)-derived astrocytes and on striatal and cortical tissue from a rapidly progressing HD mouse model (R6/2). Clustering analysis of HD human and mouse astrocytes revealed a confirmation of glutamate signaling, as well as dysregulation of astrocyte identity, maturation, and actin-mediated signaling specific to human iPSC-derived astrocytes. Proteins representative of these pathways and states showed altered levels and included alterations in the actin cytoskeleton. HD transcriptional changes reveal potential astrocyte maturation deficits and suggest regulatory roles for astrogliogenesis transcription factors, including ATF3. These data further support the hypothesis that mutant HTT induces dysregulated astrocyte cell states that may induce dysfunctional astrocytic properties, contributing to HD pathogenesis. **This work is being submitted for publication to Cell Journals.**

4.2 Introduction

Huntington's disease (HD) is a devastating, autosomal-dominant neurodegenerative disease characterized by movement abnormalities, psychiatric disturbances, and cognitive impairment with no effective disease-modifying treatment (Ross & Tabrizi, 2011). The genetic cause of HD is a CAG repeat expansion in the first exon of the *huntingtin* (*HTT*) gene, which encodes an expansion of a polyglutamine (polyQ) repeat tract in the Huntingtin (HTT) protein (The Huntington's Disease Collaborative Research Group, 1993). When the *HTT* CAG repeat is expanded to 40 CAGs or above, HD is fully penetrant (Nance & Myers, 2001; Zuccato et al., 2010). HTT is ubiquitously expressed in all cell types in the body and a broad range of cellular processes, predominantly in the brain, are impacted by chronic mutant HTT (mHTT) expression (Bates et al., 2015; Ross & Tabrizi, 2011). The mutation alters HTT structure and function, causing loss of normal HTT functions and toxic gain of function (Bates et al., 2015). While the most overt HD neuropathology involves striatal neuronal loss and cortical atrophy, modeling of human induced pluripotent stem cells (iPSCs) has been leveraged to identify HD cell-autonomous defects in non-neuronal cell types, such as endothelial cells that comprise the blood-brain barrier (Lim et al., 2017), oligodendrocytes (Osipovitch et al., 2019), and astrocytes (Benraiss et al., 2021; Garcia et al., 2019; Juopperi et al., 2012; Osipovitch et al., 2019), indicating that chronic expression of mutant HTT may induce intrinsic deficits within each cell type.

Astrocytes are the major glial cell type in the CNS, playing a critical role in regulating brain homeostasis. Astrocytes provide neurotrophic support through glutamate uptake and recycling, and contribute to synaptogenesis, neuronal maturation, and neuronal maintenance. Inter-astrocytic communication of calcium signaling is a function of astrocytes thought to help control blood flow for coupling to neuronal energy demand (Khakh & Sofroniew, 2015; Zhao et al., 2015). In addition to regulating a microenvironment that facilitates neuronal signaling, astrocytes maintain direct interactions with the brain endothelium to establish and maintain BBB and neuronal functions through soluble and physical communications (Abbott et al., 2006).

There has been growing literature characterizing the development and regulation of unique cellular states defining functional states of astrocytes. Moreover, evidence suggest impairments in these astrocyte states generate toxic functions that may contribute to neurological disorders; however, the extent and mechanisms driving these impairments are limited for HD. HD astrocyte dysfunction appears to contribute to neuronal dyshomeostasis (Jiang et al., 2016; Khakh & Sofroniew, 2014; Tong et al., 2014), including impaired glutamate signaling and K+ buffering in astrocytes from HD mice (Lee et al., 2013; Milnerwood et al., 2010; Tong et al., 2014). While glutamate-related dysfunction in HD astrocytes has primarily been characterized in HD mouse models, this phenotype has recently been demonstrated in human patient iPSC-derived cells. HD iPSC-derived astrocytes carrying juvenile-onset range CAG repeat lengths (77 CAG and 109 CAG) provided less support for functional neuronal maturation and contributed to glutamate-induced toxicity in iPSC-derived striatal neurons (Garcia et al., 2019). Other HD iPSC-astrocyte based studies revealed an increased autophagic response (Juopperi et al., 2012) and increased evoked inflammatory responses (Hsiao et al., 2015). However, studies have yet to examine the molecular heterogeneity and define overlapping and distinct astrocyte states from HD mouse models and patient iPSCs as well as potential mechanisms controlling their dysregulation.

With the development of single-cell and single-nuclei RNA-sequencing (sc- or snRNA-seq), astrocyte cell state transitions can now be compared at high resolution across multiple species, brain regions and ages. A recent snRNA-seq study on HD astrocytes from post-mortem patient cortical tissue identified heterogeneous cell states in HD human astrocytes (Al-Dalahmah et al., 2020). Increased expression of metallothionein and heatshock genes and loss of astrocyte-specific gene expression was demonstrated. To further investigate HD human astrocyte cell states, human patient iPSC-derived astrocytes allow the ability to ascertain earlier events at the single-cell level that may lead to later changes in post-mortem human tissue.

The goals of the present study are to further molecularly characterize astrocyte cell states in unaffected and an HD context, and to compare these states across human iPSC and mouse model systems. We investigated which astrocyte states exist in HD and if their transcriptional signatures can help to predict altered astrocyte functions HD. We used unbiased snRNA-seq clustering followed by pathway enrichment and systematically compared signaling states between human and mouse astrocytes. Using this approach, we found altered astrocyte cell states relating to glutamate signaling common to both HD iPSC-derived astrocytes (iAstros) and striatal and cortical R6/2 astrocytes compared to unaffected control astrocytes. We also identified disease cell states that predict activated extracellular matrix (ECM) and dysregulated actin cytoskeletal dynamics to be unique to human HD astrocytes, informing cell-autonomous dysregulation related to endogenous CAG repeat expansion in astrocytes. These transcriptional signatures were then used to identify regulatory genes that may be driving these alterations and could represent therapeutic targets. Together, this data provides a resource of astrocyte cell states and transitions that will be useful for broadening understanding of the role of diverse astrocytes in the brain. We provide data for novel astrocyte signatures that exist in HD that could directly contribute to pathogenesis and may represent targets for therapeutic intervention in HD patients.

4.3 Results

4.3.1 Astrocyte Transcriptional States in Patient-Derived iAstros Reveals Immature Cell States Regulated by Aberrant Astrogenesis Transcription in HD

To begin to understand how CAG repeat expansion may influence astrocyte function in HD, we evaluated heterogenous astrocyte cell states through quantifiable gene expression analysis at the single-cell level. We first investigated whether altered cell state changes are reflected through cell-intrinsic mechanisms in astrocytes differentiated from human HD versus control iPSCs that express mutant *HTT* in an endogenous context. HD (46Q, 53Q) and control iPSCs (18Q and 33Q)

(HD iPSC Consortium, 2013, 2017; Lim et al., 2017; Smith-Geater et al., 2020) were differentiated into astrocytes (iAstros) that express mature astrocyte markers. iPSCs were subject to prolonged neural induction to generate gliogenic neural stem cells followed by exposure to astrogliogenic factors for 60 days to induce morphologically and functionally mature astrocytes (**Figure 4.1A** and **Supplemental Figure 4.1**). We observed a significant decrease in the percentage of HD iAstros that express GLAST, a glutamate transporter expressed by functionally mature human astrocytes compared to controls (**Figure 4.1C** and **4.1D**). HD iAstros had fewer astrocytic processes (**Figure 4.1E**) and had significantly larger cell volumes (**Supplemental Figure 4.1**), indicating a potential deficit in astrocyte maturation (Zhang et al., 2016). To directly compare a purer population of HD to control mature astrocytes, GLAST-positive iAstros were isolated by FACS sorting and used for all subsequent studies (**Figure 4.1B-D**). GLAST-sorted HD and control cells express canonical astrocyte markers, like GFAP, and exhibit a classical star-like morphology (**Figure 4.1F**).

Next, unaffected control and (Cronin et al., 2019) HD GLAST-positive iAstros underwent snRNA-seq (**Figure 4.1B**). Among the 36,128 nuclei sequenced, nine distinct cell clusters were identified across HD and control iAstros representing unique astrocyte cell states (**Figure 4.2A**). HD or control-enriched clusters were identified by the number of iAstros per genotype by cluster (**Figure 4.2B**). Control-enriched cluster 0 highly expressed mature astrocyte markers (**Figure 4.2C**). Clusters 4 and 6 were also control-enriched (>60%). HD-enriched clusters 1, 2, 3, 5, and 8 expressed low levels of mature astrocyte markers, with cluster 3 expressing high levels of immature human astrocyte markers (*MKI67 and TOP2A*), as transcriptionally defined from fetal human astrocytes (Zhang et al., 2016). In addition to expression of immature astrocyte markers, HD-enriched cluster 8 had high expression of astroglial progenitor markers, *PAX6* and *HES6*. Cluster 7 also highly expressed immature astrocyte markers but was not significantly enriched by genotype (~59% HD). Based on gene expression profiling of astrocyte developmental markers, control and HD iAstros reflect various developmental states and suggest altered maturation in HD

iAstros. While most cell states exist in both control and HD iAstros, there are clear shifts in composition and full depletion of one of the control states.

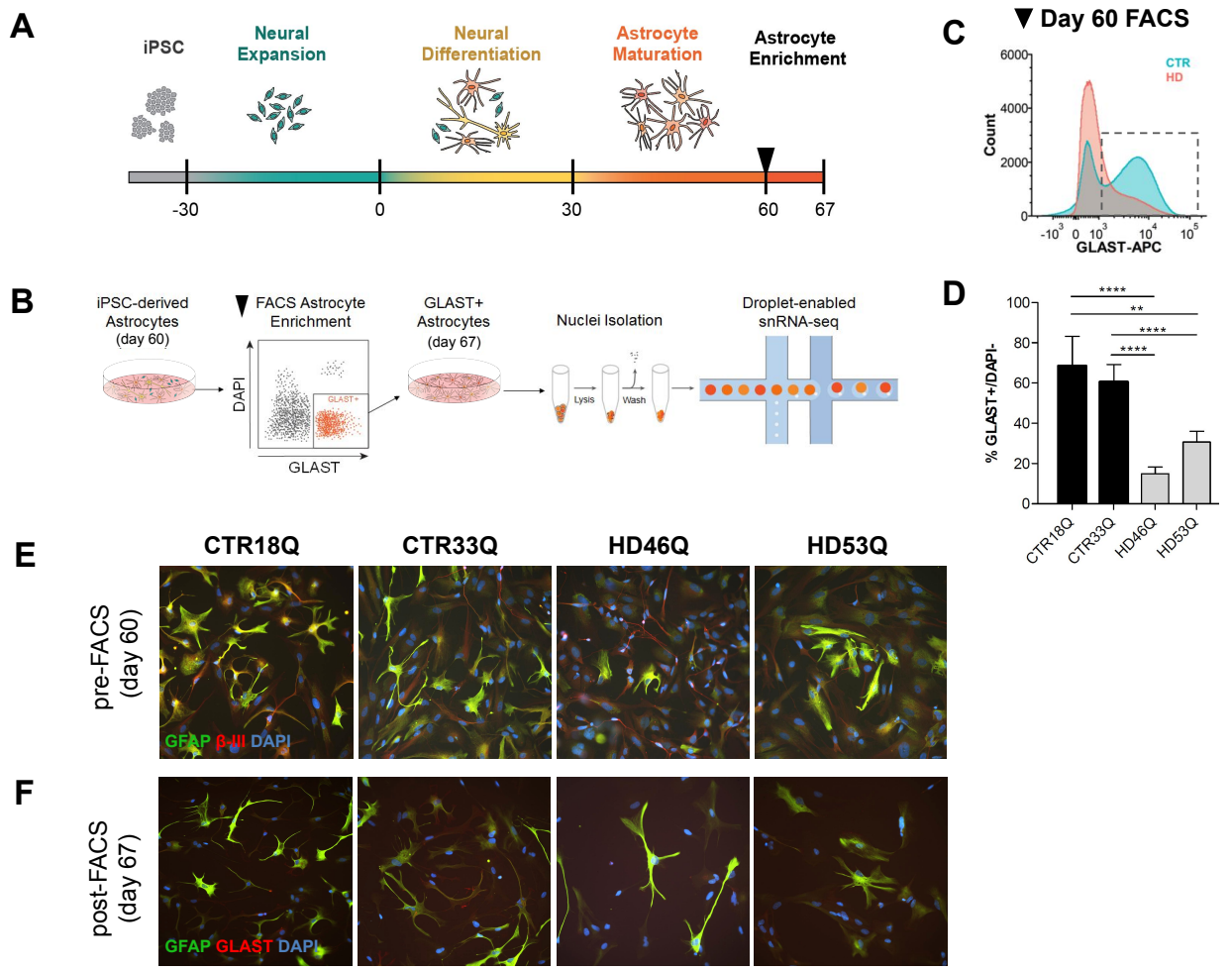

Figure 4.1. HD Induced Pluripotent Stem Cell-Derived Astrocyte Derivation. (**A**) Astrocyte Differentiation first begins with the differentiation of iPSCs into gliogenic neural stem cells (NSCs), followed by 30 days of neural differentiation and 30 days of astrocyte maturation. (**B**) At day 60, GLAST+/DAPI- FACS was performed for astrocyte-enrichment and astrocytes are subsequently matured for 7 days. At day 67, GLAST+ astrocytes underwent single-nuclei isolation prior to droplet-enabled single-nuclei RNA-sequencing (snRNA-seq). (**C**) Representative FACS histogram of HD and control iAstros GLAST expression level demonstrates HD astrocytes have decreased expression of GLAST at day 60. (**D**) FACS quantification of GLAST+/DAPI- populations in day 60 iPSC-derived astrocytes (18Qv46Q ****p<0.0001 [n=8,11], 33Qv46Q **p<0.0001 [n=8,11], 18Qv53Q **p=0.0035 [n=8,11], 33Qv53Q ****p<0.0001 [n=8,11]). (**E-F**) Immunocytochemistry for GFAP, β-III tubulin (β-III), and DAPI at day 60 prior to FACS. (E) Immunocytochemistry for GFAP, SLC1A3, and DAPI 7 days post-FACS astrocyte enrichment (F).

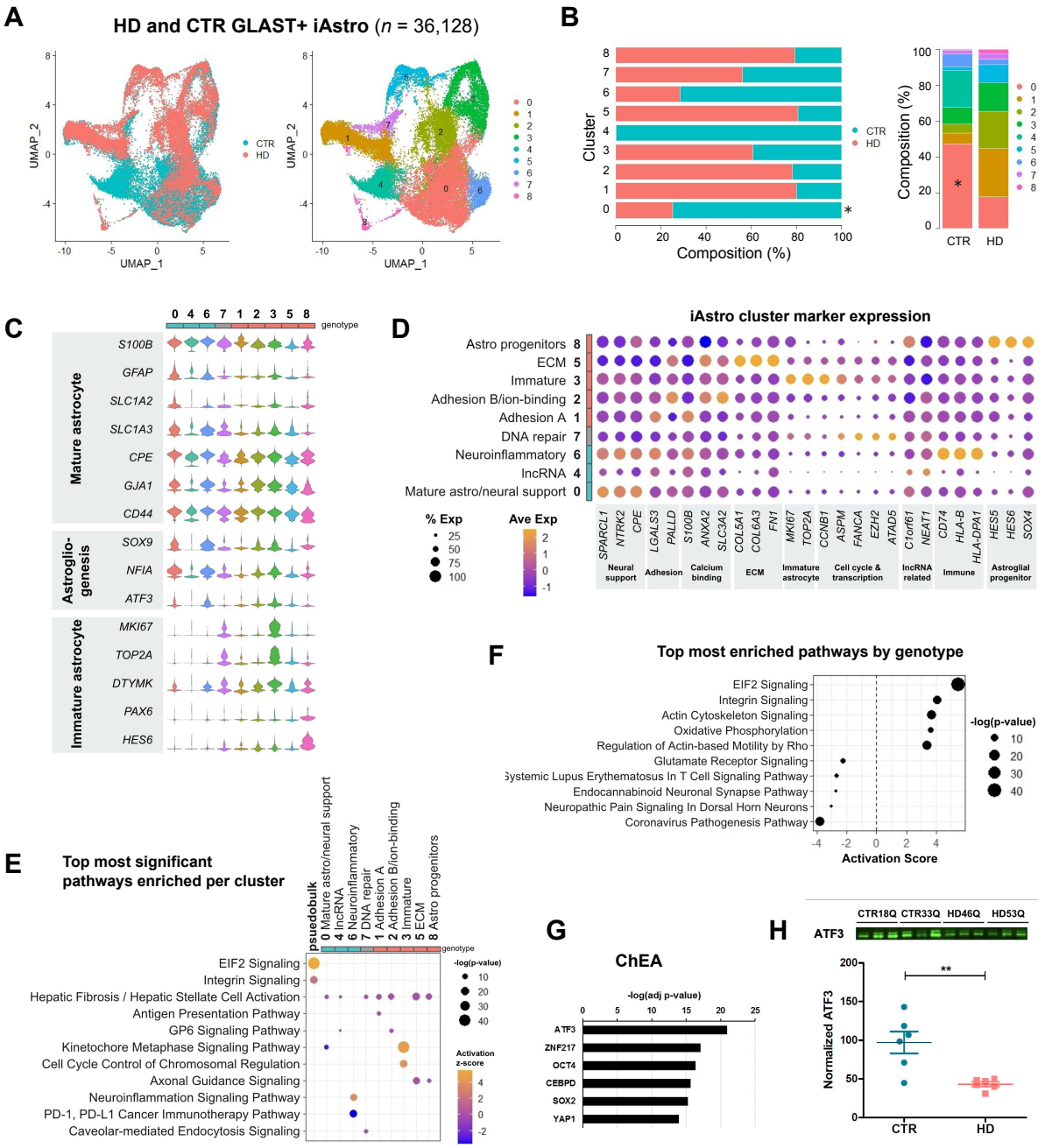

Figure 4.2. Dysregulated HD Patient-Derived Astrocytes Implicate Immature Cell States Regulated by Aberrant Astrogliogenesis Transcription. (**A**) GLAST+ iAstro snRNA-seq UMAP by genotype (CTR n=2, HD n=2) and by cluster. (**B**) Genotype composition of cells across astrocyte subclusters and by genotype (CTR n=2, HD n=2). (**C**) Astrocyte marker genes across each iAstro cluster shows a decrease in maturation gene expression in several HD-enriched subclusters. Genotype enrichment was defined by >60% of cluster, gray genotype represents 40-60%. (**D**) Top cluster markers for each cluster for cell state classification. (**E**) Top 5 most significantly activated and inhibited pathways in HD iAstros. (**F**) Top significant pathways across all iAstro clusters used to classify cell state signatures. Psuedobulk genotype pathway enrichment using DEGs from all HD iAstros compared to control iAstros is included for comparison. (**G**) Predicted transcription factor regulation in HD iAstros. (**H**) ATF3 western blot and quantification shows significant decreased ATF3 in HD iAstros (two-tailed t-test, **p=0.004, n=3 per cell line, 2 lines per genotype).

To molecularly assess the unique transcriptional signatures across iAstro clusters, the top markers per cluster were plotted and classified into gene categories (**Figure 4.2D**). Control-enriched iAstro cluster 0 and 6 had the highest expression of neural support-related markers, like astrocyte-secreted synaptogenesis regulator *SPARCL1* and brain-derived neurotrophic factor (BDNF) receptor *NTRK2*. Interestingly, immune-related genes, including *CD74* and many HLAs, were also highly expressed in control-enriched iAstro cluster 6. Control-enriched cluster 4 represents a unique cell state with the most highly expressed genes related to long non-coding RNAs like *NEAT1,* and reduced expression of ECM and progenitor markers. HD-enriched clusters 1 and 2 had high expression of adhesion-related molecules, *LGALS3* and *PALLD*, with cluster 2 also highly expressing calcium-binding molecules, *ANXA2* and *SLC3A1*. Immature astrocyte markers and cell cycle-related genes were highly expressed among HD-enriched cluster 3. Several ECM-related genes, including collagens and fibronectin, showed increased expression in HD-enriched cluster 5 along with calcium-binding and adhesion-related genes, which were also enriched in HD-enriched clusters 1 and 2. HD-enriched cluster 8 was the smallest cluster (493 nuclei; 1.4% of total nuclei sequenced) and had gene expression profile consistent with astroglial progenitors. Non-genotype enriched cluster 7 had a relatively high expression of DNA repair and transcription-related genes, like *FANCA* and *EZH2*. Overall, control states were enriched for astrocyte functions involved in neural support and neuroinflammation, while HD states were enriched for adhesion, ECM, and immature markers. These data highlight both a loss of normal astrocyte functional support, potential developmental impairments, and novel ECM and adhesion-related alterations. Furthermore, there is complete loss of a control state that shows high expression of *NEAT1* a lncRNA regulator of transcription.

To further explore the functional relevance of the iAstro clusters to biological pathways, IPA pathway enrichment was performed on the genes differentially expressed between clusters. The top 2 most significant pathways per cluster were compared to assess the transcriptional signatures unique to each iAstro cluster (**Figure 4.2E**). Hepatic Fibrosis/Hepatic Stellate Cell

Activation was a pathway among the top two significantly enriched pathways in all iAstro clusters except 3 and 6. Control-enriched cluster 0 had significant inhibition of Kinetochore Metaphase Signaling (z=-3.16, p<3e-9), composed of cyclin, centromere, and histone-related molecules (*CCNB1, CDK1, CENPE, CENPK, H2AX, H2AZ1),* which was activated in the immature HD-enriched cluster 3 (z=4.64, p<2e-43). Control-enriched cluster 4 was most significantly enriched in Hepatic Fibrosis/Hepatic Stellate Cell Activation (z=0, p<1e-5) largely due to the downregulation of several collagens (*COL1A1, COL4A1, COL4A2)*. Control-enriched cluster 6 had a significant activation of Neuroinflammatory Signaling molecules (z=3.74, p<6e-14), like HLA transcripts and *SLC1A2*. HD-enriched iAstro cluster 1 had significant enrichment of Antigen Presentation Pathway (z=0, p<3e-7) due to the expression of RNA transcripts that encode various HLA proteins (*HLA-A, HLA-C, HLA-DPA1, HLA-DRB5, HLA-E*). The significant upregulation of several collagen transcripts (*COL11A1, COL18A1, COL1A2, COL27A1, COL3A1, COL4A1, COL4A2, COL6A2*) caused HD-enriched cluster 2 to be significantly enriched in GP6 Signaling molecules (z=0, p<7e-8). HD-enriched iAstro cluster 3 had a significant activation of mitosis-related pathways, like Kinetochore Metaphase Signaling Pathway (z=4.65, p<2e-43) and Cell Cycle Control of Chromosomal Regulation (z=4, p<4e-19) with the upregulation of cyclin-related genes, like *CDK1*, that suggests a mitotic activation of HD iAstros. The dysregulation of integrins (*ITGA11, ITGA6, ITGB1, ITGB4, ITGB8*) and tubulins (*TUBA1A, TUBA1C, TUBB2A, TUBB2B, TUBB6*) induced enrichment of Axonal Guidance Signaling in cluster 5 (z=0, p<3e-16) and 8 (z=0, p<1e-6), which was comprised of 81% HD iAstros. Caveolar-mediated Endocytosis Signaling was significantly enriched (z=0, p<4e7) in cluster 7, which highly expressed integrin beta subunits. These nine iAstro clusters comprise unique transcriptional human astrocytic signatures that provide a glimpse into functionally relevant states of homeostatic and HD astrocytes.

To directly investigate genotype differences between HD and control iAstros, the top 5 significantly activated and top 5 significantly inhibited pathways by genotype were plotted by activation score (**Figure 4.2F**). Eukaryotic Initiation Factor 2 (EIF2) signaling (z=5.47, p<6e-41)

and Actin Signaling Pathways (z=3.68, p<6e-14) were the most significantly activated pathways in HD iAstros, which contained overlapping actin-related genes (*ACTA2, ACTB, ACTC1, ACTG2*). Glutamate Receptor (z=-2.24, p<0.001), Endocannabinoid Neuronal Synapse (z=-2.71, p<0.04), and Neuropathic Pain Signaling (z=-3, p<0.05) Pathways were among the inhibited pathways in HD iAstros and contained genes encoding multiple glutamate receptors, *GRIA1-2* and *GRIN2A-B*. Additional inflammatory-related signaling pathways were among the most significantly inhibited, including Systemic Lupus Erythematosus in T Cell Signaling (z=-2.65, p<0.002) and Coronavirus Pathogenesis Pathways (z=-3.78, p<1e-15) with dysregulation of transcripts in common encoding HLA proteins and ribosome subunits. Together, HD iAstro gene expression changes by cluster and by genotype highlight an inhibited glutamate receptor signaling state and unique astrocyte cell states, such as actin cytoskeletal signaling activation that may contribute to loss of neural support and altered morphology or motility.

To investigate the potential regulatory mechanisms controlling human HD astrocyte dysregulation, we used genotype DEGs in HD iAstros to predict transcription factor regulation enrichment analysis by Chromatin immunoprecipitation-X Enrichment Analysis (ChEA) (Kuleshov et al., 2016) (**Figure 4.2G**). The top predicted transcriptional regulator was an important regulator of astrogliogenesis, ATF3, followed by transcriptional repressor ZNF217 (**Figure 4.2G**). Upon further investigation, ATF3 protein levels were significantly decreased in HD compared to control iAstros, suggesting aberrant HD astrogliogenesis (**Figure 4.2H**). Other enriched transcriptional regulators included neural stem cell factor SOX2, further supporting a developmental deficit in HD iAstros. YAP1 of the HIPPO signaling pathway that has an essential role in regeneration and self-renewal, was another significantly enriched factor in HD iAstros that has previously been implicated in HD and shown to interact with Htt (Mueller et al., 2018). Overall, HD astrocyte transcriptionally dysregulated cell states may implicate an astrogliogenesis deficit that induces astrocyte dysfunctions in glutamate signaling and activation of ECM and actin cytoskeletal

signaling to potentially contribute to HD pathogenesis via altered glutamate uptake and cellular motility, respectively.

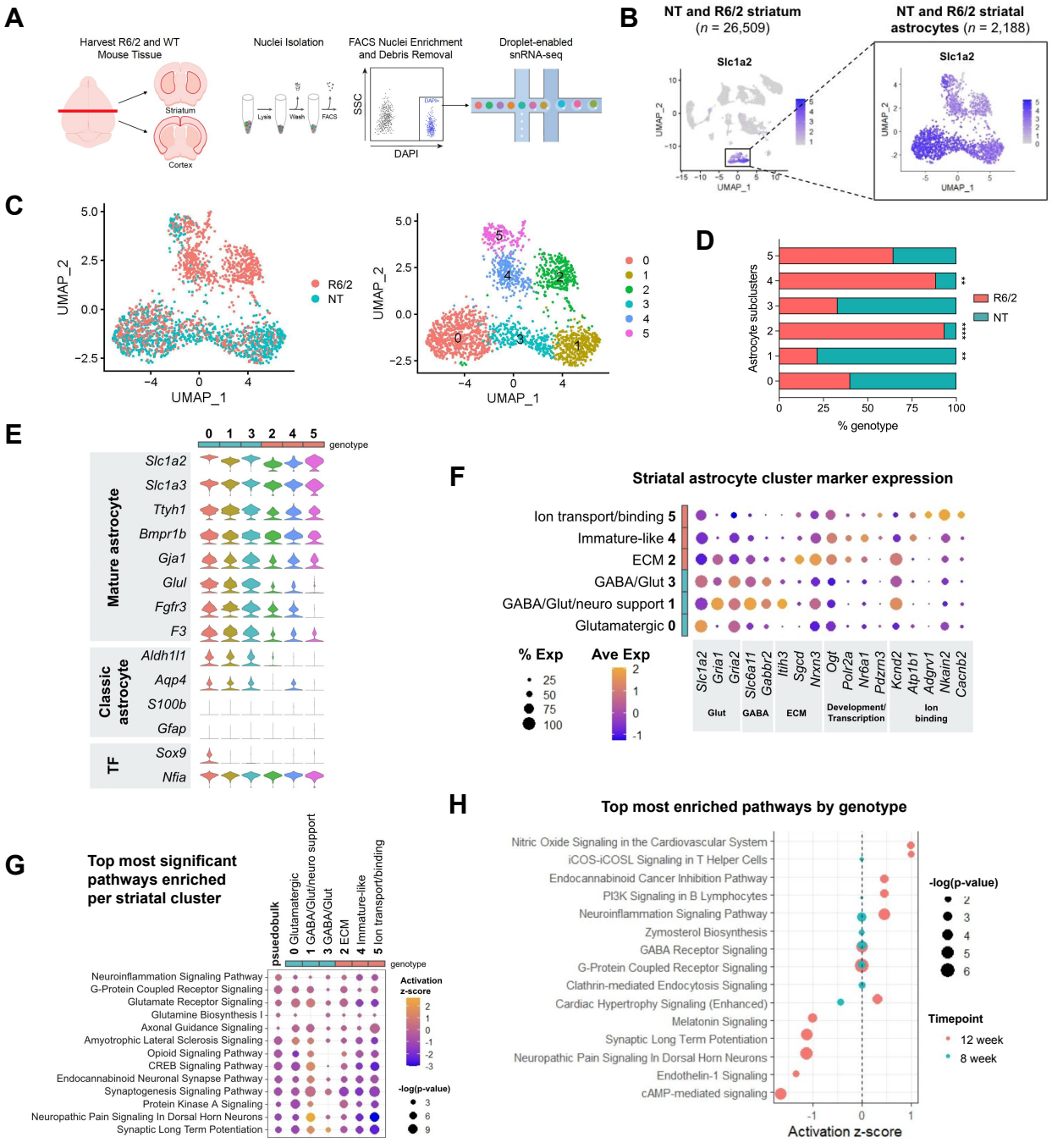

Figure 4.3. Striatal R6/2 Astrocytes Exhibit Immature and Decreased Synaptogenesis Cell States. (**A**) Experimental workflow for snRNA-seq analysis where striatal and cortical tissue was harvested from NT and R6/2 mice, dissociated, then underwent single-nuclei isolation and FACS separation prior to droplet-enabled snRNA-seq. (**B**) UMAP of all 12-week striatal snRNA-seq libraries performed on aggregated peak matrix. The astrocyte cluster was identified by expression of *Slc1a2*. (**C**) UMAP subset analysis of astrocyte

continued from previous page; cluster identified several astrocyte subclusters across R6/2 and NT. (**D**) Genotype composition of cells across astrocyte subclusters (two-way ANOVA, Bonferroni multiple comparisons test performed on number of nuclei per mouse within each subcluster adjusted p-values: cluster 0 p=0.0809, cluster 1 **p=0.0012, cluster 2 ****p<0.0001, cluster 3 p=0.5160, cluster 4 **p=0.0057, cluster 5 ns; n=3 mice/genotype). (**E**) Astrocyte marker genes across each subcluster shows a decrease in maturation gene expression in several striatal R6/2-enriched subclusters. Genotype enrichment was defined by >60% of cluster, gray genotype represents 40-60%. (**F**) Top cluster markers for each cluster for cell state classification. (**G**) Top significant pathways across all striatal astrocyte clusters used to classify cell state signatures. Psuedobulk genotype pathway enrichment using DEGs from all 12-week R6/2 striatal astrocytes compared to all 12-week NT striatal astrocytes is included for comparison. (**H**) Top most significantly enriched pathways by age for 8- and 12-week striatal R6/2 astrocytes.

4.3.2 Defining HD Striatal and Cortical Mouse Astrocyte Cell States

Human HD iAstros show shifts in cell state compositions and complete loss of a state seen in control iAstros, that may be driven by deficits in astrogliogenesis. We next compared if state changes occur in an *in vivo* animal model of HD, and whether species-specific states exist. To assess the transcriptional cell states of striatal and cortical mouse astrocytes within a well-established system that recapitulates transcriptome changes in human HD tissue (Hodges et al., 2006), we carried out snRNA-seq on striatal and cortical brain regions from the rapidly progressing R6/2 and non-transgenic (NT) mice at 8-week-old symptomatic and 12-week-old highly symptomatic time points (Mangiarini et al., 1996) (**Figure 4.3A** and **4.4A**). At the 12-week time point, we identified 13 and 16 distinct clusters from 26,509 striatal and 25,237 cortical nuclei sequenced, respectively. The *Slc1a2* astrocyte marker gene that encodes GLAST, a glutamate transporter that clears the excitatory neurotransmitter from the extracellular space at synapses, was used as an astrocyte marker and expression was plotted across all cells to identify the astrocyte cluster for each dataset (**Figure 4.3B** and **4.4B**). The cluster with the highest *Slc1a2* expression was subset to investigate R6/2 astrocyte-specific dysregulation via sub-clustering and further transcriptomic analyses. Due to a small population of cells with relatively low levels of astrocyte markers and high expression of vascular markers *Pdgfrb* and *Flt1* (Zhang et al., 2014), additional sub-setting was necessary before sub-clustering the cortical astrocyte cluster (**Supplemental Figure 4.4**). Upon sub-clustering all 12-week R6/2 astrocyte clusters, we

identified six striatal astrocyte clusters and five cortical astrocyte clusters visualized using Uniform Manifold Approximation and Projection (UMAP) plot (**Figures 4.3C** and **4.4B**). Diverse cellular states were represented across each dataset and to identify genotype composition by cluster, the total number of cells per genotype were quantified by cluster. Striatal clusters 2 and 4 were significantly enriched in R6/2 compared to NT, while cortical cluster 0 was significantly enriched in R6/2, indicating these clusters are relatively novel to the R6/2 condition (**Figures 4.3D** and **4.4C**). R6/2 striatal astrocytes had a larger number of differentially expressed genes by genotype compared to cortical astrocytes (**Supplemental Figures 4.5** and **4.6**).

Expression of mature astrocyte marker genes and transcription factors regulating astrogliogenesis were visualized across astrocyte clusters (**Figure 4.3E** and **4.4D**). R6/2-enriched striatal astrocyte clusters 2 and 4 as well as R6/2-enriched cortical cluster 0 had a lower expression of several classic astrocyte identity genes, such as *Slc1a2* and Glutamate-Ammonia Ligase (*Glul*), compared to NT-enriched clusters. Similarly, cortical astrocyte clusters 1 and 3 had a lower expression of these astrocyte identity genes compared to cluster 0. Decreased expression of astrocyte markers in R6/2-enriched clusters indicates that dysregulated cell states exist in R6/2 astrocytes that may reflect differences in astrocyte development.

4.3.3 Inhibited Synaptogenesis-Related Signaling States in R6/2 Striatal Astrocytes

We next molecularly assessed the cell states identified in striatal R6/2 and NT mouse astrocytes. First, the top most highly expressed gene markers per cluster were used to classify clusters into functionally relevant categories (**Figure 4.3F**). Several of the highest expressing genes in NT-enriched striatal clusters 0, 1, and 3 included astrocyte-enriched glutamate receptor, *Slc1a2,* and glutamate transporters, *Gria1* and *Gria2,* similar to control-enriched iAstro clusters 0 and 6. NT-enriched striatal clusters 1 and 3 also had high expression of GABA transporter *Slc6a11* and GABA receptor *Gabbr2.* Among the striatal clusters with significantly more R6/2 cells compared

to NT, striatal clusters 2 and 4 had the highest expression of developmental-related genes, RNA polymerase (*Polr2a*) and a nuclear receptor involved in neurogenesis (*Nr6a1*). R6/2-enriched striatal cluster 2 also had the highest expression of two ECM-related genes, glycoprotein-related *Sgcd* and cell adhesion molecule *Nrxn3*. Like HD-enriched iAstro clusters 1 and 2, R6/2-enriched striatal cluster 5 had the highest expression of sodium, potassium, or calcium ion binding genes, like *Adgrv1, Nkain2,* and *Cacnb2*, except for the potassium channel, *Kcnd2*, which was most highly expressed in striatal clusters 1 and 2.

To further explore the potential functional relevance of these striatal astrocyte clusters, we ran pathway enrichment analysis (IPA) on the DEGs for each cluster compared to all other striatal astrocytes (**Figure 4.3G**). The NT-enriched striatal cluster 0 had the highest activation of an Amyotrophic Lateral Sclerosis (ALS) Signaling pathway (z=1, p<4e-6) and Glutamate Receptor Signaling (z=0.38, p<1e-8) due to the high expression of overlapping genes that encode proteins responsible for glutamate-glutamine cycling in astrocytes (*Slc1a2, Glul, Gria1, Grid1,* and *Grin2c)*. Also significantly enriched in NT astrocytes, striatal cluster 1 had the highest activation in Neuropathic Pain Signaling (z=2.67, p<3e-8) and Synaptic Long Term Potentiation (z=1.6, p<7e-7), due to the overlap in upregulated genes *Gria1, Gria2,* and *Grin2c*. NT-enriched striatal cluster 3 exhibited significant activation of Synaptic Long Term Potentiation (z=2, p<0.001) and Synaptogenesis Signaling (z=-1.35, p<9e-10), with upregulation of *Gria2* in both pathways. Among the striatal astrocyte clusters significantly enriched with R6/2 cells, the most significant pathways across striatal clusters 2 and 4 were Synaptogenesis Signaling (cluster 2: z=-1.35, p<9e-10; cluster 4: z=-1.81, p<2e-7) and Glutamate Receptor Signaling (cluster 2: z=0, p<3e-7; cluster 4: z=-1.34, p<9e-7) specifically due to the downregulation of genes associated with glutamate receptors, like *Gria1* and *Gria2.* Neuropathic pain (z=-3, p<1e-9) was among the most inhibited pathways for striatal R6/2-enriched cluster 5, as well as Synaptic Long Term Potentiation (z=-2.36, p<8e-10) and cAMP response element-binding protein (CREB) Signaling (z=-2.36, p<1e-8). Overall, the data suggest a loss of glutamate signaling and synaptogenesis-related

pathways across R6/2 striatal astrocytes, and activation of ECM and immature-like astrocyte states, similar to the HD patient iAstros. These data highlight similarities with the human HD iAstros that suggest maturation impairments, with a particular focus on glutamate receptor and synaptogenesis-related dysregulation.

4.3.4 Inhibited Synaptogenesis-Related Signaling in R6/2 Cortical Astrocytes

To molecularly assess R6/2 cortical astrocytes, highly expressed genes per cluster were used to classify clusters into functionally relevant categories (**Figure 4.4E**), similar to the striatal clustering classification. NT-enriched cortical cluster 4 had a high expression of neural regulatory genes (*Anks1b and Nrg3*), axonal/synaptic related genes (*Robo2, Dlg2, and Lrtm4*), and *Kcnip4*, which encodes for a potassium channel interacting protein. Cortical clusters 1 and 2 had the highest expression of glutamate-related genes, *Slc1a2, Grin2c,* and *Glul*, and had no significant genotype enrichment (43% R6/2) or were significantly enriched in NT astrocytes, respectively. Cortical clusters 1 and 2 also had a high expression of an actin-binding gene *Clmn* and a phagocytic receptor *Mertk*. Cortical cluster 3 exhibited high expression of calcium-binding genes, *Adgrv1* and *Cacnb2*, and was not enriched by genotype, while R6/2-enriched cortical cluster 0 highly expressed *Ogt*, a glycosyltransferase regulator.

To further explore the potential functional relevance of the cortical clusters to astrocyte biology, IPA pathway enrichment was performed on the genes differentially expressed between clusters (**Figure 4.4F**). Cortical cluster 4 was largely composed of NT astrocytes and had significant activation of Synaptogenesis Signaling (z=6.97, p<7e-29) and Calcium Signaling (z=6.08, p<3e-13) through upregulation of genes that encode calcium/calmodulin-dependent protein kinases (*Camk2a, Camk3b, Camk4*) and calcium voltage-gated channel subunits (*Cacna1b, Cacna2d1, Cacnb4*). Cortical clusters 1 and 2 were significantly enriched in Glutamate Receptor Signaling due to expression of *Grin2c* and *Slc1a2*, with predicted activation in cluster 1

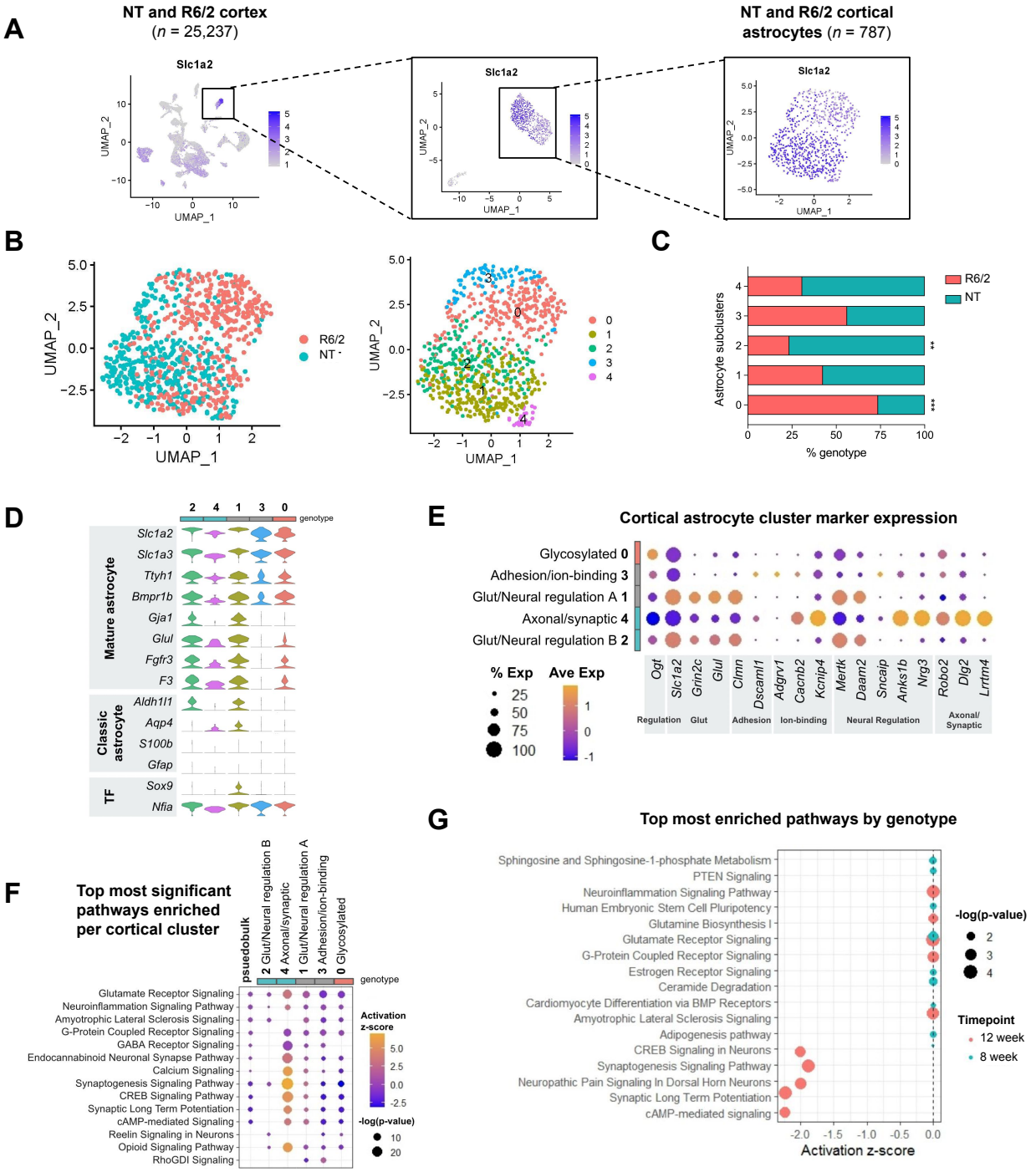

Figure 4.4. Cortical R6/2 Astrocytes Exhibit Inhibited Neuronal Homeostatic Signaling and Decreased Astrocyte Marker Expression. (**A**) UMAP of all 12-week cortical snRNA-seq libraries performed on aggregated peak matrix. The astrocyte cluster was identified by expression of astrocyte marker gene, *Slc1a2*. Additional subclustering was necessary to subset out cortical vascular cells from astrocytes. (**B**) UMAP subset analysis of astrocyte cluster identified several astrocyte subclusters across R6/2 and NT. (**C**) Genotype composition of cells across astrocyte subclusters (two-way ANOVA, Bonferroni multiple comparisons test performed on number of nuclei per mouse within each subcluster adjusted p-values: cluster 0 ***p=0.0004, cluster 1 p=0.8024, cluster 2 **p=0.0064, cluster 3 ns, cluster 4 ns; n=3 mice/genotype). (**D**) Astrocyte marker genes across each subcluster. Genotype enrichment was defined by

continued from previous page; >60% of cluster, gray genotype represents 40-60%. (**E**) Top cluster markers for each cluster for cell state classification. (**F**) Top significant pathways across all cortical astrocyte clusters used to classify cell state signatures. Psuedobulk genotype pathway enrichment using DEGs from all 12-week R6/2 cortical astrocytes compared to all 12-week NT cortical astrocytes is included for comparison (**G**) Top most significantly enriched pathways by age for 8- and 12-week cortical R6/2 astrocytes.

(z=1, p<5e-8) but no predicted activation for cluster 2 (z=0, p<0.002). Cortical cluster 1 also exhibited a predicted activation of Synaptogenesis Signaling (z=2.83, p<0.0006). Glutamate Receptor Signaling was the most significantly enriched pathway for cortical cluster 3, with a predicted inhibition (z=1.34, p<4e-11), like HD iAstros. Additionally, Rho GDP-dissociation inhibitor (RhoGDI) Signaling was predicted to be most activated and Synaptogenesis Signaling was the most inhibited predicted pathway for non-genotype-enriched cortical cluster 3. R6/2-enriched cortical cluster 0 was most significantly enriched in Glutamate Receptor Signaling (z=-1, p<7e-9), and Synaptogenesis signaling pathway was predicted to be the most inhibited pathway (z=-3.16, p<2e-6).

4.3.5 HD Mouse Astrocyte Temporal and Brain Region Comparisons

We next examined transcriptional changes that occur in R6/2 astrocytes with progressive disease. We assessed the activation scores of the top ten most significant pathways enriched in 8-week mouse astrocyte signaling states and 12-week mouse astrocyte signaling states compared to age-matched NT mouse striatal astrocytes (**Figure 4.3H**). (Luthi-Carter et al., 2002). As expected, there was overlap of many relevant pathways between the 8- and 12-week striatal R6/2 astrocytes, with the 12-week astrocytes exhibiting increased predicted activation of iCOS-iCOSL Signaling in T Helper Cells (12-week: z=1, p<0.008; 8-week: z=0, p<0.032), PI3K Signaling in B Lymphocytes (12-week: z=0.447, p<0.003; 8-week: z=0, p<0.048), and Neuroinflammation Signaling (12-week: z=0.447, p<5e-5; 8-week: z=0, p<0.001). *Chuk*, which encodes an inhibitor of the transcription factor NFκB complex, was an overlapping upregulated gene across the three

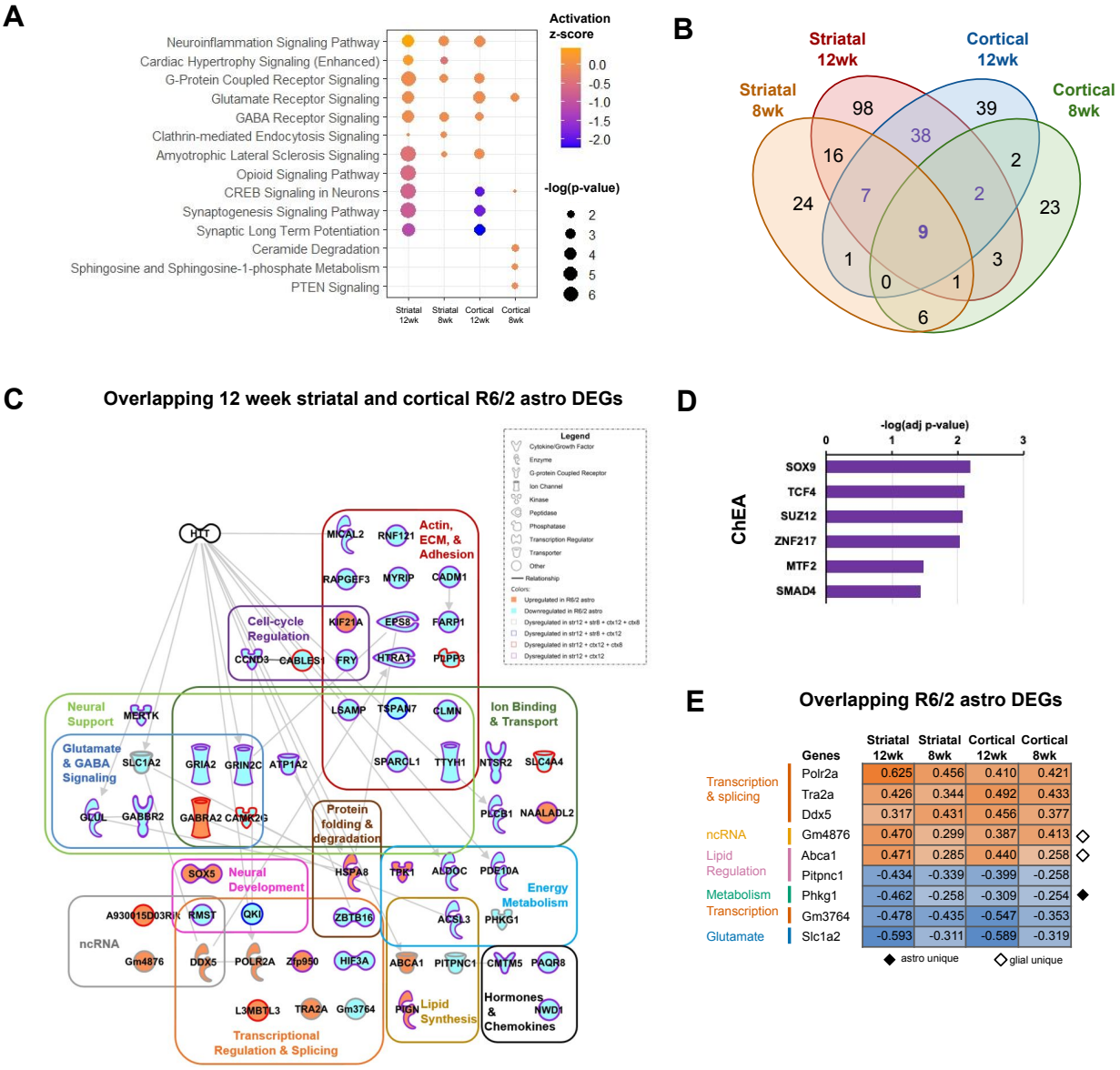

Figure 4.5. Shared R6/2 Astrocyte Dysregulation Across Brain Regions and Ages Highlights Neuronal Homeostasis Dysregulation. (**A**) Top pathways dysregulated across all four R/2 datasets (**B**) Venn diagrams of significant differentially expressed genes (DEGs) in R6/2 mouse astrocytes across time points and brain region (Exact hypergeometric probability calculated using 56 DEG overlap for 12-week striatum [174] vs 12-week cortex [98] ****p<8e-113, 33 DEG overlap for 12-week striatum [174] vs 8-week striatum [64] ***p<7e-64, 13 DEG overlap for 12-week cortex [98] vs 8-week cortex [46] *p<8e-25, 16 DEG overlap for 8-week striatum [64] vs 8-week cortex [46] **p<3e-35 using 46,206 as the number of genes with nucleotide sequence data in the mouse genome database). (**C**) Top most significant canonical pathways across brain regions and ages. (**C-D**) Overlap of 12-week striatal and cortical astrocyte DEGs highlight pathway dysregulation (C), predicted transcription factor regulation (D) in R6/2 astrocytes across both brain regions in symptomatic mice. (**E**) The nine overlapping DEGs across all datasets. Orange represents upregulated DEG and blue represents downregulated DEG. Solid black diamond denotes a DEG unique to only astrocytes, while a white diamond denotes a DEG unique to astrocytes, oligodendrocytes, and OPCs.

inflammatory pathways. The most significantly inhibited pathway in 12-week striatal astrocytes was cAMP-mediated Signaling (z=-1.67, p<3e-5). Interestingly, Cardiac Hypertrophy Signaling was the most significantly inhibited pathway predicted in the 8-week striatal R6/2 astrocytes (z=-0.447, p<0.008) but was predicted to be activated in 12-week striatal R6/2 astrocytes (z=0.302, p<6e-4). A majority of the most significantly enriched pathways in 8-week striatal astrocytes had no predicted activation or inhibition. By 12 weeks, R6/2 astrocytes had more severe predicted activation or inhibition of these overlapping pathways that correlates with increased severity in motor phenotypes (Luthi-Carter et al., 2002), suggesting increased astrocyte dysfunction with disease progression. The overlap in top pathways between 8- and 12-week with progressive dysregulation of similar genes between 8 and 12 weeks indicates that at these two timepoints, R6/2 astrocytes are similarly dysregulated in symptomatic animals. Taken together, R6/2 astrocytes exhibited inhibition of neuronal homeostatic signaling pathways, suggesting how mutant HTT expressing striatal astrocytes could contribute to neuronal dysregulation in R6/2 mice.

Temporal changes occurring in R6/2 cortical astrocytes were also compared for cortical astrocytes (**Figure 4.4G**). The most significantly enriched pathways in 12-week cortical astrocytes were predicted to be inhibited or had no activation scores. Among those were Glutamate Receptor Signaling (z=0, p<8e-5), Synaptic Long Term Potentiation (z=-2.236, p<2e-4), and Neuroinflammation Signaling Pathway (z=0, p<2e-4), with glutamate receptor *Grin2c* being a common downregulated gene across the three pathways. The most significantly enriched pathway in 8-week cortical astrocytes was Glutamate Receptor Signaling (z=0, p<0.004), which was also significantly enriched in 12-week cortical astrocytes due to downregulation of related genes (*Glul, Gria2, Grin2c,* and *Slc1a2*). The 8-week cortical astrocyte pathways had no predicted activation or inhibition (z=0), like 8-week striatal astrocytes. These findings further demonstrate dysregulated signaling in R6/2 astrocytes related to neuronal homeostasis, particularly Glutamate Receptor Signaling that overlap with HD iAstros and increase in severity with disease progression,

although diversity in cell states was less severe in R6/2 cortical astrocytes compared to R6/2 striatal astrocytes.

To determine the impact of mutant HTT on R6/2 astrocyte cell states by brain region, we directly compared striatal and cortical astrocyte pathway enrichment performed on genotype DEGs from both timepoints (**Figure 4.5A** and **Supplemental Figure 4.4**). R6/2 12-week striatal and cortical astrocytes showed significant inhibition of neural regulatory-related signaling, including Synaptic Long Term Potentiation, Synaptogenesis, and CREB Signaling in Neurons. The most significant pathways enriched in R6/2 8-week striatal and cortical astrocytes had low or no predicted activation scores, but the individual pathways were more unique to each brain region. When evaluating each region, striatal 8-week top pathways included Neuroinflammation and GABA receptor signaling, while cortical 8-week top pathways were Glutamate Receptor Signaling, Ceramide Degradation, and Sphingosine-1-phosphate (S1P) metabolism; this highlights the unique cellular processes in metabolic regulation across these two brain regions during this stage in HD pathogenesis that may drive changes at later stages. There were many overlapping significant pathways relating to Synaptogenesis Signaling in 12-week striatal and cortical timepoints but had increased predicted inhibition in cortical astrocytes. These shared and unique pathways across astrocytes in age and brain region highlight the unique astrocyte cell states that may contribute to R6/2 pathogenesis across these two highly affected brain regions.

As the overlapping pathways across time points and brain regions suggested, there was significant astrocyte genotype DEG overlap (**Figure 4.5B**). The set of 56 overlapping 12-week striatal and cortical DEGs were genes all dysregulated in the same direction and may represent common signatures in astrocytes independent of region (**Figure 4.5C**). Individual examination of each of these genes was performed to uncover commonalities contributing to transcriptional dysregulation in R6/2 mouse astrocytes at this severe disease stage. *Gria2* and *Grin2c* were present in a majority of the overlapping dysregulated signaling pathways related to neuronal support, glutamate receptor signaling, and ion binding, highlighting how aberrant R6/2 astrocytes

affect the regulation of neuronal homeostasis. There were also several genes related to both neural support and extracellular matrix/adhesion-related signaling, such as *Sparcl1, Ttyh1*, and *Tspan7*. Together, this dysregulated astrocyte signaling at 12 weeks may highlight two major dysfunctions occurring across R6/2 astrocytes and how it affects the cells they are meant to support, therefore contributing to pathogenesis.

To identify possible transcriptional regulators, we conducted transcription factor enrichment analysis (Kuleshov et al., 2016) using these 56 common 12-week DEGs. ChEA database showed SOX9, a glial developmental transcription factor, as the most significant transcription factor enriched, suggesting a role for this complex in altered gene expression in R6/2 mouse astrocytes (**Figure 4.5D**). TCF4, a transcription factor involved in nervous system development, and SUZ12, a member of the polycomb repressive complex 2 (PRC2), were also enriched, suggesting roles for these complexes in silencing astrocyte development genes (**Figure 4.5D**), that have also been implicated in HD neurons (Seong et al., 2010), endothelial genes in HD BMECs (Ferrari Bardile et al., 2019; Lim et al., 2017), and HD oligodendroglia (Ferrari Bardile et al., 2019). Another predicted transcriptional regulator in R6/2 astrocytes was the transcriptional repressor ZNF217, which was also present in HD iAstro analysis (**Figure 4.2G** & **4.5D**). For further investigation into transcription factor perturbation in R6/2 mouse astrocytes, Enrichr Transcription Factor Database was queried (**Supplemental Figure 4.5B**). Hes Family BHLH Transcription Factor 1 (HES1) overexpression was implicated as the most significant perturbation, further implicating transcriptional repression of nervous system development in R6/2. Alterations in ASCL1 and MECP2, regulators of neural development, were also predicted to contribute to common dysregulated gene sets in R6/2 striatal and cortical astrocytes. NFIA, a transcription factor that controls astrogliogenesis, was identified as being deficient, indicating a potential mechanism for altered astrocyte development in R6/2. These findings highlight potential mechanisms in astrogliogenesis and neural developmental dysregulation contributing to

downstream pathway dysregulation in mutant HTT-expressing astrocytes—a similar finding to our iAstro model of HD.

To further assess the common dysregulation across R6/2 astrocytes, we examined the nine genotype DEGs that were common across astrocytes from both brain regions and time points. These genes all had very similar expression levels that often became more severe with age, with striatal 12-week astrocytes typically having the most extreme expression of these nine common DEGs (**Figure 4.5E**). Exceptions included several splicing and transcription-related genes (*Gm3764, Tra2a, Ddx5*) that had the highest fold change in DEGs from cortical 12-week R6/2 astrocytes compared to cortical NT astrocytes. A non-coding RNA (*Gm4876*) and a lipid regulator (*Abca1*) were DEGs unique to only glial cell types (astrocytes, oligodendrocytes, and/or oligodendrocyte progenitor cells) in the larger R6/2 snRNA-seq dataset. Among these overlapping astrocyte DEGs, the downregulation of the glycogen phosphorylase activator, *Phkg1,* was unique to only astrocytes compared to other R6/2 cell types and highlights the potential dysregulation of glycogen breakdown in R6/2 astrocytes.

4.3.6 Inhibition of Glutamate Signaling in HD iAstros and R6/2 astrocytes

A significantly inhibited glutamate receptor signaling cell state was identified in HD-enriched R6/2 and iAstro clusters. The presence of these states in both the mouse and iPSC model suggest that this is core feature of HD astrocytes and likely arises intrinsically from the expression of mutant HTT. Genes that encode glutamate transporters (*SLC1A2*, *SLC1A3*) and glutamate receptors (*GRIA1, GRIA2, GRIN2A*) were significantly downregulated across both models of HD astrocytes (**Figure 4.6A** and **4.6B**). To confirm the intrinsic loss of glutamate signaling in HD astrocytes we investigated protein levels of a representative glutamate receptor 1 (GluR1), encoded by *GRIA1;* western analysis for GluR1 was performed on HD and control iAstros and showed significantly decreased GluR1 in HD iAstros compared to control iAstros (**Figure 4.6C**). Taken together,

glutamate signaling is a cell-autonomously downregulated signaling pathway in HD astrocytes that may inhibit the uptake of glutamate, which can influence HD pathogenesis by contributing to glutamate neurotoxicity.

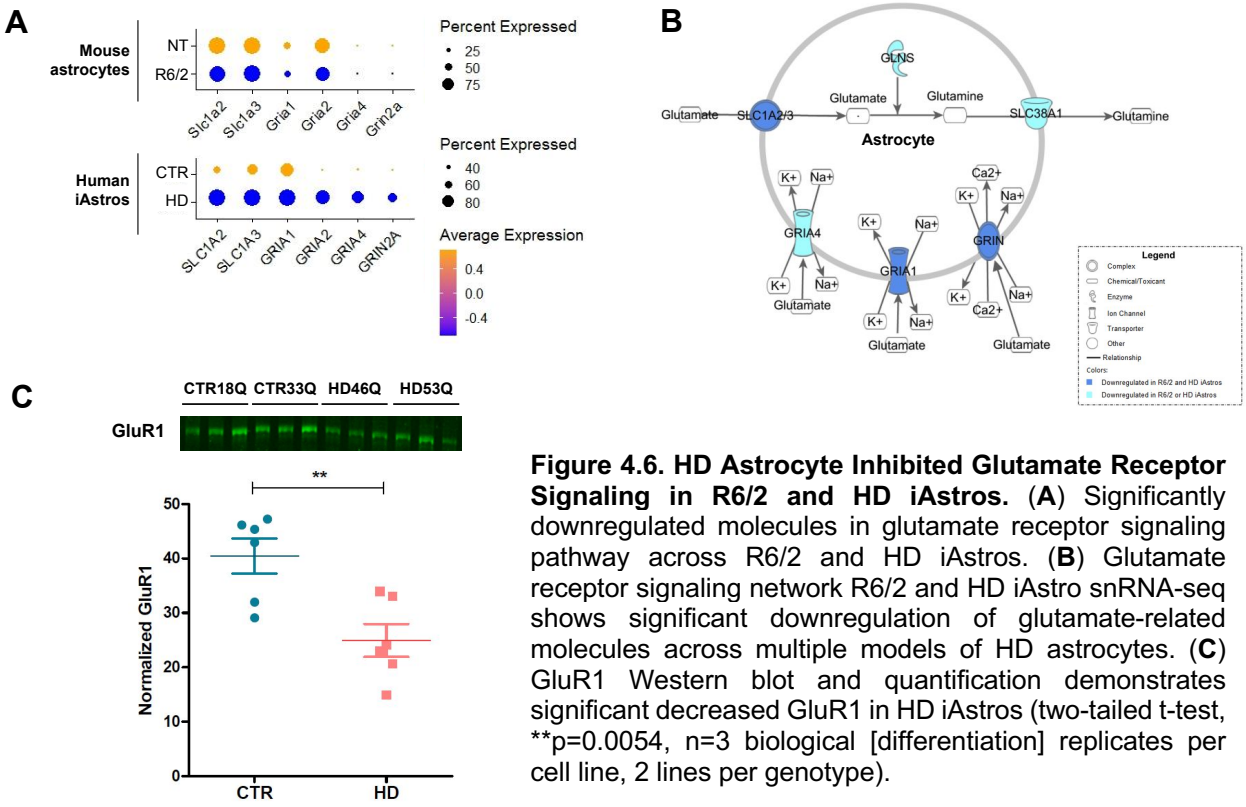

Figure 4.6. HD Astrocyte Inhibited Glutamate Receptor Signaling in R6/2 and HD iAstros. (**A**) Significantly downregulated molecules in glutamate receptor signaling pathway across R6/2 and HD iAstros. (**B**) Glutamate receptor signaling network R6/2 and HD iAstro snRNA-seq shows significant downregulation of glutamate-related molecules across multiple models of HD astrocytes. (**C**) GluR1 Western blot and quantification demonstrates significant decreased GluR1 in HD iAstros (two-tailed t-test, **p=0.0054, n=3 biological [differentiation] replicates per cell line, 2 lines per genotype).

4.3.7 Activation of ECM and Actin in HD iAstros

ECM and actin cytoskeletal signaling activation was a cell state uniquely activated in HD iAstros compared to R6/2 astrocytes. While there were several actin, ECM, and adhesion-related DEGs present in overlapping 12-week striatal and cortical R6/2 astrocytes (**Figure 4.5C**), this did not trigger significant enrichment of specific actin or ECM signaling pathways, unlike HD iAstros. We investigated the genes contributing to ECM and actin cytoskeletal signaling activation in the HD and control iAstro cell lines to determine the genes controlling these dysregulated pathways

(**Figure 4.7A**). Genes related to extracellular signaling (*ITGB1* and *ITGA3*) and those regulating actin dynamics (*ACTN1, Talin, ERM*), actin polymerization (*F-actin, PFN, and ARP2/3*), and overall cytoskeletal reorganization (*MYL and Myosin*) were all significantly upregulated in HD iAstros (**Figure 4.7B**). To investigate filamentous actin (F-actin) protein expression, Phalloidin in-cell westerns were performed on HD and control iAstros. HD iAstros had a significantly increased expression of F-actin compared to control iAstros (**Figure 4.7C**). Taken together, ECM and actin cytoskeletal signaling is a cell-autonomous and potentially early activated signaling pathway unique to patient-derived HD astrocytes that may contribute to morphological changes or increased adhesion in HD astrocytes.

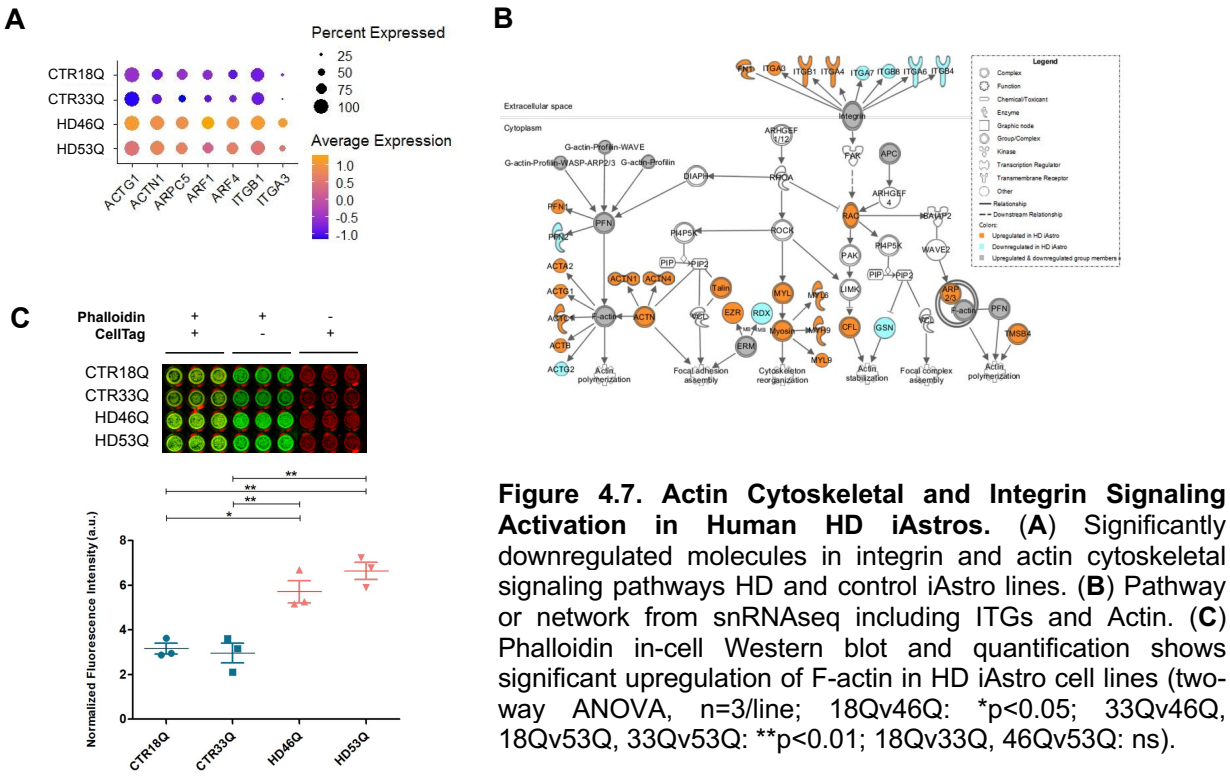

Figure 4.7. Actin Cytoskeletal and Integrin Signaling Activation in Human HD iAstros. (**A**) Significantly downregulated molecules in integrin and actin cytoskeletal signaling pathways HD and control iAstro lines. (**B**) Pathway or network from snRNAseq including ITGs and Actin. (**C**) Phalloidin in-cell Western blot and quantification shows significant upregulation of F-actin in HD iAstro cell lines (two-way ANOVA, n=3/line; 18Qv46Q: *p<0.05; 33Qv46Q, 18Qv53Q, 33Qv53Q: **p<0.01; 18Qv33Q, 46Qv53Q: ns).

4.4 Discussion

Unbiased single cell approaches to define cell states across the landscape of thousands of individual astrocytes (Trapnell, 2015), especially for cell types such as astrocytes whose function span a wide range of biological processes, provides a unique window into the cell states that arise during disease. The goal of our studies was to identify and compare astrocyte transcriptional cell states in specific systems and time points, their transitions in unaffected control and HD systems, and to elucidate regulatory signaling involved. We investigated transcriptome signatures in astrocytes from human iPSC-derived astrocytes and a transgenic mouse model to elucidate common and species-specific cell states, as well as aberrant cell states that exist in both human and mouse HD astrocytes. Both models demonstrated potential loss of cell states involved in neural support, glutamate signaling, ion-binding, and neural development. Both also suggest astrocyte developmental alterations that are predicted to be regulated by astrogliogenesis transcription factors. HD human astrocytes also exhibited a unique activation of ECM and cytoskeletal signaling that may represent a novel human state not seen in the HD mice. While most of the transcriptional cell states we identified in both human and mouse data were represented in HD and control samples, with shifts in percent composition in each condition, the iAstro data revealed a complete loss of a unique control cell state that showed high expression of *NEAT1,* a gene associated with the stability of nuclear paraspeckles and thought to function through interactions with RNA binding and other proteins and RNAs, thus affecting transcription (Clemson et al., 2009; Hirose et al., 2014). *NEAT1* has also been implicated in striatal neurons from HD patients and mouse models, with its overexpression protecting from mutant HTT-induced cytotoxicity (Cheng et al., 2018). The R6/2 astrocytic dysregulation that overlapped between regions and with the human data showed an increase in severity between 8 and 12 weeks, suggesting that astrocyte dysregulation is progressive; however, there were unique differences found in 8-week cortical astrocytes involving SP1 signaling and lipid metabolism, which may represent unique age-dependent cortical changes or early changes that give rise to the

dysregulation of molecular processes that were dysregulated at 12 weeks. Overall, the dysregulated astrocytic states identified here are anticipated to induce dysfunctional brain homeostasis and contribute to HD pathogenesis.

Single-nuclei technology has allowed us to identify diverse astrocyte states within a heterogeneous population through unsupervised computational clustering that may not have been identified using traditional bulk transcriptomic analysis (Hu et al., 2016). Homeostatic astrocyte states identified from control iAstros and NT mouse astrocytes, compared to HD iAstros or R6/2 mouse astrocytes, included activation of signaling pathways previously suggested to play roles in astrocyte functions. Synaptogenesis signaling and CREB signaling were significantly activated in NT-enriched striatal and cortical astrocyte states along with calcium-binding activation in the cortex. In control human iAstros, several synaptogenesis-related genes were among the top upregulated cluster markers (*SPARCL1*) in control iAstro state cluster 0. Glutamate receptor signaling was significantly activated across an NT-enriched striatal mouse astrocyte state relative to R6/2 striatal astrocyte clusters. Interestingly, glutamate receptor signaling was predicted to be less inhibited in an R6/2-enriched cortical astrocyte state, which could suggest that cortical R6/2 astrocytes have undergone a gain of cell state caused by the dysregulated glutamatergic circuitry that projects from the cortex to the striatum (Blumenstock & Dudanova, 2020).

4.4.1 HD Human iAstro and R6/2 Astrocyte Phenotype Comparisons

A commonly dysregulated astrocyte state across HD human iAstros and R6/2 mouse astrocytes was the inhibition of glutamate signaling. This phenotype is consistent with studies suggesting that glutamate handling is a critical feature of excitotoxicity in HD (Choi, 1988; Cross et al., 1986; Greenamyre, 1986). Astrocytes terminate the action of neurotransmitters, like glutamate and gamma-aminobutyric acid (GABA), through uptake at the tripartite synapse. In the case of glutamate, astrocytes help clear this excitatory neurotransmitter from the synaptic cleft through

transporters (GLT1 and GLAST) and with the help of transmembrane glutamate receptors (GluR1 and GluR2) that form ligand-gated ion channels (Lehre et al., 1995; Rothstein et al., 1994, 1996). Within the cytosol of astrocytes, glutamate is then degraded into the neuro-inactive state, glutamine, via glutamine synthetase (GLUL) in an ATP-dependent manner; each of these were downregulated in our present study. To begin to validate these data, decreased protein levels of the glutamate transporter GLAST in human HD iAstros upon FACS isolation, and decreased protein levels of the AMPA glutamate receptor GluR1 in GLAST-positive HD iAstros compared to GLAST-positive control iAstros was observed. Transcriptionally downregulated glutamate receptor signaling may have implications related to glutamate neurotoxicity due to the decreased glutamate transporter expression at astrocytes within the tripartite synapse. This dysregulation is present in R6/2 and other models of HD and may involve potassium ion channel Kir4.1 in R6/2 mice (Bradford et al., 2009; Faideau et al., 2010; Garcia et al., 2019; Jiang et al., 2016; Khakh et al., 2017; Lee et al., 2013). The evidence of HD iAstro glutamate downregulation presented in this study is consistent with studies demonstrating a similar phenotype in juvenile-onset HD iPSC-derived astrocytes (Garcia et al., 2019) and neurological symptoms upon loss of GLT1 expression in mice with HTT-160Q selectively expressed only in astrocytes (Bradford et al., 2009). Together, these data support a cell autonomous component of aberrant glutamate signaling inhibition in astrocytes in HD.

Axonal guidance was an inhibited pathway predicted in one HD-enriched iAstro cell state that overlapped with striatal R6/2 astrocytes. This neural developmental pathway is necessary to guide neurons to their correct targets for proper synaptogenesis, therefore inhibition of this critical process would alter neuronal circuitry homeostasis. Moreover, HD iAstro-enriched cluster 3 and R6/2-enriched striatal cluster 4 appeared to be in a more immature, proliferative cell state. Aberrant activation of cell cycle-related signaling has been demonstrated from HD mice (Conforti et al., 2013; Luthi-Carter et al., 2002), HD iPSC-derived neural models (HD iPSC Consortium, 2017; Mattis et al., 2014; Ring et al., 2015; Smith-Geater et al., 2020), and HD patient tissue

(Barnat et al., 2020; Hickman et al., 2021). Osipovitch et al also demonstrated a decrease in GFAP expression in HD patient ESC-derived astrocytes that reflects impaired astrocytic differentiation (Osipovitch et al., 2019).

Developmental alterations in HD iAstros and decreased mature astrocyte markers in a striatal R6/2 astrocyte subpopulation may be a common cell state associated with mutant HTT-induced decreased astrogliogenesis. Transcription factor analysis of R6/2 and HD iAstros identified regulators of early astrogliogenesis (NFIA, SOX9, ATF3) (Kang et al., 2012; Tiwari et al., 2018). Polycomb group proteins, like SUZ12, restrict the propensity of NPCs to differentiate into neurons by repressing pro-neuronal genes (Hirabayashi et al., 2009) and have been implicated in HD (Seong et al., 2010). HES1 overexpression was one of the most significantly enriched transcription factors in R6/2 12-week astrocytes along with the dysregulation of several HES genes in HD iAstros, consistent with epigenetic dysregulation of a HES family transcription factor (HES4) associated with striatal degeneration in HD post-mortem cortex (Bai et al., 2015). . The observed molecular phenotypes may also be due to a loss of astrocyte identity rather than a developmental alteration, as suggested in previous studies (Langfelder et al., 2016); however, the human HD iAstros data suggest a developmental phenotype given the decreased propensity for HD iPSCs to differentiate into GLAST-positive, morphologically mature astrocytes, and the likelihood that this iPSC model recapitulates early developmental stages. Both hypotheses could be occurring as HD progresses and mature cells lose their identity while progenitor cells give rise to developmentally impaired astrocytes. Nonetheless, alterations in astrocyte functions are suggested due to the lack of mature astrocyte characteristics. Rescuing these deficits may require the proper induction of transcriptional regulators that are involved in the development and maturation of astrocytes and the expression of mature functional genes.

Astrocyte reactivity has been documented in HD mouse (Lin et al., 2001; Myers et al., 1991; Reddy et al., 1998; Yu et al., 2003) and human tissue (Sapp et al., 2001; Selkoe et al.,

1982); however, the extent of cell-autonomous astrogliosis has not been extensively characterized. Surprisingly, control iAstros appeared to exhibit a more activated neuroinflammatory state compared to HD; however, this was a relatively small cell state in iAstro cluster 6, only encompassing 5% of the total nuclei sequenced. This suggests that control human iAstros may have a greater ability to mount normal inflammatory responses, including those that are a hallmark of *in vitro* cultured astrocytes (Haim et al., 2015). Neuroinflammatory signaling was enriched in R6/2 striatal and cortical genotype-specific differentially expressed genes, with minor activation in striatal 12-week astrocytes; however, looking closely into the cell states, NT-enriched cortical cluster 4 had a predicted activation of neuroinflammation signaling similar to iAstro control-enriched cluster 6. Consistent with this hypothesis, R6/2-enriched striatal cluster 4, which had the lowest expression of mature astrocyte markers, had a predicted inhibition of neuroinflammatory signaling, demonstrating a potential loss of cell function in HD. These data suggest that both activated and inhibited states may exist in HD and could be playing different roles in the disease. Furthermore, some of these neuroinflammatory states may only arise due to extrinsic signaling from other CNS cell types, as suggested by the lack of neuroinflammatory states in the HD iAstros. Since immune responses of astrocytes can induce detrimental and/or beneficial effects on neighboring cell types, it is unknown what consequences would result from this loss of cell state (Ding et al., 2021). Studies aimed at inducing reactivity through LPS or A1-activating factors (Liddelow et al., 2017), may help to determine if HD astrocytes are unable to mount appropriate responses. While a lack of inflammatory response in HD astrocytes contrasts with evidence in literature showing evidence of reactive astrocytes in HD mouse models (Lin et al., 2001; Reddy et al., 1998; Yu et al., 2003) and human post-mortem tissue (Faideau et al., 2010; Myers et al., 1991; Reddy et al., 1998; Sapp et al., 2001; Selkoe et al., 1982), more recent studies support a lack of traditional or A1-like reactive astrogliosis states in HD (Al-Dalahmah et al., 2020; Jiang et al., 2016; Tong et al., 2014).

Translational and stress response regulation was predicted to be activated in HD iAstros but not enriched in R6/2 astrocytes. HD iAstros had a significant increase in EIF2 signaling associated gene expression, including an increase in 53 transcripts that encode small and large ribosomal subunits as well as RNA polymerase subunit *POLR2A*. Since a majority of differentially expressed genes in HD iAstros and R6/2 striatal astrocytes were downregulated, the predicted activation of EIF2 protein synthesis may be a compensatory mechanism to combat the drastic downregulation of genes occurring in HD or could reflect altered stress granule dynamics that have been demonstrated in R6/2 mouse and HD patient tissue (Sanchez et al., 2021). To support this overt downregulation in HD, a recent study examined mutant HTT's involvement in protein synthesis repression through ribosome stalling in mouse HD striatal neurons *in vitro* (Eshraghi et al., 2021).

There were several dysregulated pathways common to HD human iAstros and R6/2 astrocytes; differences between systems may be due to multiple reasons including expression of an expanded repeat HTT exon 1 transgene in R6/2, while HD iAstros contain the full-length endogenous mutant HTT. A recent study identified similarities and differences across GLT1-positive astrocytes from truncated (R6/2) and full-length (zQ175) mutant HTT mouse models (Benraiss et al., 2021). These changes may also be due to the influence of other cell types within the NVU, such as activated microglia (Liddelow et al., 2017). Finally, species differences may also contribute as human astrocytes have greater development of astrocyte networks both in numbers and complexity, exhibiting significantly more multi-branched processes than rodent astrocytes (Khakh & Sofroniew, 2015; Oberheim et al., 2009). The difference in the ability of adult human and mouse astrocytes to respond to extracellular glutamate is an example that suggests adult human astrocytes may have evolved an improved capability to respond to synaptic activity (Oberheim et al., 2009; Sun et al., 2013; Zhang et al., 2016).

4.4.2 Unique HD Human iAstro Phenotypes

Signaling states unique to human HD iAstros included activation of actin cytoskeletal and integrin signaling. Additionally, HD iAstros had a decrease in matrix metalloproteinases (*MMP15 & 17*) that aid in ECM degradation. Altered actin cytoskeletal dynamics was validated by increased Phalloidin staining in HD iAstros at the protein level. This gain-of-function cell state unique to human HD iAstros suggests a cellular state transition that is most likely a cell-autonomous effect not influenced by the presence of other cell types that provide developmental cues for astrocytes. The functional relevance of actin and integrin or lncRNA activation to disease pathogenesis has yet to be determined but may relate to altered morphology, movement, and adhesion or transcriptional regulation, respectively.

4.4.3 Unique R6/2 Astrocyte Dysregulated Cell States

Cyclic adenosine monophosphate (cAMP)-mediated signaling was the most inhibited pathway in striatal and cortical R6/2 astrocytes at 12 weeks. This signaling pathway plays a vital role in cellular signaling, including the regulation of glucose and lipid metabolism. Interestingly, Phosphorylase Kinase Catalytic Subunit Gamma 1 (*Phkg1*) was a downregulated gene common across both time points and both brain regions but was unique to only astrocytes from the R6/2 snRNA-seq analysis. Since astrocytes are the primary storage site for glycogen in the brain (Sofroniew & Vinters, 2010), a decrease in *Phkg1* would reduce glycogen phosphorylase's ability to break down glycogen in astrocytes needed for the high energy demand of neurons. Decreased glucose levels have been shown in HD astrocytes purified from mouse striatum (Polyzos et al., 2019) and decreased striatal metabolism in HD patients attributed to decreased glucose uptake through GLUT3 (Ciarmiello et al., 2006; McClory et al., 2014). In addition to disrupting neuronal activity,, reduced glucose levels may impact downstream epigenetic and transcriptomic signatures.

We also described novel cellular states unique to the two brain regions assessed. Striatal R6/2 cell state differences highlighted changes in maturation and ion transport/binding astrocytic processes, while cortical R6/2 astrocytes mostly presented glycosylated cell state transition with an inhibited synaptogenesis signature. The predicted inhibition of a majority of signaling pathways was also seen in R6/2-enriched striatal and cortical clusters. Striatal R6/2 astrocytes and HD iAstros clusters had a loss of astrocyte identity genes, while this molecular phenotype was less overt in cortical R6/2 astrocytes. While there was a difference between cortical R6/2 and NT astrocytes, there appeared to be less diversity in cell states in cortical R6/2 astrocytes. Intriguingly, there were less significant differentially expressed genes across genotype for 12-week and 8-week cortical astrocytes compared to striatal, which yielded less diversity in significant pathway dysregulation. This correlates with more overt neurodegeneration in the striatum, compared to the cortex.

Taken together, our findings indicate that aberrant cell states exist in HD astrocytes that include inhibition of glutamate signaling and potential developmental alterations that may be regulated by mutant HTT's interaction with astrogliogenesis transcription factors, ATF3, NFIA, or SOX9. In addition, loss of astrocyte maturation may contribute to inhibition of glutamate signaling in human HD and R6/2 astrocytes. The identification of common and unique HD cell states across human and mouse astrocytes provides directions for further mechanistic evaluation and greater information relating to potential therapeutic interventions targeting these dysregulated astrocytic states in HD as well as predicted outcomes across model systems.

4.5 Experimental Procedures

4.5.1 iPSCs

HD and unaffected control iPSCs were generated and characterized as described (HD iPSC Consortium, 2013, 2017; Lim et al., 2017; Mattis et al., 2013; Smith-Geater et al., 2020). The five iPSC lines were maintained on Matrigel hESC-qualified matrix (Corning) with mTeSR1 (STEM CELL Technologies). Once 60-80% confluent, iPSCs were passaged using a 5-10 min incubation with Versene (Gibco) at 37°C.

Table 4.5.1 HD and Unaffected iPSC Lines Used for iAstros

Cell line	*HTT* CAG repeat	Sex	Reprogramming method	Fibroblast line	Clinical Notes
CS25iCTR18n6 (CTR18Q)	18, 17	Male	Non-integrating episomal	ND30625	Clinically Normal; brother of affected sibling; mother affected and/or gene positive; Sibling(s) affected and/or gene positive; Niece is ND31038; HD family ND31846
CS83iCTR33n1 (CTR33Q)	33, 18	Female	Non-integrating episomal	GM02183	Clinically Normal; At risk (50%) for Huntington's Disease
CS04iHD46n10 (HD46Q)	46, 26	Male	Non-integrating episomal	UCI-HDF4	Clinically Affected
CS03iHD53n3 (HD53Q)	53, ?	Male	Non-integrating episomal	UCI-HDF3	Clinically Affected
CS81iHD71n3 (HD71Q)	71, 17	Female	Non-integrating episomal	GM04281	Rigid form of HD, possible homozygote, onset at age 14 yrs; neurological exam 3/82 shows a hypokinetic variant of HD with dystonia and marked tremor, ataxic wide-based gait; maternal cousin to clinically normal GM04711 and clinically affected GM04777

4.5.2 Astrocyte Differentiation

Five iPSC lines were differentiated into neural progenitor cells (NPCs) as described (Gibco #A1647801, MAN0008031). NPCs were cultured to 90-95% confluency, then seeded at 1e5/cm^2 on hESC-qualified matrigel (Corning) for four passages before induction of astrocyte

differentiation. To begin astrocyte differentiation, passage four NPCs were seeded at 0.75e5/cm2 in Neural Expansion Medium (Gibco #A1647801, MAN0008031) and the following day (day 0), half the medium was replaced with astrocyte differentiation medium (ADM) 1. Half media changes were performed every other day for the remainder of the differentiation. All subsequent passages were performed by washing cells with HBSS without Mg Ca (Gibco) three times, then incubating in StemPro Accutase (Gibco) at 37°C for 10-15min, counting using TC20 Automated Cell Counter (Bio-Rad) with trypan blue exclusion, and seeding on hESC-qualified matrigel (Corning) at 5e4/cm^2 unless otherwise noted. On day 7, the cells were replated in ADM1. On day 15, the cells were replated in 50% ADM1, 50% ADM2. Subsequent half media changes were performed using ADM2. On day 30, day 34, and day 45, the cells were replated in 100% ADM3. On day 60, the cells were subject to astrocyte enrichment via FACS. QC immunostaining was performed at each passage time point for PSC, NPC, neural, and astrocytic markers.

Table 4.5.2a. Astrocyte Differentiation Medium 1 (ADM1)

ADM1 Component	Company	Cat. #	Concentration
DMEM, high glucose	Life Technologies	11995-065	100%
HI-FBS‡	Life Technologies	10082-147	1%
GlutaMAX [100X]	Life Technologies	35050061	1X
N2 Supplement [100X]	Life Technologies	17502048	1X
LIF*	STEMCELL Technologies	78055	100ng/mL
CNTF*	Peprotech	0117158	100ng/mL
bFGF*	STEMCELL Technologies	78003.2	50ng/mL

*added to media fresh before media change
‡Lot #: 1876835

Table 4.5.2b. Astrocyte Differentiation Medium 2 (ADM2)

ADM2 Component	Company	Cat. #	Concentration
BrainPhys	STEMCELL Technologies	05790	100%
SM1 Supplement [50X]	STEMCELL Technologies	05711	1X
LIF*	STEMCELL Technologies	78055	25ng/mL
CNTF*	Peprotech	0117158	50ng/mL
bFGF*	STEMCELL Technologies	78003.2	50ng/mL

*added to media fresh before media change

Table 4.5.2c Astrocyte Differentiation Medium 3 (ADM3)

ADM3 Component	Company	Cat. #	Concentration
DMEM, high glucose	Life Technologies	11995-065	50%
Neurobasal	Life Technologies	21103-049	50%
GlutaMAX [100X]	Life Technologies	35050061	1X
Sodium Pyruvate [100mM]	Life Technologies	11360070	1mM
SATO Supplement [100X]	-	-	1X
N-Acetylcysteine*	Sigma-Aldrich	A9165	5µg/mL
huHBEGF*	R&D Systems	259-HE	5ng/mL

*added to media fresh before media change

4.5.3 Immunofluorescence

Cells were fixed using 4% paraformaldehyde (Electron Microscopy Sciences) in PBS for 10min at room temperature. Depending on antigen, cells were permeabilized with 0.3% Triton X-100 (Sigma-Aldrich) in PBS for 10min at room temperature. Cells were blocked for 1hr in 10% goat serum (Gibco), 1% BSA (Gibco), 0.1% Triton X-100 in PBS for 1hr at room temperature. Cells were incubated with primary antibodies overnight at 4°C and then washed three times with PBS before incubation in 1:1000 Alexa-Fluor 488, 594, 647 secondary antibodies (Invitrogen) for 1hr at room temperature and subsequently incubated with Hoechst 33342 (Sigma-Aldrich) for 10min at room temperature. Stained slides were mounted with Fluoromount-G (Southern Biotech). Cells were imaged with a Nikon T-E fluorescence microscope at 10x and 20x. Analysis of images were performed by Cell Profiler (Carpenter et al., 2006).

Table 4.5.3 Primary Antibodies Used

Primary Antibody	species	dilution	Company	Cat. #
OCT4	Mouse	1:500	Millipore	MAB4401
SOX2	Rabbit	1:500	Millipore	AB5603
Nestin	Mouse	1:1000	Millipore	MAB5326
PAX6	Rabbit	1:250	Abcam	ab5790
DCX	guinea pig	1:500	Millipore	AB2253
TUJ1	Mouse	1:1000	Millipore	MAB5564
MAP2	guinea pig	1:1000	Synaptic Systems	188004
GFAP	Chicken	1:1000	Abcam	ab4674
ALDH1L1	Rabbit	1:400	Abcam	ab87117
S100β	Mouse	1:500	Abcam	ab4066

GLAST	Mouse	1:100	Miltenyi Biotec	130-095-822
GLAST-APC	Mouse	1:50	Miltenyi Biotec	130-123-555
AQP4	Rabbit	1:100	Abcam	ab81355
GluR1	Mouse	1:1000	Abcam	ab174785
ATF3	Rabbit	1:1000	Abcam	ab254268
IgG	Mouse	As needed	Invitrogen	02-6502
IgG	Rabbit	As needed	Invitrogen	02-6102

4.5.4 FACS Astrocyte Enrichment

Day 60 cells were washed with HBSS without Mg Ca (Gibco) three times then lifted using a 10-15min incubation of StemPro Accutase (Gibco) at 37°C. Cells were collected and strained through a 70um cell strainer then incubated with 100U/mL DNaseI (Qiagen) in FACS Buffer (0.5% BSA [Gibco] in PBS without Mg and Ca) for 10 min at room temperature. Cells were washed, collected, then stained for GLAST-APC (Miltenyi Biotec) in FACS Buffer for 15 min at 4°C in the dark. Cells were washed, 40um strained, then collected, then stained for DAPI in FACS Buffer for 5 min at room temperature in the dark. Cells were immediately sorted on the FACSAria Fusion Cell Sorter (BD Biosciences) into ADM3 with PenStrep (Gibco). GLAST-positive/DAPI-negative cells were replated at 0.38e6/well of a 6-well in ADM3 with 1X PenStrep. Following astrocyte-enrichment, the cells were cultured for another 7 days before harvest with half media changes every other day in ADM3 with 1X PenStrep followed by immunofluorescence quality control analysis for astrocyte markers.

4.5.5 F-Actin In-Cell Western

Day 67 GLAST-positive astrocytes were seeded into a hESC-qualified matrigel coated 96-well plate at 0.4e5/cm2 for 3 technical replicates per biological (differentiation) replicate per cell line. Two days post seeding, cells were fixed using 4% paraformaldehyde (Electron Microscopy Sciences) in PBS for 20 min at room temperature. After washing cells 3X with 0.1% Tween 20 (Sigma-Aldrich) in PBS, cells were permeabilized with 0.2% Triton X-100 (Sigma-Aldrich) in PBS

for 30 min at room temperature. Cells were then blocked for 1 hr in 5% goat serum (Gibco), 3% BSA (Gibco) in PBS for 1 hr at room temperature. Cells were incubated with Phalloidin-iFluor790 CytoPainter (ab176763) at 1:1000 for 1 hr at room temperature, followed by washing 3X with 0.1% Tween 20 (Sigma-Aldrich) in PBS. CCellTag700 (LI-COR 926-41090) at 1:500 was added as a total protein stain (for normalization purposes) and incubated for 1 hr at room temperature. Cells were then washed 3X with 0.1% Tween 20 (Sigma-Aldrich) in PBS, then solution was completely removed from wells. Wells were immediately imaged using the LI-COR Odyssey CLx and analyzed using LI-COR's Empiria Studio Software.

4.5.6 Western Blots

Day 67 GLAST-positive astrocytes were collected then broke pellets in 150uL modified RIPA buffer Sonicate 3x for 10 seconds at 40% then spun down for 20 min at 4˚C, 1000 rpm. Bradford (Thermo Scientific BioMate 3S UV-visible spectrophotometer) protein quantification was performed with cuvettes. Protein lysates were aliquoted at 5 ug for ATF3 and GluR1, then equivalent amounts of loading buffer were added. Gels were ran at 150V using Bolt™ 4-12% Bis-Tris Plus Gels, 15-well gels with MOPS, transferred onto Nitrocellulose Membrane 0.45 µm at 10 V for 1 hr at room temperature. The membrane was rinsed in water and then let dry for 15 min. Membranes were rehydrated in water and then followed the Revert 700 Total Protein Stain protocol. Membranes were blocked in Intercept (TBS) Blocking Buffer for 1 hr at room temperature. Membranes were incubated in primary antibody (ATF3 rb 1:1000, GluR1 ms 1:1000) and rotated at 4˚ overnight. Membranes were then washed 3x with TBST, then incubated in secondary antibody: ATF3 into IRDye® 800CW Goat anti-Mouse IgG 1:20,000, and GluR1 into IRDye® 800CW Goat anti-Rabbit IgG 1:20,000 for 1 hr at room temperature. Membranes were washed 3x with TBST while gently shaking for 1 hr, then washed 2x with TBS at room

temperature. Membranes were imaged using the LI-COR Odyssey CLx and analyzed using LI-COR's Empiria Studio Software.

4.5.7 snRNA-seq

4.5.7.1 Mouse snRNA-seq

Single nuclei were isolated from half hemisphere striatum or cortex in Nuclei EZ Lysis buffer (Sigma-Aldrich, NUC101-1KT) and incubated for 5 min. Samples were passed through a 70µm filter and incubated in additional lysis buffer for 5 min and centrifuged at 500 g for 5 min at 4°C before two washes in Nuclei Wash and Resuspension buffer (1xPBS, 1% BSA, 0.2U/µl RNase inhibitor). Nuclei were FACS sorted using DAPI to further isolate single nuclei and remove additional cellular debris. These nuclei were run on the 10x Chromium Single cell 3' gene expression v3 platform.

4.5.7.2 iAstro snRNA-seq

Day 67 GLAST-positive single-cell suspensions were strained using a 70 µm strainer, washed using cold 0.08% BSA (Gibco) in PBS, and counted using TC20 Automated Cell Counter (BioRad) with trypan blue exclusion as described in the 10x Genomics® Demonstrated Protocol: Single Cell Suspensions from Cultured Cell Lines for Single Cell RNA Sequencing (Document CG00054). To obtain a single-nuclei suspension, cells were lysed using Nuclei EZ Lysis Buffer (Sigma Aldrich, NUC101-1KT) for 5 min on ice. Lysed cells were centrifuged 500 rcf for 5 min at 4°C, then washed by twice resuspending in 1% BSA (Gibco), 0.2 U/µL of Human Placenta RNase Inhibitor (NEB), in PBS and centrifuged again. After two washes, the nuclei were strained using a 40 µm cell strainer, counted using the TC20 Automated Cell counter (Bio-Rad), resuspended at 1000 nuclei/µL in 0.08% BSA (Gibco) in PBS, then proceeded immediately with the 10x Genomics® Single Cell Protocol.

4.5.8 snRNA-seq Data Processing

4.5.8.1 Mouse snRNA-seq

Libraries were QCed and sequenced on the NovaSeq 6000 using 30 bases for read 1 and 98 bases for read 2, to obtain >=50K reads per a cell. A total of 109,053 cells with 6.1 billion reads were sequenced for the 24 samples with on average 4544 cells per sample with ~55.6K reads each. Alignment was done using the CellRanger pipeline v3.1.0 (10X Genomics https://github.com/10XGenomics/cellranger) to a custom pre-mRNA transcriptome built from refdata-cellranger-mm10-1.2.0 transcriptome using cellRanger mkref. UMI Count matrices were generated from BAM files using default parameters of cellRanger count command. The gene barcode matrices for each sample were imported into R using the Read10X function in the Seurat R package (Stuart et al., 2019) (v3.1.5). Replicates were combined using cellRanger aggr.

4.5.8.2 iAstros snRNA-seq

Fastq files were quality controlled and aligned to the GRCh38 reference transcriptome to obtain a gene count matrix using Cell Ranger. Before downstream tertiary analysis, quality control of sequenced nuclei was performed by filtering out low-quality nuclei and low-abundance genes (nFeature_RNA > 200 & nFeature_RNA < 6000 & percent.mt < 5) in Seurat v3.1. After quality control and expression matrix formation, normalization was performed using UMI (unique molecular identifiers), and log-transformation was used to control variance. Seurat integration was used to combine datasets from patient-derived cell lines. Dimension reduction was used to visualize and explore major features of the data using PCA and UMAP. Clustering was performed in Seurat v3.1 using PC1-20 and 0.2 resolution. To identify gene expression differences between clusters and/or samples, a non-parametric Wilcoxon rank sum test was used with Bonferroni correction and 1% FDR cutoff using Seurat v3.1. Cell types were assigned to clusters based on known cell-type markers.

4.5.9 Exploratory and Pathway Analysis

QIAGEN's Ingenuity Pathway Analysis (http://www.qiagen.com/ingenuity) and Enrichr (Kuleshov et al., 2016 and Chen et al., 2013) were used for analysis of significantly differentially expressed genes (FDR<0.1).

4.5.10 R6/2 Mouse Model

All experimental procedures were in accordance with the Guide for the Care and Use of Laboratory Animals of the NIH and animal protocols were approved by Institutional Animal Care and Use Committees at the University of California Irvine (UCI), an AAALAC accredited institution. R6/2 mice have been described elsewhere in detail (Mangiarini et al., 1996). For this study, 10 five-week-old R6/2 and non-transgenic (NT) male mice were purchased from Jackson Laboratories and housed in groups of up to five animals/cage under a 12-hr light/dark cycle with ad libitum access to chow and water. Mice were aged to 8 or 12 weeks then euthanized by pentobarbital overdose and perfused with 0.01 M PBS. Striatum and cerebral cortex were dissected out of each hemisphere and flash-frozen for snRNA-seq or biochemical analysis.

4.5.11 Author Contributions

AMRO, RGL, and LMT conceived and designed experiments. AMRO, KQW, and CS performed differentiations. AMRO, RM, and CS performed differentiation quality control analysis. AL, JR, MN, EM, JR, and VS performed mouse experiments. AMRO and NGM performed Western blots. AMRO carried out data analysis. WWP and EMA developed the differentiation paradigm. AMRO optimized the differentiation paradigm for selected cell lines. JW and RGL performed initial mouse transcriptomic data analysis. AMRO performed all mouse and human astrocyte transcriptomic analyses. AMRO wrote the original draft of manuscript. AMRO, JR, WWP, RGL, and LMT edited the manuscript. LMT supervised the project and acquired funding.

4.5.12 Acknowledgments

We thank HD patients and their families for their essential contributions to this research. We acknowledge the UCI Stem Cell Research Flow Cytometry Core and specifically, Vanessa Scarfone and Pauline Nguyen, for their FACS technical assistance. The following provided guidance or technical assistance: Dr. Sarah Hernandez provided optimized ICW protocol and experimental guidance, Jennifer Stocksdale for expansion of iPSC lines utilized in this paper, Mara Burns for her technical assistance in cellular expansion, and Marie Schulte-Bisping for technical assistance with Western blot optimization. We also acknowledge Drs. Peter Donovan, Suzanne Sandmeyer, and Jeff Rothstein for helpful discussions. This work was supported by the following NIH grants: R35 NS116872, R01834 NS089076 and P01 NS092525 (LMT), R01 Research Supplement NS089076 (AMRO), UC Bridge to Doctorate Fellowship (AMRO), NIH NRSA T32 Training Grant NS082174-05 (AMRO), Stanley Behrens Family Foundation (AMRO), and the CIRM Bridges to Stem Cell Program (CS). This work was made possible in part, through access to the Genomics High Throughput Facility Shared Resource of the Cancer Center Support Grant (P30CA-062203) at the University of California Irvine and NIH shared instrumentation grants 1S10RR025496-01, 1S10OD010794-01, and 1S10OD021718-01.

4.6 References

Abbott, N. J., Rönnbäck, L., & Hansson, E. (2006). Astrocyte–endothelial interactions at the blood–brain barrier. *Nature Reviews Neuroscience*, *7*(1), 41–53. https://doi.org/10.1038/nrn1824

Al-Dalahmah, O., Sosunov, A. A., Shaik, A., Ofori, K., Liu, Y., Vonsattel, J. P., Adorjan, I., Menon, V., & Goldman, J. E. (2020). Single-nucleus RNA-seq identifies Huntington disease astrocyte states. *Acta Neuropathologica Communications*, *8*(1). https://doi.org/10.1186/s40478-020-0880-6

Bai, G., Cheung, I., Shulha, H. P., Coelho, J. E., Li, P., Dong, X., Jakovcevski, M., Wang, Y., Grigorenko, A., Jiang, Y., Hoss, A., Patel, K., Zheng, M., Rogaev, E., Myers, R. H., Weng, Z., Akbarian, S., & Chen, J. F. (2015). Epigenetic dysregulation of hairy and enhancer of

split 4 (HES4) is associated with striatal degeneration in postmortem Huntington brains. *Human Molecular Genetics*, *24*(5), 1441–1456. https://doi.org/10.1093/hmg/ddu561

Barnat, M., Capizzi, M., Aparicio, E., Boluda, S., Wennagel, D., Kacher, R., Kassem, R., Lenoir, S., Agasse, F., Bra, B. Y., Liu, J. P., Ighil, J., Tessier, A., Zeitli, S. O., Duyckaerts, C., Dommergues, M., Durr, A., & Humbert, S. (2020). Huntington's disease alters human neurodevelopment. *Science*, *369*(6505), 787–793. https://doi.org/10.1126/science.aax3338

Bates, G. P., Dorsey, R., Gusella, J. F., Hayden, M. R., Kay, C., Leavitt, B. R., Nance, M., Ross, C. a., Scahill, R. I., Wetzel, R., Wild, E. J., & Tabrizi, S. J. (2015). Huntington disease. *Nature Reviews Disease Primers*, *April*, 15005. https://doi.org/10.1038/nrdp.2015.5

Benraiss, A., Mariani, J. N., Osipovitch, M., Cornwell, A., Windrem, M. S., Villanueva, C. B., Chandler-Militello, D., & Goldman, S. A. (2021). Cell-intrinsic glial pathology is conserved across human and murine models of Huntington's disease. *Cell Reports*, *36*. https://doi.org/10.1016/j.celrep.2021.109308ll

Blumenstock, S., & Dudanova, I. (2020). Cortical and Striatal Circuits in Huntington's Disease. In *Frontiers in Neuroscience* (Vol. 14). Frontiers Media S.A. https://doi.org/10.3389/fnins.2020.00082

Bradford, J., Shin, J., Roberts, M., Wang, C., Li, X., & Li, S. (2009). Expression of mutant huntingtin in mouse brain astrocytes causes age-dependent neurological symptoms. *PNAS*, *106*(52), 22480–22485. https://doi.org//10.1073/pnas.0911503106

Cheng, C., Spengler, R. M., Keiser, M. S., Monteys, A. M., Rieders, J. M., Ramachandran, S., & Davidson, B. L. (2018). The long non-coding RNA NEAT1 is elevated in polyglutamine repeat expansion diseases and protects from disease gene-dependent toxicities. *Human Molecular Genetics*, *27*(24), 4303–4314. https://doi.org/10.1093/hmg/ddy331

Choi, D. W. (1988). Glutamate Neurotoxicity and Diseases of the Nervous System. *Neuron*, *1*, 623–634. https://doi.org/10.1016/0896-6273(88)90162-6

Ciarmiello, A., Cannella, M., Lastoria, S., Simonelli, M., Frati, L., Rubinsztein, D. C., & Squitieri, F. (2006). Brain White-Matter Volume Loss and Glucose Hypometabolism Precede the Clinical Symptoms of Huntington's Disease. *The Journal of Nuclear Medicine*, *47*(2), 216–222.

Clemson, C. M., Hutchinson, J. N., Sara, S. A., Ensminger, A. W., Fox, A. H., Chess, A., & Lawrence, J. B. (2009). An Architectural Role for a Nuclear Noncoding RNA: NEAT1 RNA Is Essential for the Structure of Paraspeckles. *Molecular Cell*, *33*(6), 717–726. https://doi.org/10.1016/j.molcel.2009.01.026

Conforti, P., Camnasio, S., Mutti, C., Valenza, M., Thompson, M., Fossale, E., Zeitlin, S., MacDonald, M. E., Zuccato, C., & Cattaneo, E. (2013). Lack of huntingtin promotes neural stem cells differentiation into glial cells while neurons expressing huntingtin with expanded polyglutamine tracts undergo cell death. *Neurobiology of Disease*, *50*(1), 160–170. https://doi.org/10.1016/j.nbd.2012.10.015

Cross, A. J., Slatew, P., & Reynolds, G. P. (1986). Reduced High-Affinity Glutamate Uptake Sites in the Brains of Patients with Huntington's Disease. *Neuroscience Letters*, *67*(2), 198–202. https://doi.org/10.1016/0304-3940(86)90397-6

Ding, Z. bin, Song, L. J., Wang, Q., Kumar, G., Yan, Y. Q., & Ma, C. G. (2021). Astrocytes: A double-edged sword in neurodegenerative diseases. In *Neural Regeneration Research* (Vol. 16, Issue 9, pp. 1702–1710). Wolters Kluwer Medknow Publications. https://doi.org/10.4103/1673-5374.306064

Faideau, M., Kim, J., Cormier, K., Gilmore, R., Welch, M., Auregan, G., Dufour, N., Guillermier, M., Ferrante, R. J., Brouillet, E., Hantraye, P., & De, N. (2010). In vivo expression of polyglutamine-expanded huntingtin by mouse striatal astrocytes impairs glutamate transport: a correlation with Huntington's disease subjects. *Human Molecular Genetics*, *19*(15), 3053–3067. https://doi.org/10.1093/hmg/ddq212

Ferrari Bardile, C., Garcia-Miralles, M., Caron, N. S., Rayan, N. A., Langley, S. R., Harmston, N., Rondelli, A. M., Tang, R., Teo, Y., Waltl, S., Anderson, L. M., Bae, H.-G., Jung, S., Williams, A., Prabhakar, S., Petretto, E., Hayden, M. R., & Pouladi, M. A. (2019). Intrinsic mutant HTT-mediated defects in oligodendroglia cause myelination deficits and behavioral abnormalities in Huntington disease. *PNAS*, *116*(19), 9622–9627. https://doi.org/10.1073/pnas.1818042116

Garcia, V. J., Rushton, D. J., Tom, C. M., Allen, N. D., Kemp, P. J., Svendsen, C. N., & Mattis, V. B. (2019). Huntington's Disease Patient-Derived Astrocytes Display Electrophysiological Impairments and Reduced Neuronal Support. *Frontiers in Neuroscience*, *13*(June), 1–14. https://doi.org/10.3389/fnins.2019.00669

Greenamyre, J. T. (1986). The Role of Glutamate in Neurotransmission and in Neurologic Disease. *Arch Neurol*, *43*(10), 1059–1063. https://doi.org/doi:10.1001/archneur.1986.00520100062016

Haim, L. ben, Sauvage, M. C., Ceyzériat, K., & Curtin, J. F. (2015). Elusive roles for reactive astrocytes in neurodegenerative diseases. *Frontiers in Cellular Neuroscience*, *9*(August), 1–27. https://doi.org/10.3389/fncel.2015.00278

HD iPSC Consortium. (2013). Induced Pluripotent Stem Cells from Patients with Huntington's Disease Show CAG Repeat Expansion Associated Phenotypes. *Cell Stem Cell*, *11*(2), 264–278. https://doi.org/10.1016/j.stem.2012.04.027.Induced

HD iPSC Consortium. (2017). Developmental alterations in Huntington's disease neural cells and pharmacological rescue in cells and mice. *Nature Neuroscience*, *20*(5), 648–660. https://doi.org/10.1038/nn.4532

Hickman, R. A., Faust, · P L, Rosenblum, · M K, Marder, · K, Mehler, · M F, Vonsattel, · J P, & Purpura, D. P. (2021). Developmental malformations in Huntington disease: neuropathologic evidence of focal neuronal migration defects in a subset of adult brains. *Acta Neuropathologica*, *141*, 399–413. https://doi.org/10.1007/s00401-021-02269-4

Hirabayashi, Y., Suzki, N., Tsuboi, M., Endo, T. A., Toyoda, T., Shinga, J., Koseki, H., Vidal, M., & Gotoh, Y. (2009). Polycomb Limits the Neurogenic Competence of Neural Precursor Cells to Promote Astrogenic Fate Transition. *Neuron*, *63*(5), 600–613. https://doi.org/10.1016/j.neuron.2009.08.021

Hirose, T., Virnicchi, G., Tanigawa, A., Naganuma, T., Li, R., Kimura, H., Yokoi, T., Nakagawa, S., Bénard, M., Fox, A. H., & Pierron, G. (2014). NEAT1 long noncoding RNA regulates

transcription via protein sequestration within subnuclear bodies. *Molecular Biology of the Cell*, *25*(1), 169–183. https://doi.org/10.1091/mbc.E13-09-0558

Hodges, A., Strand, A. D., Aragaki, A. K., Kuhn, A., Sengstag, T., Hughes, G., Elliston, L. A., Hartog, C., Goldstein, D. R., Thu, D., Hollingsworth, Z. R., Collin, F., Synek, B., Holmans, P. A., Young, A. B., Wexler, N. S., Delorenzi, M., Kooperberg, C., Augood, S. J., … Luthi-Carter, R. (2006). Regional and cellular gene expression changes in human Huntington's disease brain. *Human Molecular Genetics*, *15*(6), 965–977. https://doi.org/10.1093/hmg/ddl013

Hsiao, H. Y., Chen, Y. C., Huang, C. H., Chen, C. C., Hsu, Y. H., Chen, H. M., Chiu, F. L., Kuo, H. C., Chang, C., & Chern, Y. (2015). Aberrant astrocytes impair vascular reactivity in Huntington disease. *Annals of Neurology*, *78*(2), 178–192. https://doi.org/10.1002/ana.24428

Hu, X., Yuan, Y., Wang, D., & Su, Z. (2016). Heterogeneous astrocytes: Active players in CNS. In *Brain Research Bulletin* (Vol. 125, pp. 1–18). Elsevier Inc. https://doi.org/10.1016/j.brainresbull.2016.03.017

Jiang, R., Diaz-Castro, B., Looger, L. L., & Khakh, B. S. (2016). Dysfunctional Calcium and Glutamate Signaling in Striatal Astrocytes from Huntington's Disease Model Mice. *Journal of Neuroscience*, *36*(12), 3453–3470. https://doi.org/10.1523/JNEUROSCI.3693-15.2016

Juopperi, T. A., Kim, W. R., Chiang, C., Yu, H., Margolis, R. L., Ross, C. A., Ming, G., & Song, H. (2012). Astrocytes generated from patient induced pluripotent stem cells recapitulate features of Huntington's disease patient cells. *Molecular Brain*, *5*(17), 1–14.

Kang, P., Lee, H. K., Glasgow, S. M., Finley, M., Donti, T., Gaber, Z. B., Graham, B. H., Foster, A. E., Novitch, B. G., Gronostajski, R. M., & Deneen, B. (2012). Sox9 and NFIA Coordinate a Transcriptional Regulatory Cascade during the Initiation of Gliogenesis. *Neuron*, *74*(1), 79–94. https://doi.org/10.1016/j.neuron.2012.01.024

Khakh, B. S., Beaumont, V., Cachope, R., Munoz-Sanjuan, I., Goldman, S. A., & Grantyn, R. (2017). Unravelling and Exploiting Astrocyte Dysfunction in Huntington's Disease. *Trends in Neurosciences*, *40*(7), 422–437. https://doi.org/10.1016/j.tins.2017.05.002

Khakh, B. S., & Sofroniew, M. v. (2014). Astrocytes and Huntington's disease. *ACS Chemical Neuroscience*, *5*(7), 494–496. https://doi.org/10.1021/cn500100r

Khakh, B. S., & Sofroniew, M. V. (2015). Diversity of astrocyte functions and phenotypes in neural circuits. *Nature Neuroscience*, *18*(7), 942–952. https://doi.org/10.1038/nn.4043

Kuleshov, M. v., Jones, M. R., Rouillard, A. D., Fernandez, N. F., Duan, Q., Wang, Z., Koplev, S., Jenkins, S. L., Jagodnik, K. M., Lachmann, A., McDermott, M. G., Monteiro, C. D., Gundersen, G. W., & Ma'ayan, A. (2016). Enrichr: a comprehensive gene set enrichment analysis web server 2016 update. *Nucleic Acids Research*, *44*(W1), W90–W97. https://doi.org/10.1093/nar/gkw377

Langfelder, P., Cantle, J. P., Chatzopoulou, D., Wang, N., Gao, F., Al-Ramahi, I., Lu, X. H., Ramos, E. M., El-Zein, K., Zhao, Y., Deverasetty, S., Tebbe, A., Schaab, C., Lavery, D. J., Howland, D., Kwak, S., Botas, J., Aaronson, J. S., Rosinski, J., … Yang, X. W. (2016).

Integrated genomics and proteomics define huntingtin CAG length-dependent networks in mice. *Nature Neuroscience*, *19*(4), 623–633. https://doi.org/10.1038/nn.4256

Lee, W., Reyes, R. C., Gottipati, M. K., Lewis, K., Lesort, M., Parpura, V., & Gray, M. (2013). Enhanced Ca2+-dependent glutamate release from astrocytes of the BACHD Huntington's disease mouse model. *Neurobiology of Disease*, *58*, 192–199. https://doi.org/10.1016/j.nbd.2013.06.002

Lehre, K. P., Levy, L. M., Ottersen, O. P., Storm-Mathisen, J., & Danbolt, N. C. (1995). Differential Expression of Two Glial Glutamate Transporters in the Rat Brain: Quantitative and Immunocytochemical Observations. *The Journal of Neuroscience*, *15*(3), 1835–1853. https://doi.org/10.1523/JNEUROSCI.15-03-01835.1995

Liddelow, S. A., Guttenplan, K. A., Clarke, L. E., Bennett, F. C., Bohlen, C. J., Schirmer, L., Bennett, M. L., Münch, A. E., Chung, W., Peterson, T. C., & Wilton, D. K. (2017). Neurotoxic reactive astrocytes are induced by activated microglia. *Nature*, *541*(7638), 481–487. https://doi.org/10.1038/nature21029

Lim, R. G., Quan, C., Reyes-Ortiz, A. M., Lutz, S. E., Kedaigle, A. J., Gipson, T. A., Wu, J., Vatine, G. D., Stocksdale, J., Casale, M. S., Svendsen, C. N., Fraenkel, E., Housman, D. E., Agalliu, D., & Thompson, L. M. (2017). Huntington's Disease iPSC-Derived Brain Microvascular Endothelial Cells Reveal WNT-Mediated Angiogenic and Blood-Brain Barrier Deficits. *Cell Reports*, *19*(7), 1365–1377. https://doi.org/10.1016/j.celrep.2017.04.021

Lin, C. H., Tallaksen-Greene, S., Chien, W. M., Cearley, J. A., Jackson, W. S., Crouse, A. B., Ren, S., Li, X. J., Albin, R. L., & Detloff, P. J. (2001). Neurological abnormalities in a knock-in mouse model of Huntington's disease. *Human Molecular Genetics*, *10*(2), 137–144. https://doi.org/10.1093/hmg/10.2.137

Luthi-Carter, R., Hanson, S. A., Strand, A. D., Bergstrom, D. A., Chun, W., Peters, N. L., Woods, A. M., Chan, E. Y., Kooperberg, C., Krainc, D., Young, A. B., Tapscott, S. J., & Olson, J. M. (2002). Dysregulation of gene expression in the R6/2 model of polyglutamine disease: parallel changes in muscle and brain. *Human Molecular Genetics*, *11*(17), 1911–1926. www.neumetrix.info.

Mangiarini, L., Sathasivam, K., Seller, M., Cozens, B., Harper, A., Hetherington, C., Lawton, M., Trottier, Y., Lehrach, H., Davies, S. W., & Bates, G. P. (1996). Exon 1 of the HD Gene with an Expanded CAG Repeat Is Sufficient to Cause a Progressive Neurological Phenotype in Transgenic Mice. *Cell*, *87*, 493–506. http://ac.els-cdn.com/S0092867400813690/1-s2.0-S0092867400813690-main.pdf?_tid=7db7695e-7afe-11e7-94f8-00000aacb35d&acdnat=1502062090_1e45eb383db00141a08e5daa67072892

Mattis, V. B., Svendsen, S. P., Ebert, A., Svendsen, C. N., King, A. R., Casale, M., Winokur, S. T., Batugedara, G., Vawter, M., Peter, J., Gillis, T., Mysore, J., Li, J., Seong, I., Shen, Y., Arbez, N., Juopperi, T., Ratovitski, T., Chiang, J. H., … Cole, R. N. (2013). Induced Pluripotent Stem Cells from Patients with Huntington's Disease Show CAG-Repeat-Expansion-Associated Phenotypes. *Cell Stem Cell*, *11*(2), 264–278. https://doi.org/10.1016/j.stem.2012.04.027.Induced

Mattis, V. B., Tom, C., Akimov, S., Saeedian, J., Østergaard, M. E., Southwell, A. L., Doty, C. N., Ornelas, L., Sahabian, A., Lenaeus, L., Mandefro, B., Sareen, D., Arjomand, J., Hayden, M. R., Ross, C. A., & Svendsen, C. N. (2014). HD iPSC-derived neural progenitors

accumulate in culture and are susceptible to BDNF withdrawal due to glutamate toxicity. *Human Molecular Genetics*, *24*(11), 3257–3271. https://doi.org/10.1093/hmg/ddv080

McClory, H., Williams, D., Sapp, E., Gatune, L. W., Wang, P., DiFiglia, M., & Li, X. (2014). Glucose transporter 3 is a rab11-dependent trafficking cargo and its transport to the cell surface is reduced in neurons of CAG140 Huntington's disease mice. *Acta Neuropathologica Communications*, *2*(179). https://doi.org/10.1186/s40478-014-0178-7

Milnerwood, A. J., Gladding, C. M., Pouladi, M. A., Kaufman, A. M., Hines, R. M., Boyd, J. D., Ko, R. W. Y., Vasuta, O. C., Graham, R. K., Hayden, M. R., Murphy, T. H., & Raymond, L. A. (2010). Early Increase in Extrasynaptic NMDA Receptor Signaling and Expression Contributes to Phenotype Onset in Huntington•s Disease Mice. *Neuron*, *65*, 178–190. https://doi.org/10.1016/j.neuron.2010.01.008

Mueller, K. A., Glajch, K. E., Huizenga, M. N., Wilson, R. A., Granucci, E. J., Dios, A. M., Tousley, A. R., Iuliano, M., Weisman, E., Laquaglia, M. J., Difiglia, M., Kegel-Gleason, K., Vakili, K., & Sadri-Vakili, G. (2018). Hippo Signaling Pathway Dysregulation in Human Huntington's Disease Brain and Neuronal Stem Cells. *Scientific Reports*, *8*(11355). https://doi.org/10.1038/s41598-018-29319-4

Myers, R. H., Vonsattel, J. P., Paskevich, P. A., Kiely, D. K., Stevens, T. J., Cupples, L. A., Jr, E. P. R., & Bird, E. D. (1991). Decreased neuronal and increased oligodendroglial densities in Huntington's disease caudate nucleus. *Journal of Neuropathology and Experimental Neurology*, *50*(6), 729–742. https://doi.org/10.1097/00005072-199111000-00005.

Nance, M. A., & Myers, R. H. (2001). Juvenile onset Huntington's disease — clinical and research perspectives. *Ment Retard Dev Disabil Res Rev.*, *7*, 153–157.

Oberheim, N. A., Takano, T., Han, X., He, W., Lin, J. H. C., Wang, F., Xu, Q., Wyatt, J. D., Pilcher, W., Ojemann, J. G., Ransom, B. R., Goldman, S. A., & Nedergaard, M. (2009). Uniquely Hominid Features of Adult Human Astrocytes. *Journal of Neuroscience*, *29*(10), 3276–3287. https://doi.org/10.1523/JNEUROSCI.4707-08.2009

Osipovitch, M., Martinez, A. A., Mariani, J. N., Cornwell, A., Dhaliwal, S., Zou, L., Chandler-Militello, D., Wang, S., Li, X., Benraiss, S.-J., Agate, R., Lampp, A., Benraiss, A., Windrem, M. S., & Goldman, S. A. (2019). Human ESC-Derived Chimeric Mouse Models of Huntington's Disease Reveal Cell-Intrinsic Defects in Glial Progenitor Cell Differentiation. *Cell Stem Cell*, *24*(1), 107–122. https://doi.org/10.1016/j.stem.2018.11.010

Reddy, P. H., Williams, M., Charles, V., Garrett, L., Pike-Buchanan, L., Whetsell, W. O., Miller, G., & Tagle, D. A. (1998). Behavioural abnormalities and selective neuronal loss in HD transgenic mice expressing mutated full-length HD cDNA. *Nature Genetics*, *20*(2), 198–202. https://doi.org/10.1038/2510

Ring, K. L., An, M. C., Zhang, N., O'Brien, R. N., Ramos, E. M., Gao, F., Atwood, R., Bailus, B. J., Melov, S., Mooney, S. D., Coppola, G., & Ellerby, L. M. (2015). Genomic Analysis Reveals Disruption of Striatal Neuronal Development and Therapeutic Targets in Human Huntington's Disease Neural Stem Cells. *Stem Cell Reports*, *5*(6), 1023–1038. https://doi.org/10.1016/j.stemcr.2015.11.005

Ross, C. A., & Tabrizi, S. J. (2011). Huntington's disease: from molecular pathogenesis to clinical treatment. *The Lancet Neurology*, *10*(1), 83–98. https://doi.org/10.1016/S1474-4422(10)70245-3

Rothstein, J. D., Dykes-Hoberg, M., Pardo, C. A., Bristol, L., Jin, L., Kuncl, R. W., Kanai, Y., Hediger, M. A., Wang, Y., Schielke, J. P., & Welty, D. (1996). Knockout of Glutamate Transporters Reveals a Major Role for Astroglial Transport in Excitotoxicity and Clearance of Glutamate. *Neuron*, *16*, 675–686. https://doi.org/10.1016/s0896-6273(00)80086-0

Rothstein, J. D., Martin, L., Levey, A. I., Dykes-Hoberg, M., Jin, L., Wu, D., Nash, N., & Kuncl, R. W. (1994). Localization of Neuronal and Glial Glutamate Transporters. *Neuron*, *13*, 713–725. https://doi.org/10.1016/0896-6273(94)90038-8

Sanchez, I. I., Nguyen, T. B., England, W. E., Lim, R. G., Vu, A. Q., Miramontes, R., Byrne, L. M., Markmiller, S., Lau, A. L., Orellana, I., Curtis, M. A., Maxwell Faull, R. L., Yeo, G. W., Fowler, C. D., Reidling, J. C., Wild, E. J., Spitale, R. C., & Thompson, L. M. (2021). Huntington's disease mice and human brain tissue exhibit increased G3BP1 granules and TDP43 mislocalization. *Journal of Clinical Investigation*, *131*(12). https://doi.org/10.1172/JCI140723

Sapp, E., Kegel, K. B., Aronin, N., Hashikawa, T., Uchiyama, Y., Tohyama, K., Bhide, P. G., Vonsattel, J. P., & Difiglia, M. (2001). Early and progressive accumulation of reactive microglia in the Huntington disease brain. *Journal of Neuropathology and Experimental Neurology*, *60*(2), 161–172. https://doi.org/10.1093/jnen/60.2.161

Selkoe, D. J., Salasar, F. J., Abraham, C., & Kosik, K. S. (1982). Huntington's disease: Changes in striatal proteins reflect astrocytic gliosis. *Brain Research*, *245*(1), 117–125. https://doi.org/10.1016/0006-8993(82)90344-4

Seong, I. S., Woda, J. M., Song, J.-J., Lloret, A., Abeyrathne, P. D., Woo, C. J., Gregory, G., Lee, J.-M., Wheeler, V. C., Walz, T., Kingston, R. E., Gusella, J. F., Conlon, R. A., & Macdonald, M. E. (2010). Huntingtin facilitates polycomb repressive complex 2. *Human Molecular Genetics*, *19*(4), 573–583. https://doi.org/10.1093/hmg/ddp524

Smith-Geater, C., Hernandez, S. J., Lim, R. G., Adam, M., Wu, J., Stocksdale, J. T., Wassie, B. T., Gold, M. P., Wang, K. Q., Miramontes, R., Kopan, L., Orellana, I., Joy, S., Kemp, P. J., Allen, N. D., Fraenkel, E., & Thompson, L. M. (2020). Aberrant Development Corrected in Adult-Onset Huntington's Disease iPSC-Derived Neuronal Cultures via WNT Signaling Modulation. *Stem Cell Reports*, *14*, 406–419. https://doi.org/10.1016/j.stemcr.2020.01.015

Sofroniew, M. v, & Vinters, H. v. (2010). Astrocytes: biology and pathology. *Acta. Neuropathol.*, *119*, 7–35. https://doi.org/10.1007/s00401-009-0619-8

Stuart, T., Butler, A., Hoffman, P., Hafemeister, C., Papalexi, E., Mauck, W. M., Hao, Y., Stoeckius, M., Smibert, P., & Satija, R. (2019). Comprehensive Integration of Single-Cell Data. *Cell*, *177*(7), 1888-1902.e21. https://doi.org/10.1016/j.cell.2019.05.031

Sun, W., McConnell, E., Pare, J.-F., Xu, Q., Chen, M., Peng, W., Lovatt, D., Han, X., Smith, Y., & Nedergaard, M. (2013). Glutamate-Dependent Neuroglial Calcium Signaling Differs Between Young and Adult Brain. *Science*, *339*(6116), 197–200. https://doi.org/10.1126/science.1226740.Glutamate-Dependent

The Huntington's Disease Collaborative Research Group. (1993). *A Novel Gene Containing a Trinucleotide That Is Expanded and Unstable on Huntington's Disease Chromosomes*. *72*, 971–983.

Tiwari, N., Pataskar, A., Péron, S., Thakurela, S., Sahu, S. K., Figueres-Oñate, M., Marichal, N., López-Mascaraque, L., Tiwari, V. K., & Berninger, B. (2018). Stage-Specific Transcription Factors Drive Astrogliogenesis by Remodeling Gene Regulatory Article Stage-Specific Transcription Factors Drive Astrogliogenesis by Remodeling Gene Regulatory Landscapes. *Cell Stem Cell*, *23*, 557–571. https://doi.org/10.1016/j.stem.2018.09.008

Tong, X., Ao, Y., Faas, G. C., Nwaobi, S. E., Xu, J., Haustein, M. D., Anderson, M. A., Mody, I., Olsen, M. L., Sofroniew, M. v., & Khakh, B. S. (2014). Astrocyte Kir4.1 ion channel deficits contribute to neuronal dysfunction in Huntington's disease model mice. *Nature Neuroscience*, *17*(5), 694–703. https://doi.org/10.1038/nn.3691

Trapnell, C. (2015). Defining cell types and states with single-cell genomics. *Genome Research*, *25*(10), 1491–1498. https://doi.org/10.1101/gr.190595.115

Yu, Z.-X., Li, S.-H., Evans, J., Pillarisetti, A., Li, H., & Li, X.-J. (2003). Mutant huntingtin causes context-dependent neurodegeneration in mice with Huntington's disease. *The Journal of Neuroscience : The Official Journal of the Society for Neuroscience*, *23*(6), 2193–2202. https://doi.org/23/6/2193 [pii]

Zhang, Y., Chen, K., Sloan, S. A., Bennett, M. L., Scholze, A. R., Keeffe, S. O., Phatnani, H. P., Guarnieri, X. P., Caneda, C., Ruderisch, N., Deng, S., Liddelow, S. A., Zhang, C., Daneman, R., Maniatis, T., Barres, X. B. A., & Wu, X. J. Q. (2014). An RNA-Sequencing Transcriptome and Splicing Database of Glia, Neurons, and Vascular Cells of the Cerebral Cortex. *The Journal of Neuroscience*, *34*(36), 11929–11947. https://doi.org/10.1523/JNEUROSCI.1860-14.2014

Zhang, Y., Sloan, S. A., Clarke, L. E., Grant, G. A., Gephart, M. G. H., Barres, B. A., Zhang, Y., Sloan, S. A., Clarke, L. E., Caneda, C., Plaza, C. A., & Blumenthal, P. D. (2016). Purification and Characterization of Progenitor and Mature Human Astrocytes Reveals Transcriptional and Functional Differences with Mouse. *Neuron*, *89*(1), 37–53. https://doi.org/10.1016/j.neuron.2015.11.013

Zhao, Z., Nelson, A. R., Betsholtz, C., & Zlokovic, B. v. (2015). Establishment and Dysfunction of the Blood-Brain Barrier. *Cell*, *163*(5), 1064–1078. https://doi.org/10.1016/j.cell.2015.10.067

Zuccato, C., Valenza, M., & Cattaneo, E. (2010). Molecular Mechanisms and Potential Therapeutical Targets in Huntington's Disease. *Physiol Rev*, *90*, 905–981. https://doi.org/10.1152/physrev.00041.2009.

4.7 Supplemental Figures

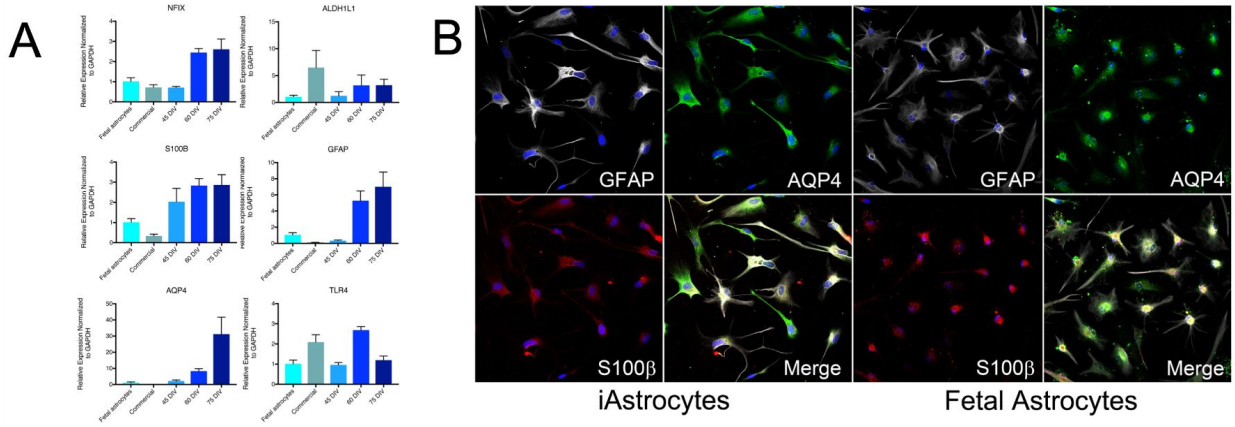

Supplemental Figure 4.1. iAstro Differentiation Compared to Other human Astrocyte Cell Lines. (A) Quantitative PCR on astrocyte marker transcripts compared to human fetal and commercially available astrocytes. (B) Immunocytochemistry of astrocyte marker proteins compared to human fetal astrocytes.

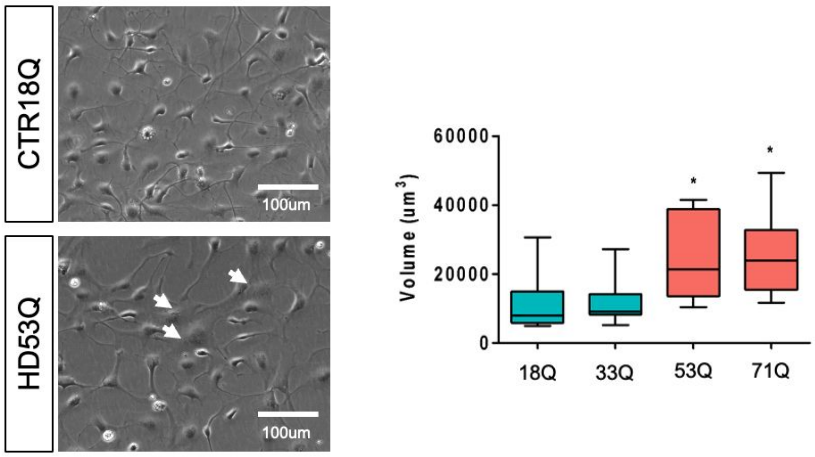

Supplemental Figure 4.2. HD and Control iAstro Morphology Differences. (A) Representative phase contrast images of unsorted day 60 iAstros morphology. HD iAstro white arrows highlight HD iAstros with enlarged cell bodies. (B) Quantification of cellular volume by confocal z-stacks of GFAP-positive iAstros at day 60. n = 3 biological (differentiation replicates) *p<0.05.

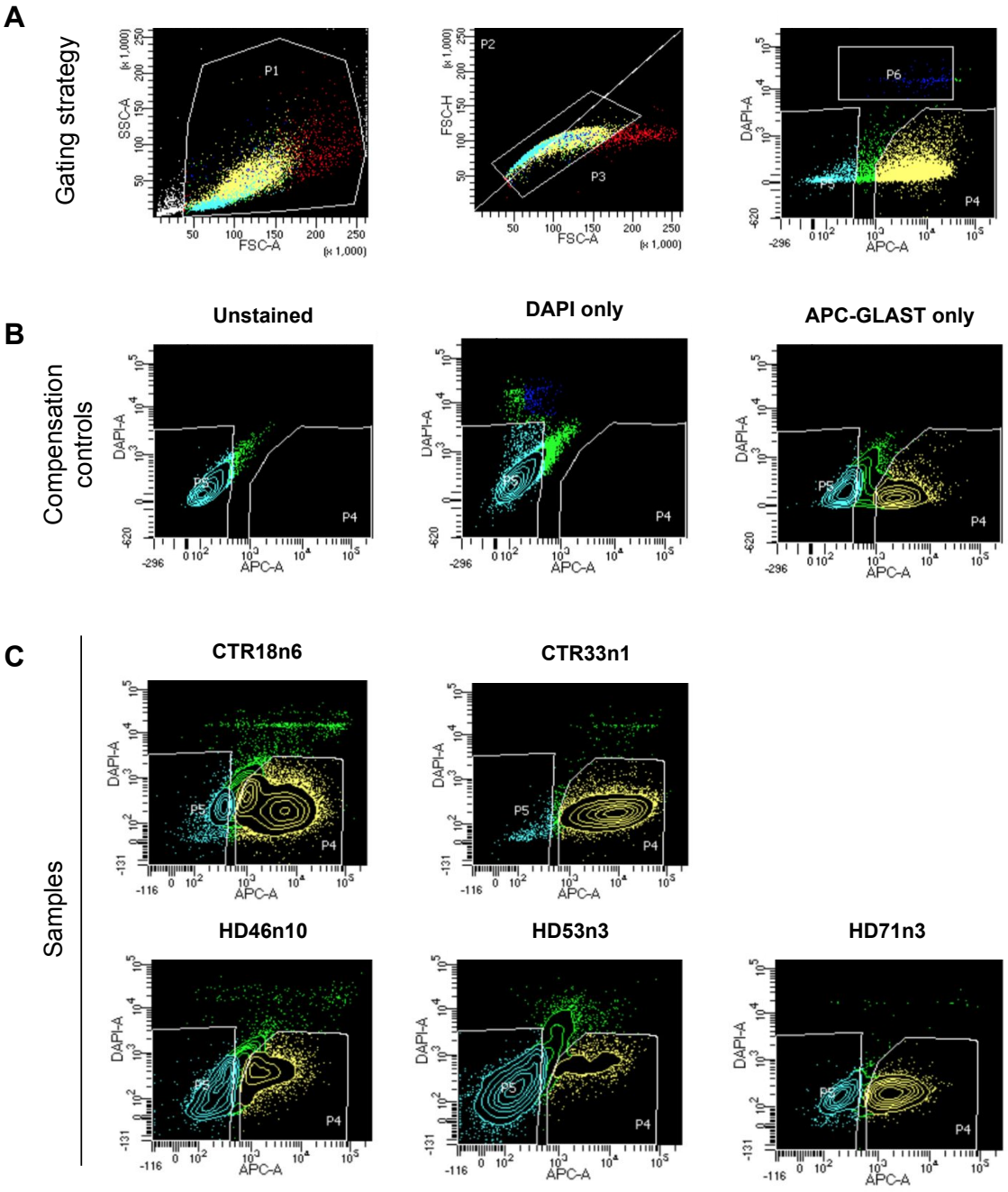

Supplemental Figure 4.3. Representative FACS Plots for iAstro Enrichment. (A) Gating strategy to remove cellular debris and select single cells. (B) Compensation controls for unstained cells and single-stains of DAPI only and APC-GLAST only. (C) Representative FACS plot for each day 60 iAstro cell line.

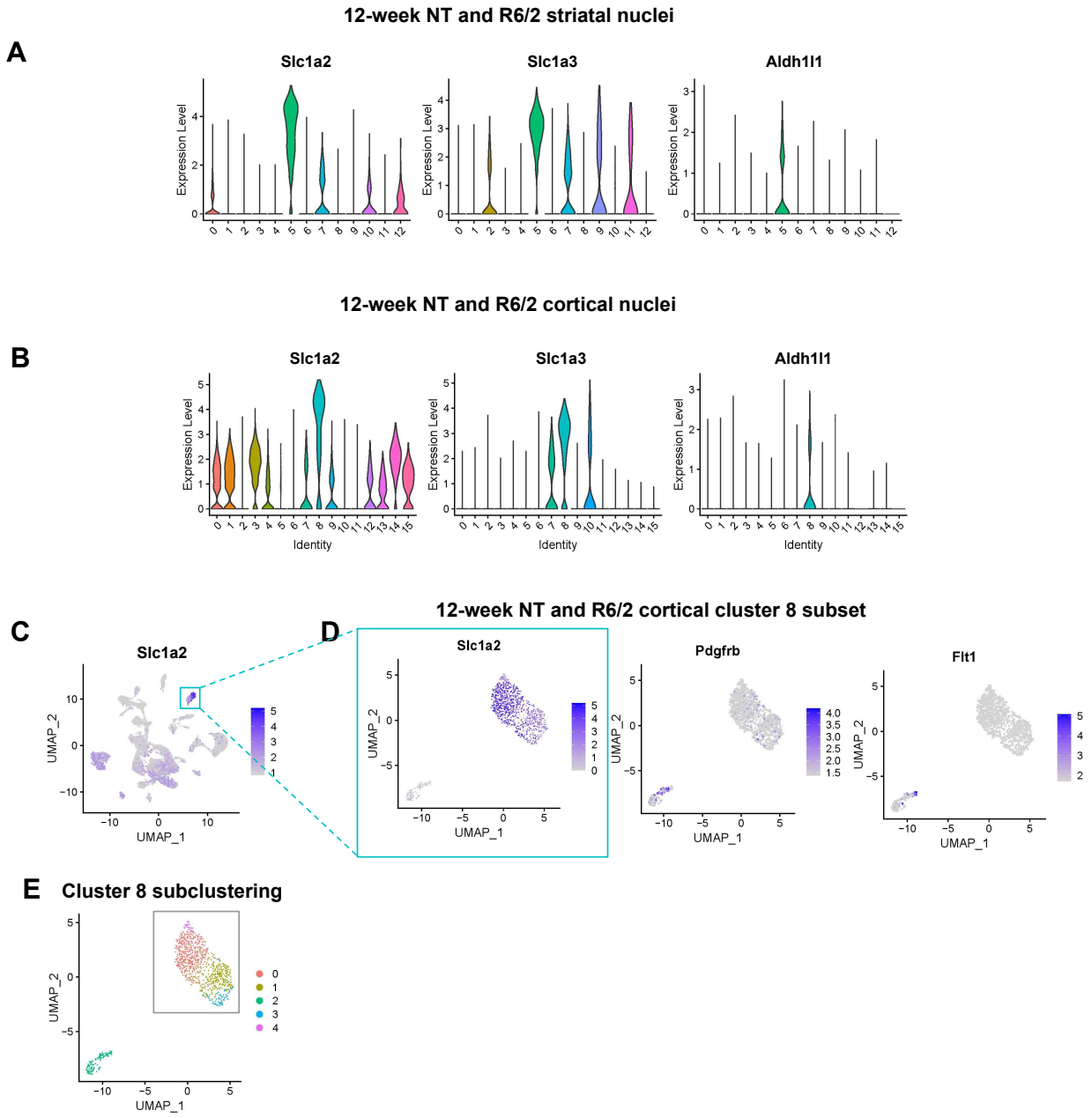

Supplemental Figure 4.4. Astrocyte Cluster Selection for NT and R6/2 12-Week Striatal and Cortical snRNA-seq. (A) Violin plots of astrocyte markers depict striatal cluster 5 as the astrocyte cluster by highest astrocyte marker expression. (B-D) Violin plots (B) and UMAP visulization (C) of astrocyte markers depict cortical cluster 8 as the astrocyte cluster by highest astrocyte marker expression. (D) Subset of cortical cluster 8 with expression astrocyte markers and vascular markers shows multiple cell types. (E) Clustering analysis of cortical cluster 8 deomstrates subcluster 2 (green) contains significantly different gene expression compared to other subclusters. Subclusters 0, 1, 3, 4 (gray box) were subset and deemed the revised cortical astrocyte cluster for subsequent cortical analyses.

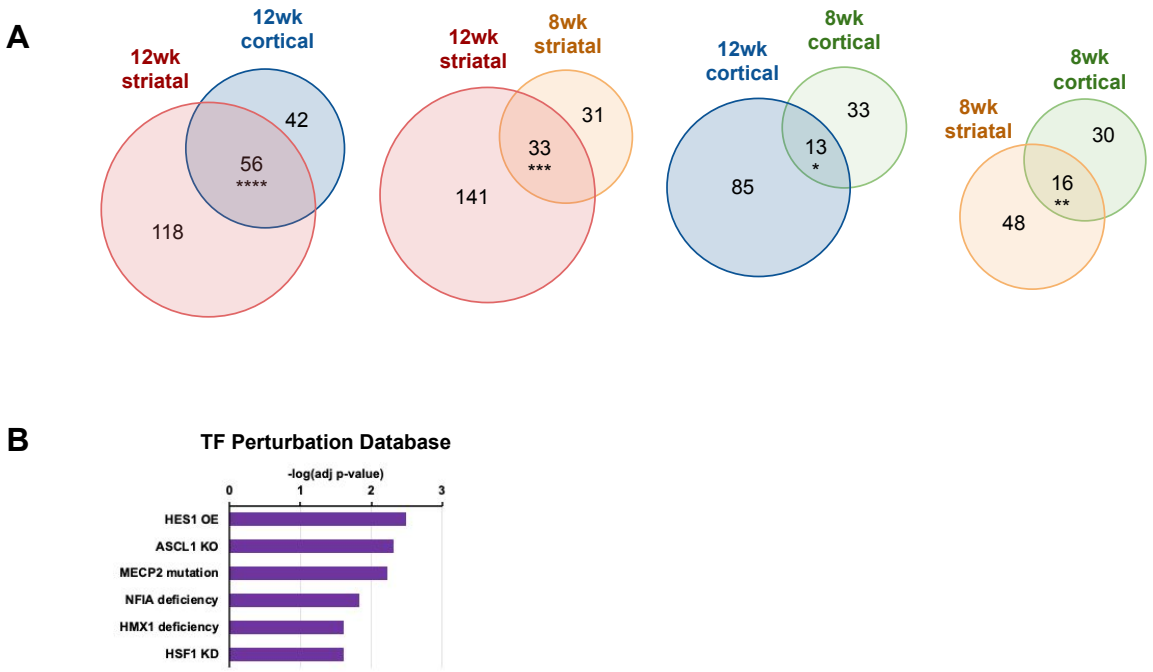

Supplemental Figure 4.5. R6/2 Astrocyte Differentially Expressed Gene Overlaps and Transcription Factor Enrichment. (A) Venn diagrams of significant differentially expressed genes (DEGs) in R6/2 mouse astrocytes across time points and brain region (Exact hypergeometric probability calculated using 56 DEG overlap for 12 week striatum [174] vs 12 week cortex [98] ****p < 7.190e-113, 33 DEG overlap for 12 week striatum [174] vs 8 week striatum [64] ***p < 6.427e-64, 13 DEG overlap for 12 week cortex [98] vs 8 week cortex [46] *p < 7.335e-25, 16 DEG overlap for 8 week striatum [64] vs 8 week cortex [46] **p < 2.281e-35 using 46,206 as the number of genes with nucleotide sequence data in the mouse genome database). (B) Overlap of R6/2 12wk striatal and 12wk cortical astrocyte DEGs predicted transcription factor regulation using Enrichr.

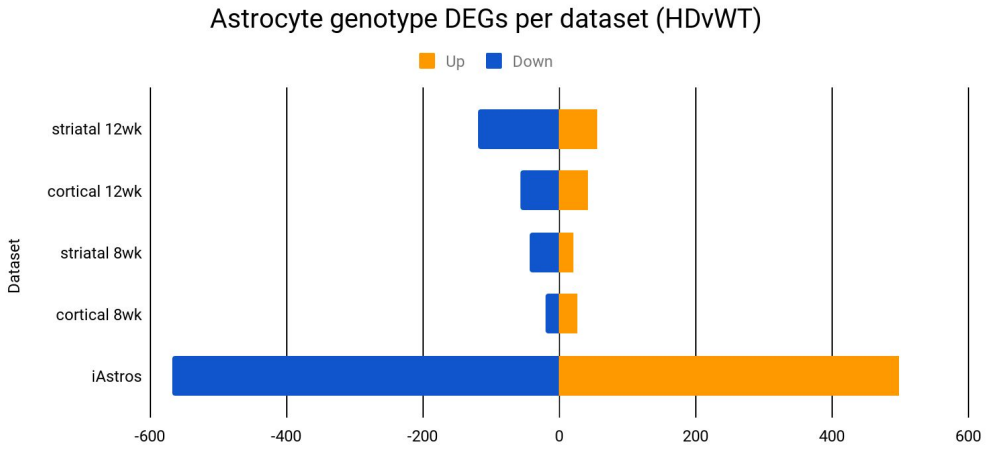

Supplemental Figure 4.6. Genotype DEG Counts. R6/2 astrocyte and HD iAstro significant differentially expressed gene count. Orange represents an upregulated gene and blue represents a downregulated gene count.

4.8 Tables

Table 4.8.1. R6/2 12-Week Striatal Astrocyte Significant Differentially Expressed Genes

Gene	p_val	avg_logFC	pct.1	pct.2	p_val_adj
Farp1	2.83E-87	-0.6025293049	0.816	0.957	7.93E-83
Slc1a2	5.26E-81	-0.5929855476	0.929	0.993	1.47E-76
Qk	2.46E-80	-0.4571416613	0.955	0.989	6.88E-76
Gm3764	7.74E-73	-0.477757083	0.932	0.982	2.17E-68
Atp1a2	7.15E-69	-0.4825047855	0.815	0.961	2.00E-64
Etnppl	3.91E-61	-0.9529915398	0.088	0.379	1.09E-56
Lsamp	1.85E-59	-0.2724676744	0.996	1	5.18E-55
Cables1	1.33E-55	-0.7162233874	0.321	0.625	3.73E-51
Ttyh1	2.02E-48	-0.467716787	0.672	0.858	5.64E-44
Sparcl1	2.16E-46	-0.4670477125	0.744	0.9	6.04E-42
Hif3a	5.94E-44	-0.685237795	0.183	0.442	1.66E-39
Mical2	1.33E-43	-0.5296972272	0.448	0.691	3.73E-39
Abca1	7.53E-43	0.4706447972	0.826	0.631	2.11E-38
Gria2	8.01E-43	-0.4319903804	0.81	0.919	2.24E-38
Acsl3	1.42E-40	-0.4745250889	0.591	0.801	3.98E-36
Glul	2.95E-40	-0.5349906258	0.439	0.694	8.26E-36
Phkg1	1.00E-39	-0.4615852365	0.661	0.842	2.80E-35
Pitpnc1	3.33E-39	-0.4343576075	0.934	0.97	9.31E-35
Kcnn2	4.63E-39	-0.6269814867	0.407	0.637	1.30E-34
Zbtb16	7.58E-37	-0.7490911955	0.122	0.337	2.12E-32
Polr2a	1.22E-36	0.6246740655	0.377	0.149	3.41E-32
Slc4a4	2.79E-36	-0.3798458463	0.91	0.954	7.81E-32
Tpk1	4.59E-36	0.6239557784	0.362	0.133	1.29E-31
D030047H15Rik	1.06E-34	-0.5105373396	0.294	0.524	2.98E-30
Igsf8	3.21E-34	-0.4476908837	0.433	0.649	8.98E-30
Paqr8	1.49E-33	-0.4832290047	0.493	0.706	4.18E-29
Ntsr2	2.58E-33	-0.4510600323	0.45	0.671	7.22E-29
Mertk	2.60E-33	-0.454028863	0.741	0.856	7.29E-29
Csrp1	2.36E-32	-0.4728301955	0.458	0.673	6.60E-28
Rnf121	5.61E-32	-0.6511529004	0.374	0.556	1.57E-27
Grin2c	4.01E-31	-0.4985858123	0.276	0.496	1.12E-26
Gm12695	4.17E-30	0.3530480096	0.118	0.001	1.17E-25
Plpp3	5.92E-30	-0.2667637487	0.849	0.963	1.66E-25
Camk2g	1.77E-29	-0.3955499825	0.657	0.806	4.96E-25
Mapk4	5.19E-29	-0.4185037171	0.607	0.774	1.45E-24
Agbl4	7.64E-29	0.5750334966	0.544	0.325	2.14E-24
Htra1	6.14E-28	-0.4364528741	0.535	0.701	1.72E-23
Guf1	8.52E-28	0.504143576	0.34	0.147	2.39E-23
Gm26704	2.34E-27	-0.4272073459	0.435	0.639	6.56E-23

Tspan7	4.33E-27	-0.3931479279	0.685	0.821	1.21E-22
Tra2a	5.03E-27	0.4256440542	0.777	0.609	1.41E-22
Nwd1	8.53E-27	-0.3643507843	0.557	0.768	2.39E-22
Angpt1	1.01E-26	0.5164732913	0.212	0.056	2.83E-22
Phka1	8.19E-26	-0.4449135135	0.586	0.715	2.29E-21
Fgf14	1.40E-25	0.320251689	0.947	0.924	3.93E-21
Ntrk2	3.82E-25	-0.3228102322	0.905	0.95	1.07E-20
Ndrg2	3.16E-24	-0.3942639065	0.499	0.672	8.83E-20
Sncaip	7.61E-24	0.4889876604	0.369	0.175	2.13E-19
Ddx5	1.24E-23	0.3171122508	0.902	0.814	3.46E-19
Fam107a	3.09E-23	-0.434815195	0.16	0.332	8.66E-19
Myrip	9.07E-23	-0.4164262887	0.23	0.413	2.54E-18
March3	3.83E-22	0.4625438487	0.375	0.189	1.07E-17
Trim9	4.79E-22	-0.309230578	0.742	0.845	1.34E-17
Sctr	1.93E-21	0.3670416091	0.158	0.037	5.40E-17
Sox5	4.00E-21	0.3053044425	0.866	0.782	1.12E-16
Pde10a	6.37E-21	-0.8146820501	0.14	0.295	1.78E-16
Agt	1.06E-20	-0.4319253084	0.05	0.173	2.98E-16
Gm4876	1.49E-20	0.4700544746	0.301	0.14	4.17E-16
Camk2d	1.50E-20	0.3447422145	0.745	0.607	4.19E-16
F3	1.63E-20	-0.4031696244	0.451	0.612	4.58E-16
Nebl	1.70E-20	-0.3574193191	0.647	0.767	4.77E-16
Sat1	2.04E-20	-0.4008576405	0.294	0.47	5.72E-16
Clmn	4.37E-20	-0.342783772	0.474	0.659	1.22E-15
Ccnd3	7.23E-20	-0.4555194088	0.272	0.444	2.02E-15
Naaladl2	7.76E-20	0.4114742439	0.625	0.45	2.17E-15
Gm44151	8.21E-20	-0.4001019152	0.251	0.421	2.30E-15
Glud1	1.19E-19	-0.3006724353	0.708	0.828	3.34E-15
Sgcd	3.70E-19	0.6877180337	0.414	0.254	1.04E-14
Galnt18	6.25E-19	-0.5388525837	0.267	0.425	1.75E-14
Ptprk	7.82E-19	0.3977055898	0.199	0.07	2.19E-14
Slc25a21	9.63E-19	0.4471674685	0.375	0.205	2.70E-14
Cst3	1.30E-18	-0.2888982262	0.707	0.841	3.65E-14
Sema6a	2.06E-18	0.4141130974	0.376	0.208	5.76E-14
Gjb6	2.58E-18	-0.3763580998	0.124	0.266	7.23E-14
Phactr3	2.70E-18	-0.2979283251	0.615	0.751	7.55E-14
Sfmbt2	3.35E-18	0.3476548869	0.191	0.066	9.37E-14
Itih3	4.58E-18	-0.6321787362	0.254	0.39	1.28E-13
Ldlr	8.58E-18	-0.3200131923	0.085	0.215	2.40E-13
A930015D03Rik	1.12E-17	0.328694302	0.332	0.171	3.14E-13
Lrig1	1.21E-17	-0.4465683365	0.464	0.594	3.39E-13
Ddx60	2.27E-17	0.2536547629	0.109	0.019	6.35E-13
Fam20a	3.20E-17	-0.3433556197	0.435	0.596	8.95E-13

Slc6a11	6.37E-17	-0.5331069297	0.609	0.696	1.78E-12
Gm6277	6.88E-17	-0.4044728132	0.111	0.244	1.93E-12
Plcb1	8.34E-17	-0.3291474029	0.812	0.893	2.33E-12
Metap1d	8.66E-17	0.3606416928	0.44	0.271	2.42E-12
5031439G07Rik	1.16E-16	-0.4318027617	0.364	0.511	3.25E-12
Mmd2	1.22E-16	-0.269293777	0.636	0.771	3.41E-12
Creb5	1.29E-16	0.3681346457	0.163	0.053	3.62E-12
Cadm1	1.47E-16	-0.2628362303	0.92	0.938	4.11E-12
Ubb	1.98E-16	0.3207481497	0.429	0.261	5.55E-12
Adrbk2	2.30E-16	-0.2573415846	0.681	0.801	6.43E-12
Gm12239	5.06E-16	-0.3354835191	0.43	0.602	1.42E-11
4930578G10Rik	6.66E-16	-0.3814275425	0.091	0.212	1.87E-11
Daam2	6.84E-16	-0.2706053202	0.521	0.674	1.92E-11
Trpm3	7.42E-16	-0.2847495697	0.907	0.944	2.08E-11
Zfp950	1.16E-15	0.3365119931	0.504	0.349	3.24E-11
Acss2	1.53E-15	-0.3049178248	0.115	0.243	4.29E-11
Rmst	1.68E-15	-0.4164845917	0.492	0.624	4.72E-11
Robo2	3.79E-15	0.4213793453	0.445	0.303	1.06E-10
4930448N21Rik	6.84E-15	-0.2896692364	0.553	0.671	1.92E-10
2310022B05Rik	9.26E-15	-0.3496843948	0.15	0.275	2.59E-10
Lhfp	1.01E-14	-0.4466906865	0.663	0.728	2.84E-10
Trim2	1.11E-14	0.342322232	0.476	0.322	3.12E-10
Gm13872	1.62E-14	-0.2913878249	0.099	0.217	4.55E-10
Akt3	1.72E-14	0.2684628896	0.777	0.675	4.83E-10
Dclk1	1.81E-14	-0.2971871069	0.731	0.801	5.07E-10
Ahcyl1	1.90E-14	-0.2847464776	0.512	0.647	5.33E-10
Dpyd	2.18E-14	0.357014608	0.532	0.384	6.10E-10
Ogt	2.54E-14	0.2834064127	0.799	0.691	7.11E-10
Arid5b	2.73E-14	0.3773733865	0.339	0.202	7.65E-10
Atp9a	3.71E-14	0.2702314688	0.174	0.067	1.04E-09
Gm9925	4.10E-14	-0.3370781019	0.222	0.355	1.15E-09
Msmo1	4.54E-14	-0.336755654	0.109	0.225	1.27E-09
Adcy2	6.51E-14	-0.2745345491	0.673	0.771	1.82E-09
Mycbp	6.70E-14	0.3130414286	0.313	0.176	1.88E-09
Vegfa	6.73E-14	-0.3454102137	0.279	0.414	1.88E-09
Ccdc148	7.45E-14	0.3642368408	0.246	0.125	2.09E-09
Wnk2	8.19E-14	-0.3543288085	0.497	0.606	2.29E-09
Mob3b	8.57E-14	0.3797574414	0.182	0.075	2.40E-09
Tsc22d3	9.36E-14	-0.3620242513	0.094	0.203	2.62E-09
Padi2	1.03E-13	-0.3915827629	0.111	0.223	2.89E-09
L3mbtl3	1.13E-13	0.3451815319	0.492	0.34	3.16E-09
Eps8	1.20E-13	-0.3083600005	0.542	0.673	3.35E-09
Nt5c2	1.55E-13	-0.2823394111	0.413	0.555	4.35E-09

Gm26835	2.13E-13	-0.3251687388	0.312	0.447	5.97E-09
Kank1	2.23E-13	-0.2653098851	0.495	0.638	6.25E-09
Gm26843	2.83E-13	-0.2941130663	0.268	0.416	7.91E-09
Smox	4.78E-13	-0.2861042703	0.25	0.386	1.34E-08
9530026P05Rik	4.81E-13	0.3743040316	0.413	0.273	1.35E-08
Nkx6-2	9.46E-13	-0.3019736895	0.035	0.113	2.65E-08
Kif21a	9.58E-13	0.2527035365	0.643	0.483	2.68E-08
Snhg20	1.42E-12	0.2661516297	0.282	0.155	3.97E-08
Ifi27	1.61E-12	0.3117998396	0.228	0.115	4.50E-08
Rapgef3	1.78E-12	-0.3016315628	0.383	0.506	4.98E-08
Prodh	2.04E-12	-0.3030223722	0.264	0.394	5.71E-08
Rtn1	2.08E-12	0.2860569449	0.482	0.34	5.82E-08
2210408I21Rik	2.10E-12	0.2878034791	0.48	0.336	5.88E-08
Chuk	2.15E-12	0.3024946002	0.352	0.223	6.02E-08
Bcl6	3.06E-12	-0.3448440862	0.221	0.34	8.57E-08
Pnpla7	3.29E-12	-0.3091624819	0.456	0.564	9.20E-08
Nrxn3	3.32E-12	0.3049656156	0.852	0.795	9.30E-08
Hmgn3	4.23E-12	-0.2828861131	0.298	0.43	1.18E-07
Tlcd1	4.37E-12	-0.2565488452	0.098	0.201	1.22E-07
Pitpnm2	4.85E-12	-0.3279068963	0.24	0.359	1.36E-07
Lamp2	4.98E-12	0.2782960627	0.511	0.372	1.40E-07
Vit	5.01E-12	0.2784897702	0.235	0.119	1.40E-07
Sox5os4	5.25E-12	0.2670633237	0.128	0.044	1.47E-07
Fads1	6.51E-12	-0.3043140626	0.189	0.308	1.82E-07
Cep85l	8.59E-12	-0.275971079	0.576	0.676	2.40E-07
Col4a5	8.76E-12	0.2692227765	0.252	0.133	2.45E-07
Dgki	1.13E-11	0.2771758806	0.481	0.341	3.15E-07
Grin2b	1.31E-11	0.2829579372	0.568	0.42	3.66E-07
Gnao1	1.36E-11	-0.2604476674	0.743	0.784	3.82E-07
Sema5b	1.77E-11	0.3101823841	0.205	0.102	4.95E-07
Cox7b	1.91E-11	0.2638651399	0.249	0.137	5.36E-07
Gm21954	2.05E-11	-0.2778766626	0.186	0.304	5.73E-07
Ccdc80	2.24E-11	0.2564261567	0.211	0.108	6.29E-07
Hes5	2.26E-11	-0.3467293729	0.346	0.461	6.32E-07
Sema4a	2.34E-11	-0.2711595413	0.187	0.301	6.54E-07
Mllt3	2.36E-11	0.286834618	0.496	0.359	6.59E-07
Ubash3b	2.39E-11	0.3380316244	0.291	0.173	6.68E-07
Sepp1	2.42E-11	-0.2953976513	0.141	0.243	6.77E-07
Aldoc	2.60E-11	-0.2973295533	0.203	0.315	7.27E-07
Cmtm5	3.32E-11	-0.2769196385	0.173	0.287	9.28E-07
Sulf1	4.31E-11	0.299765826	0.113	0.038	1.21E-06
A330093E20Rik	4.88E-11	-0.2708781279	0.116	0.222	1.37E-06
Prdm11	5.75E-11	0.2513493277	0.168	0.075	1.61E-06

Cpq	7.01E-11	0.2872371403	0.605	0.483	1.96E-06
Crebzf	7.36E-11	0.263899359	0.427	0.295	2.06E-06
Slc38a1	8.01E-11	0.3183141082	0.172	0.079	2.24E-06
Aifm3	8.25E-11	-0.2541742905	0.28	0.402	2.31E-06
Rgs7	9.29E-11	0.2942553976	0.763	0.692	2.60E-06
Gm2163	1.25E-10	-0.3045354124	0.139	0.242	3.50E-06
Igf2bp3	1.46E-10	0.3252996756	0.315	0.202	4.08E-06
Pign	1.75E-10	0.2558784767	0.276	0.163	4.89E-06
Gabra2	1.86E-10	0.2916025318	0.426	0.309	5.21E-06
Hspa8	1.98E-10	0.2591635117	0.288	0.173	5.56E-06
Trp53bp2	2.02E-10	-0.2910687358	0.266	0.38	5.64E-06
Cntn1	2.62E-10	-0.3094452953	0.389	0.513	7.34E-06
Cdh13	2.93E-10	0.2875369316	0.212	0.112	8.21E-06
Tef	4.74E-10	-0.2515068706	0.36	0.466	1.33E-05
Kdm5b	5.60E-10	-0.2956274645	0.413	0.518	1.57E-05
Arhgef28	5.95E-10	-0.3224700459	0.112	0.202	1.67E-05
Nxn	8.06E-10	-0.2986559942	0.571	0.663	2.26E-05
Emx2os	1.31E-09	-0.3120215862	0.19	0.291	3.67E-05
Kcnq1ot1	1.82E-09	0.3235375037	0.404	0.29	5.10E-05
Acyp2	1.84E-09	0.2565209428	0.522	0.393	5.17E-05
Mok	2.52E-09	0.2636374891	0.211	0.117	7.06E-05
Maml3	3.47E-09	0.294817925	0.258	0.158	9.72E-05
Cacna1a	3.65E-09	0.2885480526	0.323	0.214	0.0001021241641
Atp5o	3.67E-09	-0.2500784122	0.609	0.682	0.0001027452726
Lrrc8c	3.75E-09	-0.2642833214	0.085	0.167	0.0001049671929
Cyp4f15	6.63E-09	-0.2567472326	0.178	0.274	0.0001855900248
Ednrb	9.71E-09	-0.2559896484	0.363	0.469	0.0002717587514
Spag16	1.00E-08	0.4072273538	0.175	0.092	0.0002805459154
Folh1	1.11E-08	-0.2705739455	0.185	0.282	0.0003101891636
Slc7a10	1.19E-08	-0.2553329425	0.444	0.537	0.000332790988
Zcchc16	1.55E-08	0.3407924821	0.135	0.063	0.000433886632
Aig1	2.15E-08	0.2524048607	0.382	0.274	0.0006015253075
Gabbr2	2.37E-08	-0.2891310847	0.409	0.499	0.0006631242721
Stat1	2.46E-08	0.2736958706	0.138	0.066	0.0006895577736
Sycp2	4.83E-08	-0.2680271954	0.294	0.388	0.001351019715
A230009B12Rik	6.28E-08	-0.3016594372	0.139	0.222	0.001758031232
Fry	6.34E-08	-0.3635251354	0.582	0.639	0.001775799693
Gm11713	6.69E-08	-0.264983672	0.257	0.351	0.001873938474
Dab1	7.91E-08	-0.2501963778	0.634	0.708	0.002213833493
Plp1	8.06E-08	-0.264557635	0.171	0.259	0.002256370917
Pde1c	8.64E-08	0.303234014	0.257	0.169	0.002420259274
Neat1	9.14E-08	-0.2620266105	0.14	0.225	0.002559003086
Usp53	9.33E-08	-0.298338117	0.332	0.425	0.002612624445

Pipox	1.81E-07	-0.2513238474	0.113	0.189	0.005080643502
Gm15520	2.91E-07	-0.260298482	0.155	0.237	0.008153042439
Gm16168	7.78E-07	-0.3530193359	0.34	0.417	0.02179106278
Sorbs1	9.31E-07	-0.2743239315	0.69	0.719	0.02606181513
Gpr158	1.04E-06	-0.2803357633	0.206	0.286	0.02917356911
Igfbp5	1.34E-06	-0.2504963723	0.08	0.142	0.03746286364
Egfem1	1.57E-06	-0.298025501	0.154	0.229	0.04391705276
Adgrv1	2.06E-06	0.2873322373	0.135	0.074	0.05759995174
Ccdc85a	2.06E-06	-0.2746249525	0.61	0.668	0.05777208755
Erc2	2.26E-06	0.2608126444	0.292	0.211	0.06315598714
Sparc	2.60E-06	-0.2716249114	0.161	0.233	0.07274355483

Table 4.8.2. R6/2 12-Week Cortical Astrocyte Significant Differentially Expressed Genes

Gene	p_val	avg_logFC	pct.1	pct.2	p_val_adj
Slc1a2	6.43E-33	-0.5889318236	0.92	0.99	1.80E-28
Farp1	6.20E-29	-0.6906421185	0.728	0.899	1.74E-24
Gm3764	2.96E-28	-0.5472626671	0.866	0.942	8.30E-24
Lsamp	3.47E-28	-0.3660585643	1	0.995	9.73E-24
Nrxn1	1.44E-22	-0.271464111	0.995	0.995	4.03E-18
Mertk	4.34E-21	-0.5940070779	0.733	0.879	1.22E-16
Atp1a2	1.54E-20	-0.53748091	0.756	0.897	4.30E-16
Rnf121	2.50E-20	-0.8700672635	0.352	0.618	7.00E-16
Ntm	2.60E-17	-0.2772943029	0.985	0.975	7.28E-13
Cadm1	2.11E-16	-0.4129531681	0.884	0.937	5.91E-12
Qk	2.55E-16	-0.3934056218	0.884	0.947	7.14E-12
Mical2	2.69E-16	-0.6231133795	0.398	0.638	7.54E-12
Cables1	2.84E-16	-0.705055339	0.177	0.435	7.95E-12
Slc4a4	2.60E-15	-0.4661479204	0.807	0.905	7.27E-11
Tpk1	2.23E-14	0.6675944632	0.278	0.073	6.25E-10
Hif3a	3.03E-14	-0.6614498276	0.159	0.387	8.49E-10
Msi2	3.14E-14	-0.2839615643	0.974	0.982	8.79E-10
Luzp2	9.39E-14	-0.4882595757	0.884	0.907	2.63E-09
Acsl3	2.91E-13	-0.5617539895	0.422	0.626	8.15E-09
Zbtb16	7.94E-13	-0.8898757851	0.08	0.259	2.22E-08
Htra1	8.50E-13	-0.5795996687	0.429	0.641	2.38E-08
Gria2	9.18E-13	-0.3985834588	0.794	0.884	2.57E-08
Sparcl1	1.63E-12	-0.393693047	0.692	0.839	4.55E-08
Kirrel3	1.66E-12	-0.4210266322	0.781	0.892	4.64E-08
Aldoc	3.06E-12	-0.5664212869	0.098	0.286	8.57E-08
Pitpnc1	7.06E-12	-0.3985528792	0.9	0.927	1.98E-07
Glul	1.02E-11	-0.4944984353	0.404	0.611	2.87E-07
Nckap5	1.09E-11	0.3452282623	0.91	0.786	3.06E-07
Frmd4a	1.26E-11	-0.3392858299	0.933	0.945	3.52E-07
Dcc	1.48E-11	0.5526406014	0.656	0.445	4.14E-07
Clmn	1.59E-11	-0.4492429349	0.512	0.704	4.46E-07
Tspan7	2.64E-11	-0.359322741	0.766	0.877	7.38E-07
Plpp3	5.49E-11	-0.3467634136	0.758	0.894	1.54E-06
Ddx5	5.74E-11	0.4562136219	0.599	0.364	1.61E-06
Grin2c	8.54E-11	-0.4954675174	0.311	0.518	2.39E-06
Tra2a	1.47E-10	0.4919440497	0.648	0.44	4.11E-06
RP24-127M20.8	1.91E-10	0.5029631871	0.494	0.289	5.36E-06

Ciapin1	2.17E-10	0.4060240676	0.27	0.09	6.07E-06
Fry	2.87E-10	-0.4703515613	0.491	0.666	8.05E-06
Gm26804	4.24E-10	0.331116242	0.838	0.698	1.19E-05
Slc22a23	2.36E-09	0.4450488833	0.447	0.244	6.60E-05
Asic2	4.96E-09	-0.4506905223	0.445	0.593	0.0001389042558
Hspa8	6.28E-09	0.4023494489	0.301	0.123	0.0001759613579
Sox5	9.26E-09	0.3305522197	0.761	0.616	0.0002593748181
Gabbr1	9.61E-09	-0.4785152322	0.47	0.578	0.0002690601558
Phkg1	9.80E-09	-0.3090903357	0.62	0.781	0.0002743390464
Meis2	1.08E-08	0.330997777	0.848	0.693	0.0003030169375
Nwd1	1.20E-08	-0.3936813491	0.53	0.691	0.0003362649105
Cmss1	1.28E-08	0.3803778467	0.769	0.618	0.0003573268853
Mdga2	1.30E-08	-0.2621905626	0.931	0.94	0.0003627396804
Slc35f1	1.91E-08	0.4261932742	0.429	0.239	0.0005358973677
Eps8	2.17E-08	-0.425304891	0.481	0.636	0.0006067607046
Prex2	3.05E-08	-0.3010459376	0.833	0.882	0.0008535885876
Atp1b1	3.19E-08	0.3564954347	0.375	0.196	0.0008917844642
Ccnd3	3.88E-08	-0.5193512064	0.177	0.339	0.001086878045
Abca1	5.88E-08	0.4398429111	0.512	0.322	0.001645291869
Camk2g	6.19E-08	-0.385811783	0.568	0.681	0.001733050455
Paqr8	6.57E-08	-0.4452782185	0.483	0.628	0.001840743277
Gabbr2	7.05E-08	-0.5129271906	0.296	0.45	0.001972811145
Ntsr2	8.97E-08	-0.3894442167	0.247	0.42	0.002510778427
Naaladl2	9.51E-08	0.4372779265	0.537	0.359	0.002662944818
Son	9.88E-08	0.2678725131	0.923	0.849	0.002766845592
Palld	1.00E-07	0.404917164	0.514	0.319	0.002798427148
Polr2a	1.18E-07	0.4095346145	0.278	0.126	0.003293700415
Efr3b	1.34E-07	-0.3437759057	0.56	0.678	0.003754689541
Rmst	1.62E-07	-0.4803142365	0.465	0.598	0.004542107213
Rbfox1	1.74E-07	-0.6230965788	0.116	0.254	0.004863293501
Rbms3	2.67E-07	0.4759251189	0.301	0.151	0.007469740833
Kif21a	2.89E-07	0.3342359669	0.548	0.362	0.008086387405
Rapgef3	4.61E-07	-0.4140866505	0.386	0.53	0.01291305825
Myo1e	5.67E-07	0.3661911181	0.285	0.136	0.01587328739
L3mbtl3	5.88E-07	0.4407850221	0.388	0.229	0.01647632605
Ttyh1	6.06E-07	-0.3776183018	0.589	0.716	0.01697804247
Tnik	7.05E-07	-0.2617943722	0.892	0.91	0.01974770733
Pign	7.25E-07	0.3352596274	0.262	0.121	0.02028706056
Clock	7.31E-07	0.4175982996	0.288	0.143	0.02046115413

Bbs9	7.33E-07	0.3614669164	0.26	0.118	0.02050900073
Tmem243	7.57E-07	0.3078314959	0.486	0.304	0.02120317602
Cmtm5	8.59E-07	-0.4520133448	0.131	0.261	0.02404299638
Arl3	8.74E-07	0.3317621478	0.373	0.209	0.02448134645
PISD	9.58E-07	0.3636498414	0.45	0.284	0.02681964463
Zfp950	1.05E-06	0.332344095	0.44	0.269	0.02926487223
Ttyh2	1.17E-06	0.3129383487	0.306	0.153	0.03288527202
Slc24a3	1.19E-06	0.2779498796	0.362	0.198	0.03319715516
Aqp9	1.19E-06	0.2872943401	0.254	0.113	0.0332349553
Trip12	1.22E-06	0.3316909555	0.545	0.372	0.03424855023
Mfge8	1.28E-06	-0.4114037117	0.152	0.286	0.0357766103
Rbm26	1.33E-06	0.3035090308	0.635	0.475	0.03717175738
A930015D03Rik	1.46E-06	0.3499967694	0.278	0.136	0.04095520433
Syne1	1.62E-06	-0.3126113888	0.609	0.746	0.04535241888
Gm4876	1.73E-06	0.3868828207	0.326	0.176	0.04836792214
Nrg3	1.78E-06	-0.5203324964	0.221	0.354	0.04997045287
Ppp2r3a	1.81E-06	0.3002032183	0.496	0.327	0.05077277253
Gabra2	1.99E-06	0.3343135816	0.627	0.48	0.05585335985
Pde10a	2.08E-06	-1.167840701	0.216	0.334	0.05817088151
U2surp	2.14E-06	0.3338322991	0.401	0.234	0.06004858507
Myrip	2.71E-06	-0.42181494	0.206	0.337	0.07600007856
Plcb1	2.93E-06	-0.27557164	0.794	0.859	0.08189955298

Table 4.8.3. R6/2 8-Week Striatal Astrocyte Significant Differentially Expressed Genes

Gene	p_val	avg_logFC	pct.1	pct.2	p_val_adj
Gm3764	7.61E-64	-0.4351935798	0.924	0.956	2.13E-59
Ddx5	2.61E-44	0.4295178911	0.875	0.757	7.30E-40
Slc1a2	8.53E-39	-0.313088975	0.946	0.988	2.39E-34
Plpp3	1.40E-34	-0.292978873	0.873	0.964	3.91E-30
Sfxn5	8.94E-29	-0.2888526251	0.867	0.94	2.50E-24
Pitpnc1	2.59E-27	-0.3382444246	0.965	0.971	7.25E-23
Cst3	5.10E-25	-0.3357015619	0.762	0.866	1.43E-20
Itih3	1.17E-23	-0.660092941	0.235	0.393	3.27E-19
Phactr1	1.40E-23	-0.3866001498	0.512	0.668	3.92E-19
Tra2a	2.09E-23	0.3446941349	0.749	0.62	5.85E-19
Phkg1	2.52E-23	-0.2789870025	0.679	0.828	7.05E-19
Zfp949	1.41E-22	0.3370738198	0.497	0.304	3.96E-18
Adrbk2	2.02E-22	-0.3120062499	0.69	0.782	5.64E-18
Polr2a	2.74E-22	0.4558622848	0.301	0.147	7.66E-18
Guf1	5.09E-21	0.3680664386	0.272	0.129	1.43E-16
A930015D03Rik	8.17E-21	0.3514203868	0.308	0.153	2.29E-16
Slc4a4	6.23E-20	-0.2896068647	0.933	0.926	1.75E-15
Slc25a21	2.52E-19	0.4147977585	0.316	0.167	7.06E-15
Slc6a11	1.16E-18	-0.455436308	0.613	0.694	3.26E-14
Fgf14	1.74E-18	0.2939291202	0.905	0.844	4.88E-14
Abca1	1.84E-18	0.2872709877	0.727	0.58	5.14E-14
Chuk	2.58E-18	0.3339200031	0.314	0.17	7.23E-14
Zfp36l1	7.04E-18	-0.3810466237	0.226	0.371	1.97E-13
Slc7a11	6.24E-17	-0.3591209256	0.444	0.583	1.75E-12
Gabbr1	1.00E-16	-0.3141524463	0.489	0.609	2.81E-12
Msmo1	2.21E-16	-0.3409560137	0.146	0.276	6.18E-12
Cspg5	2.78E-16	-0.292511719	0.723	0.793	7.79E-12
Camk2g	1.06E-15	-0.2994002816	0.656	0.729	2.96E-11
Sgcd	1.67E-15	0.4507194733	0.4	0.265	4.69E-11
Cdh19	1.05E-14	0.3086095463	0.443	0.298	2.94E-10
Igf2bp3	1.11E-14	0.3453150659	0.304	0.178	3.11E-10
Galnt16	1.60E-14	-0.3170428917	0.312	0.448	4.48E-10
Clybl	2.56E-14	0.2644187031	0.663	0.523	7.16E-10
Tprkb	6.72E-14	-0.2809442053	0.466	0.596	1.88E-09
Plp1	2.77E-13	-0.3223598318	0.161	0.278	7.75E-09
1700112E06Rik	4.94E-13	0.3254657535	0.413	0.28	1.38E-08
Gm4876	7.46E-13	0.2937112636	0.257	0.143	2.09E-08

Meis1	5.38E-12	0.2795944272	0.392	0.266	1.50E-07
Mtss1l	7.08E-12	-0.2833844485	0.487	0.581	1.98E-07
9330159F19Rik	1.04E-11	0.2731116009	0.563	0.427	2.92E-07
Vegfa	3.00E-11	-0.289825691	0.271	0.375	8.41E-07
L3mbtl3	3.11E-11	0.270117953	0.457	0.333	8.71E-07
Mgat5	3.38E-11	-0.3559737586	0.539	0.612	9.47E-07
Kcnj10	4.37E-11	-0.2862726421	0.278	0.386	1.22E-06
Arpp21	7.17E-11	-0.2831766863	0.181	0.284	2.01E-06
Dlg2	7.32E-11	-0.2606400437	0.417	0.527	2.05E-06
Robo2	1.66E-10	0.3018348964	0.446	0.328	4.65E-06
Arhgef10l	2.46E-10	-0.2532097055	0.437	0.527	6.88E-06
Nrg1	2.51E-10	-0.8100417325	0.329	0.422	7.03E-06
Ptn	2.70E-10	-0.2969987031	0.696	0.744	7.57E-06
Hes5	2.96E-10	-0.2913214435	0.278	0.392	8.28E-06
Pcyt2	3.97E-10	-0.2623917185	0.358	0.455	1.11E-05
Ednrb	4.49E-10	-0.3013643835	0.394	0.488	1.26E-05
Adra1a	7.01E-10	-0.2737818966	0.169	0.267	1.96E-05
Gabra2	1.17E-09	0.2648481621	0.453	0.338	3.26E-05
Clu	1.19E-09	-0.27087683	0.44	0.537	3.32E-05
Phyhipl	1.52E-09	-0.2571326284	0.507	0.595	4.27E-05
Cables1	1.98E-09	-0.2970104779	0.473	0.555	5.54E-05
Emx2os	5.69E-09	-0.2560402279	0.214	0.306	0.0001592937273
Caskin1	9.33E-09	-0.2540783162	0.316	0.406	0.0002612318608
Ptch1	1.85E-08	-0.3925152986	0.697	0.714	0.0005169693733
Nav3	3.22E-08	-0.2553924724	0.268	0.368	0.0009007740121
Nnat	3.86E-07	-0.4027826085	0.42	0.481	0.01081258792
Lrig1	8.97E-07	-0.3495980458	0.466	0.498	0.02510430692

Table 4.8.4. R6/2 8-Week Cortical Astrocyte Significant Differentially Expressed Genes

Gene	p_val	avg_logFC	pct.1	pct.2	p_val_adj
Gm3764	8.09E-21	-0.3525800815	0.882	0.928	2.27E-16
1700112E06Rik	5.02E-17	0.5957858585	0.378	0.16	1.40E-12
Lrp1b	4.32E-16	0.3712670501	0.842	0.665	1.21E-11
Zfp949	2.71E-15	0.4568156303	0.359	0.153	7.59E-11
Slc1a2	9.18E-14	-0.3188177368	0.929	0.88	2.57E-09
Fgf14	2.01E-13	0.3297119013	0.869	0.694	5.62E-09
Qk	4.49E-13	-0.2877335002	0.894	0.908	1.26E-08
Tra2a	5.31E-13	0.4326984883	0.613	0.414	1.49E-08
Lrrc4c	6.06E-13	0.3162270496	0.844	0.697	1.70E-08
Auts2	6.76E-13	-0.3532366424	0.961	0.972	1.89E-08
Ddx5	7.00E-12	0.3772442037	0.576	0.377	1.96E-07
Lama3	1.62E-11	-0.5339719176	0.138	0.28	4.55E-07
Phactr1	3.20E-11	-0.4754103681	0.43	0.577	8.95E-07
Gm4876	4.95E-11	0.4134770043	0.269	0.114	1.39E-06
Cspg5	5.05E-11	-0.3892869268	0.647	0.732	1.41E-06
Ptprj	7.00E-11	0.3747472891	0.34	0.171	1.96E-06
Polr2a	8.55E-11	0.421172756	0.297	0.139	2.40E-06
Frmd4a	9.61E-11	-0.287058999	0.89	0.88	2.69E-06
Gpm6b	3.28E-10	-0.2575747467	0.897	0.88	9.19E-06
Fam13c	5.03E-10	-0.3884394789	0.39	0.519	1.41E-05
Tspan7	2.48E-09	-0.2770376661	0.795	0.831	6.93E-05
Grm3	3.20E-09	-0.3993224793	0.807	0.768	8.97E-05
Rgs20	4.03E-09	-0.2784579896	0.869	0.861	0.0001128197531
Cul5	1.00E-08	0.3351298041	0.346	0.194	0.0002811035721
Diaph2	1.52E-08	0.313093182	0.517	0.35	0.0004256119256
Ogt	2.39E-08	0.3007592651	0.698	0.537	0.0006689754822
Bcar3	6.05E-08	0.2950094459	0.395	0.243	0.001695032766
Dst	7.50E-08	0.3023129054	0.631	0.467	0.002100759832
Pitpnc1	1.14E-07	-0.2580057841	0.884	0.856	0.003194216304
Rbfox1	1.30E-07	-0.5674958056	0.158	0.269	0.003631808185
Dctn4	1.48E-07	0.2859192822	0.374	0.227	0.004154111739
A830082K12Rik	1.61E-07	0.3098372248	0.455	0.308	0.004515163191
Foxo1	2.05E-07	0.3101144651	0.397	0.25	0.005752329315
March7	2.79E-07	0.2604120141	0.307	0.174	0.007812115853
Sfxn5	3.16E-07	-0.2549841815	0.794	0.805	0.008848945253
Gm26843	4.34E-07	-0.3051412853	0.328	0.451	0.01215519379
Cdh19	4.37E-07	0.3471243503	0.388	0.257	0.01222535749

9530026P05Rik	4.83E-07	0.2864032874	0.276	0.153	0.01351738493
Ccdc58	6.60E-07	0.3076689282	0.391	0.252	0.01848437156
Bmpr1a	1.22E-06	0.2687074828	0.583	0.447	0.03412871891
Zfand6	1.43E-06	0.2901436886	0.328	0.204	0.04005207924
Abca1	1.60E-06	0.2575346823	0.456	0.305	0.04477353129
Klhl24	1.64E-06	0.263488401	0.279	0.158	0.04582104042
Anks1b	2.63E-06	-0.5974861514	0.167	0.268	0.07359214383
Acer3	2.68E-06	0.2918090439	0.328	0.206	0.07513124234
Phkg1	3.01E-06	-0.2542729361	0.64	0.71	0.08438140253

Table 4.8.5. R6/2 12-Week Striatal Astrocyte snRNA-seq Mouse Breakdown by Cluster

Cluster	NT #1	R6/2 #2	NT #5	NT #6	R6/2 #7	R6/2 #8	Total	Total R6/2	Total NT	%R6/2	%NT
0	186	87	118	127	105	96	*719*	288	431	40.1%	59.9%
1	142	37	55	127	41	11	*413*	89	324	21.5%	78.5%
2	10	132	7	5	86	92	*332*	310	22	93.4%	6.6%
3	91	33	53	45	36	24	*282*	93	189	33.0%	67.0%
4	12	74	8	10	83	75	*262*	232	30	88.5%	11.5%
5	16	65	29	19	28	23	*180*	116	64	64.4%	35.6%

Table 4.8.6. R6/2 12-Week Cortical Astrocyte snRNA-seq Mouse Breakdown by Cluster

Cluster	NT #1	R6/2 #2	NT #5	NT #6	R6/2 #7	R6/2 #8	Total	Total R6/2	Total NT	%R6/2	%NT
0	46	69	11	12	65	59	262	193	69	73.7%	26.3%
1	67	36	31	44	27	42	247	105	142	42.5%	57.5%
2	59	19	46	32	14	9	179	42	137	23.5%	76.5%
3	16	11	5	11	16	14	73	41	32	56.2%	43.8%
4	10	3	6	2	1	4	26	8	18	30.8%	69.2%

Table 4.8.7. HD iAstro Significant Differentially Expressed Genes

Gene	p_val	avg_logFC	pct.1	pct.2	p_val_adj
ANKRD1	0	2.1214	0.876	0.053	0
IGFBP5	0	1.7265	0.948	0.402	0
S100A11	0	1.5287	0.998	0.614	0
IGFBP3	0	1.4327	0.819	0.162	0
TAGLN	0	1.3517	1	0.959	0
TGFBI	0	1.3349	0.912	0.349	0
LMCD1	0	1.2082	0.746	0.183	0
TPM1	0	1.2070	1	0.933	0
TPM2	0	1.1859	0.99	0.674	0
NNMT	0	1.1305	0.744	0.1	0
MYL9	0	1.1212	0.823	0.288	0
S100A10	0	1.1191	0.978	0.571	0
ACTA2	0	1.1108	0.995	0.814	0
PMEPA1	0	1.0481	0.854	0.39	0
RPS4Y1	0	1.0354	0.955	0.338	0
SERPINE1	0	1.0256	0.818	0.353	0
FN1	0	1.0240	0.942	0.668	0
TAGLN2	0	0.9999	0.885	0.447	0
IER3	0	0.9961	0.945	0.599	0
COL8A1	0	0.9890	0.524	0.049	0
ID1	0	0.9559	0.608	0.057	0
HOXB2	0	0.9444	0.6	0.045	0
PLAU	0	0.9291	0.819	0.415	0
COL1A1	0	0.9045	0.964	0.758	0
LOXL1	0	0.9042	0.821	0.367	0
TPM4	0	0.8826	0.956	0.676	0
COL5A1	0	0.8651	0.804	0.412	0
CAV1	0	0.8630	0.959	0.666	0
MT-CO2	0	0.8620	0.975	0.766	0
GAS6	0	0.8500	0.714	0.286	0
IGFBP7	0	0.8043	0.881	0.483	0
PFN1	0	0.7921	0.969	0.741	0
LOX	0	0.7762	0.819	0.417	0
TNC	0	0.7684	0.898	0.674	0
MT-CYB	0	0.7654	0.992	0.899	0
ACTN1	0	0.7476	0.931	0.689	0
PDLIM7	0	0.7128	0.883	0.563	0
NEXN	0	0.7029	0.713	0.342	0
LIMS1	0	0.6994	0.804	0.491	0
S100A16	0	0.6977	0.766	0.352	0
TWIST1	0	0.6967	0.529	0.067	0
RBP1	0	0.6918	0.664	0.185	0

MT-CO3	0	0.6916	0.999	0.965	0
PKM	0	0.6901	0.97	0.819	0
MT-ATP6	0	0.6823	0.965	0.781	0
ANXA2	0	0.6767	0.998	0.954	0
CALD1	0	0.6677	0.999	0.985	0
NTM	0	0.6666	0.572	0.15	0
MEST	0	0.6635	0.875	0.582	0
LIF	0	0.6594	0.415	0.053	0
RPL22L1	0	0.6551	0.82	0.431	0
CCND1	0	0.6513	0.796	0.466	0
PTMA	0	0.6436	0.998	0.924	0
ITGA3	0	0.6327	0.551	0.15	0
PLXND1	0	0.6176	0.56	0.128	0
EEF1B2	0	0.6125	0.979	0.818	0
PTK7	0	0.6032	0.719	0.43	0
CAP1	0	0.5986	0.841	0.574	0
LGALS1	0	0.5974	0.995	0.907	0
CLIC1	0	0.5960	0.962	0.784	0
PLP2	0	0.5954	0.45	0.042	0
GLIPR2	0	0.5947	0.721	0.358	0
MYL6	0	0.5932	1	0.993	0
PLK2	0	0.5913	0.609	0.268	0
PHLDA2	0	0.5883	0.567	0.211	0
EIF4EBP1	0	0.5859	0.571	0.155	0
NPM1	0	0.5857	0.994	0.916	0
UBE2S	0	0.5839	0.777	0.44	0
ZFAS1	0	0.5811	0.889	0.616	0
HERPUD1	0	0.5786	0.755	0.472	0
IL11	0	0.5745	0.364	0.012	0
TGFB1	0	0.5736	0.546	0.166	0
NT5E	0	0.5679	0.683	0.352	0
RGCC	0	0.5647	0.472	0.145	0
ARPC2	0	0.5588	0.936	0.734	0
BEX1	0	0.5559	0.764	0.426	0
PPP1R14B	0	0.5492	0.966	0.825	0
RAN	0	0.5476	0.968	0.82	0
TSPO	0	0.5468	0.779	0.436	0
JPT1	0	0.5461	0.893	0.639	0
SLC7A5	0	0.5447	0.64	0.315	0
RPL12	0	0.5416	0.999	0.963	0
CXXC5	0	0.5415	0.815	0.576	0
MYH9	0	0.5386	0.882	0.651	0
IL32	0	0.5376	0.472	0.108	0
CAVIN1	0	0.5376	0.834	0.569	0
CHCHD2	0	0.5372	0.764	0.503	0
PRSS23	0	0.5289	0.935	0.75	0

PALLD	0	0.5251	0.929	0.776	0
MYL12A	0	0.5235	0.974	0.824	0
MT-CO1	0	0.5228	0.993	0.933	0
HES6	0	0.5209	0.447	0.141	0
MT-ND4	0	0.5184	0.824	0.608	0
CNN1	0	0.5182	0.377	0.035	0
GAPDH	0	0.5180	1	0.989	0
COL10A1	0	0.5177	0.304	0.012	0
IER5L	0	0.5164	0.605	0.279	0
ELN	0	0.5162	0.365	0.124	0
RGS3	0	0.4984	0.583	0.275	0
NUAK1	0	0.4961	0.581	0.259	0
NUPR1	0	0.4961	0.505	0.166	0
SDC1	0	0.4958	0.376	0.069	0
HSP90AB1	0	0.4952	0.989	0.921	0
CLTA	0	0.4931	0.927	0.763	0
MT-ND6	0	0.4917	0.859	0.7	0
H2AFZ	0	0.4906	0.974	0.825	0
FBN1	0	0.4906	0.464	0.227	0
SH3BGRL3	0	0.4880	0.902	0.665	0
S100A13	0	0.4877	0.864	0.599	0
L1CAM	0	0.4875	0.36	0.027	0
PAPPA	0	0.4867	0.291	0.039	0
HINT1	0	0.4863	0.985	0.886	0
ITGB1	0	0.4858	0.955	0.848	0
VASP	0	0.4850	0.542	0.208	0
RPL8	0	0.4847	0.999	0.981	0
SLC1A5	0	0.4843	0.506	0.194	0
RPL23A	0	0.4840	0.999	0.96	0
DCBLD2	0	0.4820	0.723	0.467	0
ARPC5	0	0.4813	0.837	0.591	0
RPL18A	0	0.4805	0.999	0.978	0
MRPL14	0	0.4769	0.688	0.36	0
EIF4A1	0	0.4746	0.877	0.677	0
ACTG1	0	0.4734	1	1	0
LOXL2	0	0.4730	0.565	0.251	0
HSPB1	0	0.4718	0.883	0.654	0
PHGDH	0	0.4706	0.685	0.409	0
NF2	0	0.4691	0.518	0.202	0
NAP1L1	0	0.4657	0.96	0.844	0
APOE	0	0.4653	0.333	0.093	0
PSMA7	0	0.4641	0.972	0.847	0
RPL28	0	0.4637	1	0.989	0
MT-ND1	0	0.4636	0.856	0.658	0
RPL36AL	0	0.4630	0.929	0.726	0
EIF1	0	0.4618	0.997	0.953	0

NT5DC2	0	0.4603	0.834	0.61	0
C5orf46	0	0.4588	0.351	0.032	0
EIF1AY	0	0.4557	0.48	0.124	0
ANXA3	0	0.4550	0.393	0.063	0
MT-ND5	0	0.4547	0.697	0.446	0
EIF2S2	0	0.4538	0.861	0.628	0
FBLIM1	0	0.4528	0.393	0.057	0
EZR	0	0.4511	0.582	0.298	0
TGFB1I1	0	0.4505	0.766	0.5	0
PGAM1	0	0.4499	0.848	0.638	0
RACK1	0	0.4496	1	0.979	0
ARF4	0	0.4475	0.815	0.573	0
DSTN	0	0.4451	0.979	0.852	0
ID3	0	0.4445	0.501	0.194	0
STK38L	0	0.4444	0.507	0.184	0
SLC25A3	0	0.4431	0.98	0.888	0
SLC2A1	0	0.4415	0.528	0.228	0
MYL12B	0	0.4412	0.952	0.804	0
RPLP0	0	0.4407	0.999	0.974	0
COL18A1	0	0.4405	0.724	0.463	0
CCT5	0	0.4403	0.827	0.616	0
RPS27A	0	0.4398	1	0.997	0
ADAM19	0	0.4394	0.521	0.21	0
FST	0	0.4393	0.291	0.056	0
BASP1	0	0.4366	0.895	0.709	0
UBA52	0	0.4346	0.994	0.931	0
HACD1	0	0.4340	0.482	0.149	0
CNN2	0	0.4304	0.716	0.426	0
CCL2	0	0.4281	0.952	0.749	0
PMAIP1	0	0.4278	0.348	0.032	0
PFKP	0	0.4265	0.545	0.259	0
PDGFC	0	0.4264	0.502	0.189	0
TLN1	0	0.4250	0.754	0.569	0
NME1	0	0.4227	0.815	0.562	0
RPL11	0	0.4227	1	0.994	0
REXO2	0	0.4218	0.754	0.483	0
ARF1	0	0.4205	0.792	0.568	0
RPS3	0	0.4199	1	0.987	0
BTG1	0	0.4194	0.724	0.493	0
RPL7A	0	0.4186	1	0.994	0
VIM	0	0.4183	1	1	0
SNRPE	0	0.4141	0.787	0.526	0
RPL19	0	0.4118	1	0.991	0
MFAP2	0	0.4118	0.385	0.083	0
OAZ1	0	0.4113	0.949	0.796	0
RPS2	0	0.4096	1	0.999	0

TNFRSF12A	0	0.4083	0.974	0.844	0
LAMB1	0	0.4078	0.573	0.252	0
LAYN	0	0.4066	0.394	0.096	0
TXNDC17	0	0.4051	0.772	0.502	0
NRP2	0	0.4048	0.519	0.224	0
TMSB10	0	0.4044	1	0.997	0
FHL2	0	0.4039	0.47	0.156	0
RPL35	0	0.4012	0.999	0.975	0
GADD45B	0	0.4006	0.718	0.472	0
ACTC1	0	0.4006	0.164	0.001	0
RPS6	0	0.4006	1	0.986	0
ARSJ	0	0.4005	0.476	0.192	0
RPL24	0	0.3986	0.998	0.963	0
EMILIN1	0	0.3972	0.308	0.056	0
RPL10A	0	0.3962	0.999	0.973	0
RPL4	0	0.3961	0.964	0.84	0
LIMD2	0	0.3947	0.553	0.256	0
TPI1	0	0.3943	0.916	0.747	0
P4HA2	0	0.3925	0.41	0.137	0
CLIC4	0	0.3908	0.536	0.245	0
RAB34	0	0.3901	0.609	0.321	0
RPS9	0	0.3876	1	0.988	0
PRELID1	0	0.3867	0.832	0.622	0
BTF3	0	0.3858	0.957	0.816	0
SNRPB	0	0.3848	0.833	0.62	0
IRX3	0	0.3843	0.473	0.208	0
RPS16	0	0.3830	0.999	0.97	0
EIF6	0	0.3827	0.715	0.459	0
LBH	0	0.3826	0.466	0.212	0
B4GALT1	0	0.3819	0.314	0.019	0
GARS	0	0.3810	0.533	0.276	0
SARS	0	0.3810	0.652	0.388	0
EIF5A	0	0.3797	0.808	0.582	0
KPNA2	0	0.3794	0.694	0.432	0
RPSA	0	0.3792	0.999	0.972	0
AC245595.1	0	0.3789	0.478	0.169	0
INHBA	0	0.3774	0.281	0.104	0
ACTN4	0	0.3773	0.843	0.674	0
LRRC17	0	0.3769	0.395	0.135	0
GDF6	0	0.3764	0.262	0.005	0
SRP9	0	0.3764	0.839	0.634	0
PFDN2	0	0.3764	0.719	0.452	0
RPS27L	0	0.3763	0.948	0.799	0
RPL22	0	0.3750	0.99	0.923	0
SNRPD1	0	0.3741	0.775	0.533	0
RBM8A	0	0.3724	0.81	0.591	0

RHOC	0	0.3720	0.802	0.577	0
TSPAN9	0	0.3718	0.396	0.11	0
EEF1D	0	0.3704	0.94	0.809	0
PPIA	0	0.3699	0.979	0.877	0
SVIL	0	0.3688	0.725	0.537	0
LMNA	0	0.3675	0.938	0.846	0
GCHFR	0	0.3665	0.383	0.115	0
RPS5	0	0.3664	0.997	0.961	0
SLC3A2	0	0.3660	0.907	0.794	0
ATP5MC2	0	0.3658	0.941	0.797	0
RHOBTB3	0	0.3653	0.922	0.77	0
HNRNPAB	0	0.3645	0.625	0.368	0
ANXA1	0	0.3629	0.912	0.726	0
AES	0	0.3625	0.626	0.346	0
SLC38A1	0	0.3620	0.355	0.075	0
DLG1	0	0.3618	0.494	0.275	0
RTRAF	0	0.3614	0.845	0.637	0
SLC9A3R2	0	0.3612	0.468	0.181	0
CAV2	0	0.3612	0.671	0.421	0
FILIP1L	0	0.3597	0.626	0.407	0
RPL3	0	0.3590	1	0.999	0
CCT8	0	0.3580	0.795	0.607	0
SERTAD4-AS1	0	0.3575	0.295	0.023	0
RUNX1	0	0.3571	0.493	0.231	0
PSMB5	0	0.3569	0.893	0.738	0
TP53I3	0	0.3560	0.647	0.393	0
ACTB	0	0.3551	1	1	0
FZD2	0	0.3546	0.485	0.207	0
ACTR3	0	0.3535	0.821	0.645	0
SET	0	0.3532	0.914	0.771	0
ATF4	0	0.3530	0.705	0.466	0
PBX3	0	0.3527	0.571	0.326	0
GTF2F2	0	0.3522	0.582	0.33	0
CFL1	0	0.3516	0.993	0.945	0
RPLP2	0	0.3501	0.998	0.966	0
MCM7	0	0.3493	0.5	0.269	0
WDR1	0	0.3480	0.735	0.516	0
PLEKHO1	0	0.3471	0.64	0.387	0
AMIGO2	0	0.3465	0.271	0.044	0
HMGA1	0	0.3459	0.488	0.237	0
TSPAN2	0	0.3459	0.268	0.006	0
POMP	0	0.3453	0.89	0.695	0
CCT2	0	0.3450	0.831	0.663	0
SERF2	0	0.3447	0.993	0.94	0
EBP	0	0.3444	0.58	0.345	0
IGF1R	0	0.3441	0.658	0.428	0

MT-ND2	0	0.3441	0.628	0.394	0
RPS12	0	0.3440	1	0.995	0
SNRPF	0	0.3433	0.727	0.479	0
BAX	0	0.3428	0.833	0.639	0
SSR2	0	0.3423	0.863	0.699	0
ILF2	0	0.3418	0.798	0.609	0
CENPV	0	0.3416	0.468	0.199	0
RPS13	0	0.3411	0.997	0.961	0
RPL32	0	0.3408	0.999	0.989	0
RPL6	0	0.3396	0.999	0.985	0
CCT3	0	0.3393	0.876	0.74	0
SSR3	0	0.3382	0.892	0.712	0
ENO1	0	0.3381	0.959	0.849	0
TUBB6	0	0.3378	0.76	0.54	0
P4HB	0	0.3378	0.934	0.842	0
PSMC5	0	0.3358	0.815	0.628	0
SSBP1	0	0.3355	0.858	0.665	0
CSRP1	0	0.3340	0.538	0.312	0
PDCD5	0	0.3339	0.743	0.501	0
RRAS	0	0.3328	0.483	0.228	0
SERPINH1	0	0.3325	0.857	0.708	0
NCL	0	0.3323	0.905	0.793	0
ABRACL	0	0.3320	0.347	0.075	0
PHLDA3	0	0.3319	0.634	0.404	0
PSMA5	0	0.3317	0.727	0.493	0
UQCRH	0	0.3317	0.885	0.687	0
MRPL51	0	0.3311	0.862	0.675	0
SEP11	0	0.3311	0.939	0.815	0
SMURF2	0	0.3310	0.418	0.204	0
VDAC1	0	0.3304	0.82	0.643	0
AP2S1	0	0.3291	0.83	0.631	0
CCT6A	0	0.3288	0.784	0.597	0
RPS14	0	0.3288	1	0.996	0
EEF1A1	0	0.3278	1	1	0
SEC61G	0	0.3276	0.843	0.635	0
PA2G4	0	0.3269	0.758	0.558	0
SNRPD2	0	0.3267	0.807	0.589	0
RPL5	0	0.3259	0.999	0.981	0
PDAP1	0	0.3258	0.77	0.557	0
GSTP1	0	0.3245	0.996	0.961	0
RPL15	0	0.3244	1	0.994	0
VDAC2	0	0.3242	0.829	0.642	0
EIF3J	0	0.3233	0.717	0.497	0
NACA	0	0.3225	0.996	0.963	0
HSPG2	0	0.3225	0.42	0.174	0
ILK	0	0.3223	0.703	0.481	0

NAT14	0	0.3220	0.634	0.426	0
MT-ND3	0	0.3208	0.671	0.4	0
TPT1	0	0.3206	1	0.99	0
CYCS	0	0.3202	0.715	0.482	0
EFEMP2	0	0.3198	0.522	0.3	0
ASNS	0	0.3196	0.4	0.184	0
SPDL1	0	0.3187	0.355	0.125	0
CAST	0	0.3186	0.674	0.483	0
RPS18	0	0.3181	1	0.999	0
SRI	0	0.3171	0.855	0.699	0
CD24	0	0.3161	0.382	0.132	0
RPL27	0	0.3148	0.995	0.95	0
PRMT1	0	0.3142	0.834	0.661	0
SOX4	0	0.3135	0.857	0.752	0
PSMB2	0	0.3121	0.805	0.608	0
EIF3D	0	0.3118	0.768	0.587	0
CAPZB	0	0.3117	0.709	0.503	0
AP2M1	0	0.3116	0.885	0.737	0
PXDN	0	0.3113	0.469	0.227	0
UBE2C	0	0.3110	0.384	0.172	0
SEC61B	0	0.3109	0.926	0.775	0
TARS	0	0.3107	0.541	0.299	0
NOP10	0	0.3106	0.788	0.573	0
CCNB1	0	0.3103	0.484	0.269	0
POLR2L	0	0.3102	0.916	0.771	0
RPS23	0	0.3099	1	0.995	0
NDUFS6	0	0.3092	0.878	0.714	0
TXN	0	0.3090	0.943	0.809	0
SRSF3	0	0.3087	0.858	0.689	0
SRM	0	0.3081	0.614	0.372	0
SFRP2	0	0.3062	0.183	0.027	0
NR2F6	0	0.3060	0.585	0.363	0
ANP32B	0	0.3045	0.744	0.545	0
ID2	0	0.3044	0.476	0.261	0
MTHFD2	0	0.3034	0.307	0.087	0
CDC42EP3	0	0.3021	0.553	0.334	0
EEF2	0	0.3013	0.968	0.886	0
ARPC1B	0	0.3012	0.389	0.134	0
RPS3A	0	0.3012	1	0.994	0
TOMM40	0	0.3011	0.565	0.337	0
FDPS	0	0.3007	0.887	0.77	0
PSMB1	0	0.3006	0.925	0.799	0
PSMB3	0	0.3004	0.799	0.6	0
ADRM1	0	0.3003	0.695	0.486	0
ARPC4	0	0.3000	0.643	0.414	0
APRT	0	0.2998	0.777	0.572	0

TUBA1C	0	0.2986	0.572	0.364	0
ARPC3	0	0.2983	0.923	0.783	0
ATP5MD	0	0.2980	0.85	0.652	0
CDC42EP1	0	0.2977	0.535	0.301	0
SLC25A5	0	0.2974	0.806	0.62	0
RPS11	0	0.2968	0.996	0.965	0
XRCC5	0	0.2968	0.829	0.691	0
EDN1	0	0.2955	0.319	0.147	0
RPS24	0	0.2954	1	0.995	0
PSMD2	0	0.2952	0.807	0.676	0
PRDX1	0	0.2948	0.979	0.915	0
C1QBP	0	0.2945	0.776	0.58	0
RPL13	0	0.2944	1	0.999	0
NXN	0	0.2943	0.535	0.301	0
MAP1LC3B	0	0.2939	0.7	0.491	0
HMGB2	0	0.2939	0.597	0.38	0
SNRPG	0	0.2938	0.779	0.571	0
SNRPD3	0	0.2927	0.724	0.507	0
RPL38	0	0.2927	0.99	0.924	0
STMN1	0	0.2921	0.965	0.868	0
PPA1	0	0.2919	0.723	0.525	0
BMP1	0	0.2918	0.483	0.254	0
UAP1	0	0.2916	0.406	0.175	0
ATOX1	0	0.2905	0.822	0.62	0
TWF2	0	0.2902	0.51	0.273	0
CDC20	0	0.2898	0.275	0.101	0
GFRA1	0	0.2898	0.405	0.174	0
GADD45A	0	0.2894	0.482	0.24	0
TUBA4A	0	0.2892	0.265	0.072	0
MCAM	0	0.2892	0.421	0.191	0
RPL7	0	0.2892	0.997	0.968	0
CCDC107	0	0.2891	0.661	0.458	0
ERH	0	0.2886	0.878	0.729	0
FHL3	0	0.2884	0.372	0.132	0
UBE2I	0	0.2878	0.753	0.555	0
BOP1	0	0.2877	0.422	0.19	0
CKS2	0	0.2871	0.469	0.224	0
RPS27	0	0.2867	1	0.994	0
GLIPR1	0	0.2867	0.601	0.375	0
LRRC59	0	0.2842	0.549	0.324	0
PSME2	0	0.2840	0.67	0.454	0
CREB3	0	0.2831	0.525	0.292	0
SNU13	0	0.2830	0.796	0.612	0
EEF1A2	0	0.2829	0.415	0.21	0
TYMS	0	0.2827	0.502	0.28	0
TPM3	0	0.2823	0.696	0.494	0

FADS3	0	0.2821	0.42	0.191	0
DDX21	0	0.2821	0.621	0.425	0
RPL21	0	0.2818	0.999	0.983	0
AXL	0	0.2814	0.575	0.358	0
TES	0	0.2809	0.249	0.025	0
DEK	0	0.2809	0.76	0.586	0
RPL29	0	0.2795	0.999	0.99	0
PSMA4	0	0.2794	0.765	0.567	0
TIMM13	0	0.2785	0.763	0.576	0
MSRB3	0	0.2783	0.445	0.212	0
PABPC4	0	0.2767	0.489	0.258	0
PDHB	0	0.2765	0.684	0.493	0
TK1	0	0.2755	0.285	0.099	0
ITGA4	0	0.2749	0.305	0.092	0
XBP1	0	0.2740	0.611	0.393	0
RANBP1	0	0.2740	0.753	0.57	0
SNRPN	0	0.2739	0.737	0.547	0
EIF3I	0	0.2727	0.766	0.575	0
RPL35A	0	0.2720	0.999	0.986	0
RCN1	0	0.2717	0.833	0.676	0
AURKAIP1	0	0.2707	0.801	0.624	0
PAWR	0	0.2699	0.649	0.434	0
RPS19	0	0.2697	1	0.999	0
MRPL52	0	0.2697	0.675	0.453	0
MAGOH	0	0.2692	0.568	0.353	0
PGK1	0	0.2678	0.722	0.554	0
PRICKLE1	0	0.2676	0.314	0.097	0
STRAP	0	0.2673	0.764	0.583	0
EIF4E2	0	0.2673	0.558	0.334	0
BZW2	0	0.2662	0.359	0.129	0
PPP1CA	0	0.2658	0.679	0.475	0
UQCRC1	0	0.2653	0.667	0.481	0
RPL18	0	0.2650	0.999	0.989	0
PSMD7	0	0.2648	0.774	0.607	0
RPS15	0	0.2647	1	0.995	0
PTMS	0	0.2646	0.978	0.91	0
RBX1	0	0.2645	0.849	0.682	0
GADD45GIP1	0	0.2643	0.843	0.675	0
SINHCAF	0	0.2641	0.36	0.129	0
CDV3	0	0.2638	0.673	0.497	0
CNIH4	0	0.2637	0.613	0.397	0
PSMD8	0	0.2632	0.885	0.741	0
LARP6	0	0.2630	0.447	0.23	0
NTMT1	0	0.2624	0.54	0.313	0
ARPC5L	0	0.2620	0.553	0.342	0
ANXA4	0	0.2613	0.32	0.092	0

SRP14	0	0.2604	0.993	0.949	0
DKC1	0	0.2604	0.469	0.26	0
PSMB6	0	0.2600	0.859	0.702	0
RBM3	0	0.2592	0.691	0.488	0
IKBIP	0	0.2590	0.591	0.381	0
SLC20A1	0	0.2590	0.379	0.165	0
CAPNS1	0	0.2588	0.702	0.499	0
RAC1	0	0.2586	0.934	0.818	0
RPL23	0	0.2585	0.994	0.961	0
HMGB1	0	0.2578	0.994	0.957	0
PLAUR	0	0.2569	0.269	0.079	0
ISOC2	0	0.2569	0.469	0.254	0
PSMC4	0	0.2569	0.679	0.484	0
MCTS1	0	0.2568	0.485	0.266	0
TRMT112	0	0.2566	0.788	0.624	0
YARS	0	0.2565	0.42	0.198	0
PGRMC2	0	0.2564	0.671	0.498	0
GSTO1	0	0.2563	0.616	0.412	0
EPHA2	0	0.2560	0.299	0.079	0
BIRC5	0	0.2557	0.339	0.16	0
PTTG1	0	0.2553	0.563	0.341	0
COX5A	0	0.2548	0.735	0.537	0
LDHB	0	0.2547	0.951	0.864	0
NHP2	0	0.2545	0.66	0.455	0
MRTO4	0	0.2543	0.492	0.287	0
LSM4	0	0.2539	0.717	0.527	0
HIST1H4C	0	0.2537	0.487	0.276	0
HMGB3	0	0.2528	0.577	0.37	0
BIN1	0	0.2526	0.406	0.203	0
SLC25A6	0	0.2518	0.933	0.813	0
TIMM17A	0	0.2512	0.468	0.249	0
GXYLT2	0	0.2509	0.258	0.076	0
MRPS7	0	0.2509	0.607	0.401	0
RPL39	0	0.2503	0.999	0.985	0
OSTC	0	0.2502	0.878	0.739	0
PACSIN3	0	0.2502	0.39	0.176	0
HAP1	0	-0.2507	0.032	0.151	0
PROX1	0	-0.2511	0.049	0.195	0
CTNNA2	0	-0.2527	0.025	0.188	0
ANKS1B	0	-0.2529	0.043	0.18	0
PRSS12	0	-0.2546	0.023	0.151	0
ZNF704	0	-0.2554	0.098	0.247	0
SLITRK5	0	-0.2559	0.091	0.239	0
GAS2L3	0	-0.2565	0.07	0.219	0
PPP2R2B	0	-0.2600	0.086	0.253	0
ECM2	0	-0.2609	0.038	0.209	0

NCKAP5	0	-0.2629	0.053	0.181	0
AC087477.2	0	-0.2639	0.011	0.182	0
CPNE8	0	-0.2647	0.057	0.21	0
ZMYND10	0	-0.2652	0.05	0.213	0
IFIT2	0	-0.2665	0.044	0.197	0
LARGE1	0	-0.2675	0.06	0.216	0
CFAP126	0	-0.2680	0.041	0.202	0
SNCAIP	0	-0.2688	0.076	0.221	0
PLPPR5	0	-0.2688	0.031	0.219	0
LEPR	0	-0.2731	0.068	0.227	0
F3	0	-0.2748	0.078	0.221	0
LMBRD1	0	-0.2776	0.162	0.323	0
LAMA2	0	-0.2792	0.027	0.195	0
RERG	0	-0.2797	0.021	0.202	0
C1S	0	-0.2797	0.021	0.19	0
APP	0	-0.2798	0.868	0.882	0
EN2	0	-0.2858	0.05	0.186	0
ALDH6A1	0	-0.2863	0.169	0.326	0
C21orf62	0	-0.2868	0.072	0.249	0
KCND3	0	-0.2868	0.138	0.295	0
IFIT1	0	-0.2878	0.063	0.204	0
PDE1A	0	-0.2886	0.044	0.225	0
PTPRJ	0	-0.2890	0.096	0.263	0
CPEB2	0	-0.2893	0.1	0.265	0
SOX21	0	-0.2899	0.155	0.32	0
C1orf226	0	-0.2915	0.113	0.285	0
HSP90B1	0	-0.2932	0.916	0.921	0
TMEM200C	0	-0.2978	0.126	0.278	0
GFRA2	0	-0.2996	0.011	0.2	0
MMP15	0	-0.3003	0.159	0.328	0
SOX1	0	-0.3012	0.022	0.232	0
ABAT	0	-0.3019	0.196	0.358	0
TMBIM6	0	-0.3038	0.936	0.926	0
SORBS1	0	-0.3042	0.083	0.264	0
BTBD11	0	-0.3049	0.047	0.247	0
DACH1	0	-0.3050	0.082	0.272	0
NLGN4X	0	-0.3053	0.113	0.283	0
PLEKHA4	0	-0.3080	0.206	0.37	0
ATRX	0	-0.3084	0.706	0.762	0
BAIAP3	0	-0.3084	0.072	0.231	0
SLC4A4	0	-0.3095	0.019	0.184	0
CHST7	0	-0.3126	0.13	0.306	0
SLIT2	0	-0.3128	0.172	0.338	0
KCTD12	0	-0.3143	0.089	0.266	0
DOCK5	0	-0.3152	0.135	0.286	0
MAGI2	0	-0.3158	0.09	0.272	0

NPTX2	0	-0.3167	0.049	0.177	0
TTC3	0	-0.3176	0.857	0.887	0
KLHL4	0	-0.3198	0.072	0.235	0
COX6A1	0	-0.3201	0.958	0.94	0
VCAN	0	-0.3205	0.474	0.659	0
ITM2B	0	-0.3209	0.931	0.93	0
HLA-DRB5	0	-0.3222	0.002	0.102	0
B3GAT1	0	-0.3226	0.07	0.246	0
PIFO	0	-0.3230	0.133	0.315	0
RGMA	0	-0.3235	0.111	0.285	0
TSPAN3	0	-0.3235	0.682	0.732	0
C3orf58	0	-0.3245	0.12	0.307	0
CSF1	0	-0.3252	0.117	0.307	0
DPYSL2	0	-0.3259	0.644	0.723	0
S1PR3	0	-0.3261	0.107	0.283	0
PLCE1	0	-0.3270	0.147	0.32	0
MEGF9	0	-0.3273	0.132	0.327	0
C5orf49	0	-0.3296	0.086	0.28	0
MOK	0	-0.3310	0.117	0.304	0
HMGN3	0	-0.3327	0.663	0.733	0
ADCY2	0	-0.3336	0.117	0.304	0
MLF1	0	-0.3337	0.275	0.43	0
TUBB2A	0	-0.3351	0.933	0.937	0
CACNA1C	0	-0.3356	0.041	0.221	0
H1F0	0	-0.3357	0.036	0.234	0
FAM43A	0	-0.3361	0.138	0.3	0
NR2F2-AS1	0	-0.3365	0.024	0.227	0
CSRP2	0	-0.3365	0.977	0.982	0
MLLT1	0	-0.3389	0.361	0.505	0
CACNG4	0	-0.3392	0.2	0.37	0
ESPN	0	-0.3412	0.016	0.183	0
NOS1AP	0	-0.3416	0.203	0.387	0
DTNA	0	-0.3421	0.121	0.299	0
FMN2	0	-0.3439	0.166	0.363	0
MPC1	0	-0.3448	0.319	0.478	0
RFX4	0	-0.3461	0.304	0.48	0
SSPN	0	-0.3463	0.256	0.421	0
MAP3K13	0	-0.3465	0.014	0.241	0
BBOX1	0	-0.3469	0.051	0.255	0
C1R	0	-0.3469	0.024	0.247	0
TCEAL7	0	-0.3471	0.133	0.335	0
EPN2	0	-0.3477	0.293	0.452	0
MARCKS	0	-0.3487	0.943	0.948	0
HEATR5A	0	-0.3496	0.178	0.366	0
SEMA6D	0	-0.3522	0.06	0.269	0
DNAAF4	0	-0.3522	0.252	0.416	0

BEX4	0	-0.3545	0.64	0.71	0
BCHE	0	-0.3547	0.083	0.304	0
TLE1	0	-0.3552	0.269	0.436	0
HEXA	0	-0.3572	0.545	0.652	0
AL391807.1	0	-0.3597	0.114	0.309	0
C6orf118	0	-0.3598	0.069	0.283	0
XPR1	0	-0.3602	0.168	0.352	0
ST8SIA1	0	-0.3612	0.08	0.294	0
FSTL5	0	-0.3617	0.102	0.298	0
PREX2	0	-0.3624	0.11	0.313	0
PRSS35	0	-0.3631	0.092	0.276	0
PDIA5	0	-0.3646	0.173	0.362	0
ST5	0	-0.3649	0.414	0.553	0
GRIN2B	0	-0.3652	0.022	0.216	0
MTSS1	0	-0.3652	0.029	0.245	0
DCHS1	0	-0.3654	0.359	0.525	0
RDX	0	-0.3671	0.788	0.832	0
EPHA4	0	-0.3688	0.161	0.351	0
CNR1	0	-0.3689	0.034	0.226	0
CTXND1	0	-0.3705	0.005	0.233	0
SLC27A1	0	-0.3707	0.143	0.361	0
IRS2	0	-0.3710	0.525	0.644	0
DPYSL5	0	-0.3722	0.274	0.447	0
GRID2	0	-0.3723	0.093	0.275	0
HES1	0	-0.3729	0.663	0.769	0
SOCS3	0	-0.3734	0.286	0.474	0
SELENOP	0	-0.3736	0.046	0.262	0
CCDC88A	0	-0.3755	0.481	0.608	0
PLPP3	0	-0.3790	0.065	0.297	0
DCLK2	0	-0.3790	0.305	0.473	0
KIAA1549L	0	-0.3803	0.06	0.287	0
GALNT17	0	-0.3806	0.326	0.484	0
PDE4B	0	-0.3811	0.056	0.264	0
HS6ST1	0	-0.3812	0.121	0.352	0
PIR	0	-0.3813	0.143	0.342	0
FNBP1	0	-0.3814	0.292	0.466	0
GYG2	0	-0.3814	0.137	0.35	0
SGCE	0	-0.3820	0.37	0.53	0
ATP1B2	0	-0.3839	0.077	0.318	0
ERBIN	0	-0.3843	0.448	0.578	0
RGS5	0	-0.3843	0.047	0.253	0
AFDN	0	-0.3844	0.417	0.557	0
COL13A1	0	-0.3855	0.024	0.237	0
ZNF106	0	-0.3866	0.455	0.574	0
LRRN2	0	-0.3869	0.083	0.313	0
KAZN	0	-0.3878	0.25	0.443	0

CLSTN1	0	-0.3879	0.563	0.666	0
COL26A1	0	-0.3879	0.227	0.419	0
FRRS1L	0	-0.3882	0.084	0.3	0
SLC1A2	0	-0.3890	0.04	0.239	0
NPAS3	0	-0.3914	0.407	0.572	0
CPD	0	-0.3916	0.307	0.479	0
GRIA4	0	-0.3920	0.049	0.291	0
PSAP	0	-0.3943	0.836	0.881	0
RARRES3	0	-0.3952	0.043	0.286	0
CANX	0	-0.3957	0.891	0.911	0
APLP2	0	-0.3969	0.892	0.914	0
DDX17	0	-0.3976	0.772	0.843	0
PRMT2	0	-0.3977	0.728	0.812	0
CFI	0	-0.3990	0.169	0.362	0
FAM171B	0	-0.4002	0.114	0.337	0
ADD3	0	-0.4004	0.318	0.495	0
JAM2	0	-0.4012	0.407	0.558	0
CHID1	0	-0.4017	0.6	0.7	0
FXYD6	0	-0.4018	0.367	0.52	0
PLD3	0	-0.4035	0.886	0.916	0
KIF1A	0	-0.4043	0.51	0.643	0
CLDN10	0	-0.4057	0.004	0.218	0
ARHGAP21	0	-0.4079	0.436	0.597	0
LRIG1	0	-0.4081	0.197	0.41	0
DPF3	0	-0.4095	0.084	0.309	0
RETREG1	0	-0.4097	0.124	0.34	0
GPRC5B	0	-0.4103	0.222	0.428	0
SLC22A17	0	-0.4104	0.337	0.521	0
MALAT1	0	-0.4107	1	1	0
SOX6	0	-0.4109	0.013	0.213	0
TNFRSF11B	0	-0.4115	0.078	0.301	0
IGFBP2	0	-0.4128	0.999	0.999	0
LAMP1	0	-0.4149	0.833	0.868	0
ANGPTL2	0	-0.4164	0.084	0.265	0
TCTN1	0	-0.4165	0.28	0.485	0
RAB9A	0	-0.4179	0.401	0.551	0
PEA15	0	-0.4182	0.629	0.707	0
SLN	0	-0.4190	0.015	0.154	0
LGALS3BP	0	-0.4194	0.713	0.781	0
RFX3	0	-0.4207	0.177	0.381	0
CALCRL	0	-0.4215	0.059	0.279	0
ITGB8	0	-0.4235	0.473	0.635	0
SLC44A1	0	-0.4236	0.22	0.447	0
ZIC2	0	-0.4236	0.16	0.406	0
SPRY1	0	-0.4255	0.48	0.646	0
JUN	0	-0.4257	0.753	0.831	0

TTYH3	0	-0.4267	0.611	0.708	0
PTPRA	0	-0.4275	0.561	0.681	0
SETBP1	0	-0.4288	0.165	0.405	0
CLDN5	0	-0.4299	0.004	0.172	0
SIPA1L1	0	-0.4327	0.366	0.551	0
PROM1	0	-0.4330	0.209	0.421	0
KIDINS220	0	-0.4346	0.455	0.622	0
SPAG16	0	-0.4351	0.232	0.479	0
PLEKHH2	0	-0.4368	0.063	0.295	0
LAMP2	0	-0.4369	0.633	0.726	0
LTBP3	0	-0.4372	0.414	0.615	0
RNASET2	0	-0.4373	0.147	0.396	0
TUBA1A	0	-0.4401	1	1	0
ERBB4	0	-0.4405	0.22	0.454	0
PLA2G16	0	-0.4407	0.264	0.47	0
TNIK	0	-0.4409	0.163	0.402	0
PON2	0	-0.4419	0.842	0.886	0
RUFY3	0	-0.4424	0.395	0.582	0
IQGAP2	0	-0.4432	0.248	0.447	0
TENM2	0	-0.4441	0.419	0.592	0
PSRC1	0	-0.4445	0.389	0.597	0
RIPOR2	0	-0.4480	0.12	0.374	0
LIFR	0	-0.4488	0.191	0.423	0
LRP1	0	-0.4503	0.615	0.754	0
PLPPR3	0	-0.4511	0.325	0.534	0
KIF1B	0	-0.4535	0.533	0.686	0
SEMA5B	0	-0.4549	0.118	0.36	0
PHLDA1	0	-0.4557	0.629	0.749	0
LRRC4B	0	-0.4558	0.165	0.46	0
RBM6	0	-0.4564	0.462	0.625	0
GDPD2	0	-0.4574	0.12	0.381	0
PEG10	0	-0.4579	0.782	0.836	0
ITGA6	0	-0.4583	0.138	0.378	0
LINC00461	0	-0.4595	0.546	0.685	0
MARCH6	0	-0.4603	0.536	0.684	0
SOX2	0	-0.4605	0.633	0.767	0
APC2	0	-0.4608	0.148	0.389	0
PODXL	0	-0.4610	0.182	0.42	0
NRP1	0	-0.4614	0.121	0.381	0
HLA-B	0	-0.4629	0.778	0.824	0
TCEAL4	0	-0.4656	0.708	0.785	0
IL13RA2	0	-0.4656	0.059	0.322	0
DAG1	0	-0.4674	0.406	0.594	0
RTN3	0	-0.4675	0.673	0.774	0
SMOC2	0	-0.4678	0.031	0.305	0
CDH13	0	-0.4709	0.26	0.462	0

EGR1	0	-0.4752	0.289	0.456	0
ITSN1	0	-0.4781	0.571	0.715	0
SPTBN1	0	-0.4784	0.663	0.779	0
EMC10	0	-0.4790	0.189	0.51	0
ADAM9	0	-0.4792	0.691	0.796	0
COL12A1	0	-0.4796	0.313	0.531	0
TMTC2	0	-0.4819	0.05	0.332	0
PHKB	0	-0.4831	0.297	0.527	0
APC	0	-0.4896	0.279	0.505	0
HEG1	0	-0.4900	0.382	0.542	0
EPB41L3	0	-0.4906	0.224	0.443	0
SDC3	0	-0.4924	0.212	0.465	0
ITPKB	0	-0.4941	0.225	0.485	0
ARHGAP29	0	-0.4957	0.666	0.79	0
GRIN2A	0	-0.4965	0.073	0.265	0
GSN	0	-0.4974	0.489	0.638	0
CD99	0	-0.4979	0.971	0.982	0
B2M	0	-0.4995	0.991	0.996	0
FHL1	0	-0.5003	0.526	0.708	0
DMD	0	-0.5005	0.079	0.33	0
MAPK10	0	-0.5006	0.185	0.424	0
FRZB	0	-0.5015	0.039	0.233	0
PCDH8	0	-0.5042	0.04	0.236	0
RTN1	0	-0.5068	0.231	0.482	0
SERINC1	0	-0.5073	0.496	0.658	0
FGFR1	0	-0.5101	0.513	0.687	0
EMP2	0	-0.5120	0.35	0.542	0
COL1A2	0	-0.5144	0.181	0.366	0
SEMA6A	0	-0.5155	0.347	0.564	0
SLC1A3	0	-0.5163	0.337	0.555	0
CSRNP3	0	-0.5172	0.193	0.455	0
NAV2	0	-0.5233	0.216	0.489	0
CST3	0	-0.5267	0.843	0.9	0
CD74	0	-0.5277	0.229	0.42	0
SYT11	0	-0.5281	0.53	0.701	0
USP11	0	-0.5293	0.478	0.664	0
FIGN	0	-0.5302	0.206	0.481	0
ZBTB20	0	-0.5312	0.534	0.71	0
GPC4	0	-0.5320	0.595	0.722	0
MAP1B	0	-0.5343	0.956	0.976	0
MMP17	0	-0.5344	0.08	0.349	0
TMEM47	0	-0.5347	0.367	0.583	0
PJA2	0	-0.5403	0.527	0.708	0
POLR2J3.1	0	-0.5407	0.468	0.667	0
TENT5A	0	-0.5421	0.085	0.385	0
GPC3	0	-0.5487	0.057	0.294	0

FIBIN	0	-0.5504	0.018	0.32	0
ARNT2	0	-0.5504	0.161	0.467	0
AC120042.3	0	-0.5505	0.1	0.404	0
ATP2B1	0	-0.5519	0.5	0.666	0
GAP43	0	-0.5536	0.575	0.755	0
TMEM59L	0	-0.5635	0.112	0.442	0
SRGAP1	0	-0.5664	0.383	0.609	0
BEX3	0	-0.5665	0.939	0.972	0
GLG1	0	-0.5690	0.625	0.763	0
EDNRB	0	-0.5693	0.057	0.368	0
ENPP2	0	-0.5699	0.051	0.388	0
INTU	0	-0.5749	0.33	0.576	0
FAM89A	0	-0.5763	0.292	0.528	0
CTNND2	0	-0.5779	0.196	0.499	0
IFI6	0	-0.5801	0.356	0.598	0
KIF5C	0	-0.5810	0.492	0.66	0
SAT1	0	-0.5829	0.5	0.627	0
ACTG2	0	-0.5833	0.403	0.643	0
CRB2	0	-0.5883	0.4	0.667	0
MIR99AHG	0	-0.5913	0.508	0.738	0
NEFL	0	-0.5918	0.17	0.365	0
NEAT1	0	-0.5925	0.466	0.705	0
CEBPD	0	-0.5937	0.273	0.549	0
HTRA1	0	-0.6020	0.626	0.785	0
CCND2	0	-0.6047	0.254	0.492	0
VMP1	0	-0.6048	0.862	0.927	0
CCDC102B	0	-0.6058	0.066	0.339	0
ASGR1	0	-0.6067	0.132	0.463	0
SARAF	0	-0.6097	0.884	0.936	0
ATP1A2	0	-0.6105	0.02	0.293	0
GDF10	0	-0.6113	0.137	0.371	0
SERPINE2	0	-0.6116	0.362	0.539	0
PRDX4	0	-0.6117	0.761	0.847	0
MEG3	0	-0.6146	0	0.157	0
B4GALNT4	0	-0.6197	0.292	0.585	0
ELMOD1	0	-0.6203	0.16	0.44	0
COMT	0	-0.6209	0.285	0.438	0
CTSC	0	-0.6252	0.632	0.78	0
C1orf61	0	-0.6268	0.239	0.418	0
PCDH10	0	-0.6280	0.097	0.442	0
NTRK3	0	-0.6298	0.439	0.681	0
TUBB2B	0	-0.6373	0.967	0.986	0
FZD3	0	-0.6414	0.523	0.763	0
CD44	0	-0.6415	0.806	0.877	0
LAMB2	0	-0.6423	0.489	0.72	0
B4GAT1	0	-0.6438	0.425	0.675	0

PMP22	0	-0.6454	0.817	0.905	0
LRRC4C	0	-0.6458	0.188	0.503	0
RGS6	0	-0.6484	0.075	0.454	0
METRN	0	-0.6529	0.679	0.832	0
WSCD1	0	-0.6545	0.152	0.453	0
ANK2	0	-0.6582	0.283	0.601	0
ZIC1	0	-0.6639	0.026	0.408	0
ID4	0	-0.6675	0.448	0.7	0
DDR1	0	-0.6695	0.648	0.831	0
CCDC144NL-AS1	0	-0.6700	0.203	0.558	0
WSB1	0	-0.6722	0.741	0.882	0
AP1S2	0	-0.6746	0.677	0.812	0
QKI	0	-0.6770	0.743	0.883	0
TIMP2	0	-0.6883	0.785	0.885	0
NKAIN3	0	-0.7024	0.168	0.512	0
LRP2	0	-0.7058	0.061	0.403	0
PLS3	0	-0.7064	0.35	0.607	0
CPAMD8	0	-0.7067	0.012	0.366	0
SRGAP3	0	-0.7073	0.296	0.658	0
LRRIQ1	0	-0.7108	0.159	0.51	0
PCDH9	0	-0.7125	0.295	0.598	0
PPP1CB	0	-0.7147	0.713	0.861	0
CD47	0	-0.7260	0.672	0.821	0
FYN	0	-0.7307	0.455	0.731	0
HLA-DPA1	0	-0.7364	0.114	0.348	0
ITGB4	0	-0.7408	0.258	0.608	0
FGFBP3	0	-0.7483	0.419	0.696	0
PAM	0	-0.7636	0.367	0.685	0
NDFIP1	0	-0.7659	0.733	0.87	0
CRISPLD1	0	-0.7904	0.29	0.638	0
MAP2	0	-0.7984	0.401	0.742	0
NFIA	0	-0.8043	0.283	0.638	0
NETO2	0	-0.8137	0.255	0.573	0
PTX3	0	-0.8214	0.573	0.829	0
PDPN	0	-0.8228	0.426	0.742	0
NOVA1	0	-0.8477	0.243	0.651	0
SMOC1	0	-0.8543	0.007	0.351	0
SLIT1	0	-0.8711	0.024	0.465	0
CAMK2N1	0	-0.8924	0.224	0.637	0
COL11A1	0	-0.9118	0.526	0.789	0
CP	0	-0.9132	0.254	0.711	0
PLTP	0	-0.9142	0.587	0.817	0
DCLK1	0	-0.9160	0.288	0.706	0
HLA-DRA	0	-0.9267	0.387	0.712	0
WLS	0	-0.9362	0.751	0.943	0
DST	0	-0.9371	0.795	0.946	0

FBLN5	0	-0.9405	0.216	0.622	0
SNTG1	0	-0.9497	0.225	0.612	0
GRIA1	0	-0.9724	0.325	0.738	0
IFITM1	0	-0.9746	0.05	0.552	0
SYNM	0	-0.9763	0.258	0.661	0
NR2F2	0	-0.9966	0.436	0.75	0
GFAP	0	-1.0125	0.06	0.453	0
FABP7	0	-1.0384	0.889	0.976	0
NTRK2	0	-1.0623	0.526	0.825	0
TFPI	0	-1.0795	0.168	0.572	0
ATP1B1	0	-1.1122	0.271	0.679	0
NR2F1	0	-1.1962	0.49	0.803	0
SPOCK2	0	-1.2233	0.086	0.633	0
MLC1	0	-1.2329	0.257	0.749	0
CPE	0	-1.2485	0.662	0.901	0
PI15	0	-1.2508	0.141	0.629	0
COL3A1	0	-1.2871	0.309	0.81	0
C1QL1	0	-1.3864	0.263	0.784	0
GPM6A	0	-1.4242	0.289	0.816	0
TTYH1	0	-1.4415	0.364	0.867	0
IFITM2	0	-1.4479	0.218	0.797	0
SPARCL1	0	-1.5203	0.166	0.792	0
S100B	0	-1.5696	0.481	0.952	0
IFITM3	0	-1.5748	0.512	0.977	0
PTPRZ1	0	-1.6910	0.274	0.891	0
CLU	0	-1.7279	0.707	0.983	0
A2M	0	-1.7553	0.831	0.999	0
LY6H	0	-1.9605	0.245	0.936	0
PTN	0	-1.9982	0.888	1	0
GPM6B	0	-2.0449	0.777	0.991	0
STAG2	5.46E-308	-0.3552	0.372	0.509	1.26E-303
SRSF7	1.92E-304	0.2576	0.796	0.635	4.42E-300
MTCL1	4.76E-304	-0.3515	0.265	0.418	1.10E-299
IFT57	1.16E-302	-0.3582	0.452	0.572	2.66E-298
BMP7	2.43E-301	-0.3244	0.277	0.43	5.61E-297
PIK3R1	3.15E-301	-0.2873	0.135	0.282	7.27E-297
NTN1	7.07E-300	-0.3764	0.293	0.439	1.63E-295
FEZ1	7.23E-299	-0.3017	0.682	0.733	1.67E-294
FOXJ1	5.44E-297	-0.2581	0.125	0.273	1.26E-292
TMED10	7.93E-297	-0.2824	0.753	0.78	1.83E-292
TSPAN11	9.08E-297	-0.2620	0.135	0.284	2.09E-292
KIAA1958	3.93E-293	-0.2755	0.148	0.298	9.07E-289
CDH6	6.27E-293	-0.4865	0.336	0.467	1.45E-288
STIM2	4.48E-290	-0.3236	0.204	0.353	1.03E-285
SOX9	4.78E-288	-0.3320	0.3	0.448	1.10E-283
OGFRL1	6.20E-288	-0.2560	0.117	0.259	1.43E-283

RALGPS2	7.99E-287	-0.3021	0.205	0.356	1.84E-282
NBEA	5.08E-285	-0.3183	0.228	0.38	1.17E-280
STK33	1.14E-284	-0.2976	0.176	0.325	2.63E-280
MID1	3.78E-281	-0.3891	0.368	0.501	8.72E-277
MCC	5.69E-281	-0.3067	0.163	0.308	1.31E-276
COL4A5	6.73E-281	-0.3017	0.205	0.356	1.55E-276
HMGCS1	9.78E-280	-0.3753	0.572	0.668	2.25E-275
CETN2	1.38E-279	-0.3421	0.525	0.625	3.19E-275
SPATA6	3.26E-279	-0.3175	0.132	0.274	7.51E-275
SORT1	3.72E-278	-0.3281	0.547	0.64	8.57E-274
IQCK	4.62E-276	-0.2841	0.182	0.332	1.07E-271
TMBIM4	3.34E-274	-0.3207	0.516	0.615	7.70E-270
IDH2	1.22E-273	-0.3387	0.623	0.678	2.81E-269
ARHGAP5	3.16E-273	-0.3107	0.311	0.45	7.30E-269
PCDHGA10	3.46E-272	-0.2593	0.076	0.201	7.97E-268
MAP1A	6.63E-270	-0.3116	0.43	0.556	1.53E-265
ATP6AP2	1.30E-269	-0.2716	0.763	0.788	3.00E-265
SERINC5	2.08E-267	-0.2666	0.111	0.243	4.80E-263
SRD5A1	1.73E-265	-0.2693	0.181	0.322	3.99E-261
COLGALT2	5.19E-265	-0.2731	0.104	0.233	1.20E-260
ZNRF3	7.60E-264	-0.2766	0.173	0.313	1.75E-259
THBS1	2.62E-261	0.2861	0.545	0.367	6.04E-257
DYNC2H1	3.22E-260	-0.3006	0.24	0.386	7.42E-256
SCG2	3.54E-260	-0.4735	0.157	0.299	8.16E-256
NAGLU	4.40E-260	-0.3039	0.339	0.469	1.02E-255
HLA-DPB1	1.05E-258	-0.4219	0.098	0.226	2.43E-254
FNDC4	7.11E-258	-0.3258	0.384	0.509	1.64E-253
MAGEH1	4.64E-257	-0.2879	0.277	0.419	1.07E-252
ADGRV1	1.54E-256	-0.5356	0.249	0.377	3.54E-252
HLA-DMA	4.17E-256	-0.3914	0.137	0.274	9.62E-252
GNG12	9.34E-256	-0.3183	0.393	0.507	2.15E-251
RSRP1	3.09E-255	-0.3280	0.503	0.612	7.13E-251
MEGF8	5.22E-255	-0.3058	0.369	0.497	1.20E-250
SYT1	2.67E-252	-0.3915	0.394	0.521	6.15E-248
GRN	1.07E-251	-0.2631	0.748	0.776	2.47E-247
AGAP1	3.54E-250	-0.2600	0.178	0.316	8.17E-246
TAX1BP1	6.44E-249	-0.2994	0.652	0.702	1.48E-244
LIPA	2.72E-245	-0.2988	0.218	0.35	6.27E-241
CTNNA1	3.78E-245	-0.2716	0.718	0.746	8.71E-241
SCD	1.08E-244	-0.3182	0.762	0.786	2.48E-240
SLCO3A1	2.53E-244	-0.3244	0.237	0.371	5.83E-240
FTX	2.03E-243	-0.3789	0.378	0.507	4.68E-239
GOLM1	3.19E-242	-0.3086	0.58	0.648	7.35E-238
ASAH1	1.80E-240	0.2935	0.762	0.638	4.15E-236
LHFPL6	7.01E-240	-0.3680	0.474	0.562	1.62E-235
KLF6	1.67E-239	-0.2964	0.634	0.728	3.84E-235

DUSP6	2.25E-239	-0.2554	0.112	0.239	5.19E-235
RNF13	5.41E-237	-0.2955	0.334	0.459	1.25E-232
AUTS2	5.50E-237	-0.3306	0.442	0.558	1.27E-232
NCALD	3.23E-236	-0.2801	0.193	0.328	7.45E-232
ZFP36L2	2.82E-233	-0.3037	0.381	0.513	6.51E-229
MIAT	8.83E-233	-0.3248	0.18	0.321	2.04E-228
SLC35F6	2.10E-230	-0.2989	0.288	0.412	4.83E-226
LINC00632	1.54E-228	-0.3418	0.238	0.371	3.55E-224
SLC35F1	2.08E-226	-0.2577	0.217	0.35	4.79E-222
JPX	6.59E-226	-0.3411	0.358	0.482	1.52E-221
ARGLU1	1.18E-225	-0.3152	0.715	0.764	2.72E-221
ITFG1	2.27E-225	-0.2917	0.354	0.472	5.23E-221
TCF7L2	2.72E-224	-0.2972	0.307	0.435	6.26E-220
SLC12A2	9.13E-223	-0.2938	0.255	0.381	2.11E-218
TMEM9B	1.99E-222	-0.3085	0.511	0.589	4.59E-218
EFHC1	9.91E-221	-0.3059	0.389	0.506	2.28E-216
PNISR	3.54E-219	-0.2760	0.779	0.821	8.17E-215
N4BP2	3.13E-215	-0.2565	0.193	0.321	7.23E-211
TMEM67	6.04E-214	-0.2800	0.217	0.347	1.39E-209
MICAL3	2.51E-213	-0.2613	0.193	0.32	5.79E-209
IQSEC1	3.14E-213	-0.2843	0.248	0.371	7.24E-209
HCFC1R1	7.88E-213	-0.2835	0.334	0.46	1.82E-208
LUC7L3	8.29E-213	-0.2739	0.808	0.841	1.91E-208
P4HTM	2.37E-212	-0.2782	0.424	0.533	5.48E-208
NEO1	1.04E-209	-0.2580	0.224	0.349	2.40E-205
PALMD	2.87E-209	-0.2505	0.151	0.275	6.62E-205
WRB	3.01E-207	-0.2807	0.37	0.485	6.95E-203
KIAA1109	3.82E-207	-0.2763	0.279	0.403	8.81E-203
NMB	3.90E-205	-0.3361	0.215	0.336	9.00E-201
TNRC6B	7.41E-205	-0.2871	0.601	0.67	1.71E-200
COL4A3BP	2.05E-204	-0.2952	0.28	0.397	4.72E-200
GPAA1	5.08E-203	-0.2832	0.604	0.656	1.17E-198
SERPING1	3.50E-200	-0.2696	0.255	0.377	8.07E-196
PFN2	3.51E-200	-0.2862	0.546	0.615	8.09E-196
SFXN5	5.42E-200	-0.2787	0.265	0.389	1.25E-195
TPP1	6.45E-200	-0.2635	0.269	0.389	1.49E-195
TCEAL3	1.30E-198	-0.3067	0.328	0.438	2.99E-194
IDS	4.85E-197	-0.2801	0.523	0.607	1.12E-192
DGCR2	1.53E-196	-0.2575	0.313	0.426	3.53E-192
PCGF5	2.51E-196	-0.2560	0.237	0.357	5.80E-192
COL4A2	2.59E-195	0.2582	0.894	0.837	5.96E-191
RND2	1.83E-193	-0.2821	0.257	0.377	4.23E-189
SPRY2	2.98E-192	-0.2718	0.283	0.403	6.88E-188
SPTAN1	3.25E-192	-0.2697	0.641	0.691	7.49E-188
PLCB1	1.28E-190	-0.2610	0.237	0.359	2.95E-186
PPP2CB	2.08E-189	-0.2750	0.56	0.619	4.81E-185

AKAP13	2.80E-187	-0.2830	0.473	0.561	6.46E-183
DOCK7	3.90E-187	-0.2763	0.311	0.427	9.00E-183
APCDD1	4.83E-185	-0.2780	0.112	0.22	1.11E-180
GDI1	9.86E-185	-0.2699	0.393	0.496	2.27E-180
NRBP2	3.91E-184	-0.2847	0.244	0.361	9.01E-180
MAGT1	1.28E-183	-0.2732	0.393	0.49	2.96E-179
CELSR1	1.79E-180	-0.2758	0.399	0.498	4.13E-176
JAKMIP2	2.74E-180	-0.2532	0.275	0.392	6.32E-176
SPG7	1.20E-178	-0.2895	0.546	0.622	2.76E-174
NOTCH1	1.10E-177	-0.2848	0.378	0.484	2.53E-173
STAT3	1.40E-176	-0.2707	0.487	0.572	3.22E-172
UBA1	1.93E-176	-0.2896	0.5	0.577	4.44E-172
SPAG9	3.11E-176	-0.2744	0.555	0.626	7.18E-172
ADGRG1	1.63E-175	-0.2706	0.219	0.333	3.75E-171
PCDHB2	4.40E-175	-0.2651	0.27	0.382	1.01E-170
SLC1A4	2.06E-171	-0.2675	0.177	0.283	4.76E-167
HLA-DRB1	3.95E-170	0.3247	0.273	0.153	9.10E-166
ABCA1	9.09E-169	-0.2987	0.329	0.438	2.10E-164
PTGFRN	2.08E-162	-0.2659	0.346	0.441	4.81E-158
HIPK2	3.68E-162	-0.2597	0.329	0.429	8.49E-158
PCDH7	1.52E-160	-0.2585	0.256	0.364	3.50E-156
IRS1	5.85E-160	-0.2540	0.34	0.443	1.35E-155
PCMTD1	3.49E-157	-0.2801	0.265	0.369	8.05E-153
IER5	4.00E-157	-0.2747	0.436	0.519	9.22E-153
PLEKHA5	4.83E-157	-0.2808	0.416	0.499	1.11E-152
FOS	5.24E-156	-0.3655	0.4	0.495	1.21E-151
PBX1	2.84E-155	-0.2613	0.503	0.579	6.54E-151
RGMB	4.86E-155	-0.2726	0.216	0.319	1.12E-150
NFIX	4.25E-154	-0.2604	0.552	0.616	9.79E-150
SESN3	1.43E-153	-0.2609	0.323	0.426	3.30E-149
UPP1	4.00E-150	-0.3024	0.417	0.498	9.24E-146
SYNE2	4.48E-150	-0.2983	0.372	0.471	1.03E-145
DOK5	7.76E-150	-0.2590	0.418	0.506	1.79E-145
SCPEP1	1.26E-149	-0.2530	0.376	0.463	2.90E-145
LIMCH1	1.08E-147	-0.2606	0.428	0.523	2.48E-143
COL27A1	4.49E-147	-0.3399	0.252	0.357	1.04E-142
AHNAK	7.04E-143	-0.2789	0.576	0.617	1.62E-138
LPL	1.05E-140	-0.2807	0.174	0.273	2.43E-136
MDM4	5.68E-138	-0.2795	0.375	0.465	1.31E-133
ZEB1	8.50E-135	-0.2628	0.446	0.523	1.96E-130
COL6A1	9.68E-134	-0.2827	0.667	0.728	2.23E-129
ITGA7	1.29E-133	-0.2623	0.229	0.325	2.98E-129
TCEAL8	4.14E-133	-0.2616	0.547	0.592	9.54E-129
CHD1	9.59E-131	-0.2589	0.411	0.486	2.21E-126
FBN2	1.94E-129	-0.2887	0.341	0.423	4.47E-125
ECI2	2.38E-125	-0.2582	0.439	0.51	5.50E-121

MSMO1	4.78E-125	-0.2594	0.627	0.657	1.10E-120
HLA-E	4.48E-123	-0.2628	0.426	0.49	1.03E-118
KIF21A	3.18E-122	-0.2612	0.299	0.382	7.32E-118
ANKRD12	5.86E-121	-0.2510	0.459	0.527	1.35E-116
SLC5A3	1.01E-113	-0.2526	0.274	0.357	2.34E-109
COL4A1	1.69E-110	0.2515	0.916	0.865	3.91E-106
BAALC	1.25E-109	-0.2735	0.291	0.368	2.89E-105
DNM1	3.39E-99	-0.2828	0.283	0.358	7.81E-95
SFRP1	5.91E-95	-0.4069	0.347	0.403	1.36E-90
IDH1	8.08E-88	-0.2618	0.396	0.456	1.86E-83
TMEM132A	1.51E-73	-0.2529	0.614	0.633	3.47E-69

Table 4.8.8. HD iAstro snRNA-seq Cell Line Breakdown by Cluster

cluster	CTR18n6	CTR33n1	HD46n10	HD53n3	Total	Total HD	Total CTR	%HD	%CTR
0	3777	5238	1738	1295	12048	3033	9015	25.2%	74.8%
1	971	172	1829	2740	5712	4569	1143	80.0%	20.0%
2	587	401	2451	1112	4551	3563	988	78.3%	21.7%
3	950	803	2066	634	4453	2700	1753	60.6%	39.4%
4	33	3889	4	0	3926	4	3922	0.1%	99.9%
5	0	416	986	744	2146	1730	416	80.6%	19.4%
6	600	734	278	255	1867	533	1334	28.5%	71.5%
7	68	341	217	306	932	523	409	56.1%	43.9%
8	84	18	113	278	493	391	102	79.3%	20.7%

CHAPTER IV

Dissertation Concluding Remarks

CHAPTER IV

Dissertation Concluding Remarks

5.1 Summary

Understanding the contributions of all dysregulated cell types to Huntington's disease (HD) pathogenesis is critical to understanding the disease as a whole. The data presented in this dissertation describe the cell-autonomous effects caused by *HTT* CAG repeat expansion in two cell types not yet extensively characterized in an unbiassed manner. Brain microvascular endothelial cells (BMECs) and astrocytes are cell types that are critical to regulating overall brain homeostasis. With their dysregulation in HD or other neurodegenerative disorders, complex molecular signaling regulating brain homeostasis will be compromised, making neurons more susceptible to degeneration. I was able to investigate the molecular and functional consequences of endogenous mutant HTT expression in human BMECs and astrocytes by utilizing HD patient-derived induced pluripotent stem cells (iPSC) modeling. In HD human iBMECs, I helped to determine aberrant WNT-mediated angiogenesis and migration along with compromised barrier functions. In HD human astrocytes, I identified inhibited glutamate receptor signaling and activated actin cytoskeleton-associated signaling that may be due to underlying developmental deficits in astrogliogenesis utilizing single-nuclei RNA-sequencing (snRNA-seq). To complement the HD astrocyte characterization, I also employed snRNA-seq to investigate astrocytes from a symptomatic HD mouse model (R6/2). HD mouse and human astrocytes had several common dysregulated cell states, including inhibited synaptogenesis and glutamate receptor signaling that increase in severity with age (8-weeks vs 12-weeks). Further investigation into the functional consequences of these dysregulated astrocytic cell states and how they contribute to dysfunction of the brain will provide greater understanding of the role they play in HD pathogenesis.

5.1.1 HD iBMEC Dysfunctions and Future Directions

The blood-brain barrier (BBB) regulates the movement of essential and toxic molecules between the brain and the rest of the body. We demonstrated decreased paracellular and transcellular barrier function in HD iBMECs that lead to increased BBB permeability (Chapter 1). This suggests a vulnerability in the HD BBB that may allow toxic substances to cross a leaky barrier and influx into the brain to cause harm to neurons, and subsequently induce neurodegeneration. Increased angiogenesis observed in HD iBMECs (Chapter 1) may seem like an improved aspect of the BBB; however, lack of barrier integrity in these newly formed blood vessels would likely induce further destruction to brain regions, broadening the scope of BMEC dysfunction across the HD brain. It may be possible to leverage these dysfunctional properties to enhance the transport of medicines across the leaky HD BBB that would not be able to do so in a brain with an intact BBB.

The mechanism behind HD iBMEC aberrant angiogenesis appeared to be due to the cell-autonomous activation of WNT signaling predicted via transcriptomic analysis. We demonstrated the rescue of aberrant angiogenesis via WNT inhibition in HD iBMECs (Chapters 1 and 2). Conversely, paracellular barrier function appeared to be exacerbated following WNT inhibition in HD iBMECs, raising question to the realistic therapeutic potential of this perturbation. As WNT signaling is critical for the functional maturation of the BBB, this dysregulation suggests the existence of developmental alterations in HD iBMECs. Similar developmentally altered phenotypes have been observed in other iPSC-derived cell types that include astrocytes (Chapter 3 and Osipovitch et al., 2019), neurons (HD iPSC Consortium, 2017; Smith-Geater et al., 2020), and oligodendrocytes (Osipovitch et al., 2019), as well as mouse models (Conforti et al., 2013; Luthi-Carter et al., 2002) and human tissue (Barnat et al., 2020; Hickman et al., 2021).

Many HD therapeutics undergoing clinical investigations are aimed at targeting the disease-causing DNA, RNA, or protein to ameliorate its downstream effects on cellular signaling and function (Tabrizi et al., 2019). Clustered regularly interspaced short palindromic repeats (CRISPR)/Cas9, antisense oligonucleotides (ASOs), RNA interference (RNAi), and small molecule splicing inhibitors for HTT lowering have been undergoing clinical assessment for their

therapeutic potential for HD (Tabrizi et al., 2019; Wild & Tabrizi, 2017). Unfortunately, the clinical promise of HTT lowering has had some devastating recent setbacks. The failure of several HTT lowering clinical trials this year highlights the many challenges that remain for this obvious, yet complicated, therapeutic target. These failures may be attributed to issues in drug distribution, dosing, and/or timing (Kingwell, 2021), and indicate that additional investigation into HTT lowering is necessary. It is important to understand how HTT lowering would affect individual human cell types to get a closer look into the complex cellular processes once cell type at a time. In this dissertation, I assessed how *HTT* lowering would functionally affect HD iBMECs *in vitro* (Chapter 2). I demonstrated a minor improvement in paracellular barrier function in HD iBMECs that were generated from a HD HTT knockdown iPSC line that contained a 60% reduction of *HTT*, however this interpretation was complicated by repeat instability within the clonal lines. Further functional assessments of patient knockdown iBMECs or isogenic HTT cell lines are needed to determine the magnitude of change this perturbation would produce on iBMECs. For example, angiogenic migration or transcellular function have yet to be evaluated in HD iBMECs with HTT knockdown. Additionally, the changes in molecular signaling beyond expression of several tight junction transcripts were not assessed in HD iBMECs with HTT knockdown. I hypothesize specifically mutant HTT lowering in HD iBMECs could alleviate WNT signaling activation to rescue aberrant angiogenesis and other dysfunctional properties of HD iBMECs.

While it is necessary to understand the cell-autonomous effect of individual cell types, it would be interesting to investigate how dysfunctional HD iBMECs effect other cell types in the brain. These assessments have begun to be investigated by our lab *in vitro* through implementation of iPSC-derived cellular co-culture systems. HD patient iPSC-derived astrocytes (iAstros) exacerbate BBB permeability when co-cultured in a transwell system with iBMECs, while unaffected control iAstros decrease barrier permeability in HD iBMECs (data not shown). Under the experimental conditions of a transwell co-culture system, the iAstros and iBMECs were not physically touching; this indicates astrocytes have the capacity to modulate barrier function via

secreted molecules and therefore may provide therapeutic potential if clinically targeted. Vascular reactivity of HD patient-derived and mouse model astrocytes has been shown to contribute to endothelial cell proliferation (Hsiao et al., 2015). Furthermore, co-cultures with iBMECs and HD patient iPSC-derived neurons in a transwell system could provide meaningful information as to how a leaky barrier may contribute to neuronal death. Finally, the co-culture of BMECs, astrocytes, and neurons would add further complexity of intercellular communications but could provide a more complete picture of neurovascular unit alterations in HD.

5.1.2 HD Human and Mouse Astrocyte Dysregulation and Future Directions

Astrocytes are critical regulators of brain metabolism, synaptogenesis, extracellular matrix, and the blood-brain barrier (Barres, 2008). Dysregulation of several of these properties have been demonstrated in HD astrocytes (Khakh et al., 2017; Khakh & Sofroniew, 2014). Specifically, I showed astrocyte dysregulation that implicated inhibition of glutamate receptor signaling in both human and mouse HD astrocytes (Chapter 3). The functional consequence of this dysregulated signaling pathway implicates decreased glutamate uptake through astrocytic glutamate transporters. Excessive glutamate at the synaptic cleft would over-excite neuronal glutamate receptors to induce excitotoxicity. As previously discussed, the HD iAstro dysregulation I show in this dissertation is validated by evidence of glutamate excitotoxicity caused by patient-derived and mouse model astrocytes, as well as post-mortem patient tissue (Bradford et al., 2009; Faideau et al., 2010; Garcia et al., 2019; Jiang et al., 2016; Khakh et al., 2017).

Additional studies are necessary to assess the functional consequences of HD astrocyte dysregulation. Altered expression of glutamate transporters and receptors could induce dysfunctional astrocytic glutamate uptake. Future studies quantifying the capacity for HD astrocytes to uptake glutamate is in the works. Next steps would include co-culture of iPSC-derived astrocytes with iPSC-derived striatal neurons, to better elucidate this impact with a larger context. It is critical to understand how diseased astrocytes affect neurons, either through

impaired glutamate uptake that leads to neuronal excitotoxicty or through other mechanisms. Experimental investigation into the effect of astrocytes on neuronal activity *in vitro*, perhaps utilizing microelectrode array (MEA) measurements, could also provide further evidence of the role of astrocytes on neuronal function. Additionally, as astrocytes elicit many homeostatic functions through secretion of soluble molecules, secretome studies of HD iAstros would be informative in further characterizing the functional effect of HD astrocytes on neighboring cell types. Furthermore, the effect of diseased neurons on healthy astrocytes would be an interesting avenue to investigate for non-cell autonomous mechanisms of HD pathogenesis.

Activated extracellular matrix and actin-associated signaling was another HD astrocyte phenotype I identified (Chapter 3). Actin-associated signaling activation as well as filamentous actin protein increase in HD iAstros was a novel finding as this aberrant phenotype had not been previously described in HD astrocytes. The functional consequence of activated actin-associated signaling has not yet been investigated. This may be related to increased properties in adhesion or migration of astrocytes. Alternatively, increased actin can manifest in altered astrocytic morphology, which has been described in HD-patient derived astrocytes (Chapter 3 and (Osipovitch et al., 2019). Additional functional assessments are underway for elucidation of the dysfunction associated with increased actin-related signaling in HD iAstros.

Increased cytoskeletal signaling has been associated with two major signatures in astrocytes—immaturity and reactivity (Schiweck et al., 2018). The lack of neuroinflammatory molecules in HD iAstros (Chapter 3) was slightly unexpected as this is pathological hallmark that has been demonstrated in advanced grades of HD patients (Faideau et al., 2010; Myers et al., 1991; Reddy et al., 1998; Sapp et al., 2001; Selkoe et al., 1982) and mouse models (Lin et al., 2001; Yu et al., 2003). This result indicates that reactive astrogliosis may be a non-cell autonomous phenotype occurring in HD astrocytes that may require exposure of inflammatory cytokines and chemokines from activated microglia; alternatively, the HD iAstros may not replicate aspects of late disease stages. HD iAstros can be co-cultured with activated microglia or their

neurotoxic astrocyte-inducing secreted factors (Liddelow et al., 2017) to assess the induction of reactive phenotypes in HD. Lack of clear astrogliosis signatures in HD iAstros may also suggest a dysfunction within HD iAstros, which may be associated with altered astrocyte maturation. In addition to being a hallmark of reactive astrogliosis, increases in cytoskeletal structural proteins, such as VIMENTIN, are associated with decreased astrocyte maturity (Schiweck et al., 2018).

Much of the data I showed in HD human and iPSC-derived astrocytes suggested developmental deficit that may manifest in dysfunctional astrocyte states (Chapter 3). Transcription factor enrichment analysis highlighted astrogliogenesis and neural regulatory factors as controlling HD mouse and human astrocyte dysregulation. The mechanistic evaluation of ATF3 or other astrogliogenesis transcription factors will be an informative avenue to pursue for future studies. As I demonstrated significant decreased ATF3 protein levels, it is possible the overexpression of ATF3 in HD astrocytes may rescue aberrant astrogliogenesis to restore astrocyte signaling and functions. *In vitro* and *in vivo* investigations are necessary to characterize how this astrocytic perturbation may restore neuronal homeostasis and freeze neurodegeneration in HD.

Further *in vitro* experimentation on iAstros is necessary. First, HTT knockdown in HD human astrocytes would help inform HTT lowering studies. Secondly, patient variability is a major issue when using iPSC modeling (Carcamo-Orive et al., 2017). The generation of HTT isogenic iPSCs and subsequent astrocyte differentiation would help to alleviate that. Next, the process of *in vitro* differentiation often lacks that ability to develop fully mature cells, even when using healthy control iPSCs. Aging astrocytes *in vivo* through implantation into mice would be an interesting avenue to investigate. Finally, directed astrocyte generation from patient fibroblasts would be a great opportunity to retain epigenetic marks of an adult cell type for modeling a late-onset disease, like HD. Unfortunately, this technology is not yet efficient for human cells (Caiazzo et al., 2015), most likely due to the lack of astrocyte developmental characterization in humans.

Additional computational studies for extended transcriptomic and epigenomic investigation would provide a clearer picture on HD astrocyte dysregulation and the mechanisms controlling their dysregulation. Single-cell transcriptomics performed on other HD mouse models that contain full-length HTT and better recapitulate human HD pathogenesis, like zQ175 mice, would be extremely informative. The epigenetic investigation would be a great avenue to pursue for elucidation of altered transcriptional regulation in HD astrocytes. For instance, assay for transposase-accessible chromatin using sequencing (ATAC)-seq or chromatin immunoprecipitation sequencing (ChIP)-seq can be used to identify astrogliogenesis transcription factor binding sites that differ between HD and unaffected control astrocytes. With the advancement of computational biology technologies, future multi-omic studies combining single-cell transcriptomics, epigenomics, and proteomics within the same cell will hopefully be more established and cost-effective to perform a deeper analysis into HD iAstros molecular signatures (Lee et al., 2020).

5.2 Conclusion

In this dissertation, I provided greater context into non-neuronal cell type dysregulation in HD. Through the combination of patient iPSC and mouse modeling with transcriptomic approaches, I was able to uncover dysregulated BBB signaling in HD iBMECs and dysregulated states HD iAstros. The validation of the dysfunction of HD iBMEC and the dysregulation of glutamate and actin-associated signaling in HD human astrocytes suggests a contribution for non-neuronal cell types to loss of function or gain of toxic function in HD pathogenesis. Together, my analyses provided novel insights into molecular mechanisms that contribute to disease pathogenesis and suggests the influence of mutant HTT on altered developmental patterns in HD cell types. Overall, the knowledge provided in this dissertation can be used to inform future therapeutic investigations for Huntington’s disease

5.3 References

Barnat, M., Capizzi, M., Aparicio, E., Boluda, S., Wennagel, D., Kacher, R., Kassem, R., Lenoir, S., Agasse, F., Bra, B. Y., Liu, J. P., Ighil, J., Tessier, A., Zeitli, S. O., Duyckaerts, C., Dommergues, M., Durr, A., & Humbert, S. (2020). Huntington's disease alters human neurodevelopment. *Science*, *369*(6505), 787–793. https://doi.org/10.1126/science.aax3338

Barres, B. A. (2008). The Mystery and Magic of Glia: A Perspective on Their Roles in Health and Disease. *Neuron*, *60*(3), 430–440. https://doi.org/10.1016/j.neuron.2008.10.013

Bradford, J., Shin, J., Roberts, M., Wang, C., Li, X., & Li, S. (2009). Expression of mutant huntingtin in mouse brain astrocytes causes age-dependent neurological symptoms. *Proceedings of the National Academy of Sciences*, *106*(52), 22480–22485. https://doi.org//10.1073/pnas.0911503106

Caiazzo, M., Giannelli, S., Valente, P., Lignani, G., Carissimo, A., Sessa, A., Colasante, G., Bartolomeo, R., Massimino, L., Ferroni, S., Settembre, C., Benfenati, F., & Broccoli, V. (2015). Direct Conversion of Fibroblasts into Functional Astrocytes by Defined Transcription Factors. *Stem Cell Reports*, *4*(1), 25–36. https://doi.org/10.1016/j.stemcr.2014.12.002

Carcamo-Orive, I., Hoffman, G. E., Cundiff, P., Beckmann, N. D., D'Souza, S. L., Knowles, J. W., Patel, A., Papatsenko, D., Abbasi, F., Reaven, G. M., Whalen, S., Lee, P., Shahbazi, M., Henrion, M. Y. R., Zhu, K., Wang, S., Roussos, P., Schadt, E. E., Pandey, G., … Lemischka, I. (2017). Analysis of Transcriptional Variability in a Large Human iPSC Library Reveals Genetic and Non-genetic Determinants of Heterogeneity. *Cell Stem Cell*, *20*(4), 518-532.e9. https://doi.org/10.1016/j.stem.2016.11.005

Conforti, P., Camnasio, S., Mutti, C., Valenza, M., Thompson, M., Fossale, E., Zeitlin, S., MacDonald, M. E., Zuccato, C., & Cattaneo, E. (2013). Lack of huntingtin promotes neural stem cells differentiation into glial cells while neurons expressing huntingtin with expanded polyglutamine tracts undergo cell death. *Neurobiology of Disease*, *50*(1), 160–170. https://doi.org/10.1016/j.nbd.2012.10.015

Faideau, M., Kim, J., Cormier, K., Gilmore, R., Welch, M., Auregan, G., Dufour, N., Guillermier, M., Ferrante, R. J., Brouillet, E., Hantraye, P., & De, N. (2010). In vivo expression of polyglutamine-expanded huntingtin by mouse striatal astrocytes impairs glutamate transport: a correlation with Huntington's disease subjects. *Human Molecular Genetics*, *19*(15), 3053–3067. https://doi.org/10.1093/hmg/ddq212

Garcia, V. J., Rushton, D. J., Tom, C. M., Allen, N. D., Kemp, P. J., Svendsen, C. N., & Mattis, V. B. (2019). Huntington's Disease Patient-Derived Astrocytes Display Electrophysiological Impairments and Reduced Neuronal Support. *Frontiers in Neuroscience*, *13*(June), 1–14. https://doi.org/10.3389/fnins.2019.00669

HD iPSC Consortium. (2017). Developmental alterations in Huntington's disease neural cells and pharmacological rescue in cells and mice. *Nature Neuroscience*, *20*(5), 648–660. https://doi.org/10.1038/nn.4532

Hickman, R. A., Faust, · P L, Rosenblum, · M K, Marder, · K, Mehler, · M F, Vonsattel, · J P, & Purpura, D. P. (2021). Developmental malformations in Huntington disease: neuropathologic evidence of focal neuronal migration defects in a subset of adult brains. *Acta Neuropathologica*, *141*, 399–413. https://doi.org/10.1007/s00401-021-02269-4

Hsiao, H. Y., Chen, Y. C., Huang, C. H., Chen, C. C., Hsu, Y. H., Chen, H. M., Chiu, F. L., Kuo, H. C., Chang, C., & Chern, Y. (2015). Aberrant astrocytes impair vascular reactivity in Huntington disease. *Annals of Neurology*, *78*(2), 178–192. https://doi.org/10.1002/ana.24428

Jiang, R., Diaz-Castro, B., Looger, L. L., & Khakh, B. S. (2016). Dysfunctional Calcium and Glutamate Signaling in Striatal Astrocytes from Huntington's Disease Model Mice. *Journal of Neuroscience*, *36*(12), 3453–3470. https://doi.org/10.1523/JNEUROSCI.3693-15.2016

Khakh, B. S., Beaumont, V., Cachope, R., Munoz-Sanjuan, I., Goldman, S. A., & Grantyn, R. (2017). Unravelling and Exploiting Astrocyte Dysfunction in Huntington's Disease. *Trends in Neurosciences*, *40*(7), 422–437. https://doi.org/10.1016/j.tins.2017.05.002

Khakh, B. S., & Sofroniew, M. v. (2014). Astrocytes and Huntington's disease. *ACS Chemical Neuroscience*, *5*(7), 494–496. https://doi.org/10.1021/cn500100r

Kingwell, K. (2021). Double setback for ASO trials in Huntington disease. In *Nature Reviews. Drug Discovery* (Vol. 20, Issue 6, pp. 412–413). NLM (Medline). https://doi.org/10.1038/d41573-021-00088-6

Lee, J., Hyeon, D. Y., & Hwang, D. (2020). Single-cell multiomics: technologies and data analysis methods. In *Experimental and Molecular Medicine* (Vol. 52, Issue 9, pp. 1428–1442). Springer Nature. https://doi.org/10.1038/s12276-020-0420-2

Liddelow, S. A., Guttenplan, K. A., Clarke, L. E., Bennett, F. C., Bohlen, C. J., Schirmer, L., Bennett, M. L., Münch, A. E., Chung, W., Peterson, T. C., & Wilton, D. K. (2017). Neurotoxic reactive astrocytes are induced by activated microglia. *Nature*, *541*(7638), 481–487. https://doi.org/10.1038/nature21029

Lin, C. H., Tallaksen-Greene, S., Chien, W. M., Cearley, J. A., Jackson, W. S., Crouse, A. B., Ren, S., Li, X. J., Albin, R. L., & Detloff, P. J. (2001). Neurological abnormalities in a knock-in mouse model of Huntington's disease. *Human Molecular Genetics*, *10*(2), 137–144. https://doi.org/10.1093/hmg/10.2.137

Luthi-Carter, R., Hanson, S. A., Strand, A. D., Bergstrom, D. A., Chun, W., Peters, N. L., Woods, A. M., Chan, E. Y., Kooperberg, C., Krainc, D., Young, A. B., Tapscott, S. J., & Olson, J. M. (2002). Dysregulation of gene expression in the R6/2 model of polyglutamine disease: parallel changes in muscle and brain. *Human Molecular Genetics*, *11*(17), 1911–1926. www.neumetrix.info.

Myers, R. H., Vonsattel, J. P., Paskevich, P. A., Kiely, D. K., Stevens, T. J., Cupples, L. A., Jr, E. P. R., & Bird, E. D. (1991). Decreased neuronal and increased oligodendroglial densities in Huntington's disease caudate nucleus. *Journal of Neuropathology and Experimental Neurology*, *50*(6), 729–742. https://doi.org/10.1097/00005072-199111000-00005.

Osipovitch, M., Martinez, A. A., Mariani, J. N., Cornwell, A., Dhaliwal, S., Zou, L., Chandler-Militello, D., Wang, S., Li, X., Benraiss, S.-J., Agate, R., Lampp, A., Benraiss, A., Windrem, M. S., & Goldman, S. A. (2019). Human ESC-Derived Chimeric Mouse Models of Huntington's Disease Reveal Cell-Intrinsic Defects in Glial Progenitor Cell Differentiation. *Cell Stem Cell*, *24*(1), 107–122. https://doi.org/10.1016/j.stem.2018.11.010

Reddy, P. H., Williams, M., Charles, V., Garrett, L., Pike-Buchanan, L., Whetsell, W. O., Miller, G., & Tagle, D. A. (1998). Behavioural abnormalities and selective neuronal loss in HD transgenic mice expressing mutated full-length HD cDNA. *Nature Genetics*, *20*(2), 198–202. https://doi.org/10.1038/2510

Sapp, E., Kegel, K. B., Aronin, N., Hashikawa, T., Uchiyama, Y., Tohyama, K., Bhide, P. G., Vonsattel, J. P., & Difiglia, M. (2001). Early and progressive accumulation of reactive microglia in the Huntington disease brain. *Journal of Neuropathology and Experimental Neurology*, *60*(2), 161–172. https://doi.org/10.1093/jnen/60.2.161

Schiweck, J., Eickholt, B. J., & Murk, K. (2018). Important shapeshifter: Mechanisms allowing astrocytes to respond to the changing nervous system during development, injury and disease. In *Frontiers in Cellular Neuroscience* (Vol. 12). Frontiers Media S.A. https://doi.org/10.3389/fncel.2018.00261

Selkoe, D. J., Salasar, F. J., Abraham, C., & Kosik, K. S. (1982). Huntington's disease: Changes in striatal proteins reflect astrocytic gliosis. *Brain Research*, *245*(1), 117–125. https://doi.org/10.1016/0006-8993(82)90344-4

Smith-Geater, C., Hernandez, S. J., Lim, R. G., Adam, M., Wu, J., Stocksdale, J. T., Wassie, B. T., Gold, M. P., Wang, K. Q., Miramontes, R., Kopan, L., Orellana, I., Joy, S., Kemp, P. J., Allen, N. D., Fraenkel, E., & Thompson, L. M. (2020). Aberrant Development Corrected in Adult-Onset Huntington's Disease iPSC-Derived Neuronal Cultures via WNT Signaling Modulation. *Stem Cell Reports*, *14*, 406–419. https://doi.org/10.1016/j.stemcr.2020.01.015

Tabrizi, S. J., Ghosh, R., & Leavitt, B. R. (2019). Huntingtin Lowering Strategies for Disease Modification in Huntington's Disease. In *Neuron* (Vol. 101, Issue 5, pp. 801–819). Cell Press. https://doi.org/10.1016/j.neuron.2019.01.039

Wild, E. J., & Tabrizi, S. J. (2017). Therapies targeting DNA and RNA in Huntington's disease. In *The Lancet Neurology* (Vol. 16, Issue 10, pp. 837–847). Lancet Publishing Group. https://doi.org/10.1016/S1474-4422(17)30280-6

Yu, Z.-X., Li, S.-H., Evans, J., Pillarisetti, A., Li, H., & Li, X.-J. (2003). Mutant huntingtin causes context-dependent neurodegeneration in mice with Huntington's disease. *The Journal of Neuroscience : The Official Journal of the Society for Neuroscience*, *23*(6), 2193–2202. https://doi.org/23/6/2193 [pii]

APPENDIX

Supplemental Tables corresponding to Chapter 3

Supplemental Table 4.1. R6/2 12-Week Striatal Astrocyte IPA Canonical Pathway Enrichment Analysis

Ingenuity Canonical Pathways	-log(p-value)	Ratio	z-score	Molecules
Opioid Signaling Pathway	6.69	0.048	-0.577	ADCY2,AKT3,CACNA1A,CAMK2D,CAMK2G,GNAO1,GRIN2B,GRIN2C,MAPK4,PDE1C,PLCB1,RGS7
CREB Signaling in Neurons	6.6	0.0529	-0.707	ADCY2,AKT3,CACNA1A,CAMK2D,CAMK2G,GNAO1,GRIA2,GRIN2B,GRIN2C,PLCB1,POLR2A
Synaptogenesis Signaling Pathway	6.48	0.0415	-0.832	ADCY2,AKT3,CADM1,CAMK2D,CAMK2G,DAB1,FARP1,GRIA2,GRIN2B,GRIN2C,HSPA8,Nrxn3,NTRK2
Amyotrophic Lateral Sclerosis Signaling	6.35	0.0816	-0.447	AKT3,CACNA1A,GLUL,GRIA2,GRIN2B,GRIN2C,SLC1A2,VEGFA
G-Protein Coupled Receptor Signaling	6.3	0.0441		ADCY2,AKT3,CAMK2D,CAMK2G,CHUK,GABBR2,GNAO1,PDE10A,PDE1C,PLCB1,RAPGEF3,RGS7
Endocannabinoid Neuronal Synapse Pathway	5.47	0.0625	-0.707	ADCY2,CACNA1A,GNAO1,GRIA2,GRIN2B,GRIN2C,MAPK4,PLCB1
Neuropathic Pain Signaling In Dorsal Horn Neurons	5.12	0.0686	-1.134	CAMK2D,CAMK2G,GRIA2,GRIN2B,GRIN2C,NTRK2,PLCB1
cAMP-mediated signaling	4.49	0.0396	-1.667	ADCY2,CAMK2D,CAMK2G,GABBR2,GNAO1,PDE10A,PDE1C,RAPGEF3,RGS7
Synaptic Long Term Potentiation	4.46	0.0543	-1.134	CAMK2D,CAMK2G,GRIA2,GRIN2B,GRIN2C,PLCB1,RAPGEF3
Glutamate Receptor Signaling	4.31	0.0877		GLUL,GRIA2,GRIN2B,GRIN2C,SLC1A2
Neuroinflammation Signaling Pathway	4.27	0.0332	0.447	AKT3,CHUK,GABBR2,GABRA2,GLUL,GRIN2B,GRIN2C,MAPK4,SLC1A2,SLC6A11
GABA Receptor Signaling	4.26	0.0632		ADCY2,CACNA1A,GABBR2,GABRA2,SLC6A11,Ubb
Spermine and Spermidine Degradation I	3.54	0.5		SAT1,SMOX
Cardiac Hypertrophy Signaling (Enhanced)	3.19	0.0226	0.302	ADCY2,AKT3,CACNA1A,CAMK2D,CAMK2G,CHUK,EDNRB,FGF14,PDE10A,PDE1C,PLCB1
Relaxin Signaling	3.18	0.04		ADCY2,AKT3,GNAO1,PDE10A,PDE1C,VEGFA
CDK5 Signaling	3.01	0.0463	-0.447	ADCY2,CABLES1,CACNA1A,MAPK4,NTRK2
Melatonin Signaling	2.79	0.0556	-1	CAMK2D,CAMK2G,GNAO1,PLCB1
Ephrin Receptor Signaling	2.77	0.0333	-0.447	AKT3,GNAO1,GRIN2B,GRIN2C,SORBS1,VEGFA
Protein Kinase A Signaling	2.69	0.0226	-1	ADCY2,CAMK2D,CAMK2G,CHUK,PDE10A,PDE1C,PHKG1,PLCB1,UBASH3B

Notch Signaling	2.63	0.0789		CNTN1,HES5,MAML3
PI3K Signaling in B Lymphocytes	2.54	0.0362	0.447	AKT3,CAMK2D,CAMK2G,CHUK,PLCB1
Calcium Signaling	2.48	0.0291		CACNA1A,CAMK2D,CAMK2G,GRIA2,GRIN2B,GRIN2C
Endocannabinoid Cancer Inhibition Pathway	2.46	0.0347	0.447	ADCY2,AKT3,CCND3,GNAO1,VEGFA
Thrombin Signaling	2.45	0.0287	0.447	ADCY2,AKT3,CAMK2D,CAMK2G,GNAO1,PLCB1
Role of NFAT in Cardiac Hypertrophy	2.39	0.0279		ADCY2,AKT3,CACNA1A,CAMK2D,CAMK2G,PLCB1
Nitric Oxide Signaling in the Cardiovascular System	2.27	0.04	1	AKT3,CACNA1A,PDE1C,VEGFA
Dopamine-DARPP32 Feedback in cAMP Signaling	2.23	0.0307	-0.447	ADCY2,CACNA1A,GRIN2B,GRIN2C,PLCB1
γ-linolenate Biosynthesis II (Animals)	2.21	0.118		ACSL3,FADS1
Molecular Mechanisms of Cancer	2.19	0.0204		ADCY2,AKT3,CAMK2D,CAMK2G,CCND3,GNAO1,PLCB1,RAPGEF3
Huntington's Disease Signaling	2.18	0.0252		AKT3,GRIN2B,HSPA8,PLCB1,POLR2A,Ubb
Role of Macrophages, Fibroblasts and Endothelial Cells in Rheumatoid Arthritis	2.18	0.0224		AKT3,CAMK2D,CAMK2G,CHUK,GNAO1,PLCB1,VEGFA
Glutamine Biosynthesis I	2.16	1		GLUL
Thiamin Salvage III	2.16	1		TPK1
GNRH Signaling	2.13	0.0289	-1	ADCY2,CACNA1A,CAMK2D,CAMK2G,PLCB1
iCOS-iCOSL Signaling in T Helper Cells	2.1	0.0357	1	AKT3,CAMK2D,CAMK2G,CHUK
Apelin Endothelial Signaling Pathway	2.05	0.0345		ADCY2,AKT3,GNAO1,PLCB1
Endocannabinoid Developing Neuron Pathway	2.05	0.0345		ADCY2,AKT3,GNAO1,MAPK4
Putrescine Degradation III	2.03	0.0952		SAT1,SMOX
B Cell Receptor Signaling	2	0.0269	0.447	AKT3,BCL6,CAMK2D,CAMK2G,CHUK
Endothelin-1 Signaling	1.99	0.0267	-1.342	ADCY2,EDNRB,GNAO1,MAPK4,PLCB1
Role of Tissue Factor in Cancer	1.98	0.0331		AKT3,F3,PLCB1,VEGFA
G Beta Gamma Signaling	1.97	0.0328		ADCY2,AKT3,CACNA1A,GNAO1
Gap Junction Signaling	1.88	0.0251		ADCY2,AKT3,GJB6,GRIA2,PLCB1
Cellular Effects of Sildenafil (Viagra)	1.87	0.0305		ADCY2,CACNA1A,PDE1C,PLCB1

GM-CSF Signaling	1.87	0.0423		AKT3,CAMK2D,CAMK2G
Glutamate Biosynthesis II	1.86	0.5		GLUD1
Glutamate Degradation X	1.86	0.5		GLUD1
Leptin Signaling in Obesity	1.8	0.04		ADCY2,AKT3,PLCB1
Cardiac β-adrenergic Signaling	1.77	0.0286		ADCY2,CACNA1A,PDE10A,PDE1C
IL-7 Signaling Pathway	1.74	0.038		AKT3,BCL6,CCND3
Type II Diabetes Mellitus Signaling	1.74	0.028		ACSL3,AKT3,CACNA1A,CHUK
Chemokine Signaling	1.73	0.0375		CAMK2D,CAMK2G,PLCB1
Corticotropin Releasing Hormone Signaling	1.72	0.0276		ADCY2,CACNA1A,GNAO1,VEGFA
Renal Cell Carcinoma Signaling	1.72	0.037		AKT3,Ubb,VEGFA
Proline Degradation	1.68	0.333		LOC102724788/PRODH
Axonal Guidance Signaling	1.67	0.0164		AKT3,GNAO1,NTRK2,PLCB1,ROBO2,SEMA4A,SEMA6A,VEGFA
Circadian Rhythm Signaling	1.65	0.0606		GRIN2B,GRIN2C
Gustation Pathway	1.64	0.0261		ADCY2,CACNA1A,PDE10A,PDE1C
Inhibition of Angiogenesis by TSP1	1.63	0.0588		AKT3,VEGFA
PKCθ Signaling in T Lymphocytes	1.62	0.0256		CACNA1A,CAMK2D,CAMK2G,CHUK
Gαq Signaling	1.6	0.0253		AKT3,CHUK,PLCB1,RGS7
eNOS Signaling	1.58	0.025	-1	ADCY2,AKT3,HSPA8,VEGFA
IL-1 Signaling	1.58	0.033		ADCY2,CHUK,GNAO1
Melatonin Degradation II	1.56	0.25		SMOX
Thymine Degradation	1.56	0.25		DPYD
Uracil Degradation II (Reductive)	1.56	0.25		DPYD
CXCR4 Signaling	1.52	0.0238		ADCY2,AKT3,GNAO1,PLCB1
Apelin Cardiomyocyte Signaling Pathway	1.48	0.03		AKT3,MAPK4,PLCB1
Wnt/β-catenin Signaling	1.47	0.0231		AKT3,GNAO1,SOX5,Ubb
tRNA Splicing	1.46	0.0476		PDE10A,PDE1C
Serotonin Receptor Signaling	1.44	0.0465		ADCY2,SMOX

Antioxidant Action of Vitamin C	1.41	0.028		CHUK,NXN,PLCB1
Role of NFAT in Regulation of the Immune Response	1.41	0.022		AKT3,CHUK,GNAO1,PLCB1
Arginine Biosynthesis IV	1.39	0.167		GLUD1
FAT10 Cancer Signaling Pathway	1.39	0.0435		AKT3,CHUK
Synaptic Long Term Depression	1.37	0.0214	-1	CACNA1A,GNAO1,GRIA2,PLCB1
Glioma Signaling	1.37	0.027		AKT3,CAMK2D,CAMK2G
nNOS Signaling in Neurons	1.37	0.0426		GRIN2B,GRIN2C
GPCR-Mediated Nutrient Sensing in Enteroendocrine Cells	1.36	0.0268		ADCY2,CACNA1A,PLCB1
PPARα/RXRα Activation	1.35	0.0211		ABCA1,ADCY2,CHUK,PLCB1
HIF1α Signaling	1.34	0.0263		AKT3,MAPK4,VEGFA
Clathrin-mediated Endocytosis Signaling	1.32	0.0206		FGF14,HSPA8,Ubb,VEGFA
Phosphatidylcholine Biosynthesis I	1.32	0.143		PHKA1
RAR Activation	1.32	0.0206		ADCY2,AKT3,VEGFA,ZBTB16
Thioredoxin Pathway	1.32	0.143		NXN

Supplemental Table 4.2. R6/2 12-Week Cortical Astrocyte IPA Canonical Pathway Enrichment Analysis

Ingenuity Canonical Pathways	-log(p-value)	Ratio	z-score	Molecules
Glutamate Receptor Signaling	4.11	0.0702		GLUL,GRIA2,GRIN2C,SLC1A2
Synaptic Long Term Potentiation	3.79	0.0388	-2.236	CAMK2G,GRIA2,GRIN2C,PLCB1,RAPGEF3
Neuroinflammation Signaling Pathway	3.73	0.0234		GABBR1,GABBR2,GABRA2,GLUL,GRIN2C,MFGE8,SLC1A2
Synaptogenesis Signaling Pathway	3.62	0.0224	-1.89	CADM1,CAMK2G,FARP1,GRIA2,GRIN2C,HSPA8,NRXN1
Amyotrophic Lateral Sclerosis Signaling	3.22	0.0412		GLUL,GRIA2,GRIN2C,SLC1A2
Neuropathic Pain Signaling In Dorsal Horn Neurons	3.16	0.0396	-2	CAMK2G,GRIA2,GRIN2C,PLCB1
G-Protein Coupled Receptor Signaling	3.13	0.0221		CAMK2G,GABBR1,GABBR2,PDE10A,PLCB1,RAPGEF3
CREB Signaling in Neurons	2.85	0.0242	-2	CAMK2G,GRIA2,GRIN2C,PLCB1,POLR2A
cAMP-mediated signaling	2.67	0.0219	-2.236	CAMK2G,GABBR1,GABBR2,PDE10A,RAPGEF3
Thiamin Salvage III	2.4	1		TPK1
Glutamine Biosynthesis I	2.4	1		GLUL
GABA Receptor Signaling	2.2	0.0316		GABBR1,GABBR2,GABRA2
Circadian Rhythm Signaling	2.12	0.0606		CLOCK,GRIN2C
Breast Cancer Regulation by Stathmin1	2.04	0.0118		CAMK2G,CCND3,GABBR1,GABBR2,NTSR2,PLCB1,PPP2R3A
Endocannabinoid Neuronal Synapse Pathway	1.84	0.0234		GRIA2,GRIN2C,PLCB1
Protein Kinase A Signaling	1.67	0.0125	-1.342	CAMK2G,DCC,PDE10A,PHKG1,PLCB1
D-myo-inositol-5-phosphate Metabolism	1.61	0.0191		ATP1A2,PLCB1,PPP2R3A
Necroptosis Signaling Pathway	1.61	0.0191		CAMK2G,GLUL,MERTK
Aldosterone Signaling in Epithelial Cells	1.6	0.019		ASIC2,HSPA8,PLCB1
Dopamine-DARPP32 Feedback in cAMP Signaling	1.57	0.0184		GRIN2C,PLCB1,PPP2R3A
Melatonin Signaling	1.48	0.0278		CAMK2G,PLCB1
Sucrose Degradation V (Mammalian)	1.45	0.111		ALDOC
Synaptic Long Term Depression	1.41	0.0159		GRIA2,PLCB1,PPP2R3A
PPARα/RXRα Activation	1.4	0.0158		ABCA1,CLOCK,PLCB1
Chemokine Signaling	1.4	0.025		CAMK2G,PLCB1
Cyclins and Cell Cycle Regulation	1.39	0.0247		CCND3,PPP2R3A

Superpathway of Inositol Phosphate Compounds	1.35	0.0151	ATP1A2,PLCB1,PPP2R3A
Calcium Signaling	1.31	0.0146	CAMK2G,GRIA2,GRIN2C

Supplemental Table 4.3. R6/2 8-Week Striatal Astrocyte IPA Canonical Pathway Enrichment Analysis

Ingenuity Canonical Pathways	-log(p-value)	Ratio	z-score	Molecules
Neuroinflammation Signaling Pathway	3	0.0167		CHUK,GABBR1,GABRA2,SLC1A2,SLC6A11
GABA Receptor Signaling	2.74	0.0316		GABBR1,GABRA2,SLC6A11
G-Protein Coupled Receptor Signaling	2.3	0.0148		ADRA1A,CAMK2G,CHUK,GABBR1
Cardiac Hypertrophy Signaling (Enhanced)	2.1	0.0103	-0.447	ADRA1A,CAMK2G,CHUK,EDNRB,FGF14
Clathrin-mediated Endocytosis Signaling	1.88	0.0155		CLU,FGF14,VEGFA
Zymosterol Biosynthesis	1.82	0.167		MSMO1
Osteoarthritis Pathway	1.77	0.0141		CHUK,PTCH1,VEGFA
Protein Kinase A Signaling	1.73	0.01		CAMK2G,CHUK,PHKG1,PTCH1
Phosphatidylethanolamine Biosynthesis II	1.64	0.111		PCYT2
α-Adrenergic Signaling	1.61	0.0211		ADRA1A,PHKG1
Amyotrophic Lateral Sclerosis Signaling	1.59	0.0206		SLC1A2,VEGFA
Bladder Cancer Signaling	1.59	0.0206		FGF14,VEGFA
iCOS-iCOSL Signaling in T Helper Cells	1.49	0.018		CAMK2G,CHUK
Cholesterol Biosynthesis I	1.49	0.0769		MSMO1
Cholesterol Biosynthesis II (via 24,25-dihydrolanosterol)	1.49	0.0769		MSMO1
Cholesterol Biosynthesis III (via Desmosterol)	1.49	0.0769		MSMO1
LXR/RXR Activation	1.42	0.0165		ABCA1,CLU
IL-6 Signaling	1.39	0.016		CHUK,VEGFA
Gα12/13 Signaling	1.36	0.0154		CDH19,CHUK
IL-12 Signaling and Production in Macrophages	1.35	0.0152		CHUK,CLU
Role of Macrophages, Fibroblasts and Endothelial Cells in Rheumatoid Arthritis	1.34	0.00962		CAMK2G,CHUK,VEGFA
Estrogen Receptor Signaling	1.32	0.0146		DDX5,POLR2A
PI3K Signaling in B Lymphocytes	1.32	0.0145		CAMK2G,CHUK

Supplemental Table 4.4. R6/2 8-Week Cortical Astrocyte IPA Canonical Pathway Enrichment Analysis

Ingenuity Canonical Pathways	-log(p-value)	Ratio	z-score	Molecules
Glutamate Receptor Signaling	2.37	0.0351		GRM3,SLC1A2
Ceramide Degradation	1.99	0.167		ACER3
Sphingosine and Sphingosine-1-phosphate Metabolism	1.87	0.125		ACER3
PTEN Signaling	1.7	0.0159		BMPR1A,FOXO1
Adipogenesis pathway	1.65	0.0149		BMPR1A,FOXO1
Human Embryonic Stem Cell Pluripotency	1.65	0.0148		BMPR1A,FOXO1
Estrogen Receptor Signaling	1.64	0.0146		DDX5,POLR2A
Cardiomyocyte Differentiation via BMP Receptors	1.47	0.05		BMPR1A
CREB Signaling in Neurons	1.31	0.00966		GRM3,POLR2A

Supplemental Table 4.5. R6/2 12-Week Striatal and Cortical Astrocyte Overlapping DEG Significant ChIP-X Enrichment Analysis (ChEA)

Term	Overlap	P-value	Adjusted P-value	Odds Ratio	Combined Score	Genes
SOX9 24532713 ChIP-Seq HFSC Mouse	14/1384	2.00E-05	5.83E-03	4.5192	48.9070	ABCA1;FARP1;PIGN;TPK1;ZBTB16;MICAL2;ACSL3;FRY;MERTK;CCND3;CLMN;KIF21A;PLCB1;CAMK2G
SUZ12 18974828 ChIP-Seq MESCs Mouse	17/1934	1.31E-05	5.83E-03	4.0991	46.0894	GABRA2;GRIA2;GABBR2;FARP1;L3MBTL3;ZBTB16;HTRA1;SLC1A2;MICAL2;CABLES1;MYRIP;GRIN2C;SLC4A4;PDE10A;TSPAN7;PLCB1;NTSR2
TCF4 23295773 ChIP-Seq U87 Human	24/3812	3.65E-05	7.10E-03	3.1988	32.6894	GABRA2;GRIA2;GABBR2;FARP1;L3MBTL3;TPK1;SLC1A2;LSAMP;MICAL2;CABLES1;HIF3A;MYRIP;ACSL3;MERTK;NAALADL2;PDE10A;POLR2A;PHKG1;KIF21A;RMST;PLCB1;SOX5;RNF121;NTSR2
ZNF217 24962896 ChIP-Seq MCF-7 Human	14/1522	5.71E-05	8.33E-03	4.0752	39.8181	ABCA1;GABBR2;CADM1;TPK1;SLC1A2;ACSL3;FRY;MERTK;PITPNC1;NAALADL2;CLMN;RMST;PLCB1;CAMK2G
SMAD4 21799915 ChIP-Seq A2780 Human	17/2464	2.80E-04	0.0295	3.1168	25.4995	GABRA2;GRIA2;GABBR2;HTRA1;LSAMP;MICAL2;MYRIP;FRY;SLC4A4;PITPNC1;NAALADL2;CCND3;PDE10A;TSPAN7;KIF21A;PLCB1;SOX5
MTF2 20144788 ChIP-Seq MESCs Mouse	19/2981	3.03E-04	0.0295	2.9441	23.8482	GABRA2;GRIA2;GABBR2;FARP1;L3MBTL3;CADM1;ZBTB16;HTRA1;SLC1A2;LSAMP;CABLES1;MYRIP;GRIN2C;SLC4A4;PDE10A;PHKG1;PLCB1;RAPGEF3;NTSR2
EP300 20729851 ChIP-Seq FORBRAIN MIDBRAIN LIMB HEART Mouse	15/2093	4.77E-04	0.0398	3.1455	24.0571	L3MBTL3;TTYH1;HTRA1;SLC1A2;MICAL2;ATP1A2;PITPNC1;CCND3;NWD1;PDE10A;POLR2A;SPARCL1;KIF21A;QK;SOX5
SUZ12 18692474 ChIP-Seq MESCs Mouse	14/1909	6.14E-04	0.0410	3.1748	23.4782	ABCA1;GABRA2;GRIA2;GABBR2;FARP1;ZBTB16;HTRA1;SLC1A2;CABLES1;MYRIP;GRIN2C;SLC4A4;PDE10A;NTSR2
JARID2 20075857 ChIP-Seq MESCs Mouse	11/1258	6.32E-04	0.0410	3.6651	26.9999	GABRA2;GABBR2;FARP1;PDE10A;ZBTB16;HTRA1;SLC1A2;KIF21A;MYRIP;GRIN2C;SLC4A4
JARID2 20064375 ChIP-Seq MESCs Mouse	10/1117	9.64E-04	0.0438	3.6992	25.6896	GABRA2;GABBR2;L3MBTL3;PDE10A;ZBTB16;HTRA1;SLC1A2;CABLES1;MYRIP;SLC4A4

FOXM1 26456572 ChIP-Seq MCF-7 Human	14/2000	9.76E-04	0.0438	3.0141	20.8950	ABCA1;GABBR2;SLC1A2;CABLES1;MYRIP;ACSL3;SLC4A4;PITPNC1;NAALADL2;EPS8;NWD1;CLMN;SPARCL1;PLCB1
AR 21915096 ChIP-Seq LNCaP-1F5 Human	14/2000	9.76E-04	0.0438	3.0141	20.8950	ABCA1;ZBTB16;SLC1A2;ATP1A2;HIF3A;ACSL3;FRY;MERTK;PITPNC1;NWD1;PDE10A;CLMN;SPARCL1;GLUL
ZFP281 27345836 Chip-Seq ESCs Mouse	14/2000	9.76E-04	0.0438	3.0141	20.8950	PAQR8;ABCA1;GABBR2;L3MBTL3;DDX5;CADM1;ZBTB16;A930015D03RIK;GRIN2C;PITPNC1;CCND3;POLR2A;QK;GLUL
SUZ12 18692474 ChIP-Seq MEFs Mouse	10/1135	1.09E-03	0.0454	3.6365	24.8115	ABCA1;GABRA2;GRIA2;PDE10A;HTRA1;SLC1A2;CABLES1;GRIN2C;SLC4A4;NTSR2
DMRT1 23473982 ChIP-Seq TESTES Mouse	14/2072	1.38E-03	0.0526	2.8970	19.0842	FARP1;L3MBTL3;CADM1;PIGN;HIF3A;GRIN2C;SLC4A4;PITPNC1;EPS8;CCND3;PDE10A;POLR2A;QK;SOX5
SMAD3 21741376 ChIP-Seq EPCs Human	12/1613	1.44E-03	0.0526	3.1247	20.4441	ABCA1;GABRA2;GABBR2;FARP1;PDE10A;CADM1;MICAL2;CABLES1;RMST;MYRIP;FRY;PLCB1
PPARG 20176806 ChIP-Seq MACROPHAGES Mouse	11/1408	1.59E-03	0.0546	3.2453	20.9141	EPS8;ABCA1;CCND3;TTYH1;TPK1;SLC1A2;QK;ATP1A2;SLC4A4;GLUL;CAMK2G
AR 25329375 ChIP-Seq VCAP Human	13/1906	1.95E-03	0.0632	2.8829	17.9913	FARP1;L3MBTL3;CADM1;TPK1;LSAMP;ACSL3;FRY;NAALADL2;EPS8;SPARCL1;RMST;PLCB1;SOX5
SMAD3 21741376 ChIP-Seq HESCs Human	11/1460	2.12E-03	0.0652	3.1201	19.2064	EPS8;CCND3;PDE10A;CADM1;TPK1;ZBTB16;MICAL2;FRY;PLCB1;GLUL;CAMK2G
FOXA2 19822575 ChIP-Seq HepG2 Human	17/2968	2.37E-03	0.0652	2.5101	15.1765	ABCA1;FARP1;CADM1;SLC1A2;LSAMP;MICAL2;CABLES1;MYRIP;ACSL3;FRY;MERTK;PITPNC1;NAALADL2;PLCB1;CAMK2G;RAPGEF3;SOX5
AR 19668381 ChIP-Seq PC3 Human	19/3519	2.41E-03	0.0652	2.4126	14.5462	PAQR8;GABBR2;FARP1;ZBTB16;HTRA1;SLC1A2;MICAL2;CABLES1;HIF3A;MYRIP;FRY;PITPNC1;NAALADL2;PDE10A;CLMN;TSPAN7;SPARCL1;GLUL;SOX5
SUZ12 18555785 ChIP-Seq MESCs Mouse	9/1058	2.52E-03	0.0652	3.4492	20.6409	GABBR2;PDE10A;ZBTB16;HTRA1;SLC1A2;MYRIP;GRIN2C;SLC4A4;NTSR2
TCFCP2L1 18555785 ChIP-Seq MESCs Mouse	13/1987	2.82E-03	0.0652	2.7522	16.1571	HSPA8;DDX5;HTRA1;MICAL2;HIF3A;SLC4A4;CCND3;NWD1;KIF21A;PLCB1;CAMK2G;RAPGEF3;RNF121
MNX1 26342078 ChIP-Seq MIN6-4N Mouse	13/2000	2.99E-03	0.0652	2.7322	15.8833	FARP1;CMTM5;ZBTB16;HIF3A;FRY;PDE10A;POLR2A;SPARCL1;KIF21A;QK;ALDOC;GLUL;SOX5

LXR 22158963 ChIP-Seq LIVER Mouse	13/2000	2.99E-03	0.0652	2.7322	15.8833	ABCA1;FARP1;SLC1A2;MICAL2;CABLES1;A930015D03RIK;MYRIP;FRY;SLC4A4;CLMN;QK;RMST;PLCB1
RNF2 18974828 ChIP-Seq MESCs Mouse	10/1302	3.01E-03	0.0652	3.1384	18.2178	GABBR2;L3MBTL3;PDE10A;ZBTB16;HTRA1;SLC1A2;CABLES1;MYRIP;GRIN2C;SLC4A4
EZH2 18974828 ChIP-Seq MESCs Mouse	10/1302	3.01E-03	0.0652	3.1384	18.2178	GABBR2;L3MBTL3;PDE10A;ZBTB16;HTRA1;SLC1A2;CABLES1;MYRIP;GRIN2C;SLC4A4
STAT3 24763339 ChIP-Seq IMN-ESCs Mouse	12/1788	3.42E-03	0.0714	2.7899	15.8394	FARP1;L3MBTL3;NWD1;PIGN;LSAMP;KIF21A;QK;PLCB1;GLUL;CAMK2G;PITPNC1;SOX5
HNF4A 19822575 ChIP-Seq HepG2 Human	27/6083	3.85E-03	0.0775	2.1351	11.8723	L3MBTL3;PIGN;SLC1A2;ATP1A2;FRY;PITPNC1;EPS8;CLMN;KIF21A;CAMK2G;SOX5;PAQR8;ABCA1;GABBR2;FARP1;CADM1;ZBTB16;LSAMP;MICAL2;CABLES1;ACSL3;MERTK;GRIN2C;SPARCL1;PLCB1;RAPGEF3;RNF121

Supplemental Table 4.6. R6/2 12-Week Striatal and Cortical Astrocyte Overlapping DEG Significant Transcription Factor Perturbation Database Enrichment Analysis

Term	Overlap	P-value	Adjusted P-value	Odds Ratio	Combined Score	Genes
HES1 OE MOUSE GSE54622 CREEDSID GENE 2771 DOWN	6/130	1.67E-06	2.15E-03	19.1806	255.1480	CMTM5;HTRA1;ALDOC;ATP1A2;PLPP3;GRIN2C
ASCL1 KO G523NS HUMAN GSE87615 RNASEQ UP	8/344	4.89E-06	3.14E-03	9.7262	118.9421	HSPA8;CADM1;TTYH1;HTRA1;SPARCL1;ACSL3;SLC4A4;GLUL
MECP2 MUT HUMAN GSE6955 CREEDSID GENE 2473 UP	8/375	9.18E-06	3.93E-03	8.8906	103.1175	CADM1;TSPAN7;HTRA1;ALDOC;ATP1A2;PLPP3;GRIN2C;GLUL
NFIA DEFICIENCY MOUSE GSE4623 CREEDSID GENE 667 DOWN	7/320	2.98E-05	9.56E-03	8.9598	93.3812	POLR2A;TSPAN7;HTRA1;SPARCL1;ALDOC;ATP1A2;NTSR2
HMX1 DEFICIENCY MOUSE GSE47002 CREEDSID GENE 351 UP	6/245	6.18E-05	0.0159	9.8937	95.8825	PDE10A;CMTM5;ZBTB16;ATP1A2;HIF3A;ACSL3
PLAGL2 OE MOUSE GSE21143 CREEDSID GENE 2546 UP	7/372	7.71E-05	0.0159	7.6630	72.5748	ABCA1;HSPA8;CCND3;CADM1;TTYH1;TSPAN7;GLUL
HSF1 KD HUMAN GSE3697 CREEDSID GENE 782 DOWN	7/379	8.66E-05	0.0159	7.5161	70.3082	FARP1;CCND3;ALDOC;ACSL3;PLPP3;GLUL;PITPNC1
NFKB1 ACTIVATION HUMAN GSE20736 CREEDSID GENE 2522 DOWN	6/302	1.94E-04	0.0312	7.9654	68.0777	GRIA2;TTYH1;TSPAN7;SLC1A2;SLC4A4;GLUL
HOXA10 KO MOUSE GSE6439 CREEDSID GENE 1535 DOWN	5/202	2.51E-04	0.0359	9.8273	81.4501	ZBTB16;HTRA1;SLC1A2;GLUL;SOX5
OVOL2 KO MOUSE GSE53923 CREEDSID GENE 1486 UP	6/330	3.13E-04	0.0369	7.2667	58.6449	EPS8;ABCA1;DDX5;ZBTB16;SPARCL1;GLUL
SOX9 OE MOUSE GSE34060 CREEDSID GENE 2743 UP	6/331	3.18E-04	0.0369	7.2439	58.3445	HSPA8;DDX5;CADM1;CLMN;TSPAN7;ALDOC
MECP2 KD MOUSE GSE47150 CREEDSID GENE 951 DOWN	6/336	3.44E-04	0.0369	7.1324	56.8758	TSPAN7;LSAMP;SPARCL1;ALDOC;ATP1A2;GLUL
FOXO1 KO MOUSE GSE18308 CREEDSID GENE 1168 UP	5/224	4.04E-04	0.0400	8.8302	68.9899	TSPAN7;ALDOC;ATP1A2;PLPP3;GLUL
NR1I3 KNOCKIN MOUSE GSE40120 CREEDSID GENE 3068 DOWN	5/238	5.33E-04	0.0489	8.2938	62.5082	FARP1;TSPAN7;SLC1A2;SLC4A4;GLUL
GFI1B KO MOUSE GSE20655 CREEDSID GENE 3013 UP	5/242	5.75E-04	0.0493	8.1521	60.8247	PDE10A;TPK1;MICAL2;PITPNC1;NAALADL2
PPARA KO MOUSE GSE18564 CREEDSID GENE 543 UP	5/249	6.54E-04	0.0525	7.9155	58.0381	DDX5;TSPAN7;SLC1A2;SLC4A4;GLUL

BACH2 KO MOUSE GSE54050 CREEDSID GENE 2773 UP	6/384	6.96E-04	0.0526	6.2114	45.1588	CADM1;TSPAN7;HTRA1;SLC1A2;ACSL3;PLPP3
THRB HCC MUTANT BN HUMAN GSE29159 CREEDSID GENE 1696 UP	5/270	9.41E-04	0.0672	7.2804	50.7349	EPS8;ABCA1;POLR2A;TSPAN7;ACSL3
GATA6 KO MOUSE GSE47049 CREEDSID GENE 2225 UP	5/287	1.23E-03	0.0791	6.8356	45.7788	EPS8;ABCA1;HSPA8;MERTK;GLUL
EZH2 KO MDAMB231 HUMAN GSE72524 RNASEQ UP	5/290	1.29E-03	0.0791	6.7626	44.9788	HSPA8;CADM1;MICAL2;ACSL3;GLUL
MECP2 KO MOUSE GSE8720 CREEDSID GENE 2417 UP	4/170	1.31E-03	0.0791	9.1650	60.8228	ZBTB16;LSAMP;SPARCL1;MYRIP
PLAGL2 OE MOUSE GSE21143 CREEDSID GENE 2546 DOWN	4/172	1.37E-03	0.0791	9.0549	59.7026	SPARCL1;ALDOC;ATP1A2;NTSR2
EGR1 KO MOUSE GSE16974 CREEDSID GENE 553 DOWN	5/296	1.41E-03	0.0791	6.6212	43.4393	GRIA2;HSPA8;DDX5;ACSL3;GLUL
OVOL2 OE MOUSE GSE55074 CREEDSID GENE 2603 UP	5/310	1.73E-03	0.0928	6.3128	40.1342	ABCA1;SPARCL1;ATP1A2;PLPP3;GLUL

Supplemental Table 4.7. R6/2 12-Week Striatal Astrocyte snRNA-seq Cluster Markers

Gene	p_val	avg_logFC	p_val_adj	cluster
Slc1a2	2.67E-229	1.1144	7.47E-225	0
Gnao1	8.56E-182	1.0320	2.40E-177	0
Tspan7	3.54E-164	1.0587	9.91E-160	0
Adam23	2.98E-162	1.1638	8.34E-158	0
Gm26843	7.41E-162	1.2241	2.07E-157	0
Fam13c	2.70E-135	1.0805	7.57E-131	0
Ephb1	3.09E-133	1.0533	8.65E-129	0
Fam184b	5.58E-129	0.9992	1.56E-124	0
Rcan2	2.03E-96	0.9991	5.70E-92	0
Crym	2.41E-71	1.0408	6.75E-67	0
Gria1	2.04E-174	1.6203	5.70E-170	1
Fry	2.44E-151	1.2939	6.84E-147	1
Slc6a11	2.73E-149	1.2881	7.64E-145	1
Itih3	1.38E-139	1.4135	3.85E-135	1
Erbb4	6.29E-127	1.0576	1.76E-122	1
Kcnd2	1.07E-123	1.1092	3.01E-119	1
B230323A14Rik	1.79E-110	1.2555	5.00E-106	1
Etnppl	1.06E-101	1.1838	2.97E-97	1
Car10	5.10E-82	1.0803	1.43E-77	1
Nav3	1.19E-78	1.0933	3.35E-74	1
Sgcd	1.21E-75	1.2906	3.39E-71	2
Lrp1b	3.31E-70	0.7765	9.28E-66	2
Kcnd2	1.55E-64	0.7681	4.34E-60	2
Csmd3	5.34E-60	0.8566	1.50E-55	2
Nrxn3	1.39E-51	0.7032	3.90E-47	2
B230323A14Rik	1.36E-45	0.7593	3.81E-41	2
RP23-474J16.2	2.42E-43	0.8923	6.78E-39	2
Kcnq1ot1	1.06E-35	0.6863	2.98E-31	2
Samd12	2.15E-31	0.7367	6.02E-27	2
Pde4b	3.44E-29	0.7040	9.64E-25	2
Slc4a4	2.59E-42	0.5058	7.24E-38	3
Gria2	3.01E-25	0.4606	8.43E-21	3
Gabbr2	1.82E-24	0.6172	5.09E-20	3
Cables1	5.17E-20	0.5525	1.45E-15	3
Tprkb	5.53E-20	0.4988	1.55E-15	3
Rasgrf1	2.51E-18	0.5565	7.02E-14	3

Car10	7.50E-11	0.5061	2.10E-06	3
Pigk	4.61E-06	0.5568	0.1290458731	3
Pde10a	1.99E-05	0.6946	0.5577185487	3
St6galnac5	0.000248294302	0.5729	1	3
Sctr	2.09E-34	0.6064	5.84E-30	4
Atp1b1	5.97E-25	0.5751	1.67E-20	4
Polr2a	6.35E-19	0.5453	1.78E-14	4
Guf1	1.23E-15	0.4673	3.45E-11	4
Arhgap18	4.92E-15	0.5057	1.38E-10	4
Nr6a1	8.28E-15	0.4554	2.32E-10	4
Sema5b	1.62E-12	0.4488	4.55E-08	4
Robo2	1.58E-11	0.4576	4.43E-07	4
Pdzrn3	6.25E-10	0.4313	1.75E-05	4
Eya1	1.48E-08	0.4117	0.0004156059864	4
Adamts18	2.22E-101	1.4655	6.22E-97	5
Adgrv1	2.26E-96	1.5002	6.33E-92	5
Ccdc170	1.43E-70	1.0667	4.00E-66	5
Spag16	1.08E-45	1.4156	3.03E-41	5
Nkain2	2.32E-44	1.1840	6.49E-40	5
Cfap44	3.46E-44	1.0254	9.69E-40	5
Slc38a1	8.79E-39	0.9857	2.46E-34	5
Csmd1	5.21E-38	1.1754	1.46E-33	5
Nrg1	1.86E-37	2.0843	5.21E-33	5
Cacnb2	3.36E-29	1.0401	9.40E-25	5

Supplemental Table 4.8. R6/2 12-Week Cortical Astrocyte snRNA-seq Cluster Markers

Gene	p_val	avg_logFC	p_val_adj	cluster
Grin2c	3.62E-41	1.0627	1.01E-36	0
Slc1a2	6.26E-72	0.9607	1.75E-67	0
Glul	5.46E-37	0.8199	1.53E-32	0
Clmn	1.73E-46	0.9996	4.86E-42	0
Gm26843	6.20E-32	0.9590	1.74E-27	0
Tspan7	1.21E-54	0.9397	3.40E-50	0
Mertk	6.05E-50	0.9065	1.69E-45	0
St6galnac5	1.01E-26	0.8458	2.84E-22	0
Phkg1	3.90E-39	0.8303	1.09E-34	0
Daam2	1.80E-31	0.8027	5.04E-27	0
Robo2	1.51E-06	0.3805	0.0424	1
Dpyd	2.03E-06	0.4663	0.0569	1
Slc35f1	1.72E-07	0.4581	0.0048	1
Abca1	1.53E-06	0.4563	0.0429	1
Ogt	1.01E-07	0.3981	0.0028	1
Ddx5	2.16E-06	0.3805	0.0604	1
Adgrv1	6.26E-16	1.1571	1.75E-11	3
Dscaml1	5.29E-19	1.5978	1.48E-14	3
Sncaip	3.45E-07	1.0227	0.0097	3
Anks1b	1.53E-07	0.8776	0.0043	3
Tmem132b	5.82E-07	0.9155	0.0163	3
Cacnb2	4.42E-07	0.8318	0.0124	3
Dlg2	3.46E-24	2.5071	9.68E-20	4
Nrg3	6.26E-28	2.7586	1.75E-23	4
Lrrtm4	1.91E-29	2.7219	5.34E-25	4
Kcnip4	8.06E-16	2.6745	2.26E-11	4
Gm28928	4.21E-23	2.5558	1.18E-18	4
Opcml	2.02E-27	2.5259	5.64E-23	4
Tenm2	1.06E-28	2.4862	2.96E-24	4
Lingo2	9.86E-34	2.4833	2.76E-29	4
Syt1	2.79E-30	2.4143	7.82E-26	4
Ptprd	7.69E-19	2.3525	2.15E-14	4

Supplemental Table 4.9. R6/2 12-Week Striatal Astrocyte Significant Differentially Expressed Genes Per Cluster

Gene	p_val	avg_logFC	pct.1	pct.2	p_val_adj	Cluster
Slc1a2	2.67E-229	1.1144	1	0.941	7.47E-225	0
Gnao1	8.56E-182	1.0320	0.981	0.656	2.40E-177	0
Tspan7	3.54E-164	1.0587	0.972	0.643	9.91E-160	0
Adam23	2.98E-162	1.1638	0.771	0.175	8.34E-158	0
Gm26843	7.41E-162	1.2241	0.722	0.152	2.07E-157	0
Grm3	3.42E-161	0.9863	0.992	0.784	9.58E-157	0
Frmd4a	5.49E-150	0.7989	0.994	0.921	1.54E-145	0
Erbb4	4.87E-146	-1.5601	0.452	0.848	1.36E-141	0
Fam13c	2.70E-135	1.0805	0.761	0.247	7.57E-131	0
Ephb1	3.09E-133	1.0533	0.69	0.156	8.65E-129	0
Fam184b	5.58E-129	0.9992	0.51	0.061	1.56E-124	0
Kcnd2	1.31E-120	-1.5540	0.52	0.822	3.66E-116	0
Lypd6	4.34E-118	0.9468	0.549	0.093	1.22E-113	0
Gria1	8.50E-115	-2.0694	0.172	0.639	2.38E-110	0
Grin2c	1.72E-112	0.9414	0.713	0.221	4.81E-108	0
Mertk	9.41E-112	0.8170	0.955	0.719	2.64E-107	0
Prex2	3.59E-110	0.7067	0.986	0.791	1.01E-105	0
Mgat5	2.63E-104	0.8615	0.858	0.403	7.36E-100	0
Ptn	9.00E-103	0.7798	0.933	0.636	2.52E-98	0
Gfra1	2.06E-98	0.8727	0.634	0.176	5.75E-94	0
Rcan2	2.03E-96	0.9991	0.569	0.147	5.70E-92	0
Dclk1	3.09E-96	0.7040	0.937	0.681	8.66E-92	0
Cadm1	1.20E-92	0.5878	0.993	0.897	3.35E-88	0
Rgs20	5.67E-92	0.5813	0.987	0.853	1.59E-87	0
Lama3	2.70E-91	0.8575	0.364	0.038	7.56E-87	0
Slco1c1	4.16E-91	0.7594	0.871	0.486	1.16E-86	0
Lrp1b	2.02E-89	-1.0093	0.588	0.852	5.66E-85	0
Ntm	2.01E-87	0.4036	1	0.98	5.63E-83	0
Ptprt	4.59E-87	0.5493	0.993	0.884	1.29E-82	0
Clmn	9.91E-86	0.7398	0.841	0.428	2.78E-81	0
Cspg5	5.50E-85	0.6814	0.928	0.626	1.54E-80	0
Gldc	7.40E-85	0.7882	0.659	0.231	2.07E-80	0
Msi2	5.91E-82	0.3774	1	0.993	1.66E-77	0
Daam2	1.39E-81	0.6993	0.846	0.472	3.90E-77	0
Fars2	1.13E-75	0.6086	0.933	0.676	3.16E-71	0
Emx2os	1.54E-75	0.7204	0.483	0.119	4.32E-71	0
Plpp3	1.04E-73	0.4905	0.993	0.861	2.91E-69	0
Fgf13	1.28E-73	0.8564	0.633	0.243	3.59E-69	0
Grid2	1.13E-71	0.4857	0.987	0.92	3.15E-67	0

Crym	2.41E-71	1.0408	0.335	0.052	6.75E-67	0
Unc13c	3.80E-68	0.9192	0.519	0.168	1.06E-63	0
Lsamp	4.08E-68	0.2917	1	0.997	1.14E-63	0
Rgs7	3.32E-67	0.6513	0.901	0.644	9.31E-63	0
Gpc6	2.52E-66	0.5971	0.915	0.639	7.05E-62	0
Alk	4.76E-66	0.8733	0.346	0.064	1.33E-61	0
4930544I03Rik	5.57E-66	0.7960	0.408	0.099	1.56E-61	0
Rmst	8.34E-66	0.7121	0.79	0.441	2.34E-61	0
B230323A14Rik	2.68E-65	-1.3231	0.006	0.333	7.51E-61	0
Gm26512	3.13E-65	0.6546	0.363	0.069	8.76E-61	0
St6galnac5	1.28E-64	0.7767	0.561	0.198	3.59E-60	0
B3galt1	1.51E-64	0.4398	0.993	0.93	4.23E-60	0
Htra1	1.25E-63	0.6201	0.839	0.506	3.50E-59	0
Dtna	1.20E-62	0.3834	0.996	0.971	3.37E-58	0
Hivep3	1.92E-61	0.5895	0.879	0.592	5.38E-57	0
Spon1	2.60E-61	-0.8486	0.285	0.619	7.28E-57	0
Gpm6b	8.08E-61	0.4464	0.99	0.931	2.26E-56	0
Pde4d	3.51E-60	-0.6684	0.64	0.816	9.84E-56	0
Dio2	6.62E-60	0.5775	0.249	0.026	1.85E-55	0
Wdr17	1.34E-59	0.3831	0.999	0.979	3.75E-55	0
Dgkb	2.00E-57	0.3883	0.993	0.941	5.60E-53	0
Pdzph1	7.23E-56	0.6931	0.565	0.226	2.02E-51	0
Plce1	1.66E-55	-0.8018	0.399	0.674	4.65E-51	0
Bcan	1.63E-54	0.5112	0.905	0.641	4.55E-50	0
Fry	3.97E-54	-1.0080	0.467	0.679	1.11E-49	0
Ctnnd2	1.59E-53	0.2816	0.999	0.99	4.44E-49	0
Irak2	9.48E-53	0.6319	0.651	0.316	2.65E-48	0
Prdx6	4.51E-52	0.5099	0.848	0.567	1.26E-47	0
Swap70	5.97E-52	0.6009	0.445	0.141	1.67E-47	0
Ldb2	1.06E-50	-0.9252	0.089	0.39	2.96E-46	0
Ankrd29	3.25E-50	0.5617	0.349	0.087	9.09E-46	0
Adcy8	3.26E-50	-0.8811	0.025	0.3	9.13E-46	0
Gabrb1	3.60E-50	0.3494	0.997	0.97	1.01E-45	0
Mpp6	5.50E-50	-0.8486	0.273	0.564	1.54E-45	0
Ppp1r14c	1.60E-49	-0.8029	0.054	0.343	4.47E-45	0
Luzp2	2.07E-49	0.5671	0.965	0.85	5.80E-45	0
Col11a2	3.86E-49	0.4985	0.264	0.046	1.08E-44	0
Glul	4.33E-49	0.5091	0.789	0.452	1.21E-44	0
Pde8b	4.83E-49	0.5449	0.819	0.526	1.35E-44	0
Rpe65	5.57E-49	0.5561	0.188	0.015	1.56E-44	0
Garem	8.45E-49	0.6432	0.7	0.38	2.37E-44	0
Cpe	9.76E-49	0.3725	0.994	0.893	2.73E-44	0
Fjx1	4.98E-48	0.6299	0.453	0.161	1.39E-43	0

Ptch1	1.17E-47	-0.8132	0.618	0.751	3.28E-43	0
C030018K13Rik	9.24E-46	0.3967	0.21	0.026	2.59E-41	0
Atp1a2	2.49E-45	0.3467	0.983	0.838	6.96E-41	0
Tnfrsf19	3.39E-45	0.5834	0.605	0.292	9.48E-41	0
Gli3	3.53E-45	0.4515	0.915	0.7	9.88E-41	0
Rbms1	7.28E-45	0.6011	0.533	0.231	2.04E-40	0
Magi3	2.16E-43	0.6169	0.609	0.301	6.06E-39	0
Hapln1	2.44E-43	0.4877	0.349	0.099	6.83E-39	0
Sgcd	2.74E-43	-1.0978	0.152	0.427	7.66E-39	0
Srgap1	7.77E-43	-0.7777	0.307	0.564	2.18E-38	0
Phkg1	1.52E-42	0.4336	0.917	0.666	4.25E-38	0
Sparc	3.27E-42	-0.7610	0.032	0.276	9.16E-38	0
Itih3	3.68E-42	-0.9241	0.143	0.406	1.03E-37	0
Lyrm4	1.30E-41	0.6105	0.726	0.447	3.64E-37	0
Sik3	2.15E-41	0.3977	0.954	0.827	6.02E-37	0
Rorb	3.54E-41	0.4317	0.964	0.888	9.91E-37	0
Csmd3	5.63E-41	-0.7597	0.281	0.533	1.58E-36	0
Slc6a11	9.27E-41	-0.8273	0.552	0.7	2.60E-36	0
Sgip1	3.87E-40	0.4791	0.833	0.553	1.08E-35	0
Chst2	4.76E-40	0.4732	0.293	0.076	1.33E-35	0
9630001P10Rik	5.58E-40	0.3581	0.157	0.013	1.56E-35	0
Enox1	6.61E-40	0.5350	0.533	0.232	1.85E-35	0
Itpkb	3.83E-39	-0.7860	0.167	0.428	1.07E-34	0
Ntrk3	8.96E-39	-0.7057	0.296	0.539	2.51E-34	0
Rgcc	3.26E-38	0.5225	0.445	0.175	9.12E-34	0
Dab1	3.26E-38	0.4125	0.847	0.583	9.12E-34	0
Ngef	4.84E-38	0.4846	0.512	0.225	1.36E-33	0
Cyp4f15	9.34E-38	0.4565	0.396	0.14	2.62E-33	0
Mfap3l	1.61E-37	0.4918	0.437	0.17	4.51E-33	0
Dapp1	2.62E-37	0.4480	0.332	0.103	7.34E-33	0
RP23-474J16.2	3.17E-37	-1.0324	0.045	0.275	8.88E-33	0
Fam171b	3.23E-37	0.4717	0.576	0.283	9.04E-33	0
Sptbn1	4.70E-37	0.4279	0.828	0.607	1.32E-32	0
Nphs1	4.72E-37	0.3545	0.163	0.018	1.32E-32	0
Wnk2	4.16E-36	0.4864	0.736	0.459	1.17E-31	0
Kirrel3	1.86E-35	0.3468	0.969	0.796	5.22E-31	0
Vcl	1.91E-35	0.5244	0.673	0.406	5.33E-31	0
Nrxn3	2.42E-35	-0.6023	0.793	0.84	6.77E-31	0
Hes5	4.13E-35	0.5308	0.587	0.311	1.16E-30	0
Gm12239	5.32E-34	0.6100	0.673	0.435	1.49E-29	0
Dfna5	5.76E-34	-0.6948	0.28	0.516	1.61E-29	0
Nav3	7.49E-34	-0.8763	0.17	0.399	2.10E-29	0
Prdm16	9.17E-34	0.3813	0.853	0.615	2.57E-29	0

Gm2115	9.33E-34	0.4770	0.349	0.125	2.61E-29	0
Gm13872	9.88E-34	0.4239	0.295	0.088	2.77E-29	0
Acss3	1.53E-33	-0.6690	0.046	0.259	4.30E-29	0
Lrig1	5.88E-33	-0.6853	0.399	0.59	1.65E-28	0
Ncan	6.78E-33	0.4715	0.466	0.214	1.90E-28	0
Astn2	9.83E-33	-0.5682	0.494	0.679	2.75E-28	0
Fgfr2	1.01E-32	0.3134	0.99	0.924	2.83E-28	0
Cpeb4	2.42E-32	0.4665	0.748	0.511	6.77E-28	0
Clu	2.87E-32	0.4924	0.651	0.396	8.02E-28	0
Adamts9	3.25E-32	0.5136	0.485	0.231	9.10E-28	0
Cst3	9.17E-32	0.4493	0.892	0.713	2.57E-27	0
Rev3l	1.16E-31	-0.5448	0.409	0.619	3.25E-27	0
4930578G10Rik	2.79E-31	0.3838	0.281	0.086	7.82E-27	0
Efr3b	3.48E-31	0.3976	0.833	0.589	9.75E-27	0
Gm21954	4.08E-31	0.4418	0.399	0.167	1.14E-26	0
Pcdh7	4.50E-31	0.3054	0.972	0.866	1.26E-26	0
Cntn1	1.53E-30	-0.7517	0.312	0.517	4.27E-26	0
Eda	1.53E-30	0.4612	0.566	0.293	4.29E-26	0
Tmem117	1.64E-30	-0.6734	0.099	0.31	4.58E-26	0
Gabbr1	4.36E-30	0.4160	0.747	0.479	1.22E-25	0
Clybl	5.87E-30	0.3649	0.808	0.549	1.64E-25	0
Acsl3	6.26E-30	0.3904	0.85	0.616	1.75E-25	0
Tenm3	6.49E-30	0.3804	0.855	0.666	1.82E-25	0
Sfxn5	1.23E-29	0.2930	0.972	0.89	3.45E-25	0
Tiam2	1.32E-29	-0.5396	0.305	0.522	3.70E-25	0
Trim9	1.43E-29	0.3538	0.9	0.739	3.99E-25	0
Dpyd	2.44E-29	-0.5779	0.314	0.532	6.83E-25	0
Thsd7a	3.51E-29	-0.6338	0.15	0.364	9.82E-25	0
Kcnk1	3.94E-29	0.4286	0.382	0.161	1.10E-24	0
Nme7	5.04E-29	0.4377	0.503	0.252	1.41E-24	0
Cped1	9.67E-29	-0.5718	0.025	0.201	2.71E-24	0
Zeb1	1.41E-28	0.3029	0.936	0.826	3.94E-24	0
Atxn1	1.66E-28	-0.4708	0.609	0.737	4.66E-24	0
Dab2	1.67E-28	-0.5634	0.042	0.223	4.69E-24	0
S1pr1	1.85E-28	0.4186	0.552	0.295	5.18E-24	0
Pigk	3.59E-28	0.4685	0.494	0.253	1.01E-23	0
Pantr1	4.97E-28	0.4609	0.51	0.27	1.39E-23	0
Nwd1	5.77E-28	0.3363	0.836	0.572	1.62E-23	0
Lrp4	7.07E-28	0.4652	0.47	0.234	1.98E-23	0
Dkk3	1.16E-27	0.4016	0.476	0.23	3.24E-23	0
D030055H07Rik	1.29E-27	0.3171	0.129	0.017	3.61E-23	0
Aox1	1.89E-27	0.4296	0.339	0.132	5.28E-23	0
Kcnma1	2.04E-27	0.3802	0.787	0.573	5.70E-23	0

Slc25a18	3.09E-27	-0.5594	0.131	0.337	8.64E-23	0
Adcy2	4.48E-27	0.3834	0.843	0.66	1.25E-22	0
Eogt	1.17E-26	0.3929	0.245	0.077	3.27E-22	0
Ttyh1	1.33E-26	0.3077	0.898	0.695	3.73E-22	0
Phactr3	1.38E-26	0.3763	0.819	0.613	3.86E-22	0
Sox6	1.74E-26	-0.3294	0.887	0.912	4.88E-22	0
Scg3	7.18E-26	0.4052	0.613	0.377	2.01E-21	0
Lix1	7.88E-26	0.4189	0.624	0.385	2.21E-21	0
Pde4b	9.63E-26	-0.5691	0.544	0.685	2.70E-21	0
1700112E06Rik	2.03E-25	-0.6103	0.235	0.455	5.69E-21	0
Farp1	2.08E-25	0.2769	0.957	0.848	5.82E-21	0
Grik1	2.28E-25	0.3544	0.147	0.028	6.39E-21	0
Nsmf	3.20E-25	0.3934	0.398	0.182	8.96E-21	0
Plcb4	6.15E-25	-0.4096	0.533	0.682	1.72E-20	0
Dach1	7.43E-25	0.4741	0.345	0.149	2.08E-20	0
Car10	7.83E-25	-0.7670	0.04	0.204	2.19E-20	0
Fgf14	8.47E-25	-0.3326	0.919	0.943	2.37E-20	0
Cit	1.70E-24	-0.5439	0.103	0.293	4.76E-20	0
Glis3	2.40E-24	0.3602	0.865	0.711	6.71E-20	0
Kalrn	2.43E-24	0.3578	0.801	0.615	6.79E-20	0
Mgll	2.46E-24	0.3995	0.761	0.555	6.88E-20	0
Prodh	3.27E-24	0.3741	0.484	0.251	9.16E-20	0
Celrr	3.65E-24	0.3960	0.533	0.295	1.02E-19	0
Slc7a11	4.05E-24	0.4840	0.665	0.445	1.13E-19	0
Scel	5.05E-24	0.4186	0.195	0.055	1.41E-19	0
Chrdl1	1.61E-23	0.2713	0.111	0.015	4.50E-19	0
Cdh22	2.16E-23	-0.4839	0.022	0.169	6.06E-19	0
Colec12	2.26E-23	-0.5245	0.015	0.158	6.32E-19	0
Agt	2.79E-23	-0.5126	0.015	0.155	7.82E-19	0
Smim3	3.55E-23	0.3212	0.207	0.063	9.94E-19	0
Ddah1	4.62E-23	0.4031	0.683	0.459	1.29E-18	0
Gm21798	4.69E-23	-0.4872	0.014	0.153	1.31E-18	0
Dpp6	5.53E-23	-0.5841	0.143	0.321	1.55E-18	0
A830019P07Rik	1.09E-22	0.3442	0.309	0.128	3.04E-18	0
4930448N21Rik	1.23E-22	0.3525	0.752	0.541	3.44E-18	0
Sema4d	1.28E-22	0.3685	0.444	0.225	3.60E-18	0
Lrrc7	2.06E-22	-0.5540	0.196	0.377	5.78E-18	0
Lgr4	2.62E-22	0.3993	0.533	0.308	7.33E-18	0
Oaf	3.45E-22	0.3117	0.211	0.067	9.67E-18	0
Tmcc3	4.44E-22	-0.4860	0.49	0.625	1.24E-17	0
Gcnt4	5.51E-22	0.3363	0.203	0.063	1.54E-17	0
Add3	5.55E-22	0.3667	0.702	0.51	1.55E-17	0
Id3	6.19E-22	0.4074	0.337	0.155	1.73E-17	0

Gtf2ird1	7.65E-22	-0.4757	0.203	0.389	2.14E-17	0
Mpped1	8.19E-22	0.2958	0.195	0.058	2.29E-17	0
Kank1	1.06E-21	-0.4618	0.455	0.617	2.97E-17	0
Crlf3	1.07E-21	0.3677	0.648	0.425	3.00E-17	0
Prkca	1.13E-21	-0.5110	0.312	0.491	3.16E-17	0
Clic4	1.17E-21	-0.4866	0.161	0.343	3.27E-17	0
Tank	1.32E-21	0.3627	0.414	0.205	3.71E-17	0
Appl2	1.57E-21	0.3121	0.833	0.66	4.40E-17	0
Mid1	1.75E-21	0.3643	0.485	0.265	4.91E-17	0
Igsf8	2.15E-21	0.3271	0.686	0.465	6.03E-17	0
Lhx2	4.35E-21	0.2667	0.178	0.051	1.22E-16	0
Igsf21	4.42E-21	0.3313	0.256	0.097	1.24E-16	0
Shisa4	4.51E-21	0.3672	0.405	0.204	1.26E-16	0
Mast4	4.55E-21	0.3230	0.762	0.538	1.27E-16	0
App	8.17E-21	-0.4762	0.256	0.426	2.29E-16	0
Il1rapl1	1.21E-20	-0.3667	0.772	0.872	3.38E-16	0
Camk2d	1.77E-20	-0.3731	0.594	0.719	4.94E-16	0
Spata13	2.38E-20	-0.4286	0.031	0.167	6.65E-16	0
Pdgfd	2.41E-20	-0.5863	0.029	0.165	6.75E-16	0
Nim1k	3.00E-20	0.3498	0.707	0.491	8.40E-16	0
Tmem56	4.08E-20	0.3236	0.293	0.126	1.14E-15	0
Epha5	4.34E-20	0.3432	0.448	0.239	1.21E-15	0
Kcnq3	5.12E-20	0.4483	0.491	0.297	1.43E-15	0
Il18	6.36E-20	0.3613	0.345	0.165	1.78E-15	0
Nudt3	7.41E-20	0.3305	0.503	0.29	2.07E-15	0
Skap2	9.84E-20	-0.4892	0.264	0.43	2.76E-15	0
Id4	1.06E-19	0.3461	0.298	0.132	2.96E-15	0
Arhgef10l	1.06E-19	0.3509	0.604	0.395	2.96E-15	0
Rasal2	1.40E-19	-0.4284	0.387	0.539	3.92E-15	0
Btbd17	1.49E-19	0.3116	0.27	0.112	4.17E-15	0
Arhgap26	1.74E-19	0.2750	0.904	0.767	4.88E-15	0
Usp54	2.08E-19	0.3567	0.522	0.305	5.81E-15	0
Mob3b	2.16E-19	-0.4949	0.039	0.175	6.06E-15	0
Egfem1	2.32E-19	0.4001	0.299	0.138	6.48E-15	0
Csrp1	2.68E-19	0.3344	0.702	0.494	7.52E-15	0
Csrnp3	2.83E-19	-0.4601	0.042	0.178	7.91E-15	0
Cntfr	3.36E-19	0.3410	0.505	0.298	9.41E-15	0
Gm5089	3.92E-19	0.3384	0.323	0.152	1.10E-14	0
Plekhg1	4.61E-19	0.3337	0.733	0.53	1.29E-14	0
Nol4	5.62E-19	0.3464	0.677	0.472	1.57E-14	0
Unc5c	5.63E-19	0.4527	0.332	0.164	1.58E-14	0
Grip1	6.48E-19	0.3754	0.529	0.332	1.81E-14	0
9430041J12Rik	7.49E-19	0.3108	0.563	0.338	2.10E-14	0

Lef1	8.54E-19	0.2757	0.168	0.051	2.39E-14	0
Lama2	9.15E-19	0.2613	0.879	0.694	2.56E-14	0
Gpm6a	9.39E-19	0.2965	0.892	0.741	2.63E-14	0
Me3	9.89E-19	0.2980	0.174	0.054	2.77E-14	0
Parvb	1.32E-18	-0.4475	0.096	0.249	3.71E-14	0
Chl1	1.68E-18	-0.4783	0.057	0.193	4.69E-14	0
Tle1	1.75E-18	0.3510	0.382	0.199	4.89E-14	0
Lgi1	1.90E-18	-0.4959	0.213	0.374	5.31E-14	0
Lhfp	2.06E-18	-0.3980	0.631	0.726	5.78E-14	0
Syn2	2.18E-18	-0.4757	0.299	0.448	6.09E-14	0
Hmgn3	2.39E-18	0.3545	0.497	0.296	6.68E-14	0
D030047H15Rik	3.08E-18	0.3145	0.552	0.334	8.63E-14	0
Ctnna2	3.41E-18	0.2645	0.919	0.769	9.55E-14	0
Mcc	3.60E-18	-0.3811	0.65	0.725	1.01E-13	0
Nfasc	3.72E-18	0.3544	0.389	0.206	1.04E-13	0
Pamr1	4.52E-18	0.2766	0.178	0.059	1.27E-13	0
Tprkb	5.77E-18	0.3316	0.68	0.474	1.62E-13	0
Pdgfrb	7.09E-18	0.3311	0.431	0.235	1.99E-13	0
Slc22a4	7.68E-18	-0.4319	0.074	0.214	2.15E-13	0
Smad3	9.80E-18	-0.4593	0.11	0.263	2.74E-13	0
Gm44151	1.11E-17	0.3336	0.466	0.268	3.11E-13	0
Gm2163	1.43E-17	0.2795	0.298	0.135	3.99E-13	0
Vegfa	1.55E-17	0.3755	0.471	0.283	4.34E-13	0
Caskin1	2.26E-17	0.3245	0.561	0.359	6.33E-13	0
Pitpnc1	2.30E-17	-0.3593	0.953	0.95	6.44E-13	0
Fbxw4	2.64E-17	-0.4113	0.166	0.327	7.38E-13	0
Sh3gl2	3.91E-17	-0.4011	0.042	0.166	1.09E-12	0
Fermt2	4.16E-17	0.3127	0.715	0.53	1.17E-12	0
Slit2	4.60E-17	-0.6106	0.09	0.236	1.29E-12	0
Ncam2	4.72E-17	-0.4038	0.698	0.775	1.32E-12	0
Wscd1	5.14E-17	0.2846	0.27	0.12	1.44E-12	0
Alpk1	5.68E-17	0.3268	0.303	0.146	1.59E-12	0
Angpt1	5.74E-17	-0.4554	0.049	0.179	1.61E-12	0
Bmyc	7.29E-17	0.2733	0.211	0.082	2.04E-12	0
Ttyh3	9.49E-17	0.3265	0.523	0.327	2.66E-12	0
1110004F10Rik	1.25E-16	-0.4437	0.129	0.273	3.49E-12	0
F3	1.34E-16	0.2675	0.677	0.457	3.76E-12	0
Magi1	1.60E-16	-0.3558	0.595	0.691	4.47E-12	0
Kcnq1ot1	1.78E-16	-0.4380	0.239	0.402	4.99E-12	0
Gm12394	2.14E-16	0.2724	0.17	0.058	6.00E-12	0
Eya1	2.15E-16	0.2673	0.284	0.129	6.03E-12	0
Gab2	2.19E-16	-0.4608	0.239	0.396	6.12E-12	0
Arhgap5	2.62E-16	0.2519	0.864	0.735	7.33E-12	0

Ddo	3.33E-16	-0.4154	0.259	0.41	9.31E-12	0
Aifm3	3.67E-16	0.3058	0.47	0.275	1.03E-11	0
Lair1	4.12E-16	0.2765	0.22	0.089	1.15E-11	0
Ephx2	4.46E-16	0.2909	0.275	0.128	1.25E-11	0
Prtg	4.68E-16	-0.3966	0.045	0.165	1.31E-11	0
Map3k5	5.13E-16	0.3201	0.216	0.089	1.44E-11	0
Pcsk6	6.85E-16	0.3350	0.295	0.144	1.92E-11	0
Fat3	7.66E-16	-0.4306	0.569	0.65	2.14E-11	0
Nmur2	1.20E-15	0.3093	0.263	0.12	3.35E-11	0
Zfp532	1.20E-15	0.2955	0.637	0.428	3.35E-11	0
Fnbp1l	1.34E-15	-0.4020	0.142	0.285	3.74E-11	0
Runx1t1	1.44E-15	-0.4575	0.178	0.324	4.02E-11	0
Nbea	1.67E-15	-0.3241	0.522	0.641	4.68E-11	0
Gsap	1.71E-15	0.2947	0.437	0.252	4.78E-11	0
Tmtc2	1.87E-15	-0.3663	0.723	0.764	5.24E-11	0
Ugp2	1.90E-15	0.3115	0.697	0.525	5.32E-11	0
Gpr158	2.23E-15	0.3747	0.352	0.192	6.24E-11	0
Bmp2k	2.23E-15	0.3083	0.458	0.279	6.24E-11	0
Nnat	2.35E-15	-0.6644	0.363	0.484	6.58E-11	0
Slc22a23	2.41E-15	0.2609	0.516	0.317	6.76E-11	0
Sned1	2.51E-15	0.2701	0.318	0.161	7.03E-11	0
Crot	3.69E-15	0.3250	0.345	0.185	1.03E-10	0
Mt1	3.97E-15	0.3214	0.421	0.243	1.11E-10	0
Grid1	4.38E-15	0.2781	0.814	0.641	1.23E-10	0
Ctif	4.55E-15	0.2815	0.581	0.375	1.27E-10	0
Eva1a	5.05E-15	0.2834	0.442	0.254	1.41E-10	0
Lrrc8c	5.19E-15	0.3035	0.204	0.086	1.45E-10	0
Coro2b	7.93E-15	0.2811	0.455	0.268	2.22E-10	0
Slc38a3	9.59E-15	0.2985	0.385	0.216	2.68E-10	0
Dmd	1.12E-14	-0.2945	0.866	0.868	3.14E-10	0
Cdh2	1.20E-14	0.2624	0.783	0.627	3.35E-10	0
Plscr4	1.36E-14	-0.3707	0.114	0.249	3.82E-10	0
Rasa2	1.69E-14	0.2910	0.684	0.504	4.73E-10	0
Rgs6	1.91E-14	0.2621	0.885	0.771	5.35E-10	0
Tspan5	2.68E-14	-0.3611	0.558	0.638	7.49E-10	0
Brinp3	2.76E-14	-0.4213	0.542	0.641	7.72E-10	0
Mt2	3.33E-14	0.2669	0.195	0.081	9.33E-10	0
Hlf	3.95E-14	0.2659	0.531	0.349	1.10E-09	0
Vit	5.50E-14	-0.3709	0.092	0.221	1.54E-09	0
Pam	5.67E-14	0.2909	0.444	0.265	1.59E-09	0
Ptprk	6.15E-14	-0.4117	0.06	0.174	1.72E-09	0
Sorbs2	6.29E-14	-0.3993	0.17	0.306	1.76E-09	0
Dock5	7.14E-14	-0.2963	0.024	0.12	2.00E-09	0

Adra1a	7.14E-14	0.2847	0.33	0.176	2.00E-09	0
Nkx6-2	8.01E-14	-0.3037	0.014	0.102	2.24E-09	0
Tnc	8.36E-14	0.3935	0.196	0.084	2.34E-09	0
Slc38a1	8.78E-14	-0.4328	0.053	0.163	2.46E-09	0
Marcks	1.07E-13	-0.3463	0.065	0.18	3.00E-09	0
4931406C07Rik	1.07E-13	0.2590	0.323	0.167	3.01E-09	0
Add1	1.40E-13	0.2563	0.58	0.396	3.92E-09	0
Gm29237	1.51E-13	0.2563	0.242	0.114	4.23E-09	0
Sobp	1.57E-13	-0.4106	0.257	0.397	4.39E-09	0
Shroom4	1.69E-13	0.2723	0.427	0.251	4.72E-09	0
Arhgef19	1.75E-13	0.2843	0.437	0.267	4.90E-09	0
Foxp1	1.87E-13	-0.3195	0.41	0.525	5.23E-09	0
Hif3a	1.91E-13	0.3010	0.424	0.251	5.33E-09	0
Bmp6	2.15E-13	0.2915	0.134	0.046	6.01E-09	0
Akap6	2.15E-13	-0.3329	0.636	0.701	6.02E-09	0
2210408I21Rik	2.22E-13	-0.4153	0.323	0.453	6.23E-09	0
Tnfaip8	2.38E-13	-0.3873	0.255	0.387	6.66E-09	0
Galnt10	2.52E-13	-0.3202	0.042	0.145	7.07E-09	0
Rnf121	2.73E-13	0.4230	0.556	0.416	7.64E-09	0
Kcnt1	3.42E-13	-0.3025	0.038	0.138	9.57E-09	0
Mfge8	3.96E-13	0.2826	0.412	0.243	1.11E-08	0
Pipox	4.59E-13	-0.3504	0.072	0.188	1.28E-08	0
Rapgef3	7.53E-13	0.2707	0.576	0.377	2.11E-08	0
Specc1	8.17E-13	0.2749	0.62	0.442	2.29E-08	0
Capn2	8.48E-13	0.2618	0.446	0.273	2.37E-08	0
Kcnn2	8.54E-13	0.2545	0.647	0.455	2.39E-08	0
Nr2f2	8.67E-13	-0.3332	0.047	0.15	2.43E-08	0
Glrb	9.56E-13	0.3002	0.371	0.221	2.68E-08	0
Ssbp2	9.85E-13	-0.2782	0.673	0.745	2.76E-08	0
Rbms3	1.02E-12	0.3683	0.36	0.219	2.87E-08	0
Atp2a2	1.42E-12	-0.2912	0.561	0.643	3.99E-08	0
Aldoc	1.54E-12	0.2814	0.356	0.209	4.31E-08	0
Dpf3	1.56E-12	0.2545	0.623	0.445	4.36E-08	0
Ttc28	1.60E-12	-0.3195	0.558	0.639	4.47E-08	0
2900052N01Rik	1.69E-12	0.2951	0.223	0.105	4.72E-08	0
Phactr1	1.72E-12	0.2679	0.764	0.596	4.80E-08	0
Mgat4c	1.79E-12	-0.3503	0.645	0.72	5.02E-08	0
Srgap2	2.16E-12	0.2566	0.577	0.409	6.04E-08	0
Gpatch8	2.29E-12	-0.2737	0.687	0.722	6.41E-08	0
Etnppl	3.42E-12	-0.5513	0.149	0.268	9.56E-08	0
Ankrd6	3.84E-12	0.2813	0.481	0.315	1.07E-07	0
Erc1	3.92E-12	0.2726	0.565	0.406	1.10E-07	0
Adgrv1	4.30E-12	-0.4905	0.042	0.136	1.21E-07	0

Plekha7	4.72E-12	0.2513	0.441	0.278	1.32E-07	0
Gm43477	5.27E-12	0.2624	0.234	0.116	1.48E-07	0
St3gal4	5.44E-12	0.2642	0.683	0.518	1.52E-07	0
Slc15a2	5.52E-12	0.2544	0.473	0.302	1.55E-07	0
Raver2	5.62E-12	0.2608	0.574	0.403	1.57E-07	0
Tcf12	6.15E-12	-0.2581	0.7	0.763	1.72E-07	0
Fam49b	6.52E-12	0.2905	0.527	0.357	1.82E-07	0
Heg1	7.83E-12	-0.3237	0.086	0.197	2.19E-07	0
Ccdc50	8.46E-12	0.2966	0.529	0.364	2.37E-07	0
Gli1	9.66E-12	-0.2695	0.021	0.101	2.70E-07	0
Fam107a	9.76E-12	0.2637	0.341	0.195	2.73E-07	0
Rb1	1.11E-11	0.2716	0.67	0.491	3.10E-07	0
Reln	1.23E-11	-0.3081	0.028	0.114	3.43E-07	0
Slc7a2	1.29E-11	0.2855	0.47	0.309	3.62E-07	0
C530008M17Rik	1.30E-11	-0.3705	0.167	0.292	3.65E-07	0
Fyn	1.54E-11	-0.2839	0.434	0.542	4.31E-07	0
Fgfr1	1.63E-11	0.2538	0.58	0.413	4.55E-07	0
Sh3kbp1	1.67E-11	0.2732	0.349	0.206	4.67E-07	0
Cml3	1.76E-11	0.3048	0.502	0.352	4.94E-07	0
Dcc	2.20E-11	0.4506	0.503	0.368	6.16E-07	0
Agbl4	2.27E-11	-0.4373	0.364	0.474	6.36E-07	0
Hdac7	2.47E-11	0.2633	0.277	0.152	6.92E-07	0
Trpm3	2.64E-11	-0.4318	0.957	0.909	7.39E-07	0
Pde1c	2.80E-11	0.2542	0.302	0.172	7.83E-07	0
Gpam	2.86E-11	0.2865	0.494	0.341	8.00E-07	0
Cyp2d22	4.35E-11	0.2597	0.389	0.244	1.22E-06	0
Atp13a4	4.64E-11	-0.3364	0.431	0.517	1.30E-06	0
Pitpnm2	5.28E-11	-0.3547	0.221	0.336	1.48E-06	0
Gabra2	6.09E-11	0.3117	0.477	0.317	1.70E-06	0
Sema5b	6.62E-11	-0.3627	0.086	0.189	1.85E-06	0
Syndig1	6.73E-11	-0.3020	0.025	0.103	1.88E-06	0
Sat1	7.11E-11	0.2776	0.487	0.327	1.99E-06	0
Kcnq1	7.21E-11	-0.3152	0.14	0.257	2.02E-06	0
Metap1d	8.27E-11	-0.3240	0.275	0.398	2.32E-06	0
Rgl1	1.21E-10	-0.3088	0.352	0.46	3.38E-06	0
Cacna1a	1.22E-10	-0.3458	0.193	0.308	3.42E-06	0
Pip4k2a	1.28E-10	-0.3584	0.367	0.459	3.58E-06	0
Rtn1	2.52E-10	-0.3444	0.346	0.446	7.06E-06	0
Ubash3b	2.96E-10	-0.3580	0.16	0.27	8.28E-06	0
Polr2a	3.39E-10	-0.4034	0.196	0.301	9.50E-06	0
Grik4	3.98E-10	-0.3117	0.113	0.218	1.12E-05	0
Meg3	4.11E-10	-0.3030	0.783	0.82	1.15E-05	0
Pcx	4.63E-10	-0.3420	0.296	0.402	1.30E-05	0

Sulf1	5.15E-10	-0.3184	0.026	0.101	1.44E-05	0
Mboat2	5.21E-10	-0.2723	0.517	0.607	1.46E-05	0
Samd4	5.67E-10	-0.3176	0.298	0.408	1.59E-05	0
Tra2a	5.86E-10	-0.3038	0.684	0.701	1.64E-05	0
Kcnk2	6.31E-10	0.2749	0.406	0.265	1.77E-05	0
Smyd3	6.58E-10	-0.3123	0.385	0.492	1.84E-05	0
Ntn1	7.46E-10	-0.2726	0.029	0.103	2.09E-05	0
Zfp462	9.20E-10	-0.2891	0.377	0.483	2.58E-05	0
Otud7a	9.72E-10	0.2737	0.391	0.253	2.72E-05	0
Ptchd4	9.75E-10	0.3210	0.232	0.129	2.73E-05	0
Sncaip	1.05E-09	-0.4176	0.204	0.31	2.94E-05	0
Prex1	1.06E-09	0.2719	0.566	0.423	2.98E-05	0
L3mbtl3	1.55E-09	-0.3319	0.355	0.449	4.34E-05	0
Guf1	1.62E-09	-0.3523	0.181	0.278	4.55E-05	0
Zfhx4	1.82E-09	-0.2855	0.264	0.393	5.08E-05	0
Slc25a21	3.31E-09	-0.3456	0.217	0.329	9.27E-05	0
Ntng2	3.65E-09	-0.3294	0.161	0.261	1.02E-04	0
Ednrb	4.60E-09	-0.3774	0.359	0.441	1.29E-04	0
Cux2	5.26E-09	-0.2851	0.089	0.18	1.47E-04	0
9530026P05Rik	5.74E-09	-0.3822	0.271	0.381	1.61E-04	0
Chn1	7.39E-09	-0.2729	0.278	0.385	2.07E-04	0
Cdyl2	7.78E-09	-0.2908	0.095	0.186	2.18E-04	0
Ppp1r12a	9.04E-09	-0.2515	0.506	0.573	2.53E-04	0
Rhoq	1.01E-08	-0.3015	0.364	0.453	2.82E-04	0
Gpld1	1.08E-08	-0.3291	0.452	0.513	3.03E-04	0
Fbxl7	1.20E-08	-0.4033	0.09	0.178	3.35E-04	0
Zswim6	1.31E-08	0.2719	0.626	0.498	3.66E-04	0
Csmd2	1.48E-08	-0.2964	0.171	0.272	4.13E-04	0
Cdk19	2.00E-08	-0.2708	0.481	0.549	5.61E-04	0
2310022B05Rik	2.38E-08	-0.3005	0.149	0.241	6.67E-04	0
Traf3ip2	2.74E-08	-0.2724	0.189	0.287	7.68E-04	0
Slc20a2	2.83E-08	-0.2858	0.177	0.275	7.91E-04	0
Chd6	2.84E-08	-0.2503	0.627	0.663	7.96E-04	0
Antxr1	3.03E-08	-0.3358	0.275	0.364	8.48E-04	0
Sorbs2os	3.17E-08	-0.2871	0.088	0.172	8.88E-04	0
Samd12	4.11E-08	-0.3738	0.106	0.191	1.15E-03	0
Ube2e2	4.69E-08	-0.2546	0.505	0.581	1.31E-03	0
D230017M19Rik	4.83E-08	-0.2648	0.065	0.142	1.35E-03	0
Cd38	4.85E-08	-0.2908	0.064	0.139	1.36E-03	0
Dock10	5.44E-08	-0.3246	0.038	0.105	1.52E-03	0
Upf3b	6.04E-08	-0.2606	0.223	0.312	1.69E-03	0
Mok	6.79E-08	-0.2817	0.108	0.193	1.90E-03	0
Cdh13	7.36E-08	-0.3154	0.107	0.191	2.06E-03	0

Ptprj	7.69E-08	-0.2900	0.179	0.277	2.15E-03	0
Zfp704	7.93E-08	-0.2952	0.103	0.187	2.22E-03	0
Klhl13	8.87E-08	-0.2615	0.079	0.158	2.48E-03	0
Kcnip3	1.22E-07	-0.3092	0.338	0.417	3.43E-03	0
Gm11713	1.36E-07	-0.3007	0.243	0.332	3.80E-03	0
Nmnat2	1.44E-07	-0.2626	0.039	0.103	4.03E-03	0
Lamp2	2.02E-07	-0.2523	0.396	0.466	5.66E-03	0
Nalcn	2.35E-07	-0.2849	0.099	0.178	6.58E-03	0
Prkag2	2.55E-07	-0.2687	0.129	0.212	7.13E-03	0
Meis1	2.64E-07	-0.2937	0.345	0.419	7.39E-03	0
6430573F11Rik	2.69E-07	-0.2725	0.164	0.247	7.54E-03	0
Cep164	2.92E-07	-0.2511	0.139	0.223	8.17E-03	0
Itpr1	3.02E-07	-0.2803	0.192	0.276	8.45E-03	0
Cdk17	3.27E-07	-0.2578	0.22	0.301	9.16E-03	0
Tshz2	3.43E-07	-0.2942	0.166	0.259	9.59E-03	0
Jakmip1	3.91E-07	-0.2593	0.236	0.327	0.0110	0
Creb5	4.11E-07	-0.2793	0.063	0.133	0.0115	0
2010111I01Rik	4.12E-07	-0.2509	0.364	0.442	0.0115	0
Scmh1	5.29E-07	-0.2547	0.52	0.566	0.0148	0
Arl15	5.41E-07	-0.2558	0.356	0.442	0.0151	0
Ttyh2	6.54E-07	-0.2703	0.306	0.382	0.0183	0
A330033J07Rik	7.42E-07	-0.4137	0.197	0.283	0.0208	0
Parp8	8.82E-07	-0.2825	0.316	0.385	0.0247	0
Susd6	1.09E-06	-0.2587	0.268	0.344	0.0304	0
Spef2	1.49E-06	-0.2548	0.075	0.144	0.0417	0
Sipa1l1	1.59E-06	-0.2509	0.146	0.225	0.0444	0
Ano6	1.69E-06	-0.2592	0.163	0.241	0.0472	0
Hs6st3	1.84E-06	-0.3335	0.1	0.171	0.0515	0
Kcnip4	2.40E-06	-0.3475	0.48	0.528	0.0673	0
Ccdc148	2.93E-06	-0.2852	0.139	0.211	0.0821	0
Aspa	3.48E-06	-0.2648	0.081	0.146	0.0974	0
Gria1	2.04E-174	1.6203	0.978	0.371	5.70E-170	1
Fry	2.44E-151	1.2939	0.973	0.525	6.84E-147	1
Slc6a11	2.73E-149	1.2881	0.971	0.577	7.64E-145	1
Trpm3	5.58E-146	1.0212	1	0.908	1.56E-141	1
Itih3	1.38E-139	1.4135	0.772	0.214	3.85E-135	1
Erbb4	6.29E-127	1.0576	0.993	0.654	1.76E-122	1
Kcnd2	1.07E-123	1.1092	0.993	0.66	3.01E-119	1
B230323A14Rik	1.79E-110	1.2555	0.632	0.131	5.00E-106	1
Lrig1	3.63E-108	1.0230	0.891	0.442	1.02E-103	1
Slc4a4	4.86E-104	0.7770	0.998	0.916	1.36E-99	1
Etnppl	1.06E-101	1.1838	0.613	0.14	2.97E-97	1
Pitpnc1	5.85E-93	0.7536	0.998	0.94	1.64E-88	1

Ptch1	6.97E-90	1.0209	0.93	0.655	1.95E-85	1
Sparc	7.21E-90	0.9728	0.54	0.116	2.02E-85	1
Cntn1	2.50E-83	1.0081	0.814	0.365	6.99E-79	1
Car10	5.10E-82	1.0803	0.45	0.081	1.43E-77	1
Agt	2.12E-81	0.8073	0.373	0.048	5.95E-77	1
Npas3	1.89E-79	0.4502	1	0.992	5.29E-75	1
Nav3	1.19E-78	1.0933	0.668	0.243	3.35E-74	1
Adcy8	4.82E-77	0.9025	0.54	0.133	1.35E-72	1
Sparcl1	6.37E-76	0.6903	0.981	0.782	1.78E-71	1
Srgap1	1.69E-74	0.8586	0.823	0.399	4.73E-70	1
Gnao1	9.79E-74	-1.1643	0.511	0.821	2.74E-69	1
Adgrb3	1.78E-69	0.4818	1	0.978	4.99E-65	1
Camk2g	1.18E-63	0.7116	0.913	0.686	3.31E-59	1
Gm3764	1.78E-63	0.5252	0.995	0.947	4.97E-59	1
Fat3	3.49E-59	0.7370	0.864	0.567	9.76E-55	1
Plcb1	2.50E-57	0.6747	0.976	0.823	7.01E-53	1
Cit	1.07E-56	0.7649	0.516	0.164	3.01E-52	1
Mgat5	3.77E-55	-1.1508	0.215	0.631	1.05E-50	1
Slco1c1	3.88E-55	-0.9671	0.281	0.69	1.09E-50	1
Nebl	5.34E-53	0.6417	0.923	0.655	1.50E-48	1
Fars2	7.22E-53	-0.9565	0.545	0.811	2.02E-48	1
Itpkb	1.18E-52	0.8281	0.627	0.275	3.30E-48	1
Lrp1b	2.76E-52	0.5897	0.969	0.718	7.72E-48	1
Cables1	5.56E-51	0.7346	0.748	0.403	1.56E-46	1
Dab2	1.72E-50	0.6586	0.402	0.108	4.80E-46	1
Meis2	2.48E-50	-0.7951	0.525	0.833	6.94E-46	1
Gfra1	1.26E-49	-1.1704	0.012	0.4	3.53E-45	1
Plce1	2.36E-49	0.6665	0.828	0.527	6.60E-45	1
Frmd4a	2.60E-49	-0.7417	0.918	0.952	7.28E-45	1
Gabbr2	2.60E-49	0.6753	0.746	0.384	7.29E-45	1
5031439G07Rik	1.90E-48	0.8131	0.683	0.378	5.31E-44	1
Mpp6	2.87E-48	0.7030	0.736	0.406	8.03E-44	1
Adam23	1.39E-46	-1.1327	0.061	0.443	3.88E-42	1
Ptn	3.72E-45	-0.7874	0.499	0.788	1.04E-40	1
Zbtb20	9.55E-45	-0.3671	0.998	0.997	2.67E-40	1
Grm3	1.53E-44	-0.8041	0.726	0.882	4.28E-40	1
Lyrm4	1.73E-44	-0.9293	0.235	0.609	4.83E-40	1
Ntrk3	4.69E-44	0.6971	0.717	0.399	1.31E-39	1
Nkx6-2	8.97E-44	0.5676	0.232	0.036	2.51E-39	1
Fgf13	1.13E-43	-1.1666	0.07	0.441	3.18E-39	1
Ephb1	6.80E-43	-1.1901	0.044	0.398	1.90E-38	1
Mdga2	1.88E-42	0.4088	0.998	0.938	5.25E-38	1
RP23-474J16.2	3.28E-42	0.7821	0.443	0.143	9.20E-38	1

Lhfp	1.31E-40	0.6627	0.86	0.656	3.67E-36	1
Csmd1	4.93E-40	-0.9836	0.375	0.694	1.38E-35	1
Nnat	1.68E-39	0.9847	0.656	0.395	4.70E-35	1
Gm21798	3.29E-39	0.6143	0.286	0.066	9.22E-35	1
Sik3	3.59E-39	-0.6053	0.731	0.901	1.00E-34	1
Ppp1r14c	5.08E-39	0.6279	0.492	0.192	1.42E-34	1
Tmtc2	9.05E-39	0.5787	0.891	0.718	2.53E-34	1
Gpld1	1.31E-38	0.6001	0.714	0.442	3.67E-34	1
Dclk1	2.99E-38	-0.7051	0.615	0.8	8.38E-34	1
Dpp6	6.14E-38	0.6349	0.496	0.208	1.72E-33	1
Igsf1	1.75E-37	0.5046	0.194	0.029	4.89E-33	1
Spon1	2.49E-37	0.5939	0.76	0.451	6.97E-33	1
Nhsl1	3.21E-37	0.5280	0.923	0.786	9.00E-33	1
Cep85l	5.74E-37	0.5490	0.818	0.58	1.61E-32	1
Tmem117	6.06E-37	0.6628	0.467	0.188	1.70E-32	1
Pde4d	7.69E-37	0.4633	0.93	0.718	2.15E-32	1
Dkk3	8.80E-37	-0.8724	0.048	0.372	2.46E-32	1
Fam13c	1.73E-36	-0.9102	0.148	0.478	4.84E-32	1
Cspg5	3.58E-36	-0.6983	0.506	0.776	1.00E-31	1
Atp13a4	8.69E-36	0.5918	0.709	0.438	2.43E-31	1
Tenm3	9.92E-36	-0.6495	0.523	0.776	2.78E-31	1
Kank1	1.51E-35	0.5408	0.785	0.513	4.24E-31	1
Gm26843	3.03E-35	-0.9473	0.08	0.4	8.49E-31	1
Slc6a9	8.41E-35	0.5573	0.337	0.105	2.36E-30	1
Lypd6	1.13E-34	-0.8606	0.007	0.298	3.18E-30	1
Ctnna2	1.56E-34	-0.6242	0.639	0.86	4.38E-30	1
Slc25a18	4.12E-34	0.6061	0.494	0.217	1.15E-29	1
Lgi1	5.13E-34	0.6568	0.547	0.269	1.44E-29	1
Tmcc3	5.42E-34	0.6206	0.758	0.539	1.52E-29	1
Ednrb	9.62E-34	0.6295	0.634	0.363	2.69E-29	1
2310022B05Rik	6.21E-32	0.5557	0.414	0.163	1.74E-27	1
Kif21a	1.66E-31	-0.6997	0.308	0.625	4.65E-27	1
Adgrl3	4.05E-31	0.3297	0.993	0.943	1.13E-26	1
Ptprt	6.20E-31	-0.4874	0.867	0.932	1.73E-26	1
Ndrg2	2.90E-30	0.4995	0.772	0.539	8.12E-26	1
Dfna5	3.69E-30	0.5920	0.644	0.39	1.03E-25	1
Atp1a2	8.95E-30	0.3829	0.969	0.866	2.51E-25	1
St6galnac5	1.02E-29	-1.1167	0.09	0.37	2.86E-25	1
Gpm6b	1.11E-29	-0.4452	0.906	0.961	3.11E-25	1
Tspan7	1.42E-29	-0.7788	0.644	0.776	3.99E-25	1
Nkain2	2.01E-29	-0.9977	0.407	0.647	5.63E-25	1
Dennd1a	2.70E-29	-0.4851	0.724	0.874	7.56E-25	1
Kcnt1	4.03E-29	0.4500	0.257	0.07	1.13E-24	1

Magi3	6.86E-29	-0.7375	0.157	0.459	1.92E-24	1
Ntsr2	7.03E-29	0.4674	0.753	0.512	1.97E-24	1
Gldc	7.99E-29	-0.7406	0.138	0.426	2.24E-24	1
Tmc7	2.09E-28	0.5634	0.61	0.365	5.85E-24	1
Emx2os	9.59E-28	-0.7253	0.031	0.287	2.68E-23	1
Rgs7	1.21E-27	-0.6426	0.576	0.764	3.38E-23	1
Pipox	5.27E-27	0.5209	0.317	0.111	1.48E-22	1
Rgs20	8.98E-27	-0.5035	0.843	0.91	2.52E-22	1
Qk	9.56E-27	0.2958	0.998	0.965	2.68E-22	1
Wnk2	2.61E-26	-0.6073	0.315	0.605	7.31E-22	1
Mgat4c	2.86E-26	0.4676	0.855	0.658	8.00E-22	1
Fgfr3	4.36E-26	0.4130	0.772	0.542	1.22E-21	1
B3galt1	8.32E-26	-0.3865	0.925	0.957	2.33E-21	1
Eps8	1.38E-25	0.4616	0.785	0.563	3.86E-21	1
Tlcd1	1.62E-25	0.4853	0.303	0.112	4.55E-21	1
Sorcs2	1.73E-25	0.4336	0.806	0.63	4.85E-21	1
Unc13c	2.12E-25	-0.8875	0.077	0.331	5.94E-21	1
Cdh22	3.68E-25	0.4724	0.269	0.086	1.03E-20	1
Mapk4	4.12E-25	0.4155	0.838	0.653	1.15E-20	1
Ntrk2	4.13E-25	0.3799	0.969	0.917	1.16E-20	1
Kcnj10	4.24E-25	0.5798	0.47	0.255	1.19E-20	1
Cd38	5.04E-25	0.5245	0.254	0.082	1.41E-20	1
Fam184b	6.43E-25	-0.7233	0.022	0.252	1.80E-20	1
Tcf4	6.71E-25	-0.3282	0.93	0.967	1.88E-20	1
Dock5	7.86E-25	0.4286	0.215	0.059	2.20E-20	1
Tnfrsf19	4.97E-24	-0.7173	0.182	0.445	1.39E-19	1
Rhoq	6.61E-24	0.4717	0.617	0.379	1.85E-19	1
Usp53	6.72E-24	0.5244	0.567	0.333	1.88E-19	1
Syn2	7.77E-24	0.5253	0.584	0.356	2.18E-19	1
Gpc6	8.36E-24	-0.5581	0.588	0.763	2.34E-19	1
Lrrc16a	9.37E-24	0.4246	0.833	0.672	2.62E-19	1
A330033J07Rik	1.27E-23	0.6949	0.441	0.212	3.56E-19	1
Gm5089	1.39E-23	-0.6066	0.027	0.25	3.90E-19	1
Pigk	1.91E-23	-0.8466	0.128	0.379	5.35E-19	1
Slc6a1	2.10E-23	0.4087	0.818	0.668	5.89E-19	1
Dgkb	2.48E-23	-0.3371	0.935	0.964	6.94E-19	1
Gab2	3.41E-23	0.5207	0.533	0.301	9.53E-19	1
Dab1	5.41E-23	-0.5576	0.482	0.713	1.52E-18	1
Clybl	5.95E-23	-0.5187	0.441	0.679	1.67E-18	1
Slc7a10	7.78E-23	0.4862	0.646	0.452	2.18E-18	1
Paqr8	8.13E-23	0.4351	0.785	0.552	2.28E-18	1
Prkca	1.23E-22	0.5096	0.625	0.388	3.45E-18	1
Sh3gl2	1.25E-22	0.4603	0.266	0.092	3.49E-18	1

Dmd	1.41E-22	0.3240	0.927	0.854	3.95E-18	1
Brinp3	1.64E-22	0.4349	0.782	0.568	4.59E-18	1
Brinp2	5.72E-22	0.4809	0.274	0.1	1.60E-17	1
Plcb4	6.13E-22	0.3927	0.775	0.6	1.72E-17	1
Rmst	8.76E-22	-0.6891	0.378	0.597	2.45E-17	1
Gria2	1.28E-21	0.3323	0.952	0.842	3.59E-17	1
Pde4b	2.16E-21	0.3821	0.789	0.603	6.04E-17	1
Gm26704	3.04E-21	0.4438	0.709	0.493	8.51E-17	1
Slc35f1	3.08E-21	-0.7379	0.075	0.299	8.63E-17	1
Ezr	3.28E-21	-0.5627	0.036	0.245	9.18E-17	1
Mical2	3.60E-21	0.4495	0.709	0.532	1.01E-16	1
Sema6a	4.84E-21	-0.6277	0.104	0.339	1.35E-16	1
Nmnat2	8.35E-21	0.4385	0.194	0.056	2.34E-16	1
Nme7	1.01E-20	-0.5565	0.136	0.381	2.82E-16	1
Paqr6	1.23E-20	0.4015	0.23	0.076	3.44E-16	1
Ldb2	1.27E-20	0.4426	0.477	0.248	3.57E-16	1
Mettl7a1	2.16E-20	0.4465	0.278	0.11	6.04E-16	1
Cdh20	2.31E-20	0.3818	0.838	0.659	6.46E-16	1
Ghr	2.81E-20	0.4600	0.78	0.601	7.86E-16	1
Gm11713	3.35E-20	0.5297	0.467	0.264	9.39E-16	1
Ahcyl1	3.44E-20	0.4264	0.719	0.545	9.63E-16	1
Pou2f1	3.69E-20	-0.4637	0.472	0.695	1.03E-15	1
Nedd4l	5.38E-20	-0.4555	0.472	0.708	1.51E-15	1
Dapp1	6.93E-20	-0.5489	0.022	0.215	1.94E-15	1
Dock4	8.79E-20	0.3222	0.944	0.883	2.46E-15	1
Mid1	9.15E-20	-0.5735	0.14	0.383	2.56E-15	1
Kirrel3	1.33E-19	0.3466	0.956	0.829	3.72E-15	1
Prdm16	2.07E-19	-0.5106	0.552	0.726	5.80E-15	1
Tnik	2.29E-19	0.2749	0.988	0.939	6.42E-15	1
Celf2	2.52E-19	-0.2914	0.923	0.964	7.06E-15	1
Pdzrn3	2.53E-19	-0.7005	0.022	0.208	7.08E-15	1
Garem	2.91E-19	-0.5666	0.293	0.53	8.14E-15	1
Gtf2ird1	5.39E-19	0.4443	0.494	0.29	1.51E-14	1
Ncam1	5.63E-19	0.2692	0.966	0.906	1.58E-14	1
Slc1a2	5.81E-19	-0.6730	0.985	0.954	1.63E-14	1
Sorbs1	7.76E-19	0.4877	0.797	0.682	2.17E-14	1
Astn2	8.60E-19	0.4419	0.758	0.586	2.41E-14	1
Gm26703	9.00E-19	0.4232	0.262	0.106	2.52E-14	1
Sema4d	1.00E-18	-0.5210	0.114	0.339	2.81E-14	1
Mtss1l	1.06E-18	0.4629	0.673	0.501	2.97E-14	1
Epha5	1.34E-18	-0.6838	0.131	0.349	3.76E-14	1
Rcan2	1.45E-18	-0.6481	0.111	0.326	4.07E-14	1
Fam171b	1.53E-18	-0.5488	0.194	0.423	4.27E-14	1

Luzp2	2.13E-18	-0.4986	0.826	0.903	5.96E-14	1
Tspan5	2.14E-18	0.4193	0.734	0.583	5.98E-14	1
Rgs7bp	2.16E-18	0.4732	0.516	0.317	6.05E-14	1
Acss3	2.34E-18	0.4146	0.344	0.153	6.56E-14	1
Nrxn3	2.65E-18	0.3061	0.91	0.805	7.43E-14	1
Srgap2	3.23E-18	-0.5190	0.276	0.508	9.05E-14	1
Cadm1	3.73E-18	-0.3633	0.906	0.934	1.04E-13	1
Crym	3.81E-18	-0.7698	0.01	0.177	1.07E-13	1
Ankrd29	5.37E-18	-0.4703	0.027	0.207	1.50E-13	1
Folh1	5.69E-18	0.4290	0.383	0.197	1.59E-13	1
Parvb	5.77E-18	0.4416	0.344	0.165	1.61E-13	1
Galnt10	5.78E-18	0.3744	0.23	0.083	1.62E-13	1
Sepp1	8.88E-18	0.4109	0.329	0.158	2.49E-13	1
Syt10	1.06E-17	0.2997	0.119	0.025	2.97E-13	1
Lama3	1.17E-17	-0.5984	0.012	0.176	3.29E-13	1
Tnfaip8	1.35E-17	0.4559	0.506	0.306	3.78E-13	1
Hdac8	1.43E-17	0.3004	0.949	0.883	3.99E-13	1
Alk	1.49E-17	-0.6727	0.019	0.189	4.16E-13	1
Fut9	2.41E-17	0.3908	0.78	0.655	6.74E-13	1
Rbms1	2.63E-17	-0.5456	0.153	0.371	7.38E-13	1
Pak1	2.91E-17	-0.5215	0.077	0.276	8.15E-13	1
Clic6	4.31E-17	0.3659	0.155	0.043	1.21E-12	1
Gm9925	4.84E-17	0.4311	0.438	0.251	1.35E-12	1
Serpine2	6.20E-17	0.3359	0.734	0.55	1.74E-12	1
Bbox1	6.97E-17	0.2816	0.138	0.035	1.95E-12	1
Gjb6	7.68E-17	0.3867	0.332	0.161	2.15E-12	1
Tsc22d3	8.03E-17	0.4330	0.274	0.117	2.25E-12	1
Trp63	1.32E-16	0.5241	0.179	0.059	3.70E-12	1
Lrrc7	1.64E-16	0.4143	0.475	0.281	4.60E-12	1
Setbp1	2.05E-16	-0.4802	0.46	0.658	5.75E-12	1
Grin3a	2.22E-16	0.4882	0.31	0.146	6.21E-12	1
Pip4k2a	2.34E-16	0.4307	0.574	0.395	6.56E-12	1
Adrbk2	2.84E-16	0.3092	0.86	0.711	7.96E-12	1
Ankrd6	2.94E-16	-0.5097	0.194	0.411	8.22E-12	1
Msi2	3.67E-16	-0.2619	0.998	0.995	1.03E-11	1
Fgfr2	4.09E-16	-0.2976	0.925	0.951	1.14E-11	1
Robo2	4.29E-16	-0.6450	0.213	0.414	1.20E-11	1
Daam1	4.62E-16	-0.4022	0.414	0.624	1.29E-11	1
Sox6	5.21E-16	0.2790	0.935	0.897	1.46E-11	1
Scg3	5.38E-16	-0.4706	0.278	0.496	1.51E-11	1
Chl1	5.90E-16	0.3290	0.276	0.119	1.65E-11	1
Slc22a23	9.87E-16	-0.4833	0.208	0.423	2.76E-11	1
Cpe	1.04E-15	-0.3277	0.872	0.939	2.90E-11	1

Nos1ap	1.10E-15	0.3752	0.412	0.231	3.07E-11	1
Mcu	1.16E-15	-0.4449	0.32	0.539	3.24E-11	1
Phyhipl	1.47E-15	0.3861	0.692	0.527	4.11E-11	1
Lrp4	1.65E-15	-0.5094	0.148	0.35	4.62E-11	1
Akt3	1.65E-15	-0.3615	0.596	0.758	4.62E-11	1
Dcc	2.17E-15	-0.9061	0.259	0.448	6.07E-11	1
Mertk	2.26E-15	-0.4794	0.743	0.809	6.32E-11	1
Plekha7	3.50E-15	-0.4948	0.165	0.37	9.79E-11	1
Clic4	3.57E-15	0.3745	0.436	0.248	1.00E-10	1
Ddah1	4.46E-15	-0.4616	0.375	0.569	1.25E-10	1
Grip1	5.37E-15	-0.5937	0.235	0.434	1.50E-10	1
Auts2	5.45E-15	-0.2936	0.964	0.976	1.53E-10	1
Gli1	6.89E-15	0.3103	0.165	0.054	1.93E-10	1
Vcl	7.51E-15	-0.4667	0.327	0.533	2.10E-10	1
Pitpnm2	8.09E-15	0.3850	0.436	0.266	2.27E-10	1
Hapln1	9.51E-15	-0.4323	0.048	0.212	2.66E-10	1
Abat	1.07E-14	0.3391	0.671	0.483	3.00E-10	1
Disc1	1.09E-14	0.3964	0.262	0.118	3.05E-10	1
Trim2	1.15E-14	-0.5191	0.242	0.438	3.22E-10	1
Sptbn1	1.40E-14	-0.3757	0.538	0.713	3.92E-10	1
Swap70	1.54E-14	-0.4433	0.092	0.275	4.31E-10	1
Cdc42ep1	1.60E-14	0.2923	0.186	0.068	4.48E-10	1
Pde8b	2.51E-14	-0.4283	0.484	0.655	7.04E-10	1
Kcnip3	2.77E-14	0.3980	0.528	0.359	7.76E-10	1
Pdgfd	3.22E-14	0.4689	0.228	0.095	9.01E-10	1
Immp2l	3.54E-14	-0.5212	0.155	0.35	9.92E-10	1
Prdx6	3.69E-14	-0.3857	0.525	0.691	1.03E-09	1
Gm42556	3.98E-14	0.3442	0.155	0.052	1.11E-09	1
Myrip	4.25E-14	0.4097	0.455	0.287	1.19E-09	1
Grik4	4.73E-14	0.3702	0.31	0.154	1.33E-09	1
Tox	4.77E-14	-0.3778	0.697	0.801	1.33E-09	1
Flrt2	5.33E-14	0.4097	0.337	0.183	1.49E-09	1
Mmp16	5.46E-14	-0.4941	0.073	0.24	1.53E-09	1
Lhfpl3	5.56E-14	0.5347	0.247	0.112	1.56E-09	1
Sez6l	5.73E-14	0.3033	0.128	0.036	1.60E-09	1
Eda	6.03E-14	-0.5109	0.215	0.422	1.69E-09	1
Ece1	6.83E-14	0.4029	0.322	0.171	1.91E-09	1
Csmd2	7.38E-14	0.3413	0.38	0.206	2.07E-09	1
Limk2	8.24E-14	0.3912	0.506	0.348	2.31E-09	1
Fam65b	1.14E-13	0.3960	0.298	0.15	3.19E-09	1
Syndig1	1.15E-13	0.3743	0.165	0.057	3.21E-09	1
Abhd3	1.25E-13	0.3806	0.479	0.313	3.50E-09	1
Bach2	2.59E-13	-0.3933	0.569	0.695	7.24E-09	1

Cyp2j9	4.84E-13	0.3609	0.416	0.257	1.36E-08	1
Ddo	5.67E-13	0.3269	0.499	0.328	1.59E-08	1
1700112E06Rik	7.93E-13	0.3568	0.538	0.347	2.22E-08	1
Nrp1	8.17E-13	0.3479	0.441	0.27	2.29E-08	1
Tnc	8.74E-13	-0.4589	0.017	0.145	2.45E-08	1
Srgap3	1.10E-12	-0.3232	0.663	0.799	3.07E-08	1
Fjx1	1.22E-12	-0.4374	0.116	0.29	3.41E-08	1
Rgl1	1.23E-12	0.3846	0.542	0.397	3.45E-08	1
Micalcl	1.32E-12	0.2848	0.211	0.09	3.71E-08	1
Glis3	1.40E-12	-0.3553	0.659	0.786	3.92E-08	1
Dach1	1.42E-12	-0.5064	0.087	0.243	3.97E-08	1
Kcnip1	1.47E-12	0.3573	0.121	0.036	4.11E-08	1
Igsf8	1.62E-12	0.2807	0.671	0.506	4.54E-08	1
Heyl	1.87E-12	0.2634	0.136	0.043	5.24E-08	1
Arhgef26	1.93E-12	0.3006	0.797	0.703	5.40E-08	1
Tra2a	3.08E-12	-0.3777	0.571	0.725	8.62E-08	1
Colgalt2	4.97E-12	-0.3694	0.031	0.162	1.39E-07	1
Tmtc1	6.12E-12	0.3035	0.211	0.092	1.71E-07	1
Phka1	6.32E-12	0.3184	0.758	0.623	1.77E-07	1
Mettl24	6.47E-12	0.3339	0.218	0.096	1.81E-07	1
Sntg1	7.91E-12	0.3807	0.266	0.134	2.21E-07	1
Lhx2	8.29E-12	-0.3439	0.005	0.113	2.32E-07	1
Glud1	8.81E-12	0.2628	0.835	0.75	2.47E-07	1
F3	9.08E-12	0.3616	0.637	0.504	2.54E-07	1
Celsr1	9.70E-12	-0.3299	0.005	0.113	2.72E-07	1
Colec12	1.03E-11	0.3523	0.206	0.089	2.88E-07	1
Rab34	1.05E-11	0.3591	0.472	0.332	2.95E-07	1
Grm5	1.09E-11	0.4649	0.458	0.318	3.05E-07	1
Gdpd2	1.21E-11	0.2751	0.184	0.077	3.39E-07	1
Atp1b1	1.30E-11	-0.4186	0.162	0.33	3.65E-07	1
Unc5c	1.63E-11	-0.5069	0.094	0.248	4.56E-07	1
Pam	1.73E-11	-0.4109	0.182	0.357	4.83E-07	1
Gli3	1.79E-11	-0.3030	0.678	0.793	5.00E-07	1
Maml3	2.07E-11	-0.4553	0.087	0.238	5.78E-07	1
Lef1	2.44E-11	-0.3390	0.005	0.109	6.83E-07	1
Chst2	2.49E-11	-0.3569	0.041	0.172	6.98E-07	1
Jag1	2.82E-11	0.2537	0.133	0.046	7.88E-07	1
Rb1	3.39E-11	-0.3551	0.412	0.583	9.49E-07	1
Cped1	3.43E-11	0.2751	0.247	0.119	9.61E-07	1
Fmo1	3.52E-11	-0.3805	0.102	0.255	9.87E-07	1
Fam20a	3.60E-11	0.3828	0.622	0.488	1.01E-06	1
Pdcd4	3.71E-11	-0.4019	0.199	0.371	1.04E-06	1
Gpd2	3.89E-11	0.3250	0.513	0.372	1.09E-06	1

Mdga1	3.95E-11	-0.3657	0.015	0.125	1.11E-06	1
Axin2	4.07E-11	-0.3086	0.022	0.139	1.14E-06	1
4930544I03Rik	4.49E-11	-0.4291	0.082	0.228	1.26E-06	1
Cyfip1	4.55E-11	0.3403	0.523	0.393	1.27E-06	1
Nudt3	4.62E-11	-0.3770	0.22	0.393	1.29E-06	1
Skap2	4.91E-11	0.3379	0.496	0.348	1.37E-06	1
Camk1d	4.91E-11	0.3150	0.637	0.513	1.38E-06	1
Clu	5.75E-11	-0.4121	0.339	0.512	1.61E-06	1
Kcnk10	5.92E-11	-0.3758	0.041	0.166	1.66E-06	1
Sh3pxd2b	6.12E-11	0.3380	0.518	0.387	1.71E-06	1
C030018K13Rik	6.28E-11	-0.2666	0.005	0.105	1.76E-06	1
Lifr	6.49E-11	0.3387	0.446	0.304	1.82E-06	1
Pcx	7.24E-11	0.3578	0.484	0.34	2.03E-06	1
Ubr5	7.42E-11	0.2704	0.741	0.627	2.08E-06	1
Ctif	7.52E-11	-0.3613	0.293	0.478	2.11E-06	1
Myo1e	7.83E-11	-0.4076	0.153	0.312	2.19E-06	1
Atp1b2	8.89E-11	0.3215	0.516	0.374	2.49E-06	1
Syt17	8.94E-11	-0.3662	0.012	0.117	2.50E-06	1
Wscd1	1.17E-10	-0.3301	0.061	0.195	3.27E-06	1
Timp4	1.20E-10	0.3338	0.293	0.166	3.36E-06	1
Grid2	1.22E-10	-0.2660	0.925	0.946	3.40E-06	1
Guf1	1.27E-10	-0.4057	0.126	0.274	3.55E-06	1
Csmd3	1.28E-10	0.2771	0.584	0.419	3.58E-06	1
Dlc1	1.35E-10	0.5133	0.424	0.301	3.77E-06	1
1110004F10Rik	1.53E-10	0.3333	0.337	0.2	4.29E-06	1
Epb41l2	1.63E-10	-0.3677	0.346	0.526	4.56E-06	1
Csgalnact1	1.85E-10	0.2622	0.809	0.697	5.19E-06	1
Creb5	1.86E-10	-0.3808	0.022	0.13	5.20E-06	1
Mboat2	2.12E-10	0.3012	0.685	0.552	5.93E-06	1
Fnbp1l	2.14E-10	0.2777	0.356	0.211	5.99E-06	1
Pax6	2.43E-10	-0.3286	0.104	0.255	6.80E-06	1
Jakmip1	2.56E-10	0.3784	0.409	0.271	7.18E-06	1
Pik3r1	2.66E-10	0.3342	0.617	0.504	7.46E-06	1
Pgm2	2.91E-10	0.3065	0.436	0.302	8.16E-06	1
Itga6	2.98E-10	0.3165	0.63	0.518	8.34E-06	1
Lgr4	3.25E-10	-0.3692	0.247	0.414	9.09E-06	1
Asap1	3.38E-10	0.2515	0.804	0.73	9.47E-06	1
Prex2	3.39E-10	-0.3436	0.855	0.855	9.49E-06	1
Map3k5	3.44E-10	-0.3326	0.036	0.153	9.64E-06	1
Rasgrf1	4.11E-10	0.3074	0.387	0.242	1.15E-05	1
Polr2a	4.27E-10	-0.4478	0.148	0.294	1.20E-05	1
Abcc4	4.27E-10	-0.3421	0.041	0.159	1.20E-05	1
4930578G10Rik	4.73E-10	-0.3954	0.051	0.173	1.32E-05	1

Dgki	4.82E-10	-0.3775	0.281	0.444	1.35E-05	1
Tank	5.58E-10	-0.3428	0.148	0.303	1.56E-05	1
Dio2	5.96E-10	-0.3155	0.017	0.118	1.67E-05	1
Abca5	6.41E-10	-0.3008	0.024	0.131	1.80E-05	1
Slc16a6	7.01E-10	0.3090	0.206	0.101	1.96E-05	1
Eya1	7.05E-10	-0.3387	0.073	0.205	1.98E-05	1
Ttc3	7.39E-10	-0.3262	0.496	0.657	2.07E-05	1
Mgll	8.08E-10	-0.4155	0.506	0.65	2.26E-05	1
Ttll8	8.38E-10	0.3012	0.317	0.192	2.35E-05	1
Kazn	9.08E-10	0.2667	0.14	0.056	2.54E-05	1
Pdlim5	9.30E-10	-0.3347	0.426	0.574	2.60E-05	1
Elmo2	9.53E-10	0.3210	0.327	0.201	2.67E-05	1
Ccnd2	9.54E-10	-0.3106	0.027	0.132	2.67E-05	1
Scel	9.96E-10	-0.4027	0.019	0.12	2.79E-05	1
Arhgap23	1.03E-09	-0.3750	0.199	0.349	2.88E-05	1
Whamm	1.04E-09	0.2808	0.252	0.135	2.93E-05	1
Pdzph1	1.12E-09	-0.4456	0.215	0.366	3.13E-05	1
Rgcc	1.25E-09	-0.3737	0.143	0.292	3.51E-05	1
Plscr4	1.26E-09	0.2620	0.312	0.18	3.53E-05	1
2610035D17Rik	1.45E-09	0.2780	0.714	0.603	4.06E-05	1
Gsap	1.66E-09	-0.3566	0.184	0.343	4.63E-05	1
Kcnk1	1.70E-09	-0.3241	0.116	0.261	4.77E-05	1
Fyn	1.89E-09	0.2629	0.625	0.479	5.28E-05	1
Sctr	1.96E-09	-0.3137	0.019	0.118	5.48E-05	1
Ctnnbip1	2.23E-09	-0.3272	0.065	0.186	6.26E-05	1
Gm26512	2.29E-09	-0.3599	0.068	0.189	6.40E-05	1
Galnt18	2.36E-09	0.3918	0.45	0.319	6.60E-05	1
Mcc	2.36E-09	0.2587	0.76	0.686	6.61E-05	1
Fam19a1	2.44E-09	0.4194	0.131	0.051	6.82E-05	1
Gm27247	2.62E-09	0.2749	0.126	0.048	7.34E-05	1
Sncaip	2.67E-09	-0.4048	0.155	0.303	7.48E-05	1
Dner	2.72E-09	-0.3745	0.278	0.435	7.63E-05	1
Ugp2	2.74E-09	-0.3124	0.453	0.611	7.67E-05	1
Raver2	2.74E-09	-0.3347	0.324	0.491	7.67E-05	1
Cdh2	2.76E-09	-0.3162	0.584	0.7	7.74E-05	1
Frmd4b	2.78E-09	-0.3375	0.048	0.161	7.78E-05	1
Ppp2r3a	2.80E-09	-0.3520	0.356	0.514	7.84E-05	1
Zswim5	2.96E-09	0.3887	0.387	0.264	8.28E-05	1
Enox1	3.09E-09	-0.3777	0.206	0.36	8.66E-05	1
Miat	3.16E-09	-0.3193	0.029	0.131	8.84E-05	1
Tpd52l1	3.44E-09	0.3203	0.16	0.072	9.63E-05	1
Pamr1	3.50E-09	-0.2931	0.019	0.116	9.81E-05	1
Spag16	3.80E-09	-0.5713	0.046	0.155	1.06E-04	1

Ephx2	3.89E-09	-0.3095	0.075	0.2	1.09E-04	1
Arpp21	4.05E-09	0.2956	0.344	0.218	1.14E-04	1
Slc16a2	5.30E-09	-0.3630	0.058	0.172	1.48E-04	1
Ap3s1	5.41E-09	-0.3181	0.153	0.301	1.52E-04	1
Actr3b	5.72E-09	0.3577	0.291	0.176	1.60E-04	1
Frem1	5.74E-09	0.2831	0.215	0.112	1.61E-04	1
Oaf	5.77E-09	-0.2669	0.031	0.134	1.61E-04	1
Gm4876	6.05E-09	-0.3941	0.116	0.248	1.69E-04	1
Sybu	6.42E-09	-0.2777	0.562	0.694	1.80E-04	1
Apba1	6.67E-09	-0.3666	0.201	0.357	1.87E-04	1
0610040J01Rik	6.82E-09	-0.3382	0.041	0.146	1.91E-04	1
Stxbp6	7.10E-09	-0.3635	0.082	0.206	1.99E-04	1
9630028H03Rik	7.11E-09	0.3599	0.385	0.269	1.99E-04	1
Fam214a	7.68E-09	0.3204	0.424	0.303	2.15E-04	1
Ramp1	8.16E-09	0.3084	0.298	0.183	2.28E-04	1
Notch3	8.19E-09	0.3003	0.354	0.233	2.29E-04	1
Gabra2	8.54E-09	-0.3676	0.247	0.398	2.39E-04	1
Cblb	8.87E-09	-0.3543	0.177	0.315	2.48E-04	1
Rfx3	9.00E-09	-0.2901	0.581	0.718	2.52E-04	1
Gm2163	9.46E-09	-0.3390	0.087	0.212	2.65E-04	1
Atp13a5	1.04E-08	0.3119	0.32	0.203	2.90E-04	1
Reck	1.12E-08	-0.3400	0.119	0.248	3.13E-04	1
Tle1	1.17E-08	-0.3305	0.145	0.286	3.29E-04	1
Smad3	1.21E-08	0.3163	0.308	0.19	3.40E-04	1
Lcorl	1.23E-08	-0.3440	0.269	0.432	3.45E-04	1
Pde1c	1.24E-08	-0.3560	0.109	0.239	3.47E-04	1
Nrf1	1.32E-08	-0.2846	0.508	0.654	3.71E-04	1
Foxo1	1.33E-08	-0.3225	0.312	0.471	3.73E-04	1
Eogt	1.35E-08	-0.3058	0.046	0.152	3.79E-04	1
D930015E06Rik	1.38E-08	-0.2622	0.019	0.109	3.88E-04	1
Dtx1	1.70E-08	0.2899	0.339	0.218	4.76E-04	1
Pantr1	1.80E-08	-0.3746	0.24	0.375	5.04E-04	1
Adgrl2	2.08E-08	-0.3091	0.039	0.137	5.83E-04	1
Arhgef10	2.18E-08	0.2967	0.269	0.157	6.10E-04	1
Hrh1	2.32E-08	0.2722	0.358	0.233	6.50E-04	1
Id4	2.44E-08	-0.3268	0.09	0.209	6.82E-04	1
Tiam2	2.50E-08	0.2915	0.552	0.427	6.99E-04	1
Fchsd2	2.81E-08	-0.2843	0.513	0.65	7.85E-04	1
Trib2	3.19E-08	0.3238	0.288	0.182	8.94E-04	1
Cacna2d1	3.60E-08	-0.3270	0.092	0.212	1.01E-03	1
Fam168b	3.65E-08	-0.3129	0.211	0.355	1.02E-03	1
Bmper	3.73E-08	-0.3828	0.036	0.132	1.05E-03	1
B3galt2	3.78E-08	0.2948	0.278	0.17	1.06E-03	1

Ankrd28	3.85E-08	-0.3109	0.228	0.367	1.08E-03	1
Rasgrp1	4.24E-08	-0.3156	0.07	0.181	1.19E-03	1
Adgrv1	4.32E-08	-0.4740	0.031	0.122	1.21E-03	1
Acot11	4.40E-08	0.2925	0.446	0.329	1.23E-03	1
Tpk1	4.62E-08	-0.3892	0.148	0.275	1.29E-03	1
Ccnjl	5.20E-08	-0.2812	0.039	0.135	1.45E-03	1
Rasa2	5.24E-08	-0.3030	0.438	0.593	1.47E-03	1
Nav1	6.01E-08	-0.3169	0.053	0.154	1.68E-03	1
Sall2	6.99E-08	0.2532	0.327	0.212	1.96E-03	1
Vcan	7.21E-08	-0.2852	0.031	0.122	2.02E-03	1
Strn3	7.34E-08	-0.2662	0.6	0.715	2.06E-03	1
2810459M11Rik	8.19E-08	-0.3024	0.063	0.166	2.29E-03	1
Igsf21	8.20E-08	-0.2854	0.063	0.17	2.29E-03	1
Scara3	8.23E-08	-0.2547	0.034	0.125	2.30E-03	1
Grin2c	8.23E-08	-0.3995	0.276	0.407	2.31E-03	1
Slc15a2	9.04E-08	-0.2905	0.24	0.386	2.53E-03	1
Ccdc80	9.62E-08	-0.2812	0.073	0.181	2.69E-03	1
D030047H15Rik	9.67E-08	0.2726	0.504	0.383	2.71E-03	1
Astn1	1.02E-07	0.2524	0.712	0.651	2.87E-03	1
Nr2f2	1.10E-07	0.2726	0.189	0.099	3.08E-03	1
Adgrb1	1.13E-07	0.2687	0.421	0.31	3.17E-03	1
Id3	1.21E-07	-0.3015	0.116	0.238	3.39E-03	1
Smurf2	1.33E-07	-0.2699	0.271	0.417	3.72E-03	1
Kcnk2	1.40E-07	-0.3786	0.201	0.337	3.91E-03	1
Hivep3	1.49E-07	-0.3199	0.634	0.699	4.17E-03	1
4930545L23Rik	1.62E-07	0.2952	0.177	0.091	4.53E-03	1
Mfhas1	1.70E-07	0.2902	0.39	0.278	4.76E-03	1
Fbxw4	1.71E-07	0.2676	0.37	0.251	4.79E-03	1
N4bp2	1.75E-07	-0.2963	0.07	0.174	4.91E-03	1
Zbtb16	1.83E-07	0.4178	0.315	0.206	5.13E-03	1
Stox2	1.95E-07	-0.2596	0.598	0.731	5.47E-03	1
Sfmbt2	2.09E-07	-0.3035	0.053	0.149	5.86E-03	1
6430573F11Rik	2.25E-07	0.2848	0.303	0.201	6.31E-03	1
Cdc14a	2.26E-07	-0.2877	0.189	0.325	6.32E-03	1
Cox10	2.28E-07	-0.3146	0.169	0.296	6.38E-03	1
Mfap3l	2.28E-07	-0.3124	0.155	0.282	6.39E-03	1
Garnl3	2.31E-07	-0.3786	0.08	0.183	6.47E-03	1
Cntn4	2.69E-07	0.3161	0.235	0.139	7.53E-03	1
Zfp609	2.78E-07	-0.3060	0.383	0.521	7.77E-03	1
Fgfr1	2.88E-07	-0.3010	0.346	0.496	8.06E-03	1
Arhgap18	2.89E-07	-0.2940	0.068	0.169	8.11E-03	1
Cobll1	2.99E-07	-0.2505	0.024	0.104	8.37E-03	1
Igf2bp3	3.16E-07	-0.3524	0.16	0.283	8.84E-03	1

Synpo2	3.26E-07	-0.3126	0.041	0.129	9.13E-03	1
Plekhg1	3.31E-07	-0.2604	0.489	0.621	9.26E-03	1
Sorbs2os	3.50E-07	0.2679	0.218	0.127	9.79E-03	1
Psd2	3.62E-07	0.2921	0.484	0.382	0.0101	1
Intu	3.76E-07	-0.2657	0.056	0.15	0.0105	1
Ski	3.89E-07	-0.2717	0.153	0.279	0.0109	1
Tshz2	3.94E-07	0.3080	0.317	0.208	0.0110	1
Nr2e1	3.96E-07	-0.3287	0.114	0.221	0.0111	1
Elavl3	4.11E-07	-0.3063	0.085	0.188	0.0115	1
Epb41l4b	4.13E-07	-0.3109	0.048	0.138	0.0116	1
Syne2	4.31E-07	-0.2990	0.075	0.176	0.0121	1
Rasal2	4.71E-07	0.2514	0.574	0.469	0.0132	1
Ntng2	4.76E-07	0.2525	0.32	0.207	0.0133	1
E530001K10Rik	5.31E-07	-0.3292	0.063	0.157	0.0149	1
Trpc1	5.64E-07	-0.2609	0.08	0.182	0.0158	1
Sobp	6.23E-07	0.2780	0.443	0.33	0.0174	1
Sema5b	8.45E-07	-0.3374	0.077	0.173	0.0237	1
Atl2	8.77E-07	0.2633	0.482	0.392	0.0246	1
Car8	9.29E-07	-0.2607	0.036	0.117	0.0260	1
Erc1	1.00E-06	-0.2830	0.358	0.481	0.0280	1
Ccdc50	1.15E-06	-0.2810	0.308	0.443	0.0322	1
Rbms3	1.25E-06	-0.3506	0.172	0.287	0.0351	1
Crot	1.31E-06	-0.2859	0.145	0.259	0.0368	1
Itm2b	1.33E-06	-0.2938	0.303	0.435	0.0373	1
Mef2c	1.34E-06	-0.3523	0.223	0.346	0.0376	1
Mtss1	1.45E-06	-0.2699	0.097	0.2	0.0407	1
Slc38a1	1.66E-06	-0.3635	0.058	0.143	0.0465	1
Slc10a7	1.73E-06	0.2901	0.373	0.272	0.0485	1
Gng12	1.80E-06	-0.2973	0.397	0.515	0.0503	1
Mxi1	1.87E-06	-0.2823	0.363	0.488	0.0524	1
Sep11	1.90E-06	-0.2870	0.145	0.255	0.0531	1
Zfp950	1.94E-06	-0.2512	0.312	0.456	0.0543	1
Lrp8	2.00E-06	-0.2566	0.104	0.207	0.0559	1
Cd9	2.03E-06	-0.2837	0.123	0.232	0.0568	1
Ostm1	2.16E-06	-0.3271	0.191	0.304	0.0606	1
Clmn	2.30E-06	-0.3110	0.492	0.581	0.0643	1
Pbx3	2.55E-06	-0.3116	0.153	0.26	0.0715	1
Agbl4	2.58E-06	-0.3903	0.341	0.461	0.0721	1
Tox3	2.67E-06	-0.2861	0.053	0.137	0.0748	1
Fgf12	2.77E-06	-0.2692	0.162	0.278	0.0776	1
Gprc5b	2.93E-06	0.2652	0.392	0.302	0.0821	1
Cdh4	2.94E-06	-0.3362	0.092	0.184	0.0823	1
Fstl1	3.06E-06	0.2617	0.337	0.241	0.0856	1

Pacrg	3.44E-06	-0.3119	0.45	0.567	0.0963	1
Slc1a2	3.23E-109	-1.5973	0.867	0.977	9.05E-105	2
Prex2	1.05E-93	-1.2996	0.5	0.919	2.95E-89	2
Sgcd	1.21E-75	1.2906	0.72	0.268	3.39E-71	2
Plpp3	2.35E-74	-0.9659	0.711	0.939	6.58E-70	2
Msi2	4.11E-71	-0.6405	0.988	0.997	1.15E-66	2
Atp1a2	1.67E-70	-0.9166	0.699	0.919	4.66E-66	2
Lrp1b	3.31E-70	0.7765	0.985	0.726	9.28E-66	2
Frmd4a	1.98E-68	-0.9717	0.861	0.96	5.55E-64	2
Nrxn1	1.35E-65	-0.4206	1	0.998	3.78E-61	2
Kcnd2	1.55E-64	0.7681	0.982	0.677	4.34E-60	2
Ntm	1.41E-60	-0.5237	0.997	0.984	3.94E-56	2
Tspan7	3.72E-60	-1.1696	0.446	0.805	1.04E-55	2
Csmd3	5.34E-60	0.8566	0.795	0.388	1.50E-55	2
Rgs20	3.31E-54	-0.8205	0.753	0.923	9.25E-50	2
Ptprt	2.62E-52	-0.7273	0.795	0.942	7.32E-48	2
Nrxn3	1.39E-51	0.7032	0.967	0.799	3.90E-47	2
Gnao1	3.95E-49	-1.0102	0.566	0.798	1.11E-44	2
Erbb4	1.95E-48	0.6227	0.973	0.672	5.47E-44	2
Qk	2.64E-48	-0.5604	0.934	0.978	7.40E-44	2
Gm3764	5.24E-46	-0.6486	0.946	0.958	1.47E-41	2
B230323A14Rik	1.36E-45	0.7593	0.53	0.171	3.81E-41	2
Cpe	1.01E-44	-0.7151	0.831	0.943	2.82E-40	2
RP23-474J16.2	2.42E-43	0.8923	0.476	0.15	6.78E-39	2
Sfxn5	4.73E-43	-0.6000	0.813	0.935	1.32E-38	2
Grm3	9.48E-42	-0.8552	0.732	0.874	2.65E-37	2
Clmn	1.45E-41	-0.9659	0.226	0.624	4.07E-37	2
Gabrb1	1.54E-41	-0.5093	0.964	0.982	4.31E-37	2
Glul	8.18E-41	-1.0000	0.256	0.617	2.29E-36	2
Lsamp	1.08E-40	-0.3381	1	0.997	3.03E-36	2
Spata13	1.49E-40	0.5910	0.343	0.082	4.18E-36	2
Fgf14	1.67E-40	0.5076	0.985	0.927	4.68E-36	2
Nwd1	1.60E-39	-0.7635	0.352	0.714	4.49E-35	2
Mertk	3.31E-39	-0.8332	0.633	0.826	9.27E-35	2
Grin2c	9.29E-39	-1.0381	0.06	0.44	2.60E-34	2
Pde4d	9.85E-39	0.5521	0.919	0.73	2.76E-34	2
Wdr17	1.01E-38	-0.4763	0.982	0.986	2.84E-34	2
Ttyh1	4.81E-38	-0.6981	0.536	0.802	1.35E-33	2
Phkg1	3.69E-37	-0.7391	0.512	0.791	1.03E-32	2
Farp1	4.59E-37	-0.6282	0.771	0.904	1.28E-32	2
Cst3	6.41E-37	-0.7980	0.575	0.807	1.80E-32	2
Gpc6	1.31E-36	-0.7689	0.488	0.773	3.67E-32	2
Hivep3	3.05E-36	-0.7756	0.41	0.736	8.53E-32	2

Kcnq1ot1	1.06E-35	0.6863	0.633	0.298	2.98E-31	2
Ppp1r14c	2.54E-35	0.6310	0.518	0.2	7.10E-31	2
Grid2	1.15E-34	-0.5276	0.867	0.955	3.23E-30	2
Dtna	3.44E-34	-0.4444	0.97	0.981	9.63E-30	2
Mgat5	3.48E-34	-1.0134	0.283	0.601	9.74E-30	2
Pde8b	3.86E-34	-0.7494	0.334	0.674	1.08E-29	2
Auts2	5.44E-34	-0.4717	0.922	0.983	1.52E-29	2
Gria1	4.93E-33	0.3878	0.816	0.427	1.38E-28	2
Fars2	3.72E-32	-0.8201	0.59	0.791	1.04E-27	2
Cadm1	4.27E-32	-0.5539	0.877	0.938	1.20E-27	2
Bcan	6.07E-32	-0.6394	0.512	0.767	1.70E-27	2
Efr3b	2.14E-31	-0.7223	0.425	0.713	5.99E-27	2
Samd12	2.15E-31	0.7367	0.373	0.126	6.02E-27	2
Sparcl1	4.93E-31	-0.6872	0.747	0.832	1.38E-26	2
Adam23	1.12E-30	-0.9947	0.093	0.42	3.15E-26	2
Gm12239	1.70E-30	-1.0474	0.238	0.562	4.77E-26	2
Gfra1	2.15E-30	-0.9782	0.051	0.376	6.01E-26	2
Trim9	2.96E-30	-0.6226	0.642	0.819	8.28E-26	2
Daam2	4.85E-30	-0.7554	0.337	0.641	1.36E-25	2
Cspg5	5.05E-30	-0.7130	0.536	0.759	1.41E-25	2
Angpt1	1.89E-29	0.6456	0.328	0.102	5.30E-25	2
Slc7a11	1.94E-29	-0.9031	0.238	0.567	5.44E-25	2
Acsl3	2.21E-29	-0.6669	0.485	0.73	6.20E-25	2
Pde4b	3.44E-29	0.7040	0.828	0.605	9.64E-25	2
Polr2a	5.02E-29	0.6618	0.488	0.227	1.41E-24	2
Ephb1	5.22E-29	-1.0213	0.066	0.379	1.46E-24	2
Gm26843	1.03E-28	-0.9837	0.078	0.386	2.88E-24	2
Dclk1	1.50E-28	-0.6506	0.587	0.797	4.19E-24	2
Hotairm1	1.62E-28	0.3095	0.111	0.009	4.54E-24	2
Guf1	1.83E-28	0.5886	0.473	0.206	5.12E-24	2
Mical2	1.94E-27	-0.6926	0.31	0.611	5.44E-23	2
Rmst	2.24E-27	-0.8156	0.304	0.601	6.27E-23	2
Mpp6	2.28E-27	0.5584	0.729	0.421	6.38E-23	2
Prdm16	3.10E-27	-0.6419	0.47	0.733	8.67E-23	2
Slco1c1	3.64E-27	-0.7205	0.404	0.65	1.02E-22	2
Dab1	5.44E-27	-0.7032	0.455	0.708	1.52E-22	2
Spon1	7.68E-27	0.5243	0.738	0.468	2.15E-22	2
Ctnnd2	8.99E-27	-0.2828	0.994	0.992	2.52E-22	2
Sgip1	9.53E-27	-0.6312	0.404	0.689	2.67E-22	2
Ptprk	1.46E-26	0.5231	0.322	0.103	4.10E-22	2
F3	1.81E-26	-0.7147	0.283	0.573	5.07E-22	2
Htra1	2.47E-26	-0.6981	0.404	0.654	6.93E-22	2
Gm26704	3.12E-26	-0.6943	0.277	0.58	8.73E-22	2

Dfna5	3.99E-26	0.5446	0.696	0.392	1.12E-21	2
Pdzph1	5.45E-26	-0.8371	0.084	0.383	1.52E-21	2
Rimbp2	1.20E-25	0.3813	0.202	0.044	3.35E-21	2
Adcy8	3.48E-25	0.5407	0.425	0.171	9.73E-21	2
Oasl2	4.45E-25	0.4845	0.145	0.023	1.25E-20	2
Ptn	6.65E-25	-0.6431	0.59	0.759	1.86E-20	2
Mob3b	1.55E-24	0.5057	0.307	0.099	4.34E-20	2
B3galt1	1.78E-24	-0.4106	0.895	0.961	4.99E-20	2
Camk2d	1.89E-24	0.4411	0.858	0.645	5.29E-20	2
Nr2f2	2.66E-24	0.4850	0.28	0.087	7.45E-20	2
St6galnac5	3.08E-24	-1.0994	0.084	0.359	8.62E-20	2
Elmo1	3.09E-24	0.5117	0.247	0.071	8.66E-20	2
Smad3	3.59E-24	0.5433	0.419	0.176	1.01E-19	2
Gria2	7.24E-24	-0.5318	0.783	0.877	2.03E-19	2
Gabbr1	7.92E-24	-0.6222	0.328	0.61	2.22E-19	2
Fgf13	8.31E-24	-0.9198	0.133	0.414	2.33E-19	2
Ntrk2	1.49E-23	-0.4699	0.88	0.935	4.17E-19	2
Lypd6	2.92E-23	-0.7634	0.027	0.282	8.18E-19	2
Slc1a3	3.27E-23	-0.3770	0.964	0.978	9.16E-19	2
Camk2g	7.37E-23	-0.5841	0.569	0.758	2.06E-18	2
Kirrel3	9.38E-23	-0.5158	0.753	0.871	2.63E-18	2
Tpk1	1.13E-22	0.6182	0.449	0.216	3.16E-18	2
Gli3	1.20E-22	-0.4875	0.596	0.802	3.35E-18	2
Emx2os	1.45E-22	-0.7258	0.027	0.276	4.06E-18	2
Fam13c	1.74E-22	-0.7585	0.187	0.457	4.87E-18	2
Cped1	3.19E-22	0.5502	0.313	0.113	8.94E-18	2
Prdx6	4.36E-22	-0.5211	0.464	0.695	1.22E-17	2
Hdac8	5.73E-22	-0.4380	0.81	0.911	1.60E-17	2
Gpm6b	1.46E-21	-0.4195	0.916	0.956	4.08E-17	2
Igsf8	1.99E-21	-0.5978	0.331	0.574	5.58E-17	2
Negr1	2.22E-21	-0.3826	0.907	0.965	6.20E-17	2
Meis2	3.16E-21	-0.4966	0.62	0.802	8.86E-17	2
Srgap1	3.79E-21	0.4281	0.717	0.437	1.06E-16	2
Igf2bp3	4.04E-21	0.5484	0.452	0.226	1.13E-16	2
Mapk4	1.21E-20	-0.5096	0.5	0.721	3.38E-16	2
Fam184b	1.22E-20	-0.7303	0.018	0.242	3.42E-16	2
Kcnq1	1.73E-20	0.5367	0.404	0.186	4.85E-16	2
Tprkb	1.79E-20	-0.6678	0.334	0.579	5.02E-16	2
Gldc	1.97E-20	-0.6598	0.157	0.411	5.51E-16	2
Ddx60	2.83E-20	0.3911	0.181	0.045	7.93E-16	2
Mcc	3.85E-20	0.4569	0.843	0.675	1.08E-15	2
Gm4951	6.30E-20	0.3543	0.133	0.025	1.76E-15	2
Thsd7a	7.25E-20	0.5164	0.494	0.258	2.03E-15	2

Acss3	7.40E-20	0.4692	0.37	0.157	2.07E-15	2
Tra2a	1.04E-19	0.4599	0.843	0.669	2.91E-15	2
Skap2	1.12E-19	0.4496	0.584	0.338	3.12E-15	2
Csrnp3	1.30E-19	0.4490	0.289	0.105	3.63E-15	2
Ubash3b	1.55E-19	0.4918	0.422	0.2	4.35E-15	2
Abr	1.80E-19	-0.4052	0.729	0.846	5.04E-15	2
Dpyd	1.81E-19	0.4684	0.657	0.425	5.08E-15	2
Lgr6	2.08E-19	0.3585	0.166	0.039	5.84E-15	2
Tiam2	2.15E-19	0.4340	0.663	0.413	6.01E-15	2
Ldb2	2.28E-19	0.5778	0.491	0.255	6.40E-15	2
Cables1	3.85E-19	-0.7130	0.268	0.504	1.08E-14	2
Ctnna2	5.73E-19	-0.5198	0.702	0.839	1.60E-14	2
Unc13c	6.17E-19	-0.8564	0.084	0.319	1.73E-14	2
Garem	8.77E-19	-0.6173	0.277	0.522	2.46E-14	2
Sfmbt2	1.09E-18	0.3969	0.28	0.104	3.05E-14	2
D030047H15Rik	1.15E-18	-0.5566	0.19	0.444	3.23E-14	2
Slc25a13	1.19E-18	0.3540	0.154	0.036	3.32E-14	2
Lix1	1.22E-18	-0.5931	0.253	0.501	3.42E-14	2
Pcdh9	1.36E-18	0.2583	1	0.992	3.81E-14	2
Rcan2	1.46E-18	-0.7459	0.087	0.321	4.08E-14	2
Rxrg	1.46E-18	0.2973	0.111	0.019	4.09E-14	2
Phka1	2.02E-18	-0.5736	0.485	0.678	5.66E-14	2
Wnk2	2.18E-18	-0.6310	0.377	0.581	6.11E-14	2
Rorb	3.33E-18	-0.4283	0.88	0.919	9.32E-14	2
Ngef	4.33E-18	-0.5706	0.114	0.356	1.21E-13	2
Zcchc16	7.01E-18	0.5572	0.229	0.077	1.96E-13	2
Pbx1	8.74E-18	-0.2952	0.964	0.987	2.45E-13	2
Ogt	1.06E-17	0.3736	0.852	0.727	2.96E-13	2
Gm26719	1.10E-17	0.3416	0.142	0.032	3.09E-13	2
Mllt3	1.42E-17	0.4222	0.63	0.394	3.99E-13	2
Rapgef4	1.74E-17	0.4173	0.22	0.073	4.87E-13	2
Hes5	1.83E-17	-0.6773	0.205	0.437	5.12E-13	2
Gm15345	1.93E-17	0.3643	0.157	0.04	5.40E-13	2
Prtg	2.47E-17	0.4101	0.268	0.1	6.91E-13	2
Chuk	2.54E-17	0.3943	0.488	0.254	7.12E-13	2
S1pr1	2.98E-17	-0.5290	0.172	0.416	8.33E-13	2
Kcnn2	3.63E-17	-0.6043	0.331	0.552	1.02E-12	2
Chl1	3.81E-17	0.5272	0.292	0.123	1.07E-12	2
Zeb1	4.14E-17	-0.3813	0.789	0.876	1.16E-12	2
Cdk6	5.08E-17	0.3120	0.127	0.026	1.42E-12	2
4930448N21Rik	5.34E-17	-0.5155	0.434	0.642	1.50E-12	2
Lrrn1	6.37E-17	0.3537	0.193	0.058	1.78E-12	2
Clic6	6.37E-17	0.3605	0.169	0.046	1.78E-12	2

Mid1	7.07E-17	-0.6324	0.145	0.372	1.98E-12	2
Slc22a4	1.12E-16	0.4090	0.322	0.141	3.15E-12	2
Adrbk2	1.38E-16	-0.4478	0.593	0.765	3.87E-12	2
Ubn2	1.45E-16	0.3594	0.843	0.685	4.07E-12	2
Tnfrsf19	1.48E-16	-0.6602	0.202	0.429	4.14E-12	2
Slc4a4	1.49E-16	-0.4617	0.961	0.926	4.16E-12	2
Ndrg2	1.53E-16	-0.5273	0.404	0.615	4.29E-12	2
Arsj	1.75E-16	0.2724	0.123	0.026	4.91E-12	2
Cacna1a	3.46E-16	0.4768	0.443	0.239	9.69E-12	2
Aff3	3.61E-16	0.5124	0.419	0.224	1.01E-11	2
Nebl	3.66E-16	-0.5321	0.581	0.727	1.03E-11	2
Csrp1	4.42E-16	-0.5045	0.377	0.595	1.24E-11	2
Hs6st3	5.10E-16	0.5702	0.286	0.123	1.43E-11	2
Dab2	5.26E-16	0.4541	0.313	0.137	1.47E-11	2
Irak2	6.01E-16	-0.6166	0.241	0.459	1.68E-11	2
Cp	7.55E-16	0.3048	0.127	0.029	2.11E-11	2
4930544l03Rik	1.07E-15	-0.6156	0.039	0.23	2.99E-11	2
Tmem117	1.19E-15	0.3750	0.419	0.209	3.33E-11	2
Ddx5	1.64E-15	0.3548	0.922	0.848	4.59E-11	2
Prcp	1.67E-15	0.3115	0.172	0.051	4.67E-11	2
Rgcc	1.86E-15	-0.5276	0.087	0.295	5.21E-11	2
Fam171b	2.02E-15	-0.5244	0.19	0.413	5.65E-11	2
Cyp4f15	2.38E-15	-0.5041	0.06	0.254	6.66E-11	2
Adcy2	3.86E-15	-0.4325	0.587	0.744	1.08E-10	2
Ntsr2	5.89E-15	-0.4594	0.377	0.589	1.65E-10	2
Lgi4	6.44E-15	-0.5337	0.102	0.304	1.80E-10	2
Gm26512	6.49E-15	-0.4829	0.018	0.192	1.82E-10	2
Dock10	6.94E-15	0.6515	0.19	0.064	1.94E-10	2
Etnppl	8.47E-15	-0.7828	0.069	0.258	2.37E-10	2
Brinp3	1.18E-14	0.4398	0.783	0.578	3.29E-10	2
Luzp2	1.40E-14	-0.5739	0.87	0.891	3.92E-10	2
Rnf38	1.42E-14	0.3901	0.458	0.261	3.96E-10	2
Dennd1a	1.50E-14	-0.3645	0.744	0.864	4.20E-10	2
Rapgef3	1.63E-14	-0.5073	0.262	0.475	4.57E-10	2
Metap1d	1.74E-14	0.4056	0.53	0.327	4.88E-10	2
Plce1	1.81E-14	0.3367	0.753	0.553	5.06E-10	2
Aspa	1.87E-14	0.4511	0.25	0.102	5.22E-10	2
Aifm3	2.06E-14	-0.4767	0.157	0.372	5.78E-10	2
Ncan	2.21E-14	-0.4805	0.12	0.329	6.19E-10	2
Lama3	2.30E-14	-0.5801	0.009	0.17	6.44E-10	2
Mgll	2.34E-14	-0.5032	0.482	0.648	6.55E-10	2
Coro2b	2.72E-14	-0.4593	0.151	0.361	7.61E-10	2
Lrrc7	2.81E-14	0.4203	0.491	0.287	7.87E-10	2

March3	3.24E-14	0.4770	0.446	0.256	9.06E-10	2
Phactr1	3.76E-14	-0.4155	0.5	0.678	1.05E-09	2
Nt5c2	3.97E-14	-0.4326	0.298	0.515	1.11E-09	2
Sat1	4.51E-14	-0.5036	0.202	0.411	1.26E-09	2
Rgs6	4.58E-14	-0.3962	0.699	0.828	1.28E-09	2
Kalrn	5.97E-14	-0.3893	0.533	0.702	1.67E-09	2
Rgs7	7.38E-14	-0.4955	0.63	0.746	2.07E-09	2
Mmd2	8.67E-14	-0.3685	0.551	0.728	2.43E-09	2
Hapln1	8.68E-14	-0.4512	0.036	0.207	2.43E-09	2
Caskin1	1.05E-13	-0.4639	0.241	0.459	2.94E-09	2
Arhgef10l	1.07E-13	-0.4882	0.292	0.494	2.99E-09	2
Clic4	1.16E-13	0.4215	0.443	0.255	3.26E-09	2
Lamp2	1.36E-13	0.3880	0.596	0.416	3.80E-09	2
Swap70	1.71E-13	-0.5034	0.084	0.269	4.80E-09	2
1700112E06Rik	1.89E-13	0.4479	0.563	0.351	5.28E-09	2
Fam20a	2.31E-13	-0.4610	0.337	0.545	6.47E-09	2
Crym	2.36E-13	-0.7255	0.015	0.169	6.61E-09	2
Gm4876	2.39E-13	0.4053	0.37	0.197	6.69E-09	2
Slit2	2.45E-13	0.3796	0.334	0.162	6.86E-09	2
Heg1	3.17E-13	0.3383	0.298	0.136	8.88E-09	2
4930578G10Rik	3.67E-13	-0.4953	0.018	0.173	1.03E-08	2
Itpkb	3.79E-13	0.3056	0.521	0.31	1.06E-08	2
Stx6	4.67E-13	0.3892	0.334	0.17	1.31E-08	2
9530026P05Rik	4.70E-13	0.3630	0.518	0.314	1.31E-08	2
Plag1	4.78E-13	0.2778	0.12	0.031	1.34E-08	2
Col4a5	5.36E-13	0.3973	0.334	0.169	1.50E-08	2
Ccdc58	5.99E-13	0.4406	0.494	0.308	1.68E-08	2
Slc20a2	6.00E-13	0.4072	0.392	0.216	1.68E-08	2
Glud1	6.17E-13	-0.3591	0.657	0.786	1.73E-08	2
Igsf21	7.67E-13	-0.4660	0.021	0.172	2.15E-08	2
Sobp	7.72E-13	0.3703	0.527	0.32	2.16E-08	2
Phactr3	8.82E-13	-0.3867	0.533	0.707	2.47E-08	2
Gm21954	8.83E-13	-0.4668	0.09	0.27	2.47E-08	2
Eda	1.63E-12	-0.6057	0.22	0.412	4.56E-08	2
L3mbtl3	1.72E-12	0.4410	0.563	0.392	4.83E-08	2
Mtss1l	1.78E-12	-0.4395	0.373	0.562	4.99E-08	2
Fjx1	2.22E-12	-0.5267	0.108	0.284	6.22E-08	2
Fnbp1	2.67E-12	-0.3021	0.792	0.886	7.48E-08	2
Reln	2.71E-12	0.3569	0.184	0.068	7.58E-08	2
Gja1	3.05E-12	-0.4008	0.401	0.595	8.54E-08	2
Sik3	3.05E-12	-0.3632	0.828	0.876	8.54E-08	2
Rev3l	3.24E-12	0.3318	0.705	0.523	9.07E-08	2
Celrr	3.63E-12	-0.4522	0.211	0.402	1.02E-07	2

Pnpla7	3.83E-12	-0.4404	0.355	0.536	1.07E-07	2
Prdm11	4.30E-12	0.3278	0.238	0.102	1.20E-07	2
Gm14964	4.31E-12	-0.4003	0.316	0.517	1.21E-07	2
9430041J12Rik	4.34E-12	-0.4291	0.229	0.445	1.22E-07	2
Kank1	4.38E-12	0.3268	0.714	0.537	1.23E-07	2
Gtf2ird1	4.78E-12	0.3379	0.485	0.3	1.34E-07	2
Adamts12	5.14E-12	0.3523	0.13	0.039	1.44E-07	2
Cul5	5.36E-12	0.3628	0.533	0.339	1.50E-07	2
Sntg2	5.62E-12	0.2927	0.136	0.041	1.57E-07	2
Enox1	6.09E-12	-0.4320	0.16	0.362	1.70E-07	2
Ncam2	6.12E-12	0.3321	0.867	0.728	1.71E-07	2
Dpp6	6.13E-12	0.3583	0.416	0.235	1.72E-07	2
Gm21798	6.69E-12	0.3893	0.214	0.088	1.87E-07	2
Ttll8	8.07E-12	-0.4652	0.075	0.241	2.26E-07	2
Hmgn3	8.72E-12	-0.4298	0.205	0.39	2.44E-07	2
Sptbn1	1.29E-11	-0.3800	0.575	0.698	3.61E-07	2
Arhgef4	1.29E-11	-0.4227	0.509	0.652	3.61E-07	2
Tenm3	1.35E-11	-0.3413	0.614	0.749	3.78E-07	2
Kcnk10	1.64E-11	-0.4347	0.024	0.164	4.59E-07	2
Nbea	1.72E-11	0.3347	0.732	0.578	4.81E-07	2
Pld1	2.09E-11	0.3470	0.34	0.186	5.85E-07	2
Cux2	2.20E-11	0.3225	0.271	0.128	6.16E-07	2
Vit	2.32E-11	0.3567	0.31	0.155	6.49E-07	2
Parp8	2.35E-11	0.3725	0.509	0.336	6.57E-07	2
A930015D03Rik	2.42E-11	0.3365	0.398	0.228	6.77E-07	2
Pigk	2.55E-11	-0.6176	0.184	0.358	7.13E-07	2
Tcf12	2.59E-11	0.2856	0.834	0.726	7.25E-07	2
Hist2h2bb	3.15E-11	0.2640	0.108	0.03	8.82E-07	2
Adk	3.18E-11	-0.3537	0.614	0.754	8.89E-07	2
Smyd3	3.28E-11	0.3299	0.614	0.429	9.17E-07	2
Gm2115	4.13E-11	-0.4893	0.069	0.222	1.16E-06	2
Ccnl2	4.33E-11	0.2786	0.762	0.598	1.21E-06	2
A330093E20Rik	4.41E-11	-0.4785	0.042	0.19	1.23E-06	2
Ankrd29	4.52E-11	-0.4121	0.048	0.196	1.26E-06	2
Lyrm4	4.75E-11	-0.4983	0.416	0.56	1.33E-06	2
Naaladl2	4.87E-11	0.3746	0.672	0.517	1.36E-06	2
Dapp1	4.99E-11	-0.4354	0.051	0.201	1.40E-06	2
Cmtm5	5.68E-11	-0.4057	0.09	0.253	1.59E-06	2
Ahcyl1	5.81E-11	-0.3805	0.431	0.604	1.63E-06	2
Pantr1	6.09E-11	-0.4527	0.202	0.376	1.71E-06	2
Rapgef6	6.79E-11	0.3848	0.494	0.325	1.90E-06	2
Gm2163	6.82E-11	-0.4815	0.063	0.211	1.91E-06	2
Hlf	6.95E-11	-0.4809	0.259	0.435	1.94E-06	2

Runx1t1	7.13E-11	0.4487	0.419	0.251	1.99E-06	2
Cpd	7.38E-11	0.3099	0.355	0.192	2.07E-06	2
Marcks	9.10E-11	0.3362	0.256	0.122	2.55E-06	2
Fam107a	9.59E-11	-0.4207	0.105	0.268	2.68E-06	2
Setbp1	1.15E-10	-0.3841	0.482	0.645	3.23E-06	2
Tmem108	1.18E-10	0.2722	0.123	0.039	3.32E-06	2
Hif3a	1.20E-10	-0.4557	0.16	0.335	3.35E-06	2
Gm9925	1.44E-10	-0.4294	0.142	0.312	4.04E-06	2
Mfap3l	1.60E-10	-0.4253	0.12	0.282	4.47E-06	2
Npat	1.61E-10	0.3314	0.271	0.137	4.52E-06	2
Ptprd	1.62E-10	0.3225	0.828	0.772	4.54E-06	2
Papss2	1.69E-10	-0.4551	0.075	0.223	4.74E-06	2
Ttyh3	1.76E-10	-0.3738	0.238	0.419	4.92E-06	2
Paqr8	1.89E-10	-0.3873	0.461	0.62	5.30E-06	2
Nalcn	2.04E-10	0.3768	0.262	0.133	5.71E-06	2
Arrb1	2.07E-10	-0.3907	0.256	0.435	5.79E-06	2
Aox1	2.07E-10	-0.4014	0.072	0.223	5.79E-06	2
Gas7	2.11E-10	0.2956	0.16	0.06	5.90E-06	2
Parvb	2.17E-10	0.3173	0.325	0.176	6.06E-06	2
Elk3	2.25E-10	0.2740	0.154	0.057	6.30E-06	2
Tef	2.27E-10	-0.3826	0.259	0.439	6.34E-06	2
Antxr1	2.30E-10	0.3517	0.479	0.309	6.45E-06	2
Stat1	2.59E-10	0.4123	0.199	0.086	7.24E-06	2
Col11a2	3.33E-10	-0.3352	0.015	0.136	9.32E-06	2
Prodh	3.89E-10	-0.4224	0.187	0.352	1.09E-05	2
Ptprj	4.26E-10	0.3328	0.38	0.221	1.19E-05	2
Gm26699	4.82E-10	0.3155	0.488	0.323	1.35E-05	2
Nim1k	4.88E-10	-0.4065	0.434	0.585	1.37E-05	2
Arhgap5	5.00E-10	-0.3036	0.672	0.796	1.40E-05	2
Kansl1	5.20E-10	0.2534	0.864	0.76	1.46E-05	2
Tmtc2	5.42E-10	0.2676	0.834	0.736	1.52E-05	2
Sep4	5.95E-10	0.3104	0.166	0.066	1.66E-05	2
Adora1	6.87E-10	0.2676	0.169	0.067	1.92E-05	2
D030068K23Rik	7.12E-10	0.2532	0.145	0.053	1.99E-05	2
Cobll1	7.19E-10	0.2843	0.178	0.073	2.01E-05	2
Afap1l2	7.26E-10	0.2687	0.25	0.121	2.03E-05	2
Mpped2	7.35E-10	-0.4370	0.13	0.289	2.06E-05	2
Pcsk6	7.65E-10	-0.4394	0.072	0.215	2.14E-05	2
Gpm6a	7.93E-10	-0.3094	0.711	0.805	2.22E-05	2
Gm13872	8.01E-10	-0.3733	0.045	0.176	2.24E-05	2
Ptk2	8.61E-10	0.2565	0.813	0.71	2.41E-05	2
Aig1	9.86E-10	0.3346	0.473	0.304	2.76E-05	2
Galnt10	1.02E-09	0.2702	0.208	0.094	2.86E-05	2

Cntfr	1.04E-09	-0.3834	0.229	0.391	2.91E-05	2
Uty	1.04E-09	0.3078	0.572	0.408	2.91E-05	2
Luzp1	1.14E-09	0.3547	0.566	0.4	3.20E-05	2
Cbx4	1.19E-09	0.2740	0.214	0.099	3.32E-05	2
C030018K13Rik	1.25E-09	-0.2720	0	0.102	3.51E-05	2
Gm44151	1.29E-09	-0.4323	0.199	0.357	3.61E-05	2
St3gal4	1.46E-09	-0.3866	0.431	0.598	4.09E-05	2
Cdh22	1.51E-09	0.3206	0.22	0.103	4.22E-05	2
Mboat2	1.57E-09	0.2848	0.711	0.553	4.40E-05	2
Crebzf	1.59E-09	0.3090	0.491	0.341	4.45E-05	2
Slc25a21	1.60E-09	0.3510	0.428	0.268	4.48E-05	2
Fam189a2	1.67E-09	0.2664	0.313	0.167	4.67E-05	2
Dtx4	1.86E-09	0.2632	0.169	0.07	5.22E-05	2
Sbf2	1.94E-09	0.3335	0.623	0.483	5.44E-05	2
Ankrd6	2.00E-09	-0.4303	0.232	0.394	5.60E-05	2
Alk	2.24E-09	-0.5120	0.048	0.176	6.27E-05	2
Atp9a	2.33E-09	0.2932	0.22	0.105	6.52E-05	2
Gcnt4	2.38E-09	-0.3296	0.015	0.126	6.68E-05	2
Eps15	2.39E-09	-0.3060	0.608	0.726	6.69E-05	2
Btbd1	2.48E-09	0.2845	0.515	0.342	6.94E-05	2
Syn2	2.48E-09	0.3002	0.536	0.374	6.95E-05	2
Prkag2	2.68E-09	0.3181	0.298	0.165	7.51E-05	2
Lhx2	2.82E-09	-0.3346	0.006	0.108	7.89E-05	2
Cstf3	2.93E-09	0.2816	0.605	0.434	8.20E-05	2
Pitpnc1	3.03E-09	-0.3341	0.955	0.95	8.48E-05	2
Sncaip	3.05E-09	0.3178	0.407	0.252	8.53E-05	2
Aldoc	3.20E-09	-0.3850	0.133	0.28	8.95E-05	2
Nhsl1	3.30E-09	-0.3635	0.819	0.811	9.25E-05	2
Crlf3	3.32E-09	-0.3428	0.352	0.524	9.30E-05	2
Lair1	3.54E-09	-0.3372	0.03	0.15	9.90E-05	2
Rbm20	3.54E-09	0.3155	0.238	0.119	9.91E-05	2
2210408I21Rik	3.59E-09	0.2841	0.56	0.383	1.00E-04	2
Vkorc1l1	3.73E-09	0.2884	0.301	0.165	1.05E-04	2
Tcea1	4.16E-09	0.2753	0.241	0.119	1.16E-04	2
Plscr4	4.21E-09	0.3463	0.322	0.184	1.18E-04	2
Mfge8	4.33E-09	-0.3922	0.169	0.322	1.21E-04	2
Rapgef2	4.33E-09	0.3317	0.548	0.387	1.21E-04	2
Arhgef19	4.45E-09	-0.3621	0.19	0.346	1.24E-04	2
Sema4a	4.67E-09	-0.3194	0.114	0.265	1.31E-04	2
Dkk3	4.82E-09	-0.4064	0.175	0.335	1.35E-04	2
Nsmf	4.91E-09	-0.3803	0.133	0.275	1.37E-04	2
Id3	4.99E-09	-0.4249	0.096	0.236	1.40E-04	2
Agbl4	5.17E-09	0.3026	0.578	0.413	1.45E-04	2

Ccdc148	5.34E-09	0.2943	0.301	0.167	1.49E-04	2
Cab39l	5.50E-09	0.2704	0.235	0.115	1.54E-04	2
Bcl6	5.74E-09	-0.3655	0.148	0.302	1.61E-04	2
Tspan5	6.58E-09	0.3066	0.726	0.591	1.84E-04	2
Rmdn1	6.62E-09	0.2927	0.605	0.452	1.85E-04	2
Clock	7.31E-09	0.2821	0.398	0.245	2.05E-04	2
Dio2	7.75E-09	-0.3226	0.012	0.115	2.17E-04	2
Atrn	8.56E-09	0.2970	0.506	0.356	2.40E-04	2
Tmem56	8.57E-09	-0.3137	0.069	0.201	2.40E-04	2
Slc30a9	9.47E-09	0.2910	0.355	0.214	2.65E-04	2
Acss1	1.01E-08	-0.3391	0.536	0.658	2.83E-04	2
Abhd3	1.09E-08	-0.3586	0.211	0.369	3.05E-04	2
Fam120c	1.09E-08	0.2952	0.536	0.371	3.06E-04	2
Gm6277	1.12E-08	-0.4184	0.066	0.195	3.14E-04	2
Ccdc60	1.16E-08	0.3066	0.136	0.053	3.26E-04	2
Sec22a	1.24E-08	0.2777	0.25	0.131	3.48E-04	2
Il1rapl1	1.26E-08	0.2585	0.913	0.826	3.54E-04	2
Gabrg3	1.27E-08	-0.4526	0.241	0.399	3.55E-04	2
Bptf	1.34E-08	0.3071	0.651	0.498	3.75E-04	2
Lama2	1.50E-08	-0.2719	0.654	0.773	4.20E-04	2
Fbxw4	1.64E-08	0.2711	0.404	0.251	4.58E-04	2
Map7	1.69E-08	0.3743	0.265	0.148	4.74E-04	2
Adra1a	1.84E-08	-0.3503	0.108	0.248	5.16E-04	2
Grik4	1.99E-08	0.3185	0.289	0.164	5.58E-04	2
Tlcd1	2.02E-08	-0.3363	0.048	0.165	5.66E-04	2
Rasa2	2.15E-08	-0.3360	0.446	0.585	6.03E-04	2
Nmur2	2.19E-08	-0.4032	0.063	0.186	6.13E-04	2
Sycp2	2.21E-08	-0.3353	0.211	0.363	6.17E-04	2
Fads1	2.31E-08	-0.3531	0.13	0.267	6.47E-04	2
Il18	2.45E-08	-0.3303	0.105	0.246	6.86E-04	2
Cdh20	2.47E-08	0.2773	0.786	0.676	6.91E-04	2
Dcc	2.49E-08	-0.7979	0.304	0.432	6.98E-04	2
Lef1	2.52E-08	-0.3145	0.009	0.104	7.06E-04	2
Traf3ip2	2.53E-08	0.2900	0.377	0.233	7.08E-04	2
Atrnl1	2.69E-08	0.3135	0.416	0.273	7.52E-04	2
Prpf4b	2.87E-08	0.2874	0.678	0.552	8.03E-04	2
Zcchc8	3.02E-08	0.2875	0.325	0.196	8.45E-04	2
Bahcc1	3.16E-08	0.2945	0.232	0.12	8.84E-04	2
2900052N01Rik	3.18E-08	-0.3481	0.045	0.161	8.90E-04	2
Gm13111	3.32E-08	-0.3008	0.036	0.146	9.30E-04	2
Ncald	3.54E-08	0.3030	0.232	0.12	9.90E-04	2
Stam2	3.55E-08	0.3091	0.286	0.165	9.94E-04	2
Ntrk3	3.78E-08	0.2655	0.59	0.436	1.06E-03	2

Mt1	4.09E-08	-0.3469	0.175	0.324	1.15E-03	2
Apbb2	4.14E-08	0.2811	0.566	0.422	1.16E-03	2
Nme7	4.26E-08	-0.3413	0.202	0.358	1.19E-03	2
Igfbp5	4.61E-08	-0.3727	0.024	0.126	1.29E-03	2
Slc30a10	4.72E-08	-0.3611	0.093	0.22	1.32E-03	2
Gigyf2	4.73E-08	0.2856	0.566	0.426	1.33E-03	2
Magi3	4.91E-08	-0.4170	0.277	0.425	1.37E-03	2
Frs2	4.91E-08	0.2666	0.44	0.29	1.38E-03	2
C530008M17Rik	5.11E-08	0.3116	0.37	0.23	1.43E-03	2
Smim3	5.14E-08	-0.3016	0.024	0.126	1.44E-03	2
6430573F11Rik	5.67E-08	0.2753	0.334	0.199	1.59E-03	2
Ano6	5.95E-08	0.2972	0.325	0.196	1.67E-03	2
Fzd2	6.02E-08	-0.2872	0.057	0.176	1.69E-03	2
Fgfr3	6.21E-08	-0.3050	0.473	0.606	1.74E-03	2
App	8.06E-08	0.3058	0.488	0.349	2.26E-03	2
Myrip	8.19E-08	-0.3461	0.193	0.341	2.29E-03	2
Adamts6	8.38E-08	0.3087	0.38	0.245	2.35E-03	2
Kcnk2	8.47E-08	-0.4495	0.193	0.333	2.37E-03	2
9330159F19Rik	8.88E-08	-0.3100	0.389	0.541	2.49E-03	2
Cxcl14	9.10E-08	-0.2899	0.051	0.166	2.55E-03	2
Pamr1	9.83E-08	-0.3027	0.018	0.112	2.75E-03	2
Rnf121	1.06E-07	-0.4752	0.37	0.478	2.96E-03	2
Clu	1.07E-07	-0.3561	0.364	0.5	2.98E-03	2
Mpped1	1.14E-07	-0.2747	0.021	0.117	3.19E-03	2
Ppp1r12a	1.17E-07	0.2538	0.669	0.53	3.26E-03	2
Ppm1h	1.19E-07	0.3355	0.271	0.155	3.34E-03	2
Add3	1.22E-07	-0.2809	0.449	0.595	3.42E-03	2
Pacrg	1.25E-07	-0.3318	0.416	0.568	3.50E-03	2
Uggt2	1.26E-07	0.2795	0.304	0.184	3.52E-03	2
Add1	1.33E-07	-0.2849	0.334	0.478	3.73E-03	2
Ascc3	1.36E-07	0.2617	0.47	0.318	3.80E-03	2
Susd6	1.39E-07	0.2719	0.44	0.298	3.89E-03	2
Rhoj	1.39E-07	0.2781	0.16	0.073	3.89E-03	2
Gm43477	1.39E-07	-0.3020	0.057	0.172	3.90E-03	2
Epha4	1.54E-07	-0.3660	0.096	0.219	4.30E-03	2
Sh3gl2	1.58E-07	0.2731	0.214	0.109	4.42E-03	2
Klhl23	1.62E-07	0.2628	0.127	0.051	4.55E-03	2
Cdh13	1.71E-07	0.3003	0.262	0.146	4.79E-03	2
Micalcl	1.80E-07	-0.3072	0.03	0.127	5.03E-03	2
Sirpa	1.85E-07	-0.3223	0.214	0.358	5.17E-03	2
Gm12394	1.93E-07	-0.2986	0.018	0.108	5.41E-03	2
Pcx	2.10E-07	0.2931	0.488	0.345	5.89E-03	2
Foxp1	2.33E-07	0.2964	0.605	0.466	6.52E-03	2

Atp2c1	2.41E-07	0.2713	0.554	0.431	6.76E-03	2
Adhfe1	2.50E-07	-0.3260	0.256	0.394	7.01E-03	2
Otx2os1	2.51E-07	0.2912	0.111	0.043	7.03E-03	2
Tada2a	2.64E-07	0.2545	0.286	0.166	7.38E-03	2
St6galnac3	2.69E-07	0.4644	0.136	0.059	7.53E-03	2
Npas2	2.69E-07	-0.3621	0.274	0.41	7.54E-03	2
Pak1	2.84E-07	-0.3671	0.133	0.258	7.94E-03	2
Bmper	2.87E-07	-0.4202	0.033	0.128	8.03E-03	2
Sh3pxd2b	3.07E-07	-0.3353	0.295	0.433	8.59E-03	2
Scel	3.13E-07	-0.3961	0.024	0.115	8.75E-03	2
A830019P07Rik	3.15E-07	-0.3228	0.087	0.205	8.83E-03	2
Scg3	3.22E-07	-0.3161	0.343	0.475	9.03E-03	2
Rnf213	3.40E-07	0.3563	0.292	0.174	9.53E-03	2
Id4	3.41E-07	-0.3390	0.087	0.204	9.54E-03	2
Epn2	3.49E-07	0.2599	0.44	0.305	9.78E-03	2
Zfhx4	3.52E-07	0.2609	0.479	0.328	9.84E-03	2
Sulf1	3.54E-07	0.2688	0.145	0.064	9.91E-03	2
Asrgl1	3.57E-07	-0.2837	0.41	0.544	9.98E-03	2
Grip1	3.59E-07	-0.4303	0.286	0.416	0.0100	2
Nlk	3.86E-07	0.3000	0.548	0.419	0.0108	2
Cbs	4.20E-07	-0.2904	0.193	0.331	0.0118	2
Btaf1	4.46E-07	0.2889	0.506	0.365	0.0125	2
Sorbs2	4.66E-07	0.2626	0.373	0.241	0.0131	2
Plekhg1	4.86E-07	-0.2828	0.479	0.617	0.0136	2
C130071C03Rik	5.36E-07	-0.2561	0.666	0.758	0.0150	2
Inf2	5.38E-07	-0.3197	0.084	0.193	0.0151	2
1110004F10Rik	5.58E-07	0.2980	0.325	0.208	0.0156	2
Csdc2	5.60E-07	-0.3039	0.117	0.244	0.0157	2
Magi1	5.87E-07	0.2536	0.741	0.645	0.0164	2
Rasal2	5.88E-07	0.2582	0.596	0.47	0.0165	2
Agap1	6.11E-07	0.2763	0.473	0.349	0.0171	2
Eva1a	6.49E-07	-0.3251	0.205	0.336	0.0182	2
Abtb2	6.69E-07	0.2786	0.446	0.319	0.0187	2
Anapc1	6.79E-07	0.2576	0.307	0.192	0.0190	2
Ckb	6.92E-07	-0.2512	0.548	0.661	0.0194	2
Immp1l	9.16E-07	0.2690	0.5	0.364	0.0256	2
Gli2	9.31E-07	-0.2966	0.458	0.571	0.0261	2
Btbd17	9.58E-07	-0.2710	0.072	0.18	0.0268	2
Shc3	9.66E-07	-0.2974	0.325	0.474	0.0270	2
Cpeb3	1.01E-06	0.3034	0.714	0.629	0.0282	2
Dnm1l	1.02E-06	0.2558	0.437	0.305	0.0286	2
Sned1	1.04E-06	-0.2928	0.114	0.231	0.0292	2
Myh14	1.09E-06	-0.2687	0.193	0.326	0.0305	2

Dzip1l	1.12E-06	-0.2845	0.157	0.29	0.0314	2
Shisa4	1.17E-06	-0.3101	0.166	0.289	0.0328	2
Egfem1	1.20E-06	-0.4162	0.096	0.207	0.0335	2
Ptchd4	1.28E-06	-0.3864	0.072	0.179	0.0358	2
Dennd5a	1.50E-06	0.2936	0.503	0.377	0.0420	2
Tshz2	1.51E-06	0.3170	0.331	0.21	0.0422	2
Camk2n1	1.59E-06	-0.3222	0.117	0.226	0.0446	2
Galnt18	1.60E-06	-0.4472	0.244	0.362	0.0448	2
Slc38a3	1.60E-06	-0.2850	0.166	0.291	0.0449	2
Tbcd	1.69E-06	0.2846	0.298	0.189	0.0475	2
Efna5	1.73E-06	-0.4461	0.105	0.217	0.0485	2
Gpam	1.79E-06	-0.3200	0.289	0.409	0.0500	2
Pou6f1	2.00E-06	0.2770	0.367	0.251	0.0559	2
Ccnd3	2.17E-06	-0.3510	0.247	0.375	0.0608	2
Glis3	2.20E-06	-0.2583	0.702	0.773	0.0616	2
Cep164	2.26E-06	0.2583	0.283	0.179	0.0632	2
Coq3	2.36E-06	0.2547	0.244	0.145	0.0660	2
Rasgrp1	2.45E-06	-0.2662	0.072	0.176	0.0687	2
Serbp1	2.52E-06	0.2599	0.37	0.252	0.0705	2
Colec12	2.73E-06	0.3388	0.184	0.098	0.0764	2
Rnf220	3.02E-06	0.4348	0.199	0.112	0.0846	2
Adamts9	3.18E-06	-0.3363	0.205	0.334	0.0891	2
Bhlhe40	3.31E-06	-0.2673	0.048	0.138	0.0927	2
Fbxo11	3.35E-06	0.2623	0.521	0.408	0.0937	2
Ccdc77	3.36E-06	0.2669	0.274	0.171	0.0941	2
Ror1	3.39E-06	0.2636	0.148	0.072	0.0948	2
Slc4a4	2.59E-42	0.5058	0.993	0.922	7.24E-38	3
Nrxn1	3.12E-32	0.2652	1	0.998	8.73E-28	3
Ntm	3.09E-29	0.3005	1	0.984	8.65E-25	3
Gria2	3.01E-25	0.4606	0.961	0.848	8.43E-21	3
Gabbr2	1.82E-24	0.6172	0.706	0.415	5.09E-20	3
Sparcl1	2.04E-23	0.3852	0.968	0.797	5.71E-19	3
Farp1	3.97E-21	0.3808	0.968	0.871	1.11E-16	3
Cables1	5.17E-20	0.5525	0.681	0.437	1.45E-15	3
Tprkb	5.53E-20	0.4988	0.748	0.512	1.55E-15	3
Rasgrf1	2.51E-18	0.5565	0.472	0.24	7.02E-14	3
Ephb1	2.66E-17	-0.8407	0.113	0.364	7.45E-13	3
Trpm3	5.60E-17	0.3602	0.979	0.917	1.57E-12	3
Nhsl1	7.22E-17	0.3995	0.908	0.798	2.02E-12	3
Gm3764	6.43E-16	0.2729	0.993	0.951	1.80E-11	3
Qk	1.01E-15	0.2648	0.996	0.967	2.82E-11	3
Lrig1	2.21E-15	0.4309	0.709	0.5	6.18E-11	3
Astn2	2.95E-15	0.3987	0.773	0.595	8.26E-11	3

Slc1a2	1.17E-14	0.2525	0.996	0.955	3.29E-10	3
Nwd1	2.22E-14	0.3350	0.826	0.634	6.22E-10	3
Atp1a2	3.83E-14	0.2944	0.982	0.871	1.07E-09	3
Pitpnc1	8.12E-14	0.2650	0.982	0.946	2.27E-09	3
Plpp3	4.83E-13	0.2931	0.965	0.896	1.35E-08	3
Clmn	2.44E-12	0.3103	0.762	0.535	6.82E-08	3
Cpe	8.12E-12	0.3192	0.957	0.922	2.27E-07	3
Csgalnact1	9.08E-12	0.3202	0.819	0.703	2.54E-07	3
Mical2	1.80E-11	0.3343	0.727	0.541	5.04E-07	3
Adrbk2	2.13E-11	0.3414	0.869	0.72	5.98E-07	3
Cit	2.60E-11	0.4121	0.383	0.208	7.29E-07	3
Cep85l	3.67E-11	0.3033	0.759	0.605	1.03E-06	3
Mapk4	4.55E-11	0.3043	0.801	0.671	1.27E-06	3
Plcb1	6.07E-11	0.3191	0.915	0.842	1.70E-06	3
Car10	7.50E-11	0.5061	0.277	0.132	2.10E-06	3
Guf1	1.47E-10	-0.4718	0.096	0.269	4.11E-06	3
Cspg5	1.50E-10	0.3113	0.851	0.707	4.21E-06	3
Gfra1	2.17E-10	-0.5666	0.163	0.351	6.08E-06	3
Glul	2.46E-10	0.3198	0.706	0.541	6.89E-06	3
Lypd6	3.38E-10	-0.5318	0.099	0.264	9.45E-06	3
Phkg1	3.90E-10	0.2746	0.869	0.731	1.09E-05	3
Phyhipl	6.27E-10	0.3201	0.699	0.537	1.76E-05	3
Trim9	7.94E-10	0.2911	0.869	0.781	2.22E-05	3
Kif21a	1.09E-09	-0.4116	0.418	0.587	3.05E-05	3
Eps8	1.34E-09	0.3177	0.738	0.586	3.75E-05	3
Gm26704	2.03E-09	0.3415	0.67	0.514	5.69E-05	3
Ahcyl1	4.17E-09	0.2763	0.709	0.558	1.17E-04	3
Adam23	4.84E-09	-0.5512	0.223	0.392	1.35E-04	3
Kank1	5.15E-09	0.3041	0.716	0.541	1.44E-04	3
Hdac8	6.04E-09	0.2888	0.936	0.889	1.69E-04	3
Ccdc80	6.31E-09	-0.3613	0.039	0.179	1.77E-04	3
Sorbs1	7.53E-09	0.3328	0.791	0.691	2.11E-04	3
Fam184b	7.75E-09	-0.4960	0.078	0.228	2.17E-04	3
Rbms1	8.13E-09	-0.4502	0.181	0.352	2.28E-04	3
Etnppl	1.12E-08	0.3592	0.358	0.21	3.13E-04	3
Nrxn3	1.12E-08	-0.3679	0.706	0.842	3.13E-04	3
Fam20a	1.95E-08	0.2714	0.645	0.494	5.45E-04	3
Ogt	2.43E-08	-0.3002	0.613	0.766	6.80E-04	3
Acss1	2.51E-08	0.2896	0.755	0.623	7.02E-04	3
Asrgl1	2.59E-08	0.3150	0.631	0.508	7.24E-04	3
2310022B05Rik	4.40E-08	0.3174	0.326	0.194	1.23E-03	3
Epha5	4.53E-08	-0.4839	0.174	0.327	1.27E-03	3
Pipox	5.67E-08	0.2588	0.259	0.134	1.59E-03	3

Rapgef3	7.92E-08	0.3090	0.553	0.426	2.22E-03	3
Shisa9	1.00E-07	0.3861	0.582	0.464	2.80E-03	3
Fat3	1.08E-07	0.2691	0.716	0.61	3.02E-03	3
Tnfrsf19	1.34E-07	-0.4632	0.266	0.414	3.76E-03	3
Pitpnm2	1.51E-07	0.2922	0.422	0.28	4.22E-03	3
Fry	1.65E-07	0.2504	0.73	0.591	4.62E-03	3
Igsf21	1.81E-07	0.3164	0.252	0.134	5.06E-03	3
2900052N01Rik	2.13E-07	0.2517	0.241	0.129	5.96E-03	3
Sncaip	2.27E-07	-0.4119	0.149	0.294	6.36E-03	3
Mgat4c	2.49E-07	0.2636	0.816	0.677	6.97E-03	3
Mfge8	3.10E-07	0.3019	0.411	0.282	8.69E-03	3
Dgki	3.29E-07	-0.3870	0.28	0.433	9.22E-03	3
Slc7a11	3.44E-07	0.3377	0.642	0.499	9.63E-03	3
Tenm4	4.09E-07	0.3461	0.514	0.374	0.0115	3
Slc25a18	4.71E-07	0.2898	0.39	0.251	0.0132	3
Rgma	5.34E-07	0.2912	0.762	0.636	0.0150	3
Dcc	6.03E-07	-0.7107	0.301	0.429	0.0169	3
Ednrb	6.74E-07	0.3291	0.532	0.397	0.0189	3
Kcnd3	7.30E-07	0.4367	0.23	0.126	0.0204	3
Adhfe1	7.38E-07	0.2737	0.489	0.356	0.0207	3
Galnt16	8.19E-07	0.3096	0.486	0.358	0.0229	3
Immp2l	8.20E-07	-0.4022	0.188	0.332	0.0230	3
Myrip	1.04E-06	0.2701	0.436	0.301	0.0290	3
Rnf121	1.14E-06	0.3329	0.56	0.448	0.0320	3
Ndrg2	1.21E-06	0.2570	0.688	0.567	0.0340	3
Aff3	1.66E-06	-0.3577	0.135	0.271	0.0466	3
Trim2	2.02E-06	-0.3372	0.27	0.421	0.0565	3
Prkca	2.70E-06	0.3060	0.535	0.417	0.0757	3
Ubxn7	2.94E-06	-0.3317	0.124	0.243	0.0824	3
Sh3pxd2b	2.94E-06	0.2745	0.507	0.398	0.0824	3
Sepp1	3.10E-06	0.2708	0.287	0.176	0.0867	3
Agbl4	3.39E-06	-0.4198	0.319	0.456	0.0948	3
Gm3764	3.16E-52	-0.7853	0.92	0.961	8.84E-48	4
Slc1a2	5.74E-42	-0.9776	0.969	0.959	1.61E-37	4
Sparcl1	9.18E-40	-0.8707	0.599	0.849	2.57E-35	4
Slc4a4	7.39E-38	-0.7588	0.855	0.942	2.07E-33	4
Trpm3	1.04E-35	-0.8447	0.901	0.928	2.91E-31	4
Plpp3	1.71E-35	-0.6208	0.817	0.916	4.78E-31	4
Sctr	2.09E-34	0.6064	0.309	0.071	5.84E-30	4
Lsamp	6.04E-34	-0.3413	1	0.997	1.69E-29	4
Qk	4.11E-31	-0.4951	0.939	0.976	1.15E-26	4
Fry	8.22E-31	-1.1278	0.302	0.651	2.30E-26	4
Farp1	3.62E-30	-0.5624	0.779	0.898	1.01E-25	4

Ntm	8.28E-29	-0.3756	0.992	0.985	2.32E-24	4
Nrxn1	1.11E-28	-0.2854	1	0.998	3.10E-24	4
Atp1a2	4.82E-27	-0.5684	0.821	0.895	1.35E-22	4
Cables1	8.57E-26	-0.8845	0.156	0.51	2.40E-21	4
Gria1	1.89E-25	-1.3923	0.214	0.523	5.29E-21	4
Atp1b1	5.97E-25	0.5751	0.557	0.263	1.67E-20	4
Bcan	4.76E-24	-0.6212	0.546	0.753	1.33E-19	4
Plcb1	1.91E-23	-0.6568	0.71	0.871	5.35E-19	4
Pitpnc1	1.47E-22	-0.5040	0.889	0.96	4.13E-18	4
Glul	4.09E-22	-0.7506	0.298	0.599	1.14E-17	4
Hpgd	1.00E-21	0.3608	0.107	0.012	2.80E-17	4
Gria2	3.55E-21	-0.5217	0.763	0.876	9.94E-17	4
Kcnd2	4.63E-20	-0.9608	0.584	0.742	1.30E-15	4
Phkg1	1.28E-19	-0.5211	0.557	0.775	3.59E-15	4
Hdac8	2.59E-19	-0.4737	0.824	0.905	7.25E-15	4
Igsf8	3.58E-19	-0.6050	0.309	0.569	1.00E-14	4
Polr2a	6.35E-19	0.5453	0.481	0.237	1.78E-14	4
Grin2c	9.37E-19	-0.6900	0.134	0.416	2.62E-14	4
Slc6a11	1.55E-18	-0.8207	0.466	0.677	4.35E-14	4
Ddx5	3.57E-18	0.3440	0.916	0.852	9.99E-14	4
Daam2	6.61E-18	-0.6046	0.393	0.623	1.85E-13	4
Cntn1	8.38E-18	-0.7365	0.198	0.483	2.35E-13	4
Mical2	8.50E-18	-0.5751	0.34	0.596	2.38E-13	4
Tprkb	9.97E-18	-0.6835	0.309	0.574	2.79E-13	4
B230323A14Rik	1.29E-17	-1.1020	0.019	0.253	3.61E-13	4
Eps8	4.04E-17	-0.6068	0.393	0.634	1.13E-12	4
Ndrg2	4.10E-17	-0.5896	0.363	0.613	1.15E-12	4
Ntsr2	4.11E-17	-0.5577	0.324	0.589	1.15E-12	4
Nhsl1	1.05E-16	-0.5491	0.729	0.823	2.94E-12	4
Kirrel3	1.09E-16	-0.4889	0.798	0.86	3.07E-12	4
Gabbr2	1.16E-16	-0.7094	0.221	0.484	3.25E-12	4
Msi2	3.76E-16	-0.2690	0.996	0.995	1.05E-11	4
Mapk4	4.18E-16	-0.5074	0.511	0.712	1.17E-11	4
Csrp1	4.87E-16	-0.5424	0.351	0.591	1.36E-11	4
Meis2	6.31E-16	0.3342	0.924	0.754	1.77E-11	4
B3gat2	1.16E-15	0.3780	0.237	0.08	3.26E-11	4
Guf1	1.23E-15	0.4673	0.435	0.221	3.45E-11	4
Nwd1	1.26E-15	-0.4661	0.439	0.689	3.52E-11	4
Abca1	2.18E-15	0.3456	0.874	0.712	6.12E-11	4
Sfxn5	3.35E-15	-0.3307	0.874	0.923	9.39E-11	4
Acsl3	4.56E-15	-0.4615	0.496	0.72	1.28E-10	4
Arhgap18	4.92E-15	0.5057	0.305	0.129	1.38E-10	4
Nr6a1	8.28E-15	0.4554	0.576	0.36	2.32E-10	4

Ptch1	9.73E-15	-0.6233	0.561	0.727	2.73E-10	4
Creb5	1.13E-14	0.3322	0.252	0.09	3.16E-10	4
Etnppl	1.42E-14	-0.7436	0.038	0.255	3.98E-10	4
Ppp2r3a	1.59E-14	0.3727	0.676	0.458	4.46E-10	4
Erbb4	2.40E-14	-0.7298	0.626	0.73	6.73E-10	4
Gm26843	3.25E-14	-0.6766	0.137	0.367	9.09E-10	4
Galnt18	8.55E-14	-0.6600	0.137	0.372	2.39E-09	4
Rgs6	1.01E-13	-0.4511	0.695	0.824	2.82E-09	4
Gm26704	1.17E-13	-0.5725	0.344	0.56	3.26E-09	4
Ttyh1	1.40E-13	-0.3805	0.622	0.781	3.92E-09	4
Adrbk2	1.60E-13	-0.4141	0.573	0.762	4.49E-09	4
Plag1	1.65E-13	0.3012	0.134	0.033	4.61E-09	4
Tspan7	2.09E-13	-0.5839	0.698	0.758	5.85E-09	4
D030047H15Rik	2.24E-13	-0.5142	0.198	0.434	6.28E-09	4
Dtna	3.08E-13	-0.2681	0.962	0.981	8.63E-09	4
Tra2a	3.29E-13	0.3884	0.805	0.681	9.20E-09	4
Camk2g	5.95E-13	-0.5139	0.637	0.741	1.66E-08	4
Ahcyl1	1.29E-12	-0.4629	0.405	0.601	3.60E-08	4
Sema5b	1.62E-12	0.4488	0.298	0.136	4.55E-08	4
Htra1	3.26E-12	-0.4925	0.462	0.637	9.12E-08	4
Lef1	3.49E-12	0.3762	0.202	0.074	9.76E-08	4
Nckap5	5.23E-12	0.2806	0.939	0.887	1.46E-07	4
Car10	5.79E-12	-0.7681	0.008	0.17	1.62E-07	4
Slc38a1	9.88E-12	0.3557	0.26	0.109	2.77E-07	4
Gpld1	1.26E-11	-0.4674	0.321	0.517	3.53E-07	4
Aifm3	1.46E-11	-0.4653	0.149	0.365	4.08E-07	4
Robo2	1.58E-11	0.4576	0.538	0.354	4.43E-07	4
F3	2.70E-11	-0.4736	0.344	0.555	7.55E-07	4
Nav3	2.94E-11	-0.6865	0.153	0.347	8.23E-07	4
Fam20a	3.17E-11	-0.4705	0.336	0.537	8.89E-07	4
Slc35f1	3.36E-11	0.3910	0.424	0.234	9.40E-07	4
Ttll8	3.68E-11	-0.4810	0.057	0.237	1.03E-06	4
Trim9	4.57E-11	-0.3890	0.714	0.803	1.28E-06	4
RP23-474J16.2	5.62E-11	-0.7829	0.046	0.22	1.57E-06	4
Lrig1	6.56E-11	-0.5767	0.374	0.548	1.84E-06	4
Sparc	8.55E-11	-0.5442	0.046	0.217	2.39E-06	4
0610040J01Rik	9.25E-11	0.3938	0.248	0.11	2.59E-06	4
Cep85l	1.31E-10	-0.4256	0.466	0.646	3.67E-06	4
Aox1	1.43E-10	-0.4581	0.05	0.221	4.01E-06	4
Cox7b	1.90E-10	0.3161	0.34	0.175	5.31E-06	4
Agbl4	2.35E-10	0.3760	0.603	0.416	6.59E-06	4
Adcy2	2.37E-10	-0.3206	0.588	0.738	6.63E-06	4
Abr	2.84E-10	-0.2976	0.718	0.843	7.94E-06	4

Ntrk2	2.94E-10	-0.3100	0.882	0.933	8.23E-06	4
Colgalt2	2.94E-10	0.2920	0.263	0.12	8.23E-06	4
Ogt	3.06E-10	0.3278	0.851	0.732	8.57E-06	4
Hif3a	3.09E-10	-0.4720	0.137	0.331	8.65E-06	4
Kif21a	3.37E-10	0.2728	0.737	0.542	9.44E-06	4
Kank1	4.13E-10	-0.4903	0.431	0.582	1.16E-05	4
Nnat	4.80E-10	-0.6586	0.275	0.467	1.34E-05	4
Maml3	5.83E-10	0.3536	0.355	0.19	1.63E-05	4
Gpatch8	5.86E-10	0.2962	0.79	0.7	1.64E-05	4
Pdzrn3	6.25E-10	0.4313	0.305	0.155	1.75E-05	4
Ankrd28	7.63E-10	0.3564	0.496	0.319	2.14E-05	4
Trim2	1.01E-09	0.3383	0.561	0.38	2.84E-05	4
5031439G07Rik	1.03E-09	-0.5135	0.279	0.457	2.88E-05	4
Kcnma1	1.08E-09	-0.3705	0.511	0.661	3.02E-05	4
RP23-240M8.2	1.74E-09	0.3624	0.202	0.085	4.86E-05	4
Nebl	1.96E-09	-0.4116	0.603	0.719	5.50E-05	4
Fut9	2.00E-09	-0.3861	0.546	0.697	5.61E-05	4
Crlf3	2.30E-09	-0.4118	0.332	0.521	6.45E-05	4
Pax6	2.94E-09	0.3304	0.363	0.208	8.24E-05	4
Itih3	3.46E-09	-0.6546	0.172	0.34	9.68E-05	4
Ncan	3.56E-09	-0.4316	0.141	0.318	9.96E-05	4
Sat1	4.29E-09	-0.4446	0.221	0.401	1.20E-04	4
Mmd2	5.59E-09	-0.3329	0.58	0.718	1.57E-04	4
Immp2l	5.74E-09	0.3666	0.466	0.292	1.61E-04	4
Fgfr3	5.89E-09	-0.3487	0.447	0.604	1.65E-04	4
Cmtm5	8.26E-09	-0.3300	0.084	0.248	2.31E-04	4
Fign	9.75E-09	0.2810	0.16	0.061	2.73E-04	4
Sh3pxd2b	9.77E-09	-0.3956	0.267	0.431	2.74E-04	4
Abhd3	1.01E-08	-0.3921	0.183	0.367	2.82E-04	4
Gm13872	1.15E-08	-0.3673	0.034	0.173	3.23E-04	4
Clmn	1.29E-08	-0.4087	0.431	0.582	3.61E-04	4
Rgs20	1.32E-08	-0.2872	0.87	0.901	3.70E-04	4
Eya1	1.48E-08	0.4117	0.294	0.165	4.16E-04	4
Adcy8	1.95E-08	-0.5353	0.08	0.227	5.47E-04	4
Agt	1.98E-08	-0.4312	0.008	0.123	5.55E-04	4
Lgi1	2.16E-08	-0.4171	0.172	0.342	6.06E-04	4
Dab2	2.26E-08	-0.4196	0.046	0.18	6.32E-04	4
Sema6a	2.28E-08	0.3367	0.447	0.274	6.38E-04	4
Cit	2.38E-08	-0.4438	0.092	0.249	6.66E-04	4
Sp4	2.50E-08	0.3855	0.374	0.226	7.00E-04	4
Fat3	2.53E-08	-0.4001	0.504	0.64	7.07E-04	4
Sorcs2	2.67E-08	-0.3521	0.531	0.682	7.48E-04	4
Zeb1	2.94E-08	-0.2734	0.798	0.871	8.23E-04	4

Gabra2	3.03E-08	0.3323	0.5	0.352	8.48E-04	4
Sfrp1	3.10E-08	0.2792	0.13	0.046	8.69E-04	4
Igf2bp3	3.17E-08	0.3696	0.397	0.241	8.88E-04	4
Gm5089	3.33E-08	0.3546	0.332	0.191	9.32E-04	4
Rock1	3.48E-08	0.2955	0.653	0.506	9.73E-04	4
Gm6277	3.62E-08	-0.3455	0.053	0.192	1.01E-03	4
Paqr8	3.76E-08	-0.3925	0.481	0.612	1.05E-03	4
Egfem1	5.11E-08	-0.5286	0.069	0.207	1.43E-03	4
Sfmbt2	5.54E-08	0.3302	0.237	0.116	1.55E-03	4
Dbx2	5.56E-08	-0.3664	0.263	0.435	1.56E-03	4
Tsc22d3	6.26E-08	-0.3838	0.034	0.162	1.75E-03	4
Slc25a21	7.84E-08	0.4056	0.424	0.275	2.20E-03	4
Il1rapl1	8.13E-08	0.2655	0.893	0.832	2.28E-03	4
Taf15	8.86E-08	0.3105	0.531	0.385	2.48E-03	4
Sema4a	9.26E-08	-0.3364	0.107	0.261	2.59E-03	4
Pdlim5	1.02E-07	0.2938	0.664	0.53	2.87E-03	4
Prodh	1.06E-07	-0.3628	0.179	0.347	2.96E-03	4
Scel	1.19E-07	0.3980	0.191	0.089	3.33E-03	4
Dpp6	1.29E-07	-0.4030	0.13	0.281	3.60E-03	4
Tjp1	1.31E-07	0.3376	0.779	0.692	3.68E-03	4
Micalcl	1.34E-07	-0.3340	0.015	0.126	3.74E-03	4
Tlcd1	1.44E-07	-0.3218	0.038	0.163	4.03E-03	4
9530026P05Rik	1.52E-07	0.3809	0.473	0.328	4.27E-03	4
Gm44151	1.64E-07	-0.3095	0.176	0.355	4.58E-03	4
Myo1e	1.83E-07	0.2933	0.42	0.263	5.12E-03	4
Kcnn2	1.92E-07	-0.3815	0.382	0.537	5.37E-03	4
Mycbp	1.94E-07	0.2733	0.374	0.229	5.43E-03	4
Ldlr	2.14E-07	-0.3611	0.042	0.163	5.99E-03	4
Kcnj3	2.19E-07	0.3546	0.172	0.077	6.12E-03	4
Bach2	2.30E-07	0.2985	0.763	0.658	6.43E-03	4
Car8	2.33E-07	0.3744	0.191	0.09	6.54E-03	4
Setbp1	2.38E-07	0.2574	0.725	0.606	6.67E-03	4
L3mbtl3	2.44E-07	0.3071	0.546	0.401	6.84E-03	4
Dip2b	2.93E-07	0.2851	0.634	0.498	8.21E-03	4
Phactr3	3.01E-07	-0.3148	0.595	0.693	8.44E-03	4
Slc7a10	3.37E-07	-0.3291	0.347	0.508	9.43E-03	4
Nt5c2	3.49E-07	-0.3369	0.34	0.501	9.77E-03	4
Phyhipl	3.61E-07	-0.3426	0.424	0.576	0.0101	4
Itpkb	3.61E-07	-0.4547	0.21	0.36	0.0101	4
Ccnd2	3.76E-07	0.2522	0.206	0.1	0.0105	4
Mamdc2	3.81E-07	0.2852	0.141	0.058	0.0107	4
Kcnip3	3.85E-07	-0.3633	0.252	0.41	0.0108	4
Cpeb3	3.92E-07	0.2790	0.744	0.628	0.0110	4

Syne1	4.09E-07	-0.2693	0.649	0.782	0.0115	4
Id2	4.46E-07	-0.3698	0.088	0.221	0.0125	4
Pcyt2	4.53E-07	-0.3701	0.252	0.4	0.0127	4
Slc6a9	4.95E-07	-0.3319	0.046	0.163	0.0139	4
Ccdc80	4.99E-07	0.2522	0.267	0.146	0.0140	4
Mertk	5.26E-07	-0.3867	0.767	0.801	0.0147	4
9930021J03Rik	5.41E-07	0.2687	0.592	0.443	0.0151	4
Tcf7l2	5.65E-07	-0.2716	0.656	0.772	0.0158	4
Atp5a1	5.80E-07	0.2518	0.55	0.39	0.0162	4
Rsrc1	5.84E-07	0.2965	0.538	0.406	0.0163	4
Csdc2	6.63E-07	-0.3242	0.103	0.241	0.0186	4
Thoc2	6.96E-07	0.2761	0.584	0.449	0.0195	4
Itm2b	8.32E-07	0.3166	0.538	0.393	0.0233	4
Acss1	9.68E-07	-0.2953	0.542	0.653	0.0271	4
Cdh13	9.81E-07	0.2922	0.267	0.15	0.0275	4
Btbd9	1.01E-06	0.2645	0.706	0.591	0.0282	4
Eml6	1.04E-06	0.2745	0.588	0.44	0.0293	4
Phka1	1.09E-06	-0.3380	0.561	0.66	0.0304	4
Fads1	1.10E-06	-0.3380	0.122	0.263	0.0307	4
Kalrn	1.12E-06	-0.2837	0.576	0.69	0.0313	4
Lhfp	1.25E-06	-0.3796	0.576	0.711	0.0349	4
Camk2d	1.32E-06	0.2915	0.748	0.668	0.0370	4
Tpk1	1.38E-06	0.2793	0.37	0.235	0.0386	4
Mtss1l	1.38E-06	-0.2951	0.401	0.551	0.0387	4
Efr3b	1.43E-06	-0.3309	0.569	0.683	0.0402	4
Aldh1l1	1.46E-06	-0.3519	0.221	0.369	0.0410	4
Dpf3	1.55E-06	-0.2979	0.374	0.521	0.0434	4
Tmtc2	1.65E-06	-0.3402	0.714	0.756	0.0463	4
Angpt1	1.77E-06	0.2586	0.233	0.123	0.0495	4
Cenpc1	1.77E-06	0.2749	0.401	0.266	0.0496	4
Srgap1	1.84E-06	-0.4450	0.366	0.495	0.0515	4
Pak1	1.94E-06	0.3046	0.355	0.223	0.0544	4
Igsf21	2.47E-06	-0.3074	0.05	0.163	0.0692	4
Tmcc3	2.75E-06	-0.3500	0.466	0.596	0.0769	4
Grin3a	3.03E-06	-0.3781	0.076	0.191	0.0848	4
Caskin1	3.06E-06	-0.3116	0.305	0.442	0.0857	4
Ablim1	3.16E-06	-0.2781	0.42	0.569	0.0885	4
Zbtb16	3.17E-06	-0.4582	0.115	0.241	0.0888	4
Ccdc58	3.50E-06	0.2942	0.458	0.319	0.0981	4
Adamts18	2.22E-101	1.4655	0.35	0.015	6.22E-97	5
Adgrv1	2.26E-96	1.5002	0.544	0.066	6.33E-92	5
Gpc5	7.87E-86	-1.5608	0.644	0.992	2.20E-81	5
Lsamp	9.91E-81	-0.9042	0.972	1	2.78E-76	5

Ntm	2.53E-75	-1.1279	0.85	0.999	7.09E-71	5
Slc4a4	3.74E-74	-1.5793	0.511	0.969	1.05E-69	5
Ccdc170	1.43E-70	1.0667	0.272	0.015	4.00E-66	5
Veph1	3.14E-66	0.9404	0.244	0.012	8.80E-62	5
Mdga2	1.10E-64	-1.1903	0.589	0.982	3.09E-60	5
Pcdh7	2.29E-60	-1.2575	0.406	0.945	6.41E-56	5
Sparcl1	4.07E-60	-1.4941	0.228	0.873	1.14E-55	5
Kirrel3	1.28E-55	-1.3571	0.356	0.897	3.60E-51	5
Trpm3	6.79E-51	-1.2800	0.556	0.958	1.90E-46	5
Nhsl1	2.21E-50	-1.3189	0.25	0.863	6.18E-46	5
Gm3764	1.13E-49	-1.0036	0.717	0.978	3.17E-45	5
Scml4	2.11E-48	0.8721	0.261	0.026	5.89E-44	5
Enkur	3.60E-47	0.7032	0.217	0.017	1.01E-42	5
Spag16	1.08E-45	1.4156	0.461	0.105	3.03E-41	5
Gria2	1.10E-45	-1.1028	0.456	0.899	3.09E-41	5
Adgrb3	1.99E-44	-0.7613	0.872	0.992	5.58E-40	5
Nkain2	2.32E-44	1.1840	0.878	0.577	6.49E-40	5
Cfap44	3.46E-44	1.0254	0.289	0.039	9.69E-40	5
Ncam1	3.87E-43	-0.8569	0.594	0.946	1.08E-38	5
Tspan18	4.61E-43	0.6354	0.183	0.012	1.29E-38	5
Atp1a2	3.07E-42	-0.9804	0.594	0.912	8.59E-38	5
Anxa2	4.40E-42	0.5826	0.183	0.013	1.23E-37	5
Eps8	5.03E-42	-1.3417	0.078	0.652	1.41E-37	5
Cdon	9.02E-42	0.7933	0.233	0.025	2.52E-37	5
Kcnma1	1.83E-41	-1.2980	0.122	0.69	5.11E-37	5
Fam179a	1.63E-40	0.7718	0.244	0.029	4.55E-36	5
Adgrl3	1.80E-40	-0.7742	0.7	0.975	5.04E-36	5
Npas3	2.17E-40	-0.6001	0.944	0.998	6.07E-36	5
Dock4	2.42E-40	-0.8650	0.522	0.928	6.77E-36	5
Brinp3	8.90E-40	-1.4115	0.1	0.654	2.49E-35	5
Tmem132b	1.02E-39	0.9591	0.356	0.069	2.87E-35	5
Slc38a1	8.79E-39	0.9857	0.422	0.101	2.46E-34	5
Csmd1	5.21E-38	1.1754	0.839	0.616	1.46E-33	5
Nrg1	1.86E-37	2.0843	0.656	0.335	5.21E-33	5
Cdh20	4.77E-37	-1.0860	0.189	0.738	1.34E-32	5
Ak9	5.29E-37	0.7065	0.133	0.006	1.48E-32	5
Mgat4c	9.71E-37	-1.1262	0.194	0.74	2.72E-32	5
Kif21a	1.25E-36	0.9169	0.828	0.542	3.51E-32	5
Daam2	3.80E-36	-1.2442	0.111	0.638	1.06E-31	5
Gm29260	4.38E-36	0.9252	0.172	0.014	1.23E-31	5
Appl2	7.39E-36	-0.9658	0.272	0.756	2.07E-31	5
Meg3	1.02E-35	0.9195	0.9	0.8	2.85E-31	5
Dnah9	2.09E-35	0.8244	0.161	0.012	5.86E-31	5

Tox3	2.65E-35	0.9146	0.394	0.097	7.43E-31	5
Tmem178	7.29E-35	0.4739	0.156	0.011	2.04E-30	5
Arhgap26	1.13E-33	-0.8970	0.417	0.848	3.16E-29	5
Bmper	3.38E-33	0.9738	0.372	0.091	9.46E-29	5
Gm42722	8.20E-33	0.5538	0.144	0.01	2.30E-28	5
Fry	1.87E-32	-1.4018	0.172	0.648	5.24E-28	5
Sncaip	2.97E-32	0.9432	0.594	0.247	8.32E-28	5
Epha3	3.92E-32	0.7271	0.239	0.037	1.10E-27	5
Macf1	3.93E-32	-0.4929	0.956	0.998	1.10E-27	5
Drc1	4.98E-32	0.5978	0.239	0.036	1.39E-27	5
Zbtb20	1.36E-31	0.4615	0.994	0.998	3.81E-27	5
Tnik	5.18E-31	-0.6456	0.717	0.969	1.45E-26	5
Lrrc4c	8.07E-31	-0.7379	0.661	0.95	2.26E-26	5
Kcnd2	2.79E-30	-1.4860	0.4	0.752	7.81E-26	5
Trim2	3.00E-30	0.8287	0.694	0.375	8.41E-26	5
Cadm2	5.45E-30	-0.4522	0.967	0.999	1.53E-25	5
Hydin	7.97E-30	0.5513	0.106	0.005	2.23E-25	5
Slc38a2	9.58E-30	0.6904	0.294	0.062	2.68E-25	5
Slc6a11	9.99E-30	-1.2491	0.261	0.686	2.80E-25	5
Nrcam	2.20E-29	-0.6529	0.65	0.947	6.16E-25	5
Cacnb2	3.36E-29	1.0401	0.556	0.247	9.40E-25	5
Pawr	6.67E-29	0.6659	0.183	0.023	1.87E-24	5
Srgap1	1.36E-28	-1.2619	0.061	0.517	3.82E-24	5
Eya2	1.37E-28	0.4157	0.117	0.007	3.83E-24	5
Syne1	1.71E-28	-0.6072	0.322	0.806	4.80E-24	5
Clmn	3.62E-28	-0.9517	0.128	0.603	1.01E-23	5
Fgfr3	1.15E-27	-0.9177	0.144	0.625	3.22E-23	5
Phactr3	4.46E-27	-0.8366	0.272	0.718	1.25E-22	5
Gabbr2	4.56E-27	-1.3137	0.056	0.488	1.28E-22	5
Atp13a4	8.55E-27	-0.9956	0.072	0.526	2.39E-22	5
Armc2	1.17E-26	0.8191	0.378	0.112	3.28E-22	5
Paqr8	2.59E-26	-0.9790	0.189	0.632	7.26E-22	5
Wdr17	2.97E-26	-0.5222	0.939	0.99	8.32E-22	5
Dnah5	3.91E-26	0.5368	0.133	0.012	1.09E-21	5
Ghr	9.24E-26	-0.8776	0.239	0.67	2.59E-21	5
Ak7	1.44E-25	0.7086	0.106	0.007	4.02E-21	5
Nrxn1	1.44E-25	-0.3665	0.983	1	4.03E-21	5
Col5a2	1.46E-25	0.6358	0.244	0.049	4.09E-21	5
Dnah11	1.81E-25	0.7758	0.139	0.014	5.06E-21	5
Gm26704	2.27E-25	-0.9809	0.133	0.57	6.37E-21	5
Qk	6.65E-25	-0.5376	0.894	0.978	1.86E-20	5
Cdh10	1.47E-24	-0.6885	0.483	0.852	4.12E-20	5
Slc35f1	1.56E-24	0.9537	0.522	0.233	4.37E-20	5

Slc7a10	1.97E-24	-0.8958	0.094	0.524	5.50E-20	5
Ptch1	2.10E-24	-0.9106	0.328	0.741	5.88E-20	5
Dpf3	2.30E-24	-0.8847	0.111	0.539	6.45E-20	5
Kif27	2.38E-24	0.3923	0.128	0.012	6.67E-20	5
Fat3	2.64E-24	-0.8615	0.233	0.658	7.38E-20	5
Kank1	3.59E-24	-0.8727	0.172	0.599	1.00E-19	5
Nek11	5.44E-24	0.5915	0.2	0.034	1.52E-19	5
Wdr66	1.40E-23	0.4637	0.117	0.01	3.92E-19	5
Cfap69	1.66E-23	0.6325	0.228	0.047	4.64E-19	5
Pkp2	2.67E-23	0.5120	0.15	0.019	7.47E-19	5
Dnah6	1.19E-22	0.7235	0.133	0.015	3.34E-18	5
Limch1	1.39E-22	-0.5915	0.389	0.806	3.90E-18	5
Sash1	1.55E-22	-0.5887	0.517	0.878	4.35E-18	5
Ablim1	1.67E-22	-0.8181	0.167	0.585	4.67E-18	5
Nek5	2.24E-22	0.3237	0.111	0.01	6.26E-18	5
Sorcs2	2.70E-22	-0.7445	0.278	0.698	7.57E-18	5
Srcin1	3.44E-22	0.5206	0.211	0.042	9.63E-18	5
Epb41l4b	3.93E-22	0.7254	0.333	0.102	1.10E-17	5
Sfrp1	7.24E-22	0.5409	0.211	0.042	2.03E-17	5
Bcan	9.99E-22	-0.7505	0.394	0.758	2.80E-17	5
Slc39a12	1.27E-21	-0.6167	0.339	0.775	3.54E-17	5
Thbs4	1.36E-21	0.6812	0.144	0.019	3.82E-17	5
Mertk	1.90E-21	-0.7382	0.494	0.824	5.32E-17	5
Ddhd1	2.87E-21	-0.6291	0.45	0.811	8.03E-17	5
Ank2	3.51E-21	-0.4014	0.911	0.986	9.82E-17	5
Camk2g	3.85E-21	-0.7617	0.4	0.758	1.08E-16	5
Acsbg1	4.70E-21	-0.6925	0.294	0.715	1.32E-16	5
Fam20a	5.65E-21	-0.8115	0.144	0.546	1.58E-16	5
Efhb	5.80E-21	0.6111	0.217	0.046	1.62E-16	5
Vav3	1.11E-20	-0.9371	0.028	0.391	3.12E-16	5
Dbx2	1.24E-20	-0.8806	0.067	0.446	3.48E-16	5
Cep85l	1.29E-20	-0.7327	0.272	0.656	3.60E-16	5
Cadm1	1.44E-20	-0.5464	0.767	0.943	4.03E-16	5
Mok	1.86E-20	0.7194	0.389	0.145	5.20E-16	5
Pcdh9	2.18E-20	-0.3986	0.944	0.998	6.11E-16	5
Hdac8	2.47E-20	-0.5999	0.689	0.914	6.90E-16	5
Nebl	4.25E-20	-0.7506	0.383	0.734	1.19E-15	5
Mpp6	5.19E-20	-0.9108	0.122	0.499	1.45E-15	5
Csgalnact1	6.03E-20	-0.6050	0.361	0.75	1.69E-15	5
Kif9	6.81E-20	0.6271	0.222	0.052	1.91E-15	5
Mtss1l	6.87E-20	-0.7422	0.172	0.566	1.92E-15	5
Ccdc141	8.44E-20	-0.7107	0.272	0.644	2.36E-15	5
Phka1	1.41E-19	-0.7823	0.317	0.678	3.93E-15	5

Grm3	1.49E-19	-0.7277	0.622	0.873	4.16E-15	5
Sema6a	3.04E-19	0.7737	0.528	0.274	8.51E-15	5
Son	3.62E-19	-0.4415	0.878	0.968	1.01E-14	5
Stk33	4.51E-19	0.6198	0.233	0.058	1.26E-14	5
Slc7a11	5.38E-19	-0.9690	0.178	0.548	1.51E-14	5
Gria1	5.63E-19	-1.4001	0.172	0.514	1.58E-14	5
Htra1	7.98E-19	-0.7363	0.267	0.647	2.23E-14	5
Ccdc30	1.19E-18	0.7516	0.267	0.079	3.33E-14	5
Itga6	1.21E-18	-0.7554	0.194	0.57	3.37E-14	5
Tmc7	1.22E-18	-0.8084	0.083	0.441	3.41E-14	5
Cfap43	1.35E-18	0.7389	0.167	0.032	3.79E-14	5
Ntsr2	1.48E-18	-0.7418	0.211	0.588	4.16E-14	5
Meis2	1.84E-18	0.6416	0.856	0.767	5.14E-14	5
Xylt1	2.06E-18	-0.5410	0.356	0.725	5.78E-14	5
Cntn1	3.95E-18	-1.0597	0.144	0.477	1.11E-13	5
Agbl4	3.97E-18	0.8605	0.644	0.42	1.11E-13	5
Ephb2	4.51E-18	0.4445	0.156	0.028	1.26E-13	5
Pde4b	4.63E-18	-0.8396	0.322	0.667	1.30E-13	5
Dcc	5.33E-18	0.9169	0.639	0.392	1.49E-13	5
Tprkb	5.47E-18	-0.8671	0.222	0.571	1.53E-13	5
Slc6a1	5.56E-18	-0.6139	0.378	0.725	1.56E-13	5
Nme5	6.39E-18	0.5795	0.228	0.059	1.79E-13	5
Pak3	7.83E-18	0.6818	0.244	0.069	2.19E-13	5
Cfap54	8.87E-18	0.9006	0.256	0.076	2.48E-13	5
Kalrn	1.19E-17	-0.6307	0.361	0.705	3.33E-13	5
Sycp2	1.21E-17	-0.7640	0.039	0.367	3.38E-13	5
Phkg1	1.23E-17	-0.6082	0.439	0.776	3.45E-13	5
Fgf1	1.36E-17	-0.7900	0.056	0.389	3.80E-13	5
Prex1	1.40E-17	-0.7506	0.144	0.5	3.91E-13	5
Lrp1b	1.57E-17	-0.7197	0.55	0.784	4.41E-13	5
Shc3	2.41E-17	-0.6462	0.128	0.481	6.74E-13	5
Glul	4.36E-17	-0.6773	0.25	0.591	1.22E-12	5
Dmd	5.02E-17	-0.4153	0.639	0.888	1.41E-12	5
Serpine2	5.14E-17	-0.6301	0.25	0.615	1.44E-12	5
Ssbp3	5.87E-17	0.7473	0.356	0.146	1.64E-12	5
Gabrb1	6.05E-17	-0.4219	0.894	0.987	1.69E-12	5
Rtn1	7.14E-17	0.7365	0.6	0.396	2.00E-12	5
Rgs7	7.50E-17	-0.6478	0.439	0.754	2.10E-12	5
Eno4	8.49E-17	0.3156	0.117	0.016	2.38E-12	5
Tshr	1.09E-16	0.4425	0.139	0.024	3.05E-12	5
Pdzrn3	1.22E-16	0.7264	0.383	0.154	3.41E-12	5
Shroom3	1.97E-16	0.7943	0.294	0.102	5.51E-12	5
Tmtc2	2.70E-16	-0.5909	0.422	0.78	7.55E-12	5

Miat	2.94E-16	0.6393	0.283	0.097	8.24E-12	5
Ndrg2	4.48E-16	-0.6201	0.25	0.613	1.25E-11	5
Farp1	4.78E-16	-0.4679	0.656	0.904	1.34E-11	5
Atxn1	4.84E-16	0.5930	0.794	0.686	1.36E-11	5
Fars2	5.50E-16	0.6800	0.883	0.75	1.54E-11	5
Fnbp1	6.11E-16	-0.4878	0.667	0.89	1.71E-11	5
Itpr2	6.24E-16	-0.5715	0.25	0.617	1.75E-11	5
Creb5	6.81E-16	0.6894	0.278	0.095	1.91E-11	5
Cacna2d1	9.00E-16	0.6831	0.383	0.172	2.52E-11	5
Apba2	9.54E-16	-0.5942	0.306	0.671	2.67E-11	5
Erbb4	1.01E-15	-0.8157	0.517	0.736	2.82E-11	5
Hmgcs2	2.71E-15	0.5743	0.222	0.064	7.59E-11	5
Ctnna2	3.56E-15	0.5648	0.917	0.81	9.96E-11	5
D930015E06Rik	3.94E-15	0.5176	0.244	0.079	1.10E-10	5
Igsf8	4.39E-15	-0.6063	0.217	0.566	1.23E-10	5
Dfna5	4.43E-15	-0.6498	0.139	0.465	1.24E-10	5
Ano3	4.61E-15	0.5268	0.222	0.066	1.29E-10	5
Pde7b	4.64E-15	-0.5396	0.306	0.663	1.30E-10	5
Plcb1	4.78E-15	-0.5364	0.633	0.871	1.34E-10	5
Pde4d	5.01E-15	-0.5287	0.467	0.784	1.40E-10	5
Nwd1	5.57E-15	-0.5932	0.367	0.685	1.56E-10	5
Etv5	6.82E-15	-0.7040	0.039	0.324	1.91E-10	5
Pim1	7.09E-15	0.4108	0.133	0.025	1.99E-10	5
Syne2	8.84E-15	0.6214	0.339	0.14	2.48E-10	5
Lrriq1	9.50E-15	0.6678	0.178	0.044	2.66E-10	5
Pla2g7	9.53E-15	-0.6060	0.228	0.571	2.67E-10	5
5031439G07Rik	1.10E-14	-0.7496	0.15	0.461	3.08E-10	5
Arhgef12	1.11E-14	-0.4383	0.611	0.879	3.10E-10	5
Dnah2	1.22E-14	0.6173	0.167	0.039	3.41E-10	5
Celrr	1.95E-14	-0.6209	0.094	0.398	5.46E-10	5
Gm44257	2.54E-14	-0.6693	0.056	0.344	7.10E-10	5
Efr3b	3.16E-14	-0.4913	0.372	0.696	8.86E-10	5
Lifr	4.47E-14	-0.5962	0.067	0.354	1.25E-09	5
Ggta1	4.73E-14	0.4511	0.183	0.048	1.33E-09	5
Sema5b	5.24E-14	0.6439	0.333	0.139	1.47E-09	5
Kif6	5.79E-14	0.7071	0.161	0.039	1.62E-09	5
Tspan7	5.86E-14	-0.6865	0.522	0.771	1.64E-09	5
Specc1	6.88E-14	-0.5698	0.194	0.528	1.93E-09	5
Etv4	7.23E-14	-0.6593	0.006	0.257	2.02E-09	5
Rgs6	7.43E-14	-0.5053	0.556	0.831	2.08E-09	5
Cpeb4	7.66E-14	-0.5958	0.294	0.616	2.15E-09	5
Ldb2	9.21E-14	0.4916	0.517	0.271	2.58E-09	5
Gpld1	1.12E-13	-0.5810	0.194	0.52	3.15E-09	5

Hrh1	1.15E-13	-0.6806	0.022	0.278	3.22E-09	5
Lrig1	1.21E-13	-0.7588	0.25	0.552	3.40E-09	5
Gm29514	1.22E-13	-0.7274	0.011	0.261	3.42E-09	5
Gpr156	1.68E-13	0.5150	0.239	0.081	4.72E-09	5
Vegfa	1.75E-13	-0.6668	0.083	0.368	4.90E-09	5
Auts2	1.95E-13	0.4645	0.972	0.974	5.47E-09	5
Mical2	2.23E-13	-0.5705	0.256	0.593	6.24E-09	5
Slc1a3	2.25E-13	-0.2995	0.867	0.986	6.30E-09	5
Kcnq3	2.40E-13	-0.9053	0.117	0.382	6.73E-09	5
Hmgcll1	3.00E-13	0.4583	0.222	0.072	8.40E-09	5
Trim9	3.14E-13	-0.5120	0.572	0.812	8.78E-09	5
Grid1	3.52E-13	-0.4980	0.389	0.725	9.85E-09	5
Nkx2-2os	3.91E-13	-0.7622	0.061	0.329	1.10E-08	5
Myo6	4.51E-13	-0.3996	0.689	0.88	1.26E-08	5
Arhgef26	4.66E-13	-0.5002	0.45	0.745	1.30E-08	5
Ahcyl1	4.75E-13	-0.5361	0.289	0.604	1.33E-08	5
Nrp1	4.78E-13	-0.6231	0.056	0.325	1.34E-08	5
Tjp1	5.02E-13	-0.4834	0.417	0.728	1.41E-08	5
Shisa9	6.06E-13	-0.6757	0.211	0.503	1.70E-08	5
Sntg2	6.13E-13	0.4656	0.172	0.045	1.72E-08	5
Cep112	7.83E-13	0.6377	0.356	0.164	2.19E-08	5
Grin2c	1.07E-12	-0.6813	0.122	0.406	3.00E-08	5
Ephb1	1.15E-12	0.6384	0.528	0.314	3.21E-08	5
F3	1.26E-12	-0.6046	0.256	0.554	3.54E-08	5
Skap2	1.38E-12	-0.5963	0.111	0.399	3.87E-08	5
Lrrc16a	1.65E-12	-0.4734	0.422	0.727	4.62E-08	5
Pcdh17	1.74E-12	-0.5141	0.15	0.453	4.86E-08	5
Vit	2.43E-12	0.4908	0.356	0.163	6.79E-08	5
Lgi1	2.50E-12	-0.6713	0.078	0.343	7.00E-08	5
Slc1a2	2.91E-12	-0.4989	0.844	0.971	8.14E-08	5
Atp1b2	3.26E-12	-0.5600	0.139	0.424	9.13E-08	5
Dkk3	3.26E-12	0.6200	0.489	0.295	9.13E-08	5
Slc16a2	3.79E-12	0.5814	0.311	0.136	1.06E-07	5
Wdr78	3.96E-12	0.6748	0.211	0.071	1.11E-07	5
Hes5	4.03E-12	-0.6165	0.139	0.425	1.13E-07	5
Cpne8	4.46E-12	0.4975	0.194	0.06	1.25E-07	5
6330403K07Rik	4.48E-12	0.6116	0.272	0.112	1.25E-07	5
Ppp1r14c	4.91E-12	-0.7047	0.033	0.267	1.37E-07	5
Fut9	5.00E-12	-0.4650	0.406	0.703	1.40E-07	5
Abca8a	5.39E-12	0.3595	0.133	0.031	1.51E-07	5
Erich2	5.64E-12	0.3879	0.111	0.022	1.58E-07	5
Gm44151	6.05E-12	-0.5971	0.094	0.355	1.70E-07	5
Gm11149	6.06E-12	-0.4755	0.228	0.536	1.70E-07	5

Mmd2	6.96E-12	-0.4563	0.433	0.725	1.95E-07	5
Cml3	6.97E-12	-0.5884	0.144	0.424	1.95E-07	5
Arhgap6	7.65E-12	0.7940	0.172	0.05	2.14E-07	5
St6galnac3	8.21E-12	0.4602	0.194	0.06	2.30E-07	5
Rgs7bp	8.72E-12	-0.6493	0.111	0.376	2.44E-07	5
Spred2	9.53E-12	-0.5414	0.156	0.437	2.67E-07	5
Slc24a4	1.03E-11	0.3767	0.122	0.026	2.89E-07	5
Ulk4	1.15E-11	0.5719	0.217	0.076	3.23E-07	5
Plekhm3	1.24E-11	0.6334	0.456	0.276	3.46E-07	5
Sik3	1.31E-11	0.3644	0.917	0.865	3.66E-07	5
Cables1	1.37E-11	-0.5990	0.206	0.492	3.85E-07	5
Atp1b1	1.61E-11	0.5136	0.472	0.283	4.50E-07	5
Armc3	1.71E-11	0.3720	0.15	0.04	4.79E-07	5
Abat	2.23E-11	-0.5754	0.261	0.541	6.25E-07	5
Myo1e	2.46E-11	0.5307	0.45	0.267	6.88E-07	5
Ubxn11	2.52E-11	0.4783	0.278	0.113	7.06E-07	5
Ccser1	2.84E-11	0.6655	0.5	0.332	7.96E-07	5
Vim	2.88E-11	0.3340	0.111	0.023	8.06E-07	5
Ppp3ca	2.89E-11	-0.3701	0.628	0.851	8.11E-07	5
Itih3	2.95E-11	-0.8038	0.094	0.34	8.26E-07	5
Lix1	3.50E-11	-0.5026	0.194	0.488	9.79E-07	5
Eva1a	3.57E-11	-0.5369	0.083	0.337	1.00E-06	5
Ttc28	3.86E-11	0.4505	0.733	0.601	1.08E-06	5
Kcnk10	3.93E-11	0.6012	0.289	0.129	1.10E-06	5
Adcy2	4.45E-11	-0.3621	0.461	0.744	1.25E-06	5
Abcd2	5.81E-11	-0.5563	0.078	0.323	1.63E-06	5
Sema6d	6.10E-11	-0.3580	0.539	0.827	1.71E-06	5
Gm13974	6.16E-11	0.4084	0.106	0.022	1.72E-06	5
Celsr1	6.56E-11	0.4633	0.222	0.081	1.84E-06	5
Sorcs1	6.57E-11	0.5738	0.239	0.095	1.84E-06	5
Tril	6.86E-11	-0.5554	0.017	0.223	1.92E-06	5
Ttyh1	7.55E-11	-0.4256	0.522	0.783	2.11E-06	5
Trim35	7.80E-11	0.5554	0.456	0.283	2.18E-06	5
B230323A14Rik	8.35E-11	-0.9960	0.033	0.243	2.34E-06	5
Shank2	8.94E-11	0.7184	0.189	0.064	2.50E-06	5
Trp53bp2	9.02E-11	-0.5395	0.089	0.342	2.53E-06	5
Map1b	9.17E-11	0.6311	0.261	0.112	2.57E-06	5
Gpr37l1	1.01E-10	-0.5264	0.111	0.371	2.82E-06	5
Abr	1.09E-10	-0.3655	0.6	0.849	3.05E-06	5
Cdh19	1.09E-10	-0.5688	0.122	0.376	3.06E-06	5
Mmp16	1.17E-10	0.4965	0.378	0.193	3.26E-06	5
Rasgrf1	1.18E-10	-0.6380	0.061	0.288	3.31E-06	5
A830019P07Rik	1.19E-10	-0.5413	0.006	0.204	3.32E-06	5

Frmpd1	1.21E-10	-0.4801	0.167	0.445	3.39E-06	5
Abhd3	1.45E-10	-0.5460	0.117	0.365	4.07E-06	5
Col4a6	1.48E-10	0.4114	0.111	0.025	4.13E-06	5
Synpo2	1.62E-10	0.4914	0.25	0.1	4.53E-06	5
Mboat2	1.69E-10	-0.4962	0.317	0.601	4.73E-06	5
Irak2	1.69E-10	-0.6030	0.183	0.448	4.74E-06	5
Phyhipl	1.74E-10	-0.4431	0.283	0.583	4.86E-06	5
Ntrk3	1.97E-10	-0.5306	0.206	0.482	5.51E-06	5
Hacd2	1.99E-10	-0.4235	0.222	0.504	5.58E-06	5
Abtb2	2.02E-10	-0.4085	0.106	0.359	5.65E-06	5
Rnd3	2.03E-10	0.6289	0.261	0.113	5.70E-06	5
Npas2	2.09E-10	-0.4757	0.15	0.411	5.85E-06	5
Garnl3	2.24E-10	0.7553	0.311	0.15	6.27E-06	5
Etnppl	2.35E-10	-0.8475	0.039	0.246	6.57E-06	5
Tnfaip8	2.54E-10	-0.5600	0.122	0.364	7.11E-06	5
Cpeb3	2.59E-10	-0.4317	0.383	0.665	7.25E-06	5
3300002A11Rik	2.61E-10	0.6524	0.139	0.038	7.30E-06	5
Grb14	3.19E-10	0.3944	0.117	0.028	8.93E-06	5
Dennd1a	3.21E-10	0.3679	0.911	0.84	8.99E-06	5
Ccdc148	3.22E-10	0.6466	0.333	0.174	9.02E-06	5
Gpm6a	3.26E-10	-0.3953	0.583	0.809	9.12E-06	5
Robo1	3.39E-10	-0.5007	0.239	0.519	9.48E-06	5
Igf1r	4.58E-10	0.4376	0.7	0.585	1.28E-05	5
Dixdc1	4.75E-10	0.3767	0.156	0.047	1.33E-05	5
Dscaml1	5.61E-10	0.4551	0.133	0.036	1.57E-05	5
Gfra1	6.35E-10	0.5791	0.5	0.311	1.78E-05	5
Dnaic1	6.46E-10	0.4317	0.15	0.045	1.81E-05	5
RP23-474J16.2	6.50E-10	-0.9050	0.022	0.215	1.82E-05	5
Chd9	7.13E-10	-0.3590	0.661	0.879	2.00E-05	5
Aldh1l1	8.10E-10	-0.4986	0.128	0.371	2.27E-05	5
Gjb6	8.37E-10	-0.5130	0.017	0.209	2.34E-05	5
AI854517	8.73E-10	-0.4009	0.522	0.782	2.44E-05	5
Pard3b	8.83E-10	0.3787	0.828	0.801	2.47E-05	5
Efna5	8.98E-10	0.8065	0.35	0.186	2.51E-05	5
Rapgef3	9.59E-10	-0.4709	0.194	0.465	2.69E-05	5
Atl2	1.06E-09	-0.4959	0.172	0.43	2.97E-05	5
Ust	1.07E-09	0.4778	0.206	0.079	2.99E-05	5
Rhbdl3	1.07E-09	0.5582	0.256	0.113	3.00E-05	5
Csrp1	1.23E-09	-0.4005	0.311	0.585	3.44E-05	5
Epas1	1.32E-09	-0.4738	0.106	0.339	3.69E-05	5
5330434G04Rik	1.50E-09	0.5712	0.256	0.116	4.21E-05	5
Epb41	1.75E-09	0.4867	0.228	0.094	4.90E-05	5
Cyp2d22	1.89E-09	-0.5146	0.089	0.31	5.28E-05	5

Folh1	2.08E-09	-0.4632	0.044	0.249	5.81E-05	5
Cldn10	2.16E-09	-0.4857	0.089	0.315	6.06E-05	5
S100a6	2.37E-09	0.3331	0.128	0.036	6.65E-05	5
Arhgef19	2.42E-09	-0.4868	0.106	0.342	6.77E-05	5
Abcc1	2.55E-09	0.3647	0.189	0.069	7.13E-05	5
Eda	2.83E-09	0.6082	0.533	0.37	7.93E-05	5
Jazf1	3.34E-09	0.5205	0.283	0.135	9.35E-05	5
Gabbr1	3.46E-09	-0.4264	0.317	0.59	9.68E-05	5
Adgrl2	3.66E-09	0.4386	0.244	0.108	1.02E-04	5
Prex2	3.73E-09	-0.3820	0.744	0.865	1.04E-04	5
Pou2f1	4.25E-09	0.5060	0.744	0.645	1.19E-04	5
Rhoq	4.46E-09	-0.4956	0.2	0.444	1.25E-04	5
Aqp4	4.72E-09	-0.5084	0.111	0.328	1.32E-04	5
Tspan5	4.82E-09	-0.4079	0.356	0.634	1.35E-04	5
Sel1l3	5.50E-09	0.4075	0.172	0.061	1.54E-04	5
Plcd4	5.84E-09	-0.4130	0.217	0.477	1.64E-04	5
Zfhx4	6.11E-09	0.4697	0.511	0.336	1.71E-04	5
Mir124-2hg	7.45E-09	-0.4535	0.072	0.28	2.09E-04	5
Slit2	7.69E-09	0.8795	0.328	0.176	2.15E-04	5
Sat1	8.21E-09	-0.4929	0.161	0.399	2.30E-04	5
2900026A02Rik	8.24E-09	0.2675	0.111	0.029	2.31E-04	5
Chst11	8.46E-09	-0.4479	0.25	0.492	2.37E-04	5
Ahi1	8.58E-09	0.4461	0.606	0.48	2.40E-04	5
Plch1	8.73E-09	0.4610	0.317	0.164	2.44E-04	5
Gm12239	8.74E-09	-0.3779	0.272	0.535	2.45E-04	5
Wasf3	8.82E-09	-0.4020	0.3	0.57	2.47E-04	5
Trib2	9.31E-09	-0.4537	0.033	0.217	2.61E-04	5
Mast4	9.40E-09	-0.4372	0.372	0.633	2.63E-04	5
Ap1s2	9.96E-09	0.3442	0.128	0.038	2.79E-04	5
Itpkb	1.08E-08	-0.5488	0.144	0.36	3.03E-04	5
Cadps2	1.18E-08	0.3732	0.15	0.049	3.31E-04	5
Pip5k1b	1.19E-08	0.3819	0.133	0.041	3.33E-04	5
Ubr5	1.31E-08	-0.3794	0.4	0.671	3.67E-04	5
Slc27a1	1.41E-08	-0.3461	0.294	0.573	3.95E-04	5
Cit	1.53E-08	-0.5977	0.061	0.246	4.28E-04	5
Mdga1	1.68E-08	0.5181	0.217	0.094	4.70E-04	5
Notch3	1.81E-08	-0.4636	0.078	0.271	5.08E-04	5
Ccnd2	1.82E-08	0.4279	0.228	0.102	5.11E-04	5
Psd2	1.96E-08	-0.4571	0.189	0.42	5.50E-04	5
Usp53	2.10E-08	-0.5227	0.172	0.395	5.88E-04	5
Cyfip1	2.19E-08	-0.4128	0.2	0.437	6.14E-04	5
Acsl6	2.31E-08	-0.4370	0.294	0.544	6.48E-04	5
Dlc1	2.34E-08	-0.5806	0.133	0.342	6.54E-04	5

Kcnj10	2.48E-08	-0.5041	0.106	0.312	6.94E-04	5
Agmo	2.64E-08	-0.4644	0.1	0.306	7.40E-04	5
Fam188b	2.70E-08	0.4268	0.244	0.115	7.56E-04	5
Plcl1	2.70E-08	-0.4350	0.272	0.525	7.57E-04	5
Otud7a	2.75E-08	-0.4787	0.106	0.316	7.69E-04	5
Adrbk2	3.03E-08	-0.3344	0.5	0.76	8.49E-04	5
Dner	3.05E-08	-0.4141	0.194	0.424	8.53E-04	5
Ptprk	3.08E-08	0.5563	0.261	0.125	8.62E-04	5
Mfhas1	3.09E-08	-0.4062	0.106	0.317	8.65E-04	5
Fam21	3.10E-08	-0.4578	0.128	0.338	8.67E-04	5
Cecr5	3.10E-08	-0.4477	0.111	0.314	8.68E-04	5
Igfbp5	3.24E-08	0.6838	0.222	0.1	9.06E-04	5
Arhgap5	3.39E-08	-0.3304	0.55	0.797	9.50E-04	5
Ccdc80	3.75E-08	0.4825	0.289	0.149	1.05E-03	5
2900052N01Rik	4.33E-08	-0.4687	0.006	0.156	1.21E-03	5
Hip1	4.34E-08	-0.3575	0.222	0.467	1.22E-03	5
Pter	4.39E-08	0.4657	0.178	0.071	1.23E-03	5
Plxnc1	4.55E-08	0.4567	0.261	0.128	1.27E-03	5
Cep126	4.57E-08	0.4124	0.211	0.091	1.28E-03	5
Gng12	4.75E-08	-0.3848	0.261	0.514	1.33E-03	5
Fsd1l	4.82E-08	0.4577	0.244	0.117	1.35E-03	5
Adcy8	4.93E-08	-0.5790	0.05	0.224	1.38E-03	5
Notch2	5.05E-08	0.5027	0.483	0.349	1.42E-03	5
Iqcg	5.31E-08	0.4070	0.144	0.049	1.49E-03	5
Rfx3	5.48E-08	0.4202	0.744	0.687	1.54E-03	5
Atp2c1	5.53E-08	-0.3839	0.228	0.47	1.55E-03	5
Cfap46	5.75E-08	0.6170	0.239	0.117	1.61E-03	5
Pfkp	5.89E-08	-0.4200	0.083	0.269	1.65E-03	5
Rai14	5.98E-08	0.2649	0.106	0.029	1.67E-03	5
Gm15520	6.01E-08	-0.4100	0.039	0.209	1.68E-03	5
D030047H15Rik	6.70E-08	-0.4343	0.194	0.424	1.88E-03	5
Atp13a5	6.84E-08	-0.4636	0.061	0.24	1.92E-03	5
Rab30	6.99E-08	-0.3313	0.422	0.709	1.96E-03	5
Nfix	7.33E-08	0.4324	0.494	0.358	2.05E-03	5
Ngef	8.73E-08	-0.4154	0.133	0.336	2.45E-03	5
Akt3	9.13E-08	0.3239	0.794	0.722	2.56E-03	5
Ttll5	9.25E-08	0.5045	0.389	0.247	2.59E-03	5
Aox1	9.44E-08	-0.4276	0.044	0.214	2.64E-03	5
Sorl1	1.05E-07	-0.3591	0.183	0.418	2.95E-03	5
Plekha5	1.09E-07	0.4928	0.483	0.349	3.06E-03	5
Fermt2	1.15E-07	-0.4144	0.367	0.611	3.22E-03	5
Cmya5	1.17E-07	0.4788	0.172	0.068	3.27E-03	5
Luzp2	1.20E-07	-0.4406	0.75	0.9	3.37E-03	5

Acot11	1.23E-07	-0.3850	0.15	0.369	3.43E-03	5
Aatk	1.25E-07	-0.3938	0.056	0.234	3.51E-03	5
Wwc1	1.28E-07	-0.3953	0.417	0.63	3.60E-03	5
Ptprg	1.31E-07	-0.3628	0.406	0.652	3.66E-03	5
Car2	1.32E-07	-0.3943	0.033	0.197	3.70E-03	5
Camk1d	1.40E-07	-0.3807	0.311	0.557	3.93E-03	5
Spred1	1.41E-07	-0.3596	0.233	0.475	3.94E-03	5
Actr3b	1.49E-07	-0.4156	0.044	0.211	4.17E-03	5
Slc38a3	1.50E-07	-0.4124	0.094	0.288	4.19E-03	5
Myrip	1.60E-07	-0.4275	0.133	0.335	4.47E-03	5
Mapk4	1.63E-07	-0.2989	0.461	0.708	4.55E-03	5
Mitf	1.64E-07	-0.4266	0.167	0.38	4.59E-03	5
Epha4	1.65E-07	0.4715	0.322	0.189	4.62E-03	5
Dlgap1	1.66E-07	-0.2601	0.783	0.956	4.65E-03	5
Intu	1.80E-07	0.4132	0.244	0.123	5.04E-03	5
1700112E06Rik	1.92E-07	-0.5589	0.2	0.399	5.37E-03	5
Agl	2.00E-07	-0.3359	0.267	0.499	5.60E-03	5
Spag6l	2.01E-07	0.3670	0.117	0.037	5.64E-03	5
Rreb1	2.12E-07	-0.3689	0.306	0.564	5.95E-03	5
Pik3r1	2.26E-07	-0.3829	0.317	0.544	6.32E-03	5
Fut8	2.28E-07	-0.3873	0.278	0.517	6.39E-03	5
Asap1	2.39E-07	-0.3268	0.522	0.763	6.70E-03	5
Rab34	2.40E-07	-0.3884	0.167	0.375	6.72E-03	5
Tmem44	2.58E-07	-0.4284	0.083	0.264	7.23E-03	5
Gm11417	2.67E-07	-0.3539	0.028	0.18	7.46E-03	5
Cdh4	2.68E-07	0.4355	0.289	0.156	7.50E-03	5
Cdc14a	2.68E-07	0.4160	0.428	0.287	7.51E-03	5
Eps15	2.91E-07	-0.3545	0.506	0.727	8.16E-03	5
Chst10	2.93E-07	-0.3432	0.078	0.26	8.21E-03	5
Sybu	3.06E-07	0.3175	0.722	0.664	8.56E-03	5
Braf	3.28E-07	0.3769	0.583	0.479	9.18E-03	5
Morn1	3.36E-07	0.4380	0.2	0.092	9.42E-03	5
Immp2l	3.52E-07	0.5055	0.45	0.301	9.85E-03	5
Sepp1	3.70E-07	-0.4068	0.044	0.204	0.0104	5
Mamdc2	4.10E-07	0.3924	0.156	0.06	0.0115	5
Myh14	4.11E-07	-0.3763	0.128	0.322	0.0115	5
Disc1	4.14E-07	-0.4035	0.017	0.156	0.0116	5
Anks1b	4.43E-07	0.5811	0.356	0.226	0.0124	5
Iqub	4.57E-07	0.3382	0.111	0.035	0.0128	5
Itgb8	4.80E-07	-0.3704	0.111	0.301	0.0134	5
Car10	4.82E-07	-0.6864	0.022	0.162	0.0135	5
Fyn	4.97E-07	-0.3615	0.294	0.525	0.0139	5
Slc25a18	5.04E-07	-0.4292	0.106	0.284	0.0141	5

Hapln1	5.06E-07	-0.3776	0.039	0.194	0.0142	5
Pdzd2	5.21E-07	0.4136	0.283	0.153	0.0146	5
2310022B05Rik	5.23E-07	-0.4149	0.061	0.224	0.0146	5
Nedd4l	5.28E-07	0.3827	0.744	0.656	0.0148	5
4930544l03Rik	5.30E-07	-0.4526	0.056	0.214	0.0148	5
Prkca	5.34E-07	-0.4692	0.239	0.45	0.0150	5
6430573F11Rik	5.57E-07	-0.4045	0.067	0.234	0.0156	5
Fgf14	5.71E-07	-0.2804	0.811	0.947	0.0160	5
Cd81	5.71E-07	-0.2822	0.244	0.492	0.0160	5
Adk	5.73E-07	-0.2520	0.528	0.751	0.0160	5
Caskin1	5.73E-07	-0.4147	0.233	0.443	0.0161	5
Dcdc2a	5.77E-07	0.4197	0.111	0.035	0.0161	5
Slc6a6	6.06E-07	0.4766	0.156	0.062	0.0170	5
Stambpl1	6.06E-07	-0.3915	0.083	0.255	0.0170	5
Dync2h1	6.16E-07	0.4565	0.456	0.33	0.0172	5
Shtn1	6.33E-07	0.3969	0.183	0.079	0.0177	5
Dgki	6.54E-07	0.4650	0.522	0.403	0.0183	5
Ttll3	6.68E-07	0.3242	0.144	0.055	0.0187	5
Sulf1	7.21E-07	0.4955	0.167	0.068	0.0202	5
Add3	7.50E-07	-0.3211	0.372	0.591	0.0210	5
Asrgl1	7.60E-07	-0.3696	0.306	0.543	0.0213	5
Timp4	7.63E-07	-0.3382	0.044	0.203	0.0214	5
Vwa8	8.26E-07	-0.3952	0.333	0.558	0.0231	5
Slc9a9	8.33E-07	-0.3158	0.222	0.446	0.0233	5
Cipc	8.34E-07	-0.4106	0.144	0.336	0.0233	5
Fndc3a	8.49E-07	0.3810	0.383	0.25	0.0238	5
Fam126a	8.65E-07	0.4083	0.278	0.153	0.0242	5
Ece1	8.75E-07	-0.3907	0.056	0.212	0.0245	5
Gli2	8.97E-07	-0.3640	0.339	0.573	0.0251	5
Ncan	9.35E-07	-0.3636	0.128	0.312	0.0262	5
Akap6	9.56E-07	0.3365	0.744	0.674	0.0268	5
Gm11099	1.00E-06	0.4002	0.194	0.087	0.0281	5
Pcx	1.02E-06	-0.3789	0.178	0.384	0.0284	5
Fam134b	1.03E-06	0.3621	0.294	0.165	0.0289	5
Plekhm2	1.09E-06	-0.3623	0.244	0.459	0.0305	5
Adam22	1.13E-06	0.3986	0.389	0.256	0.0318	5
St3gal4	1.17E-06	-0.2884	0.356	0.592	0.0328	5
Gm14964	1.19E-06	0.4226	0.589	0.478	0.0333	5
Slc30a10	1.20E-06	-0.3621	0.056	0.214	0.0335	5
Man1c1	1.23E-06	0.3453	0.244	0.128	0.0344	5
Gprc5b	1.23E-06	-0.3817	0.15	0.334	0.0346	5
Rabep1	1.26E-06	-0.3054	0.506	0.711	0.0353	5
Smurf1	1.31E-06	-0.3489	0.1	0.275	0.0367	5

Tbc1d10a	1.37E-06	-0.3573	0.028	0.167	0.0383	5
Mns1	1.38E-06	0.3988	0.156	0.064	0.0386	5
Iqck	1.41E-06	0.4960	0.35	0.225	0.0394	5
Timp3	1.43E-06	-0.3076	0.322	0.574	0.0399	5
Scn8a	1.46E-06	-0.3533	0.194	0.395	0.0410	5
Tmem117	1.47E-06	-0.4165	0.089	0.254	0.0410	5
Tra2a	1.47E-06	0.2995	0.728	0.693	0.0412	5
Maml3	1.49E-06	0.5344	0.328	0.199	0.0417	5
Dzip1l	1.55E-06	-0.3913	0.111	0.284	0.0435	5
Tom1	1.73E-06	-0.3348	0.15	0.345	0.0485	5
Grin3a	1.75E-06	-0.4454	0.044	0.189	0.0489	5
Slc2a13	1.84E-06	0.3918	0.261	0.14	0.0514	5
Kcnh7	1.85E-06	0.4537	0.206	0.1	0.0519	5
Cd9	1.87E-06	0.4133	0.322	0.201	0.0525	5
Rpgr	1.88E-06	0.3909	0.289	0.166	0.0525	5
Amot	1.92E-06	-0.3234	0.061	0.219	0.0539	5
Utrn	1.93E-06	-0.3060	0.433	0.651	0.0540	5
Mob3b	1.94E-06	0.5311	0.233	0.121	0.0542	5
Itpr1	1.95E-06	0.4229	0.361	0.238	0.0547	5
Prdm16	1.96E-06	0.4201	0.739	0.689	0.0548	5
Dync1i1	1.98E-06	0.2958	0.128	0.047	0.0553	5
Abi1	1.98E-06	-0.3313	0.389	0.611	0.0555	5
Sox11	2.05E-06	0.3069	0.128	0.047	0.0575	5
Snrk	2.11E-06	-0.3721	0.133	0.311	0.0592	5
App	2.18E-06	0.3880	0.478	0.361	0.0611	5
Gm15601	2.22E-06	-0.3397	0.022	0.153	0.0620	5
Slc6a9	2.26E-06	-0.3679	0.028	0.159	0.0632	5
Gm2163	2.43E-06	0.5514	0.294	0.179	0.0680	5
Mttp	2.49E-06	0.3653	0.306	0.179	0.0697	5
Dab2	2.55E-06	-0.4173	0.039	0.175	0.0713	5
Pde8b	2.80E-06	-0.3456	0.45	0.638	0.0783	5
Wdr34	2.82E-06	0.3319	0.189	0.087	0.0791	5
Rit2	2.94E-06	0.3103	0.128	0.048	0.0822	5
Setbp1	2.99E-06	0.4676	0.661	0.617	0.0836	5
Cxcl14	3.15E-06	-0.2747	0.028	0.159	0.0882	5
Spon1	3.29E-06	-0.3365	0.311	0.527	0.0922	5
Sh3pxd2b	3.33E-06	-0.3454	0.228	0.428	0.0931	5
Frmd5	3.33E-06	0.5258	0.161	0.069	0.0932	5
Ankrd6	3.37E-06	0.4192	0.489	0.359	0.0943	5
Dapp1	3.49E-06	0.5180	0.283	0.169	0.0976	5
Tmem178b	3.49E-06	-0.3551	0.272	0.478	0.0978	5

Supplemental Table 4.10. R6/2 12-Week Cortical Astrocyte Significant Differentially Expressed Genes Per Cluster

Gene	p_val	avg_logFC	pct.1	pct.2	p_val_adj	Cluster
Slc1a2	1.34E-38	-0.7730	0.924	0.971	3.76E-34	0
Clmn	7.09E-27	-0.8723	0.355	0.735	1.99E-22	0
Grin2c	8.63E-25	-0.9179	0.153	0.547	2.42E-20	0
Tspan7	4.00E-24	-0.6872	0.687	0.89	1.12E-19	0
Nrxn1	6.54E-23	-0.2757	1	0.992	1.83E-18	0
Ntm	1.02E-22	-0.3497	1	0.97	2.84E-18	0
Gm3764	6.65E-22	-0.5143	0.859	0.928	1.86E-17	0
Msi2	4.72E-21	-0.3673	0.981	0.977	1.32E-16	0
Lsamp	1.50E-20	-0.3181	1	0.996	4.20E-16	0
Qk	2.11E-20	-0.4851	0.863	0.943	5.91E-16	0
Mertk	1.23E-19	-0.6738	0.721	0.85	3.45E-15	0
Glul	1.50E-19	-0.5997	0.267	0.629	4.19E-15	0
Gnao1	1.75E-19	-0.5214	0.702	0.88	4.90E-15	0
Luzp2	2.36E-19	-0.6122	0.821	0.933	6.62E-15	0
Frmd4a	1.09E-17	-0.4243	0.939	0.939	3.06E-13	0
Cadm1	1.21E-17	-0.4511	0.851	0.941	3.38E-13	0
Gm26843	2.99E-17	-0.7742	0.179	0.491	8.36E-13	0
Plpp3	1.47E-15	-0.4259	0.729	0.876	4.12E-11	0
Atp1a2	5.34E-15	-0.4349	0.718	0.882	1.49E-10	0
Daam2	7.07E-15	-0.5974	0.382	0.651	1.98E-10	0
Slc4a4	1.32E-14	-0.4458	0.763	0.903	3.69E-10	0
St6galnac5	6.06E-14	-0.6457	0.431	0.67	1.70E-09	0
Kirrel3	1.32E-13	-0.4977	0.763	0.874	3.70E-09	0
Sparcl1	2.70E-13	-0.4338	0.634	0.832	7.56E-09	0
Phkg1	8.61E-13	-0.5020	0.55	0.777	2.41E-08	0
Gabbr2	1.63E-12	-0.7044	0.198	0.461	4.56E-08	0
D030055H07Rik	2.26E-12	-0.6855	0.011	0.192	6.32E-08	0
Irak2	3.54E-12	-0.5530	0.328	0.598	9.91E-08	0
Htra1	2.49E-11	-0.5514	0.366	0.621	6.97E-07	0
Gria2	2.72E-11	-0.3549	0.756	0.882	7.60E-07	0
Mical2	8.97E-11	-0.4300	0.328	0.615	2.51E-06	0
Prex2	1.25E-10	-0.3439	0.824	0.874	3.50E-06	0
Nwd1	2.48E-10	-0.4384	0.466	0.684	6.93E-06	0
Rgs20	3.64E-10	-0.2851	0.809	0.916	1.02E-05	0
Camk2g	4.62E-10	-0.4298	0.473	0.701	1.29E-05	0

Slc1a3	4.76E-10	-0.2928	0.935	0.96	1.33E-05	0
Mgat5	5.47E-10	-0.4843	0.389	0.615	1.53E-05	0
Pigk	6.37E-10	-0.4808	0.37	0.615	1.78E-05	0
Nhsl1	7.88E-10	-0.4313	0.641	0.77	2.21E-05	0
Cables1	2.06E-09	-0.4811	0.16	0.381	5.76E-05	0
Gm13872	2.23E-09	-0.5417	0.088	0.278	6.24E-05	0
Otud7a	2.29E-09	-0.4794	0.172	0.383	6.42E-05	0
Lama3	5.21E-09	-0.5845	0.103	0.286	0.0001	0
Rcan2	6.79E-09	-0.5727	0.149	0.343	0.0002	0
Trim9	7.20E-09	-0.3516	0.641	0.783	0.0002	0
Eps8	8.63E-09	-0.4787	0.416	0.63	0.0002	0
Ntsr2	9.42E-09	-0.3865	0.179	0.411	0.0003	0
Igsf8	1.24E-08	-0.4029	0.282	0.522	0.0003	0
Ttyh1	1.50E-08	-0.3545	0.508	0.726	0.0004	0
Farp1	1.64E-08	-0.2982	0.721	0.861	0.0005	0
Efr3b	2.09E-08	-0.3962	0.485	0.688	0.0006	0
Aifm3	2.32E-08	-0.4284	0.118	0.31	0.0007	0
Grm3	2.46E-08	-0.3526	0.821	0.876	0.0007	0
Cpeb4	2.65E-08	-0.4870	0.408	0.602	0.0007	0
Plcb1	3.41E-08	-0.3451	0.782	0.85	0.0010	0
Rapgef3	3.67E-08	-0.3990	0.309	0.533	0.0010	0
Acsl3	4.00E-08	-0.3667	0.366	0.604	0.0011	0
Dab1	4.45E-08	-0.3896	0.553	0.747	0.0012	0
Gldc	5.66E-08	-0.4207	0.271	0.486	0.0016	0
Gpm6b	5.67E-08	-0.2922	0.87	0.933	0.0016	0
Ogt	5.68E-08	0.4022	0.656	0.543	0.0016	0
Cit	6.85E-08	-0.4069	0.046	0.192	0.0019	0
Adam23	7.88E-08	-0.3907	0.21	0.429	0.0022	0
Kalrn	8.20E-08	-0.3804	0.531	0.707	0.0023	0
Trpm3	8.34E-08	-0.4873	0.729	0.81	0.0023	0
Dio2	8.42E-08	-0.4119	0.034	0.171	0.0024	0
D030047H15Rik	1.14E-07	-0.3163	0.191	0.398	0.0032	0
Rpe65	1.31E-07	-0.4444	0.011	0.124	0.0037	0
Egfem1	1.40E-07	-0.5120	0.061	0.206	0.0039	0
Pde8b	1.48E-07	-0.3468	0.5	0.703	0.0041	0
Cspg5	1.75E-07	-0.3195	0.679	0.817	0.0049	0
Sfxn5	1.86E-07	-0.2537	0.794	0.876	0.0052	0
Adcy2	2.03E-07	-0.3341	0.55	0.726	0.0057	0
Mfge8	2.30E-07	-0.4544	0.111	0.274	0.0065	0

Fam13c	2.44E-07	-0.3873	0.37	0.573	0.0068	0
Hif3a	2.90E-07	-0.4533	0.153	0.335	0.0081	0
Ttll8	3.32E-07	-0.3059	0.111	0.286	0.0093	0
Slc35f1	3.46E-07	0.4208	0.443	0.278	0.0097	0
Csrp1	3.62E-07	-0.3633	0.294	0.507	0.0101	0
Nt5c2	3.73E-07	-0.3610	0.233	0.427	0.0104	0
Angpt1	3.77E-07	0.4531	0.21	0.086	0.0106	0
Dclk1	4.01E-07	-0.2621	0.84	0.861	0.0112	0
Nckap5	4.30E-07	0.2902	0.859	0.842	0.0120	0
Sned1	4.37E-07	-0.4189	0.069	0.21	0.0122	0
Il1rapl1	4.98E-07	0.3043	0.844	0.785	0.0139	0
Gm26512	5.05E-07	-0.3880	0.122	0.29	0.0141	0
Abca1	5.11E-07	0.4764	0.504	0.371	0.0143	0
Fgfr3	5.84E-07	-0.4013	0.355	0.552	0.0164	0
Slc7a11	6.70E-07	-0.4957	0.37	0.564	0.0188	0
Phactr3	7.66E-07	-0.3492	0.515	0.693	0.0214	0
Caskin1	8.11E-07	-0.4549	0.221	0.398	0.0227	0
Acss2	8.29E-07	-0.4016	0.115	0.276	0.0232	0
4930544I03Rik	9.66E-07	-0.4235	0.145	0.31	0.0270	0
Sema4a	1.01E-06	-0.3634	0.061	0.2	0.0283	0
Tra2a	1.02E-06	0.4082	0.611	0.509	0.0287	0
Grik1	1.11E-06	-0.3537	0.019	0.126	0.0311	0
Lrrc8c	1.22E-06	-0.4701	0.073	0.208	0.0341	0
Arhgap5	1.32E-06	-0.3470	0.569	0.747	0.0369	0
Nol4	1.42E-06	-0.3309	0.435	0.644	0.0398	0
Arrb1	1.43E-06	-0.3798	0.187	0.371	0.0400	0
Robo2	1.50E-06	0.3722	0.546	0.377	0.0421	0
Dpyd	1.52E-06	0.4600	0.336	0.2	0.0425	0
Gm26704	1.82E-06	-0.3437	0.416	0.579	0.0508	0
Ddx5	2.13E-06	0.3892	0.561	0.44	0.0597	0
Msmo1	2.20E-06	-0.2782	0.107	0.263	0.0616	0
Ldlr	2.23E-06	-0.3658	0.115	0.27	0.0623	0
RP23-240M8.2	2.54E-06	0.5142	0.176	0.07	0.0712	0
Gja1	2.59E-06	-0.3558	0.233	0.423	0.0725	0
Aldh1l1	2.62E-06	-0.3206	0.179	0.354	0.0734	0
Emx2os	2.65E-06	-0.3484	0.229	0.408	0.0743	0
Fam20a	2.95E-06	-0.3200	0.263	0.453	0.0825	0
Fermt2	3.09E-06	-0.3224	0.469	0.648	0.0864	0
Hdac8	3.15E-06	-0.2580	0.721	0.836	0.0881	0

Slc1a2	7.61E-36	0.5980	1	0.935	2.13E-31	1
Ntm	2.46E-34	0.4095	1	0.97	6.89E-30	1
Luzp2	8.35E-33	0.6561	0.996	0.85	2.34E-28	1
Tspan7	1.79E-29	0.5797	0.988	0.746	5.00E-25	1
Gm3764	2.82E-29	0.5074	0.992	0.865	7.90E-25	1
Gnao1	4.43E-29	0.5624	0.984	0.746	1.24E-24	1
Frmd4a	1.47E-28	0.5046	1	0.911	4.11E-24	1
Gm26843	1.02E-27	0.7063	0.684	0.252	2.84E-23	1
Lsamp	4.55E-26	0.3326	1	0.996	1.27E-21	1
Nrxn1	1.10E-25	0.2762	1	0.993	3.08E-21	1
Grin2c	5.71E-25	0.7092	0.692	0.289	1.60E-20	1
Slc1a3	1.44E-24	0.4286	0.996	0.931	4.03E-20	1
Atp1a2	4.23E-24	0.4635	0.988	0.754	1.18E-19	1
Glul	6.45E-24	0.6295	0.777	0.385	1.80E-19	1
Clmn	8.42E-24	0.6316	0.87	0.489	2.36E-19	1
Mertk	3.13E-22	0.5249	0.951	0.741	8.76E-18	1
Slc4a4	4.15E-22	0.4339	0.992	0.794	1.16E-17	1
D030055H07Rik	4.50E-22	0.7646	0.304	0.054	1.26E-17	1
Qk	2.86E-21	0.4067	0.992	0.881	8.02E-17	1
Cadm1	4.59E-21	0.4433	0.988	0.876	1.28E-16	1
Gldc	1.45E-20	0.6378	0.668	0.298	4.06E-16	1
Nwd1	1.99E-19	0.5246	0.834	0.509	5.56E-15	1
Phkg1	5.88E-19	0.4997	0.903	0.609	1.65E-14	1
Kirrel3	6.86E-19	0.4578	0.972	0.776	1.92E-14	1
St6galnac5	7.74E-19	0.6376	0.785	0.502	2.17E-14	1
Prex2	9.65E-19	0.3985	0.972	0.806	2.70E-14	1
Lama3	1.86E-18	0.7434	0.413	0.139	5.19E-14	1
Irak2	4.31E-17	0.5618	0.737	0.404	1.21E-12	1
Grm3	5.21E-17	0.3917	0.968	0.807	1.46E-12	1
Msi2	7.47E-17	0.2766	0.996	0.97	2.09E-12	1
Ctnnd2	3.43E-16	0.2676	1	0.976	9.60E-12	1
4930544I03Rik	3.45E-16	0.5743	0.449	0.167	9.66E-12	1
Nhsl1	3.70E-16	0.4715	0.895	0.65	1.04E-11	1
Plpp3	6.51E-16	0.3623	0.96	0.767	1.82E-11	1
Daam2	7.76E-16	0.5213	0.769	0.467	2.17E-11	1
Eps8	1.33E-15	0.5135	0.781	0.457	3.72E-11	1
Pigk	1.42E-15	0.6632	0.741	0.439	3.98E-11	1
Rgs20	2.94E-15	0.3410	0.98	0.835	8.23E-11	1
Gria2	4.68E-15	0.3490	0.972	0.78	1.31E-10	1

Cspg5	7.39E-15	0.4054	0.931	0.698	2.07E-10	1
Mgat5	2.72E-14	0.5017	0.725	0.456	7.63E-10	1
Gabrb1	2.77E-14	0.2757	1	0.926	7.76E-10	1
Sparcl1	6.63E-14	0.3718	0.939	0.687	1.85E-09	1
Rpe65	7.59E-14	0.4933	0.198	0.035	2.12E-09	1
Gm26512	7.63E-14	0.5016	0.409	0.154	2.14E-09	1
Ntsr2	1.46E-13	0.4530	0.543	0.239	4.09E-09	1
Unc13c	1.79E-13	0.5655	0.672	0.407	5.01E-09	1
Slco1c1	2.05E-13	0.4061	0.826	0.537	5.73E-09	1
Cpeb4	3.95E-13	0.4647	0.709	0.459	1.10E-08	1
S1pr1	4.03E-13	0.3999	0.494	0.207	1.13E-08	1
Rcan2	5.39E-13	0.5321	0.453	0.198	1.51E-08	1
Emx2os	6.12E-13	0.4922	0.538	0.261	1.71E-08	1
Trpm3	6.23E-13	0.3306	0.923	0.719	1.74E-08	1
Rgs6	6.91E-13	0.4048	0.879	0.631	1.93E-08	1
Trim9	1.09E-12	0.3326	0.891	0.665	3.05E-08	1
Ranbp3l	1.53E-12	0.4589	0.393	0.15	4.28E-08	1
Gabbr2	3.93E-12	0.4968	0.563	0.287	1.10E-07	1
Mgll	6.53E-12	0.4229	0.866	0.624	1.83E-07	1
Aox1	7.33E-12	0.5057	0.344	0.13	2.05E-07	1
Htra1	7.35E-12	0.4175	0.729	0.448	2.06E-07	1
Fgfr3	9.16E-12	0.4523	0.7	0.389	2.57E-07	1
Rapgef3	1.33E-11	0.4439	0.64	0.376	3.72E-07	1
Pde8b	1.33E-11	0.4142	0.794	0.563	3.73E-07	1
Dpf3	2.52E-11	0.4215	0.648	0.4	7.05E-07	1
Dclk1	2.95E-11	0.3341	0.951	0.809	8.26E-07	1
Syne1	4.13E-11	0.3648	0.842	0.604	1.16E-06	1
Gja1	4.33E-11	0.3773	0.555	0.27	1.21E-06	1
Phactr3	8.00E-11	0.3842	0.814	0.552	2.24E-06	1
Igsf8	8.85E-11	0.3173	0.652	0.346	2.48E-06	1
Rorb	9.93E-11	0.3686	0.964	0.839	2.78E-06	1
Arhgap5	1.03E-10	0.3747	0.858	0.609	2.87E-06	1
Camk2g	1.28E-10	0.3873	0.794	0.548	3.59E-06	1
Prex1	1.42E-10	0.4404	0.619	0.35	3.98E-06	1
Acsl3	1.58E-10	0.3377	0.725	0.433	4.43E-06	1
Bcan	1.90E-10	0.3668	0.741	0.476	5.32E-06	1
Sfxn5	2.22E-10	0.2631	0.939	0.807	6.22E-06	1
Hes5	2.56E-10	0.4347	0.417	0.191	7.17E-06	1
Pla2g7	2.72E-10	0.3836	0.733	0.47	7.63E-06	1

Sema4a	2.81E-10	0.4383	0.279	0.096	7.86E-06	1
Lgr4	3.71E-10	0.4451	0.474	0.239	1.04E-05	1
Fnbp1	4.75E-10	0.3012	0.96	0.785	1.33E-05	1
Rbms1	5.06E-10	0.3678	0.433	0.213	1.42E-05	1
Pcdh7	5.76E-10	0.2799	0.947	0.811	1.61E-05	1
Prdm16	9.81E-10	0.3495	0.826	0.607	2.75E-05	1
Grik1	1.40E-09	0.3792	0.182	0.048	3.91E-05	1
Wdr17	1.81E-09	0.2597	0.996	0.972	5.07E-05	1
Ltbp1	2.02E-09	0.4080	0.344	0.146	5.65E-05	1
Pdzph1	2.56E-09	0.4579	0.393	0.183	7.16E-05	1
Adrbk2	2.91E-09	0.3554	0.757	0.504	8.14E-05	1
St3gal4	3.91E-09	0.4394	0.623	0.409	0.0001	1
Adcy2	4.05E-09	0.3467	0.81	0.602	0.0001	1
Gli3	8.31E-09	0.2838	0.846	0.648	0.0002	1
Slc7a11	1.01E-08	0.4240	0.652	0.43	0.0003	1
Chrdl1	1.02E-08	0.3253	0.206	0.065	0.0003	1
Fam20a	1.06E-08	0.3124	0.559	0.313	0.0003	1
Gm13872	1.22E-08	0.4242	0.344	0.156	0.0003	1
Caskin1	1.77E-08	0.4096	0.494	0.269	0.0005	1
Gm26704	1.80E-08	0.3153	0.68	0.454	0.0005	1
Cyp4f13	2.27E-08	0.3211	0.194	0.059	0.0006	1
Fam184b	2.37E-08	0.3152	0.324	0.141	0.0007	1
Meg3	2.45E-08	-0.7404	0.68	0.752	0.0007	1
Appl2	4.08E-08	0.3295	0.798	0.585	0.0011	1
Ptchd4	4.21E-08	0.3862	0.636	0.415	0.0012	1
Slc35f1	4.38E-08	-0.6374	0.211	0.389	0.0012	1
Prodh	4.46E-08	0.3707	0.381	0.185	0.0012	1
Cadps	4.60E-08	-0.7430	0.069	0.219	0.0013	1
Gm44151	5.21E-08	0.4071	0.502	0.291	0.0015	1
Lypd6	5.73E-08	0.3902	0.49	0.276	0.0016	1
Nsmf	7.03E-08	0.3381	0.328	0.152	0.0020	1
Arhgef19	7.31E-08	0.3290	0.425	0.22	0.0020	1
Ahcyl1	7.33E-08	0.3502	0.595	0.369	0.0021	1
Pbxip1	7.71E-08	0.3199	0.381	0.185	0.0022	1
Efr3b	7.77E-08	0.2888	0.781	0.546	0.0022	1
Sned1	9.10E-08	0.3362	0.271	0.113	0.0025	1
Fermt2	9.93E-08	0.3685	0.725	0.526	0.0028	1
Abhd3	1.05E-07	0.3194	0.356	0.17	0.0030	1
Hivep3	1.09E-07	0.2772	0.874	0.689	0.0030	1

Otc	1.09E-07	0.3969	0.15	0.041	0.0031	1
Sh3pxd2b	1.13E-07	0.3852	0.397	0.202	0.0032	1
Mtss1l	1.23E-07	0.2818	0.648	0.391	0.0034	1
Dio2	1.29E-07	0.3044	0.223	0.081	0.0036	1
Chrna7	1.36E-07	0.3532	0.126	0.03	0.0038	1
Hdac8	1.45E-07	0.2510	0.915	0.744	0.0041	1
Bmp2k	1.57E-07	0.3569	0.449	0.248	0.0044	1
Ldlr	1.65E-07	0.3057	0.344	0.161	0.0046	1
Fam13c	2.01E-07	0.3318	0.652	0.439	0.0056	1
Ephb1	2.04E-07	0.3547	0.652	0.433	0.0057	1
4930448N21Rik	2.05E-07	0.2811	0.785	0.574	0.0057	1
Gm44257	3.08E-07	0.3114	0.47	0.267	0.0086	1
Csrp1	3.23E-07	0.2794	0.591	0.365	0.0090	1
Kif21a	3.30E-07	-0.5378	0.36	0.496	0.0092	1
Gm29260	3.68E-07	-0.6431	0.004	0.107	0.0103	1
Ttll8	4.49E-07	0.2818	0.352	0.17	0.0126	1
Swap70	4.77E-07	0.3207	0.405	0.213	0.0134	1
Adra1a	4.96E-07	0.3123	0.389	0.2	0.0139	1
Rgs7	6.01E-07	0.2591	0.891	0.731	0.0168	1
Pmp22	8.26E-07	0.2821	0.126	0.033	0.0231	1
Tef	8.64E-07	0.3202	0.437	0.239	0.0242	1
Etv4	8.65E-07	0.2990	0.441	0.243	0.0242	1
F3	9.02E-07	0.2753	0.615	0.38	0.0253	1
C030018K13Rik	1.10E-06	0.2675	0.215	0.083	0.0307	1
Slc25a18	1.21E-06	0.2733	0.429	0.233	0.0338	1
Nphs1	1.35E-06	0.2665	0.138	0.041	0.0377	1
Tprkb	1.69E-06	0.3397	0.506	0.311	0.0473	1
Dlc1	1.83E-06	0.3278	0.381	0.215	0.0512	1
Msmo1	1.85E-06	0.2863	0.324	0.159	0.0519	1
Gabra2	1.86E-06	0.3310	0.692	0.489	0.0522	1
Ndrg2	1.92E-06	0.2821	0.482	0.274	0.0538	1
Gm15520	2.05E-06	0.3357	0.32	0.165	0.0573	1
Cep85l	2.53E-06	0.2584	0.623	0.419	0.0709	1
Vegfa	2.70E-06	0.2795	0.344	0.178	0.0756	1
Ccdc18	2.77E-06	0.2650	0.142	0.044	0.0776	1
Ptn	3.34E-06	0.3009	0.769	0.646	0.0935	1
Slc1a2	4.49E-14	0.3844	0.994	0.944	1.26E-09	2
Mertk	9.51E-12	0.4137	0.922	0.773	2.66E-07	2
Qk	2.08E-11	0.3545	0.966	0.901	5.82E-07	2

Farp1	3.19E-11	0.3933	0.922	0.783	8.93E-07	2
Gm3764	4.57E-11	0.3287	0.989	0.88	1.28E-06	2
Sparcl1	2.22E-10	0.3770	0.888	0.73	6.22E-06	2
Plpp3	6.18E-10	0.3341	0.939	0.794	1.73E-05	2
Clmn	2.18E-09	0.3811	0.777	0.559	6.11E-05	2
Tspan7	3.47E-09	0.3794	0.939	0.788	9.71E-05	2
Cables1	1.59E-08	0.4997	0.458	0.263	0.0004	2
Phkg1	2.04E-08	0.3732	0.849	0.658	0.0006	2
Paqr8	2.46E-08	0.4432	0.693	0.516	0.0007	2
Cpe	4.66E-08	0.3043	0.972	0.888	0.0013	2
Dab1	5.43E-08	0.4226	0.816	0.643	0.0015	2
Rgs20	1.24E-07	0.2557	0.983	0.85	0.0035	2
Prex2	1.38E-07	0.2875	0.955	0.829	0.0039	2
Fry	1.97E-07	0.4483	0.693	0.546	0.0055	2
Il1rapl1	8.47E-07	-0.3678	0.737	0.824	0.0237	2
Lhfp	1.11E-06	0.5074	0.575	0.429	0.0312	2
Daam2	1.12E-06	0.3217	0.693	0.523	0.0314	2
Atp1a2	1.22E-06	0.2829	0.944	0.793	0.0342	2
Etnppl	1.37E-06	0.4391	0.201	0.077	0.0384	2
D030047H15Rik	1.59E-06	0.4006	0.453	0.293	0.0446	2
Sfxn5	1.63E-06	0.2636	0.933	0.824	0.0457	2
Gpr37l1	1.96E-06	0.4138	0.346	0.199	0.0548	2
Efr3b	2.08E-06	0.3433	0.726	0.589	0.0583	2
Grin2c	2.69E-06	0.3500	0.547	0.377	0.0753	2
Ntm	2.61E-24	-0.8835	0.781	1	7.31E-20	3
Gpc5	2.89E-24	-0.9731	0.753	0.997	8.09E-20	3
Lsamp	1.35E-19	-0.6268	0.973	1	3.77E-15	3
Phkg1	5.72E-18	-1.3124	0.164	0.756	1.60E-13	3
Gm3764	1.08E-17	-0.9948	0.534	0.943	3.02E-13	3
Dscaml1	2.74E-17	1.4821	0.301	0.045	7.68E-13	3
Prex2	1.49E-16	-0.9094	0.329	0.912	4.18E-12	3
Adgrv1	1.61E-16	1.1161	0.288	0.043	4.51E-12	3
Grm3	8.73E-16	-0.9037	0.452	0.899	2.44E-11	3
Tspan7	1.43E-15	-1.0557	0.397	0.866	4.01E-11	3
Frmd4a	2.62E-15	-0.8261	0.616	0.972	7.34E-11	3
Mertk	5.51E-15	-0.8385	0.342	0.854	1.54E-10	3
Nhsl1	7.90E-15	-1.0318	0.233	0.777	2.21E-10	3
Nwd1	3.11E-14	-1.0399	0.123	0.661	8.71E-10	3
Mdga2	4.14E-14	-0.6072	0.658	0.964	1.16E-09	3

Nrxn1	6.27E-14	-0.5006	0.945	1	1.76E-09	3
Atp1a2	1.03E-13	-0.8316	0.397	0.871	2.87E-09	3
Phactr3	1.29E-13	-1.0885	0.178	0.681	3.61E-09	3
Gabrb1	1.30E-13	-0.6695	0.671	0.978	3.65E-09	3
Mgll	2.06E-13	-1.0609	0.247	0.746	5.76E-09	3
Gli3	4.89E-13	-0.8245	0.26	0.756	1.37E-08	3
Rgs7	9.27E-13	-0.8792	0.342	0.826	2.59E-08	3
Slc1a3	1.13E-12	-0.6658	0.781	0.969	3.16E-08	3
Slc1a2	1.40E-12	-0.7770	0.808	0.971	3.92E-08	3
Sparcl1	1.99E-12	-0.8360	0.301	0.814	5.58E-08	3
Grid2	2.35E-12	-0.7263	0.548	0.931	6.57E-08	3
Rorb	2.66E-12	-0.7807	0.493	0.917	7.45E-08	3
Eps8	2.69E-12	-0.8905	0.11	0.605	7.53E-08	3
Gnao1	2.84E-12	-0.8317	0.466	0.857	7.96E-08	3
Kirrel3	3.21E-12	-0.7960	0.466	0.875	9.00E-08	3
Farp1	6.93E-12	-0.7906	0.411	0.856	1.94E-07	3
Rgs20	1.42E-11	-0.6807	0.562	0.913	3.98E-07	3
Pla2g7	2.78E-11	-0.9154	0.137	0.595	7.79E-07	3
Qk	2.80E-11	-0.6795	0.699	0.938	7.84E-07	3
Slc4a4	3.03E-11	-0.5152	0.452	0.898	8.49E-07	3
Unc13c	3.04E-11	-1.1621	0.082	0.532	8.51E-07	3
Nrcam	3.21E-11	-0.6506	0.479	0.882	8.98E-07	3
Arhgap26	3.28E-11	-0.7658	0.384	0.829	9.20E-07	3
B3galt1	3.75E-11	-0.6033	0.671	0.955	1.05E-06	3
Dclk1	4.49E-11	-0.7008	0.521	0.888	1.26E-06	3
Acsbg1	1.22E-10	-0.8532	0.219	0.657	3.41E-06	3
Bcan	1.29E-10	-0.9074	0.164	0.599	3.61E-06	3
Cadm1	1.69E-10	-0.5807	0.685	0.934	4.73E-06	3
St6galnac5	2.41E-10	-1.0466	0.205	0.63	6.74E-06	3
Cpe	2.43E-10	-0.5599	0.589	0.94	6.81E-06	3
Pcdh7	3.91E-10	-0.4366	0.452	0.895	1.10E-05	3
Adgrb3	7.31E-10	-0.4600	0.699	0.987	2.05E-05	3
Macf1	1.01E-09	-0.4593	0.836	0.986	2.83E-05	3
Gria2	1.04E-09	-0.4962	0.493	0.875	2.92E-05	3
F3	1.06E-09	-0.9234	0.082	0.492	2.97E-05	3
Glul	1.12E-09	-0.8827	0.137	0.546	3.13E-05	3
Grin2c	1.29E-09	-0.8977	0.055	0.452	3.62E-05	3
Ctnnd2	1.39E-09	-0.4191	0.863	0.996	3.89E-05	3
Plpp3	1.39E-09	-0.5706	0.438	0.867	3.90E-05	3

Atp13a4	2.07E-09	-0.9574	0.027	0.394	5.78E-05	3
Clmn	2.41E-09	-0.7391	0.205	0.65	6.76E-05	3
Ptchd4	2.57E-09	-0.8424	0.11	0.522	7.20E-05	3
Vcl	3.44E-09	-0.7772	0.151	0.574	9.64E-05	3
Fnbp1	4.68E-09	-0.5219	0.493	0.875	0.0001	3
Zfp536	6.84E-09	0.6991	0.151	0.022	0.0002	3
Gpm6a	8.46E-09	-0.5386	0.384	0.796	0.0002	3
Paqr8	1.01E-08	-0.7761	0.205	0.592	0.0003	3
Gabbr2	1.06E-08	-1.0876	0.055	0.406	0.0003	3
Emx2os	1.25E-08	-0.7752	0.027	0.381	0.0004	3
Tmem132b	1.32E-08	0.9860	0.342	0.12	0.0004	3
Pak3	1.36E-08	1.0102	0.247	0.064	0.0004	3
Gm29260	1.36E-08	1.3771	0.233	0.059	0.0004	3
Grip1	1.39E-08	-0.9099	0.151	0.535	0.0004	3
Gabbr1	1.55E-08	-0.7126	0.164	0.562	0.0004	3
Htra1	1.65E-08	-0.7828	0.164	0.574	0.0005	3
Sfxn5	1.66E-08	-0.5183	0.521	0.882	0.0005	3
Csgalnact1	1.70E-08	-0.6857	0.274	0.688	0.0005	3
Itga6	1.73E-08	-0.7773	0.096	0.471	0.0005	3
Dpf3	1.80E-08	-0.6356	0.123	0.514	0.0005	3
Mgat4c	1.92E-08	-0.9204	0.123	0.506	0.0005	3
Rapgef3	2.09E-08	-0.8151	0.123	0.493	0.0006	3
Luzp2	2.17E-08	-0.5974	0.671	0.919	0.0006	3
Camk2g	2.24E-08	-0.6596	0.274	0.661	0.0006	3
Anks1b	2.45E-08	0.9575	0.425	0.175	0.0007	3
Daam2	2.48E-08	-0.7419	0.219	0.597	0.0007	3
Sncaip	2.52E-08	1.0245	0.288	0.091	0.0007	3
Pigk	3.11E-08	-0.8008	0.178	0.57	0.0009	3
Ank2	3.34E-08	-0.4645	0.726	0.972	0.0009	3
Plcb1	3.57E-08	-0.5766	0.466	0.864	0.0010	3
Cdh10	4.48E-08	-0.6416	0.342	0.731	0.0013	3
Rbl1	4.92E-08	0.4523	0.11	0.013	0.0014	3
Fry	5.24E-08	-0.7669	0.233	0.615	0.0015	3
Wdr17	7.06E-08	-0.4412	0.863	0.992	0.0020	3
Myo6	7.73E-08	-0.4652	0.452	0.843	0.0022	3
Hivep3	8.37E-08	-0.4420	0.356	0.787	0.0023	3
Pde7b	9.38E-08	-0.6602	0.192	0.566	0.0026	3
Grid1	9.64E-08	-0.6019	0.192	0.576	0.0027	3
Fut9	1.02E-07	-0.5508	0.192	0.588	0.0029	3

Apba2	1.14E-07	-0.5767	0.233	0.629	0.0032	3
Pde8b	1.17E-07	-0.6209	0.288	0.671	0.0033	3
Sorcs2	1.20E-07	-0.7348	0.137	0.489	0.0034	3
Cml3	1.38E-07	-0.7806	0.082	0.419	0.0039	3
Fgf1	1.39E-07	-0.8780	0.041	0.353	0.0039	3
Gm26704	1.41E-07	-0.5046	0.164	0.562	0.0039	3
Fam13c	1.69E-07	-0.6496	0.178	0.539	0.0047	3
Gldc	1.74E-07	-0.8119	0.11	0.445	0.0049	3
Gm26843	1.86E-07	-0.8208	0.082	0.419	0.0052	3
Syne1	2.70E-07	-0.3638	0.329	0.714	0.0075	3
Dtna	2.92E-07	-0.3289	0.658	0.947	0.0082	3
Irak2	3.15E-07	-0.5335	0.178	0.542	0.0088	3
Dbx2	3.21E-07	-0.5489	0.055	0.364	0.0090	3
Pnpla7	3.24E-07	-0.6615	0.082	0.424	0.0091	3
Appl2	3.50E-07	-0.5416	0.288	0.689	0.0098	3
Lgr4	3.54E-07	-0.7954	0.041	0.34	0.0099	3
Celrr	3.93E-07	-0.4233	0.068	0.384	0.0110	3
Fgfr3	4.11E-07	-0.5675	0.164	0.52	0.0115	3
Slco1c1	4.83E-07	-0.3605	0.247	0.667	0.0135	3
Specc1	4.90E-07	-0.6776	0.192	0.514	0.0137	3
Efr3b	5.10E-07	-0.4834	0.26	0.657	0.0143	3
Slc39a12	5.42E-07	-0.6251	0.233	0.598	0.0152	3
Prex1	5.97E-07	-0.6358	0.123	0.466	0.0167	3
Fermt2	7.74E-07	-0.6811	0.288	0.619	0.0217	3
Megf10	8.28E-07	-0.5829	0.123	0.441	0.0232	3
Tspan18	9.21E-07	0.6385	0.123	0.021	0.0258	3
Htr2c	1.22E-06	1.7192	0.11	0.017	0.0341	3
Trim9	1.23E-06	-0.2961	0.37	0.773	0.0343	3
Pitpnc1	1.25E-06	-0.3936	0.63	0.943	0.0351	3
Mmd2	1.32E-06	-0.4138	0.26	0.634	0.0370	3
Abr	1.34E-06	-0.4872	0.411	0.787	0.0376	3
Tnik	1.39E-06	-0.4131	0.616	0.93	0.0390	3
Nebl	1.66E-06	-0.5190	0.425	0.779	0.0463	3
Gabra2	1.67E-06	-0.6416	0.247	0.584	0.0467	3
Arhgef19	2.03E-06	-0.6801	0.041	0.31	0.0568	3
Arhgef12	2.15E-06	-0.4410	0.384	0.766	0.0603	3
Hdac8	2.23E-06	-0.3952	0.466	0.832	0.0625	3
Slc7a11	2.41E-06	-0.7656	0.205	0.529	0.0674	3
Arhgap5	2.45E-06	-0.4778	0.356	0.721	0.0687	3

Kcnma1	2.74E-06	-0.6660	0.164	0.489	0.0767	3
Glud1	2.75E-06	-0.5000	0.288	0.647	0.0770	3
Etv4	2.90E-06	-0.7338	0.055	0.331	0.0811	3
Slc6a11	2.92E-06	-0.5574	0.164	0.493	0.0819	3
Spata13	3.07E-06	0.7518	0.11	0.018	0.0859	3
Vav3	3.07E-06	-0.6875	0.082	0.364	0.0859	3
Psd2	3.15E-06	-0.6392	0.027	0.293	0.0883	3
Rapgef5	1.65E-104	1.3112	0.846	0.011	4.61E-100	4
Nrg3os	7.82E-103	1.7225	1	0.022	2.19E-98	4
Gm20642	7.75E-91	1.6163	0.885	0.02	2.17E-86	4
4921534H16Rik	5.33E-86	0.7141	0.5	0	1.49E-81	4
Pcnxl2	5.20E-79	0.7728	0.769	0.016	1.46E-74	4
Fstl4	2.09E-75	1.4175	0.846	0.025	5.84E-71	4
Prmt8	4.44E-75	0.8207	0.615	0.008	1.24E-70	4
Nyap2	7.71E-75	1.1060	0.769	0.018	2.16E-70	4
Cacng2	2.82E-74	0.9656	0.692	0.013	7.89E-70	4
Gm1992	8.06E-73	0.7582	0.577	0.007	2.26E-68	4
Rbfox3	4.37E-71	1.5404	0.962	0.041	1.22E-66	4
Gm11418	8.77E-71	0.5527	0.538	0.005	2.46E-66	4
Lrrc3b	1.05E-70	0.5239	0.538	0.005	2.94E-66	4
Fam189a1	1.57E-70	1.4585	0.885	0.033	4.39E-66	4
Ksr2	1.80E-70	1.1573	0.846	0.028	5.05E-66	4
Tmem132d	5.69E-70	1.6016	0.846	0.03	1.59E-65	4
Sptbn4	1.19E-69	1.0578	0.731	0.018	3.33E-65	4
Ccdc64	3.76E-69	0.7697	0.769	0.021	1.05E-64	4
Mtus2	1.87E-67	1.0894	0.808	0.026	5.23E-63	4
Oprm1	5.11E-67	1.0415	0.731	0.02	1.43E-62	4
Cacng3	5.40E-66	0.8670	0.692	0.017	1.51E-61	4
Lin7a	1.44E-65	0.8081	0.615	0.012	4.02E-61	4
Gm15810	1.46E-64	0.6293	0.5	0.005	4.08E-60	4
Dscam	3.50E-64	1.5685	0.962	0.049	9.80E-60	4
Zfyve28	6.15E-64	0.9133	0.692	0.018	1.72E-59	4
Add2	1.29E-63	0.9070	0.692	0.018	3.60E-59	4
Myt1l	9.02E-63	1.7733	1	0.059	2.53E-58	4
Mlip	1.89E-62	1.1019	0.769	0.026	5.31E-58	4
A930011G23Rik	1.91E-62	1.1077	0.692	0.02	5.35E-58	4
Mirg	2.31E-62	0.7396	0.577	0.011	6.48E-58	4
Hecw2	9.27E-62	1.6457	0.923	0.047	2.60E-57	4
Lrfn2	1.27E-61	1.0883	0.654	0.017	3.56E-57	4

Kcnh1	1.02E-60	0.9688	0.731	0.024	2.87E-56	4
Fam135b	1.25E-60	1.0856	0.808	0.032	3.50E-56	4
Clvs1	1.54E-60	0.7524	0.654	0.017	4.31E-56	4
Ica1	1.59E-60	0.9748	0.769	0.028	4.46E-56	4
Ryr2	5.93E-59	1.8611	1	0.068	1.66E-54	4
Kcnj6	1.04E-58	0.8673	0.654	0.018	2.92E-54	4
Socs2	1.77E-58	0.4839	0.462	0.005	4.96E-54	4
Pgbd5	4.36E-58	0.6909	0.654	0.018	1.22E-53	4
Hecw1	4.92E-58	1.4505	0.846	0.041	1.38E-53	4
Pak7	1.39E-57	1.3520	0.923	0.05	3.91E-53	4
Jakmip3	5.97E-57	0.6338	0.538	0.011	1.67E-52	4
Atp2b3	7.71E-57	0.5680	0.577	0.013	2.16E-52	4
Sez6l	2.12E-56	1.0696	0.769	0.032	5.95E-52	4
Csrnp3	9.16E-56	1.1063	0.808	0.037	2.57E-51	4
Kctd16	9.92E-56	2.0295	1	0.075	2.78E-51	4
Rit2	2.58E-55	0.8452	0.731	0.028	7.22E-51	4
Ralyl	3.21E-55	0.9484	0.769	0.032	8.99E-51	4
Rimbp2	8.89E-55	1.1064	0.808	0.037	2.49E-50	4
Gm15414	9.21E-55	0.6095	0.462	0.007	2.58E-50	4
Gm15398	9.22E-55	1.1652	0.577	0.014	2.58E-50	4
Dlgap3	1.60E-54	0.8316	0.654	0.021	4.49E-50	4
Cacna1b	2.97E-54	0.9495	0.731	0.029	8.30E-50	4
Rapgef4os1	3.58E-54	0.6664	0.538	0.012	1.00E-49	4
Zfp385b	5.42E-54	1.2853	0.885	0.049	1.52E-49	4
Slit3	8.74E-54	1.5541	0.885	0.051	2.45E-49	4
Zmat4	1.13E-53	1.1959	0.692	0.026	3.16E-49	4
Shank2	1.32E-53	1.2182	0.885	0.049	3.69E-49	4
Fndc9	5.03E-53	0.9390	0.692	0.026	1.41E-48	4
Clstn2	1.10E-52	1.6826	0.846	0.049	3.07E-48	4
Sidt1	3.64E-52	1.0929	0.731	0.032	1.02E-47	4
Brinp1	3.88E-52	1.4946	0.923	0.06	1.09E-47	4
Grin2a	4.31E-52	2.2390	1	0.088	1.21E-47	4
Dlgap2	4.46E-52	2.2985	0.962	0.078	1.25E-47	4
Chrm3	5.83E-52	1.6926	0.885	0.054	1.63E-47	4
Car10	5.92E-52	2.1214	1	0.084	1.66E-47	4
Ppfia2	6.74E-52	1.5175	0.923	0.059	1.89E-47	4
Spock1	2.57E-51	1.6623	0.885	0.058	7.21E-47	4
Nell1	2.74E-51	1.4873	0.654	0.025	7.67E-47	4
Nwd2	7.38E-51	1.1517	0.615	0.021	2.07E-46	4

Osbp2	7.99E-51	0.7954	0.769	0.035	2.24E-46	4
Cabp1	1.05E-50	0.8351	0.692	0.028	2.95E-46	4
Stxbp5l	1.28E-50	1.7067	0.962	0.071	3.58E-46	4
Camk2a	2.27E-50	1.6158	1	0.079	6.36E-46	4
2900055J20Rik	2.33E-50	0.9525	0.769	0.037	6.52E-46	4
Kcnb2	2.40E-50	2.0630	0.885	0.062	6.72E-46	4
Cntn3	2.71E-50	1.4435	0.846	0.051	7.59E-46	4
Crhr1	2.95E-50	0.4451	0.385	0.004	8.25E-46	4
Dnajc6	2.12E-49	1.1721	0.846	0.049	5.94E-45	4
Rnf165	2.65E-49	0.6102	0.538	0.014	7.42E-45	4
Ephb2	2.65E-49	0.5209	0.538	0.014	7.42E-45	4
Xkr4	2.72E-49	2.0082	1	0.092	7.62E-45	4
Cacna1e	5.37E-49	1.5876	0.923	0.066	1.50E-44	4
D430041D05Rik	6.16E-49	1.3570	0.808	0.046	1.73E-44	4
Cacna1i	7.81E-49	0.4598	0.423	0.007	2.19E-44	4
Sntg1	8.97E-49	1.7506	0.962	0.076	2.51E-44	4
Gm28905	9.35E-49	0.5872	0.5	0.012	2.62E-44	4
Gm12002	2.05E-48	0.4423	0.346	0.003	5.73E-44	4
Dync1i1	4.20E-48	1.2700	0.769	0.042	1.17E-43	4
Syt16	7.87E-48	0.9065	0.731	0.035	2.20E-43	4
Tmem108	1.02E-47	1.1798	0.769	0.041	2.85E-43	4
Lrfn5	1.43E-47	2.0008	0.962	0.084	3.99E-43	4
Gria4	2.02E-47	1.7252	0.923	0.07	5.66E-43	4
Gm13883	2.85E-47	0.5490	0.308	0.001	7.99E-43	4
Xirp2	4.03E-47	0.5084	0.308	0.001	1.13E-42	4
Vsnl1	7.08E-47	1.1160	0.885	0.059	1.98E-42	4
9530059O14Rik	7.38E-47	0.9867	0.654	0.028	2.07E-42	4
Ano3	8.72E-47	1.1913	0.692	0.033	2.44E-42	4
Arfgef3	9.45E-47	0.7275	0.577	0.02	2.64E-42	4
Synpo	1.49E-46	0.6520	0.5	0.013	4.16E-42	4
Epb41l3	2.38E-46	0.8340	0.769	0.041	6.68E-42	4
Rasgef1a	2.44E-46	0.7141	0.692	0.032	6.82E-42	4
Ppp2r2c	2.65E-46	0.7205	0.615	0.024	7.42E-42	4
Mkx	4.19E-46	0.6992	0.462	0.011	1.17E-41	4
Rims1	6.06E-46	2.2108	0.962	0.093	1.70E-41	4
Dpp10	7.80E-46	1.8604	0.962	0.089	2.19E-41	4
A230006K03Rik	8.06E-46	1.4536	0.769	0.047	2.26E-41	4
Glt1d1	9.14E-46	0.4284	0.423	0.008	2.56E-41	4
Satb2	1.20E-45	1.3690	0.846	0.058	3.35E-41	4

Ryr3	1.65E-45	0.9738	0.577	0.021	4.62E-41	4
Sphkap	3.86E-45	0.7914	0.692	0.033	1.08E-40	4
Osbpl10	7.49E-45	0.7295	0.577	0.021	2.10E-40	4
Svop	7.67E-45	0.9541	0.692	0.034	2.15E-40	4
Slc6a6	7.81E-45	0.7327	0.808	0.047	2.19E-40	4
Prkar1b	1.32E-44	0.7608	0.731	0.038	3.71E-40	4
Klhl29	1.97E-44	1.2254	0.923	0.07	5.52E-40	4
Ank3	2.99E-44	2.1870	1	0.113	8.37E-40	4
Cacnb4	3.22E-44	1.6092	0.962	0.085	9.01E-40	4
Celf4	4.12E-44	1.5780	0.962	0.081	1.15E-39	4
Reps2	4.67E-44	0.8761	0.731	0.039	1.31E-39	4
Khdrbs2	5.14E-44	1.2168	0.808	0.053	1.44E-39	4
A830018L16Rik	5.18E-44	1.0569	0.769	0.045	1.45E-39	4
Shtn1	9.56E-44	0.7549	0.654	0.03	2.68E-39	4
Clvs2	1.10E-43	0.7193	0.462	0.012	3.08E-39	4
Sez6l2	1.31E-43	0.6027	0.538	0.018	3.66E-39	4
Gm30382	1.56E-43	0.6151	0.462	0.012	4.38E-39	4
Slit1	1.86E-43	0.6281	0.462	0.012	5.21E-39	4
Srrm3	2.41E-43	0.8961	0.692	0.035	6.74E-39	4
Atp8a2	5.65E-43	1.0873	0.769	0.047	1.58E-38	4
Slc4a10	7.37E-43	0.9539	0.846	0.058	2.06E-38	4
Hcn1	8.73E-43	0.9954	0.769	0.047	2.44E-38	4
Pex5l	1.18E-42	1.4895	0.846	0.063	3.31E-38	4
Dgkg	1.76E-42	0.7439	0.654	0.032	4.92E-38	4
Ankrd33b	1.80E-42	0.6864	0.5	0.016	5.03E-38	4
Cdh12	1.90E-42	1.5930	0.731	0.047	5.32E-38	4
Cnksr2	2.07E-42	1.3252	0.885	0.07	5.81E-38	4
Galnt13	2.41E-42	0.9465	0.654	0.033	6.75E-38	4
Gabra5	3.12E-42	0.3427	0.308	0.003	8.73E-38	4
Vwa5b2	3.53E-42	0.5024	0.308	0.003	9.88E-38	4
Ovol2	3.53E-42	0.3859	0.308	0.003	9.88E-38	4
Wscd2	4.49E-42	0.7685	0.577	0.024	1.26E-37	4
Grin1	4.82E-42	1.3050	0.962	0.085	1.35E-37	4
Cacna1a	5.38E-42	1.8255	0.962	0.102	1.51E-37	4
Gm20696	1.40E-41	0.5735	0.577	0.024	3.92E-37	4
Wipf3	1.42E-41	0.7843	0.462	0.013	3.96E-37	4
Pcsk2	2.98E-41	1.5923	0.885	0.078	8.33E-37	4
2010300C02Rik	6.40E-41	0.9072	0.538	0.021	1.79E-36	4
Gm16351	9.26E-41	0.2808	0.269	0.001	2.59E-36	4

Gm11844	9.91E-41	0.4229	0.269	0.001	2.77E-36	4
Cacna1g	1.22E-40	0.4129	0.346	0.005	3.42E-36	4
March1	2.02E-40	1.5543	0.885	0.079	5.66E-36	4
Fam19a2	2.45E-40	1.5562	0.731	0.049	6.87E-36	4
Gm42649	2.60E-40	0.2723	0.231	0	7.28E-36	4
Pde6a	2.60E-40	0.2661	0.231	0	7.28E-36	4
5730522E02Rik	3.20E-40	1.3253	0.923	0.083	8.97E-36	4
Cers6	7.12E-40	1.0547	0.731	0.046	1.99E-35	4
4930419G24Rik	1.02E-39	0.8641	0.462	0.014	2.85E-35	4
Sorcs3	1.06E-39	1.1017	0.692	0.041	2.98E-35	4
Kcnt2	1.42E-39	0.9445	0.731	0.046	3.98E-35	4
Reep1	2.06E-39	0.8954	0.731	0.046	5.76E-35	4
Tnr	2.70E-39	1.4335	0.885	0.078	7.57E-35	4
Slc8a1	2.95E-39	1.6429	0.846	0.075	8.27E-35	4
Pde2a	4.04E-39	0.9001	0.615	0.032	1.13E-34	4
Slc35f4	5.76E-39	0.9447	0.654	0.037	1.61E-34	4
Kcnq5	7.21E-39	2.3388	0.962	0.12	2.02E-34	4
Dpp6	8.23E-39	1.3727	0.885	0.079	2.30E-34	4
Gm12064	1.72E-38	0.5395	0.423	0.012	4.82E-34	4
Iqsec3	2.85E-38	0.4570	0.423	0.012	7.97E-34	4
Wbscr17	3.20E-38	1.2437	0.692	0.045	8.95E-34	4
Phf24	4.00E-38	0.8051	0.654	0.037	1.12E-33	4
Matk	4.11E-38	0.5866	0.615	0.032	1.15E-33	4
Pde1a	4.39E-38	1.5180	0.769	0.06	1.23E-33	4
Snap91	8.53E-38	0.9084	0.769	0.054	2.39E-33	4
Col25a1	1.29E-37	0.4700	0.385	0.009	3.60E-33	4
Tmem196	1.29E-37	0.4613	0.346	0.007	3.60E-33	4
Slc7a14	1.74E-37	0.6591	0.5	0.02	4.86E-33	4
Sv2b	2.23E-37	1.0489	0.654	0.039	6.25E-33	4
Unc5d	2.39E-37	1.6859	0.846	0.079	6.68E-33	4
Grm7	2.52E-37	2.1992	1	0.138	7.05E-33	4
Sh3gl2	2.53E-37	1.1300	0.846	0.071	7.07E-33	4
Shank3	3.94E-37	0.6255	0.615	0.033	1.10E-32	4
Frmd5	4.37E-37	1.2002	0.846	0.071	1.22E-32	4
Lrrc7	9.97E-37	1.9234	1	0.141	2.79E-32	4
Fam155a	1.32E-36	2.2912	1	0.145	3.69E-32	4
Cacna1c	2.92E-36	1.4562	0.923	0.1	8.18E-32	4
Ndst3	3.52E-36	0.8191	0.462	0.017	9.85E-32	4
Bcl11a	3.56E-36	1.0202	0.808	0.066	9.97E-32	4

Elmod1	4.42E-36	0.9197	0.692	0.046	1.24E-31	4
Slc6a17	4.55E-36	0.5196	0.538	0.025	1.27E-31	4
4933413L06Rik	5.22E-36	0.3785	0.269	0.003	1.46E-31	4
Frmpd4	5.75E-36	1.7013	0.846	0.088	1.61E-31	4
Rapgef4	1.08E-35	1.2602	0.885	0.087	3.03E-31	4
Cobl	1.18E-35	0.8473	0.538	0.026	3.30E-31	4
Fmn1	1.25E-35	0.7660	0.654	0.041	3.50E-31	4
Gm15155	3.97E-35	0.6074	0.538	0.026	1.11E-30	4
Camk4	4.20E-35	0.9235	0.769	0.059	1.17E-30	4
Prkg1	7.87E-35	1.6267	0.923	0.109	2.20E-30	4
Grm1	8.18E-35	0.7445	0.577	0.032	2.29E-30	4
Pcsk2os2	8.30E-35	0.5284	0.308	0.005	2.32E-30	4
Itga8	8.30E-35	0.4542	0.308	0.005	2.32E-30	4
Slc16a7	9.42E-35	0.7118	0.423	0.014	2.64E-30	4
Gabrb2	1.04E-34	1.0341	0.731	0.057	2.90E-30	4
A330102I10Rik	1.13E-34	0.6175	0.5	0.022	3.15E-30	4
Kcnip2	1.14E-34	0.5843	0.423	0.014	3.19E-30	4
Srrm4	1.17E-34	0.8486	0.731	0.054	3.26E-30	4
St6gal2	1.51E-34	0.6243	0.5	0.022	4.23E-30	4
Arhgap20	1.66E-34	0.5323	0.423	0.014	4.66E-30	4
C77370	1.86E-34	0.5913	0.462	0.018	5.22E-30	4
Dmtn	1.90E-34	0.5924	0.5	0.022	5.31E-30	4
Osbpl3	1.93E-34	0.6168	0.462	0.018	5.41E-30	4
Bean1	2.23E-34	0.3225	0.231	0.001	6.25E-30	4
Kcnh7	2.72E-34	2.0458	1	0.16	7.61E-30	4
Mctp1	3.80E-34	1.3199	0.769	0.067	1.07E-29	4
Gm14330	5.58E-34	0.6720	0.538	0.028	1.56E-29	4
Rbfox1	7.19E-34	2.2914	1	0.158	2.01E-29	4
Tmem178	1.05E-33	0.5572	0.538	0.028	2.93E-29	4
Gm13963	1.43E-33	0.5787	0.385	0.012	4.01E-29	4
Caln1	2.87E-33	1.1052	0.577	0.034	8.04E-29	4
Ptprr	2.97E-33	0.6616	0.423	0.016	8.33E-29	4
Cadps	3.14E-33	1.5945	1	0.143	8.80E-29	4
Sgsm1	3.20E-33	0.8000	0.423	0.016	8.95E-29	4
5330417C22Rik	3.40E-33	0.6892	0.462	0.02	9.51E-29	4
Ak5	3.96E-33	1.0706	0.731	0.059	1.11E-28	4
Erc2	4.24E-33	1.7597	1	0.148	1.19E-28	4
Gabra3	4.26E-33	0.4620	0.5	0.024	1.19E-28	4
Nuak1	8.40E-33	0.5503	0.462	0.02	2.35E-28	4

Stk32c	9.83E-33	0.4418	0.423	0.016	2.75E-28	4
Gm37459	1.63E-32	0.4088	0.346	0.009	4.55E-28	4
4933406I18Rik	1.71E-32	0.6821	0.577	0.034	4.77E-28	4
Rab15	1.93E-32	0.3808	0.346	0.009	5.41E-28	4
Nmnat2	1.99E-32	0.6130	0.654	0.045	5.56E-28	4
Gm17202	2.20E-32	0.3733	0.346	0.009	6.15E-28	4
Rims4	2.20E-32	0.3384	0.346	0.009	6.15E-28	4
Rtn4rl1	2.20E-32	0.3260	0.346	0.009	6.15E-28	4
Gm42609	2.97E-32	0.2827	0.269	0.004	8.31E-28	4
Lingo2	3.06E-32	2.4758	0.923	0.145	8.58E-28	4
Gm26652	3.13E-32	0.3894	0.269	0.004	8.77E-28	4
Hs6st3	3.21E-32	2.0941	0.808	0.089	9.00E-28	4
Adarb1	3.36E-32	0.5285	0.577	0.034	9.42E-28	4
Efcab6	5.43E-32	0.4065	0.308	0.007	1.52E-27	4
Elmo1	7.62E-32	0.6832	0.538	0.03	2.13E-27	4
Aff2	9.02E-32	0.9075	0.615	0.042	2.52E-27	4
Gabrb3	1.17E-31	1.4829	0.923	0.121	3.27E-27	4
Chrm2	1.28E-31	0.6229	0.385	0.013	3.59E-27	4
Etl4	1.52E-31	1.8688	0.923	0.121	4.25E-27	4
Anks1b	1.72E-31	1.9703	1	0.171	4.81E-27	4
Dnm1	1.86E-31	0.8337	0.769	0.067	5.20E-27	4
Unc79	2.26E-31	0.8694	1	0.112	6.32E-27	4
Trpc5	2.29E-31	0.4889	0.462	0.021	6.42E-27	4
Epha6	2.70E-31	1.5420	0.769	0.079	7.57E-27	4
Ctnna3	3.21E-31	1.3780	0.923	0.11	8.98E-27	4
Chd5	5.81E-31	0.6369	0.5	0.026	1.63E-26	4
Scn1a	7.07E-31	0.8564	0.577	0.038	1.98E-26	4
Usp29	1.02E-30	0.9060	0.462	0.022	2.86E-26	4
Map6	1.15E-30	0.5270	0.577	0.037	3.23E-26	4
Gm26905	1.17E-30	0.7685	0.346	0.011	3.27E-26	4
Slc24a2	1.33E-30	1.4479	0.846	0.099	3.73E-26	4
Map1b	1.73E-30	1.2331	0.923	0.113	4.83E-26	4
Gm38112	1.97E-30	0.4937	0.346	0.011	5.52E-26	4
Cntn5	2.00E-30	2.1552	0.846	0.106	5.60E-26	4
RP24-267C3.3	2.14E-30	0.4268	0.346	0.011	5.98E-26	4
Clmp	2.51E-30	0.4571	0.346	0.011	7.02E-26	4
Rasgrf1	2.98E-30	1.0863	0.885	0.102	8.33E-26	4
Ptk2b	3.88E-30	0.5376	0.462	0.022	1.09E-25	4
Slc35f3	4.17E-30	0.6220	0.5	0.028	1.17E-25	4

Neto1	5.43E-30	0.5607	0.423	0.018	1.52E-25	4
Smoc2	5.98E-30	0.4088	0.231	0.003	1.68E-25	4
Sgk1	6.02E-30	0.5848	0.385	0.014	1.68E-25	4
Cdkl5	6.10E-30	0.7426	0.769	0.07	1.71E-25	4
Ptpro	6.24E-30	0.4400	0.385	0.014	1.75E-25	4
Nr4a1	6.34E-30	0.2701	0.231	0.003	1.77E-25	4
Gm44188	8.34E-30	0.7105	0.308	0.008	2.33E-25	4
Cntnap5b	1.04E-29	0.9018	0.5	0.029	2.90E-25	4
Tmeff2	1.04E-29	1.2150	0.808	0.085	2.90E-25	4
Baiap2	1.09E-29	0.6147	0.654	0.05	3.06E-25	4
Slain1	1.27E-29	0.4299	0.5	0.028	3.55E-25	4
Ppfia3	1.32E-29	0.5403	0.538	0.033	3.70E-25	4
Itpr1	1.52E-29	1.0662	0.846	0.093	4.25E-25	4
Hs3st4	1.55E-29	1.8445	0.615	0.049	4.33E-25	4
Gm2824	1.61E-29	0.3599	0.308	0.008	4.49E-25	4
Neurl1a	1.75E-29	0.3427	0.308	0.008	4.90E-25	4
Syt1	2.08E-29	2.4356	1	0.23	5.82E-25	4
Unc80	2.25E-29	0.8754	0.846	0.089	6.30E-25	4
Krt12	3.04E-29	0.5008	0.269	0.005	8.50E-25	4
Plekha6	3.27E-29	0.6384	0.577	0.039	9.16E-25	4
Coro2a	3.52E-29	0.3269	0.269	0.005	9.84E-25	4
Kcnc2	3.61E-29	0.9790	0.577	0.041	1.01E-24	4
Plppr5	4.53E-29	0.5813	0.5	0.029	1.27E-24	4
Prkcg	5.66E-29	0.6354	0.5	0.029	1.58E-24	4
Pcdh15	9.95E-29	1.8994	0.769	0.095	2.79E-24	4
Syn1	1.48E-28	0.7105	0.654	0.053	4.14E-24	4
Samd12	1.50E-28	1.3233	0.846	0.102	4.20E-24	4
Celf3	1.62E-28	0.3861	0.423	0.02	4.54E-24	4
Mmp24	2.28E-28	0.4396	0.385	0.016	6.39E-24	4
Nipal2	2.44E-28	0.3684	0.385	0.016	6.84E-24	4
Rnf150	2.45E-28	0.7330	0.5	0.03	6.86E-24	4
Sorbs2	2.83E-28	1.4450	0.962	0.146	7.92E-24	4
Gm28376	3.50E-28	0.8813	0.654	0.055	9.79E-24	4
Lrrtm4	3.63E-28	2.7148	0.962	0.183	1.02E-23	4
Lrrtm3	4.03E-28	1.2012	0.654	0.059	1.13E-23	4
Pacsin1	4.22E-28	1.0409	0.769	0.08	1.18E-23	4
Jph1	4.30E-28	0.5278	0.462	0.025	1.20E-23	4
Edil3	4.39E-28	1.0248	0.692	0.063	1.23E-23	4
Slc22a3	4.50E-28	0.2635	0.192	0.001	1.26E-23	4

Nell2	7.44E-28	1.0175	0.808	0.091	2.08E-23	4
Tenm2	1.01E-27	2.5082	0.962	0.197	2.83E-23	4
Sel1l3	1.63E-27	0.5857	0.577	0.042	4.56E-23	4
Dchs2	2.29E-27	0.3886	0.154	0	6.41E-23	4
Reep2	2.38E-27	0.4569	0.423	0.021	6.66E-23	4
Cpne5	2.41E-27	0.4042	0.308	0.009	6.75E-23	4
Glp2r	2.53E-27	0.7547	0.808	0.084	7.08E-23	4
Cntn4	2.76E-27	1.8665	0.846	0.129	7.72E-23	4
Celf5	3.19E-27	0.6170	0.5	0.032	8.92E-23	4
Nrg3	3.19E-27	2.7860	1	0.264	8.94E-23	4
Grm8	3.30E-27	1.3302	0.615	0.055	9.24E-23	4
D130043K22Rik	3.53E-27	0.5486	0.462	0.026	9.90E-23	4
Camkk2	3.76E-27	0.6496	0.846	0.091	1.05E-22	4
Tmem63c	4.44E-27	0.5437	0.346	0.013	1.24E-22	4
Arhgap15	4.95E-27	0.5555	0.346	0.013	1.39E-22	4
Rasgrf2	5.18E-27	0.5922	0.385	0.017	1.45E-22	4
Galnt9	5.71E-27	0.4409	0.346	0.013	1.60E-22	4
Tenm1	6.79E-27	1.1665	0.769	0.088	1.90E-22	4
Nkain3	6.89E-27	1.0234	0.654	0.058	1.93E-22	4
Trpc4	7.33E-27	0.3616	0.346	0.013	2.05E-22	4
Csmd3	8.02E-27	1.6252	0.962	0.16	2.24E-22	4
4930509J09Rik	9.39E-27	0.5479	0.269	0.007	2.63E-22	4
Gm26906	1.07E-26	0.4224	0.269	0.007	3.00E-22	4
Epha10	1.23E-26	0.5433	0.231	0.004	3.44E-22	4
Rasal1	1.34E-26	0.3185	0.269	0.007	3.75E-22	4
Mmp17	1.47E-26	0.3094	0.269	0.007	4.10E-22	4
E130309D14Rik	1.47E-26	0.3076	0.269	0.007	4.10E-22	4
Mturn	1.47E-26	0.2789	0.269	0.007	4.10E-22	4
Plxdc1	1.47E-26	0.2715	0.269	0.007	4.10E-22	4
Exph5	1.67E-26	0.3944	0.231	0.004	4.68E-22	4
Tmtc1	1.73E-26	0.7580	0.654	0.058	4.83E-22	4
Opcml	1.73E-26	2.5496	0.962	0.214	4.85E-22	4
Ccsap	1.85E-26	0.2617	0.231	0.004	5.18E-22	4
Hs3st5	2.09E-26	0.5122	0.423	0.022	5.85E-22	4
Grm5	3.64E-26	1.7282	0.962	0.196	1.02E-21	4
Ablim2	3.92E-26	0.8594	0.654	0.06	1.10E-21	4
Atp1a3	4.28E-26	0.7589	0.808	0.088	1.20E-21	4
Msra	5.13E-26	1.1027	0.885	0.122	1.44E-21	4
Tmod1	6.06E-26	0.4339	0.462	0.028	1.70E-21	4

Arpp21	8.01E-26	1.9997	0.962	0.235	2.24E-21	4
Nsg2	2.23E-25	0.5439	0.731	0.072	6.23E-21	4
Kcnab2	2.50E-25	0.3049	0.346	0.014	6.99E-21	4
Actn1	2.50E-25	0.5581	0.462	0.029	7.01E-21	4
Atcay	3.17E-25	0.4601	0.462	0.029	8.87E-21	4
Cntnap2	3.58E-25	1.6592	1	0.233	1.00E-20	4
Nav3	4.54E-25	1.9142	1	0.255	1.27E-20	4
Gda	4.68E-25	0.4599	0.462	0.029	1.31E-20	4
Gria3	5.48E-25	1.3117	0.808	0.113	1.53E-20	4
Cntn6	6.85E-25	0.6725	0.462	0.03	1.92E-20	4
Chsy3	7.70E-25	1.1048	0.846	0.114	2.15E-20	4
Arhgap10	7.94E-25	0.5343	0.5	0.035	2.22E-20	4
Susd4	9.64E-25	0.5481	0.385	0.02	2.70E-20	4
Atp9a	1.32E-24	0.5273	0.731	0.075	3.69E-20	4
Col19a1	1.42E-24	0.5450	0.269	0.008	3.97E-20	4
Pld5	1.74E-24	0.5405	0.269	0.008	4.88E-20	4
Pou2f2	2.23E-24	0.2952	0.269	0.008	6.24E-20	4
Cit	2.37E-24	0.8781	0.885	0.118	6.62E-20	4
Bend6	2.98E-24	0.4138	0.462	0.03	8.36E-20	4
Gm28928	3.05E-24	2.5922	0.731	0.11	8.55E-20	4
Rph3a	3.30E-24	0.4670	0.346	0.016	9.23E-20	4
Lrrc8b	3.76E-24	0.5638	0.615	0.055	1.05E-19	4
Ttll11	4.66E-24	0.7986	0.692	0.075	1.30E-19	4
Sytl2	4.85E-24	0.3631	0.346	0.016	1.36E-19	4
Ipcef1	5.01E-24	0.4000	0.346	0.016	1.40E-19	4
Tmem130	5.34E-24	0.3486	0.346	0.016	1.49E-19	4
Cdh8	5.34E-24	0.9003	0.577	0.053	1.50E-19	4
Npas4	5.60E-24	0.3432	0.192	0.003	1.57E-19	4
RP24-236C17.3	5.60E-24	0.2753	0.192	0.003	1.57E-19	4
Palm2	5.85E-24	0.3913	0.308	0.012	1.64E-19	4
Fhl2	6.06E-24	0.3551	0.308	0.012	1.70E-19	4
Slc6a15	6.28E-24	0.4032	0.308	0.012	1.76E-19	4
Crtac1	6.50E-24	0.4531	0.308	0.012	1.82E-19	4
Sgcz	6.77E-24	1.7367	0.885	0.152	1.89E-19	4
Bsn	6.87E-24	0.5607	0.654	0.063	1.92E-19	4
Cntnap5a	7.40E-24	1.2734	0.538	0.047	2.07E-19	4
Efna5	7.48E-24	1.2847	0.808	0.116	2.10E-19	4
Pou6f2	9.58E-24	0.3760	0.231	0.005	2.68E-19	4
Zfp804b	1.06E-23	1.0767	0.462	0.033	2.97E-19	4

5530401A14Rik	1.10E-23	0.2818	0.231	0.005	3.08E-19	4
Olfm3	1.25E-23	0.5855	0.423	0.026	3.50E-19	4
Kcnd3	1.30E-23	0.8110	0.808	0.1	3.64E-19	4
Zfp804a	1.58E-23	0.5399	0.423	0.026	4.43E-19	4
Slit2	1.68E-23	0.4064	0.462	0.032	4.69E-19	4
Rras2	2.20E-23	0.2833	0.385	0.021	6.16E-19	4
Gm12394	2.40E-23	0.6872	0.654	0.067	6.72E-19	4
Gpr158	2.53E-23	1.2421	0.923	0.17	7.08E-19	4
Lzts1	2.75E-23	0.3931	0.423	0.026	7.69E-19	4
Dlg2	2.77E-23	2.4784	1	0.35	7.76E-19	4
Fam19a1	3.09E-23	1.7700	0.692	0.084	8.64E-19	4
Sorbs2os	4.12E-23	0.9772	0.808	0.106	1.15E-18	4
Csmd2	4.46E-23	1.0873	0.923	0.146	1.25E-18	4
Tshz3	5.67E-23	0.6250	0.577	0.053	1.59E-18	4
Scn3a	5.85E-23	0.5737	0.462	0.033	1.64E-18	4
Snap25	8.23E-23	1.4365	1	0.235	2.30E-18	4
Pianp	8.38E-23	0.3330	0.346	0.017	2.35E-18	4
A830036E02Rik	8.64E-23	0.4390	0.346	0.017	2.42E-18	4
Jph4	8.91E-23	0.2900	0.346	0.017	2.49E-18	4
Slco3a1	1.28E-22	0.8122	0.577	0.055	3.58E-18	4
Gfra2	1.53E-22	0.3297	0.269	0.009	4.29E-18	4
Gm16183	1.75E-22	0.3708	0.308	0.013	4.90E-18	4
Prkar2b	2.00E-22	0.3706	0.385	0.022	5.60E-18	4
Ly6e	2.00E-22	0.3364	0.308	0.013	5.60E-18	4
Dcx	2.06E-22	0.3714	0.385	0.022	5.75E-18	4
Khdrbs3	2.91E-22	1.1220	0.962	0.172	8.15E-18	4
Srcin1	3.82E-22	0.5488	0.577	0.054	1.07E-17	4
Plxna4	4.07E-22	1.0313	0.885	0.137	1.14E-17	4
Pak3	4.76E-22	0.7206	0.615	0.063	1.33E-17	4
Vstm5	7.71E-22	0.2650	0.154	0.001	2.16E-17	4
Mir124a-1hg	8.77E-22	0.7196	0.615	0.063	2.46E-17	4
Ccser1	9.02E-22	1.3972	1	0.243	2.53E-17	4
Hook1	1.04E-21	0.3485	0.5	0.041	2.91E-17	4
Cemip	1.10E-21	0.6581	0.231	0.007	3.08E-17	4
Arhgap44	1.11E-21	0.7085	0.577	0.057	3.10E-17	4
Pparg	1.16E-21	0.4074	0.346	0.018	3.26E-17	4
Ppargc1b	1.16E-21	0.3246	0.346	0.018	3.26E-17	4
Gng2	1.21E-21	0.4065	0.423	0.029	3.39E-17	4
Vmn2r87	1.40E-21	0.4488	0.385	0.024	3.91E-17	4

RP23-407N2.2	1.43E-21	0.4361	0.385	0.024	4.01E-17	4
6530403H02Rik	1.46E-21	1.1036	0.308	0.014	4.10E-17	4
Trpc6	1.60E-21	0.3947	0.231	0.007	4.47E-17	4
Gm13629	1.89E-21	0.3017	0.231	0.007	5.28E-17	4
Trhde	2.64E-21	0.7592	0.692	0.08	7.40E-17	4
Plekhg5	2.88E-21	0.6649	0.577	0.058	8.06E-17	4
Prr16	2.90E-21	0.6870	0.731	0.091	8.13E-17	4
Epha7	3.45E-21	0.4475	0.538	0.049	9.66E-17	4
Shc2	3.66E-21	0.3496	0.308	0.014	1.03E-16	4
Slc7a8	4.03E-21	0.2853	0.308	0.014	1.13E-16	4
Shank1	4.88E-21	0.5530	0.538	0.05	1.37E-16	4
Ankef1	6.70E-21	0.2746	0.115	0	1.88E-16	4
Srrm4os	6.91E-21	0.3048	0.269	0.011	1.94E-16	4
Cdkl1	6.91E-21	0.2746	0.269	0.011	1.94E-16	4
Cacna2d3	6.98E-21	1.4163	0.769	0.12	1.95E-16	4
Gm16226	7.31E-21	0.2732	0.192	0.004	2.05E-16	4
4930590L20Rik	7.31E-21	0.2593	0.192	0.004	2.05E-16	4
Map7d2	8.45E-21	0.6318	0.731	0.089	2.37E-16	4
Unc13a	9.63E-21	0.4610	0.5	0.043	2.70E-16	4
Zkscan16	1.04E-20	0.3909	0.346	0.02	2.91E-16	4
Ptprn2	1.08E-20	1.1996	0.962	0.213	3.04E-16	4
Snca	1.10E-20	0.6505	0.577	0.059	3.07E-16	4
Tbc1d30	1.13E-20	0.3868	0.385	0.025	3.16E-16	4
Mgat4a	1.13E-20	0.3474	0.346	0.02	3.16E-16	4
Inha	1.26E-20	0.3031	0.346	0.02	3.53E-16	4
Syndig1	1.28E-20	0.6724	0.538	0.053	3.58E-16	4
Zbtb46	1.31E-20	0.2999	0.385	0.025	3.68E-16	4
Acsl1	1.35E-20	0.4068	0.462	0.037	3.78E-16	4
Trank1	1.38E-20	0.3467	0.462	0.037	3.86E-16	4
Gas7	1.44E-20	0.4909	0.615	0.066	4.02E-16	4
Zcchc16	2.61E-20	0.6985	0.577	0.06	7.32E-16	4
Elavl2	2.63E-20	0.5110	0.423	0.032	7.37E-16	4
Clstn3	3.23E-20	0.4509	0.5	0.045	9.05E-16	4
Adap1	3.43E-20	0.4484	0.5	0.045	9.61E-16	4
Pgm2l1	3.56E-20	0.4708	0.462	0.038	9.97E-16	4
Faah	5.23E-20	0.4889	0.385	0.026	1.46E-15	4
Prickle1	5.49E-20	1.3134	0.962	0.217	1.54E-15	4
Kndc1	6.00E-20	0.3220	0.308	0.016	1.68E-15	4
Fstl5	7.30E-20	0.5994	0.423	0.033	2.05E-15	4

Rnf112	8.31E-20	0.3321	0.385	0.026	2.33E-15	4
Tmem132b	8.97E-20	0.7332	0.808	0.118	2.51E-15	4
Il1rap	9.97E-20	0.5453	0.654	0.078	2.79E-15	4
Kif5a	1.17E-19	0.6172	0.462	0.039	3.29E-15	4
Sh3rf3	1.23E-19	0.6669	0.577	0.062	3.45E-15	4
4930467D21Rik	1.28E-19	0.3738	0.231	0.008	3.57E-15	4
Gng4	1.48E-19	0.3406	0.231	0.008	4.16E-15	4
Lrtm1	1.48E-19	0.2960	0.231	0.008	4.16E-15	4
4430402I18Rik	1.50E-19	0.4590	0.577	0.06	4.21E-15	4
Nalcn	1.52E-19	0.7835	0.615	0.072	4.27E-15	4
Ptgis	1.54E-19	0.3593	0.231	0.008	4.32E-15	4
Cnih3	1.59E-19	0.3489	0.269	0.012	4.46E-15	4
Ltk	1.60E-19	0.2703	0.231	0.008	4.48E-15	4
Sgpp2	1.60E-19	0.2541	0.231	0.008	4.48E-15	4
Pde4dip	2.07E-19	0.9676	0.769	0.122	5.79E-15	4
Pde10a	2.10E-19	1.3686	1	0.251	5.87E-15	4
Rap1gap2	2.18E-19	0.6212	0.615	0.071	6.11E-15	4
Nfasc	2.22E-19	0.8443	0.885	0.143	6.21E-15	4
Pitpnm3	2.50E-19	0.6453	0.346	0.022	7.00E-15	4
Sipa1l1	2.60E-19	1.1115	0.846	0.15	7.29E-15	4
Mmp16	3.35E-19	1.0567	0.923	0.176	9.38E-15	4
Gabra1	3.50E-19	0.4757	0.577	0.062	9.79E-15	4
Gm21798	3.61E-19	0.4356	0.385	0.028	1.01E-14	4
Gm10419	3.78E-19	0.4361	0.385	0.028	1.06E-14	4
Pdzrn3	4.15E-19	1.1123	0.808	0.138	1.16E-14	4
Sorcs1	4.42E-19	0.6354	0.577	0.064	1.24E-14	4
Gdap1	5.13E-19	0.3886	0.346	0.022	1.44E-14	4
Adcy1	5.24E-19	0.3790	0.5	0.047	1.47E-14	4
Tenm4	5.61E-19	1.3238	0.923	0.21	1.57E-14	4
Myo5a	6.32E-19	0.6880	0.808	0.12	1.77E-14	4
Rtn4r	6.79E-19	0.3420	0.346	0.022	1.90E-14	4
Slc2a3	6.88E-19	0.3892	0.423	0.034	1.93E-14	4
Tmem229b	7.12E-19	0.3009	0.308	0.017	1.99E-14	4
Olfm2	7.12E-19	0.2534	0.308	0.017	1.99E-14	4
B230334C09Rik	8.00E-19	0.3779	0.423	0.034	2.24E-14	4
Stxbp1	8.72E-19	0.6905	0.692	0.092	2.44E-14	4
Runx1t1	1.15E-18	0.7518	0.654	0.085	3.21E-14	4
Gucy1a2	1.29E-18	0.8467	0.808	0.129	3.60E-14	4
Aff3	1.51E-18	0.7522	0.846	0.137	4.24E-14	4

Gprin3	1.57E-18	0.3026	0.192	0.005	4.41E-14	4
Cntnap3	1.57E-18	0.2944	0.192	0.005	4.41E-14	4
Myo5b	1.64E-18	0.3034	0.192	0.005	4.60E-14	4
Pcsk1	1.64E-18	0.2928	0.192	0.005	4.60E-14	4
Nav1	1.65E-18	0.5887	0.692	0.091	4.61E-14	4
Slc45a1	1.71E-18	0.3175	0.192	0.005	4.80E-14	4
Prkg2	1.71E-18	0.3117	0.192	0.005	4.80E-14	4
Cntnap5c	2.08E-18	0.6150	0.346	0.024	5.83E-14	4
Slitrk5	2.36E-18	0.2918	0.385	0.029	6.60E-14	4
Ptprd	3.14E-18	2.3704	1	0.689	8.79E-14	4
Trim46	4.04E-18	0.4420	0.346	0.024	1.13E-13	4
Phactr1	4.16E-18	1.8380	1	0.549	1.16E-13	4
Pla2g3	4.24E-18	0.4051	0.346	0.024	1.19E-13	4
Kif5c	4.41E-18	0.6355	0.808	0.122	1.23E-13	4
Rgs17	4.63E-18	0.5439	0.5	0.051	1.30E-13	4
Tctn3	5.98E-18	0.3013	0.231	0.009	1.67E-13	4
Nrxn3	6.01E-18	1.8625	1	0.459	1.68E-13	4
Pla2g4e	6.05E-18	0.3629	0.308	0.018	1.69E-13	4
Gm20754	7.13E-18	0.6787	0.423	0.038	2.00E-13	4
Stx1a	7.14E-18	0.4810	0.615	0.075	2.00E-13	4
Gm26854	7.91E-18	0.3868	0.385	0.03	2.22E-13	4
Meg3	9.64E-18	2.0461	1	0.72	2.70E-13	4
Nrg1	9.72E-18	1.5612	1	0.361	2.72E-13	4
Kcnj3	9.84E-18	0.6679	0.846	0.143	2.76E-13	4
Kcnq2	1.09E-17	0.5821	0.346	0.025	3.06E-13	4
Pde4a	1.25E-17	0.5601	0.538	0.06	3.50E-13	4
Ptprn	1.48E-17	0.6952	0.538	0.062	4.14E-13	4
Klhl3	1.56E-17	0.4727	0.462	0.045	4.38E-13	4
Snhg11	1.88E-17	1.7806	1	0.711	5.26E-13	4
Syt7	1.98E-17	0.4564	0.538	0.06	5.54E-13	4
Sema3a	2.02E-17	0.4119	0.346	0.025	5.66E-13	4
Cacna2d1	2.21E-17	1.2532	0.885	0.223	6.17E-13	4
St6galnac3	2.42E-17	0.3948	0.577	0.068	6.77E-13	4
Ank1	2.50E-17	0.4321	0.346	0.025	6.99E-13	4
Ccdc30	2.82E-17	0.3937	0.385	0.032	7.88E-13	4
Fscn1	3.64E-17	0.3173	0.269	0.014	1.02E-12	4
Trpm4	3.97E-17	0.3362	0.269	0.014	1.11E-12	4
Nipsnap1	4.04E-17	0.3213	0.385	0.032	1.13E-12	4
Lrrfip1	4.15E-17	0.6318	0.577	0.072	1.16E-12	4

Stx3	4.85E-17	0.2609	0.308	0.02	1.36E-12	4
Ptpn3	4.98E-17	0.3295	0.308	0.02	1.39E-12	4
Kcnma1	5.95E-17	1.4087	1	0.44	1.67E-12	4
Slc2a13	6.05E-17	1.0220	0.769	0.147	1.69E-12	4
Necab1	6.58E-17	0.6038	0.346	0.026	1.84E-12	4
Ube3a	7.67E-17	1.3317	0.962	0.351	2.15E-12	4
Ppm1h	8.11E-17	0.6825	0.846	0.143	2.27E-12	4
Slc17a5	8.58E-17	0.4817	0.615	0.08	2.40E-12	4
Dgkh	1.13E-16	0.5845	0.769	0.121	3.17E-12	4
Epb41l1	1.22E-16	0.4663	0.538	0.063	3.41E-12	4
Mtmr7	1.34E-16	0.2796	0.423	0.039	3.75E-12	4
Gm15561	1.46E-16	0.2929	0.192	0.007	4.09E-12	4
Nsun2	1.48E-16	0.3843	0.615	0.08	4.14E-12	4
Gabrg2	1.79E-16	0.5580	0.462	0.049	5.00E-12	4
Ergic1	1.99E-16	0.3634	0.731	0.106	5.56E-12	4
Serp2	2.14E-16	0.2979	0.462	0.047	5.99E-12	4
Susd1	2.97E-16	0.2919	0.308	0.021	8.31E-12	4
Tspan33	3.12E-16	0.3419	0.308	0.021	8.73E-12	4
Fbxo16	3.12E-16	0.3031	0.308	0.021	8.73E-12	4
Adamts17	3.26E-16	0.4257	0.269	0.016	9.13E-12	4
Mast1	3.54E-16	0.3126	0.269	0.016	9.91E-12	4
Plppr4	3.71E-16	0.3996	0.462	0.049	1.04E-11	4
Agpat4	3.95E-16	0.2799	0.269	0.016	1.11E-11	4
Rapgefl1	3.95E-16	0.2752	0.269	0.016	1.11E-11	4
Cx3cl1	4.14E-16	0.2995	0.423	0.041	1.16E-11	4
Celf2	4.27E-16	1.2637	1	0.933	1.20E-11	4
Ppm1l	4.41E-16	0.7415	0.731	0.12	1.23E-11	4
D630045J12Rik	5.64E-16	0.4957	0.654	0.093	1.58E-11	4
Gnaz	5.70E-16	0.3051	0.385	0.034	1.60E-11	4
Tspan13	5.92E-16	0.3232	0.346	0.028	1.66E-11	4
Agbl4	5.94E-16	1.2036	0.923	0.263	1.66E-11	4
Nphp4	6.19E-16	0.2537	0.346	0.028	1.73E-11	4
Olfm1	7.05E-16	0.5175	0.577	0.076	1.97E-11	4
Csmd1	7.80E-16	1.5817	1	0.59	2.18E-11	4
Grin2b	8.91E-16	1.2668	1	0.436	2.50E-11	4
Gm12371	9.67E-16	0.3418	0.115	0.001	2.71E-11	4
Cacnb2	9.81E-16	0.6104	0.769	0.131	2.75E-11	4
Amph	9.92E-16	0.6426	0.769	0.13	2.78E-11	4
Itgbl1	1.29E-15	0.4910	0.385	0.035	3.62E-11	4

C530008M17Rik	1.31E-15	0.5221	0.577	0.078	3.68E-11	4
Elavl3	1.37E-15	0.5999	0.885	0.163	3.85E-11	4
Ulk4	1.42E-15	0.4238	0.385	0.035	3.99E-11	4
Camk2b	1.59E-15	0.4683	0.462	0.051	4.45E-11	4
Tmem117	1.60E-15	0.3641	0.385	0.035	4.48E-11	4
Junb	1.70E-15	0.3757	0.385	0.035	4.75E-11	4
Eml2	1.71E-15	0.3199	0.538	0.067	4.80E-11	4
Cpne6	1.80E-15	0.3571	0.231	0.012	5.03E-11	4
Tmem191c	1.88E-15	0.4723	0.538	0.068	5.27E-11	4
Far2	2.00E-15	0.4726	0.462	0.051	5.61E-11	4
Cyfip2	2.05E-15	0.5043	0.615	0.085	5.75E-11	4
Basp1	2.15E-15	0.4950	0.731	0.117	6.01E-11	4
Kcnj9	2.50E-15	0.2931	0.346	0.029	7.00E-11	4
Lrrn2	2.82E-15	0.3590	0.5	0.059	7.88E-11	4
Madd	3.08E-15	0.5718	0.577	0.08	8.63E-11	4
Hid1	3.29E-15	0.2904	0.269	0.017	9.20E-11	4
Kcnip4	3.94E-15	2.6934	1	0.445	1.10E-10	4
Gap43	4.42E-15	0.4055	0.385	0.037	1.24E-10	4
Scn2a1	4.51E-15	0.6992	0.808	0.146	1.26E-10	4
Pdzrn4	4.94E-15	1.0571	0.5	0.07	1.38E-10	4
Ablim3	5.20E-15	0.2644	0.192	0.008	1.46E-10	4
Kifc2	5.53E-15	0.2847	0.385	0.037	1.55E-10	4
Foxp1	5.72E-15	0.8828	0.846	0.185	1.60E-10	4
Adam22	6.09E-15	0.5980	0.846	0.156	1.70E-10	4
Gria1	6.59E-15	1.1343	0.885	0.216	1.85E-10	4
Asxl3	6.84E-15	0.3252	0.308	0.024	1.91E-10	4
Smpd4	8.71E-15	0.2808	0.346	0.03	2.44E-10	4
St8sia5	8.88E-15	0.3015	0.346	0.03	2.49E-10	4
Nkain2	9.74E-15	1.4735	1	0.43	2.73E-10	4
Kcnb1	1.67E-14	0.7040	0.538	0.076	4.68E-10	4
Adcy5	1.84E-14	0.2656	0.269	0.018	5.14E-10	4
Prkag2	1.86E-14	0.6779	0.769	0.145	5.20E-10	4
Rab3c	1.98E-14	0.4276	0.346	0.032	5.53E-10	4
Fam78b	1.98E-14	0.2614	0.269	0.018	5.53E-10	4
Map7	2.03E-14	0.5318	0.577	0.083	5.68E-10	4
Frmpd3	2.13E-14	0.2731	0.269	0.018	5.95E-10	4
A230050P20Rik	2.36E-14	0.2987	0.346	0.032	6.60E-10	4
Pkig	2.40E-14	0.6008	0.692	0.116	6.73E-10	4
Sh3pxd2a	2.52E-14	0.2725	0.231	0.013	7.06E-10	4

Gm16214	2.59E-14	0.2815	0.231	0.013	7.26E-10	4
Pde1b	2.59E-14	0.2594	0.231	0.013	7.26E-10	4
Hs3st2	2.73E-14	0.4247	0.308	0.025	7.64E-10	4
Vopp1	2.76E-14	0.3843	0.346	0.032	7.72E-10	4
Zdhhc14	3.10E-14	0.6233	0.654	0.108	8.67E-10	4
Nol4l	3.16E-14	0.4678	0.423	0.047	8.84E-10	4
Rab40b	3.17E-14	0.3030	0.308	0.025	8.88E-10	4
Egfem1	3.40E-14	0.8644	0.731	0.138	9.52E-10	4
Klc2	3.58E-14	0.4019	0.385	0.039	1.00E-09	4
Zfp697	3.66E-14	0.3896	0.577	0.083	1.02E-09	4
Jakmip2	4.46E-14	0.5732	0.692	0.118	1.25E-09	4
Cpne4	4.46E-14	0.7570	0.462	0.059	1.25E-09	4
A330015K06Rik	5.07E-14	0.4933	0.346	0.033	1.42E-09	4
Scn8a	5.18E-14	0.7771	1	0.248	1.45E-09	4
Ptprk	6.16E-14	0.7756	0.731	0.143	1.73E-09	4
Rap1gap	6.21E-14	0.5345	0.538	0.076	1.74E-09	4
Ypel2	7.86E-14	0.5413	0.462	0.059	2.20E-09	4
4930578G10Rik	7.95E-14	0.6294	0.615	0.1	2.23E-09	4
Asic2	8.17E-14	1.1941	1	0.503	2.29E-09	4
Dixdc1	8.97E-14	0.3153	0.346	0.033	2.51E-09	4
Scube1	9.92E-14	0.3656	0.423	0.049	2.78E-09	4
Zbtb20	9.94E-14	-1.0317	1	0.997	2.78E-09	4
Sobp	1.03E-13	0.7255	0.923	0.213	2.88E-09	4
Pgr	1.03E-13	0.3365	0.269	0.02	2.90E-09	4
Slc44a5	1.06E-13	0.2962	0.269	0.02	2.96E-09	4
Nin	1.06E-13	0.3379	0.538	0.075	2.97E-09	4
Cfap54	1.10E-13	0.4665	0.423	0.05	3.09E-09	4
Gpr176	1.20E-13	0.2548	0.192	0.009	3.35E-09	4
Nrg2	1.29E-13	0.4764	0.654	0.108	3.62E-09	4
Psmd9	1.33E-13	0.3766	0.577	0.085	3.71E-09	4
Cdh6	1.41E-13	0.5116	0.385	0.042	3.94E-09	4
Kcnq3	1.46E-13	1.0556	1	0.38	4.09E-09	4
Gm27247	1.50E-13	0.3978	0.231	0.014	4.19E-09	4
Runx2	1.67E-13	0.7015	0.577	0.093	4.67E-09	4
Cnnm1	1.99E-13	0.2683	0.231	0.014	5.58E-09	4
Gfod1	2.05E-13	0.4851	0.538	0.079	5.75E-09	4
Myo16	2.29E-13	0.5979	0.615	0.102	6.40E-09	4
Adcy8	2.45E-13	0.4732	0.5	0.068	6.85E-09	4
Myh10	2.53E-13	0.2574	0.5	0.067	7.07E-09	4

Otud7a	2.55E-13	0.9434	0.962	0.29	7.13E-09	4
Plxna2	2.59E-13	0.5202	0.769	0.143	7.24E-09	4
Gm38393	2.66E-13	0.3514	0.423	0.05	7.44E-09	4
Flrt2	3.50E-13	0.6142	0.654	0.117	9.81E-09	4
Gm43948	4.39E-13	0.4164	0.269	0.021	1.23E-08	4
Ptpre	4.39E-13	0.3379	0.269	0.021	1.23E-08	4
Plec	4.59E-13	0.3433	0.423	0.051	1.29E-08	4
Ephx4	4.69E-13	0.3519	0.269	0.021	1.31E-08	4
Dgkz	4.89E-13	0.5112	0.654	0.112	1.37E-08	4
Arsb	6.19E-13	0.4741	0.654	0.114	1.73E-08	4
Npas3	6.28E-13	-1.0402	1	0.983	1.76E-08	4
Ano4	6.29E-13	0.3456	0.346	0.035	1.76E-08	4
Hiatl1	6.52E-13	0.2854	0.423	0.051	1.83E-08	4
Homer1	6.78E-13	0.6979	0.731	0.143	1.90E-08	4
RP23-231J2.1	6.91E-13	1.0932	0.308	0.029	1.94E-08	4
Apex2	7.09E-13	0.3597	0.731	0.133	1.98E-08	4
Jazf1	8.41E-13	0.5874	0.577	0.093	2.36E-08	4
Cdh9	9.34E-13	0.4668	0.231	0.016	2.62E-08	4
Slc17a7	9.36E-13	0.3993	0.5	0.071	2.62E-08	4
Mef2c	1.04E-12	1.0969	0.962	0.327	2.90E-08	4
Col26a1	1.12E-12	0.3011	0.115	0.003	3.15E-08	4
Gm43376	1.17E-12	0.5150	0.5	0.074	3.27E-08	4
Klf10	1.19E-12	0.2960	0.231	0.016	3.34E-08	4
Prkcb	1.22E-12	0.9410	0.923	0.263	3.41E-08	4
Prkcz	1.26E-12	0.4347	0.577	0.091	3.53E-08	4
Gm14703	1.28E-12	0.3462	0.308	0.029	3.58E-08	4
A330008L17Rik	1.31E-12	0.3299	0.192	0.011	3.67E-08	4
Mest	1.35E-12	0.3065	0.231	0.016	3.78E-08	4
Lmf1	1.35E-12	0.2875	0.423	0.053	3.78E-08	4
Calb1	1.38E-12	0.3188	0.231	0.016	3.87E-08	4
Ptpru	1.39E-12	0.3112	0.192	0.011	3.89E-08	4
Herc3	1.40E-12	0.4669	0.654	0.114	3.91E-08	4
Ldlrad4	1.44E-12	0.7425	0.692	0.141	4.04E-08	4
Brinp2	1.54E-12	0.5291	0.615	0.104	4.32E-08	4
Kcnab1	1.55E-12	0.5302	0.615	0.106	4.35E-08	4
Stmn2	1.62E-12	0.4271	0.5	0.074	4.52E-08	4
Slc8a3	1.65E-12	0.3482	0.269	0.022	4.62E-08	4
Cttnbp2	1.65E-12	0.9221	0.962	0.357	4.62E-08	4
Snx7	1.76E-12	0.2678	0.385	0.045	4.93E-08	4

Ldb2	1.82E-12	0.8465	0.615	0.118	5.11E-08	4
Kcnc1	1.89E-12	0.3010	0.346	0.037	5.30E-08	4
Cntnap4	2.00E-12	0.2709	0.269	0.022	5.59E-08	4
Man2a1	2.00E-12	0.4085	0.462	0.063	5.60E-08	4
Slc24a5	2.33E-12	0.4278	0.462	0.064	6.52E-08	4
Gnptg	2.57E-12	0.3168	0.423	0.054	7.19E-08	4
Greb1l	2.83E-12	0.5508	0.385	0.047	7.93E-08	4
Pip5k1b	3.23E-12	0.3911	0.308	0.03	9.04E-08	4
1700025G04Rik	3.42E-12	0.3062	0.615	0.104	9.59E-08	4
Gpc5	3.78E-12	-1.0439	1	0.974	1.06E-07	4
Swi5	3.78E-12	0.3310	0.385	0.046	1.06E-07	4
Ap3b2	4.48E-12	0.3138	0.385	0.046	1.25E-07	4
Nbea	4.76E-12	0.9613	0.962	0.422	1.33E-07	4
Tmem178b	5.15E-12	0.9098	1	0.357	1.44E-07	4
Cnrip1	5.21E-12	0.3951	0.5	0.074	1.46E-07	4
Ptprz1	5.44E-12	-1.1701	1	0.953	1.52E-07	4
Ntrk3	5.48E-12	1.0203	0.846	0.254	1.54E-07	4
Gm13052	5.93E-12	0.3583	0.231	0.017	1.66E-07	4
Tgfbr3	6.21E-12	0.3340	0.231	0.017	1.74E-07	4
Apobec4	6.31E-12	0.3525	0.269	0.024	1.77E-07	4
Galntl6	8.61E-12	1.4960	0.615	0.13	2.41E-07	4
Tro	8.87E-12	0.3295	0.346	0.039	2.48E-07	4
Gm5441	9.66E-12	0.3469	0.423	0.057	2.70E-07	4
Eml1	1.01E-11	0.3943	0.538	0.088	2.83E-07	4
Nfia	1.11E-11	-1.0763	1	0.961	3.12E-07	4
Ptprj	1.17E-11	0.6032	0.962	0.244	3.28E-07	4
Kif26b	1.20E-11	0.3477	0.192	0.012	3.36E-07	4
Epha3	1.30E-11	0.3836	0.385	0.049	3.65E-07	4
Ankfn1	1.34E-11	0.2751	0.192	0.012	3.74E-07	4
Gsg1l	1.34E-11	0.2769	0.308	0.032	3.74E-07	4
Rims2	1.34E-11	0.9256	1	0.353	3.75E-07	4
Zfp704	1.36E-11	0.4568	0.577	0.1	3.80E-07	4
Lmo7	1.36E-11	0.2765	0.308	0.032	3.81E-07	4
Chchd6	1.44E-11	0.3571	0.577	0.097	4.03E-07	4
Cux2	1.48E-11	0.6613	0.577	0.108	4.16E-07	4
Ust	1.59E-11	0.4409	0.269	0.025	4.46E-07	4
Pip5k1c	1.87E-11	0.2699	0.462	0.067	5.22E-07	4
Raph1	1.89E-11	0.3467	0.692	0.131	5.28E-07	4
2900011O08Rik	1.89E-11	0.4879	0.462	0.07	5.29E-07	4

Fbxo41	2.05E-11	0.3263	0.269	0.025	5.74E-07	4
Gm26691	2.10E-11	0.3994	0.577	0.101	5.87E-07	4
Grik4	2.18E-11	0.3851	0.385	0.05	6.11E-07	4
Slc1a3	2.30E-11	-1.2085	0.962	0.951	6.45E-07	4
Ahi1	2.35E-11	0.9410	1	0.382	6.57E-07	4
Ralgapa2	2.38E-11	0.5113	0.692	0.138	6.67E-07	4
Hivep2	2.48E-11	0.8903	1	0.51	6.95E-07	4
Mtcl1	2.58E-11	0.3523	0.654	0.122	7.23E-07	4
Cdh18	2.72E-11	0.9512	0.615	0.134	7.62E-07	4
Numbl	2.80E-11	0.3097	0.231	0.018	7.84E-07	4
Myo1d	2.82E-11	0.3117	0.308	0.033	7.90E-07	4
Frrs1l	3.01E-11	0.4269	0.615	0.11	8.42E-07	4
Tcte2	3.22E-11	0.4674	0.577	0.104	9.01E-07	4
2900026A02Rik	3.53E-11	0.2845	0.308	0.033	9.87E-07	4
Syt14	4.20E-11	0.3022	0.462	0.07	1.18E-06	4
Fntb	4.31E-11	0.3751	0.5	0.079	1.21E-06	4
1700111E14Rik	4.52E-11	0.4192	0.538	0.092	1.26E-06	4
Grik3	4.98E-11	0.4092	0.269	0.026	1.39E-06	4
Klhl2	5.04E-11	0.4626	0.692	0.142	1.41E-06	4
Pkia	5.12E-11	0.4238	0.654	0.126	1.43E-06	4
Tacc1	5.58E-11	0.5743	0.923	0.227	1.56E-06	4
Tmem169	5.68E-11	0.3380	0.269	0.026	1.59E-06	4
Prickle2	5.83E-11	0.8055	0.962	0.357	1.63E-06	4
Fgf12	6.02E-11	0.6946	0.923	0.261	1.69E-06	4
Gnal	6.20E-11	0.3521	0.308	0.034	1.74E-06	4
Nob1	6.63E-11	0.3541	0.577	0.104	1.86E-06	4
N4bp2l1	6.81E-11	0.2951	0.423	0.06	1.91E-06	4
Arhgef3	6.93E-11	0.2703	0.385	0.051	1.94E-06	4
Mgat5b	8.00E-11	0.3590	0.192	0.013	2.24E-06	4
Dgki	8.09E-11	0.8357	0.962	0.348	2.26E-06	4
Fhod3	8.09E-11	0.4774	0.692	0.143	2.26E-06	4
Trpc3	8.50E-11	0.2671	0.308	0.034	2.38E-06	4
Ppp1r14c	8.81E-11	0.3340	0.462	0.072	2.47E-06	4
Wdr17	9.48E-11	-1.0638	1	0.979	2.66E-06	4
Dock3	9.53E-11	0.7897	1	0.384	2.67E-06	4
Ptpn5	1.01E-10	0.3831	0.346	0.043	2.83E-06	4
Sulf2	1.07E-10	0.2581	0.231	0.02	3.00E-06	4
Cacna1d	1.09E-10	0.7673	0.885	0.254	3.05E-06	4
Mthfr	1.09E-10	0.3163	0.231	0.02	3.06E-06	4

Sdk1	1.19E-10	0.6474	0.385	0.057	3.32E-06	4
Ncald	1.19E-10	0.8069	0.769	0.209	3.33E-06	4
Rgs7bp	1.21E-10	0.5814	0.885	0.233	3.38E-06	4
Cpa6	1.24E-10	0.2911	0.231	0.02	3.47E-06	4
Fam69a	1.25E-10	0.2632	0.385	0.053	3.49E-06	4
Trafd1	1.34E-10	0.3733	0.5	0.083	3.76E-06	4
Ankrd45	1.35E-10	0.2504	0.231	0.02	3.77E-06	4
Gm15440	1.37E-10	0.2566	0.231	0.02	3.85E-06	4
Gm15738	1.47E-10	0.4083	0.462	0.074	4.12E-06	4
Arhgef7	1.55E-10	0.3326	0.615	0.116	4.34E-06	4
R3hdm1	1.60E-10	0.9427	1	0.455	4.48E-06	4
St3gal5	1.62E-10	0.3137	0.462	0.074	4.53E-06	4
Oxr1	1.66E-10	0.9725	0.923	0.424	4.65E-06	4
Lpgat1	1.72E-10	0.3604	0.462	0.074	4.80E-06	4
Slc44a1	1.75E-10	0.4184	0.615	0.118	4.89E-06	4
Gm26835	1.75E-10	0.7978	0.962	0.325	4.90E-06	4
Rims3	1.88E-10	0.3530	0.269	0.028	5.25E-06	4
Scai	1.92E-10	0.5426	0.923	0.235	5.38E-06	4
Lhfpl3	2.00E-10	0.4291	0.423	0.066	5.60E-06	4
Ccdc148	2.01E-10	0.3329	0.538	0.096	5.64E-06	4
Sept3	2.08E-10	0.2609	0.308	0.035	5.82E-06	4
Tmx4	2.09E-10	0.2610	0.5	0.084	5.85E-06	4
Plcl2	2.19E-10	0.5338	0.577	0.11	6.15E-06	4
Vash1	2.34E-10	0.3418	0.385	0.054	6.54E-06	4
Baiap2l1	2.36E-10	0.2632	0.269	0.028	6.62E-06	4
Syngr1	3.18E-10	0.2836	0.577	0.106	8.89E-06	4
Sugp1	3.23E-10	0.3382	0.615	0.118	9.04E-06	4
Dscaml1	3.24E-10	0.5990	0.385	0.058	9.06E-06	4
Cdyl2	3.31E-10	0.4384	0.615	0.125	9.27E-06	4
Pxk	3.61E-10	0.2926	0.577	0.106	1.01E-05	4
Gpr137c	3.64E-10	0.3133	0.538	0.097	1.02E-05	4
Kcnh5	3.66E-10	0.5644	0.423	0.068	1.03E-05	4
Kalrn	3.80E-10	0.9771	1	0.636	1.06E-05	4
Efnb2	4.33E-10	0.2561	0.308	0.037	1.21E-05	4
Sema3e	4.42E-10	0.3117	0.231	0.021	1.24E-05	4
Gm1043	4.42E-10	0.2854	0.231	0.021	1.24E-05	4
Dnm3	4.79E-10	0.5878	0.731	0.175	1.34E-05	4
Sept11	4.94E-10	0.3963	0.846	0.198	1.38E-05	4
Me3	5.15E-10	0.6367	0.615	0.134	1.44E-05	4

Mkl2	6.20E-10	0.6306	0.808	0.209	1.74E-05	4
Uggt1	6.23E-10	0.2898	0.5	0.087	1.75E-05	4
Fnbp1l	6.87E-10	0.3494	0.538	0.099	1.92E-05	4
Phf6	7.04E-10	0.3025	0.615	0.121	1.97E-05	4
Whsc1	7.35E-10	0.3827	0.769	0.173	2.06E-05	4
Ildr2	7.78E-10	0.5212	0.577	0.116	2.18E-05	4
Osbpl6	8.37E-10	0.4952	0.692	0.158	2.34E-05	4
Ftx	8.62E-10	0.4656	0.692	0.151	2.41E-05	4
Ccdc3	8.86E-10	0.2695	0.154	0.009	2.48E-05	4
Aig1	8.93E-10	0.4311	0.846	0.201	2.50E-05	4
Zdhhc21	9.26E-10	0.3107	0.808	0.184	2.59E-05	4
Tmem57	9.79E-10	0.3922	0.731	0.162	2.74E-05	4
Sept9	9.89E-10	0.2546	0.423	0.068	2.77E-05	4
Lmtk2	1.03E-09	0.4035	0.692	0.155	2.88E-05	4
Msi2	1.09E-09	-0.8625	1	0.978	3.05E-05	4
Syn2	1.09E-09	0.6436	0.923	0.271	3.05E-05	4
Nhsl2	1.13E-09	0.4201	0.231	0.022	3.16E-05	4
Smim14	1.29E-09	0.2777	0.385	0.058	3.61E-05	4
Dgkd	1.30E-09	0.2664	0.577	0.112	3.65E-05	4
Stau2	1.39E-09	0.3816	0.731	0.166	3.89E-05	4
Pclo	1.52E-09	0.5845	0.923	0.273	4.25E-05	4
Gtdc1	1.54E-09	0.4893	0.808	0.201	4.30E-05	4
Rab11fip4	1.55E-09	0.3774	0.654	0.138	4.34E-05	4
Ankrd44	1.55E-09	0.2722	0.346	0.049	4.35E-05	4
Arid5b	1.67E-09	0.3293	0.731	0.163	4.68E-05	4
Slc43a2	1.72E-09	0.2633	0.577	0.114	4.80E-05	4
Acot7	1.84E-09	0.2552	0.538	0.101	5.16E-05	4
Lmbr1	1.96E-09	0.2932	0.654	0.135	5.49E-05	4
Apoe	2.03E-09	-1.2653	0.846	0.894	5.69E-05	4
Prdm10	2.14E-09	0.2786	0.5	0.091	5.98E-05	4
Atrnl1	2.36E-09	0.6733	0.846	0.242	6.61E-05	4
Mical3	2.50E-09	0.5043	0.846	0.223	7.01E-05	4
Nos1ap	2.52E-09	0.4483	0.846	0.213	7.04E-05	4
Gm10516	2.72E-09	0.2882	0.423	0.07	7.61E-05	4
Gm38251	2.72E-09	0.3035	0.385	0.06	7.62E-05	4
Iqgap2	2.80E-09	0.3135	0.269	0.032	7.83E-05	4
Bcl11b	3.25E-09	0.2561	0.231	0.024	9.10E-05	4
Xkr6	3.56E-09	0.4928	0.808	0.204	9.95E-05	4
Fras1	3.63E-09	0.3787	0.346	0.051	0.0001	4

Tnfrsf21	3.66E-09	0.2656	0.308	0.041	0.0001	4
Htr1f	3.72E-09	0.5138	0.615	0.138	0.0001	4
Lancl1	3.77E-09	0.2537	0.462	0.083	0.0001	4
Pcbp3	3.86E-09	0.2620	0.462	0.081	0.0001	4
Ube4a	3.95E-09	0.3235	0.692	0.156	0.0001	4
Sv2a	4.24E-09	0.2674	0.385	0.06	0.0001	4
Faim2	4.24E-09	0.2864	0.346	0.051	0.0001	4
5330434G04Rik	4.29E-09	0.4430	0.538	0.112	0.0001	4
Sptbn2	4.36E-09	0.3602	0.308	0.042	0.0001	4
Macf1	4.83E-09	-0.7046	1	0.971	0.0001	4
Pdzd2	4.96E-09	0.4382	0.5	0.097	0.0001	4
Simc1	5.05E-09	0.3089	0.5	0.096	0.0001	4
Plppr1	5.09E-09	0.2820	0.462	0.083	0.0001	4
Apba1	5.34E-09	0.4377	0.923	0.261	0.0001	4
Megf8	5.45E-09	0.3746	0.423	0.074	0.0002	4
Plcxd3	5.69E-09	0.6794	0.231	0.025	0.0002	4
Fgf14	6.20E-09	0.6609	1	0.863	0.0002	4
Dlgap4	7.19E-09	0.4624	0.808	0.208	0.0002	4
Dock9	8.96E-09	0.4771	0.654	0.152	0.0003	4
Arhgap39	1.01E-08	0.3615	0.808	0.205	0.0003	4
Dhx57	1.01E-08	0.4211	0.654	0.155	0.0003	4
Garnl3	1.09E-08	0.7897	0.654	0.163	0.0003	4
Palm	1.09E-08	0.2800	0.615	0.134	0.0003	4
Nrp2	1.10E-08	0.3546	0.269	0.034	0.0003	4
Sntb2	1.11E-08	0.4729	0.615	0.139	0.0003	4
Lrrc28	1.16E-08	0.2899	0.462	0.085	0.0003	4
Zbtb16	1.23E-08	0.2696	0.654	0.154	0.0003	4
Dennd5b	1.41E-08	0.4217	0.846	0.226	0.0004	4
Inpp4a	1.42E-08	0.2921	0.423	0.076	0.0004	4
Upp2	1.45E-08	0.5223	0.846	0.244	0.0004	4
RP24-274B19.1	1.52E-08	0.5311	0.577	0.133	0.0004	4
Eif2b5	1.54E-08	0.3007	0.308	0.045	0.0004	4
C2cd5	1.64E-08	0.3703	0.885	0.239	0.0005	4
Stxbp5	1.69E-08	0.3453	0.769	0.189	0.0005	4
Snrpn	1.82E-08	0.4093	0.231	0.026	0.0005	4
Pknox2	1.89E-08	0.4380	0.731	0.188	0.0005	4
Sntg2	1.94E-08	0.2925	0.231	0.026	0.0005	4
Pam	1.95E-08	0.6788	0.885	0.289	0.0005	4
Pvrl1	2.11E-08	0.2871	0.192	0.018	0.0006	4

Dlg4	2.16E-08	0.2791	0.692	0.163	0.0006	4
Enox1	2.25E-08	0.7247	0.846	0.263	0.0006	4
Slc25a27	2.37E-08	0.3372	0.577	0.126	0.0007	4
Zc2hc1a	2.61E-08	0.3194	0.423	0.078	0.0007	4
App	3.03E-08	0.5310	0.923	0.292	0.0008	4
Prosc	3.04E-08	0.2623	0.462	0.091	0.0009	4
Eefsec	3.07E-08	0.3124	0.5	0.104	0.0009	4
Calm2	3.09E-08	0.4719	0.846	0.242	0.0009	4
Gabra4	3.32E-08	0.3957	0.615	0.147	0.0009	4
Spock3	3.64E-08	0.2911	0.308	0.046	0.0010	4
Dmxl2	3.78E-08	0.3082	0.692	0.17	0.0011	4
Lmo3	3.82E-08	0.4151	0.346	0.058	0.0011	4
Wasf1	3.91E-08	0.2659	0.462	0.089	0.0011	4
Ndfip1	4.08E-08	0.3148	0.923	0.26	0.0011	4
Smarca1	4.96E-08	0.2595	0.269	0.037	0.0014	4
Tanc2	5.61E-08	0.7014	1	0.453	0.0016	4
Rasgrp1	5.93E-08	0.3469	0.538	0.121	0.0017	4
Zfp618	5.94E-08	0.2722	0.115	0.007	0.0017	4
Ntm	6.05E-08	-0.6326	1	0.979	0.0017	4
Hs6st2	6.15E-08	0.3417	0.192	0.02	0.0017	4
Bdnf	6.15E-08	0.2674	0.192	0.02	0.0017	4
Hspa12a	6.15E-08	0.2532	0.192	0.02	0.0017	4
Cdc40	6.28E-08	0.2679	0.692	0.168	0.0018	4
Rgs20	6.65E-08	-1.1226	0.846	0.882	0.0019	4
Nrgn	6.77E-08	0.3511	0.462	0.096	0.0019	4
Pi4ka	6.84E-08	0.5490	0.962	0.372	0.0019	4
Fbxw7	6.84E-08	0.2710	0.692	0.171	0.0019	4
Kitl	8.81E-08	0.2755	0.269	0.038	0.0025	4
Gm3764	9.19E-08	-1.0564	1	0.901	0.0026	4
Il1rapl1	9.21E-08	0.6358	1	0.798	0.0026	4
Sclt1	9.39E-08	0.3980	0.654	0.164	0.0026	4
Ly6h	9.53E-08	0.3096	0.462	0.095	0.0027	4
Ppm1e	1.00E-07	0.6189	0.923	0.33	0.0028	4
Kcnd2	1.01E-07	0.7855	1	0.549	0.0028	4
Abhd2	1.03E-07	0.2538	0.462	0.095	0.0029	4
Cadps2	1.09E-07	0.5489	0.462	0.101	0.0031	4
Atxn1	1.11E-07	0.6541	0.962	0.501	0.0031	4
Nptn	1.13E-07	0.5082	0.962	0.332	0.0032	4
Atp2b4	1.19E-07	0.3854	0.423	0.085	0.0033	4

Atp2b2	1.25E-07	0.5750	1	0.426	0.0035	4
Slc30a3	1.25E-07	0.2840	0.154	0.013	0.0035	4
Frmd6	1.34E-07	0.3495	0.538	0.127	0.0038	4
Plekha5	1.39E-07	0.5058	0.846	0.264	0.0039	4
Gm26911	1.70E-07	0.2580	0.192	0.021	0.0048	4
Adcy9	1.75E-07	0.3391	0.885	0.255	0.0049	4
Gabbr2	1.85E-07	0.5605	0.962	0.353	0.0052	4
Galnt18	1.87E-07	0.4745	0.731	0.219	0.0052	4
Trps1	2.06E-07	-0.8560	0.962	0.903	0.0058	4
Phlpp2	2.17E-07	0.2668	0.538	0.125	0.0061	4
Son	2.46E-07	-0.9649	0.846	0.887	0.0069	4
Cdk14	2.60E-07	0.5603	0.923	0.307	0.0073	4
Nckap5	2.65E-07	-1.0138	0.962	0.844	0.0074	4
Arl15	2.78E-07	0.5077	0.846	0.29	0.0078	4
Sdk2	3.15E-07	0.4466	0.423	0.088	0.0088	4
Heatr3	3.24E-07	0.3361	0.5	0.114	0.0091	4
Ptprs	3.40E-07	0.3905	0.808	0.235	0.0095	4
Mios	3.42E-07	0.2736	0.308	0.053	0.0096	4
Zfp654	3.50E-07	0.2539	0.577	0.141	0.0098	4
Flnb	3.53E-07	0.2832	0.538	0.126	0.0099	4
Qk	3.68E-07	-0.9620	1	0.913	0.0103	4
Pitpnc1	4.03E-07	-0.9408	0.923	0.913	0.0113	4
Samd5	4.35E-07	0.3086	0.269	0.042	0.0122	4
Pacs1	4.38E-07	0.3157	0.769	0.214	0.0123	4
Fam208b	4.57E-07	0.3336	0.615	0.159	0.0128	4
Dtna	4.63E-07	-0.7852	0.962	0.919	0.0130	4
Cdk17	4.74E-07	0.3687	0.808	0.229	0.0133	4
Rap1gds1	5.04E-07	0.3546	0.654	0.173	0.0141	4
Dym	5.16E-07	0.2662	0.731	0.193	0.0144	4
Il1rapl2	5.21E-07	1.2386	0.346	0.079	0.0146	4
Gabrg3	6.01E-07	0.8331	0.615	0.206	0.0168	4
Rasal2	6.07E-07	0.5410	0.885	0.331	0.0170	4
Atp1a2	6.20E-07	-1.0945	0.808	0.828	0.0173	4
Dlgap1	7.06E-07	0.4947	1	0.876	0.0198	4
Trio	7.60E-07	0.5430	1	0.413	0.0213	4
Sept6	7.63E-07	0.2774	0.308	0.054	0.0214	4
Fam63b	7.66E-07	0.2603	0.654	0.173	0.0214	4
Prex2	7.86E-07	-1.0334	0.923	0.855	0.0220	4
Flrt3	8.01E-07	0.2555	0.385	0.078	0.0224	4

Gabrb1	8.45E-07	-0.6868	1	0.947	0.0237	4
Atp2b1	8.48E-07	0.4694	0.885	0.294	0.0237	4
Ncs1	8.48E-07	0.3063	0.462	0.104	0.0237	4
Ube2w	8.78E-07	0.2760	0.615	0.159	0.0246	4
Dync1i2	8.96E-07	0.3557	0.846	0.252	0.0251	4
Trim35	9.63E-07	0.3058	0.615	0.163	0.0270	4
Nav2	9.83E-07	0.5680	0.962	0.574	0.0275	4
Trim2	1.10E-06	0.3081	0.846	0.268	0.0307	4
Iqsec1	1.10E-06	0.3785	0.808	0.242	0.0309	4
Dnajc21	1.20E-06	0.2805	0.346	0.068	0.0337	4
Ncoa7	1.26E-06	0.3560	0.577	0.152	0.0351	4
Rps6ka3	1.30E-06	0.3865	0.654	0.191	0.0364	4
Ttc7b	1.34E-06	0.4967	0.731	0.229	0.0376	4
Uvrag	1.38E-06	0.3897	0.654	0.185	0.0385	4
Lsamp	1.40E-06	-0.5481	1	0.997	0.0391	4
Sash1	1.42E-06	-1.0512	0.808	0.795	0.0397	4
Large	1.46E-06	0.6404	0.923	0.51	0.0407	4
Sfxn5	1.49E-06	-0.9249	0.885	0.848	0.0417	4
Gm36975	1.63E-06	0.4221	0.769	0.243	0.0457	4
Tiam1	1.79E-06	0.2676	0.192	0.025	0.0501	4
Mllt4	2.09E-06	0.2553	0.731	0.206	0.0586	4
Gls	2.14E-06	0.3911	0.808	0.265	0.0599	4
Macrod2	2.43E-06	0.5848	1	0.687	0.0680	4
Dapk1	2.57E-06	0.3646	0.615	0.177	0.0719	4
Ptpn1	2.58E-06	0.3057	0.615	0.167	0.0722	4
Prkce	2.96E-06	0.6424	0.885	0.451	0.0829	4
Map2k4	3.02E-06	0.3052	0.808	0.25	0.0846	4
Gm2163	3.03E-06	0.5845	0.577	0.173	0.0849	4
Nlk	3.15E-06	0.5718	0.885	0.361	0.0883	4
Plekhm3	3.22E-06	0.2875	0.462	0.112	0.0903	4

Supplemental Table 4.11. R6/2 12-Week Striatal Astrocyte IPA Canonical Pathway Enrichment Analysis Per Cluster

Ingenuity Canonical Pathways	-log(p-value)	Ratio	z-score	Molecules	Cluster
Protein Kinase A Signaling	8.61	0.0729	-1	ADCY2,ADCY8,ADD1,ADD3,AKAP6,CAMK2D,CREB5,DCC,EYA1,GLI3,ITPR1,LEF1,NTN1,PDE1C,PDE4B,PDE8B,PHKG1,PLCB4,PLCE1,PPP1R12A,PPP1R14C,PRKAG2,PRKCA,PTCH1,PTPRJ,PTPRK,PTPRT,SMAD3,UBASH3B	0
Glutamate Receptor Signaling	7.84	0.193	0.378	GLUL,GRIA1,GRID1,GRID2,GRIK1,GRIK4,GRIN2C,GRIP1,GRM3,SLC1A2,SLC38A1	0
CREB Signaling in Neurons	7.4	0.0918	-1	ADCY2,ADCY8,CACNA1A,CAMK2D,CREB5,GNAO1,GRIA1,GRID1,GRID2,GRIK1,GRIK4,GRIN2C,GRM3,ITPR1,PLCB4,PLCE1,POLR2A,PRKAG2,PRKCA	0
Synaptogenesis Signaling Pathway	7.04	0.0737	-0.626	ADCY2,ADCY8,CADM1,CAMK2D,CDH13,CDH2,CDH22,CHN1,CREB5,DAB1,EPHA5,EPHB1,FARP1,FYN,GRIA1,GRIN2C,GRM3,ITPR1,KALRN,Nrxn3,PRKAG2,RELN,SYN2	0
Synaptic Long Term Potentiation	6.49	0.109	-1.069	ADCY8,CAMK2D,CREB5,GRIA1,GRIN2C,GRM3,ITPR1,PLCB4,PLCE1,PPP1R12A,PPP1R14C,PRKAG2,PRKCA,RAPGEF3	0
Axonal Guidance Signaling	5.73	0.0558		ADAM23,ADAMTS9,BMP6,DCC,EPHA5,EPHB1,FYN,GLI1,GLI3,GNAO1,KALRN,NGEF,NTN1,NTNG2,NTRK3,PDGFD,PLCB4,PLCE1,PRKAG2,PRKCA,PTCH1,SEMA4D,SLIT2,SRGAP1,SRGAP2,UNC5C,VEGFA	0
Sperm Motility	5.55	0.0762	-1.89	ALK,EPHA5,EPHB1,ERBB4,FGFR1,FGFR2,FYN,ITPR1,MERTK,NTRK3,PDE1C,PDE4B,PDGFRB,PLCB4,PLCE1,PRKAG2,PRKCA	0
Amyotrophic Lateral Sclerosis Signaling	5.42	0.113	1	CACNA1A,CAPN2,GLUL,GRIA1,GRID1,GRID2,GRIK1,GRIK4,GRIN2C,SLC1A2,VEGFA	0
G-Protein Coupled Receptor Signaling	4.99	0.0662		ADCY2,ADCY8,ADRA1A,CAMK2D,CREB5,FYN,GABBR1,GNAO1,GRM3,PDE1C,PDE4B,PDE8B,PLCB4,PRKAG2,PRKCA,RAPGEF3,RGS7,S1PR1	0
Molecular Mechanisms of Cancer	4.83	0.0563		ADCY2,ADCY8,ARHGEF19,BMP6,CAMK2D,CDK17,CDK19,CTNNA2,FYN,GAB2,GLI1,GNAO1,LEF1,MAP3K5,PLCB4,PRKAG2,PRKCA,PTCH1,RAPGEF3,RB1,RHOQ,SMAD3	0
Dopamine-DARPP32 Feedback in cAMP Signaling	4.59	0.0798	-1.155	ADCY2,ADCY8,ATP2A2,CACNA1A,CREB5,GRIN2C,ITPR1,PLCB4,PLCE1,PPP1R12A,PPP1R14C,PRKAG2,PRKCA	0

Neuropathic Pain Signaling In Dorsal Horn Neurons	4.46	0.099	-1.265	CAMK2D,GRIA1,GRIN2C,GRM3,ITPR1,KCNQ3,PLCB4,PLCE1,PRKAG2,PRKCA	0
Corticotropin Releasing Hormone Signaling	4.44	0.0828	-0.333	ADCY2,ADCY8,CACNA1A,CREB5,GLI1,GLI3,GNAO1,ITPR1,PRKAG2,PRKCA,PTCH1,VEGFA	0
Cardiac Hypertrophy Signaling (Enhanced)	4.28	0.0493	-1.043	ADCY2,ADCY8,ADRA1A,AGT,ATP2A2,CACNA1A,CAMK2D,Eda,EDNRB,FGF13,FGF14,FGFR1,FGFR2,HDAC7,IL18,ITPR1,MAP3K5,PDE1C,PDE4B,PDE8B,PLCB4,PLCE1,PRKAG2,PRKCA	0
Endocannabinoid Neuronal Synapse Pathway	4.27	0.0859	-0.632	ADCY2,ADCY8,CACNA1A,GNAO1,GRIA1,GRIN2C,ITPR1,MGLL,PLCB4,PLCE1,PRKAG2	0
White Adipose Tissue Browning Pathway	4.24	0.0853	0.905	ADCY2,ADCY8,CACNA1A,CREB5,DIO2,FGFR1,FGFR2,PRDM16,PRKAG2,RUNX1T1,VEGFA	0
Cellular Effects of Sildenafil (Viagra)	4.18	0.084		ADCY2,ADCY8,CACNA1A,ITPR1,KCNQ3,PDE1C,PDE4B,PLCB4,PLCE1,PPP1R12A,PRKAG2	0
Cardiac β-adrenergic Signaling	3.89	0.078	0	ADCY2,ADCY8,AKAP6,ATP2A2,CACNA1A,PDE1C,PDE4B,PDE8B,PPP1R12A,PPP1R14C,PRKAG2	0
Opioid Signaling Pathway	3.84	0.0607	-1.807	ADCY2,ADCY8,CACNA1A,CAMK2D,CREB5,FYN,GNAO1,GRIN2C,ITPR1,PDE1C,PRKAG2,PRKCA,RGS20,RGS6,RGS7	0
IL-15 Production	3.79	0.0826	1.265	ALK,EPHA5,EPHB1,ERBB4,FGFR1,FGFR2,FYN,MERTK,NTRK3,PDGFRB	0
Hepatic Fibrosis Signaling Pathway	3.76	0.0516	0.688	AGT,CACNA1A,COL11A2,CREB5,FGFR1,GLI1,GLI3,IL18,IL1RAPL1,IRAK2,LEF1,PDGFD,PDGFRB,PRKAG2,PRKCA,PTCH1,RHOQ,SMAD3,VEGFA	0
cAMP-mediated signaling	3.67	0.0614	0.832	ADCY2,ADCY8,AKAP6,CAMK2D,CREB5,GABBR1,GNAO1,GRM3,PDE1C,PDE4B,PDE8B,RAPGEF3,RGS7,S1PR1	0
FGF Signaling	3.56	0.0952	0	CREB5,FGF13,FGF14,FGFR1,FGFR2,ITPR1,MAP3K5,PRKCA	0
Osteoarthritis Pathway	3.46	0.0616	1	CREB5,CTNNA2,FGFR1,GLI1,GLI3,HTRA1,IL1RAPL1,LEF1,PRKAG2,PTCH1,SIK3,SMAD3,VEGFA	0
Melatonin Signaling	3.23	0.0972	-0.378	CAMK2D,GNAO1,PLCB4,PLCE1,PRKAG2,PRKCA,RORB	0
GABA Receptor Signaling	3.19	0.0842		ADCY2,ADCY8,CACNA1A,GABBR1,GABRA2,GABRB1,KCNQ3,SLC6A11	0
Phospholipase C Signaling	3.15	0.0545	-0.632	ADCY2,ADCY8,ARHGEF19,CREB5,FYN,GPLD1,HDAC7,ITPR1,PLCB4,PLCE1,PPP1R12A,PRKCA,RAPGEF3,RHOQ	0
Ephrin Receptor Signaling	2.98	0.0611	0.816	ANGPT1,CREB5,EPHA5,EPHB1,FYN,GNAO1,GRIN2C,KALRN,NGEF,PDGFD,VEGFA	0
Hepatic Fibrosis / Hepatic Stellate Cell Activation	2.87	0.0591		AGT,COL11A2,EDNRB,FGFR1,FGFR2,IL1RAPL1,LHX2,PDGFD,PDGFRB,SMAD3,VEGFA	0

Human Embryonic Stem Cell Pluripotency	2.8	0.0667		BMP6,FGFR1,FGFR2,LEF1,NTRK3,PDGFD,PDGFRB,S1PR1,SMAD3	0
GPCR-Mediated Nutrient Sensing in Enteroendocrine Cells	2.73	0.0714	-2.121	ADCY2,ADCY8,CACNA1A,ITPR1,PLCB4,PLCE1,PRKAG2,PRKCA	0
Apelin Endothelial Signaling Pathway	2.66	0.0696	-1.414	ADCY2,ADCY8,ANGPT1,GNAO1,PLCB4,PRKAG2,PRKCA,SMAD3	0
Sphingosine-1-phosphate Signaling	2.61	0.0684	-0.707	ADCY2,ADCY8,PDGFD,PDGFRB,PLCB4,PLCE1,RHOQ,S1PR1	0
Sonic Hedgehog Signaling	2.6	0.138	0	GLI1,GLI3,PRKAG2,PTCH1	0
GNRH Signaling	2.59	0.0578	-1.667	ADCY2,ADCY8,CACNA1A,CAMK2D,CREB5,ITPR1,MAP3K5,PLCB4,PRKAG2,PRKCA	0
Calcium Signaling	2.52	0.0534	-1.667	ATP2A2,CACNA1A,CAMK2D,CREB5,GRIA1,GRIK1,GRIN2C,HDAC7,ITPR1,PRKAG2,RCAN2	0
α-Adrenergic Signaling	2.5	0.0729	0	ADCY2,ADCY8,ADRA1A,ITPR1,PHKG1,PRKAG2,PRKCA	0
GPCR-Mediated Integration of Enteroendocrine Signaling Exemplified by an L Cell	2.47	0.0822	0	ADCY2,ADCY8,ITPR1,PLCB4,PLCE1,PRKAG2	0
RhoGDI Signaling	2.46	0.0556	0	ARHGAP5,ARHGEF19,CDH13,CDH2,CDH22,GNAO1,GRIP1,PPP1R12A,PRKCA,RHOQ	0
Nitric Oxide Signaling in the Cardiovascular System	2.43	0.0707	-0.378	ATP2A2,CACNA1A,ITPR1,PDE1C,PRKAG2,PRKCA,VEGFA	0
Role of NFAT in Cardiac Hypertrophy	2.4	0.0514	-2.53	ADCY2,ADCY8,CACNA1A,CAMK2D,HDAC7,ITPR1,PLCB4,PLCE1,PRKAG2,PRKCA,RCAN2	0
Role of Macrophages, Fibroblasts and Endothelial Cells in Rheumatoid Arthritis	2.37	0.0449		CAMK2D,CREB5,DKK3,GNAO1,IL18,IL1RAPL1,IRAK2,LEF1,PDGFD,PLCB4,PLCE1,PRKCA,TRAF3IP2,VEGFA	0
Synaptic Long Term Depression	2.31	0.0529	-0.632	CACNA1A,GNAO1,GRIA1,GRID1,GRID2,GRM3,ITPR1,PLCB4,PLCE1,PRKCA	0
Regulation of the Epithelial-Mesenchymal Transition Pathway	2.26	0.0521		CDH2,FGF13,FGF14,FGFR1,FGFR2,LEF1,PDGFD,PDGFRB,SMAD3,ZEB1	0
Gαs Signaling	2.24	0.0654	-1.134	ADCY2,ADCY8,ADD1,ADD3,CREB5,PRKAG2,RAPGEF3	0
Neuroinflammation Signaling Pathway	2.11	0.0433	-0.378	APP,CREB5,GABBR1,GABRA2,GABRB1,GLUL,GRIA1,GRIN2C,IL18,IRAK2,MFGE8,SLC1A2,SLC6A11	0
Thrombin Signaling	2.03	0.0481	-2.121	ADCY2,ADCY8,CAMK2D,GNAO1,ITPR1,PLCB4,PLCE1,PPP1R12A,PRKCA,RHOQ	0
Netrin Signaling	2.02	0.0769	-0.447	CACNA1A,DCC,NTN1,PRKAG2,UNC5C	0
Relaxin Signaling	1.97	0.0533	0	ADCY2,ADCY8,GNAO1,PDE1C,PDE4B,PDE8B,PRKAG2,VEGFA	0

Integrin Signaling	1.96	0.0469	0.378	ARHGAP26,ARHGAP5,CAPN2,FYN,PARVB,PPP1R12A,RHOQ,TSPAN5,TSPAN7,VCL	0
Hepatic Cholestasis	1.91	0.0486		ADCY2,ADCY8,Eda,IL18,IL1RAPL1,IRAK2,PRKAG2,PRKCA,SLCO1C1	0
Gustation Pathway	1.9	0.0519		ADCY2,ADCY8,CACNA1A,ITPR1,PDE1C,PDE4B,PDE8B,PRKAG2	0
Gαi Signaling	1.89	0.056	1.134	ADCY2,ADCY8,GABBR1,GRM3,PRKAG2,RGS7,S1PR1	0
D-myo-inositol (1,4,5)-Trisphosphate Biosynthesis	1.88	0.12		PIP4K2A,PLCB4,PLCE1	0
PTEN Signaling	1.87	0.0556	-1.134	FGFR1,FGFR2,MAGI1,MAGI3,NTRK3,PDGFRB,PREX2	0
Endothelin-1 Signaling	1.86	0.0479	-1.667	ADCY2,ADCY8,EDNRB,GNAO1,GPLD1,ITPR1,PLCB4,PLCE1,PRKCA	0
P2Y Purigenic Receptor Signaling Pathway	1.85	0.0551	-1.89	ADCY2,ADCY8,CREB5,PLCB4,PLCE1,PRKAG2,PRKCA	0
Basal Cell Carcinoma Signaling	1.84	0.0694		BMP6,GLI1,GLI3,LEF1,PTCH1	0
Apelin Liver Signaling Pathway	1.83	0.115		AGT,COL11A2,PDGFRB	0
Reelin Signaling in Neurons	1.82	0.0543	-0.378	APP,CAMK2D,CDH2,DAB1,FYN,GRIN2C,RELN	0
Leptin Signaling in Obesity	1.79	0.0676		ADCY2,ADCY8,PLCB4,PLCE1,PRKAG2	0
Glioblastoma Multiforme Signaling	1.74	0.0485	-1.414	ITPR1,LEF1,PDGFD,PDGFRB,PLCB4,PLCE1,RB1,RHOQ	0
Adipogenesis pathway	1.74	0.0522		FGFR1,FGFR2,HDAC7,NR2F2,RB1,RUNX1T1,SMAD3	0
Gap Junction Signaling	1.73	0.0455		ADCY2,ADCY8,GRIA1,GRIK1,ITPR1,PLCB4,PLCE1,PRKAG2,PRKCA	0
Dopamine Receptor Signaling	1.72	0.0649		ADCY2,ADCY8,PPP1R12A,PPP1R14C,PRKAG2	0
Glutamine Biosynthesis I	1.7	1		GLUL	0
CDK5 Signaling	1.67	0.0556	0	ADCY2,ADCY8,CACNA1A,PPP1R12A,PPP1R14C,PRKAG2	0
Cardiac Hypertrophy Signaling	1.64	0.0417	-1	ADCY2,ADCY8,ADRA1A,CACNA1A,GNAO1,MAP3K5,PLCB4,PLCE1,PRKAG2,RHOQ	0
Endocannabinoid Cancer Inhibition Pathway	1.6	0.049	-0.378	ADCY2,ADCY8,CREB5,GNAO1,LEF1,PRKAG2,VEGFA	0
Endocannabinoid Developing Neuron Pathway	1.55	0.0522	-0.447	ADCY2,ADCY8,CREB5,GNAO1,MGLL,PRKAG2	0
Breast Cancer Regulation by Stathmin1	1.53	0.0321		ADGRV1,ADRA1A,ARHGEF19,BMP6,CAMK2D,CREB5,EDNRB,GABBR1,GPR158,GRM3,LGR4,NMUR2,PLCB4,PPP1R12A,PPP1R14C,PRKAG2,PRKCA,S1PR1,VEGFA	0

Factors Promoting Cardiogenesis in Vertebrates	1.5	0.0467	-1.134	BMP6,CAMK2D,CREB5,LEF1,PLCB4,PLCE1,PRKCA	0
Renin-Angiotensin Signaling	1.5	0.0508	-2	ADCY2,ADCY8,AGT,ITPR1,PRKAG2,PRKCA	0
GP6 Signaling Pathway	1.49	0.0504	0	COL11A2,FYN,ITPR1,LAMA2,LAMA3,PRKCA	0
Estrogen Receptor Signaling	1.48	0.0366	-1.732	ADCY2,ADCY8,AGT,CACNA1A,CREB5,GNAO1,PLCB4,PLCE1,PPP1R12A,PRKAG2,PRKCA,VEGFA	0
Wnt/Ca+ pathway	1.45	0.0645	-2	CREB5,PLCB4,PLCE1,PRKCA	0
IL-1 Signaling	1.44	0.0549		ADCY2,ADCY8,GNAO1,IRAK2,PRKAG2	0
PPARα/RXRα Activation	1.42	0.0421	0	ADCY2,ADCY8,IL1RAPL1,PLCB4,PLCE1,PRKAG2,PRKCA,SMAD3	0
ILK Signaling	1.42	0.0421	0.378	CREB5,FERMT2,LEF1,PARVB,PPP1R12A,RHOQ,VCL,VEGFA	0
D-myo-inositol-5-phosphate Metabolism	1.42	0.0449	-1.134	EPHX2,NUDT3,PIP4K2A,PLCB4,PLCE1,PPP1R12A,PTPRJ	0
Xenobiotic Metabolism PXR Signaling Pathway	1.4	0.0417	0	CAMK2D,CHST2,GRIP1,HS6ST3,PPP1R12A,PPP1R14C,PRKAG2,PRKCA	0
Gαq Signaling	1.4	0.0443	-1.89	ADRA1A,GPLD1,ITPR1,PLCB4,PRKCA,RGS7,RHOQ	0
Fcγ Receptor-mediated Phagocytosis in Macrophages and Monocytes	1.39	0.0532	-2.236	DGKB,FYN,GAB2,GPLD1,PRKCA	0
Clathrin-mediated Endocytosis Signaling	1.39	0.0415		CLU,DAB2,FGF13,FGF14,PDGFD,SH3GL2,SH3KBP1,VEGFA	0
RAR Activation	1.38	0.0412		ADCY2,ADCY8,MAP3K5,NR2F2,PRKAG2,PRKCA,SMAD3,VEGFA	0
Calcium-induced T Lymphocyte Apoptosis	1.37	0.0606	-1	ATP2A2,CAPN2,ITPR1,PRKCA	0
Adrenomedullin signaling pathway	1.35	0.0406	-0.707	ADCY2,ADCY8,IL18,ITPR1,KCNQ3,PLCB4,PLCE1,PRKAG2	0
Superpathway of Inositol Phosphate Compounds	1.34	0.0404	-1.414	EPHX2,ITPKB,NUDT3,PIP4K2A,PLCB4,PLCE1,PPP1R12A,PTPRJ	0
Apelin Cardiomyocyte Signaling Pathway	1.31	0.0505	-2.236	ATP2A2,ITPR1,PLCB4,PLCE1,PRKCA	0
Synaptogenesis Signaling Pathway	11.8	0.0994	0.365	ADCY8,AKT3,CACNA2D1,CADM1,CAMK2G,CDH2,CDH20,CDH22,CDH4,CREB5,DAB1,EPHA5,EPHB1,FYN,GRIA1,GRIA2,GRIN2C,GRIN3A,GRM3,GRM5,LRP8,Nrxn3,NTRK2,PAK1,PIK3R1,RASGRF1,RASGRP1,STXBP6,SYN2,SYT10,SYT17	1

CREB Signaling in Neurons	7.64	0.0966	1.5	ADCY8,AKT3,CACNA2D1,CAMK2G,CREB5,GNAO1,GNG12,GRIA1,GRIA2,GRID2,GRIK4,GRIN2C,GRM3,GRM5,PIK3R1,PLCB1,PLCB4,PLCE1,POLR2A,PRKCA	1
Glutamate Receptor Signaling	7.53	0.193	0.816	GRIA1,GRIA2,GRID2,GRIK4,GRIN2C,GRIN3A,GRIP1,GRM3,GRM5,SLC1A2,SLC38A1	1
Neuropathic Pain Signaling In Dorsal Horn Neurons	7.48	0.139	2.673	CAMK1D,CAMK2G,GRIA1,GRIA2,GRIN2C,GRIN3A,GRM3,GRM5,NTRK2,PIK3R1,PLCB1,PLCB4,PLCE1,PRKCA	1
Axonal Guidance Signaling	7.16	0.064		ADAM23,AKT3,DCC,EPHA5,EPHB1,FYN,GLI1,GLI3,GNAO1,GNG12,LIMK2,MMP16,NRP1,NTNG2,NTRK2,NTRK3,PAK1,PDGFD,PIK3R1,PLCB1,PLCB4,PLCE1,PRKCA,PTCH1,ROBO2,SEMA4D,SEMA6A,SRGAP1,SRGAP2,SRGAP3,UNC5C	1
Synaptic Long Term Potentiation	6.14	0.109	1.604	ADCY8,CAMK2G,CREB5,GRIA1,GRIA2,GRIN2C,GRIN3A,GRM3,GRM5,PLCB1,PLCB4,PLCE1,PPP1R14C,PRKCA	1
Molecular Mechanisms of Cancer	5.87	0.0639		ADCY8,AKT3,ARHGEF10,CAMK2G,CCND2,CTNNA2,FOXO1,FYN,GAB2,GLI1,GNAO1,LEF1,MAP3K5,PAK1,PIK3R1,PLCB1,PLCB4,PRKCA,PTCH1,RASGRF1,RASGRP1,RB1,RHOQ,SMAD3,TCF4	1
Sperm Motility	5.78	0.0807	1.89	ABHD3,ALK,EPHA5,EPHB1,ERBB4,FGFR1,FGFR2,FGFR3,FYN,MERTK,NTRK2,NTRK3,PDE1C,PDE4B,PLCB1,PLCB4,PLCE1,PRKCA	1
Endocannabinoid Neuronal Synapse Pathway	5.42	0.102	1.155	ADCY8,CACNA2D1,GNAO1,GRIA1,GRIA2,GRIN2C,GRIN3A,GRM5,MAPK4,MGLL,PLCB1,PLCB4,PLCE1	1
G-Protein Coupled Receptor Signaling	5.15	0.0699		ADCY8,AKT3,CAMK2G,CREB5,FYN,GABBR2,GNAO1,GRM3,GRM5,HRH1,PDE1C,PDE4B,PDE8B,PIK3R1,PLCB1,PLCB4,PRKCA,RASGRP1,RGS7	1
FGF Signaling	4.91	0.119	-1.265	AKT3,CREB5,FGF12,FGF13,FGFR1,FGFR2,FGFR3,MAP3K5,PIK3R1,PRKCA	1
Human Embryonic Stem Cell Pluripotency	4.46	0.0889		AKT3,FGFR1,FGFR2,FGFR3,FOXO1,LEF1,NTRK2,NTRK3,PDGFD,PIK3R1,SMAD3,TCF4	1
RhoGDI Signaling	4.45	0.0778	-0.905	ARHGEF10,CDH2,CDH20,CDH22,CDH4,DLC1,EZR,GNAO1,GNG12,GRIP1,LIMK2,PAK1,PRKCA,RHOQ	1
Amyotrophic Lateral Sclerosis Signaling	4.36	0.103	1	AKT3,GRIA1,GRIA2,GRID2,GRIK4,GRIN2C,GRIN3A,PAK1,PIK3R1,SLC1A2	1
IL-15 Production	4.23	0.0909	-0.302	ALK,EPHA5,EPHB1,ERBB4,FGFR1,FGFR2,FGFR3,FYN,MERTK,NTRK2,NTRK3	1
Regulation of the Epithelial-Mesenchymal Transition Pathway	4.15	0.0729		AKT3,CDH2,FGF12,FGF13,FGFR1,FGFR2,FGFR3,JAG1,LEF1,NOTCH3,PDGFD,PIK3R1,SMAD3,TCF4	1

PTEN Signaling	4.07	0.0873	0.632	AKT3,FGFR1,FGFR2,FGFR3,FOXO1,GHR,MAGI3,NTRK2,NTRK3,PIK3R1,PREX2	1
Opioid Signaling Pathway	4.04	0.0648	1	ADCY8,AKT3,CACNA2D1,CAMK1D,CAMK2G,CREB5,FYN,GNAO1,GRIN2C,GRIN3A,MAPK4,PDE1C,PLCB1,PRKCA,RGS20,RGS7	1
Reelin Signaling in Neurons	3.97	0.0853	0.302	AKT3,ARHGEF10,CAMK2G,CDH2,DAB1,FYN,GRIN2C,GRIN3A,ITGA6,LRP8,PIK3R1	1
Ephrin Receptor Signaling	3.85	0.0722	-0.632	AKT3,CREB5,EPHA5,EPHB1,FYN,GNAO1,GNG12,GRIN2C,GRIN3A,LIMK2,PAK1,PDGFD,SORBS1	1
Calcium Signaling	3.82	0.068	0.333	CACNA2D1,CAMK1D,CAMK2G,CREB5,GRIA1,GRIA2,GRIN2C,GRIN3A,HDAC8,MCU,MEF2C,RCAN2,TP63,TRPC1	1
Fcγ Receptor-mediated Phagocytosis in Macrophages and Monocytes	3.73	0.0957	1	AKT3,DGKB,EZR,FYN,GAB2,GPLD1,PAK1,PIK3R1,PRKCA	1
Breast Cancer Regulation by Stathmin1	3.69	0.0457		ADGRB1,ADGRB3,ADGRL3,ADGRV1,ARHGEF10,CAMK1D,CAMK2G,CCND2,CELSR1,CREB5,EDNRB,GABBR2,GNG12,GPRC5B,GRM3,GRM5,HRH1,LGR4,NTSR2,PAK1,PIK3R1,PLCB1,PLCB4,PPP1R14C,PPP2R3A,PRKCA,SCTR	1
Role of NFAT in Cardiac Hypertrophy	3.65	0.0654	1.732	ADCY8,AKT3,CACNA2D1,CAMK1D,CAMK2G,GNG12,HDAC8,MEF2C,PIK3R1,PLCB1,PLCB4,PLCE1,PRKCA,RCAN2	1
Synaptic Long Term Depression	3.64	0.0688	1.387	ABHD3,CACNA2D1,GNAO1,GRIA1,GRIA2,GRID2,GRM3,GRM5,PLCB1,PLCB4,PLCE1,PPP2R3A,PRKCA	1
Signaling by Rho Family GTPases	3.58	0.0615	1.387	ARHGEF10,CDC42EP1,CDH2,CDH20,CDH22,CDH4,CIT,CYFIP1,EZR,GNAO1,GNG12,LIMK2,PAK1,PIK3R1,RHOQ	1
Thyroid Cancer Signaling	3.54	0.101	0	AKT3,ALK,FOXO1,LEF1,NTRK2,NTRK3,PIK3R1,TCF4	1
Cardiac Hypertrophy Signaling (Enhanced)	3.43	0.0472	0.426	ADCY8,AGT,AKT3,CAMK2G,Eda,EDNRB,FGF12,FGF13,FGFR1,FGFR2,FGFR3,GHR,HDAC8,MAP3K5,MEF2C,PDE1C,PDE4B,PDE8B,PIK3R1,PLCB1,PLCB4,PLCE1,PRKCA	1
Protein Kinase A Signaling	3.39	0.0503	1.291	ADCY8,CAMK2G,CREB5,DCC,EYA1,GLI3,GNG12,LEF1,PDE1C,PDE4B,PDE8B,PLCB1,PLCB4,PLCE1,PPP1R14C,PRKCA,PTCH1,PTPRT,SMAD3,TCF4	1
Thrombin Signaling	3.24	0.0625	2.111	ADCY8,AKT3,ARHGEF10,CAMK1D,CAMK2G,GNAO1,GNG12,PIK3R1,PLCB1,PLCB4,PLCE1,PRKCA,RHOQ	1
Gαq Signaling	3.21	0.0696	2.53	AKT3,GNG12,GPLD1,GRM5,HRH1,PIK3R1,PLCB1,PLCB4,PRKCA,RGS7,RHOQ	1
Osteoarthritis Pathway	3.18	0.0616	-0.333	CREB5,CTNNA2,FGFR1,FGFR3,GLI1,GLI3,JAG1,LEF1,MEF2C,PTCH1,SIK3,SMAD3,TCF4	1
Endothelin-1 Signaling	3.11	0.0638	2.111	ABHD3,ADCY8,ECE1,EDNRB,GNAO1,GPLD1,MAPK4,PIK3R1,PLCB1,PLCB4,PLCE1,PRKCA	1

Dopamine-DARPP32 Feedback in cAMP Signaling	3.1	0.0675	0.632	ADCY8,CREB5,GRIN2C,GRIN3A,KCNJ10,PLCB1,PLCB4,PLCE1,PPP1R14C,PPP2R3A,PRKCA	1
Apelin Endothelial Signaling Pathway	3.08	0.0783	0.333	ADCY8,AKT3,GNAO1,MEF2C,PIK3R1,PLCB1,PLCB4,PRKCA,SMAD3	1
Role of Tissue Factor in Cancer	3.03	0.0769		AKT3,F3,FYN,ITGA6,LIMK2,PAK1,PIK3R1,PLCB1,PRKCA	1
CXCR4 Signaling	3.01	0.0659	0.707	ADCY8,AKT3,ELMO2,GNAO1,GNG12,PAK1,PIK3R1,PLCB1,PLCB4,PRKCA,RHOQ	1
Leptin Signaling in Obesity	2.99	0.0946		ADCY8,AKT3,FOXO1,PIK3R1,PLCB1,PLCB4,PLCE1	1
Notch Signaling	2.96	0.135		CNTN1,DTX1,JAG1,MAML3,NOTCH3	1
P2Y Purigenic Receptor Signaling Pathway	2.78	0.0709	1.414	ADCY8,AKT3,CREB5,GNG12,PIK3R1,PLCB1,PLCB4,PLCE1,PRKCA	1
Semaphorin Signaling in Neurons	2.75	0.1		FYN,LIMK2,NRP1,PAK1,RHOQ,SEMA4D	1
D-myo-inositol (1,4,5)-Trisphosphate Biosynthesis	2.74	0.16	2	PIP4K2A,PLCB1,PLCB4,PLCE1	1
White Adipose Tissue Browning Pathway	2.73	0.0698	-1.667	ADCY8,CACNA2D1,CREB5,DIO2,FGFR1,FGFR2,FGFR3,NRF1,PRDM16	1
Estrogen Receptor Signaling	2.69	0.0488	0.5	ADCY8,AGT,AKT3,CREB5,FOXO1,GNAO1,LIMK2,MCU,MMP16,NRF1,PAK1,PIK3R1,PLCB1,PLCB4,PLCE1,PRKCA	1
Glioblastoma Multiforme Signaling	2.52	0.0606	1.897	AKT3,FOXO1,LEF1,PDGFD,PIK3R1,PLCB1,PLCB4,PLCE1,RB1,RHOQ	1
Endocannabinoid Developing Neuron Pathway	2.48	0.0696	-0.707	ADCY8,AKT3,CREB5,GNAO1,MAPK4,MGLL,PAX6,PIK3R1	1
Sphingosine-1-phosphate Signaling	2.43	0.0684	1.414	ADCY8,AKT3,PDGFD,PIK3R1,PLCB1,PLCB4,PLCE1,RHOQ	1
Phospholipase C Signaling	2.42	0.0506	1.897	ADCY8,ARHGEF10,CREB5,FYN,GNG12,GPLD1,HDAC8,MEF2C,PLCB1,PLCB4,PLCE1,PRKCA,RHOQ	1
Germ Cell-Sertoli Cell Junction Signaling	2.41	0.0585		CDH2,CTNNA2,ITGA6,LIMK2,MAP3K5,PAK1,PIK3R1,RHOQ,SORBS1,VCL	1
Corticotropin Releasing Hormone Signaling	2.39	0.0621	0	ADCY8,CACNA2D1,CREB5,GLI1,GLI3,GNAO1,MEF2C,PRKCA,PTCH1	1
Wnt/β-catenin Signaling	2.38	0.0578	-1.414	AKT3,AXIN2,CDH2,DKK3,GNAO1,LEF1,PPP2R3A,SOX6,TCF4,TLE1	1
GABA Receptor Signaling	2.37	0.0737		ABAT,ADCY8,CACNA2D1,GABBR2,GABRA2,SLC6A1,SLC6A11	1
Melatonin Signaling	2.35	0.0833	0.816	CAMK2G,GNAO1,PLCB1,PLCB4,PLCE1,PRKCA	1
Factors Promoting Cardiogenesis in Vertebrates	2.29	0.06	0.333	CAMK2G,CREB5,LEF1,MEF2C,PLCB1,PLCB4,PLCE1,PRKCA,TCF4	1

p53 Signaling	2.29	0.0714	0.816	ADGRB1,AKT3,CCND2,PIK3R1,RB1,SERPINE2,TP63	1
Apelin Cardiomyocyte Signaling Pathway	2.27	0.0707	1.89	AKT3,MAPK4,PIK3R1,PLCB1,PLCB4,PLCE1,PRKCA	1
Epithelial Adherens Junction Signaling	2.26	0.0592		AKT3,CDH2,CTNNA2,FGFR1,LEF1,NOTCH3,SORBS1,TCF4,VCL	1
14-3-3-mediated Signaling	2.22	0.063	1.134	AKT3,FOXO1,MAP3K5,PIK3R1,PLCB1,PLCB4,PLCE1,PRKCA	1
Hepatic Fibrosis Signaling Pathway	2.21	0.0435	1	AGT,AKT3,CREB5,FGFR1,FOXO1,GLI1,GLI3,LEF1,PDCD4,PDGFD,PIK3R1,PRKCA,PTCH1,RHOQ,SMAD3,TCF4	1
Integrin Signaling	2.19	0.0516	0.333	AKT3,ASAP1,FYN,ITGA6,PAK1,PARVB,PIK3R1,RHOQ,TSPAN5,TSPAN7,VCL	1
p70S6K Signaling	2.18	0.062	2.121	AGT,AKT3,PIK3R1,PLCB1,PLCB4,PLCE1,PPP2R3A,PRKCA	1
Mouse Embryonic Stem Cell Pluripotency	2.17	0.068	-1.134	AKT3,ID3,ID4,LEF1,LIFR,PIK3R1,TCF4	1
IL-3 Signaling	2.16	0.0759	0.816	AKT3,FOXO1,GAB2,PAK1,PIK3R1,PRKCA	1
BEX2 Signaling Pathway	2.16	0.0759	-0.816	AKT3,CDH2,LEF1,PPP2R3A,SWAP70,TCF4	1
Gα12/13 Signaling	2.16	0.0615	-0.707	AKT3,CDH2,CDH20,CDH22,CDH4,MAP3K5,MEF2C,PIK3R1	1
Chemokine Signaling	2.13	0.075	2.449	CAMK1D,CAMK2G,LIMK2,PLCB1,PLCB4,PRKCA	1
Actin Cytoskeleton Signaling	2.12	0.0505	-0.378	CYFIP1,EZR,FGF12,FGF13,GNG12,LIMK2,PAK1,PDGFD,PIK3R1,TIAM2,VCL	1
Role of Macrophages, Fibroblasts and Endothelial Cells in Rheumatoid Arthritis	2.11	0.0449		AKT3,CAMK2G,CREB5,DAAM1,DKK3,GNAO1,LEF1,PDGFD,PIK3R1,PLCB1,PLCB4,PLCE1,PRKCA,TCF4	1
Adipogenesis pathway	2.08	0.0597		FGFR1,FGFR2,FGFR3,FOXO1,HDAC8,NR2F2,RB1,SMAD3	1
CDK5 Signaling	2.06	0.0648	0	ADCY8,CABLES1,ITGA6,MAPK4,NTRK2,PPP1R14C,PPP2R3A	1
Glioma Signaling	2.02	0.0636	1.633	AKT3,CAMK1D,CAMK2G,PDGFD,PIK3R1,PRKCA,RB1	1
PI3K Signaling in B Lymphocytes	2.01	0.058	1.414	AKT3,CAMK2G,DAPP1,FYN,PIK3R1,PLCB1,PLCB4,PLCE1	1
Leukocyte Extravasation Signaling	1.99	0.0508	-1	CTNNA2,DLC1,EZR,ITGA6,MMP16,PIK3R1,PRKCA,RASGRP1,TIMP4,VCL	1
cAMP-mediated signaling	1.98	0.0482	0.302	ADCY8,CAMK1D,CAMK2G,CREB5,GABBR2,GNAO1,GRM3,PDE1C,PDE4B,PDE8B,RGS7	1
GPCR-Mediated Nutrient Sensing in Enteroendocrine Cells	1.98	0.0625	1.134	ADCY8,CACNA2D1,GNG12,PLCB1,PLCB4,PLCE1,PRKCA	1

Gap Junction Signaling	1.98	0.0505		ADCY8,AKT3,GJB6,GRIA1,GRIA2,PIK3R1,PLCB1,PLCB4,PLCE1,PRKCA	1
Wnt/Ca+ pathway	1.98	0.0806	1.342	CREB5,PLCB1,PLCB4,PLCE1,PRKCA	1
Phospholipases	1.95	0.0794	2.236	ABHD3,GPLD1,PLCB1,PLCB4,PLCE1	1
Endocannabinoid Cancer Inhibition Pathway	1.92	0.0559	0.707	ADCY8,AKT3,CCND2,CREB5,GNAO1,LEF1,PIK3R1,TCF4	1
GNRH Signaling	1.91	0.052	0.707	ADCY8,CACNA2D1,CAMK2G,CREB5,MAP3K5,PAK1,PLCB1,PLCB4,PRKCA	1
Prostate Cancer Signaling	1.87	0.0659		AKT3,CREB5,FOXO1,LEF1,PIK3R1,RB1	1
Cell Cycle: G1/S Checkpoint Regulation	1.84	0.0746	-0.447	CCND2,FOXO1,HDAC8,RB1,SMAD3	1
NF-κB Signaling	1.82	0.0503	0.707	AKT3,FGFR1,FGFR2,FGFR3,GHR,NTRK2,NTRK3,PIK3R1,TANK	1
Relaxin Signaling	1.81	0.0533		ADCY8,AKT3,GNAO1,GNG12,PDE1C,PDE4B,PDE8B,PIK3R1	1
Role of NFAT in Regulation of the Immune Response	1.79	0.0497	0.707	AKT3,FYN,GNAO1,GNG12,MEF2C,PIK3R1,PLCB1,PLCB4,RCAN2	1
FAK Signaling	1.79	0.0632		AKT3,ASAP1,FYN,PAK1,PIK3R1,VCL	1
CCR3 Signaling in Eosinophils	1.76	0.0565	1.342	GNG12,LIMK2,PAK1,PIK3R1,PLCB1,PLCB4,PRKCA	1
Ephrin A Signaling	1.75	0.0851		EPHA5,FYN,PAK1,PIK3R1	1
Phagosome Formation	1.74	0.056		PIK3R1,PLCB1,PLCB4,PLCE1,PRKCA,RHOQ,SCARA3	1
B Cell Receptor Signaling	1.73	0.0486	-0.333	AKT3,CAMK2G,CREB5,DAPP1,FOXO1,GAB2,MAP3K5,MEF2C,PIK3R1	1
Basal Cell Carcinoma Signaling	1.72	0.0694		GLI1,GLI3,LEF1,PTCH1,TCF4	1
Thiamin Salvage III	1.67	1		TPK1	1
PPARα/RXRα Activation	1.67	0.0474	-0.816	ADCY8,GHR,GPD2,MEF2C,PLCB1,PLCB4,PLCE1,PRKCA,SMAD3	1
Chronic Myeloid Leukemia Signaling	1.63	0.0583		AKT3,GAB2,HDAC8,PIK3R1,RB1,SMAD3	1
Neurotrophin/TRK Signaling	1.63	0.0658		CREB5,MAP3K5,NTRK2,NTRK3,PIK3R1	1
Macropinocytosis Signaling	1.63	0.0658	1	PAK1,PDGFD,PIK3R1,PRKCA,RAB34	1
Clathrin-mediated Endocytosis Signaling	1.63	0.0466		AP3S1,CLU,DAB2,FGF12,FGF13,MYO1E,PDGFD,PIK3R1,SH3GL2	1
Sonic Hedgehog Signaling	1.63	0.103		GLI1,GLI3,PTCH1	1

PD-1, PD-L1 cancer immunotherapy pathway	1.58	0.0566	0	AKT3,CBLB,PDCD4,PIK3R1,RASGRP1,SMAD3	1
Superpathway of Inositol Phosphate Compounds	1.57	0.0455	1	EPHX2,ITPKB,NUDT3,PIK3R1,PIP4K2A,PLCB1,PLCB4,PLCE1,PPP2R3A	1
G Protein Signaling Mediated by Tubby	1.55	0.0968		GNG12,PLCB1,PLCB4	1
Neuroinflammation Signaling Pathway	1.54	0.04	0.378	AKT3,CREB5,GABBR2,GABRA2,GRIA1,GRIN2C,GRIN3A,MAPK4,PIK3R1,SLC1A2,SLC6A1,SLC6A11	1
Huntington's Disease Signaling	1.49	0.0422	1.633	AKT3,CREB5,GNG12,GRM5,HDAC8,PIK3R1,PLCB1,PLCB4,POLR2A,PRKCA	1
Cardiac β-adrenergic Signaling	1.49	0.0496	0	ADCY8,GNG12,PDE1C,PDE4B,PDE8B,PPP1R14C,PPP2R3A	1
Circadian Rhythm Signaling	1.48	0.0909		CREB5,GRIN2C,GRIN3A	1
TR/RXR Activation	1.47	0.0595		AKT3,DIO2,PIK3R1,RCAN2,SLC16A2	1
HER-2 Signaling in Breast Cancer	1.47	0.0595		AKT3,FOXO1,MAP3K5,PIK3R1,PRKCA	1
Cardiac Hypertrophy Signaling	1.46	0.0417	1.414	ADCY8,GNAO1,GNG12,MAP3K5,MEF2C,PIK3R1,PLCB1,PLCB4,PLCE1,RHOQ	1
Endometrial Cancer Signaling	1.4	0.0667		AKT3,CTNNA2,LEF1,PIK3R1	1
Choline Biosynthesis III	1.4	0.133		GPLD1,PHKA1	1
β-alanine Degradation I	1.37	0.5		ABAT	1
Glutamate Biosynthesis II	1.37	0.5		GLUD1	1
Glutamate Degradation X	1.37	0.5		GLUD1	1
Colorectal Cancer Metastasis Signaling	1.33	0.0395	0	ADCY8,AKT3,DCC,GNG12,LEF1,MMP16,PIK3R1,RHOQ,SMAD3,TCF4	1
Docosahexaenoic Acid (DHA) Signaling	1.33	0.0789		AKT3,FOXO1,PIK3R1	1
Hepatic Fibrosis / Hepatic Stellate Cell Activation	1.32	0.043		AGT,ECE1,EDNRB,FGFR1,FGFR2,LHX2,PDGFD,SMAD3	1
G Beta Gamma Signaling	1.32	0.0492	-1.633	AKT3,CACNA2D1,GNAO1,GNG12,PAK1,PRKCA	1
Synaptogenesis Signaling Pathway	9.05	0.0865	-1.347	ADCY2,ADCY8,CADM1,CAMK2D,CAMK2G,CDH13,CDH20,CDH22,DAB1,EFNA5,EPHA4,EPHB1,FARP1,GRIA1,GRIA2,GRIN2C,GRM3,KALRN,NRXN1,Nrxn3,NTRK2,PAK1,PRKAG2,RASGRP1,RELN,SHC3,SYN2	2
Protein Kinase A Signaling	6.82	0.0678	0	ADCY2,ADCY8,ADD1,ADD3,ANAPC1,CAMK2D,CAMK2G,CHUK,DCC,GLI3,LEF1,MPPED2,PDE4B,PDE8B,PHKG1,PLCE1,PPP1R12A,PPP1R14C,PRKAG2,PTK2,Ptprd,PTPRJ,PTPRK,PTPRT,SIRPA,SMAD3,UBASH3B	2

Glutamate Receptor Signaling	6.5	0.175	0	GLUL,GRIA1,GRIA2,GRID2,GRIK4,GRIN2C,GRIP1,GRM3,SLC1A2,SLC1A3	2
G-Protein Coupled Receptor Signaling	5.16	0.0699		ADCY2,ADCY8,ADORA1,ADRA1A,CAMK2D,CAMK2G,CHUK,GABBR1,GNAO1,GRM3,MPPED2,PDE4B,PDE8B,PRKAG2,RAPGEF3,RAPGEF4,RASGRP1,RGS7,S1PR1	2
Synaptic Long Term Potentiation	4.67	0.093	-0.577	ADCY8,CAMK2D,CAMK2G,GRIA1,GRIA2,GRIN2C,GRM3,PLCE1,PPP1R12A,PPP1R14C,PRKAG2,RAPGEF3	2
CREB Signaling in Neurons	4.38	0.0725	0	ADCY2,ADCY8,CACNA1A,CAMK2D,CAMK2G,GNAO1,GRIA1,GRIA2,GRID2,GRIK4,GRIN2C,GRM3,PLCE1,POLR2A,PRKAG2	2
IL-15 Production	4.24	0.0909	-0.302	ALK,EPHA4,EPHB1,ERBB4,FGFR3,MERTK,NTRK2,NTRK3,PTK2,ROR1,STAT1	2
Endocannabinoid Neuronal Synapse Pathway	4.01	0.0859	-0.632	ADCY2,ADCY8,CACNA1A,GNAO1,GRIA1,GRIA2,GRIN2C,MAPK4,MGLL,PLCE1,PRKAG2	2
Molecular Mechanisms of Cancer	3.94	0.0537		ADCY2,ADCY8,ARHGEF19,ARHGEF4,CAMK2D,CAMK2G,CCND3,CDK6,CTNNA2,FNBP1,FZD2,GNAO1,LEF1,NLK,PAK1,PRKAG2,PTK2,RAPGEF3,RASGRP1,RHOJ,SMAD3	2
cAMP-mediated signaling	3.91	0.0658	-0.535	ADCY2,ADCY8,ADORA1,CAMK2D,CAMK2G,GABBR1,GNAO1,GRM3,MPPED2,PDE4B,PDE8B,RAPGEF3,RAPGEF4,RGS7,S1PR1	2
Amyotrophic Lateral Sclerosis Signaling	3.63	0.0928	-0.378	CACNA1A,GLUL,GRIA1,GRIA2,GRID2,GRIK4,GRIN2C,PAK1,SLC1A2	2
Neuropathic Pain Signaling In Dorsal Horn Neurons	3.5	0.0891	-0.333	CAMK2D,CAMK2G,GRIA1,GRIA2,GRIN2C,GRM3,NTRK2,PLCE1,PRKAG2	2
Axonal Guidance Signaling	3.48	0.0475		ADAM23,ADAMTS12,ADAMTS6,ADAMTS9,DCC,EFNA5,EPHA4,EPHB1,FZD2,GLI2,GLI3,GNAO1,KALRN,NGEF,NTRK2,NTRK3,PAK1,PLCE1,PRKAG2,PTK2,SEMA4A,SLIT2,SRGAP1	2
Sperm Motility	3.47	0.0628	1.342	ABHD3,ALK,EPHA4,EPHB1,ERBB4,FGFR3,MERTK,NTRK2,NTRK3,PDE4B,PLCE1,PRKAG2,PTK2,ROR1	2
RhoGDI Signaling	3.29	0.0667	0.632	ARHGAP5,ARHGEF19,ARHGEF4,CDH13,CDH20,CDH22,FNBP1,GNAO1,GRIP1,PAK1,PPP1R12A,RHOJ	2
CDK5 Signaling	3.29	0.0833	-0.333	ADCY2,ADCY8,CABLES1,CACNA1A,MAPK4,NTRK2,PPP1R12A,PPP1R14C,PRKAG2	2
White Adipose Tissue Browning Pathway	2.74	0.0698	-0.333	ADCY2,ADCY8,CACNA1A,DIO2,FGFR3,PRDM16,PRKAG2,RUNX1T1,RXRG	2
Osteoarthritis Pathway	2.69	0.0569	-0.333	CHUK,CTNNA2,FGFR3,FZD2,GLI2,GLI3,HTRA1,IL1RAPL1,LEF1,PRKAG2,SIK3,SMAD3	2

Gαs Signaling	2.68	0.0748	1.414	ADCY2,ADCY8,ADD1,ADD3,PRKAG2,RAPGEF2,RAPGEF3,RAPGEF4	2
Neuroinflammation Signaling Pathway	2.67	0.05	0.333	APP,CHUK,GABBR1,GABRB1,GABRG3,GLUL,GRIA1,GRIN2C,IL18,IRAK2,MAPK4,MFGE8,SLC1A2,SLC1A3,STAT1	2
Acetate Conversion to Acetyl-CoA	2.58	0.5		ACSS1,ACSS3	2
Opioid Signaling Pathway	2.58	0.0526	0.832	ADCY2,ADCY8,ARRB1,CACNA1A,CAMK2D,CAMK2G,GNAO1,GRIN2C,MAPK4,PRKAG2,RGS20,RGS6,RGS7	2
Ephrin A Signaling	2.5	0.106		EFNA5,EPHA4,NGEF,PAK1,PTK2	2
Cardiac β-adrenergic Signaling	2.47	0.0638	0	ADCY2,ADCY8,CACNA1A,MPPED2,PDE4B,PDE8B,PPP1R12A,PPP1R14C,PRKAG2	2
Cardiac Hypertrophy Signaling (Enhanced)	2.36	0.0411	0.471	ADCY2,ADCY8,ADRA1A,CACNA1A,CAMK2D,CAMK2G,CHUK,Eda,FGF13,FGF14,FGFR3,FZD2,HDAC8,IL18,MPPED2,PDE4B,PDE8B,PLCE1,PRKAG2,PTK2	2
Melatonin Signaling	2.36	0.0833	0	CAMK2D,CAMK2G,GNAO1,PLCE1,PRKAG2,RORB	2
Calcium Signaling	2.31	0.0534	0.378	ATP2C1,CACNA1A,CAMK2D,CAMK2G,GRIA1,GRIA2,GRIN2C,HDAC8,MYH14,PRKAG2,RCAN2	2
Thrombin Signaling	2.28	0.0529	0	ADCY2,ADCY8,ARHGEF4,CAMK2D,CAMK2G,FNBP1,GNAO1,PLCE1,PPP1R12A,PTK2,RHOJ	2
Gαi Signaling	2.26	0.064	-0.707	ADCY2,ADCY8,ADORA1,GABBR1,GRM3,PRKAG2,RGS7,S1PR1	2
Ephrin Receptor Signaling	2.26	0.0556	-1.633	ANGPT1,EFNA5,EPHA4,EPHB1,GNAO1,GRIN2C,KALRN,NGEF,PAK1,PTK2	2
PTEN Signaling	2.24	0.0635	0	CHUK,FGFR3,MAGI1,MAGI3,NTRK2,NTRK3,PREX2,PTK2	2
Signaling by Rho Family GTPases	2.19	0.0492	0.302	ARHGEF19,ARHGEF4,CDH13,CDH20,CDH22,FNBP1,GNAO1,PAK1,PLD1,PPP1R12A,PTK2,RHOJ	2
Necroptosis Signaling Pathway	2.17	0.0573	-0.333	CAMK2D,CAMK2G,CHUK,DNM1L,GLUD1,GLUL,MERTK,SLC25A13,STAT1	2
Cellular Effects of Sildenafil (Viagra)	2.14	0.0611		ADCY2,ADCY8,CACNA1A,MYH14,PDE4B,PLCE1,PPP1R12A,PRKAG2	2
Sphingosine-1-phosphate Signaling	1.89	0.0598	0.378	ADCY2,ADCY8,FNBP1,PLCE1,PTK2,RHOJ,S1PR1	2
IL-1 Signaling	1.88	0.0659		ADCY2,ADCY8,CHUK,GNAO1,IRAK2,PRKAG2	2
Hepatic Fibrosis Signaling Pathway	1.88	0.0408	-0.535	CACNA1A,CHUK,COL11A2,FNBP1,FZD2,GLI2,GLI3,IL18,IL1RAPL1,IRAK2,LEF1,PRKAG2,PTK2,RHOJ,SMAD3	2
Renin-Angiotensin Signaling	1.87	0.0593	0	ADCY2,ADCY8,PAK1,PRKAG2,PTK2,SHC3,STAT1	2
GABA Receptor Signaling	1.79	0.0632		ADCY2,ADCY8,CACNA1A,GABBR1,GABRB1,GABRG3	2

RhoA Signaling	1.78	0.0569	1.134	ARHGAP5,NGEF,PLD1,PPP1R12A,PTK2,RAPGEF2,RAPGEF6	2
Role of Macrophages, Fibroblasts and Endothelial Cells in Rheumatoid Arthritis	1.76	0.0417		CAMK2D,CAMK2G,CHUK,DKK3,FZD2,GNAO1,IL18,IL1RAPL1,IRAK2,LEF1,NLK,PLCE1,TRAF3IP2	2
Hepatic Cholestasis	1.74	0.0486		ADCY2,ADCY8,CHUK,Eda,IL18,IL1RAPL1,IRAK2,PRKAG2,SLCO1C1	2
Ephrin B Signaling	1.72	0.0694	-1.342	EPHB1,GNAO1,KALRN,PAK1,PTK2	2
Colorectal Cancer Metastasis Signaling	1.68	0.0435	0	ADCY2,ADCY8,ARRB1,DCC,FNBP1,FZD2,LEF1,PRKAG2,RHOJ,SMAD3,STAT1	2
Reelin Signaling in Neurons	1.68	0.0543	-0.378	APP,ARHGEF4,CAMK2D,CAMK2G,DAB1,GRIN2C,RELN	2
Thiamin Salvage III	1.67	1		TPK1	2
Glutamine Biosynthesis I	1.67	1		GLUL	2
Adenine and Adenosine Salvage VI	1.67	1		ADK	2
Phospholipase C Signaling	1.64	0.0428	-1.414	ADCY2,ADCY8,ARHGEF19,ARHGEF4,FNBP1,HDAC8,PLCE1,PLD1,PPP1R12A,RAPGEF3,RHOJ	2
ERK/MAPK Signaling	1.63	0.0466	0.333	ELK3,PAK1,PPP1R12A,PPP1R14C,PRKAG2,PTK2,RAPGEF3,RAPGEF4,STAT1	2
Sonic Hedgehog Signaling	1.63	0.103		GLI2,GLI3,PRKAG2	2
Dopamine-DARPP32 Feedback in cAMP Signaling	1.62	0.0491	0	ADCY2,ADCY8,CACNA1A,GRIN2C,PLCE1,PPP1R12A,PPP1R14C,PRKAG2	2
Dopamine Receptor Signaling	1.61	0.0649		ADCY2,ADCY8,PPP1R12A,PPP1R14C,PRKAG2	2
Adipogenesis pathway	1.6	0.0522		CLOCK,FGFR3,FZD2,HDAC8,NR2F2,RUNX1T1,SMAD3	2
Human Embryonic Stem Cell Pluripotency	1.58	0.0519		FGFR3,FZD2,LEF1,NTRK2,NTRK3,S1PR1,SMAD3	2
Adrenomedullin signaling pathway	1.58	0.0457	0.333	ADCY2,ADCY8,IL18,MAPK4,PLCE1,PRKAG2,PTK2,RXRG,SHC3	2
CXCR4 Signaling	1.56	0.0479	0	ADCY2,ADCY8,ELMO1,FNBP1,GNAO1,PAK1,PTK2,RHOJ	2
Oleate Biosynthesis II (Animals)	1.52	0.154		FADS1,PTPRT	2
Ethanol Degradation II	1.52	0.0938		ACSS1,ACSS3,ADHFE1	2
Apelin Adipocyte Signaling Pathway	1.51	0.061	-0.447	ADCY2,ADCY8,MAPK4,PRDX6,PRKAG2	2
GNRH Signaling	1.48	0.0462	0.378	ADCY2,ADCY8,CACNA1A,CAMK2D,CAMK2G,PAK1,PRKAG2,PTK2	2
Circadian Rhythm Signaling	1.48	0.0909		BHLHE40,CLOCK,GRIN2C	2

GPCR-Mediated Nutrient Sensing in Enteroendocrine Cells	1.48	0.0536	1.633	ADCY2,ADCY8,CACNA1A,PLCE1,PRKAG2,RAPGEF4	2
Endocannabinoid Cancer Inhibition Pathway	1.47	0.049	0.378	ADCY2,ADCY8,CCND3,GNAO1,LEF1,PRKAG2,PTK2	2
Corticotropin Releasing Hormone Signaling	1.44	0.0483	-0.816	ADCY2,ADCY8,CACNA1A,GLI2,GLI3,GNAO1,PRKAG2	2
Endocannabinoid Developing Neuron Pathway	1.43	0.0522	-0.447	ADCY2,ADCY8,GNAO1,MAPK4,MGLL,PRKAG2	2
Apelin Endothelial Signaling Pathway	1.43	0.0522	0.816	ADCY2,ADCY8,ANGPT1,GNAO1,PRKAG2,SMAD3	2
Semaphorin Signaling in Neurons	1.41	0.0667		FNBP1,PAK1,PTK2,RHOJ	2
Choline Biosynthesis III	1.4	0.133		PHKA1,PLD1	2
Integrin Signaling	1.4	0.0423	-0.816	ARHGAP5,FNBP1,PAK1,PARVB,PPP1R12A,PTK2,RHOJ,TSPAN5,TSPAN7	2
Role of NFAT in Cardiac Hypertrophy	1.39	0.0421	1.414	ADCY2,ADCY8,CACNA1A,CAMK2D,CAMK2G,HDAC8,PLCE1,PRKAG2,RCAN2	2
Asparagine Degradation I	1.37	0.5		ASRGL1	2
Sulfate Activation for Sulfonation	1.37	0.5		PAPSS2	2
Cysteine Biosynthesis/Homocysteine Degradation	1.37	0.5		CBS/CBSL	2
Glutamate Biosynthesis II	1.37	0.5		GLUD1	2
Glutamate Degradation X	1.37	0.5		GLUD1	2
Relaxin Signaling	1.37	0.0467		ADCY2,ADCY8,GNAO1,MPPED2,PDE4B,PDE8B,PRKAG2	2
Hepatic Fibrosis / Hepatic Stellate Cell Activation	1.33	0.043		COL11A2,COL4A5,IGFBP5,IL1RAPL1,LHX2,MYH14,SMAD3,STAT1	2
Gustation Pathway	1.32	0.0455		ADCY2,ADCY8,CACNA1A,MPPED2,PDE4B,PDE8B,PRKAG2	2
Endothelin-1 Signaling	1.31	0.0426	-0.707	ABHD3,ADCY2,ADCY8,GNAO1,MAPK4,PLCE1,PLD1,SHC3	2
Production of Nitric Oxide and Reactive Oxygen Species in Macrophages	1.31	0.0426	-0.707	CHUK,CLU,FNBP1,PPP1R12A,PPP1R14C,RHOJ,SIRPA,STAT1	2
Synaptogenesis Signaling Pathway	3.77	0.0224	0.378	EPHA5,EPHB1,FARP1,GRIA2,NRXN1,Nrxn3,RASGRF1	3
Glutamate Receptor Signaling	2.89	0.0526		GLUL,GRIA2,SLC1A2	3
Synaptic Long Term Potentiation	2.85	0.031	2	GRIA2,PLCB1,PRKCA,RAPGEF3	3

Glutamine Biosynthesis I	2.43	1		GLUL	3
Neuroinflammation Signaling Pathway	2.27	0.0167		GABBR2,GLUL,MAPK4,MFGE8,SLC1A2	3
Endothelin-1 Signaling	2.26	0.0213	2	EDNRB,MAPK4,PLCB1,PRKCA	3
Amyotrophic Lateral Sclerosis Signaling	2.24	0.0309		GLUL,GRIA2,SLC1A2	3
Apelin Cardiomyocyte Signaling Pathway	2.21	0.0303		MAPK4,PLCB1,PRKCA	3
Ethanol Degradation II	2.2	0.0625		ACSS1,ADHFE1	3
Neuropathic Pain Signaling In Dorsal Horn Neurons	2.19	0.0297		GRIA2,PLCB1,PRKCA	3
Asparagine Degradation I	2.13	0.5		ASRGL1	3
Axonal Guidance Signaling	2.02	0.0124		ADAM23,DCC,EPHA5,EPHB1,PLCB1,PRKCA	3
Sperm Motility	2.01	0.0179		EPHA5,EPHB1,PLCB1,PRKCA	3
Endocannabinoid Neuronal Synapse Pathway	1.91	0.0234		GRIA2,MAPK4,PLCB1	3
Acetate Conversion to Acetyl-CoA	1.83	0.25		ACSS1	3
Phospholipase C Signaling	1.8	0.0156	2	HDAC8,PLCB1,PRKCA,RAPGEF3	3
Lysine Degradation V	1.73	0.2		PIPOX	3
G-Protein Coupled Receptor Signaling	1.72	0.0147		GABBR2,PLCB1,PRKCA,RAPGEF3	3
Chondroitin and Dermatan Biosynthesis	1.65	0.167		CSGALNACT1	3
Wnt/Ca+ pathway	1.65	0.0323		PLCB1,PRKCA	3
Serotonin Degradation	1.58	0.0299		ADHFE1,CSGALNACT1	3
Melatonin Signaling	1.52	0.0278		PLCB1,PRKCA	3
Ephrin Receptor Signaling	1.52	0.0167		EPHA5,EPHB1,SORBS1	3
Synaptic Long Term Depression	1.47	0.0159		GRIA2,PLCB1,PRKCA	3
Chemokine Signaling	1.44	0.025		PLCB1,PRKCA	3
Glycine Betaine Degradation	1.43	0.1		PIPOX	3
Gap Junction Signaling	1.42	0.0152		GRIA2,PLCB1,PRKCA	3
CREB Signaling in Neurons	1.37	0.0145		GRIA2,PLCB1,PRKCA	3
Role of NFAT in Cardiac Hypertrophy	1.33	0.014		HDAC8,PLCB1,PRKCA	3

Pregnenolone Biosynthesis	1.32	0.0769		MICAL2	3
Synaptogenesis Signaling Pathway	6.71	0.0481	-1.807	ADCY2,ADCY8,CAMK2D,CAMK2G,CDH13,CREB5,FARP1,GRIA1,GRIA2,GRIN2C,GRIN3A,KALRN,NRXN1,NTRK2,PAK1	4
Glutamate Receptor Signaling	6.07	0.123	-1.342	GLUL,GRIA1,GRIA2,GRIN2C,GRIN3A,SLC1A2,SLC38A1	4
Endocannabinoid Neuronal Synapse Pathway	5.56	0.0703	-1	ADCY2,ADCY8,GRIA1,GRIA2,GRIN2C,GRIN3A,KCNJ3,MAPK4,PLCB1	4
Synaptic Long Term Potentiation	5.54	0.0698	-1.667	ADCY8,CAMK2D,CAMK2G,CREB5,GRIA1,GRIA2,GRIN2C,GRIN3A,PLCB1	4
Opioid Signaling Pathway	5.52	0.0486	-0.577	ADCY2,ADCY8,CAMK2D,CAMK2G,CREB5,GRIN2C,GRIN3A,KCNJ3,MAPK4,PLCB1,RGS20,RGS6	4
Neuropathic Pain Signaling In Dorsal Horn Neurons	5.39	0.0792	-2.121	CAMK2D,CAMK2G,GRIA1,GRIA2,GRIN2C,GRIN3A,NTRK2,PLCB1	4
CREB Signaling in Neurons	4.67	0.0483	-1.667	ADCY2,ADCY8,CAMK2D,CAMK2G,CREB5,GRIA1,GRIA2,GRIN2C,PLCB1,POLR2A	4
Amyotrophic Lateral Sclerosis Signaling	4.52	0.0722	-0.816	GLUL,GRIA1,GRIA2,GRIN2C,GRIN3A,PAK1,SLC1A2	4
Neuroinflammation Signaling Pathway	3.99	0.0367	-0.816	CREB5,GABBR2,GABRA2,GLUL,GRIA1,GRIN2C,GRIN3A,KCNJ3,MAPK4,SLC1A2,SLC6A11	4
Dopamine-DARPP32 Feedback in cAMP Signaling	3.89	0.0491	-1.134	ADCY2,ADCY8,CREB5,GRIN2C,GRIN3A,KCNJ3,PLCB1,PPP2R3A	4
Protein Kinase A Signaling	3.51	0.0302	-1	ADCY2,ADCY8,CAMK2D,CAMK2G,CREB5,EYA1,LEF1,PHKG1,PLCB1,PTCH1,ROCK1,TCF7L2	4
Endocannabinoid Cancer Inhibition Pathway	3.46	0.049	-0.378	ADCY2,ADCY8,CCND2,CREB5,LEF1,ROCK1,TCF7L2	4
Factors Promoting Cardiogenesis in Vertebrates	3.33	0.0467	0.378	CAMK2D,CAMK2G,CREB5,LEF1,PLCB1,ROCK1,TCF7L2	4
CDK5 Signaling	3.33	0.0556	-0.816	ADCY2,ADCY8,CABLES1,MAPK4,NTRK2,PPP2R3A	4
Calcium Signaling	3.2	0.0388	-1.134	CAMK2D,CAMK2G,CREB5,GRIA1,GRIA2,GRIN2C,GRIN3A,HDAC8	4
GNRH Signaling	2.97	0.0405	-0.378	ADCY2,ADCY8,CAMK2D,CAMK2G,CREB5,PAK1,PLCB1	4
Ephrin Receptor Signaling	2.87	0.0389	0	ANGPT1,CREB5,GRIN2C,GRIN3A,KALRN,PAK1,ROCK1	4
GABA Receptor Signaling	2.75	0.0526		ADCY2,ADCY8,GABBR2,GABRA2,SLC6A11	4
Role of Macrophages, Fibroblasts and Endothelial Cells in Rheumatoid Arthritis	2.63	0.0288		CAMK2D,CAMK2G,CREB5,IL1RAPL1,LEF1,PLCB1,ROCK1,SFRP1,TCF7L2	4

Estrogen Receptor Signaling	2.49	0.0274	-0.333	ADCY2,ADCY8,AGT,ATP5F1A,CREB5,DDX5,PAK1,PLCB1,ROCK1	4
Osteoarthritis Pathway	2.48	0.0332	-0.378	CREB5,FGFR3,HTRA1,IL1RAPL1,LEF1,PTCH1,TCF7L2	4
Circadian Rhythm Signaling	2.48	0.0909		CREB5,GRIN2C,GRIN3A	4
Endocannabinoid Developing Neuron Pathway	2.39	0.0435	1.342	ADCY2,ADCY8,CREB5,MAPK4,PAX6	4
Axonal Guidance Signaling	2.3	0.0227		ABLIM1,KALRN,NTRK2,PAK1,PLCB1,PTCH1,ROBO2,ROCK1,SEMA4A,SEMA6A,SRGAP1	4
Endothelin-1 Signaling	2.11	0.0319	-0.816	ABHD3,ADCY2,ADCY8,GPLD1,MAPK4,PLCB1	4
Choline Biosynthesis III	2.1	0.133		GPLD1,PHKA1	4
Thiamin Salvage III	2.04	1		TPK1	4
Glutamine Biosynthesis I	2.04	1		GLUL	4
Gap Junction Signaling	2.01	0.0303		ADCY2,ADCY8,GRIA1,GRIA2,PLCB1,TJP1	4
Molecular Mechanisms of Cancer	2	0.023		ADCY2,ADCY8,CAMK2D,CAMK2G,CCND2,LEF1,PAK1,PLCB1,PTCH1	4
γ-linolenate Biosynthesis II (Animals)	1.99	0.118		ACSL3,FADS1	4
Thrombin Signaling	1.91	0.0288	0.816	ADCY2,ADCY8,CAMK2D,CAMK2G,PLCB1,ROCK1	4
G-Protein Coupled Receptor Signaling	1.9	0.0257		ADCY2,ADCY8,CAMK2D,CAMK2G,CREB5,GABBR2,PLCB1	4
Role of NFAT in Cardiac Hypertrophy	1.86	0.028	-1.342	ADCY2,ADCY8,CAMK2D,CAMK2G,HDAC8,PLCB1	4
Sperm Motility	1.78	0.0269		ABHD3,ERBB4,FGFR3,MERTK,NTRK2,PLCB1	4
cAMP-mediated signaling	1.74	0.0263	-0.816	ADCY2,ADCY8,CAMK2D,CAMK2G,CREB5,GABBR2	4
CXCR4 Signaling	1.73	0.0299	1.342	ADCY2,ADCY8,PAK1,PLCB1,ROCK1	4
Phospholipases	1.7	0.0476		ABHD3,GPLD1,PLCB1	4
Apelin Endothelial Signaling Pathway	1.67	0.0348	1	ADCY2,ADCY8,ANGPT1,PLCB1	4
Renin-Angiotensin Signaling	1.64	0.0339		ADCY2,ADCY8,AGT,PAK1	4
LXR/RXR Activation	1.6	0.0331	-2	ABCA1,AGT,IL1RAPL1,LDLR	4
IL-15 Production	1.6	0.0331	-2	ERBB4,FGFR3,MERTK,NTRK2	4
Proline Degradation	1.57	0.333		LOC102724788/PRODH	4
Melatonin Signaling	1.55	0.0417		CAMK2D,CAMK2G,PLCB1	4
Basal Cell Carcinoma Signaling	1.55	0.0417		LEF1,PTCH1,TCF7L2	4

Ephrin B Signaling	1.55	0.0417		KALRN,PAK1,ROCK1	4
P2Y Purigenic Receptor Signaling Pathway	1.54	0.0315	-1	ADCY2,ADCY8,CREB5,PLCB1	4
GPCR-Mediated Integration of Enteroendocrine Signaling Exemplified by an L Cell	1.54	0.0411		ADCY2,ADCY8,PLCB1	4
Synaptic Long Term Depression	1.53	0.0265	-2.236	ABHD3,GRIA1,GRIA2,PLCB1,PPP2R3A	4
Leptin Signaling in Obesity	1.52	0.0405		ADCY2,ADCY8,PLCB1	4
PPARα/RXRα Activation	1.52	0.0263	-1	ABCA1,ADCY2,ADCY8,IL1RAPL1,PLCB1	4
Reelin Signaling in Neurons	1.51	0.031	-1	CAMK2D,CAMK2G,GRIN2C,GRIN3A	4
White Adipose Tissue Browning Pathway	1.51	0.031	-1	ADCY2,ADCY8,CREB5,FGFR3	4
Phospholipase C Signaling	1.51	0.0233		ADCY2,ADCY8,CREB5,GPLD1,HDAC8,PLCB1	4
Regulation of the Epithelial-Mesenchymal Transition Pathway	1.5	0.026		FGFR3,ID2,LEF1,TCF7L2,ZEB1	4
Dopamine Receptor Signaling	1.48	0.039		ADCY2,ADCY8,PPP2R3A	4
Cardiac Hypertrophy Signaling (Enhanced)	1.45	0.0185	-1	ADCY2,ADCY8,AGT,CAMK2D,CAMK2G,FGFR3,HDAC8,PLCB1,ROCK1	4
Human Embryonic Stem Cell Pluripotency	1.45	0.0296		FGFR3,LEF1,NTRK2,TCF7L2	4
Thyroid Cancer Signaling	1.45	0.038		LEF1,NTRK2,TCF7L2	4
BEX2 Signaling Pathway	1.45	0.038		LEF1,PPP2R3A,TCF7L2	4
Spermine and Spermidine Degradation I	1.44	0.25		SAT1	4
Acetate Conversion to Acetyl-CoA	1.44	0.25		ACSS1	4
Chemokine Signaling	1.43	0.0375		CAMK2D,CAMK2G,PLCB1	4
Cyclins and Cell Cycle Regulation	1.42	0.037		CCND2,HDAC8,PPP2R3A	4
PEDF Signaling	1.41	0.0366		ROCK1,TCF7L2,ZEB1	4
Apelin Adipocyte Signaling Pathway	1.41	0.0366		ADCY2,ADCY8,MAPK4	4
Corticotropin Releasing Hormone Signaling	1.36	0.0276	0	ADCY2,ADCY8,CREB5,PTCH1	4
Notch Signaling	1.35	0.0541		CNTN1,MAML3	4
Breast Cancer Regulation by Stathmin1	1.35	0.0169		CAMK2D,CAMK2G,CCND2,CREB5,GABBR2,NTSR2,PAK1,PLCB1,PPP2R3A,SCTR	4

Synaptogenesis Signaling Pathway	11.9	0.103	-1.257	ADCY2,ADCY8,AKT3,BRAF,CACNA2D1,CADM1,CAMK2G,CDH10,CDH19,CDH20,CDH4,CREB5,EFNA5,EPHA3,EPHA4,EPHB1,EPHB2,FARP1,FYN,GRIA1,GRIA2,GRIN2C,GRIN3A,GRM3,ITPR1,KALRN,MAP1B,NRXN1,PIK3R1,RASGRF1,SHC3,THBS4	5
Axonal Guidance Signaling	9.89	0.0764		ABLIM1,ADAM22,ADAMTS18,AKT3,ARHGEF12,DCC,EFNA5,EPHA3,EPHA4,EPHB1,EPHB2,FYN,GLI2,GNG12,KALRN,LRRC4C,MMP16,NGEF,NRP1,NTRK3,PAK3,PIK3R1,PLCB1,PLCD4,PLCH1,PLCL1,PLXNC1,PPP3CA,PRKCA,PTCH1,ROBO1,SEMA6A,SEMA6D,SHANK2,SLIT2,SRGAP1,VEGFA	5
Synaptic Long Term Potentiation	9.11	0.14	-2.357	ADCY8,CAMK2G,CREB5,GRIA1,GRIA2,GRIN2C,GRIN3A,GRM3,ITPR1,ITPR2,PLCB1,PLCD4,PLCH1,PLCL1,PPP1R14C,PPP3CA,PRKCA,RAPGEF3	5
Neuropathic Pain Signaling In Dorsal Horn Neurons	8.99	0.158	-3	CAMK1D,CAMK2G,GRIA1,GRIA2,GRIN2C,GRIN3A,GRM3,ITPR1,ITPR2,KCNQ3,PIK3R1,PLCB1,PLCD4,PLCH1,PLCL1,PRKCA	5
CREB Signaling in Neurons	7.95	0.101	-2.357	ADCY2,ADCY8,AKT3,CACNA2D1,CACNB2,CAMK2G,CREB5,GNG12,GRIA1,GRIA2,GRID1,GRIN2C,GRM3,ITPR1,ITPR2,PIK3R1,PLCB1,PLCD4,PLCH1,PLCL1,PRKCA	5
Sperm Motility	7.38	0.0942	-1.897	AATK,ABHD3,EPHA3,EPHA4,EPHB1,EPHB2,ERBB4,FGFR3,FYN,IGF1R,ITPR1,ITPR2,MERTK,NTRK3,PDE4B,PLA2G7,PLCB1,PLCD4,PLCH1,PLCL1,PRKCA	5
Endocannabinoid Neuronal Synapse Pathway	6.66	0.117	-0.775	ADCY2,ADCY8,CACNA2D1,CACNB2,GRIA1,GRIA2,GRIN2C,GRIN3A,ITPR1,MAPK4,PLCB1,PLCD4,PLCH1,PLCL1,PPP3CA	5
Role of NFAT in Cardiac Hypertrophy	6.34	0.0888	-1.213	ADCY2,ADCY8,AKT3,CACNA2D1,CACNB2,CAMK1D,CAMK2G,GNG12,HDAC8,IGF1R,ITPR1,ITPR2,PIK3R1,PLCB1,PLCD4,PLCH1,PLCL1,PPP3CA,PRKCA	5
Glutamate Receptor Signaling	6.27	0.175	-1.633	GLUL,GRIA1,GRIA2,GRID1,GRIN2C,GRIN3A,GRM3,SLC1A2,SLC1A3,SLC38A1	5
Ephrin Receptor Signaling	6.11	0.0944	-1.265	ABI1,AKT3,CREB5,EFNA5,EPHA3,EPHA4,EPHB1,EPHB2,FGF1,FYN,GNG12,GRIN2C,GRIN3A,KALRN,NGEF,PAK3,VEGFA	5
Dopamine-DARPP32 Feedback in cAMP Signaling	6.01	0.0982	-1.604	ADCY2,ADCY8,CREB5,GRIN2C,GRIN3A,ITPR1,ITPR2,KCNJ10,PAWR,PLCB1,PLCD4,PLCH1,PLCL1,PPP1R14C,PPP3CA,PRKCA	5
Opioid Signaling Pathway	6	0.081	-0.894	ADCY2,ADCY8,AKT3,BRAF,CACNA2D1,CACNB2,CAMK1D,CAMK2G,CREB5,FYN,GRIN2C,GRIN3A,ITPR1,ITPR2,MAPK4,PLCB1,PPP3CA,PRKCA,RGS6,RGS7	5

Thrombin Signaling	5.88	0.0865	-1.213	ADCY2,ADCY8,AKT3,ARHGEF12,CAMK1D,CAMK2G,FNBP1,GNG12,ITPR1,ITPR2,PIK3R1,PLCB1,PLCD4,PLCH1,PLCL1,PRKCA,RHOQ,RND3	5
Endothelin-1 Signaling	5.84	0.0904	-1.5	ABHD3,ADCY2,ADCY8,BRAF,ECE1,GPLD1,ITPR1,ITPR2,MAPK4,PIK3R1,PLA2G7,PLCB1,PLCD4,PLCH1,PLCL1,PRKCA,SHC3	5
Protein Kinase A Signaling	5.81	0.0653	-1.46	ADCY2,ADCY8,ADD3,AKAP6,BRAF,CAMK2G,CREB5,DCC,EYA2,GNG12,ITPR1,ITPR2,PDE4B,PDE7B,PDE8B,PHKG1,PLCB1,PLCD4,PLCH1,PLCL1,PPP1R14C,PPP3CA,PRKCA,PTCH1,PTPRG,PTPRK	5
PI3K Signaling in B Lymphocytes	5.5	0.101	-1.387	AKT3,CAMK2G,CD81,DAPP1,FYN,ITPR1,ITPR2,PIK3R1,PLCB1,PLCD4,PLCH1,PLCL1,PPP3CA,VAV3	5
RhoGDI Signaling	5.44	0.0889	1.291	ARHGAP5,ARHGAP6,ARHGEF12,ARHGEF19,CDH10,CDH19,CDH20,CDH4,DLC1,FNBP1,GNG12,PAK3,PIP5K1B,PRKCA,RHOQ,RND3	5
Synaptic Long Term Depression	5.17	0.0847	-1.5	ABHD3,CACNA2D1,CACNB2,GRIA1,GRIA2,GRID1,GRM3,IGF1R,ITPR1,ITPR2,PLA2G7,PLCB1,PLCD4,PLCH1,PLCL1,PRKCA	5
Phospholipase C Signaling	5.15	0.0739	-1.941	ADCY2,ADCY8,ARHGEF12,ARHGEF19,CREB5,FNBP1,FYN,GNG12,GPLD1,HDAC8,ITPR1,ITPR2,PLCB1,PLCD4,PPP3CA,PRKCA,RAPGEF3,RHOQ,RND3	5
GPCR-Mediated Nutrient Sensing in Enteroendocrine Cells	5.04	0.107	-1.155	ADCY2,ADCY8,CACNA2D1,CACNB2,GNG12,ITPR1,ITPR2,PLCB1,PLCD4,PLCH1,PLCL1,PRKCA	5
GABA Receptor Signaling	5	0.116		ABAT,ADCY2,ADCY8,CACNA2D1,CACNB2,GABBR1,GABBR2,GABRB1,KCNQ3,SLC6A1,SLC6A11	5
Gap Junction Signaling	4.91	0.0808		ADCY2,ADCY8,AKT3,GJB6,GRIA1,GRIA2,ITPR1,ITPR2,PIK3R1,PLCB1,PLCD4,PLCH1,PLCL1,PPP3CA,PRKCA,TJP1	5
Amyotrophic Lateral Sclerosis Signaling	4.91	0.113	-1.667	AKT3,GLUL,GRIA1,GRIA2,GRID1,GRIN2C,GRIN3A,PIK3R1,PPP3CA,SLC1A2,VEGFA	5
Gαq Signaling	4.82	0.0886	-1.387	AKT3,FNBP1,GNG12,GPLD1,HRH1,ITPR1,ITPR2,PIK3R1,PLCB1,PPP3CA,PRKCA,RGS7,RHOQ,RND3	5
G-Protein Coupled Receptor Signaling	4.8	0.0699		ADCY2,ADCY8,AKT3,BRAF,CAMK2G,CREB5,FYN,GABBR1,GABBR2,GRM3,HRH1,PDE4B,PDE7B,PDE8B,PIK3R1,PLCB1,PRKCA,RAPGEF3,RGS7	5
Signaling by Rho Family GTPases	4.35	0.0697	-1.5	ARHGEF12,ARHGEF19,CDH10,CDH19,CDH20,CDH4,CIT,CYFIP1,FNBP1,GNG12,PAK3,PIK3R1,PIP5K1B,RHOQ,RND3,VIM,WASF3	5

cAMP-mediated signaling	4.16	0.0702	-2.324	ADCY2,ADCY8,AKAP6,BRAF,CAMK1D,CAMK2G,CREB5,GABBR1,GABBR2,GRM3,PDE4B,PDE7B,PDE8B,PPP3CA,RAPGEF3,RGS7	5
Sphingosine-1-phosphate Signaling	4.14	0.094	-0.302	ADCY2,ADCY8,AKT3,FNBP1,PIK3R1,PLCB1,PLCD4,PLCH1,PLCL1,RHOQ,RND3	5
Calcium Signaling	4.12	0.0728	-1.155	ATP2C1,CACNA2D1,CACNB2,CAMK1D,CAMK2G,CREB5,GRIA1,GRIA2,GRIN2C,GRIN3A,HDAC8,ITPR1,ITPR2,MYH14,PPP3CA	5
Ephrin A Signaling	4.08	0.149		EFNA5,EPHA3,EPHA4,FYN,NGEF,PIK3R1,VAV3	5
IL-15 Production	4.01	0.0909	-0.302	AATK,EPHA3,EPHA4,EPHB1,EPHB2,ERBB4,FGFR3,FYN,IGF1R,MERTK,NTRK3	5
Integrin Signaling	3.96	0.0704	-0.832	AKT3,ARHGAP26,ARHGAP5,ASAP1,BRAF,FNBP1,FYN,ITGA6,ITGB8,PAK3,PIK3R1,RHOQ,RND3,TSPAN5,TSPAN7	5
CXCR4 Signaling	3.94	0.0778	0	ADCY2,ADCY8,AKT3,FNBP1,GNG12,ITPR1,ITPR2,PAK3,PIK3R1,PLCB1,PRKCA,RHOQ,RND3	5
Corticotropin Releasing Hormone Signaling	3.93	0.0828	-1	ADCY2,ADCY8,BRAF,CACNA2D1,CACNB2,CREB5,GLI2,ITPR1,ITPR2,PRKCA,PTCH1,VEGFA	5
P2Y Purigenic Receptor Signaling Pathway	3.82	0.0866	-1.265	ADCY2,ADCY8,AKT3,CREB5,GNG12,PIK3R1,PLCB1,PLCD4,PLCH1,PLCL1,PRKCA	5
Adrenomedullin signaling pathway	3.77	0.0711	-1.604	ADCY2,ADCY8,AKT3,BRAF,ITPR1,ITPR2,KCNQ3,MAPK4,PIK3R1,PLCB1,PLCD4,PLCH1,PLCL1,SHC3	5
Neuroinflammation Signaling Pathway	3.74	0.06	-0.632	AKT3,APP,CREB5,GABBR1,GABBR2,GABRB1,GLUL,GRIA1,GRIN2C,GRIN3A,IRAK2,MAPK4,PIK3R1,PPP3CA,SLC1A2,SLC1A3,SLC6A1,SLC6A11	5
Cellular Effects of Sildenafil (Viagra)	3.7	0.084		ADCY2,ADCY8,ITPR1,ITPR2,KCNQ3,MYH14,PDE4B,PLCB1,PLCD4,PLCH1,PLCL1	5
GPCR-Mediated Integration of Enteroendocrine Signaling Exemplified by an L Cell	3.62	0.11	0	ADCY2,ADCY8,ITPR1,ITPR2,PLCB1,PLCD4,PLCH1,PLCL1	5
Leptin Signaling in Obesity	3.58	0.108		ADCY2,ADCY8,AKT3,PIK3R1,PLCB1,PLCD4,PLCH1,PLCL1	5
Glioblastoma Multiforme Signaling	3.41	0.0727	-0.577	AKT3,FNBP1,IGF1R,ITPR1,ITPR2,PIK3R1,PLCB1,PLCD4,PLCH1,PLCL1,RHOQ,RND3	5
Semaphorin Signaling in Neurons	3.4	0.117		ARHGEF12,FNBP1,FYN,NRP1,PAK3,RHOQ,RND3	5
Apelin Cardiomyocyte Signaling Pathway	3.38	0.0909	-1	AKT3,ITPR1,MAPK4,PIK3R1,PLCB1,PLCD4,PLCH1,PLCL1,PRKCA	5
Clathrin-mediated Endocytosis Signaling	3.32	0.0674		AP1S2,DAB2,EPHB2,EPS15,FGF1,FGF14,HIP1,ITGB8,MYO1E,MYO6,PIK3R1,PPP3CA,VEGFA	5

Wnt/Ca+ pathway	3.31	0.113	-1.134	CREB5,PLCB1,PLCD4,PLCH1,PLCL1,PPP3CA,PRKCA	5
Phospholipases	3.27	0.111	-1.89	ABHD3,GPLD1,PLA2G7,PLCB1,PLCD4,PLCH1,PLCL1	5
Leukocyte Extravasation Signaling	3.24	0.066	0	ARHGAP5,ARHGAP6,CLDN10,CTNNA2,DLC1,ITGA6,MMP16,PIK3R1,PRKCA,RAPGEF3,TIMP3,TIMP4,VAV3	5
FGF Signaling	3.2	0.0952	-0.707	AKT3,CREB5,FGF1,FGF14,FGFR3,ITPR1,PIK3R1,PRKCA	5
Molecular Mechanisms of Cancer	3.18	0.0512		ADCY2,ADCY8,AKT3,ARHGEF12,ARHGEF19,BRAF,CAMK2G,CCND2,CTNNA2,FNBP1,FYN,PAK3,PIK3R1,PLCB1,PRKCA,PTCH1,RAPGEF3,RASGRF1,RHOQ,RND3	5
Reelin Signaling in Neurons	3.14	0.0775	-1.265	AKT3,APP,ARHGEF12,CAMK2G,FYN,GRIN2C,GRIN3A,ITGA6,MAP1B,PIK3R1	5
Cardiac Hypertrophy Signaling (Enhanced)	3.1	0.0472	-2.558	ADCY2,ADCY8,AKT3,CAMK2G,Eda,FGF1,FGF14,FGFR3,GHR,HDAC8,IGF1R,ITPR1,ITPR2,PDE4B,PDE7B,PDE8B,PIK3R1,PLCB1,PLCD4,PLCH1,PLCL1,PPP3CA,PRKCA	5
Melatonin Signaling	2.92	0.0972	-0.816	BRAF,CAMK2G,PLCB1,PLCD4,PLCH1,PLCL1,PRKCA	5
Notch Signaling	2.85	0.135		CNTN1,HES5,MAML3,NOTCH2,NOTCH3	5
RhoA Signaling	2.71	0.0732	-0.333	ARHGAP5,ARHGAP6,ARHGEF12,CIT,DLC1,IGF1R,NGEF,PIP5K1B,RND3	5
GNRH Signaling	2.69	0.0636	-1	ADCY2,ADCY8,CACNA2D1,CACNB2,CAMK2G,CREB5,ITPR1,ITPR2,PAK3,PLCB1,PRKCA	5
IL-8 Signaling	2.68	0.06	-0.905	AKT3,BRAF,CCND2,FNBP1,GNG12,GPLD1,IRAK2,PIK3R1,PRKCA,RHOQ,RND3,VEGFA	5
Phagosome Formation	2.66	0.072		FNBP1,PIK3R1,PLCB1,PLCD4,PLCH1,PLCL1,PRKCA,RHOQ,RND3	5
Breast Cancer Regulation by Stathmin1	2.65	0.0423		ADGRB3,ADGRL3,ADGRV1,ARHGEF12,ARHGEF19,CAMK1D,CAMK2G,CCND2,CELSR1,CREB5,GABBR1,GABBR2,GNG12,GPR156,GPR37L1,GPRC5B,GRM3,HRH1,NTSR2,PIK3R1,PLCB1,PPP1R14C,PRKCA,TSHR,VEGFA	5
Relaxin Signaling	2.65	0.0667	-0.816	ADCY2,ADCY8,AKT3,BRAF,GNG12,PDE4B,PDE7B,PDE8B,PIK3R1,VEGFA	5
D-myo-inositol (1,4,5)-Trisphosphate Biosynthesis	2.65	0.16	0	PIP5K1B,PLCB1,PLCD4,PLCH1	5
Fatty Acid Activation	2.56	0.231		ACSBG1,ACSL6,SLC27A1	5
Cardiac Hypertrophy Signaling	2.47	0.0542	-1.732	ADCY2,ADCY8,FNBP1,GNG12,IGF1R,PIK3R1,PLCB1,PLCD4,PLCH1,PLCL1,PPP3CA,RHOQ,RND3	5
ILK Signaling	2.38	0.0579	-1.265	AKT3,CREB5,FERMT2,FNBP1,ITGB8,MYH14,PIK3R1,RHOQ,RND3,VEGFA,VIM	5
Role of Tissue Factor in Cancer	2.29	0.0684		AKT3,F3,FYN,ITGA6,PIK3R1,PLCB1,PRKCA,VEGFA	5

Renin-Angiotensin Signaling	2.26	0.0678	-0.816	ADCY2,ADCY8,ITPR1,ITPR2,PAK3,PIK3R1,PRKCA,SHC3	5
Cholecystokinin/Gastrin-mediated Signaling	2.24	0.0672	-0.707	EPHA4,FNBP1,ITPR1,ITPR2,PLCB1,PRKCA,RHOQ,RND3	5
Ephrin B Signaling	2.24	0.0833	-0.447	ABI1,EPHB1,EPHB2,GNG12,KALRN,VAV3	5
α-Adrenergic Signaling	2.21	0.0729	-1	ADCY2,ADCY8,GNG12,ITPR1,ITPR2,PHKG1,PRKCA	5
γ-linolenate Biosynthesis II (Animals)	2.21	0.176		ACSBG1,ACSL6,SLC27A1	5
Mitochondrial L-carnitine Shuttle Pathway	2.21	0.176		ACSBG1,ACSL6,SLC27A1	5
Glioma Invasiveness Signaling	2.18	0.0811	0	FNBP1,PIK3R1,RHOQ,RND3,TIMP3,TIMP4	5
EGF Signaling	2.1	0.0909	-0.447	AKT3,ITPR1,ITPR2,PIK3R1,PRKCA	5
14-3-3-mediated Signaling	2.08	0.063	-0.707	AKT3,PIK3R1,PLCB1,PLCD4,PLCH1,PLCL1,PRKCA,VIM	5
Gustation Pathway	2.07	0.0584		ADCY2,ADCY8,CACNA2D1,CACNB2,ITPR1,ITPR2,PDE4B ,PDE7B,PDE8B	5
Chondroitin Sulfate Biosynthesis	2.06	0.0893	-1.342	CHST10,CHST11,CSGALNACT1,UST,XYLT1	5
Osteoarthritis Pathway	2.05	0.0521	-0.707	ANXA2,CREB5,CTNNA2,EPAS1,FGFR3,GLI2,HTRA1,PTC H1,SIK3,TIMP3,VEGFA	5
White Adipose Tissue Browning Pathway	2.04	0.062	0	ADCY2,ADCY8,CACNA2D1,CACNB2,CREB5,FGFR3,PRD M16,VEGFA	5
Aldosterone Signaling in Epithelial Cells	2	0.057	-1	ITPR1,ITPR2,PIK3R1,PIP5K1B,PLCB1,PLCD4,PLCH1,PLC L1,PRKCA	5
eNOS Signaling	1.98	0.0566	-1.633	ADCY2,ADCY8,AKT3,AQP4,ITPR1,ITPR2,PIK3R1,PRKCA, VEGFA	5
Dermatan Sulfate Biosynthesis	1.97	0.0847	-1.342	CHST10,CHST11,CSGALNACT1,UST,XYLT1	5
Gαs Signaling	1.96	0.0654	0	ADCY2,ADCY8,ADD3,BRAF,CREB5,GNG12,RAPGEF3	5
Antioxidant Action of Vitamin C	1.92	0.0642	1.89	ABHD3,GPLD1,PLA2G7,PLCB1,PLCD4,PLCH1,PLCL1	5
Role of Macrophages, Fibroblasts and Endothelial Cells in Rheumatoid Arthritis	1.92	0.0449		AKT3,CAMK2G,CREB5,DKK3,IRAK2,PIK3R1,PLCB1,PLCD 4,PLCH1,PLCL1,PPP3CA,PRKCA,SFRP1,VEGFA	5
Tec Kinase Signaling	1.9	0.0549	-1.414	FNBP1,FYN,GNG12,PAK3,PIK3R1,PRKCA,RHOQ,RND3,V AV3	5
Pyrimidine Deoxyribonucleotides De Novo Biosynthesis I	1.89	0.136		AK7,AK9,NME5	5
Colorectal Cancer Metastasis Signaling	1.88	0.0474	-0.905	ADCY2,ADCY8,AKT3,BRAF,DCC,FNBP1,GNG12,MMP16, PIK3R1,RHOQ,RND3,VEGFA	5

Cardiac β-adrenergic Signaling	1.82	0.0567	-1.633	ADCY2,ADCY8,AKAP6,GNG12,PDE4B,PDE7B,PDE8B,PPP1R14C	5
Type II Diabetes Mellitus Signaling	1.8	0.0563		ACSBG1,ACSL6,AKT3,CACNA2D1,CACNB2,PIK3R1,PRKCA,SLC27A1	5
Netrin Signaling	1.8	0.0769	0.447	ABLIM1,CACNA2D1,CACNB2,DCC,PPP3CA	5
Endocannabinoid Developing Neuron Pathway	1.8	0.0609	1.134	ADCY2,ADCY8,AKT3,BRAF,CREB5,MAPK4,PIK3R1	5
Endocannabinoid Cancer Inhibition Pathway	1.79	0.0559	0	ADCY2,ADCY8,AKT3,CCND2,CREB5,PIK3R1,VEGFA,VIM	5
fMLP Signaling in Neutrophils	1.78	0.0603	-1.633	GNG12,ITPR1,ITPR2,PIK3R1,PLCB1,PPP3CA,PRKCA	5
Estrogen Receptor Signaling	1.74	0.0427	-1.069	ADCY2,ADCY8,AKT3,CREB5,IGF1R,MMP16,PIK3R1,PLCB1,PLCD4,PLCH1,PLCL1,PRKCA,SHC3,VEGFA	5
GP6 Signaling Pathway	1.73	0.0588	0.378	AKT3,COL4A6,COL5A2,FYN,ITPR1,PIK3R1,PRKCA	5
Fcγ Receptor-mediated Phagocytosis in Macrophages and Monocytes	1.7	0.0638	-1.633	AKT3,FYN,GPLD1,PIK3R1,PRKCA,VAV3	5
FAK Signaling	1.68	0.0632		AKT3,ARHGAP26,ASAP1,FYN,PAK3,PIK3R1	5
GM-CSF Signaling	1.67	0.0714		AKT3,CAMK2G,PIK3R1,PIM1,PPP3CA	5
nNOS Signaling in Neurons	1.67	0.0851		GRIN2C,GRIN3A,PPP3CA,PRKCA	5
Stearate Biosynthesis I (Animals)	1.67	0.0851		ACOT11,ACSBG1,ACSL6,SLC27A1	5
Glutamine Biosynthesis I	1.65	1		GLUL	5
Adenine and Adenosine Salvage VI	1.65	1		ADK	5
CCR3 Signaling in Eosinophils	1.64	0.0565	-1	GNG12,ITPR1,ITPR2,PAK3,PIK3R1,PLCB1,PRKCA	5
Salvage Pathways of Pyrimidine Ribonucleotides	1.64	0.0619	2.236	AK7,AK9,BRAF,NME5,PAK3,PIM1	5
Chondroitin Sulfate Biosynthesis (Late Stages)	1.64	0.0833	-1	CHST10,CHST11,CSGALNACT1,UST	5
Gαi Signaling	1.62	0.056	0	ADCY2,ADCY8,GABBR1,GABBR2,GNG12,GRM3,RGS7	5
UVA-Induced MAPK Signaling	1.62	0.0612	-1.633	PIK3R1,PLCB1,PLCD4,PLCH1,PLCL1,PRKCA	5
Ketogenesis	1.61	0.182		HMGCLL1,HMGCS2	5
PTEN Signaling	1.61	0.0556	0.816	AKT3,FGFR3,GHR,IGF1R,NTRK3,PIK3R1,PREX2	5
Non-Small Cell Lung Cancer Signaling	1.6	0.0685	-0.447	AKT3,ITPR1,ITPR2,PIK3R1,PRKCA	5
Nitric Oxide Signaling in the Cardiovascular System	1.6	0.0606	-0.816	AKT3,ITPR1,ITPR2,PIK3R1,PRKCA,VEGFA	5

PKCθ Signaling in T Lymphocytes	1.6	0.0516	-2.236	CACNA2D1,CACNB2,CAMK2G,FYN,PIK3R1,POU2F1,PPP3CA,VAV3	5
Melanoma Signaling	1.58	0.08		AKT3,BRAF,MITF,PIK3R1	5
Actin Cytoskeleton Signaling	1.56	0.0459	-1.134	ARHGEF12,CYFIP1,FGF1,FGF14,GNG12,MYH14,PAK3,PIK3R1,PIP5K1B,VAV3	5
p70S6K Signaling	1.56	0.0543	-1.134	AKT3,PIK3R1,PLCB1,PLCD4,PLCH1,PLCL1,PRKCA	5
Gα12/13 Signaling	1.54	0.0538	0.378	AKT3,CDH10,CDH19,CDH20,CDH4,PIK3R1,VAV3	5
Macropinocytosis Signaling	1.54	0.0658	-2	ABI1,ITGB8,PIK3R1,PRKCA,RAB34	5
PPARα/RXRα Activation	1.53	0.0474	-1.342	ADCY2,ADCY8,GHR,PLCB1,PLCD4,PLCH1,PLCL1,PRKCA,SLC27A1	5
Regulation of the Epithelial-Mesenchymal Transition Pathway	1.51	0.0469		AKT3,BRAF,FGF1,FGF14,FGFR3,NOTCH2,NOTCH3,PIK3R1,SMURF1	5
Agrin Interactions at Neuromuscular Junction	1.47	0.0633	0	ERBB4,ITGA6,Nrg1,PAK3,UTRN	5
Virus Entry via Endocytic Pathways	1.46	0.0561		AP1S2,FYN,ITGA6,ITGB8,PIK3R1,PRKCA	5
Fatty Acid β-oxidation I	1.45	0.0938		ACSBG1,ACSL6,SLC27A1	5
CDK5 Signaling	1.44	0.0556	-0.447	ADCY2,ADCY8,CABLES1,ITGA6,MAPK4,PPP1R14C	5
Superpathway of Inositol Phosphate Compounds	1.43	0.0455	-1	HACD2,ITPKB,PAWR,PIK3R1,PIP5K1B,PLCB1,PLCD4,PLCH1,PPP3CA	5
Circadian Rhythm Signaling	1.42	0.0909		CREB5,GRIN2C,GRIN3A	5
Glioma Signaling	1.41	0.0545	-0.816	AKT3,CAMK1D,CAMK2G,IGF1R,PIK3R1,PRKCA	5
iCOS-iCOSL Signaling in T Helper Cells	1.39	0.0541	-1	AKT3,CAMK2G,ITPR1,ITPR2,PIK3R1,PPP3CA	5
Inhibition of Angiogenesis by TSP1	1.39	0.0882		AKT3,FYN,VEGFA	5
Germ Cell-Sertoli Cell Junction Signaling	1.38	0.0468		CTNNA2,FNBP1,ITGA6,PAK3,PIK3R1,RHOQ,RND3,TJP1	5
VEGF Family Ligand-Receptor Interactions	1.38	0.0595	-1	AKT3,NRP1,PIK3R1,PRKCA,VEGFA	5
Cancer Drug Resistance By Drug Efflux	1.37	0.069		ABCC1,AKT3,BRAF,PIK3R1	5
Huntington's Disease Signaling	1.35	0.0422	0.378	AKT3,CREB5,GNG12,HDAC8,HIP1,IGF1R,ITPR1,PIK3R1,PLCB1,PRKCA	5
Choline Biosynthesis III	1.35	0.133		GPLD1,PHKA1	5
Asparagine Degradation I	1.35	0.5		ASRGL1	5

β-alanine Degradation I	1.35	0.5		ABAT	5
Apelin Endothelial Signaling Pathway	1.33	0.0522	0	ADCY2,ADCY8,AKT3,PIK3R1,PLCB1,PRKCA	5

Supplemental Table 4.12. R6/2 12-Week Cortical Astrocyte IPA Canonical Pathway Enrichment Analysis Per Cluster

Ingenuity Canonical Pathways	-log(p-value)	Ratio	z-score	Molecules	Cluster
G-Protein Coupled Receptor Signaling	4.5	0.0294	0	ADCY2,CAMK2G,GABBR2,GNAO1,GRM3,PDE8B,PLCB1,RAPGEF3	0
Neuroinflammation Signaling Pathway	3.39	0.0234	0	GABBR2,GLUL,GRIN2C,IRAK2,MFGE8,SLC1A2,SLC1A3	0
Reelin Signaling in Neurons	1.69	0.0233	0	CAMK2G,DAB1,GRIN2C	0
Glutamate Receptor Signaling	8.19	0.123	-1	GLUL,GRIA2,GRIK1,GRIN2C,GRM3,SLC1A2,SLC1A3	0
Amyotrophic Lateral Sclerosis Signaling	4.12	0.0515	-1	GLUL,GRIA2,GRIK1,GRIN2C,SLC1A2	0
Opioid Signaling Pathway	3.9	0.0283	-1.134	ADCY2,ARRB1,CAMK2G,GNAO1,GRIN2C,PLCB1,RGS20	0
Endocannabinoid Neuronal Synapse Pathway	3.55	0.0391	-1.342	ADCY2,GNAO1,GRIA2,GRIN2C,PLCB1	0
Neuropathic Pain Signaling In Dorsal Horn Neurons	4.03	0.0495	-2.236	CAMK2G,GRIA2,GRIN2C,GRM3,PLCB1	0
Calcium Signaling	3.47	0.0291	-2	CAMK2G,GRIA2,GRIK1,GRIN2C,HDAC8,RCAN2	0
Synaptic Long Term Potentiation	4.59	0.0465	-2.449	CAMK2G,GRIA2,GRIN2C,GRM3,PLCB1,RAPGEF3	0
CREB Signaling in Neurons	5.36	0.0386	-2.646	ADCY2,CAMK2G,GNAO1,GRIA2,GRIK1,GRIN2C,GRM3,PLCB1	0
cAMP-mediated signaling	4.12	0.0307	-2.646	ADCY2,CAMK2G,GABBR2,GNAO1,GRM3,PDE8B,RAPGEF3	0
Apelin Endothelial Signaling Pathway	2.74	0.0348	0	ADCY2,ANGPT1,GNAO1,PLCB1	0
Gap Junction Signaling	2.7	0.0253	0	ADCY2,GJA1,GRIA2,GRIK1,PLCB1	0
Role of NFAT in Cardiac Hypertrophy	2.55	0.0234	-1	ADCY2,CAMK2G,HDAC8,PLCB1,RCAN2	0
Melatonin Signaling	2.38	0.0417	0	CAMK2G,GNAO1,PLCB1	0
Glutamine Biosynthesis I	2.35	1	0	GLUL	0
TR/RXR Activation	2.19	0.0357	0	DIO2,LDLR,RCAN2	0
IL-1 Signaling	2.1	0.033	0	ADCY2,GNAO1,IRAK2	0
Ephrin Receptor Signaling	2.05	0.0222	0	ANGPT1,GNAO1,GRIN2C,KALRN	0

Synaptic Long Term Depression	1.98	0.0212	-2	GNAO1,GRIA2,GRM3,PLCB1	0
PPARα/RXRα Activation	1.97	0.0211	0	ABCA1,ADCY2,IL1RAPL1,PLCB1	0
Role of Macrophages, Fibroblasts and Endothelial Cells in Rheumatoid Arthritis	1.88	0.016	0	CAMK2G,GNAO1,IL1RAPL1,IRAK2,PLCB1	0
Uracil Degradation II (Reductive)	1.87	0.333	0	DPYD	0
Thyronamine and Iodothyronamine Metabolism	1.87	0.333	0	DIO2	0
Thymine Degradation	1.87	0.333	0	DPYD	0
Thyroid Hormone Metabolism I (via Deiodination)	1.87	0.333	0	DIO2	0
Thrombin Signaling	1.84	0.0192	0	ADCY2,CAMK2G,GNAO1,PLCB1	0
LXR/RXR Activation	1.76	0.0248	0	ABCA1,IL1RAPL1,LDLR	0
Acetate Conversion to Acetyl-CoA	1.75	0.25	0	ACSS2	0
LPS/IL-1 Mediated Inhibition of RXR Function	1.74	0.0179	0	ABCA1,ACSL3,ALDH1L1,IL1RAPL1	0
Gαi Signaling	1.73	0.024	0	ADCY2,GABBR2,GRM3	0
Synaptogenesis Signaling Pathway	5.84	0.0321	-3.162	ADCY2,CADM1,CAMK2G,DAB1,FARP1,GRIA2,GRIN2C,GRM3,KALRN,NRXN1	0
White Adipose Tissue Browning Pathway	1.69	0.0233	0	ADCY2,DIO2,FGFR3	0
Axonal Guidance Signaling	1.66	0.0124	0	ADAM23,GNAO1,KALRN,PLCB1,ROBO2,SEMA4A	0
Cardiac Hypertrophy Signaling (Enhanced)	1.65	0.0123	-1.633	ADCY2,CAMK2G,FGFR3,HDAC8,PDE8B,PLCB1	0
Glycine Cleavage Complex	1.58	0.167	0	GLDC	0
Zymosterol Biosynthesis	1.58	0.167	0	MSMO1	0
Phospholipase C Signaling	1.54	0.0156	0	ADCY2,HDAC8,PLCB1,RAPGEF3	0
Relaxin Signaling	1.52	0.02	0	ADCY2,GNAO1,PDE8B	0
Molecular Mechanisms of Cancer	1.5	0.0128	0	ADCY2,CAMK2G,GNAO1,PLCB1,RAPGEF3	0
Necroptosis Signaling Pathway	1.47	0.0191	0	CAMK2G,GLUL,MERTK	0
Protein Kinase A Signaling	1.47	0.0125	-2.236	ADCY2,CAMK2G,PDE8B,PHKG1,PLCB1	0
Dopamine-DARPP32 Feedback in cAMP Signaling	1.43	0.0184	0	ADCY2,GRIN2C,PLCB1	0
CXCR4 Signaling	1.4	0.018	0	ADCY2,GNAO1,PLCB1	0

Ephrin B Signaling	1.38	0.0278	0	GNAO1,KALRN	0
GPCR-Mediated Integration of Enteroendocrine Signaling Exemplified by an L Cell	1.37	0.0274	0	ADCY2,PLCB1	0
GNRH Signaling	1.37	0.0173	0	ADCY2,CAMK2G,PLCB1	0
Leptin Signaling in Obesity	1.36	0.027	0	ADCY2,PLCB1	0
Role of NFAT in Regulation of the Immune Response	1.32	0.0166	0	GNAO1,PLCB1,RCAN2	0
Synaptogenesis Signaling Pathway	3.25	0.0256	2.828	ADCY2,CADM1,CAMK2G,EPHB1,GRIA2,GRIN2C,GRM3,NRXN1	1
CREB Signaling in Neurons	3.62	0.0338	2.449	ADCY2,CAMK2G,GNAO1,GRIA2,GRIK1,GRIN2C,GRM3	1
cAMP-mediated signaling	5.04	0.0395	2.333	ADCY2,CAMK2G,GABBR2,GNAO1,GRM3,PDE8B,RAPGEF3,RGS7,S1PR1	1
Calcium Signaling	3.63	0.034	2.236	CAMK2G,CHRNA7,GRIA2,GRIK1,GRIN2C,HDAC8,RCAN2	1
Synaptic Long Term Potentiation	2.98	0.0388	2.236	CAMK2G,GRIA2,GRIN2C,GRM3,RAPGEF3	1
Amyotrophic Lateral Sclerosis Signaling	4.6	0.0619	1.342	GLUL,GRIA2,GRIK1,GRIN2C,SLC1A2,VEGFA	1
Glutamate Receptor Signaling	7.34	0.123	1	GLUL,GRIA2,GRIK1,GRIN2C,GRM3,SLC1A2,SLC1A3	1
Endocannabinoid Neuronal Synapse Pathway	3	0.0391	1	ADCY2,GNAO1,GRIA2,GRIN2C,MGLL	1
Opioid Signaling Pathway	3.16	0.0283	0.378	ADCY2,CAMK2G,GNAO1,GRIN2C,RGS20,RGS6,RGS7	1
Gαi Signaling	3.04	0.04	0.447	ADCY2,GABBR2,GRM3,RGS7,S1PR1	1
G-Protein Coupled Receptor Signaling	5.27	0.0368	0	ADCY2,ADRA1A,CAMK2G,GABBR2,GNAO1,GRM3,PDE8B,RAPGEF3,RGS7,S1PR1	1
Neuroinflammation Signaling Pathway	3.37	0.0268	0	GABBR2,GABRA2,GABRB1,GLUL,GRIN2C,IRAK2,SLC1A2,SLC1A3	1
White Adipose Tissue Browning Pathway	2.98	0.0388	2.236	ADCY2,DIO2,FGFR3,PRDM16,VEGFA	1
Citrulline Biosynthesis	2.91	0.222	0	LOC102724788/PRODH,OTC	1
GABA Receptor Signaling	2.6	0.0421	0	ADCY2,GABBR2,GABRA2,GABRB1	1
Neuropathic Pain Signaling In Dorsal Horn Neurons	2.51	0.0396	2	CAMK2G,GRIA2,GRIN2C,GRM3	1

Superpathway of Citrulline Metabolism	2.46	0.133	0	LOC102724788/PRODH,OTC	1
RhoGDI Signaling	2.35	0.0278	-2	ARHGAP5,ARHGEF19,DLC1,FNBP1,GNAO1	1
Synaptic Long Term Depression	2.26	0.0265	2.236	ABHD3,GNAO1,GRIA2,GRM3,PLA2G7	1
Glutamine Biosynthesis I	2.23	1	0	GLUL	1
Citrulline Degradation	2.23	1	0	OTC	1
Breast Cancer Regulation by Stathmin1	2.05	0.0152	0	ADRA1A,ARHGEF19,CAMK2G,GABBR2,GRM3,LGR4,NTSR2,S1PR1,VEGFA	1
Melatonin Signaling	2.04	0.0417	0	CAMK2G,GNAO1,RORB	1
Sperm Motility	1.97	0.0224	0	ABHD3,EPHB1,FGFR3,MERTK,PLA2G7	1
Corticotropin Releasing Hormone Signaling	1.96	0.0276	0	ADCY2,GLI3,GNAO1,VEGFA	1
Relaxin Signaling	1.91	0.0267	0	ADCY2,GNAO1,PDE8B,VEGFA	1
TR/RXR Activation	1.86	0.0357	0	DIO2,LDLR,RCAN2	1
IL-1 Signaling	1.77	0.033	0	ADCY2,GNAO1,IRAK2	1
Proline Degradation	1.75	0.333	0	LOC102724788/PRODH	1
Thyronamine and Iodothyronamine Metabolism	1.75	0.333	0	DIO2	1
Thyroid Hormone Metabolism I (via Deiodination)	1.75	0.333	0	DIO2	1
Phospholipase C Signaling	1.73	0.0195	2	ADCY2,ARHGEF19,FNBP1,HDAC8,RAPGEF3	1
α-Adrenergic Signaling	1.71	0.0312	0	ADCY2,ADRA1A,PHKG1	1
Ephrin Receptor Signaling	1.65	0.0222	0	EPHB1,GNAO1,GRIN2C,VEGFA	1
Endothelin-1 Signaling	1.59	0.0213	1	ABHD3,ADCY2,GNAO1,PLA2G7	1
Proline Biosynthesis II (from Arginine)	1.53	0.2	0	OTC	1
α-tocopherol Degradation	1.53	0.2	0	CYP4F3	1
Molecular Mechanisms of Cancer	1.53	0.0153	0	ADCY2,ARHGEF19,CAMK2G,FNBP1,GNAO1,RAPGEF3	1
Gap Junction Signaling	1.51	0.0202	0	ADCY2,GJA1,GRIA2,GRIK1	1
Endocannabinoid Developing Neuron Pathway	1.51	0.0261	0	ADCY2,GNAO1,MGLL	1
Triacylglycerol Degradation	1.5	0.0426	0	MGLL,RPE65	1
Sphingosine-1-phosphate Signaling	1.49	0.0256	0	ADCY2,FNBP1,S1PR1	1

Arginine Biosynthesis IV	1.45	0.167	0	OTC	1
Urea Cycle	1.45	0.167	0	OTC	1
Glycine Cleavage Complex	1.45	0.167	0	GLDC	1
Zymosterol Biosynthesis	1.45	0.167	0	MSMO1	1
IL-15 Production	1.45	0.0248	0	EPHB1,FGFR3,MERTK	1
Thrombin Signaling	1.45	0.0192	0	ADCY2,CAMK2G,FNBP1,GNAO1	1
Osteoarthritis Pathway	1.43	0.019	0	FGFR3,GLI3,HTRA1,VEGFA	1
Role of NFAT in Cardiac Hypertrophy	1.41	0.0187	0	ADCY2,CAMK2G,HDAC8,RCAN2	1
Atherosclerosis Signaling	1.4	0.0236	0	ABHD3,F3,PLA2G7	1
Glutamate Receptor Signaling	2.75	0.0351	0	GRIN2C,SLC1A2	2
Synaptogenesis Signaling Pathway	2.33	0.00962	0	DAB1,FARP1,GRIN2C	2
Amyotrophic Lateral Sclerosis Signaling	2.29	0.0206	0	GRIN2C,SLC1A2	2
Reelin Signaling in Neurons	2.06	0.0155	0	DAB1,GRIN2C	2
Opioid Signaling Pathway	1.52	0.0081	0	GRIN2C,RGS20	2
Circadian Rhythm Signaling	1.45	0.0303	0	GRIN2C	2
Neuroinflammation Signaling Pathway	1.37	0.00669	0	GRIN2C,SLC1A2	2
Triacylglycerol Biosynthesis	1.34	0.0238	0	PLPP3	2
Glutamate Receptor Signaling	10.4	0.158	-1.342	GLUL,GRIA2,GRID1,GRID2,GRIN2C,GRIP1,GRM3,SLC1A2,SLC1A3	3
G-Protein Coupled Receptor Signaling	6.25	0.0404	0	CAMK2G,GABBR1,GABBR2,GNAO1,GRM3,HTR2C,PDE7B,PDE8B,PLCB1,RAPGEF3,RGS7	3
cAMP-mediated signaling	5.12	0.0395	-2.333	CAMK2G,GABBR1,GABBR2,GNAO1,GRM3,PDE7B,PDE8B,RAPGEF3,RGS7	3
Neuroinflammation Signaling Pathway	5	0.0334	0	GABBR1,GABBR2,GABRA2,GABRB1,GLUL,GRIN2C,IRAK2,SLC1A2,SLC1A3,SLC6A11	3
RhoGDI Signaling	4.98	0.0444	1.633	ARHGAP5,ARHGEF12,ARHGEF19,CDH10,FNBP1,GNAO1,GRIP1,PAK3	3
Amyotrophic Lateral Sclerosis Signaling	4.66	0.0619	-1.342	GLUL,GRIA2,GRID1,GRID2,GRIN2C,SLC1A2	3
CREB Signaling in Neurons	4.54	0.0386	-2.646	CAMK2G,GNAO1,GRIA2,GRID1,GRID2,GRIN2C,GRM3,PLCB1	3

Synaptic Long Term Potentiation	3.97	0.0465	-2.449	CAMK2G,GRIA2,GRIN2C,GRM3,PLCB1,RAPGEF3	3
Synaptic Long Term Depression	3.92	0.037	-2.646	GNAO1,GRIA2,GRID1,GRID2,GRM3,PLA2G7,PLCB1	3
GABA Receptor Signaling	3.63	0.0526	0	GABBR1,GABBR2,GABRA2,GABRB1,SLC6A11	3
Integrin Signaling	3.6	0.0329	-0.816	ARHGAP26,ARHGAP5,FNBP1,ITGA6,PAK3,TSPAN7,VCL	3
Neuropathic Pain Signaling In Dorsal Horn Neurons	3.51	0.0495	-2.236	CAMK2G,GRIA2,GRIN2C,GRM3,PLCB1	3
Molecular Mechanisms of Cancer	3.32	0.023	0	ARHGEF12,ARHGEF19,CAMK2G,FNBP1,GNAO1,PAK3,PLCB1,RAPGEF3,RBL1	3
Synaptogenesis Signaling Pathway	3.31	0.0256	-2.828	CADM1,CAMK2G,CDH10,FARP1,GRIA2,GRIN2C,GRM3,NRXN1	3
Breast Cancer Regulation by Stathmin1	3.17	0.0186	0	ADGRB3,ADGRV1,ARHGEF12,ARHGEF19,CAMK2G,GABBR1,GABBR2,GRM3,HTR2C,LGR4,PLCB1	3
Melatonin Signaling	3.08	0.0556	-1	CAMK2G,GNAO1,PLCB1,RORB	3
Endocannabinoid Neuronal Synapse Pathway	3.04	0.0391	-2	GNAO1,GRIA2,GRIN2C,MGLL,PLCB1	3
Necroptosis Signaling Pathway	2.65	0.0318	-1.342	CAMK2G,GLUD1,GLUL,MERTK,RBL1	3
Signaling by Rho Family GTPases	2.51	0.0246	-1.342	ARHGEF12,ARHGEF19,CDH10,FNBP1,GNAO1,PAK3	3
Opioid Signaling Pathway	2.49	0.0243	-0.816	CAMK2G,GNAO1,GRIN2C,PLCB1,RGS20,RGS7	3
Phospholipase C Signaling	2.4	0.0233	-2.449	ARHGEF12,ARHGEF19,FNBP1,HDAC8,PLCB1,RAPGEF3	3
Semaphorin Signaling in Neurons	2.29	0.05	0	ARHGEF12,FNBP1,PAK3	3
Glutamine Biosynthesis I	2.24	1	0	GLUL	3
Leukocyte Extravasation Signaling	2.23	0.0254	-1	ARHGAP5,ITGA6,RAPGEF3,VAV3,VCL	3
Gαi Signaling	2.21	0.032	-1	GABBR1,GABBR2,GRM3,RGS7	3
Reelin Signaling in Neurons	2.17	0.031	-2	ARHGEF12,CAMK2G,GRIN2C,ITGA6	3
Semaphorin Neuronal Repulsive Signaling Pathway	2.15	0.0308	-1	ARHGEF12,BCAN,FARP1,PAK3	3
Thrombin Signaling	2.13	0.024	-2	ARHGEF12,CAMK2G,FNBP1,GNAO1,PLCB1	3
Actin Cytoskeleton Signaling	2.05	0.0229	-1	ARHGEF12,FGF1,PAK3,VAV3,VCL	3
Glutamate Biosynthesis II	1.94	0.5	0	GLUD1	3

Glutamate Degradation X	1.94	0.5	0	GLUD1	3
Gαq Signaling	1.86	0.0253	0	FNBP1,HTR2C,PLCB1,RGS7	3
Tec Kinase Signaling	1.81	0.0244	0	FNBP1,GNAO1,PAK3,VAV3	3
CXCR4 Signaling	1.79	0.024	0	FNBP1,GNAO1,PAK3,PLCB1	3
Germ Cell-Sertoli Cell Junction Signaling	1.75	0.0234	0	FNBP1,ITGA6,PAK3,VCL	3
FAK Signaling	1.74	0.0316	0	ARHGAP26,PAK3,VCL	3
Ephrin Receptor Signaling	1.68	0.0222	0	FGF1,GNAO1,GRIN2C,PAK3	3
Cardiac Hypertrophy Signaling (Enhanced)	1.63	0.0144	-1.89	CAMK2G,FGF1,FGFR3,HDAC8,PDE7B,PDE8B,PLCB1	3
Paxillin Signaling	1.6	0.0278	0	ITGA6,PAK3,VCL	3
tRNA Splicing	1.59	0.0465	0	PDE7B,PDE8B	3
Protein Kinase A Signaling	1.53	0.015	-2.236	CAMK2G,GLI3,PDE7B,PDE8B,PHKG1,PLCB1	3
Triacylglycerol Degradation	1.52	0.0426	0	MGLL,PNPLA7	3
Role of Tissue Factor in Cancer	1.51	0.0256	0	F3,ITGA6,PLCB1	3
Calcium Signaling	1.49	0.0194	0	CAMK2G,GRIA2,GRIN2C,HDAC8	3
Arginine Biosynthesis IV	1.46	0.167	0	GLUD1	3
Chondroitin and Dermatan Biosynthesis	1.46	0.167	0	CSGALNACT1	3
Glycine Cleavage Complex	1.46	0.167	0	GLDC	3
Sperm Motility	1.39	0.0179	0	FGFR3,MERTK,PLA2G7,PLCB1	3
Adipogenesis pathway	1.36	0.0224	0	FGF1,FGFR3,HDAC8	3
PI3K Signaling in B Lymphocytes	1.33	0.0217	0	CAMK2G,PLCB1,VAV3	3
Synaptogenesis Signaling Pathway	28.2	0.205	6.971	ADCY1,ADCY5,ADCY8,ADCY9,APOE,ARHGEF7,BDNF,CACNA1B,CACNA2D1,CACNB4,Calm1 (includes others),CAMK2A,CAMK2B,CAMK4,CDH12,CDH18,CDH6,CDH8,CDH9,CNTNAP2,DLG4,EFNA5,EFNB2,EPHA10,EPHA3,EPHA6,EPHA7,EPHB2,GRIA1,GRIA3,GRIA4,GRIN1,GRIN2A,GRIN2B,GRM1,GRM5,GRM7,GRM8,ITPR1,KALRN,MAP1B,Nrxn3,PRKAG2,PRKAR1B,PRKAR2B,PRKCE,RASGRF1,RASGRP1,RRAS2,SHC2,SNAP25,SNCA,STX1A,STX	4

				BP1,STXBP5,SYN1,SYN2,SYT1,SYT14,SYT16,SYT7,TIAM1,UNC13A,WASF1	
CREB Signaling in Neurons	22.8	0.227	5.477	ADCY1,ADCY5,ADCY8,ADCY9,CACNA1A,CACNA1B,CACNA1C,CACNA1D,CACNA1E,CACNA1G,CACNA1I,CACNA2D1,CACNA2D3,CACNB2,CACNB4,CACNG2,CACNG3,Calm1 (includes others),CAMK2A,CAMK2B,CAMK4,GNAL,GNAZ,GNG2,GNG4,GRIA1,GRIA3,GRIA4,GRIK3,GRIK4,GRIN1,GRIN2A,GRIN2B,GRM1,GRM5,GRM7,GRM8,ITPR1,PLCL2,PRKAG2,PRKAR1B,PRKAR2B,PRKCB,PRKCE,PRKCG,PRKCZ,RRAS2	4
Endocannabinoid Neuronal Synapse Pathway	22	0.289	3.333	ADCY1,ADCY5,ADCY8,ADCY9,CACNA1A,CACNA1B,CACNA1C,CACNA1D,CACNA1E,CACNA1G,CACNA1I,CACNA2D1,CACNA2D3,CACNB2,CACNB4,CACNG2,CACNG3,FAAH,GNAL,GNG2,GRIA1,GRIA3,GRIA4,GRIN1,GRIN2A,GRIN2B,GRM1,GRM5,ITPR1,KCNJ3,KCNJ6,KCNJ9,PLCL2,PRKAG2,PRKAR1B,PRKAR2B,RIMS1	4
Opioid Signaling Pathway	19.4	0.19	5.898	ADCY1,ADCY5,ADCY8,ADCY9,CACNA1A,CACNA1B,CACNA1C,CACNA1D,CACNA1E,CACNA1G,CACNA1I,CACNA2D1,CACNA2D3,CACNB2,CACNB4,CACNG2,CACNG3,Calm1 (includes others),CAMK2A,CAMK2B,CAMK4,GNAL,GNG2,GRIN1,GRIN2A,GRIN2B,ITPR1,KCNJ3,KCNJ6,KCNJ9,MAP2K4,OPRM1,PDE1A,PDE1B,PRKAG2,PRKAR1B,PRKAR2B,PRKCB,PRKCE,PRKCG,PRKCZ,RGS17,RGS20,RPS6KA3,RRAS2,RYR2,RYR3	4
GABA Receptor Signaling	19.2	0.316	0	ADCY1,ADCY5,ADCY8,ADCY9,CACNA1A,CACNA1B,CACNA1C,CACNA1D,CACNA1E,CACNA1G,CACNA1I,CACNA2D1,CACNA2D3,CACNB2,CACNB4,CACNG2,CACNG3,DNM1,GABBR2,GABRA1,GABRA3,GABRA4,GABRA5,GABRB1,GABRB2,GABRB3,GABRG2,GABRG3,KCNQ2,KCNQ3	4
Calcium Signaling	18.6	0.204	6.083	ATP2B1,ATP2B2,ATP2B3,ATP2B4,CACNA1A,CACNA1B,CACNA1C,CACNA1D,CACNA1E,CACNA1G,CACNA1I,CACNA2D1,CACNA2D3,CACNB2,CACNB4,CACNG2,CACNG3,Calm1 (includes others),CAMK2A,CAMK2B,CAMK4,CAMKK2,GRIA1,GRIA3,GRIA4,GRIN1,GRIN2A,GRIN2B,ITPR1,MEF2C,MYH10,PRKAG2,PRKAR1B,PRKAR2B,RYR	4

				2,RYR3,SLC8A1,SLC8A3,TRPC3,TRPC4,TRPC5, TRPC6	
Synaptic Long Term Depression	17.5	0.206	5.604	CACNA1A,CACNA1B,CACNA1C,CACNA1D,CACN A1E,CACNA1G,CACNA1I,CACNA2D1,CACNA2D3 ,CACNB2,CACNB4,CACNG2,CACNG3,CRHR1,G NAL,GNAZ,GRIA1,GRIA3,GRIA4,GRM1,GRM5,GR M7,GRM8,GUCY1A2,ITPR1,PLA2G3,PLA2G4E,PL CL2,PPM1L,PPP2R2C,PRKCB,PRKCE,PRKCG,P RKCZ,PRKG1,PRKG2,RRAS2,RYR2,RYR3	4
GPCR-Mediated Nutrient Sensing in Enteroendocrine Cells	15.9	0.259	5.385	ADCY1,ADCY5,ADCY8,ADCY9,CACNA1A,CACNA 1B,CACNA1C,CACNA1D,CACNA1E,CACNA1G,C ACNA1I,CACNA2D1,CACNA2D3,CACNB2,CACNB 4,CACNG2,CACNG3,GNG2,GNG4,ITPR1,PLCL2, PRKAG2,PRKAR1B,PRKAR2B,PRKCB,PRKCE,P RKCG,PRKCZ,RAPGEF4	4
GNRH Signaling	15.5	0.202	4.472	ADCY1,ADCY5,ADCY8,ADCY9,CACNA1A,CACNA 1B,CACNA1C,CACNA1D,CACNA1E,CACNA1G,C ACNA1I,CACNA2D1,CACNA2D3,CACNB2,CACNB 4,CACNG2,CACNG3,Calm1 (includes others),CAMK2A,CAMK2B,CAMK4,GNG2,ITPR1,M AP2K4,PAK3,PAK5,PRKAG2,PRKAR1B,PRKAR2 B,PRKCB,PRKCE,PRKCG,PRKCZ,PTK2B,RRAS2	4
Corticotropin Releasing Hormone Signaling	15.3	0.221	0.73	ADCY1,ADCY5,ADCY8,ADCY9,BDNF,CACNA1A, CACNA1B,CACNA1C,CACNA1D,CACNA1E,CACN A1G,CACNA1I,CACNA2D1,CACNA2D3,CACNB2, CACNB4,CACNG2,CACNG3,Calm1 (includes others),CAMK4,CRHR1,GUCY1A2,ITPR1,MEF2C, NR4A1,PRKAG2,PRKAR1B,PRKAR2B,PRKCB,PR KCE,PRKCG,PRKCZ	4
Netrin Signaling	14.9	0.338	4.264	ABLIM2,ABLIM3,CACNA1A,CACNA1B,CACNA1C, CACNA1D,CACNA1E,CACNA1G,CACNA1I,CACN A2D1,CACNA2D3,CACNB2,CACNB4,CACNG2,CA CNG3,PRKAG2,PRKAR1B,PRKAR2B,PRKG1,RY R2,RYR3,UNC5D	4
G Beta Gamma Signaling	14.9	0.238	5.014	ADCY1,CACNA1A,CACNA1B,CACNA1C,CACNA1 D,CACNA1E,CACNA1G,CACNA1I,CACNA2D1,CA CNA2D3,CACNB2,CACNB4,CACNG2,CACNG3,G NAL,GNAZ,GNG2,GNG4,KCNJ3,KCNJ6,KCNJ9,P RKAG2,PRKAR1B,PRKAR2B,PRKCB,PRKCE,PR KCG,PRKCZ,RRAS2	4

nNOS Signaling in Skeletal Muscle Cells	14.7	0.439	0	CACNA1A,CACNA1B,CACNA1C,CACNA1D,CACNA1E,CACNA1G,CACNA1I,CACNA2D1,CACNA2D3,CACNB2,CACNB4,CACNG2,CACNG3,Calm1 (includes others),CAMK4,RYR2,RYR3,SNTB2	4
Role of NFAT in Cardiac Hypertrophy	14	0.173	6	ADCY1,ADCY5,ADCY8,ADCY9,CACNA1A,CACNA1B,CACNA1C,CACNA1D,CACNA1E,CACNA1G,CACNA1I,CACNA2D1,CACNA2D3,CACNB2,CACNB4,CACNG2,CACNG3,Calm1 (includes others),CAMK2A,CAMK2B,CAMK4,GNG2,GNG4,ITPR1,MAP2K4,MEF2C,PLCL2,PRKAG2,PRKAR1B,PRKAR2B,PRKCB,PRKCE,PRKCG,PRKCZ,RRAS2,SLC8A1,SLC8A3	4
Glutamate Receptor Signaling	14	0.351	3.317	Calm1 (includes others),CAMK4,DLG4,GLS,GNG2,GRIA1,GRIA3,GRIA4,GRIK3,GRIK4,GRIN1,GRIN2A,GRIN2B,GRM1,GRM5,GRM7,GRM8,HOMER1,SLC17A7,SLC1A3	4
Dopamine-DARPP32 Feedback in cAMP Signaling	13.8	0.196	5.014	ADCY1,ADCY5,ADCY8,ADCY9,CACNA1A,CACNA1C,CACNA1D,CACNA1E,Calm1 (includes others),CAMK4,CAMKK2,GRIN1,GRIN2A,GRIN2B,GUCY1A2,ITPR1,KCNJ3,KCNJ6,KCNJ9,PLCL2,PPM1L,PPP1R14C,PPP2R2C,PRKAG2,PRKAR1B,PRKAR2B,PRKCB,PRKCE,PRKCG,PRKCZ,PRKG1,PRKG2	4
Synaptic Long Term Potentiation	13.3	0.217	4.707	ADCY1,ADCY8,CACNA1C,Calm1 (includes others),CAMK2A,CAMK2B,CAMK4,GRIA1,GRIA3,GRIA4,GRIN1,GRIN2A,GRIN2B,GRM1,GRM5,GRM7,GRM8,ITPR1,PLCL2,PPP1R14C,PRKAG2,PRKAR1B,PRKAR2B,PRKCB,PRKCE,PRKCG,PRKCZ,RRAS2	4
Neuropathic Pain Signaling In Dorsal Horn Neurons	13.3	0.248	5	BDNF,CAMK2A,CAMK2B,CAMK4,GRIA1,GRIA3,GRIA4,GRIN1,GRIN2A,GRIN2B,GRM1,GRM5,GRM7,GRM8,ITPR1,KCNQ2,KCNQ3,PLCL2,PRKAG2,PRKAR1B,PRKAR2B,PRKCB,PRKCE,PRKCG,PRKCZ	4
Cellular Effects of Sildenafil (Viagra)	13.1	0.214	0	ADCY1,ADCY5,ADCY8,ADCY9,CACNA1A,CACNA1C,CACNA1D,CACNA1E,CACNG2,CACNG3,Calm1 (includes others),CAMK4,GUCY1A2,ITPR1,KCNQ2,KCNQ3,MYH10,PDE1A,PDE1B,PDE2A,PDE4A,PLCL2,PR	4

				KAG2,PRKAR1B,PRKAR2B,PRKG1,PRKG2,SLC4A10	
White Adipose Tissue Browning Pathway	12.4	0.209	4.811	ADCY1,ADCY5,ADCY8,ADCY9,BDNF,CACNA1A,CACNA1B,CACNA1C,CACNA1D,CACNA1E,CACNA1G,CACNA1I,CACNA2D1,CACNA2D3,CACNB2,CACNB4,CACNG2,CACNG3,CAMKK2,GUCY1A2,PPARG,PRKAG2,PRKAR1B,PRKAR2B,PRKG1,PRKG2,RUNX1T1	4
CCR5 Signaling in Macrophages	12.2	0.245	2.828	CACNA1A,CACNA1B,CACNA1C,CACNA1D,CACNA1E,CACNA1G,CACNA1I,CACNA2D1,CACNA2D3,CACNB2,CACNB4,CACNG2,CACNG3,Calm1 (includes others),CAMK4,GNG2,GNG4,MAP2K4,PRKCB,PRKCE,PRKCG,PRKCZ,PTK2B	4
Gustation Pathway	12.1	0.188	0	ADCY1,ADCY5,ADCY8,ADCY9,ASIC2,CACNA1A,CACNA1B,CACNA1C,CACNA1D,CACNA1E,CACNA1G,CACNA1I,CACNA2D1,CACNA2D3,CACNB2,CACNB4,CACNG2,CACNG3,GNG2,ITPR1,PDE10A,PDE1A,PDE1B,PDE2A,PDE4A,PDE6A,PRKAG2,PRKAR1B,PRKAR2B	4
Cardiac β-adrenergic Signaling	11.5	0.191	2.558	ADCY1,ADCY5,ADCY8,ADCY9,CACNA1A,CACNA1C,CACNA1D,CACNA1E,GNG2,GNG4,PDE10A,PDE1A,PDE1B,PDE2A,PDE4A,PDE6A,PKIA,PKIG,PPM1L,PPP1R14C,PPP2R2C,PRKAG2,PRKAR1B,PRKAR2B,RYR2,SLC8A1,SLC8A3	4
Androgen Signaling	11.1	0.191	4.69	CACNA1A,CACNA1B,CACNA1C,CACNA1D,CACNA1E,CACNA1G,CACNA1I,CACNA2D1,CACNA2D3,CACNB2,CACNB4,CACNG2,CACNG3,Calm1 (includes others),CAMK4,GNAL,GNAZ,GNG2,GNG4,PRKAG2,PRKAR1B,PRKAR2B,PRKCB,PRKCE,PRKCG,PRKCZ	4
Protein Kinase A Signaling	10.1	0.113	1.372	ADCY1,ADCY5,ADCY8,ADCY9,ADD2,Calm1 (includes others),CAMK2A,CAMK2B,CAMK4,FLNB,GNG2,GNG4,ITPR1,MYH10,PDE10A,PDE1A,PDE1B,PDE2A,PDE4A,PDE6A,PLCL2,PPP1R14C,PRKAG2,PRKAR1B,PRKAR2B,PRKCB,PRKCE,PRKCG,PRKCZ,PTK2B,PTPN1,PTPN3,PTPN5,Ptprd,PTPRE,PT	4

				PRJ,PTPRK,PTPRN,PTPRO,PTPRR,PTPRS,PTPRU,PTPRZ1,RYR2,RYR3	
Nitric Oxide Signaling in the Cardiovascular System	9.94	0.212	4.025	CACNA1A,CACNA1C,CACNA1D,CACNA1E,Calm1 (includes others),CAMK4,GUCY1A2,ITPR1,PDE1A,PDE1B,PDE2A,PRKAG2,PRKAR1B,PRKAR2B,PRKCB,PRKCE,PRKCG,PRKCZ,PRKG1,PRKG2,RYR2	4
G-Protein Coupled Receptor Signaling	9.52	0.129	0	ADCY1,ADCY5,ADCY8,ADCY9,CAMK2A,CAMK2B,CAMK4,CHRM2,CHRM3,CRHR1,GABBR2,GNAL,GRM1,GRM5,GRM7,GRM8,HTR1F,OPRM1,PDE10A,PDE1A,PDE1B,PDE2A,PDE4A,PDE6A,PRKAG2,PRKAR1B,PRKAR2B,PRKCB,PRKCE,PRKCG,PTK2B,RAP1GAP,RAPGEF4,RASGRP1,RRAS2	4
Sperm Motility	8.71	0.135	4.69	CACNA1G,Calm1 (includes others),CAMK4,EPHA3,EPHA6,EPHB2,GUCY1A2,ITPR1,LMTK2,LTK,MAP2K4,MATK,NTRK3,PDE1A,PDE1B,PDE2A,PDE4A,PLA2G3,PLA2G4E,PLCL2,PRKAG2,PRKAR1B,PRKAR2B,PRKCB,PRKCE,PRKCG,PRKCZ,PRKG1,PRKG2,PTK2B	4
α-Adrenergic Signaling	8.52	0.198	3.162	ADCY1,ADCY5,ADCY8,ADCY9,Calm1 (includes others),CAMK4,GNG2,GNG4,ITPR1,PRKAG2,PRKAR1B,PRKAR2B,PRKCB,PRKCE,PRKCG,PRKCZ,RRAS2,SLC8A1,SLC8A3	4
Insulin Secretion Signaling Pathway	8.42	0.128	5.209	ADCY1,ADCY5,ADCY8,ADCY9,CACNA1A,CACNA1C,CACNA1D,CACNA1E,CACNA1G,CAMK2A,CAMK2B,CHRM3,EIF2B5,ITPR1,KCNB1,NALCN,PCSK1,PCSK2,PLCL2,PRKAG2,PRKAR1B,PRKAR2B,PRKCB,PRKCE,PRKCG,PRKCZ,RAPGEF4,RYR2,RYR3,SLC2A3,SNAP25	4
Type II Diabetes Mellitus Signaling	8.38	0.162	1.134	ACSL1,CACNA1A,CACNA1B,CACNA1C,CACNA1D,CACNA1E,CACNA1G,CACNA1I,CACNA2D1,CACNA2D3,CACNB2,CACNB4,CACNG2,CACNG3,MAP2K4,PPARG,PRKAG2,PRKCB,PRKCE,PRKCG,PRKCZ,SMPD4,SOCS2	4
cAMP-mediated signaling	7.89	0.127	3.528	ADCY1,ADCY5,ADCY8,ADCY9,Calm1 (includes others),CAMK2A,CAMK2B,CAMK4,CHRM2,CHRM3,CRHR1,GABBR2,GNAL,GRM7,GRM8,HTR1F,OPRM1,PDE10A,PDE1A,PDE1B,PDE2A,PDE4A,PDE6A,PKIA,PKIG,PRKAR1B,PRKAR2B,RAP1GAP,RAPGEF4	4

Axonal Guidance Signaling	7.03	0.0909	0	ABLIM2,ABLIM3,ADAM22,ADAMTS17,ARHGEF7,BAIAP2,BDNF,EFNA5,EFNB2,EPHA10,EPHA3,EPHA6,EPHA7,EPHB2,GNAL,GNAZ,GNG2,GNG4,KALRN,MMP16,MMP17,MMP24,NRP2,NTRK3,PAK3,PAK5,PLCL2,PLXNA2,PRKAG2,PRKAR1B,PRKAR2B,PRKCB,PRKCE,PRKCG,PRKCZ,RRAS2,RTN4R,SEMA3A,SEMA3E,SHANK2,SLIT1,SLIT2,SLIT3,UNC5D	4
FcγRIIB Signaling in B Lymphocytes	6.92	0.2	0	CACNA1A,CACNA1B,CACNA1C,CACNA1D,CACNA1E,CACNA1G,CACNA1I,CACNA2D1,CACNA2D3,CACNB2,CACNB4,CACNG2,CACNG3,MAP2K4,RRAS2	4
nNOS Signaling in Neurons	6.89	0.255	2.646	Calm1 (includes others),CAMK2A,CAMK4,DLG2,DLG4,GRIN1,GRIN2A,GRIN2B,PRKCB,PRKCE,PRKCG,PRKCZ	4
Renin-Angiotensin Signaling	6.3	0.153	3.742	ADCY1,ADCY5,ADCY8,ADCY9,ITPR1,MAP2K4,PAK3,PAK5,PRKAG2,PRKAR1B,PRKAR2B,PRKCB,PRKCE,PRKCG,PRKCZ,PTK2B,RRAS2,SHC2	4
Melatonin Signaling	5.55	0.181	2.496	Calm1 (includes others),CAMK2A,CAMK2B,CAMK4,MAP2K4,PLCL2,PRKAG2,PRKAR1B,PRKAR2B,PRKCB,PRKCE,PRKCG,PRKCZ	4
Neuroinflammation Signaling Pathway	5.39	0.097	3.153	APP,BDNF,CALB1,CX3CL1,GABBR2,GABRA1,GABRA3,GABRA4,GABRA5,GABRB1,GABRB2,GABRB3,GABRG2,GABRG3,GLS,GRIA1,GRIN1,GRIN2A,GRIN2B,KCNJ3,KCNJ6,KCNJ9,MAP2K4,PLA2G3,PLA2G4E,PRKCG,SLC1A3,SNCA,TGFBR3	4
Relaxin Signaling	5.36	0.127	3.162	ADCY1,ADCY5,ADCY8,ADCY9,GNAL,GNAZ,GNG2,GNG4,GUCY1A2,PDE10A,PDE1A,PDE1B,PDE2A,PDE4A,PDE6A,PRKAG2,PRKAR1B,PRKAR2B,PRKCZ	4
Gαi Signaling	5.28	0.136	0	ADCY1,ADCY5,ADCY8,ADCY9,CHRM2,GABBR2,GNG2,GNG4,GRM7,GRM8,HTR1F,OPRM1,PRKAG2,PRKAR1B,PRKAR2B,RAP1GAP,RRAS2	4
Adrenomedullin signaling pathway	5.19	0.112	4.69	ADCY1,ADCY5,ADCY8,ADCY9,Calm1 (includes others),CAMK4,GUCY1A2,ITPR1,KCNQ2,KCNQ3,MAP2K4,MATK,PLCL2,PPARG,PRKAG2,PRKAR1B,PRKAR2B,PRKG1,PRKG2,PTK2B,RRAS2,SHC2	4

Gαs Signaling	4.89	0.14	3.207	ADCY1,ADCY5,ADCY8,ADCY9,ADD2,CHRM3,CRHR1,GNG2,GNG4,PRKAG2,PRKAR1B,PRKAR2B,RAPGEF4,RYR2,RYR3	4
Rac Signaling	4.65	0.134	3.606	ANK1,BAIAP2,CYFIP2,IQGAP2,MAP2K4,PAK3,PAK5,PI4KA,PIP5K1B,PIP5K1C,PRKCZ,PTK2B,RRAS2,TIAM1,WASF1	4
Gap Junction Signaling	4.64	0.106	0	ADCY1,ADCY5,ADCY8,ADCY9,GRIA1,GRIA3,GRIA4,GRIK3,GUCY1A2,ITPR1,PLCL2,PRKAG2,PRKAR1B,PRKAR2B,PRKCB,PRKCE,PRKCG,PRKCZ,PRKG1,PRKG2,RRAS2	4
Estrogen Receptor Signaling	4.62	0.0884	5.014	ADCY1,ADCY5,ADCY8,ADCY9,CACNA1A,CACNA1C,CACNA1D,CACNA1E,DLG4,EIF2B5,GNAL,GNAZ,GNG2,MMP16,MMP17,MMP24,PGR,PLCL2,PRKAG2,PRKAR1B,PRKAR2B,PRKCB,PRKCE,PRKCG,PRKCZ,RRAS2,RUNX2,SHC2,ZDHHC21	4
Cardiac Hypertrophy Signaling (Enhanced)	4.6	0.078	6.164	ADCY1,ADCY5,ADCY8,ADCY9,CACNA1A,CACNA1C,CACNA1D,CACNA1E,Calm1 (includes others),CAMK2A,CAMK2B,CAMK4,EIF2B5,FGF12,FGF14,GNG2,ITPR1,MAP2K4,MEF2C,PDE10A,PDE1A,PDE1B,PDE2A,PDE4A,PDE6A,PLCL2,PRKAG2,PRKAR1B,PRKAR2B,PRKCB,PRKCE,PRKCG,PRKCZ,PRKG1,RRAS2,RYR2,RYR3,TGFBR3	4
Apelin Endothelial Signaling Pathway	4.51	0.13	1.807	ADCY1,ADCY5,ADCY8,ADCY9,Calm1 (includes others),CAMK4,GNAL,MAP2K4,MEF2C,PRKAG2,PRKCB,PRKCE,PRKCG,PRKCZ,RRAS2	4
eNOS Signaling	4.44	0.113	4.123	ADCY1,ADCY5,ADCY8,ADCY9,Calm1 (includes others),CAMK4,CHRM2,CHRM3,GUCY1A2,ITPR1,PRKAG2,PRKAR1B,PRKAR2B,PRKCB,PRKCE,PRKCG,PRKCZ,PRKG1	4
IL-1 Signaling	4.41	0.143	2.236	ADCY1,ADCY5,ADCY8,ADCY9,GNAL,GNAZ,GNG2,GNG4,IL1RAP,MAP2K4,PRKAG2,PRKAR1B,PRKAR2B	4
Huntington's Disease Signaling	4.4	0.097	2.138	BDNF,CACNA1B,DLG4,DNM1,DNM3,GLS,GNG2,GNG4,GRIN2B,GRM1,GRM5,ITPR1,MAP2K4,PACSIN1,PRKCB,PRKCE,PRKCG,PRKCZ,RPH3A,SGK1,SNAP25,SNCA,STX1A	4
CDK5 Signaling	4.22	0.13	3.207	ADCY1,ADCY5,ADCY8,ADCY9,BDNF,CACNA1A,GNAL,PPM1L,PPP1R14C,PPP2R2C,PRKAG2,PRKAR1B,PRKAR2B,RRAS2	4

CXCR4 Signaling	4.16	0.108	1.604	ADCY1,ADCY5,ADCY8,ADCY9,ELMO1,GNAL,GNAZ,GNG2,GNG4,ITPR1,MAP2K4,PAK3,PAK5,PRKCB,PRKCE,PRKCG,PRKCZ,RRAS2	4
Amyotrophic Lateral Sclerosis Signaling	4.11	0.134	3	CACNA1A,CACNA1C,CACNA1D,CACNA1E,GRIA1,GRIA3,GRIA4,GRIK3,GRIK4,GRIN1,GRIN2A,GRIN2B,HECW1	4
PKCθ Signaling in T Lymphocytes	4.06	0.11	2	CACNA1A,CACNA1B,CACNA1C,CACNA1D,CACNA1E,CACNA1G,CACNA1I,CACNA2D1,CACNA2D3,CACNB2,CACNB4,CACNG2,CACNG3,CAMK2A,CAMK2B,MAP2K4,RRAS2	4
GPCR-Mediated Integration of Enteroendocrine Signaling Exemplified by an L Cell	4.03	0.151	2.111	ADCY1,ADCY5,ADCY8,ADCY9,CHRM2,GLP2R,ITPR1,PLCL2,PRKAG2,PRKAR1B,PRKAR2B	4
P2Y Purigenic Receptor Signaling Pathway	4.01	0.118	3.742	ADCY1,ADCY5,ADCY8,ADCY9,GNG2,GNG4,PLCL2,PRKAG2,PRKAR1B,PRKAR2B,PRKCB,PRKCE,PRKCG,PRKCZ,RRAS2	4
Semaphorin Neuronal Repulsive Signaling Pathway	3.89	0.115	1.807	GUCY1A2,MAP2K4,NRP2,PAK3,PAK5,PDE4A,PIP5K1C,PLXNA2,PRKAG2,PRKAR1B,PRKAR2B,PRKG1,PRKG2,SEMA3A,SEMA3E	4
Cardiac Hypertrophy Signaling	3.88	0.0917	3.9	ADCY1,ADCY5,ADCY8,ADCY9,CACNA1A,CACNA1C,CACNA1D,CACNA1E,Calm1 (includes others),CAMK4,EIF2B5,GNAL,GNAZ,GNG2,GNG4,MAP2K4,MEF2C,PLCL2,PRKAG2,PRKAR1B,PRKAR2B,RRAS2	4
Dopamine Receptor Signaling	3.82	0.143	2.121	ADCY1,ADCY5,ADCY8,ADCY9,NCS1,PPM1L,PPP1R14C,PPP2R2C,PRKAG2,PRKAR1B,PRKAR2B	4
Signaling by Rho Family GTPases	3.77	0.0902	4.123	ARHGEF3,ARHGEF7,BAIAP2,CDH12,CDH18,CDH6,CDH8,CDH9,CIT,GNAL,GNAZ,GNG2,GNG4,MAP2K4,PAK3,PAK5,PI4KA,PIP5K1B,PIP5K1C,PRKCZ,PTK2B,WASF1	4
RhoGDI Signaling	3.74	0.1	-3.742	ARHGEF3,ARHGEF7,CDH12,CDH18,CDH6,CDH8,CDH9,DGKZ,GNAL,GNAZ,GNG2,GNG4,PAK3,PAK5,PI4KA,PIP5K1B,PIP5K1C,WASF1	4
Ephrin Receptor Signaling	3.74	0.1	3.317	EFNA5,EFNB2,EPHA10,EPHA3,EPHA6,EPHA7,EPHB2,GNAL,GNAZ,GNG2,GNG4,GRIN1,GRIN2A,GRIN2B,KALRN,PAK3,PAK5,RRAS2	4
CCR3 Signaling in Eosinophils	3.58	0.113	3	Calm1 (includes others),CAMK4,GNG2,GNG4,ITPR1,PAK3,PAK5,PLA2G3,PLA2G4E,PRKCB,PRKCE,PRKCG,PRKCZ,RRAS2	4

Endothelin-1 Signaling	3.51	0.0957	1.698	ADCY1,ADCY5,ADCY8,ADCY9,GNAL,GNAZ,GUCY1A2,ITPR1,PLA2G3,PLA2G4E,PLCL2,PLD5,PRKCB,PRKCE,PRKCG,PRKCZ,RRAS2,SHC2	4
Calcium Transport I	3.44	0.4	2	ATP2B1,ATP2B2,ATP2B3,ATP2B4	4
Thrombin Signaling	3.41	0.0913	1.807	ADCY1,ADCY5,ADCY8,ADCY9,ARHGEF3,CAMK2A,CAMK2B,CAMK4,GNAL,GNAZ,GNG2,GNG4,ITPR1,PLCL2,PRKCB,PRKCE,PRKCG,PRKCZ,RRAS2	4
Chondroitin Sulfate Biosynthesis (Late Stages)	3.39	0.167	2.828	CHSY3,HS3ST2,HS3ST4,HS3ST5,HS6ST2,HS6ST3,NDST3,UST	4
Endocannabinoid Developing Neuron Pathway	3.37	0.113	-0.632	ADCY1,ADCY5,ADCY8,ADCY9,GNAL,GNG2,MAP2K4,PRKAG2,PRKAR1B,PRKAR2B,RAP1GAP,RRAS2,STMN2	4
Phospholipase C Signaling	3.06	0.0817	3.742	ADCY1,ADCY5,ADCY8,ADCY9,ARHGEF3,ARHGEF7,Calm1 (includes others),CAMK4,GNG2,GNG4,ITPR1,MEF2C,PLA2G3,PLA2G4E,PLD5,PRKCB,PRKCE,PRKCG,PRKCZ,RPS6KA3,RRAS2	4
PPARα/RXRα Activation	3.01	0.0895	0.775	ADCY1,ADCY5,ADCY8,ADCY9,CHD5,IL1RAP,IL1RAPL1,IL1RAPL2,MAP2K4,MEF2C,PLCL2,PRKAG2,PRKAR1B,PRKAR2B,PRKCB,RRAS2,TGFBR3	4
Xenobiotic Metabolism PXR Signaling Pathway	2.96	0.0885	1.213	CAMK2A,CAMK2B,HS3ST2,HS3ST4,HS3ST5,HS6ST2,HS6ST3,NDST3,PPP1R14C,PRKAG2,PRKAR1B,PRKAR2B,PRKCB,PRKCE,PRKCG,PRKCZ,UST	4
ERK/MAPK Signaling	2.94	0.0881	2.5	PAK3,PAK5,PLA2G3,PLA2G4E,PPARG,PPM1L,PPP1R14C,PPP2R2C,PRKAG2,PRKAR1B,PRKAR2B,PRKCB,PRKCE,PRKCG,PTK2B,RAPGEF4,RRAS2	4
Chondroitin Sulfate Biosynthesis	2.92	0.143	2.828	CHSY3,HS3ST2,HS3ST4,HS3ST5,HS6ST2,HS6ST3,NDST3,UST	4
Dermatan Sulfate Biosynthesis (Late Stages)	2.79	0.152	2.646	HS3ST2,HS3ST4,HS3ST5,HS6ST2,HS6ST3,NDST3,UST	4
Dermatan Sulfate Biosynthesis	2.77	0.136	2.828	CHSY3,HS3ST2,HS3ST4,HS3ST5,HS6ST2,HS6ST3,NDST3,UST	4
Hepatic Cholestasis	2.72	0.0865	0	ADCY1,ADCY5,ADCY8,ADCY9,IL1RAP,IL1RAPL1,IL1RAPL2,MAP2K4,PRKAG2,PRKAR1B,PRKAR2B,PRKCB,PRKCE,PRKCG,PRKCZ,SLCO3A1	4

Molecular Mechanisms of Cancer	2.66	0.0691	0	ADCY1,ADCY5,ADCY8,ADCY9,ARHGEF3,ARHGEF7,CAMK2A,CAMK2B,CDK14,CDK17,GNAL,GNAZ,MAP2K4,NLK,PAK3,PAK5,PRKAG2,PRKAR1B,PRKAR2B,PRKCB,PRKCE,PRKCG,PRKCZ,RASGRF1,RASGRF2,RASGRP1,RRAS2	4
Aldosterone Signaling in Epithelial Cells	2.54	0.0886	3.317	ASIC2,DNAJC21,DNAJC6,HSPA12A,ITPR1,PI4KA,PIP5K1B,PIP5K1C,PLCL2,PRKCB,PRKCE,PRKCG,PRKCZ,SGK1	4
Gαq Signaling	2.54	0.0886	3.464	Calm1 (includes others),CAMK4,CHRM3,GNG2,GNG4,GRM1,GRM5,ITPR1,PLD5,PRKCB,PRKCE,PRKCG,PRKCZ,PTK2B	4
UVC-Induced MAPK Signaling	2.52	0.137	2.646	MAP2K4,PRKCB,PRKCE,PRKCG,PRKCZ,RRAS2,SMPD4	4
Melanocyte Development and Pigmentation Signaling	2.52	0.106	3.162	ADCY1,ADCY5,ADCY8,ADCY9,KITLG,PRKAG2,PRKAR1B,PRKAR2B,RPS6KA3,RRAS2	4
ErbB Signaling	2.52	0.106	3.162	MAP2K4,NRG2,NRG3,PAK3,PAK5,PRKCB,PRKCE,PRKCG,PRKCZ,RRAS2	4
Calcium-induced T Lymphocyte Apoptosis	2.46	0.121	2.828	Calm1 (includes others),CAMK4,ITPR1,NR4A1,PRKCB,PRKCE,PRKCG,PRKCZ	4
Neuregulin Signaling	2.45	0.104	2.53	DLG4,MATK,NRG2,NRG3,PRKCB,PRKCE,PRKCG,PRKCZ,RRAS2,TMEFF2	4
Reelin Signaling in Neurons	2.42	0.093	3.317	APOE,APP,ARHGEF3,CAMK2A,CAMK2B,DCX,GRIN1,GRIN2A,GRIN2B,MAP1B,MAP2K4,WASF1	4
ErbB4 Signaling	2.42	0.119	2.828	Nrg1,NRG2,NRG3,PRKCB,PRKCE,PRKCG,PRKCZ,RRAS2	4
Nur77 Signaling in T Lymphocytes	2.38	0.118	2.828	Calm1 (includes others),CAMK4,NR4A1,PRKCB,PRKCE,PRKCG,PRKCZ,RPS6KA3	4
Actin Cytoskeleton Signaling	2.38	0.078	3.207	ACTN1,ARHGEF7,BAIAP2,CYFIP2,FGF12,FGF14,IQGAP2,MATK,MYH10,PAK3,PAK5,PIP5K1B,PIP5K1C,RRAS2,TIAM1,TRIO,WASF1	4
tRNA Splicing	2.27	0.14	2.449	PDE10A,PDE1A,PDE1B,PDE2A,PDE4A,PDE6A	4
Leptin Signaling in Obesity	2.16	0.108	0	ADCY1,ADCY5,ADCY8,ADCY9,PLCL2,PRKAG2,PRKAR1B,PRKAR2B	4
Leukocyte Extravasation Signaling	2.07	0.0761	2.84	ACTN1,CTNNA3,EDIL3,MAP2K4,MMP16,MMP17,MMP24,PRKCB,PRKCE,PRKCG,PRKCZ,PTK2B,RAP1GAP,RAPGEF4,RASGRP1	4

Agrin Interactions at Neuromuscular Junction	2.02	0.103	2.828	ARHGEF7,MAP2K4,Nrg1,NRG2,NRG3,PAK3,PAK5,RRAS2	4
Tec Kinase Signaling	2	0.0793	3	GNAL,GNAZ,GNG2,GNG4,MAP2K4,PAK3,PAK5,PRKCB,PRKCE,PRKCG,PRKCZ,PTK2B,TNFRSF21	4
PAK Signaling	1.94	0.0928	2.828	ARHGAP10,ARHGEF7,DSCAM,EPHA3,MAP2K4,PAK3,PAK5,PTK2B,RRAS2	4
fMLP Signaling in Neutrophils	1.89	0.0862	3	Calm1 (includes others),CAMK4,GNG2,GNG4,ITPR1,PRKCB,PRKCE,PRKCG,PRKCZ,RRAS2	4
Xenobiotic Metabolism CAR Signaling Pathway	1.87	0.0741	1.069	HS3ST2,HS3ST4,HS3ST5,HS6ST2,HS6ST3,MAP2K4,NDST3,PPM1L,PPP2R2C,PRKCB,PRKCE,PRKCG,PRKCZ,UST	4
UVB-Induced MAPK Signaling	1.87	0.115	2.449	MAP2K4,PRKCB,PRKCE,PRKCG,PRKCZ,RPS6KA3	4
VEGF Family Ligand-Receptor Interactions	1.84	0.0952	2.646	NRP2,PLA2G3,PLA2G4E,PRKCB,PRKCE,PRKCG,PRKCZ,RRAS2	4
GP6 Signaling Pathway	1.81	0.084	3.162	Calm1 (includes others),CAMK4,COL19A1,COL25A1,COL26A1,ITPR1,PRKCB,PRKCE,PRKCG,PRKCZ	4
IL-15 Production	1.77	0.0826	3.162	EPHA3,EPHA6,EPHB2,LMTK2,LTK,MAP2K4,MATK,NTRK3,PRKCZ,PTK2B	4
Heparan Sulfate Biosynthesis (Late Stages)	1.74	0.0986	2.646	HS3ST2,HS3ST4,HS3ST5,HS6ST2,HS6ST3,NDST3,UST	4
Breast Cancer Regulation by Stathmin1	1.74	0.0558	0	ARHGEF3,ARHGEF7,CAMK2A,CAMK2B,CAMK4,CHRM2,CHRM3,CRHR1,GABBR2,GLP2R,GNG2,GNG4,GPR137C,GPR158,GPR176,GRM1,GRM5,GRM7,GRM8,HTR1F,OPRM1,PPM1L,PPP1R14C,PPP2R2C,PRKAG2,PRKAR1B,PRKAR2B,PRKCB,PRKCE,PRKCG,PRKCZ,RPS6KA3,RRAS2	4
Mechanisms of Viral Exit from Host Cells	1.72	0.122	0	PRKCB,PRKCE,PRKCG,PRKCZ,SH3GL2	4
Ephrin B Signaling	1.71	0.0972	2.236	EFNB2,EPHB2,GNAL,GNAZ,GNG2,GNG4,KALRN	4
Endocannabinoid Cancer Inhibition Pathway	1.68	0.0769	-0.302	ADCY1,ADCY5,ADCY8,ADCY9,CAMKK2,GNAL,MAP2K4,PRKAG2,PRKAR1B,PRKAR2B,SMPD4	4
Glioma Signaling	1.61	0.0818	3	Calm1 (includes others),CAMK2A,CAMK2B,CAMK4,PRKCB,PRKCE,PRKCG,PRKCZ,RRAS2	4
3-phosphoinositide Biosynthesis	1.6	0.0723	3.317	ATP1A2,MTMR7,PI4KA,PIP5K1B,PIP5K1C,PPFIA2,PPFIA3,PPM1H,PTPN1,PTPRJ,PTPRN,PTPRO	4

Xenobiotic Metabolism Signaling	1.58	0.0627	0	CAMK2A,CAMK2B,CAMK4,HS3ST2,HS3ST4,HS3ST5,HS6ST2,HS6ST3,MAP2K4,NDST3,PPM1L,PPP2R2C,PRKCB,PRKCE,PRKCG,PRKCZ,RRAS2,UST	4
Heparan Sulfate Biosynthesis	1.54	0.0897	2.646	HS3ST2,HS3ST4,HS3ST5,HS6ST2,HS6ST3,NDST3,UST	4
Ephrin A Signaling	1.49	0.106	0	EFNA5,EPHA10,EPHA3,EPHA6,EPHA7	4
Chemokine Signaling	1.49	0.0875	2.646	Calm1 (includes others),CAMK2A,CAMK2B,CAMK4,PRKCB,PTK2B,RRAS2	4
Salvage Pathways of Pyrimidine Ribonucleotides	1.48	0.0816	2.828	AK5,DAPK1,MAP2K4,PAK3,PAK5,PRKCE,SGK1,UPP2	4
RAR Activation	1.46	0.067	0	ADCY1,ADCY5,ADCY8,ADCY9,MAP2K4,PRKAG2,PRKAR1B,PRKAR2B,PRKCB,PRKCE,PRKCG,PRKCZ,ZBTB16	4
Apelin Cardiomyocyte Signaling Pathway	1.46	0.0808	2.449	ITPR1,PLCL2,PRKCB,PRKCE,PRKCG,PRKCZ,SLC8A1,SLC8A3	4
Apelin Adipocyte Signaling Pathway	1.44	0.0854	-1.89	ADCY1,ADCY5,ADCY8,ADCY9,PRKAG2,PRKAR1B,PRKAR2B	4
Cholecystokinin/Gastrin-mediated Signaling	1.42	0.0756	3	ITPR1,MAP2K4,MEF2C,PRKCB,PRKCE,PRKCG,PRKCZ,PTK2B,RRAS2	4
Pyridoxal 5'-phosphate Salvage Pathway	1.41	0.0909	2.449	DAPK1,MAP2K4,PAK3,PAK5,PRKCE,SGK1	4
Amyloid Processing	1.39	0.1	0	APP,PRKAG2,PRKAR1B,PRKAR2B,PRKCE	4
Insulin Receptor Signaling	1.39	0.0714	0.632	ASIC2,EIF2B5,PPP1R14C,PRKAG2,PRKAR1B,PRKAR2B,PRKCZ,PTPN1,RRAS2,SGK1	4
BMP signaling pathway	1.37	0.0824	2.646	CAMK4,MAP2K4,PRKAG2,PRKAR1B,PRKAR2B,RRAS2,RUNX2	4
RhoA Signaling	1.35	0.0732	2.828	BAIAP2,CIT,NRP2,PI4KA,PIP5K1B,PIP5K1C,PLEKHG5,PTK2B,WASF1	4
LPS/IL-1 Mediated Inhibition of RXR Function	1.32	0.0625	1.633	ACSL1,APOE,HS3ST2,HS3ST4,HS3ST5,HS6ST2,HS6ST3,IL1RAP,IL1RAPL1,IL1RAPL2,MAP2K4,NDST3,PPARGC1B,UST	4

Supplemental Table 4.13 HD iAstro IPA Canonical Pathway Enrichment Analysis

Ingenuity Canonical Pathways	-log(p-value)	Ratio	z-score	Molecules
EIF2 Signaling	40.2	0.321	5.466	ACTA2,ACTB,ACTC1,ACTG2,ATF4,CCND1,EIF1,EIF1AY,EIF2S2,EIF3D,EIF3I,EIF3J,EIF4A1,IGF1R,PIK3R1,PPP1CA,PPP1CB,RPL10A,RPL11,RPL12,RPL13,RPL15,RPL18,RPL18A,RPL19,RPL21,RPL22,RPL22L1,RPL23,RPL23A,RPL24,RPL27,RPL28,RPL29,RPL3,RPL32,RPL35,RPL35A,RPL36AL,RPL38,RPL39,RPL4,RPL5,RPL6,RPL7,RPL7A,RPL8,RPLP0,RPLP2,RPS11,RPS12,RPS13,RPS14,RPS15,RPS16,RPS18,RPS19,RPS2,RPS23,RPS24,RPS27,RPS27A,RPS27L,RPS3,RPS3A,RPS4Y1,RPS5,RPS6,RPS9,RPSA,RRAS,UBA52
Integrin Signaling	18	0.216	2.16	ACTA2,ACTB,ACTC1,ACTG1,ACTG2,ACTN1,ACTN4,ACTR3,ARF1,ARF4,ARHGAP5,ARPC1B,ARPC2,ARPC3,ARPC4,ARPC5,ARPC5L,CAPNS1,CAV1,FNBP1,FYN,GSN,ILK,ITGA3,ITGA4,ITGA6,ITGA7,ITGB1,ITGB4,ITGB8,LIMS1,MYL12A,MYL12B,MYL9,PFN1,PFN2,PIK3R1,PPP1CB,RAC1,RHOC,RND2,RRAS,TLN1,TSPAN2,TSPAN3,VASP
Remodeling of Epithelial Adherens Junctions	15.9	0.368	2.121	ACTA2,ACTB,ACTC1,ACTG1,ACTG2,ACTN1,ACTN4,ACTR3,APC,ARPC1B,ARPC2,ARPC3,ARPC4,ARPC5,ARPC5L,CTNNA1,CTNNA2,DNM1,NME1,TUBA1A,TUBA1C,TUBA4A,TUBB2A,TUBB2B,TUBB6
Regulation of eIF4 and p70S6K Signaling	15.9	0.236	1.667	EIF1,EIF1AY,EIF2S2,EIF3D,EIF3I,EIF3J,EIF4A1,EIF4EBP1,IRS1,ITGA3,ITGA4,ITGB1,PIK3R1,PPP2CB,PPP2R2B,RPS11,RPS12,RPS13,RPS14,RPS15,RPS16,RPS18,RPS19,RPS2,RPS23,RPS24,RPS27,RPS27A,RPS27L,RPS3,RPS3A,RPS4Y1,RPS5,RPS6,RPS9,RPSA,RRAS
Coronavirus Pathogenesis Pathway	14.9	0.233	-3.773	ATF4,BAX,CCL2,CCND1,EEF1A1,EEF1A2,FOS,JUN,MAPK10,NPM1,PA2G4,RPS11,RPS12,RPS13,RPS14,RPS15,RPS16,RPS18,RPS19,RPS2,RPS23,RPS24,RPS27,RPS27A,RPS27L,RPS3,RPS3A,RPS4Y1,RPS5,RPS6,RPS9,RPSA,SERPINE1,STAT3,TGFB1
Hepatic Fibrosis / Hepatic Stellate Cell Activation	14.9	0.21		A2M,ACTA2,BAX,CCL2,CERT1,COL10A1,COL11A1,COL12A1,COL13A1,COL18A1,COL1A1,COL1A2,COL26A1,COL27A1,COL3A1,COL4A1,COL4A2,COL4A5,COL5A1,COL6A1,COL8A1,CSF1,EDN1,EDNRB,FGFR1,FN1,IGF1R,IGFBP3,IGFBP5,KLF6,LEPR,MYH9,MYL6,MYL9,PDGFC,SERPINE1,TGFB1,TIMP2,TNFRSF11B
Epithelial Adherens Junction Signaling	14.7	0.23		ACTA2,ACTB,ACTC1,ACTG1,ACTG2,ACTN1,ACTN4,ACTR3,AFDN,APC,ARPC1B,ARPC2,ARPC3,ARPC4,ARPC5,ARPC5L,CTNNA1,CTNNA2,EPN2,FGFR1,MAGI2,MYH9,MYL6,MYL9,NOTCH1,RAC1,RRAS,SORBS1,TCF7L2,TUBA1A,TUBA1C,TUBA4A,TUBB2A,TUBB2B,TUBB6

ILK Signaling	14.5	0.205	2.197	ACTA2,ACTB,ACTC1,ACTG1,ACTG2,ACTN1,ACTN4,ATF4,CCND1,CFL1,CREB3,FBLIM1,FN1,FNBP1,FOS,ILK,IRS1,IRS2,ITGB1,ITGB4,ITGB8,JUN,LIMS1,MAPK10,MYH9,MYL6,MYL9,NACA,PDGFC,PIK3R1,PPP1R14B,PPP2CB,PPP2R2B,RAC1,RHOC,RND2,TGFB1I1,TMSB10/TMSB4X,VIM
Regulation of Actin-based Motility by Rho	14	0.287	3.4	ACTA2,ACTB,ACTC1,ACTG2,ACTR3,ARPC1B,ARPC2,ARPC3,ARPC4,ARPC5,ARPC5L,CFL1,FNBP1,GSN,ITGA3,ITGA4,ITGB1,MYL12A,MYL12B,MYL6,MYL9,PFN1,PFN2,PPP1CB,RAC1,RHOC,RND2
Actin Cytoskeleton Signaling	13.2	0.183	3.683	ACTA2,ACTB,ACTC1,ACTG1,ACTG2,ACTN1,ACTN4,ACTR3,APC,APC2,ARPC1B,ARPC2,ARPC3,ARPC4,ARPC5,ARPC5L,CFL1,EZR,FN1,GNG12,GSN,IQGAP2,ITGA3,ITGA4,ITGB1,MYH9,MYL12A,MYL12B,MYL6,MYL9,PDGFC,PFN1,PFN2,PIK3R1,PPP1CB,RAC1,RDX,RRAS,TLN1,TMSB10/TMSB4X
Germ Cell-Sertoli Cell Junction Signaling	12.3	0.199		A2M,ACTA2,ACTB,ACTC1,ACTG1,ACTG2,ACTN1,ACTN4,AFDN,CFL1,CTNNA1,CTNNA2,EPN2,FNBP1,GSN,ILK,ITGA3,ITGA6,ITGB1,MAP3K13,MAPK10,PIK3R1,RAC1,RHOC,RND2,RRAS,SORBS1,TGFB1,TUBA1A,TUBA1C,TUBA4A,TUBB2A,TUBB2B,TUBB6
Sertoli Cell-Sertoli Cell Junction Signaling	12	0.189		A2M,ACTA2,ACTB,ACTC1,ACTG1,ACTG2,ACTN1,ACTN4,AFDN,CLDN10,CLDN5,CTNNA1,CTNNA2,DLG1,EPN2,ILK,ITGA3,ITGA4,ITGB1,JAM2,JUN,MAGI2,MAP3K13,MAPK10,RAC1,RRAS,SORBS1,SPTAN1,SPTBN1,TUBA1A,TUBA1C,TUBA4A,TUBB2A,TUBB2B,TUBB6
Axonal Guidance Signaling	11.9	0.126		ACTR3,ADAM19,ADAM9,ARPC1B,ARPC2,ARPC3,ARPC4,ARPC5,ARPC5L,BMP1,BMP7,CFL1,DPYSL2,DPYSL5,EPHA2,EPHA4,FYN,FZD2,FZD3,GNG12,ITGA3,ITGA4,ITGB1,ITSN1,L1CAM,LRRC4C,MMP15,MMP17,MYL12A,MYL12B,MYL6,MYL9,NRP1,NRP2,NTN1,NTRK2,NTRK3,PAPPA,PDGFC,PFN1,PFN2,PIK3R1,PLCB1,PLCE1,PLXND1,RAC1,RGS3,RRAS,SEMA6A,SEMA6D,SLIT1,SLIT2,SRGAP1,SRGAP3,TUBA1A,TUBA1C,TUBA4A,TUBB2A,TUBB2B,TUBB6,VASP
RhoA Signaling	11.8	0.228	4.041	ACTA2,ACTB,ACTC1,ACTG1,ACTG2,ACTR3,ARHGAP5,ARPC1B,ARPC2,ARPC3,ARPC4,ARPC5,ARPC5L,CDC42EP1,CDC42EP3,CFL1,EZR,IGF1R,MYL12A,MYL12B,MYL6,MYL9,NRP2,PFN1,PFN2,PPP1CB,RDX,SEPTIN11
mTOR Signaling	11.7	0.176	0.577	EIF3D,EIF3I,EIF3J,EIF4A1,EIF4EBP1,FNBP1,IRS1,PDGFC,PIK3R1,PLD3,PPP2CB,PPP2R2B,RAC1,RHOC,RND2,RPS11,RPS12,RPS13,RPS14,RPS15,RPS16,RPS18,RPS19,RPS2,RPS23,RPS24,RPS27,RPS27A,RPS27L,RPS3,RPS3A,RPS4Y1,RPS5,RPS6,RPS9,RPSA,RRAS
Signaling by Rho Family GTPases	10.9	0.16	2.137	ACTA2,ACTB,ACTC1,ACTG1,ACTG2,ACTR3,ARPC1B,ARPC2,ARPC3,ARPC4,ARPC5,ARPC5L,CDC42EP1,CDC42EP3,CDH13,CDH6,CFL1,EZR,FNBP1,FOS,GFAP,GNG12,ITGA3,ITGA4,ITGB1,JUN,MAPK10,MYL12A,MYL12B,MYL6,MYL9,PIK3R1,RAC1,RDX,RHOC,RND2,SEPTIN11,STMN1,VIM
Virus Entry via Endocytic Pathways	10.9	0.234		ACTA2,ACTB,ACTC1,ACTG1,ACTG2,AP1S2,AP2M1,AP2S1,B2M,CAV1,CLTA,DNM1,FYN,HLA-B,HLA-E,ITGA3,ITGA4,ITGA6,ITGB1,ITGB4,ITGB8,ITSN1,PIK3R1,RAC1,RRAS

Cdc42 Signaling	10.5	0.186	2.132	ACTR3,APC,APC2,ARPC1B,ARPC2,ARPC3,ARPC4,ARPC5,ARPC5L,B2M,CFL1,FOS,HLA-B,HLA-DMA,HLA-DPA1,HLA-DPB1,HLA-DRA,HLA-DRB1,HLA-DRB5,HLA-E,IQGAP2,ITGA3,ITGA4,ITGB1,JUN,MAPK10,MYL12A,MYL12B,MYL6,MYL9,PPP1CB
RhoGDI Signaling	9.64	0.172	-2.191	ACTA2,ACTB,ACTC1,ACTG1,ACTG2,ACTR3,ARHGAP5,ARPC1B,ARPC2,ARPC3,ARPC4,ARPC5,ARPC5L,CD44,CDH13,CDH6,CFL1,EZR,FNBP1,GNG12,ITGA3,ITGA4,ITGB1,MYL12A,MYL12B,MYL6,MYL9,RAC1,RDX,RHOC,RND2
Caveolar-mediated Endocytosis Signaling	9.27	0.26		ACTA2,ACTB,ACTC1,ACTG1,ACTG2,B2M,CAV1,CAVIN1,FYN,HLA-B,HLA-E,ITGA3,ITGA4,ITGA6,ITGA7,ITGB1,ITGB4,ITGB8,ITSN1
GP6 Signaling Pathway	9.04	0.202	-0.816	CERT1,COL10A1,COL11A1,COL12A1,COL13A1,COL18A1,COL1A1,COL1A2,COL26A1,COL27A1,COL3A1,COL4A1,COL4A2,COL4A5,COL5A1,COL6A1,COL8A1,FYN,LAMA2,LAMB1,LAMB2,PIK3R1,RAC1,TLN1
Synaptogenesis Signaling Pathway	8.25	0.128	-0.48	ACTR3,ADCY2,AFDN,AP2M1,AP2S1,APOE,ARPC1B,ARPC2,ARPC3,ARPC4,ARPC5,ARPC5L,ATF4,CDH13,CDH6,CFL1,CREB3,EIF4EBP1,EPHA2,EPHA4,FYN,GPAA1,GRIA1,GRIA4,GRIN2A,GRIN2B,ITSN1,LRP1,MAP1B,MARCKS,NAP1L1,NLGN4X,NTRK2,PIK3R1,RAC1,RRAS,SYT1,SYT11,THBS1,TLN1
Leukocyte Extravasation Signaling	8.05	0.152	0.784	ACTA2,ACTB,ACTC1,ACTG1,ACTG2,ACTN1,ACTN4,AFDN,ARHGAP5,CD44,CD99,CLDN10,CLDN5,CTNNA1,CTNNA2,EZR,ITGA3,ITGA4,ITGA6,ITGB1,JAM2,MAPK10,MMP15,MMP17,MYL6,PIK3R1,RAC1,RDX,TIMP2,VASP
Antigen Presentation Pathway	7.97	0.333		B2M,CANX,CD74,HLA-B,HLA-DMA,HLA-DPA1,HLA-DPB1,HLA-DRA,HLA-DRB1,HLA-DRB5,HLA-E,PSMB5,PSMB6
Reelin Signaling in Neurons	7.62	0.178	0	ACTR3,AFDN,APOE,APP,ARPC1B,ARPC2,ARPC3,ARPC4,ARPC5,ARPC5L,CFL1,CNR1,FYN,GRIN2A,GRIN2B,ITGA3,ITGA4,ITGA6,ITGB1,MAP1B,MAPK10,PIK3R1,RAC1
Sirtuin Signaling Pathway	7.59	0.127	-0.816	ABCA1,APP,BAX,DUSP6,GADD45A,GADD45B,H1-0,IDH2,JUN,LDHB,MAP1LC3B,MT-ATP6,MT-CYB,MT-ND1,MT-ND2,MT-ND3,MT-ND4,MT-ND5,MT-ND6,NDUFS6,PGAM1,PGK1,SLC25A5,SLC25A6,SLC2A1,STAT3,TIMM13,TIMM17A,TOMM40,TSPO,TUBA1A,TUBA1C,TUBA4A,VDAC1,VDAC2,XRCC5,ZIC2
Semaphorin Neuronal Repulsive Signaling Pathway	7.55	0.177	-0.209	CD44,CFL1,DPYSL2,DPYSL5,FYN,ITGA3,ITGA4,ITGB1,MYL12A,MYL12B,MYL6,MYL9,NRP1,NRP2,PDE4B,PIK3R1,PLXND1,PPP1CB,RAC1,RRAS,SEMA6A,SEMA6D,VCAN
Fcγ Receptor-mediated Phagocytosis in Macrophages and Monocytes	7.31	0.202	2.524	ACTA2,ACTB,ACTC1,ACTG1,ACTG2,ACTR3,ARPC1B,ARPC2,ARPC3,ARPC4,ARPC5,ARPC5L,EZR,FYN,PIK3R1,PLD3,RAC1,TLN1,VASP
Agrin Interactions at Neuromuscular Junction	7.11	0.218	1.069	ACTA2,ACTB,ACTC1,ACTG1,ACTG2,DAG1,ERBB4,ITGA3,ITGA4,ITGA6,ITGB1,JUN,LAMA2,LAMB1,MAPK10,RAC1,RRAS

Paxillin Signaling	6.99	0.185	2.5	ACTA2,ACTB,ACTC1,ACTG1,ACTG2,ACTN1,ACTN4,ARF1,ITGA3,ITGA4,ITGA6,ITGA7,ITGB1,ITGB4,ITGB8,MAPK10,PIK3R1,RAC1,RRAS,TLN1
Actin Nucleation by ARP-WASP Complex	6.86	0.222	3	ACTR3,ARPC1B,ARPC2,ARPC3,ARPC4,ARPC5,ARPC5L,FNBP1,ITGA3,ITGA4,ITGB1,RAC1,RHOC,RND2,RRAS,VASP
Hepatic Fibrosis Signaling Pathway	6.71	0.111	0.16	ACTA2,ATF4,CACNA1C,CCDC88A,CCL2,CCND1,CNR1,COL10A1,COL18A1,COL1A1,COL1A2,COL3A1,CREB3,EDN1,FGFR1,FNBP1,FOS,FZD2,FZD3,IRS2,ITGA3,ITGA4,ITGB1,JUN,LEPR,MAPK10,MYL12A,MYL12B,MYL6,MYL9,PDGFC,PIK3R1,RAC1,RHOC,RND2,RRAS,SERPINE1,STAT3,TCF7L2,TGFB1,TNFRSF11B
Ephrin Receptor Signaling	6.6	0.144	1.46	ACTR3,ARPC1B,ARPC2,ARPC3,ARPC4,ARPC5,ARPC5L,ATF4,CFL1,CREB3,EPHA2,EPHA4,FYN,GNG12,GRIN2A,GRIN2B,ITGA3,ITGA4,ITGB1,ITSN1,PDGFC,RAC1,RGS3,RRAS,SORBS1,STAT3
Clathrin-mediated Endocytosis Signaling	6.54	0.14		ACTA2,ACTB,ACTC1,ACTG1,ACTG2,ACTR3,AP1S2,AP2M1,AP2S1,APOE,ARPC1B,ARPC2,ARPC3,ARPC4,ARPC5,ARPC5L,CLTA,CLU,DNM1,ITGB1,ITGB4,ITGB8,PDGFC,PIK3R1,RAC1,RPS27A,UBA52
Wnt/β-catenin Signaling	6.37	0.145	1.091	APC,APC2,CCND1,CD44,FRZB,FZD2,FZD3,ILK,JUN,LRP1,PPP2CB,PPP2R2B,RPS27A,SFRP1,SFRP2,SOX1,SOX2,SOX21,SOX4,SOX6,SOX9,TCF7L2,TGFB1,TLE1,UBA52
Tight Junction Signaling	6.05	0.143		ACTA2,ACTB,ACTC1,ACTG1,ACTG2,AFDN,CLDN10,CLDN5,CTNNA1,FOS,GPAA1,JAM2,JUN,MAGI2,MYH9,MYL6,MYL9,PPP2CB,PPP2R2B,RAC1,SPTAN1,TGFB1,TNFRSF11B,VASP
Cellular Effects of Sildenafil (Viagra)	5.02	0.145		ACTA2,ACTB,ACTC1,ACTG1,ACTG2,ADCY2,CACNA1C,CACNG4,MYH9,MYL12A,MYL12B,MYL6,MYL9,PABPC4,PDE1A,PDE4B,PLCB1,PLCE1,PPP1CB
CD28 Signaling in T Helper Cells	5	0.15	0.832	ACTR3,ARPC1B,ARPC2,ARPC3,ARPC4,ARPC5,ARPC5L,FOS,FYN,HLA-B,HLA-DMA,HLA-DRA,HLA-DRB1,HLA-DRB5,JUN,MAPK10,PIK3R1,RAC1
Oxidative Phosphorylation	4.98	0.156	3.638	ATP5MC2,COX5A,COX6A1,CYCS,MT-ATP6,MT-CO1,MT-CO2,MT-CO3,MT-CYB,MT-ND1,MT-ND2,MT-ND3,MT-ND4,MT-ND5,NDUFS6,UQCRC1,UQCRH
Protein Ubiquitination Pathway	4.97	0.11		B2M,CDC20,HLA-B,HLA-E,HSP90AB1,HSP90B1,HSPB1,PSMA4,PSMA5,PSMA7,PSMB1,PSMB2,PSMB3,PSMB5,PSMB6,PSMC4,PSMC5,PSMD2,PSMD7,PSMD8,PSME2,RBX1,RPS27A,SMURF2,UBA1,UBA52,UBE2C,UBE2I,UBE2S,USP11
Mitochondrial Dysfunction	4.85	0.129		APP,ATP5MC2,COX5A,COX6A1,CYCS,MAPK10,MT-ATP6,MT-CO1,MT-CO2,MT-CO3,MT-CYB,MT-ND1,MT-ND2,MT-ND3,MT-ND4,MT-ND5,MT-ND6,NDUFS6,UQCRC1,UQCRH,VDAC1,VDAC2
Rac Signaling	4.82	0.152	2.183	ACTR3,ARPC1B,ARPC2,ARPC3,ARPC4,ARPC5,ARPC5L,CD44,CFL1,IQGAP2,ITGA3,ITGA4,ITGB1,JUN,PIK3R1,RAC1,RRAS
Apelin Liver Signaling Pathway	4.82	0.308	0	COL10A1,COL18A1,COL1A1,COL1A2,COL3A1,EDN1,IRS1,MAPK10
Osteoarthritis Pathway	4.8	0.118	1.147	ANXA2,ATF4,COL10A1,CREB3,CTNNA1,CTNNA2,FGFR1,FN1,FRZB,FZD2,FZD3,HES1,HMGB1,HTRA1,ITGA3,ITGA4,ITGB1,LRP1,NOTCH1,PDGFC,RAC1,S1PR3,SOX9,TCF7L2,TGFB1

Atherosclerosis Signaling	4.65	0.142		APOE,CCL2,CLU,COL10A1,COL18A1,COL1A1,COL1A2,COL3A1,CSF1,F3,GLG1,ITGA4,LPL,PDGFC,PLAAT3,PLAAT4,TGFB1,TNFRSF12A
Agranulocyte Adhesion and Diapedesis	4.5	0.119		ACTA2,ACTB,ACTC1,ACTG1,ACTG2,CCL2,CD99,CLDN10,CLDN5,EZR,FN1,GLG1,ITGA3,ITGA4,ITGA6,ITGB1,MMP15,MMP17,MYH9,MYL6,MYL9,PODXL,RDX
Phagosome Maturation	4.15	0.126		B2M,CANX,CTSC,DYNC2H1,GPAA1,HLA-B,HLA-DRA,HLA-DRB1,HLA-DRB5,HLA-E,LAMP1,LAMP2,PRDX1,TUBA1A,TUBA1C,TUBA4A,TUBB2A,TUBB2B,TUBB6
FAK Signaling	3.94	0.147		ACTA2,ACTB,ACTC1,ACTG1,ACTG2,CAPNS1,FYN,ITGA3,ITGA4,ITGB1,PIK3R1,RAC1,RRAS,TLN1
Dendritic Cell Maturation	3.93	0.115	-1.342	ATF4,B2M,COL10A1,COL18A1,COL1A1,COL1A2,COL3A1,CREB3,HLA-B,HLA-DMA,HLA-DRA,HLA-DRB1,HLA-DRB5,HLA-E,IL32,LEPR,MAPK10,PIK3R1,PLCB1,PLCE1,TNFRSF11B
Inhibition of Angiogenesis by TSP1	3.9	0.235	-0.816	CD47,FYN,HSPG2,JUN,MAPK10,SDC1,TGFB1,THBS1
Glycolysis I	3.87	0.269	2.646	ENO1,GAPDH,PFKP,PGAM1,PGK1,PKM,TPI1
Amyotrophic Lateral Sclerosis Signaling	3.84	0.144	0	BAX,CACNA1C,CAPNS1,CYCS,GRIA1,GRIA4,GRID2,GRIN2A,GRIN2B,NEFL,PDGFC,PIK3R1,RAC1,SLC1A2
p53 Signaling	3.79	0.143	1.265	BAX,BIRC5,CCND1,CCND2,GADD45A,GADD45B,HIPK2,JUN,MDM4,PIK3R1,PMAIP1,SERPINE2,THBS1,TP53I3
Regulation of Cellular Mechanics by Calpain Protease	3.75	0.169	1.134	ACTN1,ACTN4,CAPNS1,CAST,CCND1,EZR,ITGA3,ITGA4,ITGB1,RRAS,TLN1
GDNF Family Ligand-Receptor Interactions	3.74	0.158	-1.508	DOK5,FOS,GFRA1,GFRA2,IRS1,IRS2,JUN,MAPK10,PDLIM7,PIK3R1,RAC1,RRAS
Role of Osteoblasts, Osteoclasts and Chondrocytes in Rheumatoid Arthritis	3.63	0.105		APC,APC2,BMP1,BMP7,COL1A1,CSF1,FOS,FRZB,FZD2,FZD3,GSN,IL11,ITGA3,ITGB1,JUN,LRP1,MAPK10,PIK3R1,SFRP1,SFRP2,TCF7L2,TGFB1,TNFRSF11B
14-3-3-mediated Signaling	3.59	0.126	-1.414	BAX,FOS,GFAP,JUN,MAPK10,PIK3R1,PLCB1,PLCE1,RRAS,TUBA1A,TUBA1C,TUBA4A,TUBB2A,TUBB2B,TUBB6,VIM
Mouse Embryonic Stem Cell Pluripotency	3.56	0.136	-0.535	APC,FZD2,FZD3,ID1,ID2,ID3,ID4,LIF,LIFR,PIK3R1,RRAS,SOX2,STAT3,TCF7L2
Role of Macrophages, Fibroblasts and Endothelial Cells in Rheumatoid Arthritis	3.52	0.0929		APC,APC2,ATF4,CCL2,CCND1,CEBPD,CREB3,CSF1,FN1,FOS,FRZB,FZD2,FZD3,IL32,JUN,LRP1,PDGFC,PIK3R1,PLCB1,PLCE1,RAC1,RRAS,SFRP1,SFRP2,SOCS3,STAT3,TCF7L2,TGFB1,TNFRSF11B
Estrogen Receptor Signaling	3.51	0.0915	-0.577	ADCY2,ATF4,CACNA1C,CAV1,CCND1,CFL1,CREB3,EIF4EBP1,FOS,HES1,HSP90AB1,HSP90B1,IGF1R,JUN,LEPR,MMP15,MMP17,MT-ATP6,MT-

				CYB,MYL12A,MYL12B,MYL6,MYL9,NOTCH1,PDGFC,PIK3R1,PLCB1,PLCE1,PPP1CB,RRAS
Semaphorin Signaling in Neurons	3.41	0.167		CFL1,DPYSL2,DPYSL5,FNBP1,FYN,ITGB1,NRP1,RAC1,RHOC,RND2
CDK5 Signaling	3.34	0.13	-0.905	ADCY2,EGR1,ITGA3,ITGA6,ITGB1,LAMB1,MAPK10,NTRK2,PPP1CA,PPP1CB,PPP1R14B,PPP2CB,PPP2R2B,RRAS
PAK Signaling	3.28	0.134	2.309	CFL1,ITGA3,ITGA4,ITGB1,MAPK10,MYL12A,MYL12B,MYL6,MYL9,PDGFC,PIK3R1,RAC1,RRAS
HIF1α Signaling	3.25	0.102	0.894	EDN1,EIF4EBP1,JUN,LDHB,MMP15,MMP17,P4HTM,PDGFC,PIK3R1,PKM,RACK1,RAN,RBX1,RPS6,RRAS,SAT1,SERPINE1,SLC2A1,STAT3,TGFB1,VIM
Tec Kinase Signaling	3.22	0.11	0	ACTA2,ACTB,ACTC1,ACTG1,ACTG2,FNBP1,FOS,FYN,GNG12,ITGA3,ITGA4,ITGB1,MAPK10,PIK3R1,RAC1,RHOC,RND2,STAT3
VEGF Signaling	3.2	0.131	1.897	ACTA2,ACTB,ACTC1,ACTG1,ACTG2,ACTN1,ACTN4,EIF1,EIF1AY,EIF2S2,PDGFC,PIK3R1,RRAS
ERK/MAPK Signaling	3.19	0.104	1.342	ATF4,CREB3,DUSP6,EIF4EBP1,FOS,FYN,HSPB1,ITGA3,ITGA4,ITGB1,PIK3R1,PPP1CA,PPP1CB,PPP1R14B,PPP2CB,PPP2R2B,RAC1,RRAS,STAT3,TLN1
Molecular Mechanisms of Cancer	3.17	0.0844		ADCY2,APC,BAX,BMP1,BMP7,CCND1,CCND2,CTNNA1,CTNNA2,CYCS,FNBP1,FOS,FYN,FZD2,FZD3,HIPK2,IRS1,ITGA3,ITGA4,ITGB1,JUN,LRP1,MAPK10,NOTCH1,PA2G4,PIK3R1,PLCB1,PMAIP1,RAC1,RHOC,RND2,RRAS,TGFB1
Colorectal Cancer Metastasis Signaling	3.14	0.0949	-1.091	ADCY2,APC,BAX,BIRC5,CCND1,FNBP1,FOS,FZD2,FZD3,GNG12,JUN,LRP1,MAPK10,MMP15,MMP17,PDGFC,PIK3R1,RAC1,RHOC,RND2,RRAS,STAT3,TCF7L2,TGFB1
Mitotic Roles of Polo-Like Kinase	3.07	0.152	0.447	CCNB1,CDC20,HSP90AB1,HSP90B1,PLK2,PPP2CB,PPP2R2B,PTTG1,STAG2,TGFB1
Insulin Secretion Signaling Pathway	3.03	0.0947	0.426	ADCY2,ATF4,CACNA1C,CPE,CREB3,EIF1,EIF2S2,EIF4A1,EIF4EBP1,FYN,GPAA1,PDHB,PIK3R1,PLCB1,PLCE1,SEC61B,SEC61G,SLC2A1,SRP14,SRP9,SSR2,SSR3,STAT3
Aryl Hydrocarbon Receptor Signaling	3.02	0.112	-1.155	ALDH6A1,BAX,CCND1,CCND2,FOS,GSTO1,GSTP1,HSP90AB1,HSP90B1,HSPB1,JUN,MCM7,NFIA,NFIX,NR2F1,TGFB1
BEX2 Signaling Pathway	3	0.139	0.905	BEX1,CCND1,JUN,LGALS1,MAP2,MAPK10,PDGFC,PPP2CB,PPP2R2B,STAT3,TCF7L2
IGF-1 Signaling	3	0.125	-1	FOS,IGF1R,IGFBP2,IGFBP3,IGFBP5,IGFBP7,IRS1,IRS2,JUN,PIK3R1,RRAS,SOCS3,STAT3
Role of Tissue Factor in Cancer	2.99	0.12		CFL1,CSF1,EGR1,F3,FYN,ITGA3,ITGA6,ITGB1,P4HB,PIK3R1,PLAUR,PLCB1,RAC1,RRAS
Glutamate Receptor Signaling	2.95	0.158	-2.236	GRIA1,GRIA4,GRID2,GRIN2A,GRIN2B,SLC1A2,SLC1A3,SLC1A4,SLC38A1
GADD45 Signaling	2.85	0.263		CCNB1,CCND1,CCND2,GADD45A,GADD45B

Human Embryonic Stem Cell Pluripotency	2.83	0.111		APC,BMP1,BMP7,FGFR1,FZD2,FZD3,INHBA,NTRK2,NTRK3,PDGFC,PIK3R1,S1PR3,SOX2,TCF7L2,TGFB1
PCP pathway	2.78	0.15	-0.707	CELSR1,FZD2,FZD3,JUN,MAPK10,PFN1,PFN2,PRICKLE1,RAC1
Cardiac Hypertrophy Signaling	2.74	0.0917	-0.447	ADCY2,CACNA1C,FNBP1,GNG12,HSPB1,IGF1R,IRS1,JUN,MAP3K13,MAPK10,MYL12A,MYL12B,MYL6,MYL9,PIK3R1,PLCB1,PLCE1,RAC1,RHOC,RND2,RRAS,TGFB1
Systemic Lupus Erythematosus In T Cell Signaling Pathway	2.74	0.0838	-2.646	ATF4,B2M,CD44,CREB3,EZR,FNBP1,FOS,GADD45A,HLA-B,HLA-DMA,HLA-DPA1,HLA-DPB1,HLA-DRA,HLA-DRB1,HLA-DRB5,HLA-E,JUN,LEPR,PIK3R1,PPP2CB,PPP2R2B,RAC1,RDX,RHOC,RND2,RRAS,S1PR3,STAT3
Inhibition of Matrix Metalloproteases	2.73	0.179	0	A2M,HSPG2,LRP1,MMP15,MMP17,SDC1,TIMP2
CXCR4 Signaling	2.71	0.102	0.258	ADCY2,EGR1,FNBP1,FOS,GNG12,JUN,MAPK10,MYL12A,MYL12B,MYL6,MYL9,PIK3R1,PLCB1,RAC1,RHOC,RND2,RRAS
Phospholipase C Signaling	2.7	0.0895	1.342	ADCY2,AHNAK,ATF4,CREB3,FNBP1,FYN,GNG12,ITGA3,ITGA4,ITGB1,MARCKS,MYL12A,MYL12B,MYL6,MYL9,PLCB1,PLCE1,PLD3,PPP1CB,RAC1,RHOC,RND2,RRAS
PTEN Signaling	2.68	0.111	-0.832	CCND1,FGFR1,IGF1R,ILK,ITGA3,ITGA4,ITGB1,MAGI2,NTRK2,NTRK3,PIK3R1,PREX2,RAC1,RRAS
Glioma Invasiveness Signaling	2.68	0.135	0.333	CD44,FNBP1,PIK3R1,PLAU,PLAUR,RAC1,RHOC,RND2,RRAS,TIMP2
Hypoxia Signaling in the Cardiovascular System	2.68	0.135		ATF4,CREB3,EDN1,HSP90AB1,HSP90B1,JUN,P4HB,UBE2C,UBE2I,UBE2S
β-alanine Degradation I	2.67	1		ABAT,ALDH6A1
Gap Junction Signaling	2.67	0.096		ACTA2,ACTB,ACTC1,ACTG1,ACTG2,ADCY2,CAV1,GRIA1,GRIA4,PIK3R1,PLCB1,PLCE1,RRAS,TUBA1A,TUBA1C,TUBA4A,TUBB2A,TUBB2B,TUBB6
IL-8 Signaling	2.62	0.095	-0.243	BAX,CCND1,CCND2,EIF4EBP1,FNBP1,FOS,GNG12,JUN,MAPK10,MYL12B,MYL9,PDGFC,PIK3R1,PLD3,RAC1,RHOC,RND2,RRAS,VASP
Neurotrophin/TRK Signaling	2.59	0.132	0.707	ATF4,CREB3,FOS,JUN,NTRK2,NTRK3,PIK3R1,RRAS,SPRY1,SPRY2
Macropinocytosis Signaling	2.59	0.132	0.447	ACTN4,CSF1,ITGB1,ITGB4,ITGB8,PDGFC,PIK3R1,RAB34,RAC1,RRAS
CTLA4 Signaling in Cytotoxic T Lymphocytes	2.58	0.124		AP1S2,AP2M1,AP2S1,B2M,CLTA,FYN,HLA-B,HLA-E,PIK3R1,PPP2CB,PPP2R2B
Crosstalk between Dendritic Cells and Natural Killer Cells	2.58	0.124	-1	ACTA2,ACTB,ACTC1,ACTG1,ACTG2,HLA-B,HLA-DRA,HLA-DRB1,HLA-DRB5,HLA-E,TLN1
OX40 Signaling Pathway	2.54	0.122		B2M,HLA-B,HLA-DMA,HLA-DPA1,HLA-DPB1,HLA-DRA,HLA-DRB1,HLA-DRB5,HLA-E,JUN,MAPK10

T Cell Exhaustion Signaling Pathway	2.5	0.0971	0	FOS,HLA-B,HLA-DMA,HLA-DPA1,HLA-DPB1,HLA-DRA,HLA-DRB1,HLA-DRB5,HLA-E,JUN,MAPK10,PIK3R1,PPP2CB,PPP2R2B,RRAS,STAT3,TGFB1
Thyroid Cancer Signaling	2.47	0.127	-1.897	CCND1,FOS,IRS1,IRS2,JUN,NTRK2,NTRK3,PIK3R1,RRAS,TCF7L2
Huntington's Disease Signaling	2.47	0.0886	-0.577	ATF4,BAX,CAPNS1,CLTA,CREB3,CYCS,DNM1,GNG12,GPAA1,GRIN2B,HAP1,IFT57,IGF1R,JUN,PIK3R1,PLCB1,POLR2L,PSME2,RPS27A,UBA52,UBE2S
PD-1, PD-L1 cancer immunotherapy pathway	2.44	0.113	1.667	B2M,HLA-B,HLA-DMA,HLA-DPA1,HLA-DPB1,HLA-DRA,HLA-DRB1,HLA-DRB5,HLA-E,PIK3R1,TGFB1,TNFRSF11B
Renal Cell Carcinoma Signaling	2.43	0.125	-0.447	FOS,JUN,PIK3R1,RAC1,RBX1,RPS27A,RRAS,SLC2A1,TGFB1,UBA52
HMGB1 Signaling	2.38	0.097	0.258	CCL2,FNBP1,FOS,HMGB1,IL11,JUN,LIF,MAPK10,PIK3R1,RAC1,RHOC,RND2,RRAS,SERPINE1,TGFB1,TNFRSF11B
Coagulation System	2.31	0.171	0.816	A2M,F3,PLAU,PLAUR,SERPINE1,TFPI
MSP-RON Signaling Pathway	2.3	0.138		ACTA2,ACTB,ACTC1,ACTG1,ACTG2,CCL2,CSF1,PIK3R1
ATM Signaling	2.29	0.113	-1	ATF4,CCNB1,CREB3,GADD45A,GADD45B,JUN,MAPK10,MDM4,PPP2CB,PPP2R2B,ZEB1
HGF Signaling	2.28	0.108	0	CCND1,FOS,ITGA3,ITGA4,ITGB1,JUN,MAP3K13,MAPK10,PIK3R1,RAC1,RRAS,STAT3
Interferon Signaling	2.24	0.167	-1.633	BAX,IFI6,IFIT1,IFITM1,IFITM2,IFITM3
Lipid Antigen Presentation by CD1	2.21	0.192		AP2M1,AP2S1,B2M,CANX,PSAP
Neuroinflammation Signaling Pathway	2.19	0.0803	-1.528	APP,ATF4,B2M,BIRC5,CCL2,CREB3,FOS,GRIA1,GRIN2A,GRIN2B,HLA-B,HLA-DMA,HLA-DRA,HLA-DRB1,HLA-DRB5,HLA-E,HMGB1,JUN,MAPK10,PIK3R1,S100B,SLC1A2,SLC1A3,TGFB1
Production of Nitric Oxide and Reactive Oxygen Species in Macrophages	2.19	0.0904	-1.213	APOE,CLU,FNBP1,FOS,JUN,MAP3K13,MAPK10,PIK3R1,PPP1CA,PPP1CB,PPP1R14B,PPP2CB,PPP2R2B,RAC1,RHOC,RND2,TNFRSF11B
Regulation Of The Epithelial Mesenchymal Transition By Growth Factors Pathway	2.19	0.0904	-0.728	EGR1,FGFR1,FOS,ID2,JUN,MAPK10,MEST,PDGFC,PIK3R1,RAC1,RRAS,STAT3,TGFB1,TNFRSF11B,TWIST1,VIM,ZEB1
Synaptic Long Term Potentiation	2.17	0.101	-1.155	ATF4,CACNA1C,CREB3,GRIA1,GRIA4,GRIN2A,GRIN2B,PLCB1,PLCE1,PPP1CA,PPP1CB,PPP1R14B,RRAS
Calcium Signaling	2.13	0.0874	-1.667	ACTA2,ACTC1,ATF4,ATP2B1,CACNA1C,CACNG4,CREB3,GRIA1,GRIA4,GRIN2A,GRIN2B,MYH9,MYL6,MYL9,TPM1,TPM2,TPM3,TPM4
fMLP Signaling in Neutrophils	2.13	0.103	2.111	ACTR3,ARPC1B,ARPC2,ARPC3,ARPC4,ARPC5,ARPC5L,GNG12,PIK3R1,PLCB1,RAC1,RRAS
RAR Activation	2.06	0.0876		ACTB,ADCY2,FOS,IGFBP3,JUN,MAPK10,NR2F1,NR2F2,NR2F6,PIK3R1,PRMT1,PRMT2,PSMC5,RAC1,RBP1,RPL7A,TGFB1

Prostate Cancer Signaling	2.03	0.11		ATF4,CCND1,CREB3,GSTP1,HSP90AB1,HSP90B1,PA2G4,PIK3R1,RRAS,SRD5A1
Granulocyte Adhesion and Diapedesis	2.02	0.0889		CCL2,CD99,CLDN10,CLDN5,EZR,GLG1,ITGA3,ITGA4,ITGA6,ITGB1,MMP15,MMP17,RDX,SDC1,SDC3,TNFRSF11B
Glioblastoma Multiforme Signaling	2.01	0.0909	0.258	APC,CCND1,FNBP1,FZD2,FZD3,IGF1R,NF2,PDGFC,PIK3R1,PLCB1,PLCE1,RAC1,RHOC,RND2,RRAS
Factors Promoting Cardiogenesis in Vertebrates	2.01	0.0933	0.277	APC,ATF4,BMP1,BMP7,CCND1,CREB3,FZD2,FZD3,LRP1,MAPK10,PLCB1,PLCE1,TCF7L2,TGFB1
Granzyme A Signaling	2	0.211		H1-0,HMGB2,NME1,SET
Pancreatic Adenocarcinoma Signaling	1.92	0.101	-0.333	BIRC5,CCND1,MAPK10,NOTCH1,PA2G4,PDGFC,PIK3R1,PLD3,RAC1,STAT3,TGFB1
PKCθ Signaling in T Lymphocytes	1.89	0.0903	-1.732	CACNA1C,CACNG4,FOS,FYN,HLA-B,HLA-DMA,HLA-DRA,HLA-DRB1,HLA-DRB5,JUN,MAP3K13,PIK3R1,RAC1,RRAS
Phagosome Formation	1.88	0.096		FN1,FNBP1,ITGA3,ITGA4,ITGB1,MARCKS,PIK3R1,PLCB1,PLCE1,RAC1,RHOC,RND2
Neuregulin Signaling	1.88	0.104	0	ERBB4,ERBIN,HSP90AB1,HSP90B1,ITGA3,ITGA4,ITGB1,PIK3R1,RPS6,RRAS
Type I Diabetes Mellitus Signaling	1.86	0.0991	0	CPE,CYCS,HLA-B,HLA-DMA,HLA-DRA,HLA-DRB1,HLA-DRB5,HLA-E,MAPK10,SOCS3,TNFRSF11B
NRF2-mediated Oxidative Stress Response	1.83	0.0847	1.89	ACTA2,ACTB,ACTC1,ACTG1,ACTG2,ATF4,FOS,GSTO1,GSTP1,HERPUD1,JUN,PIK3R1,PRDX1,RBX1,RRAS,TXN
Sperm Motility	1.8	0.0807	-1.89	AXL,DDR1,EPHA2,EPHA4,ERBB4,FGFR1,FYN,IGF1R,NTRK2,NTRK3,PDE1A,PDE4B,PLAAT3,PLAAT4,PLCB1,PLCE1,PTK7,SLC12A2
Growth Hormone Signaling	1.79	0.113	-1.134	A2M,FOS,IGF1R,IGFBP3,IRS1,PIK3R1,SOCS3,STAT3
IL-4 Signaling	1.78	0.106		HLA-B,HLA-DMA,HLA-DRA,HLA-DRB1,HLA-DRB5,HMGA1,IRS1,PIK3R1,RRAS
HOTAIR Regulatory Pathway	1.78	0.0875	0	CD44,COL1A1,COL1A2,JAM2,MMP15,MMP17,PCDH10,PIK3R1,RHOC,STAT3,TCF7L2,TGFB1,TWIST1,VIM
IL-9 Signaling	1.77	0.152	-1.342	IRS1,IRS2,PIK3R1,SOCS3,STAT3
Polyamine Regulation in Colon Cancer	1.77	0.182		APC,OAZ1,PSME2,SAT1
Allograft Rejection Signaling	1.75	0.105		B2M,HLA-B,HLA-DMA,HLA-DPA1,HLA-DPB1,HLA-DRA,HLA-DRB1,HLA-DRB5,HLA-E
Kinetochore Metaphase Signaling Pathway	1.74	0.099	0.632	BIRC5,CCNB1,CDC20,H2AZ1,PPP1CA,PPP1CB,PPP1R14B,PTTG1,SPDL1,STAG2
T Helper Cell Differentiation	1.72	0.11		HLA-B,HLA-DMA,HLA-DRA,HLA-DRB1,HLA-DRB5,STAT3,TGFB1,TNFRSF11B

Dopamine-DARPP32 Feedback in cAMP Signaling	1.72	0.0859	-1.941	ADCY2,ATF4,CACNA1C,CREB3,GRIN2A,GRIN2B,PAWR,PLCB1,PLCE1,PPP1CA,PPP1CB,PPP1R14B,PPP2CB,PPP2R2B
Acute Phase Response Signaling	1.71	0.0838	-0.302	A2M,C1R,C1S,CP,FN1,FOS,JUN,PIK3R1,RBP1,RRAS,SERPINE1,SERPING1,SOCS3,STAT3,TNFRSF11B
Role of PKR in Interferon Induction and Antiviral Response	1.71	0.094	-0.632	BAX,CYCS,FOS,HMGB1,HSP90AB1,HSP90B1,JUN,MAPK10,NPM1,PDGFC,STAT3
Sphingosine-1-phosphate Signaling	1.71	0.094	-0.632	ADCY2,ASAH1,FNBP1,PDGFC,PIK3R1,PLCB1,PLCE1,RAC1,RHOC,RND2,S1PR3
Endometrial Cancer Signaling	1.69	0.117	1.633	APC2,CCND1,CTNNA1,CTNNA2,ILK,PIK3R1,RRAS
Ceramide Signaling	1.69	0.102	-1	CYCS,FOS,JUN,PIK3R1,PPP2CB,PPP2R2B,RRAS,S1PR3,TNFRSF11B
Ephrin A Signaling	1.69	0.128		CFL1,EPHA2,EPHA4,FYN,PIK3R1,RAC1
Estrogen-Dependent Breast Cancer Signaling	1.68	0.108	0.707	ATF4,CCND1,CREB3,FOS,IGF1R,JUN,PIK3R1,RRAS
Sumoylation Pathway	1.68	0.0971	0	FNBP1,FOS,JUN,MAPK10,RAC1,RAN,RHOC,RND2,UBE2I,ZEB1
Opioid Signaling Pathway	1.68	0.0769	-0.688	ADCY2,AP2M1,AP2S1,ATF4,CACNA1C,CACNG4,CLTA,CREB3,FOS,FYN,GRIN2A,GRIN2B,PDE1A,PLCB1,RAC1,RGS3,RGS5,RGS6,RRAS
Acute Myeloid Leukemia Signaling	1.66	0.101	-0.447	CCND1,EIF4EBP1,IDH1,IDH2,PIK3R1,RRAS,RUNX1,STAT3,TCF7L2
Induction of Apoptosis by HIV1	1.66	0.115	1.134	BAX,CYCS,MAPK10,SLC25A3,SLC25A5,SLC25A6,TNFRSF11B
Role of NANOG in Mammalian Embryonic Stem Cell Pluripotency	1.66	0.0924	-0.816	APC,BMP1,BMP7,FZD2,FZD3,LIF,LIFR,PIK3R1,RRAS,SOX2,STAT3
Graft-versus-Host Disease Signaling	1.65	0.125		HLA-B,HLA-DMA,HLA-DRA,HLA-DRB1,HLA-DRB5,HLA-E
Vitamin-C Transport	1.64	0.167	2	GSTO1,NXN,SLC2A1,TXN
Th2 Pathway	1.62	0.0882	-2	HLA-B,HLA-DMA,HLA-DPA1,HLA-DPB1,HLA-DRA,HLA-DRB1,HLA-DRB5,JUN,NOTCH1,PIK3R1,SOCS3,TGFB1
B Cell Development	1.62	0.139		HLA-B,HLA-DMA,HLA-DRA,HLA-DRB1,HLA-DRB5
IL-15 Production	1.61	0.0909	-0.905	AXL,DDR1,EPHA2,EPHA4,ERBB4,FGFR1,FYN,IGF1R,NTRK2,NTRK3,PTK7
Th1 Pathway	1.61	0.0909	-1.667	HLA-B,HLA-DMA,HLA-DPA1,HLA-DPB1,HLA-DRA,HLA-DRB1,HLA-DRB5,NOTCH1,PIK3R1,SOCS3,STAT3
Autoimmune Thyroid Disease Signaling	1.61	0.122		HLA-B,HLA-DMA,HLA-DRA,HLA-DRB1,HLA-DRB5,HLA-E
Death Receptor Signaling	1.61	0.0989	1	ACTA2,ACTB,ACTC1,ACTG1,ACTG2,CYCS,HSPB1,LMNA,SPTAN1

PI3K Signaling in B Lymphocytes	1.58	0.087	-1	ATF4,FOS,FYN,IRS1,IRS2,JUN,PIK3R1,PLCB1,PLCE1,PLEKHA4,RAC1,RRAS
Cell Cycle Regulation by BTG Family Proteins	1.57	0.135		BTG1,CCND1,PPP2CB,PPP2R2B,PRMT1
Complement System	1.57	0.135	-0.447	C1QBP,C1R,C1S,CFI,SERPING1
Antioxidant Action of Vitamin C	1.53	0.0917	2.449	GSTO1,MAPK10,NXN,PLAAT3,PLAAT4,PLCB1,PLCE1,PLD3,SLC2A1,TXN
Gluconeogenesis I	1.52	0.154	2	ENO1,GAPDH,PGAM1,PGK1
IL-6 Signaling	1.52	0.088	-0.905	A2M,COL1A1,FOS,HSPB1,JUN,MAPK10,PIK3R1,RRAS,SOCS3,STAT3,TNFRSF11B
CREB Signaling in Neurons	1.51	0.0773	-1.732	ADCY2,ATF4,CACNA1C,CACNG4,CREB3,GNG12,GRIA1,GRIA4,GRID2,GRIN2A,GRIN2B,PIK3R1,PLCB1,PLCE1,POLR2L,RRAS
Protein Kinase A Signaling	1.5	0.0677	-0.655	ADCY2,ADD3,AKAP13,ATF4,CREB3,DUSP6,GNG12,H1-0,MYL12A,MYL12B,MYL6,MYL9,NTN1,PDE1A,PDE4B,PHKB,PLCB1,PLCE1,PPP1CA,PPP1CB,PPP1R14B,PTPRA,PTPRJ,PTPRZ1,TCF7L2,TGFB1,VASP
GABA Receptor Signaling	1.5	0.0947		ABAT,ADCY2,AP2M1,AP2S1,CACNA1C,CACNG4,DNM1,RPS27A,UBA52
PI3K/AKT Signaling	1.48	0.08	2.714	CCND1,EIF4EBP1,HSP90AB1,HSP90B1,IL13RA2,ILK,ITGA3,ITGA4,ITGB1,LIMS1,PIK3R1,PPP2CB,PPP2R2B,RRAS
Prolactin Signaling	1.48	0.0988	-1.414	FOS,FYN,IRS1,JUN,PIK3R1,RRAS,SOCS3,STAT3
Regulation of the Epithelial-Mesenchymal Transition Pathway	1.48	0.0781		APC,EGR1,FGFR1,FZD2,FZD3,ID2,LOX,NOTCH1,PIK3R1,RRAS,STAT3,TCF7L2,TGFB1,TWIST1,ZEB1
TGF-β Signaling	1.47	0.0938	0	BMP7,FOS,INHBA,JUN,PMEPA1,RRAS,SERPINE1,SMURF2,TGFB1
Endocannabinoid Cancer Inhibition Pathway	1.47	0.0839	0	ADCY2,ATF4,CCND1,CCND2,CNR1,CREB3,NUPR1,PDGFC,PIK3R1,TCF7L2,TWIST1,VIM
Endocannabinoid Neuronal Synapse Pathway	1.45	0.0859	-2.714	ADCY2,CACNA1C,CACNG4,CNR1,GRIA1,GRIA4,GRIN2A,GRIN2B,MAPK10,PLCB1,PLCE1
Transcriptional Regulatory Network in Embryonic Stem Cells	1.42	0.111		H4C3,L1CAM,RFX4,SET,SOX2,STAT3
Thioredoxin Pathway	1.42	0.286		NXN,TXN
Mechanisms of Viral Exit from Host Cells	1.4	0.122		ACTA2,ACTB,ACTC1,ACTG1,ACTG2
Apelin Cardiomyocyte Signaling Pathway	1.4	0.0909	-0.333	MAPK10,MYL12A,MYL12B,MYL6,MYL9,PIK3R1,PLCB1,PLCE1,TGFB1
Natural Killer Cell Signaling	1.39	0.0761	0.258	B2M,CFL1,COL10A1,COL18A1,COL1A1,COL1A2,COL3A1,FYN,HLA-B,HLA-E,ITGB1,MAP3K13,PIK3R1,RAC1,RRAS

Endocannabinoid Developing Neuron Pathway	1.39	0.087	0.632	ADCY2,ATF4,CCND1,CNR1,CREB3,MAPK10,PIK3R1,RAC1,RRAS,STAT3
RAN Signaling	1.38	0.176		KPNA2,RAN,RANBP1
HIPPO signaling	1.37	0.0941	1	CD44,DLG1,NF2,PPP1CA,PPP1CB,PPP1R14B,PPP2CB,PPP2R2B
Superpathway of Cholesterol Biosynthesis	1.37	0.138	0	EBP,FDPS,HMGCS1,MSMO1
Intrinsic Prothrombin Activation Pathway	1.36	0.119	0.447	COL10A1,COL18A1,COL1A1,COL1A2,COL3A1
Unfolded protein response	1.36	0.107	0	ATF4,CANX,CEBPD,HSP90B1,P4HB,XBP1
Neuropathic Pain Signaling In Dorsal Horn Neurons	1.36	0.0891	-3	FOS,GRIA1,GRIA4,GRIN2A,GRIN2B,NTRK2,PIK3R1,PLCB1,PLCE1
Cardiac Hypertrophy Signaling (Enhanced)	1.34	0.0637	-0.898	ADCY2,AKAP13,CACNA1C,DLG1,EDN1,EDNRB,EIF4EBP1,FGFR1,FZD2,FZD3,HSPB1,IGF1R,IL11,IL13RA2,ITGA3,ITGA4,ITGB1,JUN,LIF,MAP3K13,MAPK10,PDE1A,PDE4B,PIK3R1,PLCB1,PLCE1,RPS6,RRAS,STAT3,TGFB1,TNFRSF11B
Asparagine Biosynthesis I	1.34	1		ASNS
Adipogenesis pathway	1.33	0.0821		BMP7,CEBPD,FGFR1,FZD2,FZD3,LPL,NR2F2,RBP1,SOX9,TGFB1,XBP1
FAT10 Signaling Pathway	1.32	0.167		MAP1LC3B,PSME2,UBA1
Basal Cell Carcinoma Signaling	1.32	0.0972	-1	APC,APC2,BMP1,BMP7,FZD2,FZD3,TCF7L2
STAT3 Pathway	1.31	0.0815	0	FGFR1,IGF1R,IL13RA2,MAPK10,NTRK2,NTRK3,RAC1,RRAS,SOCS3,STAT3,TGFB1
Cholecystokinin/Gastrin-mediated Signaling	1.31	0.084	-1.667	EPHA4,FNBP1,FOS,JUN,MAPK10,PLCB1,RAC1,RHOC,RND2,RRAS

Supplemental Table 4.14. HD iAstro Top 25 Significant ChIP-X Enrichment Analysis (ChEA)

Term	Overlap	P-value	Adjusted P-value	Odds Ratio	Combined Score	Genes
ATF3 23680149 ChIP-Seq GBM1-GSC Human	228/2189	1.78E-24	1.15E-21	2.3578	128.9408	RPL3;RPL32;SERPINE1;ENO1;SOX21;IFIT2;PSMD8;SOX2;RPS14;RPS16;RPL36AL;PSMD2;DPYSL2;SOX9;RPS13;RPL21;ACTN1;ACTN4;HSPG2;RUNX1;MYL6;RBP1;RPL24;TAGLN2;RPL27;TLN1;EPHA2;PFN2;C5ORF46;TTYH3;BEX1;PCDH10;TWIST1;NUAK1;RRAS;S100A16;PRDX1;S100A13;FAM43A;S100A10;MCTS1;EGR1;JUN;XBP1;DTNA;GADD45B;IQSEC1;GADD45A;PLK2;FN1;NR2F1;PA2G4;LARP6;EIF1;PCDHGA10;ALDH6A1;ID1;ID3;HIST1H4C;DDR1;ARF4;NRP2;CLIC4;BTG1;HERPUD1;TUBA1C;MAP1LC3B;GLIPR1;TUBA1A;CSRP1;GLIPR2;PEA15;ANKRD1;IDS;KIF1B;SEC61B;FGFBP3;LMCD1;SPTAN1;CLIC1;CDV3;EDN1;CHST7;ANXA1;TNFRSF12A;ANXA2;ANXA3;HEG1;MRPS7;RGMB;RHOC;F3;DUSP6;NME1;GCHFR;ITPKB;SLC7A5;TUBB2B;PXDN;CDC42EP3;CKS2;FIBIN;CDC42EP1;ANGPTL2;GARS;WRB;RPL12;AMIGO2;CCDC107;PRICKLE1;TCEAL7;NT5E;PSMB2;PSMB3;LMNA;PDPN;CCT5;RPL19;GSN;STAT3;KLHL4;DCBLD2;AXL;RAB9A;RPL22L1;SLC27A1;PLXND1;TNC;IRS2;GXYLT2;SRP14;COMT;SAT1;CLU;CHCHD2;RGS3;SLN;PTTG1;PLAU;LAMP2;HCFC1R1;IL13RA2;PHLDA1;AP2M1;CAST;TPM4;IGFBP3;TPM2;NEAT1;ATP1B1;ILF2;EEF1A1;PLA2G16;COL4A2;SNRPG;MALAT1;RTN3;NNMT;FBLIM1;SLC1A3;TARS;SLC1A5;EIF4EBP1;PMAIP1;NPTX2;PLTP;YARS;CAV2;UBE2C;CAV1;HMGA1;LAYN;ASNS;INHBA;EIF2S2;CYCS;MDM4;UBA1;NF2;TGFBI;HSP90AB1;B4GALT1;MCM7;WDR1;FHL1;FHL2;HMGB2;SLC2A1;ILK;HSPB1;RND2;CAPZB;PDE4B;PMEPA1;UPP1;DST;HMGCS1;ITGA3;H2AFZ;PJA2;CREB3;RCN1;NOS1AP;EFHC1;ITGA7;MYH9;TMBIM6;ITGA6;PFDN2;PLEKHH2;USP11;CCL2;HES1;PCDH7;PDAP1;RPL35A;RPL23A;ATOX1;KLF6;APC;SYT11;EIF3I;SPRY2;SPRY1;VIM;SSBP1;PFKP;TNRC6B
ZNF217 24962896 ChIP-Seq MCF-7 Human	168/1522	2.39E-20	7.69E-18	2.4319	109.8762	TES;IRS1;CTNND2;ABAT;ENO1;BZW2;HS6ST1;LOXL1;IGF1R;CDH6;PPP1CB;SOX2;RGS3;CCND1;KIF5C;BASP1;ENPP2;BAALC;PTGFRN;SOX9;SOX6;IER5;TMSB10;PHLDA1;RGS6;SOX4;ANKS1B;CAST;EPHA4;SLC38A1;WSB1;TLE1;SEMA6A;LIMCH1;ACTN1;IGFBP3;TPM1;ACTN4;NEAT1;ATP1B1;RUNX1;STIM2;SNRPE;MALAT1;VDAC1;TNIK;SCG2;XPR1;PFN2;TMED10;PCDH10;SLC1A2;RHOBTB3;AGAP1;TMTC2;TNFRSF11B;SLC1A4;PIK3R1;SLC1A5;IQGAP2;GLG1;ZFP36L2;NPAS3;MAP2;PODXL;ZNF704;TSPAN2;FAM43A;SRGAP3;LRRC4C;SRGAP1;S100A11;SPTBN1;S100A10;ABCA1;XBP1;UBE2I;DTNA;AUTS2;SYT1;SMURF2;IQSEC1;PLK2

						;FN1;LIF;DSTN;NR2F2;CP;PBX1;QKI;DCLK1;COL5A1;NBEA;ID2;ID1;ID4;SDC1;MDM4;NF2;MAP3K13;PAM;SERINC5;SPAG16;NRP1;COL18A1;BTG1;SLC44A1;HSPB1;PTPRJ;ARHGAP5;CHD1;PRSS23;RERG;SYNE2;AKAP13;CSRP1;SEC61B;C3ORF58;CDV3;EDN1;ANXA2;ANXA4;HEG1;PAWR;EMP2;GFRA1;FOS;NAV2;DUSP6;MTSS1;SLC7A5;ZEB1;SETBP1;PALLD;PXDN;CDC42EP3;NOS1AP;ITGA6;CD47;PLCB1;AHNAK;AMIGO2;FIGN;PRICKLE1;CXXC5;TFPI;THBS1;NCALD;FSTL5;PGRMC2;ERBB4;AP2S1;LRIG1;HES1;CACNG4;NTRK2;BCHE;SVIL;GSN;NTRK3;PLEKHA5;HIPK2;KLF6;MARCKS;SLCO3A1;NFIA;NOVA1;MEGF9
OCT4 18692474 ChIP-Seq MEFs Mouse	200/1992	1.86E-19	4.00E-17	2.2119	95.3925	IFITM3;EIF4A1;RPL5;RPL3;ITSN1;ENO1;RPL8;IFIT1;HS6ST1;ACTB;SOX2;RPS14;PSMD7;RPS16;SOX1;CAPNS1;RPS19;RPS18;KIF21A;SNRPD3;RPS11;SOX4;IER3;DDX17;HES6;RPL21;FNBP1;RPL22;6-MAR;ACTN4;CLDN5;SFRP1;SFRP2;FNDC4;UQCRC1;SPARCL1;RPL27;VDAC1;RPL29;TLN1;SET;TTYH1;PDE1A;TWF2;OAZ1;LDHB;PRDX4;RRAS;PRDX1;PDGFC;APOE;PROM1;FZD3;DTNA;XRCC5;LRRN2;GADD45A;FN1;PBX3;LIF;PA2G4;NR2F6;ID2;ID1;ID3;GPAA1;HEXA;PTPRJ;MAP1LC3B;HINT1;TUBA1A;CSRP1;SEC61G;NEFL;KCND3;SSR2;FOS;PROX1;RHOC;AES;NME1;SLC7A5;GPRC5B;MRPL51;CANX;CKS2;CD47;GRN;TOMM40;AHNAK;COX5A;TCEAL8;CST3;NT5E;PSMB3;CAMK2N1;PDPN;RPS3;GPC4;RPS2;RPL18;JAM2;RANBP1;NPM1;SORT1;STAT3;SORBS1;NFIA;PLP2;ZBTB20;SRP14;ESPN;EEF1B2;CDH6;CHCHD2;RGS3;DACH1;CCND1;CFL1;KPNA2;TMSB10;AP2M1;PHLDA3;CAST;SNRPN;SEMA6A;RPS5;IGFBP2;SARS;ATP1B2;MID1;TUBA4A;ADAM19;EEF1A1;RAB34;ERH;RTN3;NNMT;NOTCH1;SLC1A2;SLC1A3;SLC1A4;SLC1A5;CACNA1C;PLD3;NPAS3;SLC9A3R2;SOCS3;PODXL;PMAIP1;NPTX2;IDH1;DSTN;EEF2;EIF2S2;LSM4;NACA;ARPC3;MDM4;NF2;FGFR1;SLC25A3;WDR1;RNF13;SLC2A1;HMGB3;HSPB1;SGCE;RPL7A;CAPZB;ZIC2;UPP1;DGCR2;DST;H2AFZ;PLAUR;RPS3A;EPN2;CREB3;PSRC1;MYH9;CDH13;GAPDH;CEBPD;NXN;POMP;SLC3A2;LRP2;CXXC5;NTN1;HES1;SLC12A2;NTRK2;TCF7L2;PCDH8;KLF6;ACTC1;SPRY2;SPRY1;PFKP
CEBPD 21427703 ChIP-Seq 3T3-L1 Mouse	179/1735	1.43E-18	2.31E-16	2.2565	92.7119	EIF4A1;TES;IFITM2;SERPINE2;IRS1;COL12A1;ZBTB20;IRS2;GXYLT2;RPL10A;SAT1;ACTB;PPP1CB;RPS14;LGALS1;CCND2;SESN3;BASP1;DPYSL2;PEG10;ENPP2;SOX9;KPNA2;NCKAP5;IER5;PHLDA1;RPS13;SOX4;WLS;RPS12;CAST;RPS9;WSB1;TPM4;IGFBP3;SEMA6D;ANK2;ACTN4;NEAT1;RUNX1;STIM2;COL4A1;PAPPA;MALAT1;UBA52;CALCRL;INTU;PCDH10;PDE1A;HTRA1;AGAP1;SLC1A3;TARS;TWIST1;LPL;TNFRSF11B;PIK3R1;CACNA1C;ZFP36L2;FBLN5;SOCS3;CALD1;PODXL;ARSJ;PRDX1;PDGFC;PSAP;STK38L;FAM43A;SRGAP1;ABCA1;XBP1;FZD2;SYT1;GADD45B;SMURF2;XRCC5;IQSEC1;GADD45A;CAV1;PLK2;IDH1;FN1;DCLK2;NR2F2;INHBA;CP;LARP6;PBX1;DCLK1;COL1A2;NBEA;ID1;ID3;HIST1

						H4C;SFXN5;ITM2B;FBN1;FGFR1;NRP1;DOCK5;NRP2;ECM2;WDR1;ARPC1B;RPLP0;HMGB1;FMN2;TSPAN11;PRSS23;RERG;SGCE;SEC61G;ITGB8;NEO1;EDN1;TPI1;ANXA1;ANXA2;GSTO1;H2AFZ;PAWR;GFRA1;RPS3A;RGMB;GFRA2;SRP9;DUSP6;RGMA;EPN2;RCN1;VCAN;ZEB1;SETBP1;PALLD;CDC42EP3;TAX1BP1;ANGPTL2;CDH13;CD47;SLC25A5;GAS6;PLCB1;PTMA;NFIX;LRRC17;IER5L;SLC3A2;PRICKLE1;PTN;CXXC5;ADD3;THBS1;NT5E;PGRMC2;PALMD;PDPN;LRIG1;CCL2;SLIT2;FILIP1L;SVIL;ARNT2;PCGF5;PCDH7;STAT3;ATP2B1;DCBLD2;HIPK2;COL3A1;KLF6;MARCKS;SLCO3A1;NFIA;SYT11;SPRY2;PTX3;VIM;LIMS1
SOX2 18692474 ChIP-Seq MEFs Mouse	196/1991	4.12E-18	5.30E-16	2.1537	86.2159	IFITM3;EIF4A1;IFITM1;RPL3;ITSN1;ENO1;HS6ST1;PSMD8;SOX2;RPS14;PSMD7;CAPNS1;RPS19;RPS18;MAGOH;PLCE1;KIF21A;PTGFRN;RPS11;DDX17;EPHA4;RPL21;FNBP1;RPL23;RPL22;ACTN4;CLDN5;FNDC4;RFX4;RUFY3;RPL27;VDAC1;RPL29;PFN1;RPL28;SET;TTYH1;PDE1A;TWF2;OAZ1;LDHB;RRAS;PDGFC;S100A13;SERPINH1;APOE;MCTS1;FZD3;FZD2;DTNA;GADD45B;XRCC5;ST8SIA1;LRRN2;GADD45A;RDX;FN1;BTBD11;EIF1;NR2F6;PTK7;ID1;ID3;RPS23;DDR1;GPAA1;HEXA;CSRP1;NEFL;CCT3;TPI1;SSR2;EMP2;FOS;RGMB;DUSP6;NME1;SLC7A5;GPRC5B;TUBB2B;MRPL51;CANX;CD47;PTMA;ASAH1;TOMM40;AHNAK;TIMM13;RPS27L;FIGN;COX5A;TCEAL8;CST3;NT5E;CAMK2N1;PDPN;DMD;GPC4;RPL18;JAM2;SORT1;STAT3;SORBS1;ZBTB20;ESPN;CDH6;CHCHD2;PHLDA2;TMSB10;AP2M1;RGS6;SNRPN;TLE1;TPM3;RPS5;TPM1;IGFBP2;SARS;ATP1B1;GTF2F2;ADAM19;EEF1A1;COL4A2;COL4A1;SNRPG;RTN3;NNMT;TMED10;NOTCH1;FBLIM1;SLC1A3;SLC1A4;SLC1A5;CACNA1C;PLD3;ZFP36L2;NPAS3;SOCS3;PODXL;PMAIP1;NPTX2;ASNS;EEF2;PIR;CPE;MDM4;NF2;FGFR1;DOCK5;HSP90AB1;B4GALT1;WDR1;RNF13;DOCK7;HMGB3;HSPB1;HMGB1;TSPAN11;SGCE;CAPZB;ZIC2;UPP1;DGCR2;DST;H2AFZ;ATRX;PLAUR;RPS3A;EPN2;RCN1;MYH9;CDH13;GAPDH;CEBPD;NXN;POMP;IER5L;SLC3A2;LRP2;PDHB;CXXC5;TFPI;NTN1;PTPRZ1;NT5DC2;LRIG1;SLC12A2;SPAG9;TCF7L2;FOXJ1;KLF6;MARCKS;ACTC1;SPRY2;P4HB;VIM
YAP1 20516196 ChIP-Seq MESCs Mouse	215/2329	1.06E-16	1.14E-14	2.0126	74.0262	APP;RPL8;HS6ST1;ACTB;RPL6;PSMD7;SOX1;CAPNS1;DPYSL5;PLCE1;RPL38;PTGFRN;SOX9;SOX4;ANKS1B;EPHA4;LIMCH1;RFX3;ANK2;ACTN4;RUNX1;SFRP2;RFX4;SPARCL1;PFN1;INTU;PCDH10;MRPL14;PIK3R1;GRIN2A;NKAIN3;PRDX1;A2M;ARGLU1;XBP1;FZD2;DTNA;GADD45B;IQSEC1;ST8SIA1;GADD45A;FN1;LIF;DCLK2;BTBD11;NR2F2;GNG12;GRIN2B;DCLK1;ID2;ID4;SFXN5;COL18A1;ARF1;BTG1;SLC35F1;FMN2;AKAP13;SEC61G;PCMTD1;ANXA1;ANXA2;KCND3;ANXA4;EMP2;PROX1;RGMB;RHOC;PRSS12;GFRA2;SRP9;ITFG1;MTSS1;RGMA;ITPKB;CANX;GARS;PTMA;ASAH1;NFIX;PRICKLE1;PTN;COX5A;LMNA;RPS3;CTNNA1;DMD;CTNNA2;SVIL;ARNT2;STAT3;PLEKHA5;KLHL4;PPP1CA;NFIA;MEGF

						9;SEMA5B;IRS1;CTNND2;TNC;ZBTB20;SAT1;IGF1R;CDH6;TUBB6;COL4A3BP;CCND2;DACH1;SESN3;SLN;CCND1;BASP1;CFL1;TMSB10;RGS6;CAST;RPS9;SNRPN;SEMA6A;IGFBP3;RPS5;APLP2;TPM1;MAGI2;MID1;PDIA5;EEF1A1;COL4A2;STIM2;COL4A1;COL4A5;SNRPE;SNRPB;GRIA1;LRRC59;SLC1A3;SLC1A4;SLC1A5;CACNA1C;SPATA6;FBLN5;NPAS3;ARHGAP21;PODXL;IGFBP7;NPTX2;LRRC4C;AUTS2;WSCD1;IDH2;ASNS;PHKB;INHBA;EEF2;MCC;BMP7;LSM4;DLG1;P4HA2;CPE;MDM4;MAP3K13;FGFR1;HSP90AB1;WDR1;RNF13;FHL1;SLC2A1;TSPAN11;SYNE2;SCPEP1;CAPZB;PDE4B;IFT57;EIF5A;GRID2;DST;ATP6AP2;NAV2;GAP43;SETBP1;PALLD;NOS1AP;BIRC5;MYH9;CDH13;LAMA2;SLC3A2;SPG7;ADD3;NTN1;NCALD;SLIT1;LRIG1;S1PR3;HES1;SLIT2;PDLIM7;SLC12A2;NTRK2;TCF7L2;PCDH9;LAMB2;NTRK3;IRX3;MAPK10;KLF6;MARCKS;ACTC1;APC;PPP2R2B;PMP22;SPRY2;PTX3;PFKP
WT1 25993318 ChIP-Seq PODOCYTE Human	289/3464	1.40E-16	1.29E-14	1.8486	67.4877	APP;IFITM1;FAM89A;ITSN1;ENO1;SOX21;HS6ST1;RPS14;LGALS1;EDNRB;DPYSL5;DPYSL2;DAG1;PLCE1;DPF3;PTGFRN;SOX6;NCKAP5;IER5;SOX4;IER3;ANKS1B;RPS12;EPHA4;WSB1;FNBP1;ACTN1;RFX3;ACTN4;RUNX1;MAP1B;PAPPA;MAP1A;RPL24;SERPING1;VDAC2;RPL27;KCTD12;EPHA2;PFN2;COL13A1;CFI;AGAP1;TMTC2;PIK3R1;APCDD1;MYL12A;MYL12B;LDHB;GRIN2A;NKAIN3;RRAS;S100A16;PDGFC;EPB41L3;TSPAN2;TSPAN3;N4BP2;ARGLU1;S100A11;SERF2;B4GALNT4;EGR1;JUN;NDFIP1;XRCC5;LRRN2;PLK2;MCAM;PBX3;MICAL3;LIF;DCLK2;BTBD11;NR2F2;GNG12;GRIN2B;LARP6;PBX1;NR2F6;ID1;SSPN;DCHS1;FXYD6;CPEB2;PAM;RPS24;ITM2B;DDR1;COL18A1;NRP2;CLIC4;SLC44A1;ELN;HEXA;CLTA;PTPRJ;PRSS23;AKAP13;SIPA1L1;CSRP1;GLIPR2;SLC22A17;NEFL;PHGDH;LMCD1;CTSC;PCMTD1;RALGPS2;EDN1;GSTO1;SSR2;ANXA4;SSR3;PAWR;GFRA1;FOS;PROX1;RGMB;RHOC;DUSP6;MTSS1;AES;SLC7A5;ZEB1;HEATR5A;PXDN;CDC42EP1;PTMA;CRB2;AMIGO2;ABRACL;ADCY2;FIGN;PRICKLE1;CAMK2N1;LMNA;AP2S1;CTNNA1;DMD;P4HTM;GDF10;SVIL;ARNT2;CENPV;GSN;GOLM1;PLEKHA5;BBOX1;SORBS1;DCBLD2;HIPK2;BOP1;SMOC2;SLCO3A1;NFIA;AXL;SMOC1;TTC3;MEGF8;MEGF9;SEMA5B;IRS1;CTNND2;PDCD5;TNC;ZBTB20;GXYLT2;CELSR1;ESPN;LOXL1;IGF1R;FADS3;CDH6;COL4A3BP;RGS3;CCND2;DACH1;SESN3;KIF5C;LAMP2;TMSB10;RGS6;PHLDA3;SEMA6A;IGFBP5;SEMA6D;TPM1;MAGI2;KAZN;NEAT1;ATP1B1;PDIA5;RBX1;COL4A2;DKC1;STIM2;COL4A1;MALAT1;TNIK;NUPR1;SCG2;NOTCH1;NTM;RHOBTB3;CACNA1C;PLD3;NPAS3;SLC9A3R2;SOCS3;CALD1;PODXL;IGFBP7;SRGAP3;SRGAP1;PLTP;FDPS;IDH1;IDH2;ARHGAP29;PHKB;ARPC5;MCC;BMP7;LSM4;ARPC2;CPD;TPP1;NF2;TGFBI;SERINC5;FGFR1;ITGB1;DOCK5;HSP90AB1;B4GALT1;SLC2A1;TSPAN11;CAPZB;NTMT1;PMEPA1;ITGB8;EMILIN1;SPDL1;IFT57;ACTR3;GRID2;DST;ITGA3;H2AFZ;NAV2;RE

						XO2;PJA2;EPN2;C1QL1;RCN1;VCAN;SETBP1;PALLD;MYH9;PLEKHH2;LRP1;NXN;POMP;CXXC5;ADD3;NTN1;THBS1;NCALD;ZNRF3;ERBB4;SLIT1;LRIG1;FYN;HES1;CACNG4;SLC12A2;NTRK2;TCF7L2;COL26A1;PCDH9;IRX3;LAMB1;NAP1L1;MAPK10;KLF6;PI15;SPRY2;SPRY1
XRN2 22483619 ChIP-Seq HELA Human	158/1529	1.91E-16	1.53E-14	2.2317	80.7804	RPL4;EIF4A1;RPL5;RPL3;RPL32;RPL8;RPL10A;BZW2;SAT1;SOX21;ACTB;RPL6;ACTG1;CDC20;RPS14;CHCHD2;CCND2;DACH1;SNRPD2;CCND1;RPS19;RPS18;MAGOH;HCFC1R1;RPL35;RPL38;TMSB10;B2M;AP2M1;SOX4;RPS12;DYNC2H1;RPS9;WSB1;ACTN1;RPL23;RPS5;RPL22;RPS6;SARS;RPSA;NEAT1;MID1;ILF2;HLA-E;EEF1A1;MYL6;NCL;PSME2;RPL24;TAGLN2;RPL27;MALAT1;RPL29;PFN1;EZR;PPIA;RPL28;ATF4;SNRPB;RTN3;SET;RBM8A;SLC1A3;SLC1A5;TXN;OAZ1;ZFP36L2;HSP90B1;PRDX1;PGK1;S100A13;PMAIP1;SERF2;FDPS;JUN;DTNA;GADD45B;UBE2C;GADD45A;TMEM132A;NR2F1;HMGA1;PA2G4;EEF2;GNG12;QKI;EIF1;CCT6A;RPS27;UBE2S;ID2;ID1;ID4;ID3;CYCS;TPP1;SERINC1;RPS24;ARF4;HSP90AB1;BTG1;MCM7;WDR1;RPLP0;ILK;TUBA1C;RPL7A;TUBA1A;SEC61G;RPLP2;TK1;SPTAN1;EIF5A;ACTR3;CCT2;TPI1;TNFRSF12A;HMGCS1;H2AFZ;SSR2;MRPS7;APRT;NME1;CKS2;CDC42EP1;BIRC5;ITGA7;TMBIM6;GAPDH;PTMA;TOMM40;RPL12;RPL11;SLC3A2;SPG7;PSMB2;RPL13;HES1;RPS2;RPL15;RPL18;P4HTM;RPL19;POLR2L;NPM1;PCDH9;PCDH7;STAT3;RPL35A;RPL23A;HNRNPAB;AXL;RPL22L1;P4HB;SSBP1;RAN;TNRC6B
EKLF 21900194 ChIP-Seq ERYTHROCYTE Mouse	135/1239	6.41E-16	4.38E-14	2.3445	82.0206	RPL4;RPL3;RPL32;ITSN1;ENO1;RPL10A;SAT1;RPL6;ACTG1;LOXL2;RPL7;CDC20;RPS14;CHCHD2;LGALS1;CCND2;RPS16;SNRPD2;SNRPD1;RPS18;STMN1;CFL1;MAGOH;RPL35;KPNA2;RPS11;SOX6;SLC38A1;RPS9;TPM4;SARS;ATP1B2;GTF2F2;ILF2;EEF1A1;MYL6;NCL;UQCRC1;SNRPG;PSME2;RPL24;TAGLN2;RPL27;SNRPE;ERH;VDAC1;SNRPF;RPL29;PFN1;PPIA;SNRPB;LRRC59;SET;TMED10;TARS;MRPL14;SLC1A5;PLD3;ZFP36L2;CNN2;PODXL;PSAP;EIF4EBP1;PGK1;TSPAN3;VASP;UBE2I;TGFB1;UBE2C;GADD45A;IDH2;MICAL3;HMGA1;ASNS;PA2G4;EEF2;GFAP;H1F0;PIR;RPS24;ITM2B;RPS23;SLC25A3;MCM7;WDR1;GPAA1;ARPC1B;SLC2A1;HMGB3;AKAP13;HINT1;TUBA1A;CAPZB;RPLP2;SH3BGRL3;TK1;CLIC1;EIF5A;CCT3;TPI1;GSTO1;PRMT1;SSR2;REXO2;SRP9;AES;PSMA5;PSMA4;TMBIM4;TAX1BP1;MYH9;SLC25A5;PTMA;CD44;TOMM40;ADD3;THBS1;SRM;CST3;PSMB5;PSMB3;NT5DC2;RPS3;RPL15;RPS27A;CCT5;RPL19;TCF7L2;NAP1L1;SORBS1;PPP1CA;BOP1;PSMC5;PSMC4;VIM
SUZ12 18692474 ChIP-	127/1135	6.81E-16	4.38E-14	2.4080	84.0935	SEMA5B;APP;PLXND1;CSF1;IRS1;CTNND2;COL12A1;SLC4A4;CLU;CDH6;CCND2;DACH1;SOX1;EDNRB;DPYSL5;LEPR;DPF3;SOX9;PHLDA2;SOX6;IER5;RGS6;SOX4;EPHA4;SEMA6A;IGFBP5;FST;TPM1;RUNX1;CLDN5;SFRP1;LOX;COL4A2;COL4A1;RFX4;PAPPA;EEF1A2;LY6H;FBN2;CO

Seq MEFs Mouse						L13A1;PCDH10;SLC1A2;HTRA1;TWIST1;LPL;CACNA1C;NPAS3;GRIN2A;SNTG1;PODXL;TSPAN2;NPTX2;PROM1;GPM6B;ABCA1;JUN;FZD3;FZD2;DTNA;TGFB1;ST8SIA1;LRRN2;CAV1;PBX3;NR2F1;NR2F2;GRIN2B;BMP7;LARP6;BMP1;CPD;ID1;ID4;ID3;TGFBI;PAM;FBN1;NRP1;NRP2;FHL2;TSPAN11;ZIC2;ZIC1;NEFL;KIF1A;GRID2;EDN1;KCND3;EN2;GFRA1;PROX1;PRSS12;GFRA2;SRP9;MLF1;C1QL1;MMP15;EEF1D;MMP17;ITGA7;CDH13;PLEKHO1;GAS6;NFIX;LRP2;NTN1;NT5E;PTPRZ1;FRZB;CAMK2N1;CNR1;ERBB4;SLIT1;SLIT2;JAM2;CACNG4;GDF10;NTRK2;PCDH7;NTRK3;IRX3;PCDH8;SNCAIP;HIPK2;SMOC2;NFIA;PTX3
SMARCA4 23332759 ChIP-Seq OLIGODENDROCYTES Mouse	224/2522	1.62E-15	9.48E-14	1.9283	65.6716	APP;RPL32;SERPINE2;FAM89A;ENO1;LIPA;TXNDC17;PREX2;SOX2;PSMD7;EDNRB;SNRPD1;DPYSL2;STMN1;RPL35;DPF3;PTGFRN;SOX6;IER5;DYNC2H1;EPHA4;FNBP1;LIMCH1;RFX3;RUNX1;CLDN5;PPA1;BIN1;MAP1B;COL8A1;EZR;PDE1A;SDC3;TMTC2;SLC5A3;MYL12B;NUAK1;NKAIN3;S100A16;MAP2;ARSJ;PDGFC;EPB41L3;TSPAN2;TSPAN3;ARGLU1;GPM6B;ABCA1;XBP1;FZD2;GADD45A;RDX;PBX3;NR2F1;MICAL3;DCLK2;NR2F2;GDF6;CP;LARP6;DCLK1;ID2;ID4;SPAG16;DDR1;NRP2;BTG1;SLC44A1;HEXA;PTPRJ;SLC35F1;ARHGAP5;PRSS23;ASGR1;CSRP1;SEC61G;ANKRD1;NEFL;KIF1B;LMCD1;CDV3;ANXA1;KCND3;PAWR;GFRA1;F3;GFRA2;DUSP6;ITFG1;ZEB1;TAX1BP1;FIBIN;ANGPTL2;PLCB1;PTMA;ASAH1;LRRC17;FIGN;PTN;CST3;LMNA;CTNNA1;DMD;CTNNA2;JAM2;NPM1;GSN;PCGF5;KIDINS220;STAT3;BBOX1;DCBLD2;HIPK2;SMOC2;COL3A1;SLCO3A1;NFIA;SEMA5B;PLXND1;IRS1;ZBTB20;ACTG1;IGF1R;CDH6;NRBP2;TUBB6;CCND2;SESN3;BASP1;CFL1;BAALC;TMSB10;PHLDA1;SLC38A1;TLE1;IGFBP3;SEMA6D;SARS;LIFR;ADAM19;EEF1A1;STIM2;COL4A1;TNIK;XPR1;SNRPB;FBN2;NNMT;TMED10;RTN1;CALCRL;NTM;SLC1A3;TARS;LPL;ARHGAP21;SNTG1;PODXL;PSAP;PMAIP1;IGFBP7;LRRC4C;SRGAP1;SYT1;WSCD1;SRD5A1;CAV1;DSTN;LAYN;ASNS;MCC;DLG1;PTPRA;CPE;MDM4;NF2;MAP3K13;SERINC5;B4GALT1;WDR1;HSPB1;ZIC1;TIMM17A;PDE4B;ITGB8;GRID2;ITGA4;RPS3A;NAV2;EPN2;LMBRD1;GAP43;EEF1D;CDH13;PON2;SPG7;ADD3;NCALD;OGFRL1;PTPRZ1;PALMD;CNR1;ERBB4;SLITRK5;FYN;NTRK2;TCF7L2;PCDH9;PCDH7;NTRK3;IRX3;B3GAT1;ATP2B1;KLF6;APC;ST5;PPP2R2B;EIF3I;PMP22;SPRY2;SPRY1;VIM;PFKP;TNRC6B
CLOCK 20551151 ChIP-Seq 293T Human	64/407	5.35E-15	2.87E-13	3.4656	113.8825	COL18A1;HSP90AB1;ELN;SERPINE1;HMGB3;COMT;CLU;ACTB;LOXL1;HERPUD1;RBM3;TUBA1A;TMSB10;CCT3;HES6;ANXA2;ACTN1;FOS;MTSS1;ADAM19;CLDN5;TUBB2A;COL4A2;COL4A1;RAB34;NCL;COL6A1;ANGPTL2;MYH9;ITGA6;SLC25A5;MYL9;ATF4;BEX1;COL13A1;TARS;ATP1A2;PDHB;HSP90B1;SLC9A3R2;CALD1;LMNA;SERPINH1;CCT5;S100A10;ABCA1;EGR1;XBP1;GADD45B;AUTS2;GADD45A;STAT3;NAP1L1;NR2F2;EEF2;EIF1;MARCKS;H1F0;ACTC1;ST5;FABP7;ID1;SERINC1;PFKP

RUNX2 24764292 ChIP-Seq MC3T3 Mouse	184/2000	4.18E-14	2.07E-12	1.9688	60.6491	IFITM3;IFITM1;RPL3;IRS1;ITSN1;SERPINE1;TNC;GXYLT2;HS6ST1;ACTB;ACTG1;LOXL2;IFIT2;FADS3;LGALS1;CAPNS1;CCND1;RPL18A;RPS19;KIF5C;DAG1;PTGFRN;SOX9;SOX6;IER5;TMSB10;PHLDA1;WLS;IER3;PHLDA3;CHID1;EPHA4;TLE1;IGFBP5;TPM4;FNBP1;TPM3;FST;ACTN1;TPM2;APLP2;TPM1;LIFR;NEAT1;HSPG2;RBX1;EEF1A1;PLA2G16;SFRP2;BIN1;COL8A1;TAGLN2;MALAT1;NUPR1;PFN1;TLN1;TTYH3;NNMT;NOTCH1;SDC3;HTRA1;TARS;ZFP36L2;MYL12B;CNN2;SOCS3;NUAK1;RRAS;CALD1;S100A16;PDGFC;SERPINH1;N4BP2;PLTP;S100A11;SMURF2;IDH1;FN1;LIF;EIF1;COL1A1;COL1A2;COL5A1;ARPC3;PTK7;UBE2S;ID2;OSTC;SDC1;ID3;NF2;ANP32B;FGFR1;DDR1;NRP2;CLIC4;HSP90AB1;B4GALT1;MCM7;RNF13;FHL2;ILK;PTPRJ;SGCE;TUBA1C;TRMT112;MAP1LC3B;GLIPR1;CSRP1;GLIPR2;TIMP2;ANKRD1;PHGDH;EMILIN1;RAC1;LMCD1;CLIC1;EIF5A;CAP1;ANXA1;TNFRSF12A;ANXA2;GSTO1;H2AFZ;PGAM1;SSR2;PLAUR;FOS;MRPS7;RGMB;RHOC;PJA2;DNM1;AES;SLC7A5;IQCK;PSRC1;PXDN;CDC42EP3;CKS2;CDC42EP1;BIRC5;ANGPTL2;MYH9;PFDN2;GAS6;PTMA;C1S;LRP1;AHNAK;CEBPD;SLC20A1;AMIGO2;IER5L;SLC3A2;PTN;THBS1;NCALD;PGRMC2;CAMK2N1;TMEM67;LMNA;PDPN;AP2S1;HES1;RPL19;TCF7L2;PPP1R14B;NPM1;GSN;LAMB2;STAT3;S100B;HIPK2;COL3A1;NFIA;AXL;TTC3;PMP22;PTX3;P4HB;VIM;LIMS1;MEGF9
RELA 24523406 ChIP-Seq FIBROSARCOMA Human	125/1182	7.89E-14	3.63E-12	2.2492	67.8602	APP;SERPINE2;CSF1;PDCD5;SERPINE1;TNC;ENO1;EFEMP2;LGALS1;CCND2;CAPNS1;CCND1;PLAU;PLCE1;SOX9;IER5;PHLDA1;B2M;IER3;TLE1;TPM4;TPM1;IGFBP2;HLA-B;HSPG2;MID1;ADAM19;PAPPA;PSME2;PFN1;NNMT;TWIST1;TMTC2;GRIN2A;CALD1;PGK1;S100A13;SERPINH1;APOE;SRGAP1;S100A10;ABCA1;EGR1;JUN;SYT1;GADD45B;ST8SIA1;CAV1;FN1;DSTN;INHBA;LARP6;QKI;COL1A2;TP53I3;CPD;ITGB1;DDR1;ARF1;CLIC4;ECM2;MCM7;CLTA;AKAP13;CSRP2;ITGB8;UPP1;NEO1;CLIC1;PCMTD1;IL11;EDN1;HMGCS1;PRMT1;LRRIQ1;PAWR;GFRA1;FOS;NAV2;F3;DUSP6;PJA2;SLC7A5;CREB3;TMBIM4;MYH9;PTMA;CD44;GRN;PLEKHH2;C1S;AHNAK;CEBPD;GSTP1;CCDC107;SLC3A2;ATP1A2;CXXC5;THBS1;LMNA;CCL2;SLITRK5;HES1;RPS2;RPS27A;PDLIM7;IL32;SPAG9;CD74;ARNT2;TCF7L2;PPP1R14B;GSN;LAMB2;NTRK3;RPL23A;SNCAIP;ATOX1;MARCKS;ST5;BAX;PTX3;VIM;PFKP;TPT1
EP300 20729851 ChIP-Seq FORBR	189/2093	1.02E-13	4.39E-12	1.9299	57.7247	SEMA5B;RPL32;PLXND1;CSF1;CTNND2;ITSN1;PDCD5;ZBTB20;IRS2;RPL10A;SOX21;HS6ST1;ACTB;ACTG2;IGF1R;FADS3;SOX2;RPS14;RGS3;CCND2;DACH1;SOX1;CCND1;NAGLU;BASP1;STMN1;LEPR;KIF21A;SOX9;KPNA2;SOX6;PHLDA1;SOX4;HES6;EPHA4;GAS2L3;WSB1;SEMA6A;TPM4;FNBP1;FST;ACTN1;SEMA6D;TPM1;RPS6;IGFBP2;RFX3;ACTN4;HSPG2;PDIA5;RBX1;ADAM19;EEF1A1;MTHFD2;STIM2;RFX4;SPARCL1;T

AIN MIDBRAIN LIMB HEART Mouse						AGLN2;NUPR1;PFN1;MYL9;RPL28;XPR1;EPHA2;FBN2;NOTCH1;TTYH1;SLC1A2;HTRA1;SLC1A3;TWIST1;SLC1A5;IQGAP2;ZFP36L2;NPAS3;CNN1;EPB41L3;SERPINH1;PROM1;VASP;EGR1;JUN;FZD3;AUTS2;GADD45B;UBE2C;MCAM;IDH2;FN1;PBX3;NR2F1;MICAL3;LIF;DCLK2;NR2F2;BMP7;PBX1;COL1A1;PTK7;P4HA2;ID2;ID1;ID3;ANP32B;TGFBI;PAM;RPS24;FGFR1;ITGB1;NRP1;COL18A1;CLIC4;HSP90AB1;MCM7;SLC2A1;RND2;PTMS;TMEM47;MAP1LC3B;TUBA1A;CSRP2;LBH;ZIC2;GLIPR2;ZIC1;TIMP2;ANKRD1;ITGB8;KIF1A;CCT2;GRID2;ANXA2;METRN;PABPC4;HEG1;EN2;GFRA1;FOS;PROX1;RGMB;RHOC;F3;DUSP6;DNM1;RGMA;VCAN;TUBB2B;COL6A1;ANGPTL2;MYH9;CDH13;PLEKHO1;GAPDH;PTMA;TOMM40;AHNAK;IER5L;RPS27L;ATP1A2;PRICKLE1;NTN1;NCALD;OGFRL1;ZNRF3;FRZB;CAMK2N1;ERBB4;LMNA;SLIT1;LRIG1;SLITRK5;HES1;MEST;PDLIM7;SVIL;TCF7L2;GOLM1;PLEKHA5;SNCAIP;HIPK2;KLF6;ACTC1;NFIA;NOVA1;PMP22;SPRY2;VIM;PLP2;TNRC6B
MYC 19079543 ChIP-ChIP MESCs Mouse	144/1458	1.94E-13	7.81E-12	2.0967	61.3709	RPL4;EIF4A1;RPL5;RPL3;RPL32;ARPC5L;ENO1;RPL8;ACTB;RPL6;ACTG1;RPL7;EEF1B2;RPS15;SOX2;RPS14;PSMD7;RGS3;RPS16;SLN;CCND1;RPL18A;RPS19;RPL36AL;RPS18;RPL35;RPL38;KPNA2;RPS11;RPL39;RPS13;RPS12;DDX17;RPS9;RPL21;ACTN1;RPL23;RPS5;RPL22;RPS6;IGFBP2;RPSA;LIFR;EEF1A1;NCL;SNRPG;RPL24;ADAM9;RPL27;VDAC1;LY6H;RPL29;PPIA;RPL28;UBA52;EPHA2;RTN3;SET;TMED10;PCDH10;TARS;ZFP36L2;CCNB1;EIF4EBP1;SRGAP3;PLTP;B4GALNT4;YARS;FDPS;XBP1;NMB;ST8SIA1;TMEM132A;HMGA1;EEF2;CCT6A;RPS27;NACA;FXYD6;MDM4;ANP32B;RPS24;RPS23;FGFR1;LGALS3BP;MCM7;HMGB2;PRSS23;RBM3;RPL7A;TIMM17A;TIMP2;RPLP2;TK1;EIF5A;ACTR3;CDV3;TPI1;DST;GSTO1;PRMT1;RPS3A;PRSS12;RGMA;NME1;MRPL52;CANX;CKS2;BIRC5;PTMA;RPL12;RPL11;RPS27L;DDX21;SLC3A2;CXXC5;TYMS;NTN1;SRM;PSMB6;LMNA;RPS3;HES1;CCT8;RPS2;RPL15;RPS27A;RPL18;CCT5;RPL19;GADD45GIP1;RANBP1;NPM1;STAT3;RPL35A;RPL23A;DEK;BOP1;BAX;P4HB;PLP2;SSBP1;RAN;TPT1
NUCKS1 24931609 ChIP-Seq HEPATOCYTES Mouse	77/588	2.15E-13	7.95E-12	2.8099	81.9547	ITGB1;RPL5;ARF4;EIF4A1;COL18A1;CSF1;IRS1;ARPC1B;ITSN1;SLC2A1;HSPB1;IRS2;PTPRJ;CLU;CSRP2;CCND1;RAC1;KPNA2;B2M;ACTR3;TLE1;ITGA3;PRMT1;FST;PAWR;GFRA1;FOS;ACTN4;F3;DUSP6;DNM1;AES;NME1;BIN1;NCL;BIRC5;STRAP;ITGA6;TLN1;GAPDH;PTMA;ATF4;CEBPD;SLC3A2;PIK3R1;HSP90B1;SOCS3;CCNB1;RRAS;EIF4EBP1;LRIG1;HES1;SPAG9;VASP;EGR1;JUN;UBE2I;GADD45A;STAT3;PBX3;FN1;HMGA1;PA2G4;ARPC5;SORBS1;EEF2;BMP7;HIPK2;PPP1CA;DLG1;ARPC2;APC;PTPRA;ID2;CPE;CYCS;BAX

MTF2 20144788 ChIP-Seq MESCs Mouse	246/2981	2.22E-13	7.95E-12	1.7791	51.8362	CPNE8;APP;SERPINE2;COL12A1;SOX21;SLC4A4;RPL7;SOX1;EDNRB;DPF3;SOX9;SOX6;IER5;B2M;SOX4;RPS12;HES6;EPHA4;LIMCH1;RUNX1;CLDN5;SFRP1;SFRP2;FNDC4;BIN1;FEZ1;RFX4;PAPPA;HOXB2;KCTD12;COL13A1;INTU;PCDH10;SDC3;TWIST1;APCDD1;GRIN2A;NUAK1;NKAIN3;EPB41L3;PROM1;GPM6B;B4GALNT4;EGR1;JUN;FZD3;FZD2;ST8SIA1;LRRN2;PLK2;MCAM;PBX3;NR2F1;BTBD11;NETO2;NR2F2;GDF6;GNG12;GRIN2B;LARP6;DCLK1;PCDHGA10;ID2;ID4;SDC1;ID3;CPEB2;NRP1;NRP2;PTPRJ;SLC35F1;PRSS23;AKAP13;SLC22A17;TIMP2;NEFL;KIF1A;FGFBP3;CHST7;KCND3;HEG1;ELMOD1;EN2;EMP2;GFRA1;PROX1;RGMB;PRSS12;GFRA2;MLF1;RGMA;GCHFR;ITPKB;CLDN10;GPRC5B;ZEB1;MMP15;PXDN;CDC42EP3;MMP17;CDC42EP1;PLEKHO1;GAS6;PLCB1;NFIX;AHNAK;AMIGO2;NEXN;ADCY2;FIGN;PRICKLE1;NT5E;FRZB;CAMK2N1;GDF10;ARNT2;GSN;SNCAIP;HIPK2;SMOC2;SLCO3A1;NFIA;MSRB3;SEMA5B;SLC27A1;PLXND1;CSF1;IRS1;CTNND2;CLSTN1;CELSR1;ESPN;LOXL1;IGF1R;FADS3;CDH6;CCND2;DACH1;LEPR;PHLDA2;HMGN3;PHLDA1;RGS6;COL27A1;TLE1;SEMA6A;IGFBP5;FST;IGFBP3;TPM2;SEMA6D;APLP2;TPM1;ATP1B2;ILF2;PDIA5;LOX;COL4A2;COL4A1;LY6H;FBN2;RTN1;TMEM59L;SLC1A2;HTRA1;RHOBTB3;LPL;LTBP3;FBLN5;NPAS3;SNTG1;PODXL;PGK1;PMAIP1;IGFBP7;NPTX2;GRIA4;TGFB1;WSCD1;CAV2;CAV1;ARHGAP29;INHBA;MCC;BMP7;H1F0;BMP1;COL5A1;NBEA;PTPRA;P4HA2;CPD;CPE;TPP1;TGFBI;FBN1;ITGB4;FHL2;HMGB3;RERG;SYNE2;LBH;ZIC2;ZIC1;PMEPA1;ITGB8;GRID2;ITGA3;NAV2;DNM1;C1QL1;VCAN;TMBIM4;EEF1D;NOS1AP;ITGA7;CDH13;PLEKHH2;CEBPD;NXN;PON2;LRP2;ADD3;NTN1;NCALD;PTPRZ1;CNR1;ERBB4;SPOCK2;SLIT1;LRIG1;SLITRK5;SLIT2;CACNG4;NTRK2;PCDH7;NTRK3;IRX3;PCDH8;ATP2B1;MARCKS;PPP2R2B;PMP22;PTX3;SPRY1;VIM
SUZ12 20075857 ChIP-Seq MESCs Mouse	329/4356	7.03E-13	2.35E-11	1.6548	46.3072	CPNE8;APP;TES;SERPINE2;FAM89A;COL12A1;ABAT;SOX21;SLC4A4;RPL7;PREX2;SOX1;EDNRB;RPL18A;DPYSL5;DPYSL2;PEG10;DPF3;KIF21A;SOX9;IER5;B2M;SOX4;ANKS1B;HES6;LIMCH1;RUNX1;CLDN5;SFRP1;SFRP2;FNDC4;BIN1;RFX4;PAPPA;RBP1;HOXB2;KCTD12;RPL28;PFN2;COL13A1;PCDH10;SDC3;TWIST1;TMTC2;GRIN2A;NUAK1;NKAIN3;ARSJ;PDGFC;EPB41L3;SERPINH1;TSPAN2;FAM43A;PROM1;N4BP2;GPM6B;EGR1;JUN;FZD3;FZD2;LRRN2;PLK2;MCAM;PBX3;NR2F1;LIF;BTBD11;NR2F2;L1CAM;GDF6;GNG12;GRIN2B;LARP6;DCLK1;NR2F6;PCDHGA10;PCDHB2;ID2;ID4;SDC1;ID3;DCHS1;CPEB2;PAM;SFXN5;TMEM9B;DDR1;NRP1;NRP2;SYNM;ELN;HEXA;PTPRJ;SLC35F1;FMN2;NAT14;PRSS23;SLC22A17;TIMP2;NEFL;KIF1A;FGFBP3;CTSC;APC2;IL11;EDN1;CHST7;TNFRSF12A;GSTO1;KCND3;METRN;HEG1;ELMOD1;EN2;EMP2;GFRA1;FOS;PROX1;RGMB;F3;PRSS12;GFRA2;DUSP6;MLF1;RGMA;MRPL52;GCHFR;ITPKB;GPRC5B;ZEB1;MMP15;PXDN;CDC42EP3;MMP17;FIBI

						N;CDC42EP1;PLEKHO1;GAS6;PLCB1;CD44;NFIX;AHNAK;AMIGO2;NEXN;ADCY2;FIGN;PRICKLE1;PTN;PSMB6;NT5E;FRZB;GPC4;CTNNA2;P4HTM;GDF10;ARNT2;CENPV;GSN;SORT1;MIAT;SNCAIP;HIPK2;SMOC2;SLCO3A1;NFIA;SMOC1;MSRB3;FAM171B;MEGF9;SEMA5B;PLXND1;CSF1;IRS1;CTNND2;CLSTN1;IRS2;CELSR1;ESPN;LOXL1;IGF1R;FADS3;CDH6;NRBP2;CCND2;DACH1;SESN3;NAGLU;PLAU;KIF5C;LEPR;PHLDA2;HMGN3;PHLDA1;RGS6;PHLDA3;COL27A1;SEMA6A;IGFBP5;FST;IGFBP3;TPM2;SEMA6D;TPM1;ATP1B2;PDIA5;PLA2G16;LOX;COL4A2;DOK5;STIM2;COL4A1;RAB34;EEF1A2;TNIK;LY6H;FBN2;RTN1;NTM;ANKRD12;TMEM59L;SLC1A2;HTRA1;RHOBTB3;LPL;SLC1A4;LTBP3;ZFP36L2;FBLN5;NPAS3;CNN2;CNN1;STK33;SNTG1;PODXL;PACSIN3;PMAIP1;IGFBP7;NPTX2;LRRC4C;GRIA4;LRRC4B;TGFB1;AUTS2;SYT1;WSCD1;CAV2;CAV1;ARHGAP29;INHBA;EEF2;MCC;BMP7;GFAP;H1F0;BMP1;COL5A1;NBEA;PTPRA;P4HA2;CPD;CPE;TGFBI;SERINC5;FBN1;FGFR1;ITGB4;FHL2;TSPAN11;RERG;SYNE2;SGCE;LBH;ZIC2;ZIC1;PMEPA1;ITGB8;GRID2;ITGA4;ITGA3;NAV2;DNM1;C1QL1;VCAN;SETBP1;EEF1D;NOS1AP;ITGA7;CDH13;ZMYND10;PLEKHH2;LAMA2;CEBPD;NXN;PON2;IER5L;SRI;LRP2;ADD3;NTN1;THBS1;NCALD;PTPRZ1;PALMD;CNR1;ERBB4;SPOCK2;NT5DC2;SLIT1;LRIG1;SLITRK5;S1PR3;SLIT2;MEST;CACNG4;SLC12A2;NTRK2;PCDH9;PCDH7;NTRK3;IRX3;PCDH8;B3GAT1;FOXJ1;BAIAP3;MARCKS;PPP2R2B;PMP22;PTX3;SPRY1
NANOG 18692474 ChIP-Seq MEFs Mouse	179/1989	7.29E-13	2.35E-11	1.9115	53.4212	SEMA5B;IFITM1;IFITM2;ITSN1;ZBTB20;ENO1;IFIT1;SAT1;HS6ST1;CDH6;SOX2;RPS14;CHCHD2;PSMD7;CAPNS1;RPS19;BASP1;STMN1;MAGOH;PLCE1;KIF21A;PTGFRN;TMSB10;AP2M1;RGS6;RPS13;SOX4;CAST;DDX17;SNRPN;SEMA6A;RPL21;FNBP1;TPM3;RPL23;TPM1;IGFBP2;SARS;ACTN4;ATP1B2;ATP1B1;TUBA4A;ADAM19;EEF1A1;SFRP1;RFX4;SPARCL1;ADAM9;VDAC1;LY6H;EPHA2;RTN3;SET;NNMT;NOTCH1;TTYH1;PDE1A;TWF2;SLC1A3;UQCRH;ZFP36L2;SOCS3;LDHB;ARHGAP21;PRDX4;PODXL;PRDX1;PDGFC;EIF4EBP1;S100A13;PMAIP1;APOE;PROM1;PLTP;S100A10;MCTS1;FZD2;DTNA;XRCC5;ST8SIA1;LRRN2;GADD45A;RDX;FN1;DSTN;ASNS;BTBD11;EIF2S2;PBX1;EIF1;UBE2S;ID2;ID1;PIR;ID3;MDM4;NF2;TGFBI;PAM;RPS23;FGFR1;DDR1;DOCK5;NRP2;B4GALT1;WDR1;RNF13;HEXA;SLC2A1;HMGB3;HMGB1;PRSS23;SGCE;MAP1LC3B;HINT1;TUBA1A;CAPZB;ZIC2;CSRP1;SEC61G;NEFL;SH3BGRL3;UPP1;RAC1;DGCR2;RALGPS2;EDN1;DST;SSR2;HEG1;RPS3A;RGMB;DUSP6;EPN2;NME1;GPRC5B;RCN1;LMBRD1;TUBB2B;MRPL51;PXDN;MYH9;CDH13;ITGA6;CD47;GAPDH;TOMM40;AHNAK;GSTP1;POMP;IER5L;SLC3A2;LRP2;NTN1;COX5A;CST3;NT5E;PTPRZ1;PDPN;LRIG1;DMD;HES1;CCT8;GPC4;SLIT2;JAM2;SLC12A2;NTRK2;RANBP1;TCF7L2;PPP1R14B;PLEKHA4;SORBS1;ACTC1;PPP2R2B;PMP22;SPRY2;VIM;PFKP

SUZ12 18974828 ChIP-Seq MESCs Mouse	175/1934	8.72E-13	2.67E-11	1.9200	53.3145	CPNE8;SEMA5B;APP;SERPINE2;PLXND1;CSF1;IRS1;CTNND2;COL12A1;CLSTN1;LIPA;SOX21;SLC4A4;LOXL1;CDH6;CCND2;DACH1;SOX1;EDNRB;CCND1;DPYSL5;PLAU;LEPR;DPF3;SOX9;PHLDA2;SOX6;IER5;HMGN3;B2M;RGS6;SOX4;EPHA4;COL27A1;SEMA6A;IGFBP5;FST;IGFBP3;SEMA6D;TPM1;RUNX1;CLDN5;SFRP2;LOX;COL4A2;DOK5;BIN1;COL4A1;RFX4;PAPPA;HOXB2;KCTD12;LY6H;FBN2;COL13A1;PCDH10;SLC1A2;HTRA1;TWIST1;LPL;FBLN5;NPAS3;GRIN2A;SNTG1;PODXL;ARSJ;PGK1;TSPAN2;IGFBP7;NPTX2;PROM1;GPM6B;EGR1;JUN;FZD2;TGFB1;AUTS2;LRRN2;CAV2;CAV1;PBX3;NR2F1;ARHGAP29;BTBD11;NR2F2;GDF6;GRIN2B;BMP7;BMP1;COL5A1;ID4;SDC1;ID3;CPEB2;FBN1;NRP1;NRP2;TGFB1I1;FHL2;PTPRJ;SLC35F1;PRSS23;RERG;LBH;ZIC2;ZIC1;TIMP2;NEFL;ITGB8;KIF1A;FGFBP3;GRID2;EDN1;CHST7;ITGA4;KCND3;EN2;GFRA1;PROX1;RGMB;PRSS12;GFRA2;RGMA;C1QL1;ITPKB;GPRC5B;VCAN;MMP15;PXDN;CDC42EP3;MMP17;CDC42EP1;ITGA7;CDH13;PLEKHO1;GAS6;PLCB1;CD44;PLEKHH2;NFIX;CEBPD;PON2;AMIGO2;NEXN;LRP2;PRICKLE1;NTN1;THBS1;NCALD;NT5E;FRZB;CNR1;GPC3;SLIT1;SLITRK5;SLIT2;CACNG4;GDF10;NTRK2;SORT1;PCDH7;NTRK3;IRX3;PCDH8;PDAP1;SNCAIP;SMOC2;SLCO3A1;NFIA;PPP2R2B;PMP22;RPL22L1;PTX3;VIM;MEGF9
KLF4 19030024 ChIP-ChIP MESCs Mouse	144/1502	1.92E-12	5.61E-11	2.0237	54.5990	RPL4;EIF4A1;RPL5;IFITM1;RPL3;IFITM2;SERPINE2;CLSTN1;ARPC5L;ENO1;RPL8;ACTB;ACTG1;RPL7;IFIT2;CDC20;SOX2;CHCHD2;CCND2;SOX1;SESN3;CCND1;RPL18A;DPYSL5;KIF5C;RPS18;STMN1;CFL1;RPL38;SOX9;RPS11;RPS9;SNRPN;TLE1;RPL21;IGFBP5;TPM4;RPS5;RPL22;IGFBP2;RPSA;RUNX1;RFX4;NCL;COL4A5;TAGLN2;RPL27;PPIA;UBA52;ATF4;SET;TMED10;RTN1;NOTCH1;PCDH10;PDE1A;TMEM59L;SLC1A5;LDHB;CCNB1;TSPAN9;PODXL;PRDX1;PDGFC;APOE;VASP;FDPS;JUN;FZD2;TGFB1;FN1;NR2F1;HMGA1;ASNS;NR2F2;PA2G4;GNG12;EIF2S2;PCDHGA10;CCT6A;ID2;ANP32B;RPS23;COL18A1;NRP2;CLIC4;HSP90AB1;RNF13;SLC44A1;PTPRJ;NAT14;RERG;LIMD2;RPL7A;MAP1LC3B;TUBA1A;ZIC1;NEFL;PCMTD1;EIF5A;DST;SSR2;EN2;GFRA1;FOS;PROX1;RGMA;ITPKB;RCN1;TUBB2B;MMP15;COL6A1;BIRC5;STRAP;GAPDH;PTMA;RPL12;DDX21;SLC3A2;FIGN;NTN1;THBS1;TCEAL8;SLIT2;RPL15;MEST;JAM2;RPL19;PPP1R14B;NPM1;PCDH7;IRX3;PCDH8;LAMB1;ATOX1;HIPK2;PSMC5;KLF6;NFIA;PMP22;SPRY2;VIM;SSBP1;MEGF9
SOX9 24532713 ChIP-Seq	135/1384	3.05E-12	8.54E-11	2.0555	54.5036	CPNE8;APP;SLC27A1;IFITM2;ITSN1;TNC;EMC10;ENO1;CELSR1;HS6ST1;IGF1R;RPL18A;KIF21A;SNRPD3;NCKAP5;PHLDA3;RPS12;ACTN1;RPL23;RFX3;MID1;GTF2F2;RUNX1;SFRP1;COL4A2;COL4A1;RPL24;TAGLN2;VDAC1;TNIK;EZR;EPHA2;NTM;TARS;SLC1A4;CACNA1C;IQGAP2;NUAK1;NKAIN3;TSPAN9;PRDX1;PSAP;IGFBP7;APOE;N4BP2;SRGAP1;ABCA1;FZD2;AUTS2;GADD45B;SRD5A1;IQSEC1;CAV1;PBX3;MICAL3;BTBD

HFSC Mouse						11;ARPC5;MCC;PBX1;CCT6A;CCDC88A;COL5A1;ID2;ID4;PIR;SDC1;CPE;SFXN5;ITM2B;DDR1;NRP1;COL18A1;ARF1;TENM2;RNF13;SLC2A1;MAP1LC3B;LBH;TIMP2;PDE4B;ITGB8;TK1;CLIC1;PCMTD1;ACTR3;CDV3;DST;ANXA2;PRMT2;PABPC4;PAWR;EMP2;FOS;NAV2;SRP9;DUSP6;NME1;ITPKB;PKM;PALLD;TAX1BP1;BIRC5;MYH9;ITGA6;PLCB1;PTMA;CD44;NFIX;TOMM40;LAMA2;AHNAK;NXN;PON2;SLC3A2;PTN;SPG7;NCALD;PALMD;PSMB3;NT5DC2;LMNA;GPC3;HES1;TCF7L2;GSN;PCDH7;BBOX1;ATP2B1;ATOX1;KLF6;SMOC1;MSRB3;FAM171B;PFKP;TPT1
WT1 20215353 ChIP-ChIP NEPHRON PROGENITOR Mouse	154/1663	4.51E-12	1.21E-10	1.9521	50.9999	APP;SLC27A1;IRS1;COL12A1;CLSTN1;ARPC5L;CELSR1;SLC4A4;LOXL1;ACTG1;IGF1R;FADS3;SOX2;COL4A3BP;LGALS1;CCND2;DACH1;SESN3;DPYSL5;KIF5C;DPF3;SOX4;COL27A1;TLE1;SEMA6A;TPM4;TPM3;FST;ACTN1;SEMA6D;IGFBP2;RUNX1;BIN1;RBP1;COL4A5;VDAC1;LY6H;PPIA;XPR1;PFN2;FBN2;NOTCH1;COL13A1;FBLIM1;RHOBTB3;TWIST1;TMTC2;UAP1;PIK3R1;ZFP36L2;SLC9A3R2;SOCS3;LDHB;GRIN2A;NUAK1;PDGFC;EIF4EBP1;S100A11;VASP;EGR1;JUN;NDFIP1;TGFB1;SMURF2;UBE2C;MCAM;TMEM132A;NR2F1;HMGA1;NR2F2;ARPC5;L1CAM;GNG12;BMP7;LARP6;PBX1;NR2F6;COL1A2;COL5A1;PTPRA;PTK7;CPD;FXYD6;TPP1;ANP32B;TGFBI;ITGB1;DDR1;COL18A1;HSP90AB1;WDR1;SLC2A1;CHD1;SLC22A17;PEA15;SH3BGRL3;PHGDH;KIF1A;NEO1;CLIC1;RALGPS2;EIF5A;TNFRSF12A;GSTO1;ITGA3;H2AFZ;SSR3;GFRA1;PRSS12;DUSP6;MTSS1;DNM1;APRT;RGMA;RCN1;LMBRD1;TUBB2B;SLC25A5;LRP1;COL11A1;USP11;POMP;MLLT1;FIGN;PTN;CXXC5;ADD3;NTN1;COX5A;THBS1;FRZB;LMNA;PDPN;FYN;GPC4;PDLIM7;GDF10;SVIL;ARNT2;TCF7L2;PCDH7;IRX3;ATP2B1;DEK;SNCAIP;DCBLD2;HIPK2;KLF6;SLCO3A1;NFIA;AXL;SPRY2;PFKP;MEGF9
NELFA 20434984 ChIP-Seq ESCs Mouse	176/2000	8.09E-12	2.08E-10	1.8572	47.4349	EIF4A1;RPL3;ARPC5L;ENO1;SRP14;RPL8;RPL10A;ESPN;ACTB;RPL6;PSMD8;CDC20;PPP1CB;RPS15;TUBB6;CHCHD2;PSMD7;SNRPD2;PTTG1;RPS18;PSMD2;STMN1;CFL1;LAMP2;HCFC1R1;KPNA2;RPS11;IER5;TMSB10;RPS13;IER3;RPS12;HES6;RPS9;WSB1;RPL21;FNBP1;RPL23;APLP2;RPS6;RFX3;ACTN4;ATP1B2;ATP1B1;ILF2;TUBA4A;EEF1A1;MYL6;PPA1;STIM2;NCL;UQCRC1;SNRPG;ADAM9;VDAC2;TAGLN2;VDAC1;AURKAIP1;PPIA;RPL28;ATF4;EPHA2;RTN3;RBM8A;SLC1A4;SLC1A5;SLC5A3;GLG1;ZFP36L2;HSP90B1;SOCS3;PRDX1;PSAP;EIF4EBP1;PMAIP1;APOE;NPTX2;BTF3;NMB;NDFIP1;GADD45B;SMURF2;UBE2C;GADD45A;IDH1;FN1;HMGA1;ASNS;BTBD11;PA2G4;EEF2;RPS27;ARPC2;NACA;HIST1H4C;CNIH4;SERINC5;RPS24;FGFR1;ARF1;SLC25A3;CLIC4;HSP90AB1;BTG1;B4GALT1;WDR1;HMGB2;SLC2A1;CLTA;HMGB1;HINT1;CSRP2;SEC61G;RPLP2;PCMTD1;DGCR2;RBM6;CAP1;TPI1;TNFRSF12A;H2AFZ;RGMB;DUSP6;APRT;ITPKB;SLC7A5;IQCK;PSMA4;EEF1D;CANX;CKS2;TAX1BP1;BIRC5;MYH9;GAPDH;PTMA;ASAH1;SLC20A1;RPL12;RPL11;I

	ER5L;RPS27L;DDX21;SLC3A2;SPG7;ADD3;PSMA7;PSMB6;ZNRF3;PSMB2;PSMB3;PSMB1;RPS3;RPL13;HES1;CCT8;RPS2;RPS27A;CCT5;PDLIM7;RPL19;GADD45GIP1;RANBP1;NPM1;PDAP1;RPL23A;ATOX1;PPP1CA;BOP1;KLF6;APC;PSMC4;RPL22L1;P4HB;SSBP1;MEGF9

Supplemental Table 4.15. HD iAstro snRNA-seq Cluster Markers

Gene	p_val	avg_logFC	p_val_adj	cluster
SPARCL1	0	0.7403	0	0
GPM6B	0	0.6376	0	0
PTPRZ1	0	0.6120	0	0
NTRK2	0	0.6024	0	0
ATP1B1	0	0.5812	0	0
PTN	0	0.5769	0	0
SPOCK2	0	0.5769	0	0
TTYH1	0	0.5621	0	0
CPE	0	0.5513	0	0
NKAIN3	0	0.5481	0	0
S100B	9.59E-188	0.4977	1.92E-184	1
COL27A1	1.99E-50	0.4337	3.98E-47	1
LGALS3	1.30E-154	0.3689	2.60E-151	1
B2M	0	0.3388	0	1
ACAT2	7.81E-27	0.2914	1.56E-23	1
IFITM3	2.18E-205	0.2765	4.35E-202	1
IGFBP7	1.89E-296	0.5507	3.79E-293	2
PLAU	2.48E-273	0.4555	4.97E-270	2
LBH	5.27E-287	0.4497	1.05E-283	2
COL4A1	0	0.4392	0	2
CAV1	0	0.4372	0	2
SLC3A2	8.96E-285	0.4299	1.79E-281	2
CALD1	0	0.4072	0	2
PALLD	0	0.4057	0	2
ANXA2	0	0.4004	0	2
FILIP1L	2.29E-225	0.3934	4.58E-222	2
CENPF	0	1.7564	0	3
TOP2A	0	1.5341	0	3
MKI67	0	1.4276	0	3
NUSAP1	0	1.1215	0	3
CCNB1	0	1.0219	0	3
HMGB2	0	1.0106	0	3
SMC2	0	0.9605	0	3
KPNA2	0	0.9597	0	3
H2AFX	0	0.9514	0	3
ASPM	0	0.9315	0	3

SNTG1	3.53E-72	0.8295	7.06E-69	4
NEAT1	3.50E-06	0.5850	0.007004755687	4
MIAT	8.82E-44	0.4959	1.76E-40	4
LRRC4C	1.61E-48	0.4704	3.22E-45	4
CCDC102B	7.65E-279	0.4443	1.53E-275	4
ADGRV1	1.80E-89	0.4134	3.60E-86	4
COL27A1	1.00E-99	0.4090	2.00E-96	4
LRRIQ1	1.27E-122	0.3699	2.54E-119	4
C1orf61	5.63E-12	0.3674	1.13E-08	4
SOX6	0	0.3347	0	4
FN1	0	2.3829	0	5
COL6A3	0	2.3107	0	5
POSTN	0	2.2967	0	5
COL1A1	0	2.0793	0	5
COL6A2	0	2.0338	0	5
GREM1	0	1.9964	0	5
COL6A1	0	1.9851	0	5
COL1A2	0	1.8093	0	5
COL5A1	0	1.4095	0	5
COL3A1	0	1.3881	0	5
HLA-DPA1	0	2.1445	0	6
HLA-DRA	0	2.0929	0	6
HLA-DPB1	0	1.6887	0	6
CD74	0	1.6603	0	6
HLA-DRB5	0	1.4570	0	6
HLA-DMA	0	1.3676	0	6
HLA-DQA1	0	1.3040	0	6
HLA-B	0	1.2242	0	6
HLA-DQB1	0	1.2133	0	6
HLA-DRB1	0	1.0935	0	6
C21orf58	2.05E-136	1.1320	4.10E-133	7
PIF1	2.54E-06	0.9252	0.005075050874	7
ASPM	1.60E-42	0.8882	3.20E-39	7
NUSAP1	6.85E-76	0.8227	1.37E-72	7
FANCA	5.15E-93	0.8188	1.03E-89	7
HELLS	2.06E-38	0.7768	4.13E-35	7
MIS18BP1	1.14E-20	0.7724	2.27E-17	7
EZH2	1.40E-80	0.7477	2.79E-77	7
ATAD5	1.43E-53	0.7331	2.86E-50	7

ORC6	5.58E-44	0.6835	1.12E-40	7
HES5	5.43E-289	2.1540	1.09E-285	8
HES6	1.56E-192	2.0216	3.13E-189	8
STMN2	9.66E-49	1.4012	1.93E-45	8
THSD7A	1.05E-41	1.3843	2.11E-38	8
SOX4	3.57E-131	1.2963	7.13E-128	8
CD24	8.29E-117	1.2784	1.66E-113	8
MIAT	1.01E-101	1.2709	2.03E-98	8
SOX11	9.74E-118	1.2532	1.95E-114	8
ROBO3	2.25E-47	1.0343	4.50E-44	8
DCC	4.57E-75	0.9090	9.14E-72	8

Supplemental Table 4.16. HD iAstro Significant Differentially Expressed Genes Per Cluster

Gene	p_val	avg_logFC	pct.1	pct.2	p_val_adj	Cluster
SPARCL1	0	0.7403367652	0.969	0.913	0	0
GPM6B	0	0.6375989349	1	0.999	0	0
PTPRZ1	0	0.6119934756	0.994	0.949	0	0
NTRK2	0	0.6024082282	0.978	0.902	0	0
ATP1B1	0	0.5811963294	0.902	0.803	0	0
PTN	0	0.5769481789	1	1	0	0
SPOCK2	0	0.5768829042	0.916	0.857	0	0
TTYH1	0	0.5620733809	0.991	0.947	0	0
CPE	0	0.5512512361	0.997	0.96	0	0
NKAIN3	0	0.5480882172	0.879	0.806	0	0
CCND2	0	0.5353226647	0.886	0.82	0	0
GPM6A	0	0.5156195573	0.988	0.93	0	0
MLC1	0	0.5122056543	0.939	0.84	0	0
A2M	0	0.5031541774	1	1	0	0
PLTP	0	0.5007941996	0.97	0.893	0	0
DDR1	0	0.496637271	0.983	0.901	0	0
PI15	0	0.4919402177	0.82	0.817	0	0
FBLN5	0	0.48776111	0.87	0.826	0	0
HTRA1	0	0.4826288505	0.97	0.899	0	0
FGFBP3	0	0.4808108115	0.926	0.873	0	0
SMOC1	0	0.4789943232	0.806	0.803	0	0
CRISPLD1	0	0.4744906609	0.882	0.792	0	0
CTGF	0	0.4700303077	0.996	0.985	0	0
SERPINE2	0	0.4643326089	0.891	0.824	0	0
WLS	0	0.4604012596	0.997	0.97	0	0
CLU	0	0.4580670753	1	0.993	0	0
SARAF	0	0.457892451	0.997	0.962	0	0
SYT11	0	0.4548670975	0.928	0.818	0	0
ID4	0	0.4508887584	0.931	0.847	0	0
PLPPR3	0	0.4478238493	0.901	0.813	0	0
APLP2	0	0.4438268053	0.996	0.945	0	0
AC120042.3	0	0.4374222687	0.807	0.735	0	0
KIF5C	0	0.4366028849	0.943	0.852	0	0
SYNM	0	0.4356887943	0.936	0.868	0	0
NTN1	0	0.4283840339	0.85	0.724	0	0

C1QL1	0	0.4223115703	0.987	0.938	0	0
PEG10	0	0.4221894627	0.965	0.852	0	0
CRB2	0	0.4211333956	0.895	0.809	0	0
TMEM47	0	0.4207209658	0.895	0.801	0	0
LY6H	0	0.4041888828	0.99	0.967	0	0
GRIA1	0	0.4006603948	0.96	0.889	0	0
WSCD1	0	0.3964236855	0.844	0.803	0	0
CP	0	0.3938408832	0.917	0.874	0	0
PCSK1N	0	0.387994304	0.945	0.836	0	0
APLP1	0	0.3860091128	0.877	0.735	0	0
PON2	0	0.3853257319	0.991	0.942	0	0
GDF10	0	0.3808389644	0.846	0.824	0	0
SOX2	0	0.3739615954	0.973	0.883	0	0
PCDH10	0	0.372022714	0.788	0.784	0	0
SFRP1	0	0.3706621764	0.859	0.791	0	0
NFIA	0	0.3675646925	0.855	0.783	0	0
TMEM132A	0	0.3663585509	0.926	0.831	0	0
SLIT1	0	0.3636431286	0.741	0.73	0	0
ENPP2	0	0.3632020774	0.829	0.788	0	0
FJX1	0	0.3611744463	0.852	0.767	0	0
FAM171B	0	0.3610295939	0.793	0.765	0	0
APP	0	0.3602616385	0.992	0.91	0	0
EDNRB	0	0.3557967499	0.787	0.777	0	0
CYR61	0	0.3506233235	0.993	0.959	0	0
LRRC4B	0	0.348549959	0.811	0.685	0	0
FIBIN	0	0.342541175	0.805	0.792	0	0
GPRC5B	0	0.3413046925	0.839	0.778	0	0
ADAM9	0	0.3411353725	0.971	0.888	0	0
NETO2	0	0.3407283979	0.88	0.817	0	0
PAM	0	0.3386035518	0.924	0.856	0	0
MAP1B	0	0.3383162473	1	0.989	0	0
PLD3	0	0.3378624053	0.994	0.946	0	0
APC2	0	0.3338890039	0.81	0.77	0	0
DKK3	0	0.3337304525	0.958	0.855	0	0
CDH6	0	0.3317149158	0.901	0.845	0	0
GPC4	0	0.3295927408	0.959	0.891	0	0
GPC3	0	0.3262326703	0.818	0.798	0	0
LRP2	0	0.3254982976	0.841	0.821	0	0
FSTL5	0	0.3238701089	0.765	0.777	0	0

SDC3	0	0.3229178677	0.85	0.796	0	0
DCLK1	0	0.3180995892	0.93	0.873	0	0
ATP1B2	0	0.3179535407	0.722	0.687	0	0
HSPA5	0	0.3171625551	0.997	0.963	0	0
GRN	0	0.3159455768	0.96	0.844	0	0
RTN1	0	0.3079953065	0.748	0.726	0	0
IGFBP2	0	0.3076682792	1	0.999	0	0
ITM2B	0	0.3064191315	0.996	0.953	0	0
CEBPD	0	0.3062810893	0.814	0.808	0	0
SOCS3	0	0.3062699088	0.789	0.723	0	0
MAP2	0	0.3050914062	0.93	0.872	0	0
TENM2	0	0.3012003349	0.913	0.835	0	0
ZNF106	0	0.2986749123	0.83	0.742	0	0
PODXL2	0	0.2959989712	0.71	0.571	0	0
TFPI	0	0.2956763227	0.775	0.759	0	0
PCDH9	0	0.2944497702	0.911	0.866	0	0
ATP2B1	0	0.2915601542	0.886	0.789	0	0
KIF1A	0	0.2897551097	0.862	0.741	0	0
COL11A1	0	0.2897068192	0.921	0.861	0	0
SDC2	0	0.2892598591	0.958	0.819	0	0
GSN	0	0.2892150039	0.913	0.84	0	0
JAM2	0	0.2890899366	0.834	0.725	0	0
LAPTM4B	0	0.2880094323	0.916	0.774	0	0
TUBB2B	0	0.2864246866	0.999	0.994	0	0
ITGA6	0	0.2836208227	0.664	0.63	0	0
LRRN3	0	0.2802799611	0.832	0.649	0	0
PROM1	0	0.2763790467	0.779	0.776	0	0
RETREG1	0	0.2751740721	0.729	0.747	0	0
PLS3	0	0.2730548743	0.929	0.872	0	0
TENM3	0	0.271152974	0.939	0.827	0	0
NR2F1	0	0.2707154931	0.951	0.916	0	0
TM7SF2	0	0.2699754208	0.849	0.712	0	0
RAB31	0	0.2674503159	0.871	0.801	0	0
JUN	0	0.26727202	0.982	0.901	0	0
SSPN	0	0.266994353	0.745	0.682	0	0
NDFIP1	0	0.2663999673	0.98	0.925	0	0
SPRY1	0	0.2658191214	0.878	0.819	0	0
NEFL	0	0.2653812459	0.857	0.834	0	0
EFNB2	0	0.2640179789	0.915	0.793	0	0

C1GALT1	0	0.2625007865	0.828	0.773	0	0
BCHE	0	0.2615192104	0.698	0.697	0	0
CALCRL	0	0.2600363978	0.76	0.744	0	0
NPTX2	0	0.2588078703	0.69	0.623	0	0
ITGB8	0	0.2570023649	0.887	0.841	0	0
SOX9	0	0.2562125001	0.818	0.749	0	0
LYPD1	0	0.2556371486	0.923	0.818	0	0
NPAS3	0	0.2546851734	0.877	0.791	0	0
EMC10	0	0.2528623775	0.801	0.703	0	0
MSMO1	0	0.2514572781	0.86	0.731	0	0
DOK5	0	0.2505443277	0.807	0.708	0	0
HLA-DQA1	0	-0.2536004928	0.606	0.76	0	0
TAGLN	0	-0.296527538	0.984	0.976	0	0
TUBA1B	0	-0.3255185339	0.997	0.988	0	0
TPM1	0	-0.333450833	0.973	0.964	0	0
S100A10	0	-0.3648596087	0.676	0.78	0	0
S100A11	0	-0.3662638696	0.801	0.855	0	0
H2AFZ	0	-0.4433674676	0.902	0.898	0	0
LGALS1	0	-0.5295469868	0.947	0.949	0	0
GREM1	0	-0.6174014179	0.549	0.66	0	0
COL1A1	0	-0.8998830212	0.972	0.978	0	0
POSTN	0	-0.9527296206	0.759	0.845	0	0
FN1	0	-1.19144229	0.938	0.953	0	0
PLPP3	1.15E-278	0.2677509549	0.632	0.644	2.30E-275	0
IQGAP2	1.59E-277	0.2575513918	0.788	0.771	3.19E-274	0
MKI67	2.18E-269	-0.6855415172	0.349	0.542	4.36E-266	0
COL6A3	3.48E-254	-0.8699737708	0.716	0.814	6.97E-251	0
MMP15	1.00E-241	0.2522342496	0.696	0.692	2.00E-238	0
HLA-DPB1	6.55E-223	-0.3428260612	0.655	0.789	1.31E-219	0
GDPD2	4.35E-202	0.2736654533	0.689	0.722	8.71E-199	0
IGFBP7	2.10E-200	-0.3918004343	0.829	0.819	4.19E-197	0
HMGN2	6.22E-196	-0.3427780002	0.818	0.8	1.24E-192	0
GFAP	1.08E-186	0.444486928	0.79	0.831	2.16E-183	0
CALD1	1.35E-183	-0.3268755296	0.999	0.993	2.70E-180	0
TGFBI	1.40E-182	-0.3744636477	0.721	0.75	2.80E-179	0
C21orf58	4.36E-182	-0.3072167121	0.422	0.579	8.71E-179	0
C1orf61	1.72E-178	0.2567760216	0.86	0.867	3.43E-175	0
PCDH8	8.77E-173	0.3736587797	0.747	0.766	1.75E-169	0
STMN1	1.54E-161	-0.2683812767	0.944	0.9	3.08E-158	0

DLGAP5	6.96E-151	-0.2693951708	0.258	0.451	1.39E-147	0
TOP2A	1.70E-149	-0.7953417364	0.361	0.528	3.39E-146	0
CENPK	1.55E-145	-0.260175266	0.463	0.59	3.11E-142	0
HLA-DRA	2.76E-144	-0.545911737	0.913	0.935	5.51E-141	0
SGO2	5.18E-137	-0.3029219334	0.412	0.556	1.04E-133	0
TNFRSF11B	6.42E-137	0.2722680524	0.66	0.724	1.28E-133	0
TMPO	9.06E-135	-0.3369302355	0.373	0.518	1.81E-131	0
HLA-DPA1	4.33E-134	-0.4993065626	0.721	0.82	8.66E-131	0
MYH9	3.26E-133	-0.3265998811	0.772	0.756	6.52E-130	0
CENPM	5.49E-128	-0.2553359829	0.279	0.457	1.10E-124	0
TPM4	1.14E-121	-0.2521072581	0.849	0.824	2.28E-118	0
CD74	6.48E-120	-0.3849538703	0.748	0.829	1.30E-116	0
SMC2	1.98E-112	-0.3315599298	0.575	0.682	3.96E-109	0
COL6A2	8.74E-108	-0.6456548734	0.813	0.864	1.75E-104	0
PRSS35	4.41E-106	0.2624783096	0.572	0.635	8.82E-103	0
NUSAP1	1.64E-105	-0.5585909384	0.312	0.466	3.28E-102	0
TPX2	2.13E-103	-0.3721057528	0.302	0.461	4.25E-100	0
HMGB2	2.68E-100	-0.5046153245	0.479	0.557	5.36E-97	0
ATP1A2	9.44E-98	0.3586023491	0.695	0.75	1.89E-94	0
CENPE	2.50E-90	-0.3724301269	0.461	0.549	5.00E-87	0
CENPF	4.49E-88	-0.9825389284	0.523	0.571	8.98E-85	0
COL5A1	7.86E-88	-0.3881574558	0.595	0.654	1.57E-84	0
PHGDH	2.21E-85	-0.3324528737	0.635	0.659	4.42E-82	0
NNMT	9.27E-83	-0.3017225876	0.52	0.566	1.85E-79	0
ASPM	1.07E-82	-0.4548474724	0.31	0.461	2.15E-79	0
CYP1B1	3.21E-79	-0.3475720803	0.498	0.583	6.43E-76	0
LOX	4.09E-65	-0.2586216035	0.581	0.636	8.17E-62	0
HELLS	1.78E-64	-0.2686052247	0.48	0.575	3.56E-61	0
NUF2	2.40E-64	-0.2603313047	0.296	0.438	4.79E-61	0
KPNA2	5.62E-60	-0.4329825364	0.578	0.604	1.12E-56	0
KCNQ1OT1	2.41E-55	-0.3592922655	0.569	0.676	4.82E-52	0
TYMS	5.49E-52	-0.3577460755	0.407	0.5	1.10E-48	0
CDK1	3.71E-47	-0.3817627502	0.359	0.473	7.42E-44	0
INHBA	5.50E-45	-0.2929559941	0.517	0.46	1.10E-41	0
FBN1	2.29E-44	-0.3209340638	0.46	0.538	4.59E-41	0
ZWINT	5.21E-43	-0.2585659486	0.352	0.464	1.04E-39	0
PTTG1	1.18E-36	-0.384756496	0.506	0.55	2.36E-33	0
UBE2S	1.52E-35	-0.2947123318	0.631	0.633	3.04E-32	0
SCG2	1.08E-31	0.3055769844	0.773	0.791	2.16E-28	0

PBK	4.84E-25	-0.296078243	0.414	0.497	9.68E-22	0
RRM2	1.23E-24	-0.2703661711	0.261	0.317	2.46E-21	0
DCBLD2	3.22E-23	-0.2884113896	0.766	0.71	6.44E-20	0
H2AFX	4.73E-22	-0.3523925165	0.672	0.658	9.46E-19	0
HIST1H4C	9.22E-21	-0.2503981427	0.362	0.445	1.84E-17	0
SLC1A5	1.04E-19	-0.2708568153	0.469	0.515	2.08E-16	0
MXD3	1.64E-19	-0.251117158	0.334	0.37	3.27E-16	0
UBE2T	2.26E-16	-0.2535520922	0.319	0.419	4.51E-13	0
CKS2	5.27E-14	-0.2983174275	0.359	0.441	1.05E-10	0
CCNB1	3.76E-11	-0.4518440444	0.423	0.471	7.53E-08	0
LAMB1	1.89E-10	-0.2595449754	0.614	0.591	3.77E-07	0
HES6	1.85E-09	-0.2555781203	0.426	0.436	3.70E-06	0
COL6A1	2.88E-09	-0.5168278607	0.929	0.908	5.77E-06	0
UBE2C	9.08E-08	-0.40794192	0.335	0.415	0.0001816121821	0
MCM7	3.23E-07	-0.2764900547	0.399	0.468	0.0006454807488	0
PCLAF	5.03E-07	-0.3254344523	0.365	0.437	0.001005549325	0
BIRC5	5.25E-07	-0.2681445972	0.234	0.373	0.001050120929	0
TACC3	2.16E-06	-0.3040844788	0.319	0.405	0.004329037677	0
CLSPN	1.70E-05	-0.341176869	0.374	0.405	0.03405686469	0
SMC4	1.89E-05	-0.3821131065	0.606	0.568	0.03786019621	0
KIF20B	8.63E-05	-0.2890216893	0.428	0.446	0.1726470558	0
B2M	0	0.3388170772	1	0.997	0	1
DACH1	0	-0.2520667739	0.585	0.659	0	1
MIS18BP1	0	-0.2528853392	0.176	0.494	0	1
SIPA1L2	0	-0.2570550951	0.392	0.697	0	1
SLIT2	0	-0.2587346661	0.568	0.645	0	1
FRRS1L	0	-0.2600897015	0.4	0.645	0	1
ZNRF3	0	-0.2661949298	0.268	0.596	0	1
RRBP1	0	-0.2681567077	0.552	0.735	0	1
ABCA1	0	-0.2693640955	0.887	0.79	0	1
SPRY2	0	-0.2716146119	0.57	0.742	0	1
ATP1B2	0	-0.2740484764	0.661	0.706	0	1
JUNB	0	-0.275387215	0.574	0.688	0	1
TGFB2	0	-0.2779451306	0.392	0.651	0	1
JAM2	0	-0.2786292583	0.693	0.774	0	1
HLA-DPA1	0	-0.2900848137	0.981	0.751	0	1
HLA-E	0	-0.2959530774	0.699	0.733	0	1
P4HB	0	-0.2968958359	0.85	0.913	0	1
PPP1R14C	0	-0.297091434	0.799	0.739	0	1

LRRN3	0	-0.2973625643	0.548	0.741	0	1
OLFML2B	0	-0.2995978841	0.48	0.662	0	1
DPYSL5	0	-0.3027661626	0.692	0.729	0	1
TNIK	0	-0.304960233	0.481	0.703	0	1
ZMAT3	0	-0.3051923697	0.475	0.718	0	1
CALCRL	0	-0.3076065274	0.865	0.727	0	1
NPTX2	0	-0.3102430569	0.447	0.683	0	1
LHFPL6	0	-0.3157293723	0.628	0.746	0	1
LPL	0	-0.3222411393	0.461	0.532	0	1
SDC2	0	-0.3278627755	0.744	0.888	0	1
EGR1	0	-0.3297067277	0.871	0.811	0	1
NFIA	0	-0.3315711917	0.869	0.795	0	1
SUPT16H	0	-0.3329419624	0.404	0.688	0	1
NPAS3	0	-0.3330714183	0.825	0.819	0	1
HSP90AB1	0	-0.3333109406	0.943	0.955	0	1
SOCS3	0	-0.3375473103	0.758	0.743	0	1
TACC1	0	-0.3388528825	0.806	0.806	0	1
MAP1B	0	-0.3433712385	0.999	0.991	0	1
ENPP2	0	-0.3446234378	0.973	0.769	0	1
GPM6B	0	-0.3503923004	1	0.999	0	1
SARAF	0	-0.3565484741	0.989	0.971	0	1
APLP2	0	-0.3577177576	0.99	0.957	0	1
DDR1	0	-0.3625127122	0.989	0.917	0	1
SEPT11	0	-0.3648029353	0.805	0.888	0	1
PLS3	0	-0.3650364136	0.985	0.874	0	1
NR2F2	0	-0.368197869	0.918	0.859	0	1
FIBIN	0	-0.3704947047	0.975	0.763	0	1
NR2F1	0	-0.3709424899	0.992	0.915	0	1
AKAP12	0	-0.3724383345	0.506	0.743	0	1
FOS	0	-0.3831312459	0.875	0.829	0	1
MLC1	0	-0.383365879	0.927	0.863	0	1
MARCKSL1	0	-0.3900850972	0.84	0.926	0	1
HSPA5	0	-0.3976976753	0.977	0.974	0	1
CCND2	0	-0.3999755197	0.963	0.819	0	1
PTMA	0	-0.4003536095	0.977	0.955	0	1
LRRC4B	0	-0.4017862409	0.636	0.744	0	1
ID4	0	-0.4054473602	0.917	0.867	0	1
COL5A2	0	-0.4127447852	0.741	0.86	0	1
TOP2A	0	-0.4144167398	0.286	0.507	0	1

PRKDC	0	-0.4182782393	0.707	0.849	0	1
SYT11	0	-0.4286555889	0.89	0.848	0	1
GPC4	0	-0.4311040715	0.983	0.901	0	1
NTN1	0	-0.4330663535	0.745	0.77	0	1
PKM	0	-0.4368551008	0.873	0.895	0	1
CRISPLD1	0	-0.446867492	0.847	0.817	0	1
ATP2B1	0	-0.4486660231	0.83	0.82	0	1
AC120042.3	0	-0.449339337	0.809	0.749	0	1
KIF5C	0	-0.4512611904	0.983	0.864	0	1
CXXC5	0	-0.4580292834	0.554	0.758	0	1
SNTG1	0	-0.4580699386	0.935	0.885	0	1
SERPINE2	0	-0.4584166237	0.963	0.825	0	1
CDH6	0	-0.4587096278	0.955	0.846	0	1
PALLD	0	-0.4678133643	0.747	0.871	0	1
CRB2	0	-0.4745145955	0.897	0.826	0	1
PTPRZ1	0	-0.4791296407	0.995	0.959	0	1
NTRK2	0	-0.4807817034	0.987	0.916	0	1
JUN	0	-0.4852742051	0.927	0.928	0	1
MYH10	0	-0.4930894212	0.543	0.811	0	1
CENPF	0	-0.4943814037	0.396	0.585	0	1
NKAIN3	0	-0.4970851654	0.969	0.804	0	1
APP	0	-0.4990171694	0.92	0.94	0	1
ATP1B1	0	-0.5024442515	0.891	0.826	0	1
ARID5B	0	-0.509098872	0.77	0.886	0	1
ITGB1	0	-0.5375124118	0.885	0.923	0	1
SOX4	0	-0.5500091522	0.703	0.885	0	1
SPOCK2	0	-0.5921533284	0.982	0.857	0	1
PEG10	0	-0.6542701626	0.815	0.903	0	1
COL12A1	1.69E-305	-0.3229386534	0.928	0.824	3.39E-302	1
TENM3	1.97E-305	-0.3380286588	0.824	0.872	3.95E-302	1
NASP	1.79E-302	-0.3284318078	0.577	0.803	3.58E-299	1
RHOBTB3	5.20E-302	-0.3720504511	0.923	0.929	1.04E-298	1
COL11A1	2.87E-300	-0.3901046018	0.907	0.876	5.74E-297	1
APLP1	3.80E-300	-0.3671885671	0.791	0.781	7.60E-297	1
FAM20C	5.85E-300	-0.2512283251	0.724	0.658	1.17E-296	1
CAMK2N1	1.34E-287	-0.3237855271	0.981	0.851	2.68E-284	1
TFPI	4.41E-285	-0.3425890845	0.871	0.745	8.82E-282	1
SFRP1	6.84E-284	-0.5467688806	0.964	0.785	1.37E-280	1
EFNB2	2.73E-282	-0.3640197336	0.8	0.84	5.46E-279	1

PARP1	9.66E-282	-0.2621052086	0.651	0.771	1.93E-278	1
SOX2	9.58E-280	-0.4187053601	0.979	0.901	1.92E-276	1
GRIA1	1.88E-278	-0.2836342073	0.984	0.9	3.76E-275	1
ENC1	7.17E-278	-0.2737690812	0.578	0.787	1.43E-274	1
CPE	1.13E-273	-0.2936705279	0.995	0.968	2.26E-270	1
MAP1A	2.57E-273	-0.3288115084	0.888	0.774	5.14E-270	1
ASAH1	7.46E-273	-0.2754572962	0.586	0.782	1.49E-269	1
HERPUD1	1.39E-272	-0.2573976941	0.53	0.697	2.79E-269	1
MMP15	3.98E-271	-0.2636343388	0.756	0.682	7.95E-268	1
FJX1	5.56E-266	-0.4066122306	0.862	0.782	1.11E-262	1
FILIP1L	5.59E-262	-0.2906960391	0.617	0.766	1.12E-258	1
HLA-C	2.86E-261	-0.3947798763	0.785	0.873	5.73E-258	1
WSCD1	1.84E-258	-0.4282985428	0.976	0.787	3.68E-255	1
ZNF106	1.14E-254	-0.3262558336	0.828	0.761	2.29E-251	1
GRN	3.39E-254	-0.3210867184	0.928	0.874	6.78E-251	1
CALU	1.35E-253	-0.267000649	0.8	0.876	2.70E-250	1
PCDH9	3.35E-253	-0.2654811539	0.972	0.864	6.70E-250	1
MMP2	3.87E-251	-0.3785676443	0.887	0.883	7.73E-248	1
PAM	3.45E-247	-0.2541558024	0.983	0.859	6.91E-244	1
COL4A2	8.22E-241	-0.2783357469	0.905	0.92	1.64E-237	1
LYPD1	5.94E-239	-0.2981181733	0.868	0.851	1.19E-235	1
FBLN5	1.79E-227	-0.3865236964	0.919	0.826	3.57E-224	1
MT-CO1	1.31E-226	-0.2536849503	0.979	0.968	2.62E-223	1
APC2	8.02E-226	-0.3105697952	0.961	0.75	1.60E-222	1
PEA15	7.62E-224	-0.2716408756	0.719	0.83	1.52E-220	1
KIF1A	4.83E-220	-0.3312530426	0.801	0.778	9.67E-217	1
SPARCL1	6.34E-220	-0.4393395821	0.991	0.921	1.27E-216	1
GPC1	1.14E-214	-0.2686947713	0.863	0.823	2.29E-211	1
FAM89A	8.82E-214	-0.2556559012	0.934	0.827	1.76E-210	1
SMC1A	1.40E-212	-0.2705785051	0.791	0.731	2.81E-209	1
DKK3	1.90E-208	-0.2839470937	0.892	0.889	3.81E-205	1
CEBPD	7.19E-208	-0.3342375557	0.956	0.783	1.44E-204	1
GSN	2.64E-206	-0.2851840269	0.961	0.846	5.28E-203	1
TUBB	3.28E-206	-0.2672762079	0.94	0.968	6.55E-203	1
COL4A1	1.10E-205	-0.3128627706	0.939	0.936	2.20E-202	1
SYNM	1.62E-205	-0.3156932563	0.986	0.873	3.24E-202	1
IFITM3	2.18E-205	0.2765188609	0.998	0.986	4.35E-202	1
PMEPA1	2.77E-189	-0.2549869194	0.717	0.769	5.54E-186	1
MYH9	3.07E-189	-0.3193956951	0.682	0.776	6.15E-186	1

S100B	9.59E-188	0.4976913459	0.998	0.982	1.92E-184	1
LRP2	4.13E-184	-0.2887481386	0.983	0.799	8.26E-181	1
PLTP	5.15E-174	-0.252928198	0.979	0.907	1.03E-170	1
FAM171B	1.80E-167	-0.2596207981	0.945	0.742	3.60E-164	1
SLC3A2	6.02E-167	-0.2677711011	0.873	0.908	1.20E-163	1
MKI67	1.88E-164	-0.3302066623	0.482	0.477	3.77E-161	1
CYR61	8.47E-161	-0.3505027062	0.973	0.969	1.69E-157	1
GPM6A	5.72E-159	-0.257042491	0.989	0.942	1.14E-155	1
TMEM47	1.54E-155	-0.274484611	0.979	0.805	3.09E-152	1
LGALS3	1.30E-154	0.3689462352	0.953	0.938	2.60E-151	1
SERPINE1	3.34E-154	-0.2972718784	0.57	0.626	6.67E-151	1
GDF10	2.67E-143	-0.3150183531	0.978	0.804	5.34E-140	1
HLA-A	2.19E-142	-0.2637243523	0.848	0.879	4.38E-139	1
MEST	3.88E-135	-0.277242432	0.688	0.743	7.77E-132	1
CTGF	1.34E-124	-0.4014150633	0.993	0.988	2.68E-121	1
COL3A1	3.17E-97	-0.2735246391	0.959	0.881	6.34E-94	1
SPRY1	1.16E-93	-0.2540994106	0.966	0.815	2.31E-90	1
TPM2	3.17E-92	-0.3886303773	0.842	0.775	6.33E-89	1
NETO2	2.90E-80	-0.2721727089	0.972	0.813	5.80E-77	1
PCDH10	7.15E-72	-0.2644590315	0.975	0.75	1.43E-68	1
IQGAP2	1.92E-70	-0.2622543052	0.97	0.741	3.83E-67	1
SLIT1	1.75E-63	-0.2628837904	0.857	0.711	3.50E-60	1
COL27A1	1.99E-50	0.4336548904	0.89	0.663	3.98E-47	1
HLA-DRB5	2.02E-29	-0.2606922346	0.967	0.664	4.05E-26	1
ACAT2	7.81E-27	0.2914045529	0.694	0.686	1.56E-23	1
SMOC1	3.97E-11	-0.3829519183	0.977	0.772	7.94E-08	1
IGFBP7	2.31E-10	-0.2883661166	0.849	0.817	4.61E-07	1
COL4A1	0	0.439154737	0.995	0.928	0	2
CAV1	0	0.4371708259	0.961	0.799	0	2
CALD1	0	0.4071927632	0.999	0.994	0	2
PALLD	0	0.4057296334	0.976	0.833	0	2
ANXA2	0	0.400402495	0.997	0.972	0	2
TAGLN	0	0.38774272	0.996	0.976	0	2
AL139393.2	0	0.3784852457	0.813	0.552	0	2
MYH9	0	0.367899153	0.948	0.734	0	2
CAVIN1	0	0.3670720881	0.915	0.667	0	2
MYLK	0	0.3342070322	0.939	0.704	0	2
PKM	0	0.3153687357	0.984	0.878	0	2
TRAM2	0	0.2548842245	0.841	0.53	0	2

FABP7	0	-0.4249181464	1	0.998	0	2
A2M	0	-0.4254602223	1	1	0	2
S100B	0	-0.524135142	0.997	0.983	0	2
LY6H	0	-0.5468970205	0.994	0.972	0	2
PTN	0	-0.6673829822	1	1	0	2
IGFBP7	1.89E-296	0.550650368	0.927	0.807	3.79E-293	2
SVIL	7.30E-296	0.3434237374	0.929	0.756	1.46E-292	2
COL18A1	1.97E-289	0.3145588451	0.884	0.612	3.94E-286	2
SH3BP4	2.47E-289	0.2877673616	0.964	0.773	4.94E-286	2
LBH	5.27E-287	0.4496543848	0.724	0.439	1.05E-283	2
GPM6A	1.11E-286	-0.4792970385	0.99	0.943	2.22E-283	2
AHNAK2	1.06E-285	0.3244228055	0.779	0.527	2.12E-282	2
SLC3A2	8.96E-285	0.4299459561	0.983	0.891	1.79E-281	2
HSP90AB1	2.95E-282	0.2593139753	0.997	0.947	5.90E-279	2
HERPUD1	1.25E-280	0.3493599848	0.882	0.64	2.50E-277	2
SLC7A5	2.41E-280	0.344045667	0.874	0.642	4.83E-277	2
TPM1	4.13E-280	0.3035587987	0.994	0.963	8.25E-277	2
PLAU	2.48E-273	0.4555381881	0.852	0.638	4.97E-270	2
C1QL1	9.01E-270	-0.4486000494	0.991	0.949	1.80E-266	2
S100A16	1.74E-269	0.2810121947	0.867	0.633	3.48E-266	2
ITGB1	6.34E-266	0.2718961332	0.988	0.907	1.27E-262	2
MEST	3.59E-262	0.3749124648	0.908	0.709	7.19E-259	2
NRP2	3.96E-259	0.3424236253	0.813	0.589	7.91E-256	2
IER3	7.14E-241	0.3774992763	0.943	0.811	1.43E-237	2
ARID5B	1.04E-240	0.3631332564	0.982	0.851	2.07E-237	2
COL4A2	1.93E-236	0.2731197565	0.989	0.907	3.86E-233	2
FILIP1L	2.29E-225	0.393399158	0.894	0.721	4.58E-222	2
ACTN1	7.73E-225	0.25733092	0.966	0.833	1.55E-221	2
ITGA3	7.81E-225	0.2805734442	0.682	0.342	1.56E-221	2
FBXO32	1.71E-224	0.3739886503	0.935	0.753	3.41E-221	2
PTPRZ1	7.42E-219	-0.4884973849	0.992	0.96	1.48E-215	2
DCBLD2	7.45E-213	0.3093118459	0.893	0.705	1.49E-209	2
TTYH1	6.70E-210	-0.4320380988	0.991	0.958	1.34E-206	2
SLC1A5	6.44E-209	0.2993650167	0.732	0.466	1.29E-205	2
C1orf61	1.58E-204	-0.5428585722	0.961	0.851	3.16E-201	2
ARL4C	9.69E-201	0.2927559975	0.958	0.828	1.94E-197	2
COL11A1	3.00E-194	0.2976200956	0.984	0.866	6.01E-191	2
CLU	3.21E-192	-0.3988547738	1	0.995	6.43E-189	2
TUBB2B	4.91E-190	-0.2858589564	1	0.995	9.82E-187	2

SERPINE1	3.14E-172	0.303623506	0.802	0.59	6.28E-169	2
AKAP12	1.63E-170	0.2524674296	0.884	0.679	3.26E-167	2
ACTG2	1.00E-158	0.3050372097	0.971	0.87	2.00E-155	2
PLK2	8.96E-157	0.3004034138	0.743	0.519	1.79E-153	2
SQSTM1	2.54E-152	0.2616987607	0.93	0.757	5.08E-149	2
IGFBP5	4.48E-148	0.2931292945	0.885	0.748	8.96E-145	2
JUNB	6.56E-144	0.253359902	0.843	0.645	1.31E-140	2
SPARCL1	1.12E-141	-0.5255387658	0.983	0.924	2.25E-138	2
CP	7.99E-139	-0.409826378	0.977	0.875	1.60E-135	2
CEBPB	5.59E-134	0.2716758567	0.738	0.519	1.12E-130	2
HLA-DPB1	1.40E-132	-0.2950919586	0.932	0.717	2.80E-129	2
SGO2	4.71E-129	-0.2762745213	0.492	0.51	9.41E-126	2
PCSK1N	3.65E-110	-0.2958695719	0.956	0.86	7.29E-107	2
GPM6B	2.66E-106	-0.2619589555	1	0.999	5.32E-103	2
HLA-DRA	1.16E-104	-0.7324236637	0.984	0.919	2.32E-101	2
SLC1A2	9.64E-94	-0.2707721964	0.928	0.733	1.93E-90	2
HMGB2	3.22E-91	-0.4510798538	0.56	0.527	6.45E-88	2
PROM1	1.75E-86	-0.3019347595	0.88	0.762	3.49E-83	2
ANKRD1	2.45E-81	0.3884160921	0.601	0.406	4.90E-78	2
MKI67	5.79E-80	-0.4944240179	0.728	0.442	1.16E-76	2
HTRA1	9.82E-63	-0.282365182	0.982	0.914	1.96E-59	2
TOP2A	2.32E-61	-0.5808857058	0.743	0.433	4.64E-58	2
HELLS	3.78E-61	-0.2510092035	0.564	0.54	7.57E-58	2
LINC00461	7.44E-59	-0.2950111565	0.967	0.89	1.49E-55	2
FGFBP3	9.49E-54	-0.322563055	0.973	0.879	1.90E-50	2
CENPE	2.28E-47	-0.2580490977	0.734	0.489	4.55E-44	2
UBE2C	2.45E-41	-0.2802762671	0.42	0.383	4.90E-38	2
CCNB1	3.00E-41	-0.3572985558	0.495	0.449	6.00E-38	2
H2AFZ	2.95E-40	-0.2764121323	0.959	0.89	5.89E-37	2
C21orf58	1.67E-32	-0.2598909789	0.593	0.517	3.34E-29	2
COL6A2	1.68E-30	-0.2534749937	0.962	0.83	3.36E-27	2
SRGAP3	2.29E-30	-0.3415719701	0.929	0.832	4.58E-27	2
NUSAP1	2.74E-28	-0.415114284	0.477	0.406	5.48E-25	2
SNTG1	2.29E-27	-0.4362906588	0.97	0.882	4.57E-24	2
PSRC1	4.19E-27	-0.2839034559	0.949	0.823	8.39E-24	2
CCDC102B	2.40E-26	-0.3417268321	0.921	0.779	4.80E-23	2
SLIT1	2.15E-20	-0.2825057665	0.903	0.709	4.31E-17	2
GFAP	9.67E-19	-0.448159568	0.948	0.798	1.93E-15	2
COL27A1	1.74E-17	-0.2634603033	0.86	0.675	3.49E-14	2

H2AFX	7.24E-16	-0.3181650403	0.749	0.65	1.45E-12	2
FN1	1.73E-14	-0.5621717329	0.98	0.944	3.45E-11	2
POSTN	1.12E-12	-0.6555206917	0.952	0.797	2.24E-09	2
COL3A1	5.76E-11	-0.2980162766	0.977	0.881	1.15E-07	2
CD74	7.40E-10	-0.362364796	0.934	0.784	1.48E-06	2
CLSPN	1.21E-09	-0.2656945102	0.467	0.384	2.41E-06	2
CENPF	3.54E-08	-0.709081616	0.661	0.54	7.09E-05	2
CRISPLD1	4.87E-08	-0.2711039115	0.948	0.804	9.75E-05	2
GREM1	5.21E-06	-0.4085331405	0.765	0.603	0.01042214298	2
COL1A2	4.62E-05	-0.6209562634	0.949	0.801	0.09249475535	2
CENPF	0	1.756447044	0.947	0.5	0	3
TOP2A	0	1.534094087	0.928	0.408	0	3
MKI67	0	1.427597405	0.856	0.424	0	3
NUSAP1	0	1.121492842	0.898	0.347	0	3
CCNB1	0	1.021916611	0.816	0.404	0	3
HMGB2	0	1.010558341	0.908	0.478	0	3
SMC2	0	0.9604897593	0.958	0.603	0	3
KPNA2	0	0.9596732534	0.883	0.555	0	3
H2AFX	0	0.9514441201	0.944	0.623	0	3
ASPM	0	0.9315330686	0.805	0.355	0	3
H2AFZ	0	0.9132369322	0.994	0.886	0	3
SMC4	0	0.8824446732	0.894	0.537	0	3
CLSPN	0	0.8810247116	0.766	0.343	0	3
PTTG1	0	0.8474608221	0.864	0.489	0	3
PBK	0	0.8325951619	0.862	0.414	0	3
TUBB4B	0	0.8324405086	0.989	0.866	0	3
PCLAF	0	0.8285215121	0.853	0.351	0	3
CENPE	0	0.8279645936	0.798	0.48	0	3
CDK1	0	0.822912355	0.799	0.384	0	3
TUBA1B	0	0.8146940833	1	0.99	0	3
TPX2	0	0.8002536945	0.776	0.356	0	3
UBE2C	0	0.7927305326	0.732	0.34	0	3
FEN1	0	0.7921229167	0.806	0.433	0	3
GTSE1	0	0.7621434995	0.782	0.324	0	3
MCM7	0	0.7548005018	0.858	0.387	0	3
SGO2	0	0.7510414372	0.891	0.454	0	3
UBE2S	0	0.7510272286	0.901	0.595	0	3
TACC3	0	0.744357487	0.771	0.321	0	3
BIRC5	0	0.7258286102	0.77	0.264	0	3

KIF20B	0	0.7148470973	0.788	0.391	0	3
LMNB1	0	0.714818303	0.834	0.359	0	3
NUCKS1	0	0.7054483608	0.993	0.873	0	3
CCNB2	0	0.7054390028	0.718	0.29	0	3
TMPO	0	0.6979634631	0.857	0.415	0	3
TYMS	0	0.6955924547	0.86	0.414	0	3
TUBB	0	0.6948047246	1	0.959	0	3
MXD3	0	0.6866171536	0.824	0.293	0	3
ATAD2	0	0.6854946016	0.768	0.421	0	3
NASP	0	0.6811348518	0.976	0.737	0	3
DEK	0	0.6671519957	0.954	0.691	0	3
HMGN2	0	0.6628020594	0.973	0.783	0	3
HMGB1	0	0.6524942384	1	0.971	0	3
RRM1	0	0.6521371199	0.829	0.473	0	3
MCM4	0	0.6430401891	0.781	0.365	0	3
RRM2	0	0.6363060918	0.703	0.241	0	3
PCNA	0	0.6359941774	0.834	0.494	0	3
DLGAP5	0	0.6351915217	0.702	0.342	0	3
NUF2	0	0.6259362188	0.8	0.333	0	3
STMN1	0	0.6255826825	0.994	0.904	0	3
C21orf58	0	0.6171912328	0.805	0.488	0	3
CKAP2	0	0.6152661963	0.743	0.407	0	3
SYNE2	0	0.6127750848	0.942	0.725	0	3
DTYMK	0	0.6107668161	0.898	0.544	0	3
DNMT1	0	0.5872842306	0.871	0.528	0	3
MCM3	0	0.5752132638	0.742	0.443	0	3
ZWINT	0	0.5711816095	0.803	0.373	0	3
CENPK	0	0.5710379716	0.872	0.503	0	3
E2F1	0	0.5642715222	0.704	0.455	0	3
PTMA	0	0.5562571294	0.998	0.953	0	3
ORC6	0	0.5550498919	0.785	0.389	0	3
HELLS	0	0.553723024	0.763	0.512	0	3
CCDC34	0	0.5495752769	0.938	0.613	0	3
KIFC1	0	0.543189432	0.706	0.255	0	3
SMC1A	0	0.5409443005	0.924	0.715	0	3
MIS18BP1	0	0.5359215617	0.8	0.393	0	3
HMMR	0	0.5332346871	0.713	0.266	0	3
CDKN2C	0	0.5294302628	0.87	0.522	0	3
CHAF1A	0	0.520533571	0.728	0.392	0	3

MAD2L1	0	0.5192223458	0.76	0.328	0	3
UBE2T	0	0.5170884899	0.741	0.336	0	3
PARP1	0	0.508570706	0.951	0.724	0	3
PRKDC	0	0.5066311597	0.98	0.805	0	3
SUPT16H	0	0.4994306984	0.905	0.607	0	3
KIF2C	0	0.4992263911	0.694	0.371	0	3
ESCO2	0	0.4990125129	0.767	0.244	0	3
TUBB6	0	0.4905133346	0.917	0.637	0	3
ANP32E	0	0.4899996184	0.871	0.574	0	3
CKS2	0	0.4879906059	0.738	0.368	0	3
KIF23	0	0.4876332677	0.709	0.35	0	3
CKAP5	0	0.4826917127	0.92	0.629	0	3
PRC1	0	0.4768879091	0.684	0.275	0	3
BARD1	0	0.471564772	0.834	0.529	0	3
BRCA2	0	0.4713101643	0.802	0.542	0	3
SGO1	0	0.4703579805	0.765	0.347	0	3
KNL1	0	0.4696536153	0.735	0.29	0	3
CENPA	0	0.4693897533	0.805	0.4	0	3
CDCA3	0	0.4689014598	0.677	0.244	0	3
CENPM	0	0.4675063243	0.756	0.347	0	3
BRCA1	0	0.4613445998	0.784	0.506	0	3
RAD21	0	0.4580270872	0.959	0.719	0	3
UHRF1	0	0.4573748777	0.691	0.331	0	3
ECT2	0	0.4558127856	0.735	0.322	0	3
HMGB3	0	0.4549046998	0.838	0.504	0	3
MELK	0	0.4532216235	0.741	0.281	0	3
NDC80	0	0.452472747	0.665	0.35	0	3
CCNA2	0	0.4486048049	0.697	0.28	0	3
KIF11	0	0.4405583075	0.802	0.338	0	3
USP1	0	0.438308895	0.816	0.539	0	3
SHCBP1	0	0.4365855567	0.709	0.316	0	3
SPC24	0	0.4356823192	0.798	0.282	0	3
CDCA2	0	0.4323021122	0.788	0.414	0	3
FBXO5	0	0.4310635191	0.696	0.349	0	3
NCAPG	0	0.4259175811	0.66	0.355	0	3
ANLN	0	0.4212143669	0.642	0.325	0	3
PIMREG	0	0.4146536969	0.78	0.312	0	3
FANCI	0	0.4118647969	0.682	0.383	0	3
MCM10	0	0.4067231422	0.711	0.348	0	3

CDKN3	0	0.4066059854	0.791	0.288	0	3
RAD51AP1	0	0.4058088714	0.772	0.334	0	3
TK1	0	0.4006477371	0.675	0.242	0	3
LIG1	0	0.3986822844	0.715	0.393	0	3
KIF22	0	0.3984659702	0.745	0.412	0	3
CKAP2L	0	0.3979902656	0.717	0.307	0	3
HJURP	0	0.3966260569	0.732	0.312	0	3
EZH2	0	0.3918583723	0.742	0.397	0	3
SPAG5	0	0.3877541141	0.664	0.383	0	3
CDCA5	0	0.3852468293	0.608	0.29	0	3
GINS2	0	0.3799874364	0.759	0.454	0	3
BUB1	0	0.3771482646	0.669	0.333	0	3
DHFR	0	0.3726220985	0.76	0.49	0	3
KIF14	0	0.3715725212	0.771	0.418	0	3
TCF19	0	0.3698663949	0.766	0.371	0	3
H1FX	0	0.3695263385	0.903	0.675	0	3
DNAJC9	0	0.3681232212	0.726	0.41	0	3
KNSTRN	0	0.3652235528	0.691	0.36	0	3
PKM	0	0.3603068201	0.986	0.878	0	3
CEP55	0	0.3586396014	0.74	0.36	0	3
TMEM97	0	0.3557657807	0.708	0.39	0	3
CENPH	0	0.3556304571	0.733	0.313	0	3
KIF4A	0	0.3491165743	0.674	0.383	0	3
DEPDC1	0	0.3484210333	0.712	0.323	0	3
CKS1B	0	0.3468555926	0.758	0.424	0	3
FOXM1	0	0.346513949	0.66	0.332	0	3
SAC3D1	0	0.3456186768	0.775	0.464	0	3
TMEM106C	0	0.3436623045	0.909	0.647	0	3
CIP2A	0	0.3436618368	0.753	0.49	0	3
SCARA3	0	0.3415658897	0.929	0.711	0	3
NCAPD3	0	0.3413130913	0.766	0.297	0	3
GMNN	0	0.3391726733	0.668	0.308	0	3
RFC3	0	0.3384646698	0.614	0.287	0	3
FANCA	0	0.3384266643	0.74	0.322	0	3
PHF19	0	0.3383953799	0.691	0.383	0	3
PHGDH	0	0.3360250968	0.882	0.618	0	3
FDPS	0	0.3338448974	0.974	0.816	0	3
KIF15	0	0.3329439711	0.765	0.417	0	3
BTG3	0	0.3312793154	0.822	0.509	0	3

CENPU	0	0.3305625782	0.738	0.355	0	3
HSP90AA1	0	0.3298783898	1	0.994	0	3
BUB1B	0	0.3266756793	0.687	0.375	0	3
EMP2	0	0.3172660389	0.938	0.719	0	3
PIF1	0	0.313513311	0.672	0.241	0	3
POLD3	0	0.3091594256	0.718	0.42	0	3
MND1	0	0.2995135742	0.698	0.296	0	3
SAPCD2	0	0.2982101899	0.637	0.301	0	3
ASRGL1	0	0.295682729	0.658	0.321	0	3
RACGAP1	0	0.2924413531	0.687	0.307	0	3
NEK2	0	0.2897714675	0.636	0.292	0	3
CLDN10	0	0.2881699166	0.929	0.76	0	3
TIMELESS	0	0.2880334671	0.693	0.38	0	3
POC1A	0	0.2812322188	0.652	0.296	0	3
FAM111B	0	0.2787179881	0.614	0.244	0	3
TRIP13	0	0.2711192769	0.662	0.354	0	3
NCAPG2	0	0.2666508539	0.702	0.494	0	3
CENPN	0	0.2665190413	0.793	0.319	0	3
HIRIP3	0	0.2634282622	0.709	0.451	0	3
CNIH2	0	0.26229795	0.901	0.61	0	3
RECQL4	0	0.2526649835	0.672	0.4	0	3
PSMC3IP	0	0.2515409614	0.624	0.277	0	3
ENO1	8.33E-303	0.2842200718	0.989	0.889	1.67E-299	3
CENPW	2.62E-299	0.2779478122	0.641	0.298	5.24E-296	3
SPC25	3.85E-299	0.3610586984	0.629	0.35	7.71E-296	3
ATAD5	1.59E-290	0.3114828282	0.69	0.454	3.18E-287	3
BUB3	4.09E-290	0.3129753629	0.783	0.524	8.19E-287	3
ARL6IP1	1.71E-288	0.5152883583	0.944	0.798	3.42E-285	3
SMS	3.57E-286	0.3194762652	0.946	0.771	7.15E-283	3
MZT1	9.76E-285	0.2861076726	0.733	0.458	1.95E-281	3
PLK1	2.24E-281	0.4873170002	0.623	0.34	4.48E-278	3
MYH10	2.14E-276	0.3220388098	0.951	0.743	4.28E-273	3
SAMD1	2.17E-274	0.2573251193	0.838	0.605	4.33E-271	3
RFC4	5.69E-272	0.347052748	0.653	0.343	1.14E-268	3
AURKB	3.17E-270	0.4218480473	0.631	0.324	6.34E-267	3
CDC20	7.48E-266	0.5349067838	0.593	0.225	1.50E-262	3
CHEK1	4.79E-258	0.3083628821	0.634	0.288	9.59E-255	3
FBLN1	1.29E-254	0.2702119908	0.81	0.508	2.57E-251	3
DSN1	6.90E-250	0.2524153983	0.634	0.369	1.38E-246	3

DBF4	2.36E-249	0.3227873129	0.599	0.313	4.72E-246	3
DUT	1.22E-248	0.315592848	0.879	0.68	2.44E-245	3
CKB	2.09E-245	0.3053143802	0.994	0.924	4.18E-242	3
YWHAH	3.04E-243	0.2652269309	0.852	0.603	6.08E-240	3
DIAPH3	3.44E-241	0.3650699288	0.632	0.373	6.88E-238	3
DHCR24	1.45E-236	0.2530541566	0.835	0.604	2.89E-233	3
PRR11	5.72E-231	0.3361211971	0.604	0.342	1.14E-227	3
SLBP	9.77E-222	0.3066987781	0.724	0.459	1.95E-218	3
SPDL1	6.20E-216	0.2754263635	0.629	0.348	1.24E-212	3
MCM5	1.15E-214	0.4044739882	0.657	0.426	2.30E-211	3
HIST1H4C	1.79E-207	0.2919760654	0.668	0.382	3.57E-204	3
ASF1B	1.45E-200	0.3011087267	0.576	0.288	2.90E-197	3
SOX2	5.37E-196	0.3092601019	0.991	0.902	1.07E-192	3
MSH6	1.10E-190	0.3462221722	0.708	0.491	2.20E-187	3
PEG10	3.56E-189	0.2751643205	0.987	0.876	7.12E-186	3
MCM2	1.65E-188	0.3732417624	0.61	0.351	3.30E-185	3
NCL	4.64E-188	0.2683412141	0.979	0.856	9.28E-185	3
CCDC85B	6.05E-185	0.2602055372	0.904	0.728	1.21E-181	3
ARL4C	2.20E-181	0.2747610342	0.959	0.828	4.41E-178	3
JPT1	5.17E-180	0.2889980399	0.918	0.751	1.03E-176	3
NCAPD2	1.60E-176	0.2794142024	0.582	0.314	3.19E-173	3
RANGAP1	2.65E-176	0.2852771024	0.653	0.41	5.29E-173	3
TTK	1.77E-174	0.2740331731	0.583	0.345	3.55E-171	3
LY6H	3.43E-174	-0.3746967572	0.992	0.973	6.85E-171	3
MYBL2	1.50E-172	0.2857278964	0.556	0.236	3.01E-169	3
FN1	4.77E-170	-0.8663793483	0.967	0.946	9.54E-167	3
CDT1	3.20E-169	0.2882706132	0.581	0.334	6.41E-166	3
COL1A2	2.26E-165	-0.701766146	0.898	0.809	4.52E-162	3
S100B	4.54E-160	-0.409397421	0.996	0.983	9.07E-157	3
COL1A1	4.34E-137	-0.6977743536	0.989	0.975	8.67E-134	3
TMEM158	6.78E-135	0.2724959925	0.95	0.79	1.36E-131	3
FANCD2	3.73E-132	0.2873840864	0.545	0.281	7.46E-129	3
CDCA8	1.20E-129	0.2911353261	0.487	0.19	2.41E-126	3
COL3A1	4.11E-120	-0.46129458	0.955	0.885	8.22E-117	3
NCAPH	1.48E-118	0.2802594539	0.517	0.287	2.96E-115	3
AURKA	1.07E-114	0.3885007018	0.5	0.238	2.13E-111	3
PAQR4	6.33E-110	0.2931922171	0.631	0.489	1.27E-106	3
SAT1	6.77E-110	-0.3733627505	0.96	0.903	1.35E-106	3
NEAT1	9.05E-109	-0.8111146291	0.937	0.897	1.81E-105	3

CDC45	2.04E-108	0.3013194013	0.551	0.322	4.08E-105	3
CDC6	9.78E-106	0.272762387	0.537	0.297	1.96E-102	3
POSTN	1.14E-104	-0.8285276738	0.893	0.805	2.28E-101	3
ARHGAP11A	6.37E-101	0.3861419152	0.545	0.34	1.27E-97	3
MCM6	5.32E-96	0.2936461005	0.613	0.469	1.06E-92	3
RTKN2	5.17E-94	0.2530149405	0.559	0.367	1.03E-90	3
CLU	1.31E-91	-0.3145871692	1	0.995	2.62E-88	3
CALD1	1.37E-84	-0.3383268664	0.999	0.994	2.75E-81	3
NDFIP1	1.20E-82	-0.2586239677	0.987	0.937	2.40E-79	3
HLA-DRA	1.25E-81	-0.540457763	0.969	0.922	2.51E-78	3
POLA2	3.36E-72	0.2610374156	0.544	0.386	6.72E-69	3
GREM1	6.07E-70	-0.4717054015	0.628	0.623	1.21E-66	3
S100A11	2.15E-67	-0.2966216177	0.891	0.829	4.31E-64	3
LGALS3	2.60E-67	-0.2508626885	0.975	0.936	5.20E-64	3
CYP1B1	1.70E-50	-0.2815452212	0.548	0.555	3.40E-47	3
IGFBP5	1.20E-47	-0.3413218933	0.794	0.761	2.40E-44	3
COL6A3	3.28E-45	-0.7532375368	0.88	0.768	6.57E-42	3
CP	1.16E-40	-0.2801387482	0.954	0.879	2.31E-37	3
COL6A1	2.67E-40	-0.4972210487	0.968	0.908	5.34E-37	3
ELMOD1	3.03E-35	-0.2561966955	0.92	0.822	6.07E-32	3
LUM	1.11E-32	-0.3034522731	0.593	0.573	2.22E-29	3
KCNQ1OT1	3.08E-11	-0.3864036124	0.711	0.63	6.17E-08	3
COL6A2	1.51E-06	-0.4616276733	0.925	0.836	0.003028195366	3
PI15	5.42E-06	-0.271545367	0.882	0.809	0.01083480267	3
SOX6	0	0.3347451865	0.193	0.827	0	4
SCN1A	0	0.3130798005	0.116	0.747	0	4
GRIN2B	0	0.2930670725	0.17	0.785	0	4
PDE4B	0	0.2818399213	0.206	0.827	0	4
MAP1A	0	-0.2522884998	0.2	0.865	0	4
ARL6IP1	0	-0.2657834549	0.301	0.879	0	4
SFRP1	0	-0.2849008875	0.263	0.881	0	4
HSP90AA1	0	-0.3144437854	0.959	0.999	0	4
APLP1	0	-0.3294320005	0.224	0.851	0	4
GRN	0	-0.3514736484	0.415	0.94	0	4
APLP2	0	-0.3975989917	0.766	0.986	0	4
TLN1	1.15E-294	-0.2750468837	0.224	0.791	2.31E-291	4
MT-ND4	7.65E-294	-0.2960986629	0.274	0.834	1.53E-290	4
CCDC102B	7.65E-279	0.4442861636	0.286	0.86	1.53E-275	4
SOX2	1.44E-277	-0.311090461	0.475	0.966	2.89E-274	4

IGFBP5	1.33E-276	-0.3206794692	0.285	0.823	2.66E-273	4
CCDC85B	5.25E-266	-0.2679756882	0.254	0.811	1.05E-262	4
ITM2B	1.22E-247	-0.3251335366	0.786	0.989	2.43E-244	4
HSP90AB1	5.79E-245	-0.2985840885	0.735	0.98	1.16E-241	4
NTRK2	2.32E-243	-0.3853191428	0.558	0.972	4.63E-240	4
HSPA5	4.97E-228	-0.3340897991	0.849	0.989	9.94E-225	4
FABP7	6.86E-217	0.2685828544	0.991	0.999	1.37E-213	4
SPARC	1.24E-214	-0.2538747657	0.964	0.999	2.47E-211	4
ITM2C	1.41E-211	-0.2706574644	0.383	0.889	2.82E-208	4
PLTP	6.24E-209	-0.2551797324	0.517	0.967	1.25E-205	4
DDR1	3.85E-208	-0.2703002736	0.556	0.974	7.71E-205	4
NUCKS1	6.17E-205	-0.323401425	0.519	0.933	1.23E-201	4
MT-CO1	2.13E-204	-0.3002741392	0.811	0.989	4.26E-201	4
CALU	2.16E-200	-0.2755964648	0.458	0.914	4.31E-197	4
ELMOD1	9.11E-199	0.2613105656	0.337	0.894	1.82E-195	4
DKK3	6.95E-196	-0.279363416	0.506	0.936	1.39E-192	4
APP	5.78E-194	-0.2949760686	0.682	0.968	1.16E-190	4
MT-CYB	1.68E-192	-0.3096219676	0.742	0.983	3.36E-189	4
GPM6B	2.42E-192	-0.4119107483	0.997	1	4.83E-189	4
CPE	5.75E-192	-0.4222268749	0.802	0.993	1.15E-188	4
MAP1B	5.92E-192	-0.3037749554	0.941	0.999	1.18E-188	4
NCL	6.97E-192	-0.2789661577	0.48	0.918	1.39E-188	4
IGFBP2	2.73E-189	-0.2945035536	0.997	1	5.45E-186	4
MMP2	5.41E-179	-0.2794251883	0.506	0.93	1.08E-175	4
SARAF	1.67E-178	-0.2673602205	0.82	0.992	3.34E-175	4
COL4A2	8.44E-171	-0.2698282511	0.593	0.957	1.69E-167	4
HTRA1	3.91E-165	-0.2594636604	0.553	0.968	7.81E-162	4
SCRG1	1.33E-156	0.3010307193	0.289	0.798	2.66E-153	4
PEG10	3.59E-154	-0.3018912451	0.543	0.932	7.18E-151	4
COL4A1	4.79E-139	-0.2770706038	0.684	0.968	9.57E-136	4
CCDC80	8.11E-139	-0.2871944609	0.559	0.942	1.62E-135	4
LRRIQ1	1.27E-122	0.369943569	0.352	0.863	2.54E-119	4
GFAP	2.76E-122	0.2734898072	0.374	0.871	5.53E-119	4
COL27A1	1.00E-99	0.4089609423	0.285	0.749	2.00E-96	4
LGALS1	3.41E-90	0.3089548012	0.801	0.966	6.83E-87	4
ADGRV1	1.80E-89	0.4134446576	0.399	0.902	3.60E-86	4
SNTG1	3.53E-72	0.8294975168	0.614	0.927	7.06E-69	4
MKI67	8.04E-61	-0.2798463798	0.093	0.524	1.61E-57	4
COL1A1	1.33E-56	-0.2523265984	0.908	0.985	2.67E-53	4

SRGAP3	1.92E-49	0.2744366452	0.43	0.895	3.84E-46	4
LRRC4C	1.61E-48	0.4704275935	0.42	0.899	3.22E-45	4
CLU	8.40E-48	-0.26881975	0.968	0.999	1.68E-44	4
GRID2	3.53E-45	0.3236112557	0.165	0.582	7.05E-42	4
MIAT	8.82E-44	0.4959371844	0.291	0.704	1.76E-40	4
CENPF	1.37E-26	-0.3883227472	0.227	0.595	2.73E-23	4
KCNQ1OT1	2.91E-14	0.2759054549	0.318	0.679	5.82E-11	4
C1orf61	5.63E-12	0.3674309852	0.492	0.91	1.13E-08	4
NEAT1	3.50E-06	0.585038108	0.62	0.936	0.007004755687	4
LINC00461	9.58E-06	0.2615650351	0.548	0.943	0.01915825443	4
FN1	0	2.382870271	0.995	0.945	0	5
COL6A3	0	2.310683006	0.986	0.769	0	5
POSTN	0	2.296733664	0.979	0.806	0	5
COL1A1	0	2.079309316	0.999	0.975	0	5
COL6A2	0	2.033797724	0.992	0.838	0	5
GREM1	0	1.996438099	0.972	0.601	0	5
COL6A1	0	1.985147551	0.996	0.91	0	5
COL1A2	0	1.809297357	0.937	0.813	0	5
COL5A1	0	1.409490433	0.956	0.614	0	5
COL3A1	0	1.388061306	0.978	0.888	0	5
INHBA	0	1.360432293	0.837	0.456	0	5
CYP1B1	0	1.215611898	0.838	0.536	0	5
ADAMTS6	0	1.15033238	0.787	0.591	0	5
CALD1	0	1.133800956	1	0.994	0	5
COL5A3	0	1.110092228	0.9	0.475	0	5
APCDD1	0	1.109013841	0.923	0.73	0	5
TGFBI	0	1.089021095	0.937	0.728	0	5
LUM	0	1.076404454	0.877	0.557	0	5
TPM2	0	1.073060535	0.959	0.775	0	5
FBN1	0	1.05846921	0.85	0.49	0	5
EMILIN1	0	1.037200035	0.776	0.357	0	5
PDGFRB	0	1.016520426	0.896	0.443	0	5
ANKRD28	0	0.9974060699	0.966	0.684	0	5
DLG1	0	0.9646936819	0.866	0.494	0	5
MYH9	0	0.9477006573	0.947	0.75	0	5
AKAP12	0	0.9269074091	0.897	0.693	0	5
PCOLCE	0	0.9216077541	0.879	0.417	0	5
CCDC80	0	0.9189472222	0.965	0.897	0	5
ITGA11	0	0.918676027	0.861	0.417	0	5

DDR2	0	0.908809238	0.898	0.523	0	5
LGALS1	0	0.8747544055	0.986	0.946	0	5
NNMT	0	0.8676054496	0.828	0.533	0	5
KCNQ1OT1	0	0.8643769503	0.956	0.62	0	5
TPM4	0	0.8484474168	0.965	0.824	0	5
DCBLD2	0	0.8359582945	0.936	0.716	0	5
IGFBP7	0	0.8092055526	0.934	0.815	0	5
TWIST1	0	0.8039376334	0.742	0.414	0	5
SERPINF1	0	0.8009943111	0.822	0.438	0	5
COL8A1	0	0.7947095025	0.745	0.411	0	5
S100A11	0	0.794295858	0.958	0.829	0	5
SRPX2	0	0.7831076287	0.943	0.728	0	5
LMNA	0	0.7743283937	0.972	0.898	0	5
WNT5A	0	0.7651705452	0.926	0.629	0	5
HOXB2	0	0.7612847765	0.75	0.454	0	5
PHGDH	0	0.7517934502	0.876	0.637	0	5
CACNA2D3	0	0.7493101283	0.911	0.558	0	5
LAMB1	0	0.7425810345	0.889	0.58	0	5
COLEC12	0	0.7419657724	0.865	0.461	0	5
SLC1A5	0	0.7217377776	0.761	0.483	0	5
TNFRSF19	0	0.7146990107	0.905	0.559	0	5
PTK7	0	0.7146358385	0.886	0.662	0	5
LOX	0	0.7106800309	0.863	0.602	0	5
PXDN	0	0.7067178667	0.782	0.508	0	5
MFAP4	0	0.7003555695	0.814	0.521	0	5
COL5A2	0	0.6928918453	0.948	0.835	0	5
SEPT11	0	0.6580555915	0.976	0.869	0	5
UNC5B	0	0.6514605347	0.802	0.407	0	5
CARMN	0	0.6484325895	0.69	0.33	0	5
RRBP1	0	0.6330687174	0.882	0.695	0	5
TPM1	0	0.6199127023	0.996	0.965	0	5
NPR3	0	0.6140972401	0.722	0.371	0	5
HOXB3	0	0.6105850853	0.886	0.346	0	5
OLFM2	0	0.6034179787	0.843	0.375	0	5
TPBG	0	0.6029977075	0.771	0.316	0	5
CH25H	0	0.5677248922	0.877	0.668	0	5
HMGA2	0	0.5644153282	0.903	0.459	0	5
COL25A1	0	0.5632322523	0.883	0.313	0	5
DLC1	0	0.5510017466	0.713	0.307	0	5

TIMP3	0	0.5265342195	0.743	0.216	0	5
GAS1	0	0.5259456302	0.877	0.475	0	5
SYTL2	0	0.4943439002	0.906	0.526	0	5
IGFBP4	0	0.4841136924	0.865	0.598	0	5
MIR503HG	0	0.478493454	0.864	0.466	0	5
FZD1	0	0.4662560424	0.837	0.547	0	5
MEG8	0	0.445713053	0.884	0.652	0	5
CALB2	0	0.4404369126	0.814	0.59	0	5
PHLDB2	0	0.4295334536	0.687	0.236	0	5
HMCN1	0	0.4282038243	0.806	0.484	0	5
HOXB4	0	0.42102682	0.861	0.397	0	5
AK5	0	0.4158978728	0.829	0.424	0	5
DNM3OS	0	0.414374667	0.842	0.436	0	5
TWIST2	0	0.4114390567	0.865	0.558	0	5
MFAP5	0	0.4007187448	0.753	0.363	0	5
ADAMTS14	0	0.4006332644	0.782	0.514	0	5
CLMP	0	0.3911670189	0.812	0.489	0	5
HAS2	0	0.3890023342	0.848	0.622	0	5
FOSB	0	0.3770624518	0.85	0.645	0	5
DCN	0	0.3739414904	0.852	0.622	0	5
SORCS2	0	0.3695584179	0.842	0.598	0	5
GREM2	0	0.3448331157	0.747	0.398	0	5
WNT11	0	0.3429607152	0.849	0.599	0	5
MIS18BP1	0	0.3369199546	0.828	0.419	0	5
FAP	0	0.3339578544	0.691	0.235	0	5
NTN4	0	0.3321479645	0.852	0.382	0	5
CRABP2	0	0.3320856366	0.759	0.221	0	5
TSHZ2	0	0.3232239163	0.886	0.623	0	5
LSAMP	0	0.3213744877	0.89	0.709	0	5
SGCD	0	0.313615581	0.771	0.422	0	5
MGP	0	0.3133284673	0.846	0.65	0	5
LTBP1	0	0.3072312754	0.823	0.509	0	5
TXNIP	0	0.2994969068	0.849	0.482	0	5
CD248	0	0.296727475	0.745	0.352	0	5
TMEM119	0	0.2876269566	0.804	0.513	0	5
BICC1	0	0.2811199183	0.719	0.249	0	5
FOXD1	0	0.2803807399	0.843	0.366	0	5
SPON2	0	0.2760362963	0.816	0.512	0	5
NKD2	0	0.2747532932	0.86	0.528	0	5

BMP2	0	0.2736564802	0.837	0.386	0	5
PERP	0	0.2689215583	0.686	0.247	0	5
MYO1D	0	0.2510012941	0.788	0.492	0	5
RGMA	0	-0.300095083	0.42	0.737	0	5
MOXD1	0	-0.3024620482	0.571	0.747	0	5
PLP1	0	-0.3830958105	0.713	0.753	0	5
SLC1A2	0	-0.3883681812	0.802	0.755	0	5
SEMA5B	0	-0.4464657884	0.821	0.787	0	5
NOS1AP	0	-0.471799141	0.639	0.761	0	5
SOX9	0	-0.4738695561	0.417	0.794	0	5
GPRC5B	0	-0.4871052123	0.678	0.806	0	5
B2M	0	-0.4926804118	0.999	0.998	0	5
ELMOD1	0	-0.5175626671	0.833	0.834	0	5
TUBA1A	0	-0.5238770582	1	1	0	5
SMOC1	0	-0.532251955	0.849	0.801	0	5
WSCD1	0	-0.5591532094	0.767	0.82	0	5
LRP2	0	-0.5625578626	0.842	0.827	0	5
CSRP2	0	-0.5652944341	0.98	0.991	0	5
GDF10	0	-0.5887605043	0.844	0.83	0	5
PLPPR3	0	-0.5981379846	0.827	0.843	0	5
IFITM3	0	-0.5997595239	0.985	0.988	0	5
APP	0	-0.6187354586	0.902	0.939	0	5
CD99	0	-0.6254451434	0.995	0.993	0	5
NKAIN3	0	-0.6304527237	0.833	0.83	0	5
LRRC4C	0	-0.6547398445	0.675	0.858	0	5
SARAF	0	-0.6550764016	0.976	0.974	0	5
APLP1	0	-0.6623435458	0.578	0.795	0	5
MAP1B	0	-0.6659244999	0.991	0.992	0	5
LYPD1	0	-0.6775327926	0.782	0.858	0	5
PON2	0	-0.6791136743	0.946	0.959	0	5
ITGB4	0	-0.6968072091	0.844	0.817	0	5
ADAM9	0	-0.701593544	0.822	0.922	0	5
NDFIP1	0	-0.7109107915	0.926	0.944	0	5
DCLK1	0	-0.7151446552	0.87	0.894	0	5
CDH6	0	-0.7276176621	0.817	0.867	0	5
ADGRV1	0	-0.7344130682	0.823	0.849	0	5
DKK3	0	-0.7360167894	0.775	0.897	0	5
FABP7	0	-0.7373673806	0.996	0.998	0	5
TUBB2A	0	-0.7431156521	0.953	0.975	0	5

PCSK1N	0	-0.7436870775	0.808	0.876	0	5
ATP1B1	0	-0.7437471303	0.838	0.836	0	5
CYR61	0	-0.7482576164	0.952	0.971	0	5
IGFBP2	0	-0.7530842545	1	1	0	5
CRB2	0	-0.7619758458	0.8	0.84	0	5
CPE	0	-0.7659526803	0.965	0.973	0	5
SRGAP3	0	-0.766773122	0.826	0.845	0	5
NTRK3	0	-0.7756754207	0.843	0.85	0	5
PPP1CB	0	-0.7794147782	0.918	0.954	0	5
PCDH9	0	-0.7844516089	0.855	0.882	0	5
FGFBP3	0	-0.789182119	0.888	0.891	0	5
KIF5C	0	-0.7936996142	0.747	0.891	0	5
PLTP	0	-0.8001566484	0.921	0.918	0	5
S100B	0	-0.8218542116	0.979	0.985	0	5
MAP2	0	-0.8288334702	0.851	0.894	0	5
MLC1	0	-0.831284069	0.88	0.873	0	5
PMP22	0	-0.8330199068	0.949	0.953	0	5
GRIA1	0	-0.8672325977	0.882	0.915	0	5
SYNM	0	-0.8695437147	0.869	0.892	0	5
TUBB2B	0	-0.8712463876	0.993	0.996	0	5
PI15	0	-0.8823592595	0.858	0.816	0	5
APLP2	0	-0.8958368396	0.914	0.965	0	5
LY6H	0	-0.8990496816	0.969	0.975	0	5
SPOCK2	0	-0.8999763721	0.87	0.877	0	5
SNTG1	0	-0.9003725305	0.842	0.896	0	5
CP	0	-0.9088321597	0.876	0.889	0	5
LINC00461	0	-0.9225518856	0.763	0.908	0	5
SOX2	0	-0.9355719789	0.858	0.916	0	5
DDR1	0	-0.940336705	0.904	0.93	0	5
WLS	0	-0.9829793291	0.965	0.98	0	5
CKB	0	-0.9901537243	0.826	0.94	0	5
PTN	0	-1.063644499	1	1	0	5
GPM6A	0	-1.068744717	0.917	0.951	0	5
NTRK2	0	-1.069008737	0.882	0.93	0	5
TTYH1	0	-1.098245066	0.944	0.963	0	5
A2M	0	-1.099243672	1	1	0	5
C1QL1	0	-1.126460988	0.928	0.956	0	5
NR2F1	0	-1.154409666	0.855	0.932	0	5
PTPRZ1	0	-1.157196398	0.92	0.967	0	5

CLU	0	-1.172633262	0.989	0.996	0	5
SPARCL1	0	-1.176154639	0.908	0.933	0	5
GPM6B	0	-1.39826033	0.998	1	0	5
NBL1	3.14E-307	0.3936292296	0.743	0.394	6.29E-304	5
SLFN5	1.57E-304	0.4289357928	0.712	0.365	3.14E-301	5
CNR1	7.05E-303	-0.3173475295	0.791	0.761	1.41E-299	5
MMP14	1.16E-302	0.6894395683	0.789	0.532	2.33E-299	5
PCDH10	4.26E-302	-0.4912331502	0.807	0.784	8.51E-299	5
PDPN	1.72E-301	-0.6204980267	0.891	0.889	3.44E-298	5
LOXL2	4.70E-299	0.672609526	0.787	0.51	9.40E-296	5
OGFRL1	6.05E-297	-0.268236545	0.449	0.687	1.21E-293	5
NEFL	2.46E-295	-0.4800234911	0.861	0.84	4.92E-292	5
SFRP1	1.82E-294	-0.6573232385	0.569	0.829	3.64E-291	5
PLD3	9.58E-292	-0.5165122812	0.968	0.962	1.92E-288	5
KIF1A	3.73E-291	-0.6439305455	0.597	0.793	7.46E-288	5
OLFML3	2.50E-288	0.4709997959	0.702	0.371	5.00E-285	5
CD47	1.14E-287	-0.6316815809	0.876	0.902	2.27E-284	5
EDNRB	1.06E-284	-0.4178529206	0.827	0.777	2.12E-281	5
TMEM47	6.53E-283	-0.5576384886	0.652	0.844	1.31E-279	5
PODXL	1.83E-278	-0.4698767775	0.747	0.761	3.65E-275	5
ESPN	6.27E-275	-0.2827868813	0.659	0.738	1.25E-271	5
RGS6	1.68E-271	-0.4770643146	0.822	0.786	3.35E-268	5
NPAS3	3.16E-271	-0.6246238649	0.747	0.825	6.31E-268	5
SNAI2	7.17E-265	0.4009244311	0.708	0.369	1.43E-261	5
IQGAP2	1.65E-263	-0.4341516089	0.619	0.787	3.30E-260	5
PSRC1	1.14E-261	-0.5602914974	0.777	0.843	2.27E-258	5
ENPP2	9.73E-260	-0.4281747578	0.834	0.799	1.95E-256	5
EFNB2	1.60E-259	-0.6378363669	0.687	0.843	3.20E-256	5
LIMCH1	2.86E-259	-0.5347456803	0.617	0.794	5.72E-256	5
FNDC4	1.12E-256	-0.4957286274	0.734	0.827	2.24E-253	5
CRISPLD1	1.75E-253	-0.6749148322	0.83	0.821	3.49E-250	5
HSP90AA1	3.28E-252	-0.3509735266	0.996	0.994	6.55E-249	5
CADM1	7.43E-251	-0.5416469562	0.848	0.903	1.49E-247	5
LRRC4B	7.72E-249	-0.4788681911	0.634	0.733	1.54E-245	5
CAMK2N1	1.11E-248	-0.5751566665	0.885	0.871	2.21E-245	5
ZNF503	4.79E-247	0.4585676114	0.702	0.327	9.58E-244	5
GFAP	3.04E-246	-0.6354953364	0.866	0.814	6.07E-243	5
GARS	3.16E-244	0.5201412229	0.766	0.493	6.32E-241	5
ITSN1	2.35E-243	-0.6194174549	0.763	0.856	4.71E-240	5

C21orf62	1.84E-242	-0.2899025192	0.793	0.724	3.68E-239	5
SOX6	8.75E-240	-0.2745579807	0.8	0.755	1.75E-236	5
SCD	1.80E-239	-0.6275263829	0.793	0.896	3.59E-236	5
ANXA2	1.93E-239	0.3969215168	0.991	0.974	3.86E-236	5
AC120042.3	1.23E-238	-0.4641557378	0.729	0.761	2.47E-235	5
SYNJ2	2.42E-238	0.2930462444	0.906	0.619	4.84E-235	5
HTRA1	2.82E-238	-0.6446553431	0.932	0.922	5.63E-235	5
MYO1B	3.27E-238	0.4034780294	0.718	0.412	6.54E-235	5
PTX3	9.15E-238	-0.6413927584	0.932	0.937	1.83E-234	5
EPB41L3	4.63E-237	-0.4181064122	0.615	0.782	9.26E-234	5
ADAMTS1	2.36E-235	0.4391003825	0.773	0.524	4.72E-232	5
FRRS1L	2.87E-234	-0.3399845243	0.429	0.618	5.75E-231	5
NAT8L	2.96E-233	-0.3101368297	0.363	0.6	5.92E-230	5
DAB2	3.67E-231	0.391012598	0.744	0.39	7.34E-228	5
FAT3	4.31E-231	-0.2947545116	0.492	0.679	8.61E-228	5
ITM2B	2.66E-229	-0.4288916595	0.966	0.967	5.32E-226	5
NTM	3.28E-228	0.4625022993	0.773	0.463	6.55E-225	5
CTSC	1.28E-227	-0.6465818653	0.92	0.922	2.56E-224	5
NETO2	8.42E-227	-0.5777229687	0.844	0.838	1.68E-223	5
CAVIN1	1.47E-226	0.486979833	0.884	0.686	2.94E-223	5
PRSS23	3.00E-222	-0.5752117982	0.894	0.913	5.99E-219	5
S1PR3	1.41E-219	-0.2683622477	0.762	0.758	2.81E-216	5
MTSS1	5.91E-218	-0.285545343	0.794	0.746	1.18E-214	5
NRCAM	1.67E-217	-0.4851322506	0.649	0.741	3.34E-214	5
TMEM200C	4.49E-216	-0.276001209	0.72	0.755	8.98E-213	5
ANKS1B	6.36E-216	0.2880450827	0.807	0.593	1.27E-212	5
APC2	1.56E-215	-0.3882108041	0.664	0.791	3.12E-212	5
PLA2G16	7.27E-212	-0.4458051978	0.832	0.815	1.45E-208	5
FBLN5	2.73E-211	-0.6059627801	0.859	0.84	5.46E-208	5
LPCAT2	4.72E-209	-0.438690438	0.58	0.764	9.44E-206	5
ACTN1	1.15E-208	0.3675781818	0.956	0.843	2.30E-205	5
C1orf61	4.39E-206	-0.5698101515	0.889	0.863	8.78E-203	5
IFITM1	3.77E-205	-0.3820030363	0.856	0.751	7.54E-202	5
LPP	1.42E-203	0.4172057609	0.889	0.655	2.84E-200	5
COLGALT2	2.65E-203	-0.2505814352	0.761	0.752	5.31E-200	5
PDE4B	4.14E-203	-0.303375898	0.721	0.762	8.28E-200	5
KCND3	2.34E-201	-0.3234187048	0.677	0.715	4.67E-198	5
NES	2.52E-201	-0.4749957883	0.914	0.94	5.05E-198	5
HLA-C	7.37E-201	-0.5691235578	0.83	0.861	1.47E-197	5

JAM2	8.39E-201	-0.5039313321	0.67	0.767	1.68E-197	5
CHST7	4.36E-200	-0.2953283381	0.679	0.744	8.72E-197	5
CTGF	1.03E-199	-0.6053104575	0.981	0.989	2.06E-196	5
GPC3	9.13E-199	-0.3241822129	0.862	0.801	1.83E-195	5
FHL1	1.54E-198	-0.5239720726	0.846	0.888	3.08E-195	5
WWC1	7.41E-197	-0.3753775406	0.378	0.612	1.48E-193	5
SERPINE1	1.20E-195	0.5567189181	0.826	0.604	2.40E-192	5
PRRX1	1.59E-195	0.5771077473	0.778	0.543	3.19E-192	5
HLA-B	1.96E-195	-0.6370231259	0.849	0.912	3.93E-192	5
FAM171B	1.63E-194	-0.3299131682	0.788	0.774	3.27E-191	5
ITGA6	5.34E-194	-0.3478383473	0.527	0.649	1.07E-190	5
PROM1	3.23E-193	-0.4542046222	0.815	0.775	6.45E-190	5
DNER	1.63E-192	-0.2676040789	0.816	0.728	3.26E-189	5
SPRY1	2.20E-190	-0.5326200268	0.777	0.843	4.40E-187	5
GDPD2	4.29E-190	-0.3939878166	0.715	0.711	8.57E-187	5
C1GALT1	2.28E-188	-0.3782907966	0.673	0.799	4.55E-185	5
NFIA	6.67E-187	-0.5437600012	0.789	0.808	1.33E-183	5
NELL2	1.26E-185	-0.3005526241	0.804	0.753	2.52E-182	5
FAM213A	1.56E-185	-0.5025136671	0.743	0.837	3.13E-182	5
SLC7A5	1.59E-183	0.451867313	0.823	0.662	3.19E-180	5
TAGLN3	6.00E-183	-0.3335624484	0.548	0.699	1.20E-179	5
B3GAT1	5.39E-182	-0.2975456947	0.728	0.717	1.08E-178	5
TRIB3	1.40E-181	0.3688552611	0.666	0.391	2.79E-178	5
SLIT1	1.69E-179	-0.4261048636	0.833	0.727	3.38E-176	5
PEG10	3.24E-177	-0.5970933979	0.888	0.889	6.48E-174	5
PCDH8	3.57E-177	-0.3789209704	0.801	0.757	7.15E-174	5
SYT11	4.51E-176	-0.5611416675	0.843	0.855	9.03E-173	5
TNFRSF11B	1.31E-175	-0.3285896992	0.717	0.702	2.62E-172	5
SUGCT	1.62E-175	0.3440300144	0.651	0.384	3.24E-172	5
FTH1	3.17E-175	-0.2999647859	0.998	0.998	6.34E-172	5
FAM89A	4.93E-175	-0.459876588	0.812	0.846	9.87E-172	5
CFI	7.21E-173	-0.4021320282	0.767	0.734	1.44E-169	5
NCALD	1.78E-172	-0.3081117957	0.754	0.768	3.56E-169	5
AMOTL1	1.78E-172	0.2809697826	0.795	0.545	3.56E-169	5
FSTL5	2.20E-172	-0.3274287358	0.831	0.769	4.40E-169	5
UPP1	3.89E-171	-0.4046261958	0.651	0.81	7.77E-168	5
GBX2	2.67E-170	-0.2688731976	0.599	0.759	5.34E-167	5
GRIN2B	4.19E-170	-0.2915482274	0.807	0.713	8.38E-167	5
DST	9.34E-170	-0.4783919948	0.982	0.98	1.87E-166	5

MEGF10	1.64E-169	-0.2705045029	0.394	0.617	3.27E-166	5
DPYSL5	1.60E-167	-0.4842645135	0.707	0.724	3.20E-164	5
NET1	1.81E-167	0.2989224795	0.652	0.371	3.62E-164	5
COL11A1	5.12E-167	-0.5196938686	0.813	0.885	1.02E-163	5
HERPUD1	8.64E-165	0.3878569842	0.85	0.659	1.73E-161	5
CDH11	2.20E-164	0.4127052586	0.765	0.521	4.39E-161	5
TMEM45A	2.44E-164	0.4984048499	0.631	0.321	4.87E-161	5
PSAP	1.82E-163	-0.3835696873	0.952	0.948	3.64E-160	5
ADGRG1	7.64E-163	-0.3655087513	0.753	0.734	1.53E-159	5
BGN	3.55E-161	0.5875866476	0.633	0.399	7.11E-158	5
NTN1	8.52E-161	-0.4444279316	0.685	0.771	1.70E-157	5
P4HA2	9.17E-157	0.450183968	0.683	0.45	1.83E-153	5
CD44	4.75E-155	-0.4189090727	0.931	0.923	9.50E-152	5
LRRIQ1	1.24E-153	-0.4781377094	0.836	0.806	2.48E-150	5
PPFIBP1	2.07E-152	0.4094364409	0.721	0.472	4.15E-149	5
FBN2	3.96E-152	0.2943996865	0.884	0.65	7.92E-149	5
ID4	7.65E-152	-0.5487287881	0.896	0.873	1.53E-148	5
TM7SF2	2.18E-151	-0.4682639336	0.655	0.764	4.36E-148	5
RAB31	7.41E-149	-0.3857130615	0.771	0.828	1.48E-145	5
LGALS3	1.63E-148	-0.4863952947	0.929	0.942	3.26E-145	5
FRMD6	1.19E-147	0.4256750521	0.642	0.391	2.38E-144	5
POU3F2	1.72E-147	-0.3377658491	0.425	0.67	3.44E-144	5
NMB	2.71E-145	-0.335580784	0.825	0.779	5.41E-142	5
HOXB-AS1	1.43E-144	0.3742182429	0.57	0.309	2.86E-141	5
BMP7	6.74E-144	-0.3597587287	0.612	0.689	1.35E-140	5
TAGLN	1.26E-143	0.3250053852	0.991	0.978	2.52E-140	5
KLF6	5.07E-143	0.4371115549	0.942	0.867	1.01E-139	5
LTBP2	1.72E-142	0.5094657479	0.632	0.404	3.44E-139	5
NLRP1	2.67E-142	-0.4914602799	0.748	0.788	5.34E-139	5
DOK5	2.57E-140	-0.4267266573	0.656	0.747	5.15E-137	5
ALKAL2	7.36E-140	-0.2617248811	0.363	0.557	1.47E-136	5
ENAH	3.17E-139	-0.4214080011	0.876	0.927	6.34E-136	5
COL26A1	1.00E-138	0.345921597	0.845	0.631	2.01E-135	5
FJX1	1.58E-138	-0.4920363466	0.739	0.799	3.16E-135	5
CCL2	3.28E-138	-0.5872913239	0.799	0.827	6.56E-135	5
TUBA1C	1.45E-137	0.5619352725	0.705	0.448	2.90E-134	5
CXXC5	1.78E-136	0.3613103274	0.861	0.717	3.56E-133	5
PREX2	3.57E-134	-0.333967874	0.755	0.727	7.14E-131	5
SLC20A1	4.36E-133	0.4442196997	0.664	0.427	8.72E-130	5

SDC2	9.10E-133	-0.3588305572	0.871	0.865	1.82E-129	5
SEMA6D	1.82E-131	-0.2782047185	0.815	0.718	3.64E-128	5
THBS1	3.58E-131	0.4376094017	0.739	0.478	7.16E-128	5
TENM3	3.98E-130	-0.4286372045	0.839	0.866	7.96E-127	5
BBOX1	3.03E-129	-0.2781868306	0.809	0.716	6.06E-126	5
MT-CYB	5.28E-128	-0.373798028	0.972	0.956	1.06E-124	5
EPHA4	9.04E-128	-0.2863913386	0.492	0.6	1.81E-124	5
TMEM132A	1.81E-127	-0.4763293895	0.818	0.866	3.61E-124	5
ABAT	1.01E-126	-0.3426593915	0.793	0.734	2.01E-123	5
NKD1	1.03E-126	0.2836543211	0.583	0.32	2.06E-123	5
RHOBTB3	2.66E-126	-0.4240626807	0.928	0.928	5.31E-123	5
S100A10	4.25E-126	0.3026010493	0.897	0.736	8.49E-123	5
MYL9	8.42E-126	0.3901487697	0.708	0.459	1.68E-122	5
IL13RA2	1.20E-123	-0.3075534863	0.755	0.661	2.40E-120	5
IFITM2	1.57E-123	-0.3125262808	0.93	0.888	3.14E-120	5
DUSP1	9.13E-122	0.2671643954	0.704	0.516	1.83E-118	5
ATP2B1	1.11E-121	-0.4354876539	0.745	0.826	2.22E-118	5
ZIC2	3.13E-121	-0.2664436285	0.637	0.698	6.26E-118	5
ITGB8	3.94E-120	-0.3991765868	0.89	0.854	7.89E-117	5
CCDC102B	1.43E-119	-0.3703882913	0.834	0.795	2.86E-116	5
PHLDA1	7.92E-119	-0.410150733	0.91	0.898	1.58E-115	5
ARL6IP1	5.46E-118	-0.4301035858	0.736	0.821	1.09E-114	5
ADAM12	7.64E-118	0.2632430843	0.851	0.64	1.53E-114	5
GAP43	5.11E-117	-0.4546484464	0.919	0.902	1.02E-113	5
RASSF2	7.44E-117	-0.3102612564	0.66	0.667	1.49E-113	5
GJA1	2.03E-116	-0.4238493062	0.63	0.733	4.06E-113	5
FSTL1	8.85E-115	0.2974195665	0.924	0.835	1.77E-111	5
ASAH1	1.94E-114	-0.3970557531	0.655	0.757	3.87E-111	5
HLA-A	1.75E-110	-0.4250421402	0.855	0.875	3.50E-107	5
LRRN3	4.60E-110	-0.5197621409	0.681	0.712	9.20E-107	5
PIFO	7.94E-110	-0.281588513	0.727	0.672	1.59E-106	5
SDC3	7.28E-108	-0.3170723192	0.839	0.812	1.46E-104	5
SEZ6L2	1.13E-106	0.3709481718	0.601	0.373	2.26E-103	5
FBXO32	9.33E-106	-0.5265378751	0.76	0.777	1.87E-102	5
VCAN	2.48E-104	0.3328885258	0.877	0.823	4.95E-101	5
COTL1	2.52E-104	-0.4073235927	0.709	0.802	5.04E-101	5
ITGB1	9.95E-104	0.2707002491	0.952	0.915	1.99E-100	5
VEGFA	1.12E-103	0.333472734	0.588	0.324	2.24E-100	5
PEA15	9.30E-102	-0.4314339802	0.808	0.813	1.86E-98	5

HES6	6.37E-101	-0.3133546256	0.274	0.443	1.27E-97	5
IFI6	2.00E-100	-0.4060133645	0.815	0.777	3.99E-97	5
TNIK	7.51E-99	-0.3359624839	0.624	0.67	1.50E-95	5
SERPINE2	2.89E-98	-0.404933141	0.76	0.852	5.78E-95	5
HSPG2	6.50E-97	0.2859286835	0.64	0.41	1.30E-93	5
HLA-DRA	4.91E-96	-0.8631602414	0.949	0.926	9.82E-93	5
CALCRL	5.12E-96	-0.3091452722	0.805	0.745	1.02E-92	5
PPP1R14C	4.00E-95	-0.3259595791	0.782	0.746	7.99E-92	5
ASNS	5.70E-95	0.386421021	0.663	0.493	1.14E-91	5
HEG1	1.18E-94	-0.3154987766	0.633	0.741	2.36E-91	5
CEBPD	7.24E-94	-0.4382541561	0.858	0.807	1.45E-90	5
DPYSL2	9.31E-94	-0.3625562608	0.832	0.828	1.86E-90	5
SMURF2	9.93E-93	0.4259313381	0.649	0.423	1.99E-89	5
GRN	1.87E-92	-0.3330286304	0.87	0.884	3.74E-89	5
SPRY2	1.34E-91	-0.3095268775	0.674	0.718	2.67E-88	5
NAV1	7.54E-91	0.3476745835	0.663	0.479	1.51E-87	5
SCG2	1.98E-89	-0.2876346004	0.773	0.786	3.95E-86	5
FOXP1	8.83E-89	0.3233981976	0.762	0.633	1.77E-85	5
HLA-DPA1	1.53E-88	-0.6743045075	0.857	0.783	3.07E-85	5
ABLIM1	1.87E-85	-0.2872676553	0.332	0.489	3.74E-82	5
SDC1	3.17E-85	0.3557821863	0.566	0.296	6.33E-82	5
IER3	5.08E-84	0.3088814973	0.918	0.822	1.02E-80	5
RBP1	5.59E-84	0.297010681	0.698	0.565	1.12E-80	5
AC092807.3	1.05E-83	0.3748933134	0.708	0.543	2.10E-80	5
PDLIM1	7.26E-80	-0.3276127235	0.671	0.762	1.45E-76	5
ATP1A2	2.46E-79	-0.3627783154	0.825	0.725	4.91E-76	5
PAPPA	2.53E-79	0.7955077777	0.534	0.317	5.07E-76	5
EMC10	3.03E-79	-0.3097618836	0.746	0.735	6.06E-76	5
TUBB6	1.93E-78	0.2592077738	0.823	0.662	3.87E-75	5
HSPA5	7.88E-78	-0.2704115813	0.977	0.974	1.58E-74	5
FHL2	6.38E-77	0.3091481737	0.646	0.492	1.28E-73	5
CD74	1.32E-76	-0.5589565881	0.865	0.798	2.63E-73	5
LAPTM4B	3.64E-75	-0.3351082301	0.813	0.822	7.28E-72	5
MFAP2	3.72E-75	0.3240273687	0.567	0.284	7.44E-72	5
ZFP36L1	5.57E-75	0.2599422949	0.874	0.735	1.11E-71	5
IGFBP3	8.74E-75	0.3733135249	0.595	0.361	1.75E-71	5
LRRN1	1.93E-74	-0.3366903397	0.51	0.603	3.86E-71	5
LMO7	1.98E-74	0.323396455	0.548	0.289	3.95E-71	5
CEBPB	2.42E-74	0.3090782965	0.681	0.538	4.84E-71	5

RTN1	2.85E-74	-0.4067141279	0.825	0.727	5.71E-71	5
THY1	4.94E-74	0.2992675104	0.795	0.701	9.87E-71	5
SORBS2	3.00E-73	-0.3892498507	0.68	0.741	6.01E-70	5
HES1	4.37E-73	-0.3623618031	0.858	0.917	8.73E-70	5
CSRNP3	1.00E-72	-0.4162271585	0.714	0.661	2.00E-69	5
SLC2A1	1.44E-72	0.2914377738	0.668	0.489	2.87E-69	5
PTGFRN	4.49E-72	-0.2867876212	0.71	0.731	8.98E-69	5
ARSJ	2.14E-70	0.2939558796	0.629	0.399	4.28E-67	5
TACC1	1.41E-68	-0.3024754551	0.748	0.81	2.82E-65	5
GPC4	2.57E-67	-0.3296483666	0.933	0.913	5.14E-64	5
HLA-DMA	1.20E-64	-0.3909422527	0.785	0.726	2.41E-61	5
CAV2	3.74E-64	-0.2969100037	0.586	0.673	7.47E-61	5
TENM2	4.90E-64	-0.2669880785	0.748	0.868	9.79E-61	5
GXYLT2	2.16E-62	0.3447459625	0.515	0.322	4.33E-59	5
HLA-DRB5	3.72E-62	-0.2588508484	0.819	0.705	7.44E-59	5
NUPR1	1.68E-61	0.2693520706	0.652	0.514	3.35E-58	5
CXADR	9.98E-60	-0.2544865228	0.442	0.543	2.00E-56	5
TGFB2	4.70E-59	-0.2867233208	0.528	0.616	9.39E-56	5
FILIP1L	5.91E-59	-0.3234176665	0.691	0.746	1.18E-55	5
AHR	7.21E-59	0.2691750405	0.618	0.435	1.44E-55	5
SLC38A1	2.27E-57	0.2729427771	0.544	0.255	4.54E-54	5
DPYSL3	3.54E-57	-0.2912721347	0.823	0.877	7.07E-54	5
CDH13	4.50E-57	-0.258088559	0.612	0.709	9.01E-54	5
SMC4	1.25E-56	0.2503664689	0.747	0.57	2.51E-53	5
ATP1B2	1.54E-56	-0.2814549257	0.814	0.691	3.08E-53	5
PSAT1	6.53E-55	0.2707799102	0.72	0.646	1.31E-51	5
GAS6	1.07E-54	0.2825331829	0.68	0.514	2.14E-51	5
PGPEP1	3.01E-54	-0.2743853251	0.624	0.639	6.01E-51	5
RETREG1	1.89E-53	-0.2807514377	0.816	0.736	3.78E-50	5
MMP15	9.84E-53	-0.2779932966	0.788	0.688	1.97E-49	5
FAM129B	5.79E-50	0.2510423103	0.657	0.527	1.16E-46	5
JUN	7.56E-48	-0.2630309058	0.926	0.928	1.51E-44	5
LPL	1.22E-43	-0.3426375044	0.505	0.522	2.43E-40	5
TMEM106C	1.29E-43	-0.3005472341	0.676	0.679	2.58E-40	5
TENT5A	6.02E-42	-0.2881308346	0.809	0.704	1.20E-38	5
MT2A	1.21E-41	0.2985452963	0.811	0.68	2.43E-38	5
MEST	1.68E-41	0.2600743679	0.823	0.728	3.35E-38	5
ADAMTS12	4.02E-41	0.2651262279	0.584	0.446	8.05E-38	5
GRID2	6.51E-41	-0.2958012852	0.56	0.535	1.30E-37	5

COL27A1	5.47E-40	-0.32923997	0.685	0.7	1.09E-36	5
IRX3	5.21E-39	0.2707003759	0.613	0.476	1.04E-35	5
STC2	5.53E-39	0.5005606813	0.5	0.312	1.11E-35	5
RNF19A	8.39E-39	-0.317717114	0.719	0.712	1.68E-35	5
CHODL	1.95E-37	-0.3328243512	0.418	0.481	3.90E-34	5
ZFP36L2	6.99E-36	-0.2857030168	0.818	0.778	1.40E-32	5
SESN3	7.42E-35	-0.2589737675	0.851	0.808	1.48E-31	5
SLC2A3	1.39E-34	0.2679602143	0.584	0.424	2.78E-31	5
MIAT	2.30E-34	-0.3729336502	0.718	0.656	4.60E-31	5
SLC7A11	2.70E-34	0.2619345045	0.586	0.466	5.39E-31	5
CNIH2	1.20E-33	-0.2610623747	0.682	0.643	2.39E-30	5
MTHFD2	4.57E-33	0.2686618392	0.52	0.327	9.14E-30	5
HES5	2.28E-28	-0.2707820075	0.626	0.569	4.56E-25	5
MMP17	3.62E-26	-0.2832322542	0.817	0.69	7.24E-23	5
PMAIP1	6.44E-23	0.2643838012	0.466	0.343	1.29E-19	5
CCND2	2.27E-21	-0.2641376484	0.883	0.839	4.53E-18	5
COL10A1	5.65E-19	0.3931719417	0.452	0.29	1.13E-15	5
TFPI	8.48E-19	-0.2701440025	0.858	0.759	1.70E-15	5
CREB3L1	3.56E-16	0.2513127061	0.481	0.337	7.12E-13	5
HHIP	9.34E-14	0.4260798513	0.459	0.234	1.87E-10	5
SFRP2	3.58E-11	0.3196777251	0.442	0.333	7.15E-08	5
HLA-DPA1	0	2.144494922	0.981	0.776	0	6
HLA-DRA	0	2.092880304	0.998	0.924	0	6
HLA-DPB1	0	1.688743795	0.966	0.732	0	6
CD74	0	1.660325803	0.987	0.792	0	6
HLA-DRB5	0	1.457001513	0.902	0.701	0	6
HLA-DMA	0	1.367616773	0.967	0.717	0	6
HLA-DQA1	0	1.303974147	0.874	0.7	0	6
HLA-B	0	1.224241624	0.999	0.904	0	6
HLA-DQB1	0	1.213317548	0.864	0.663	0	6
HLA-DRB1	0	1.093508822	0.798	0.195	0	6
HLA-C	0	1.024048046	0.997	0.851	0	6
HLA-A	0	0.7270740382	0.988	0.868	0	6
HLA-E	0	0.7268774045	0.96	0.715	0	6
SFRP1	0	0.6950668078	0.962	0.805	0	6
HLA-DMB	0	0.6748731394	0.837	0.524	0	6
NDFIP1	0	0.5742234512	0.999	0.94	0	6
HLA-DOA	0	0.480723812	0.796	0.569	0	6
B2M	0	0.4142692723	1	0.998	0	6

ESPN	1.80E-283	0.347207542	0.817	0.728	3.60E-280	6
APP	2.95E-281	0.4158508873	0.999	0.934	5.91E-278	6
FAM89A	4.68E-278	0.4637352812	0.958	0.838	9.37E-275	6
LYPD1	2.57E-274	0.4830779097	0.976	0.847	5.14E-271	6
LPL	1.21E-270	0.5170903802	0.794	0.506	2.42E-267	6
CP	1.00E-268	0.5655071614	0.981	0.883	2.01E-265	6
GPM6B	4.13E-266	0.4060149543	1	0.999	8.27E-263	6
MEGF10	3.60E-264	0.375964264	0.858	0.59	7.20E-261	6
TFPI	6.22E-258	0.431583135	0.917	0.756	1.24E-254	6
PEA15	5.90E-251	0.5047979771	0.973	0.804	1.18E-247	6
IFITM3	1.62E-250	0.3450325903	0.999	0.987	3.23E-247	6
ITM2B	3.36E-244	0.3403110539	0.999	0.966	6.71E-241	6
DKK3	4.07E-242	0.4371814104	0.995	0.884	8.13E-239	6
CCDC140	1.05E-237	0.252785335	0.698	0.559	2.09E-234	6
SLN	5.87E-230	0.5185337079	0.79	0.743	1.17E-226	6
SPARC	9.28E-226	0.3025827943	1	0.995	1.86E-222	6
CCDC3	6.33E-221	0.2795987967	0.756	0.66	1.27E-217	6
IFITM2	5.25E-214	0.3583105781	0.979	0.886	1.05E-210	6
NCALD	3.32E-210	0.3054843866	0.894	0.76	6.65E-207	6
NTRK2	3.79E-207	0.4029663214	0.994	0.924	7.57E-204	6
IFITM1	3.47E-201	0.3289331474	0.884	0.75	6.94E-198	6
CDH6	8.20E-201	0.4265970464	0.959	0.858	1.64E-197	6
RHOBTB3	2.54E-200	0.4403058453	0.998	0.924	5.09E-197	6
S100B	4.94E-196	0.3560026249	0.997	0.984	9.89E-193	6
TMEM178A	2.17E-195	0.276991847	0.821	0.573	4.33E-192	6
C1R	4.81E-191	0.2548606214	0.751	0.574	9.63E-188	6
MMP2	8.39E-191	0.4655339066	0.991	0.878	1.68E-187	6
MMP17	1.19E-190	0.3347867049	0.829	0.69	2.39E-187	6
S100A16	1.34E-180	0.3427100789	0.893	0.65	2.69E-177	6
COMT	1.59E-177	0.3740984999	0.727	0.456	3.19E-174	6
NR2F2	8.73E-177	0.3490823585	0.974	0.863	1.75E-173	6
PLTP	4.31E-176	0.3376221549	0.993	0.914	8.62E-173	6
SARAF	1.15E-175	0.2954024694	0.999	0.972	2.30E-172	6
TPM1	6.46E-172	-0.4726585009	0.984	0.966	1.29E-168	6
FN1	2.22E-170	-1.082302043	0.949	0.948	4.43E-167	6
LGALS1	4.96E-170	-0.5289305183	0.951	0.948	9.92E-167	6
THBS2	1.46E-168	0.2521023716	0.766	0.652	2.91E-165	6
OLFML2B	1.15E-166	0.3586551984	0.843	0.622	2.29E-163	6
CAV2	9.80E-165	0.308412629	0.923	0.654	1.96E-161	6

PSAP	2.54E-164	0.2884039508	0.997	0.946	5.08E-161	6
FTL	4.76E-163	0.2694509343	1	0.995	9.51E-160	6
IGFBP5	5.08E-160	0.5458401138	0.92	0.756	1.02E-156	6
GDF10	1.37E-155	0.285638468	0.902	0.827	2.73E-152	6
CAMK2N1	5.21E-154	0.3800226236	0.958	0.867	1.04E-150	6
CFI	2.39E-153	0.2993269252	0.849	0.729	4.79E-150	6
ID2	6.50E-153	0.2938200623	0.704	0.398	1.30E-149	6
CADM1	5.72E-146	0.3321105603	0.993	0.895	1.14E-142	6
SESN3	2.35E-144	0.266354562	0.912	0.805	4.70E-141	6
CTSC	2.50E-143	0.388280419	0.983	0.918	5.00E-140	6
RAI14	7.22E-138	0.2539217024	0.887	0.641	1.44E-134	6
SLIT1	2.06E-137	0.2767909773	0.829	0.728	4.11E-134	6
JAM2	6.33E-136	0.2653801551	0.922	0.753	1.27E-132	6
PCDH7	4.76E-132	0.2504573203	0.807	0.662	9.52E-129	6
LIMCH1	1.21E-131	0.2731534495	0.923	0.776	2.41E-128	6
CRISPLD1	2.27E-124	0.278249593	0.934	0.816	4.55E-121	6
SVIL	6.30E-124	0.3347792766	0.938	0.769	1.26E-120	6
PTGDS	1.38E-123	0.2866375846	0.72	0.61	2.75E-120	6
FAM213A	2.99E-122	0.2510837161	0.952	0.825	5.98E-119	6
NR2F1	3.11E-122	0.2946526304	0.992	0.924	6.22E-119	6
PCSK1N	1.37E-120	0.2787847872	0.976	0.867	2.73E-117	6
CD44	1.03E-119	0.283812548	0.992	0.92	2.05E-116	6
RND3	7.13E-119	0.2680404454	0.96	0.829	1.43E-115	6
GRN	5.49E-118	0.2624662676	0.985	0.877	1.10E-114	6
C1QL1	1.04E-117	0.259006789	0.995	0.952	2.09E-114	6
NMB	4.74E-117	0.2559061506	0.843	0.779	9.47E-114	6
FBLN5	8.53E-117	0.3029868119	0.933	0.836	1.71E-113	6
MLC1	8.90E-117	0.2685750217	0.951	0.869	1.78E-113	6
CEBPD	6.76E-116	0.2972253582	0.91	0.805	1.35E-112	6
ITM2C	8.60E-110	0.2665807619	0.967	0.826	1.72E-106	6
TAGLN	6.51E-109	-0.3089427133	0.993	0.978	1.30E-105	6
CPE	4.03E-100	0.2670271473	1	0.971	8.07E-97	6
SCD	3.08E-98	0.3484934147	0.98	0.885	6.17E-95	6
TTYH1	1.10E-97	0.2900889911	0.994	0.96	2.20E-94	6
SLC1A2	1.14E-97	-0.2532393097	0.665	0.763	2.29E-94	6
SPARCL1	1.27E-97	0.2802367596	0.978	0.929	2.53E-94	6
PMP22	4.36E-96	0.2800910785	0.997	0.951	8.73E-93	6
LGALS3	2.02E-93	0.3281623953	0.995	0.938	4.03E-90	6
CAV1	8.34E-87	0.2736544962	0.959	0.812	1.67E-83	6

CIITA	1.27E-76	0.2768740259	0.605	0.583	2.55E-73	6
SMOC1	9.76E-76	-0.3323398822	0.734	0.808	1.95E-72	6
FBXO32	3.43E-71	0.288383299	0.92	0.768	6.85E-68	6
COL6A3	5.84E-68	-0.7586790576	0.728	0.785	1.17E-64	6
COL1A1	2.65E-64	-0.4815820039	0.984	0.976	5.30E-61	6
CALD1	2.85E-59	-0.3497115062	0.999	0.995	5.70E-56	6
POSTN	6.77E-59	-0.8783679343	0.778	0.818	1.35E-55	6
ACTG2	6.43E-57	-0.3569776103	0.886	0.882	1.29E-53	6
MKI67	5.20E-47	-0.5540187923	0.329	0.486	1.04E-43	6
H2AFZ	1.77E-43	-0.3423001333	0.943	0.896	3.53E-40	6
STMN1	2.99E-35	-0.2598578195	0.976	0.912	5.97E-32	6
TPM4	6.72E-31	-0.2601466001	0.896	0.829	1.34E-27	6
HMGN2	3.76E-25	-0.2861924819	0.89	0.802	7.52E-22	6
COL1A2	1.07E-24	-0.4548509323	0.783	0.822	2.13E-21	6
GREM1	5.28E-24	-0.4875785755	0.576	0.626	1.06E-20	6
ASPM	6.35E-22	-0.3246098601	0.506	0.406	1.27E-18	6
SGO2	1.66E-15	-0.2529846515	0.434	0.512	3.33E-12	6
CENPF	1.10E-13	-0.8663679148	0.551	0.555	2.20E-10	6
HMGB2	6.60E-13	-0.439768649	0.528	0.531	1.32E-09	6
PBK	6.70E-13	-0.253257939	0.395	0.474	1.34E-09	6
ADAMTS6	9.50E-11	-0.2645441666	0.565	0.605	1.90E-07	6
NRP2	2.81E-09	-0.3121796225	0.633	0.617	5.62E-06	6
DCBLD2	3.06E-09	-0.2758207138	0.78	0.726	6.12E-06	6
PHGDH	1.54E-08	-0.3023908217	0.724	0.647	3.09E-05	6
FILIP1L	5.72E-08	-0.2571552992	0.822	0.739	0.0001143386287	6
TYMS	9.63E-07	-0.3130081073	0.448	0.47	0.001925077802	6
UBE2S	7.06E-06	-0.2693010713	0.688	0.63	0.01411980567	6
COL6A1	9.76E-06	-0.4497767831	0.952	0.913	0.01951152292	6
VIM	4.40E-210	-0.3961777987	1	1	8.80E-207	7
ACTB	4.03E-139	-0.3144625763	1	1	8.07E-136	7
HSPA5	9.33E-139	-0.5624822196	0.918	0.976	1.87E-135	7
C21orf58	2.05E-136	1.132029589	0.737	0.521	4.10E-133	7
FIBIN	1.65E-126	-0.2972683505	0.686	0.799	3.29E-123	7
APLP1	3.60E-124	-0.5069680223	0.48	0.79	7.20E-121	7
SPARC	4.40E-124	-0.4146831483	0.982	0.995	8.80E-121	7
GRN	2.27E-123	-0.5801009237	0.65	0.889	4.54E-120	7
HSP90AA1	4.43E-123	-0.3888586219	0.986	0.995	8.85E-120	7
HSP90AB1	6.70E-122	-0.4534248387	0.873	0.956	1.34E-118	7
TUBA1A	2.24E-117	-0.3608161454	1	1	4.48E-114	7

GPM6B	1.99E-115	-0.6003755641	0.996	1	3.98E-112	7
APP	7.60E-111	-0.5170004457	0.829	0.94	1.52E-107	7
ITM2B	9.72E-111	-0.4636933949	0.928	0.968	1.94E-107	7
PLD3	1.10E-107	-0.4597028479	0.884	0.964	2.19E-104	7
APLP2	2.12E-107	-0.5018700268	0.903	0.964	4.23E-104	7
ITGB1	5.62E-105	-0.4743624839	0.758	0.921	1.12E-101	7
PLS3	1.52E-101	-0.4148863193	0.791	0.894	3.03E-98	7
ZMAT3	6.65E-101	-0.3499000943	0.349	0.689	1.33E-97	7
BMP7	5.26E-100	-0.2851771321	0.396	0.692	1.05E-96	7
NTRK2	5.59E-99	-0.6228066243	0.837	0.93	1.12E-95	7
BRCA2	7.24E-98	0.614227479	0.707	0.57	1.45E-94	7
IGFBP2	1.19E-97	-0.4106241312	0.999	1	2.37E-94	7
MARCKSL1	2.03E-97	-0.4615099791	0.776	0.916	4.05E-94	7
CPE	9.74E-97	-0.5612526864	0.939	0.973	1.95E-93	7
DDR1	1.55E-96	-0.4895966004	0.796	0.932	3.11E-93	7
RAB31	2.67E-94	-0.3509852414	0.662	0.828	5.34E-91	7
FANCA	5.15E-93	0.8187984537	0.597	0.367	1.03E-89	7
SDC2	1.00E-92	-0.4534278465	0.656	0.871	2.01E-89	7
PMP22	1.19E-92	-0.5196791923	0.879	0.955	2.37E-89	7
PLPPR3	6.07E-92	-0.3521574164	0.708	0.846	1.21E-88	7
SFRP1	7.47E-90	-0.5465335298	0.683	0.817	1.49E-86	7
APOLD1	1.46E-89	0.4788710258	0.641	0.437	2.93E-86	7
SESN3	2.14E-89	-0.3143437592	0.657	0.815	4.28E-86	7
FAM89A	5.57E-88	-0.2934071541	0.664	0.849	1.11E-84	7
PNRC1	1.30E-87	-0.280974537	0.31	0.622	2.59E-84	7
EMP2	2.15E-84	-0.2550629557	0.464	0.753	4.29E-81	7
HLA-E	2.38E-84	-0.3365630035	0.473	0.734	4.76E-81	7
SQSTM1	6.99E-83	-0.4101383739	0.489	0.786	1.40E-79	7
A2M	4.58E-82	-0.4608665166	0.999	1	9.17E-79	7
SPARCL1	5.53E-81	-0.5819656942	0.858	0.934	1.11E-77	7
EZH2	1.40E-80	0.7476530952	0.631	0.435	2.79E-77	7
GPC4	3.99E-80	-0.4334172502	0.811	0.917	7.98E-77	7
CCND2	4.07E-80	-0.3677122697	0.735	0.845	8.15E-77	7
E2F8	2.41E-78	0.3165686461	0.608	0.486	4.82E-75	7
PTGFRN	8.08E-78	-0.2857284876	0.513	0.735	1.62E-74	7
SARAF	1.01E-76	-0.3883055749	0.931	0.975	2.01E-73	7
LAPTM4B	1.82E-76	-0.3907594146	0.541	0.829	3.65E-73	7
NUSAP1	6.85E-76	0.8227113842	0.648	0.409	1.37E-72	7
F2R	7.01E-76	-0.2563606968	0.274	0.605	1.40E-72	7

DIAPH3	2.68E-75	0.6563584858	0.6	0.4	5.35E-72	7
ADAM9	3.38E-75	-0.4146758487	0.805	0.919	6.76E-72	7
PSAP	7.70E-73	-0.3589465434	0.858	0.951	1.54E-69	7
LHFPL6	2.45E-72	-0.3318136492	0.476	0.734	4.89E-69	7
TFPI	1.56E-71	-0.3170036848	0.633	0.768	3.13E-68	7
P4HB	1.80E-71	-0.3534545918	0.779	0.907	3.61E-68	7
MAP1A	3.07E-71	-0.2887797557	0.597	0.797	6.14E-68	7
PLTP	8.28E-71	-0.4281162843	0.814	0.921	1.66E-67	7
NDFIP1	2.46E-70	-0.4134020471	0.845	0.946	4.92E-67	7
CENPF	3.36E-70	0.6666705727	0.716	0.551	6.72E-67	7
GSN	3.07E-69	-0.3715974607	0.741	0.868	6.15E-66	7
PCSK1N	2.01E-68	-0.4313531318	0.708	0.877	4.01E-65	7
PAM	5.91E-68	-0.310109196	0.773	0.881	1.18E-64	7
SOCS3	1.82E-67	-0.2568286304	0.545	0.751	3.65E-64	7
ATP2B1	1.91E-66	-0.3249399106	0.611	0.827	3.83E-63	7
ATP1B1	3.15E-66	-0.3965886793	0.734	0.839	6.29E-63	7
MLC1	3.39E-66	-0.3980068015	0.763	0.876	6.79E-63	7
WSCD1	8.71E-66	-0.3132958218	0.711	0.82	1.74E-62	7
SPOCK2	4.01E-65	-0.4778168691	0.773	0.879	8.03E-62	7
PKM	1.02E-63	-0.3555011746	0.776	0.895	2.05E-60	7
ASAH1	1.91E-63	-0.357637911	0.485	0.758	3.82E-60	7
PEG10	6.26E-63	-0.4874667187	0.749	0.893	1.25E-59	7
DKK3	1.41E-62	-0.4152863917	0.754	0.893	2.81E-59	7
CCDC85B	6.81E-62	-0.275074785	0.443	0.758	1.36E-58	7
CEBPD	1.24E-61	-0.3588793673	0.709	0.813	2.48E-58	7
ZNF106	2.41E-61	-0.2609207629	0.534	0.778	4.83E-58	7
HSPA8	5.60E-61	-0.2972712984	0.908	0.971	1.12E-57	7
OLFML2B	9.33E-61	-0.2748198745	0.431	0.639	1.87E-57	7
CRISPLD1	1.35E-60	-0.3078754691	0.66	0.826	2.69E-57	7
GDF10	2.58E-59	-0.2788719521	0.745	0.833	5.16E-56	7
TTYH1	5.46E-59	-0.3995492909	0.913	0.963	1.09E-55	7
NLRP1	2.17E-58	-0.3048706563	0.535	0.792	4.35E-55	7
LRRC4B	5.40E-58	-0.2814997519	0.575	0.731	1.08E-54	7
ENO1	1.43E-57	-0.3159720635	0.799	0.904	2.86E-54	7
TUBB2A	1.47E-57	-0.3477441139	0.928	0.975	2.94E-54	7
HLA-A	1.45E-55	-0.4161255816	0.73	0.878	2.90E-52	7
TMEM47	1.73E-55	-0.3015353868	0.725	0.835	3.47E-52	7
GJA1	5.83E-55	-0.3533668801	0.476	0.734	1.17E-51	7
FJX1	7.33E-55	-0.322530874	0.629	0.799	1.47E-51	7

CALU	8.83E-55	-0.2999813516	0.679	0.869	1.77E-51	7
CAMK2N1	9.84E-55	-0.2885579633	0.755	0.875	1.97E-51	7
SSPN	1.88E-54	-0.2610550465	0.567	0.706	3.76E-51	7
MAP1B	4.26E-54	-0.3275685986	0.982	0.993	8.51E-51	7
ATAD5	1.43E-53	0.7330637942	0.616	0.48	2.86E-50	7
FBLN5	2.10E-53	-0.3948586015	0.721	0.844	4.20E-50	7
HTRA1	4.19E-53	-0.3911018536	0.829	0.925	8.39E-50	7
ITGB4	4.92E-53	-0.2684700465	0.697	0.822	9.83E-50	7
MMP2	1.96E-52	-0.3931670095	0.755	0.887	3.92E-49	7
ANLN	5.26E-52	0.4097829086	0.546	0.359	1.05E-48	7
NKAIN3	5.98E-52	-0.3583029269	0.695	0.834	1.20E-48	7
TUBB2B	8.80E-52	-0.3148288161	0.988	0.996	1.76E-48	7
PHLDA1	1.40E-51	-0.3235908738	0.785	0.902	2.79E-48	7
CRB2	9.83E-51	-0.3176899071	0.734	0.84	1.97E-47	7
AC120042.3	1.52E-50	-0.2698061393	0.671	0.761	3.03E-47	7
PRSS23	2.23E-50	-0.3859004905	0.785	0.915	4.45E-47	7
MCM8	3.82E-50	0.4073869582	0.546	0.429	7.64E-47	7
CDH6	4.10E-50	-0.3041773867	0.774	0.866	8.20E-47	7
KIF20B	1.37E-49	0.6314488769	0.593	0.436	2.75E-46	7
HLA-C	1.61E-49	-0.4085976611	0.707	0.863	3.22E-46	7
CYR61	2.21E-49	-0.426573391	0.921	0.971	4.41E-46	7
TIMP2	2.85E-49	-0.3159250223	0.884	0.955	5.70E-46	7
CAVIN1	3.06E-49	-0.292479902	0.455	0.704	6.13E-46	7
JAM2	6.52E-49	-0.2542849269	0.613	0.765	1.30E-45	7
TMEM132A	7.12E-49	-0.3101358832	0.748	0.866	1.42E-45	7
FHL1	9.92E-49	-0.2618443396	0.724	0.89	1.98E-45	7
ITM2C	4.12E-48	-0.3508061843	0.662	0.838	8.24E-45	7
HMGB2	3.68E-47	0.4866292093	0.653	0.528	7.37E-44	7
LYPD1	6.32E-47	-0.3088374635	0.729	0.857	1.26E-43	7
KIF23	7.08E-47	0.3605308971	0.557	0.39	1.42E-43	7
PEA15	7.26E-47	-0.3062102961	0.589	0.818	1.45E-43	7
COL5A2	1.71E-46	-0.3164394045	0.649	0.846	3.41E-43	7
XRCC2	2.44E-46	0.5600975614	0.564	0.451	4.89E-43	7
SCD	3.32E-46	-0.3453811544	0.718	0.895	6.65E-43	7
SGO2	1.03E-45	0.4090962612	0.645	0.504	2.06E-42	7
CXXC5	2.72E-45	-0.2641487239	0.467	0.733	5.44E-42	7
DPYSL2	6.75E-45	-0.2737514559	0.646	0.833	1.35E-41	7
SERPINE2	9.22E-45	-0.3556879461	0.741	0.849	1.84E-41	7
KIF18B	1.04E-44	0.4749345246	0.511	0.37	2.08E-41	7

SOX2	2.99E-44	-0.3140635253	0.807	0.916	5.98E-41	7
CLU	4.25E-44	-0.3292398311	0.987	0.995	8.49E-41	7
ORC6	5.58E-44	0.6834703905	0.576	0.434	1.12E-40	7
ATP1A2	6.41E-44	-0.2653389069	0.668	0.733	1.28E-40	7
SYT11	9.82E-44	-0.2972260166	0.737	0.858	1.96E-40	7
COL4A1	1.78E-43	-0.3201296879	0.838	0.939	3.57E-40	7
CP	1.34E-42	-0.352429747	0.776	0.891	2.67E-39	7
ASPM	1.60E-42	0.8882158784	0.563	0.407	3.20E-39	7
FSTL1	4.16E-42	-0.2872382613	0.679	0.844	8.32E-39	7
CENPU	1.55E-41	0.3098432402	0.547	0.398	3.09E-38	7
SLC3A2	3.10E-41	-0.3128546068	0.776	0.906	6.20E-38	7
PTX3	2.32E-40	-0.4090741847	0.87	0.938	4.63E-37	7
MDK	2.64E-40	-0.2686125736	0.767	0.906	5.27E-37	7
GPM6A	8.28E-39	-0.3020107254	0.9	0.95	1.66E-35	7
HELLS	2.06E-38	0.7767690103	0.613	0.542	4.13E-35	7
FGFBP3	3.96E-38	-0.3310002014	0.795	0.893	7.92E-35	7
SYNE2	1.02E-37	0.5814585984	0.796	0.75	2.05E-34	7
SORBS2	8.17E-36	0.5427614788	0.732	0.738	1.63E-32	7
C1QL1	1.05E-35	-0.3079344983	0.889	0.956	2.10E-32	7
COL27A1	2.28E-35	0.5151677646	0.756	0.697	4.57E-32	7
HMGN2	2.70E-35	0.3299415988	0.813	0.806	5.39E-32	7
RTKN2	3.80E-35	0.5676027855	0.519	0.388	7.60E-32	7
NCAPD3	2.08E-34	0.3282724708	0.496	0.351	4.16E-31	7
PTN	3.82E-34	-0.3552562204	1	1	7.64E-31	7
SOX4	1.03E-33	-0.2942388329	0.707	0.861	2.07E-30	7
ARID5B	2.89E-33	-0.3027207718	0.719	0.871	5.79E-30	7
MT-CYB	4.74E-32	-0.2506590623	0.906	0.958	9.49E-29	7
CTSC	1.32E-31	-0.287236871	0.844	0.924	2.65E-28	7
CCDC80	3.65E-31	-0.3161262398	0.775	0.904	7.30E-28	7
COL11A1	9.09E-30	-0.2811061864	0.809	0.883	1.82E-26	7
CCDC18	1.83E-29	0.5395818252	0.494	0.352	3.66E-26	7
HLA-B	1.85E-29	-0.349438588	0.82	0.911	3.70E-26	7
IGFBP5	2.65E-29	-0.4497031448	0.631	0.768	5.29E-26	7
TMPO	2.85E-29	0.4988950756	0.561	0.467	5.70E-26	7
TROAP	6.36E-28	0.2580009722	0.2	0.293	1.27E-24	7
COL3A1	3.16E-27	-0.3417140469	0.829	0.895	6.32E-24	7
CTGF	5.73E-24	-0.3865946208	0.983	0.989	1.15E-20	7
LGALS3	1.12E-23	-0.281161671	0.844	0.943	2.24E-20	7
HJURP	9.23E-22	0.4442815663	0.471	0.36	1.85E-18	7

TOP2A	8.28E-21	0.4990903332	0.552	0.47	1.66E-17	7
MIS18BP1	1.14E-20	0.772394497	0.519	0.441	2.27E-17	7
CENPK	3.40E-20	0.3411658257	0.611	0.546	6.80E-17	7
NDC80	1.83E-18	0.2728003943	0.48	0.386	3.67E-15	7
WEE1	2.52E-18	0.4150168718	0.742	0.786	5.03E-15	7
HES1	2.85E-18	0.3665407971	0.9	0.914	5.69E-15	7
SMC4	4.69E-18	0.5222954335	0.595	0.581	9.37E-15	7
BUB1B	4.41E-16	0.2502014971	0.309	0.416	8.81E-13	7
KIF18A	9.64E-16	0.4220228611	0.425	0.348	1.93E-12	7
ESCO2	6.92E-15	0.4179711245	0.422	0.306	1.38E-11	7
UHRF1	7.01E-15	0.2881056873	0.459	0.373	1.40E-11	7
IGFBP7	1.00E-14	-0.3337382649	0.702	0.825	2.00E-11	7
COL6A1	1.36E-14	-0.3459688506	0.829	0.917	2.71E-11	7
CHAF1A	2.14E-14	0.2753288583	0.312	0.437	4.29E-11	7
BRIP1	2.03E-13	0.3992272154	0.422	0.337	4.06E-10	7
RAD51AP1	3.26E-13	0.3816817173	0.458	0.386	6.52E-10	7
MKI67	3.72E-13	0.5319367482	0.543	0.476	7.45E-10	7
SGO1	3.89E-12	0.2747214351	0.317	0.4	7.77E-09	7
CKAP2L	2.09E-11	0.3074860087	0.283	0.36	4.18E-08	7
AURKB	1.10E-10	0.503962097	0.453	0.36	2.21E-07	7
SLC4A7	1.21E-10	0.2893180596	0.501	0.45	2.42E-07	7
LIG1	1.93E-10	0.3137064949	0.492	0.431	3.86E-07	7
FANCD2	2.54E-10	0.2735920632	0.393	0.311	5.08E-07	7
KIF15	1.02E-09	0.2967332716	0.482	0.459	2.03E-06	7
G2E3	1.09E-09	0.376156411	0.528	0.495	2.19E-06	7
CLSPN	1.73E-09	0.5633583147	0.459	0.393	3.46E-06	7
NCAPG	4.52E-09	0.4451102952	0.455	0.391	9.04E-06	7
IQGAP3	5.83E-09	0.3089394626	0.283	0.332	1.17E-05	7
DNMT1	7.73E-09	0.3210574027	0.552	0.571	1.55E-05	7
HMGA2	1.14E-08	0.2686765072	0.515	0.485	2.28E-05	7
MXD3	1.28E-08	0.5622027292	0.437	0.356	2.56E-05	7
MYBL2	1.36E-08	0.3299542321	0.347	0.274	2.72E-05	7
CDCA7	2.69E-08	0.3924502104	0.529	0.525	5.39E-05	7
ADGRV1	3.15E-08	0.4938689797	0.804	0.848	6.29E-05	7
POLQ	4.48E-08	0.3461501728	0.482	0.457	8.96E-05	7
COL1A1	6.39E-08	-0.2771542201	0.958	0.977	0.0001278842277	7
GPSM2	2.92E-07	0.2934476588	0.421	0.539	0.0005847572367	7
PI15	3.32E-07	-0.2695952608	0.735	0.82	0.0006642023776	7
GTSE1	4.60E-07	0.677903716	0.446	0.379	0.0009198656008	7

ARHGAP11A	1.14E-06	0.3680483957	0.311	0.367	0.002282812142	7
LRRC4C	1.63E-06	0.3275451075	0.853	0.847	0.003259128698	7
PIF1	2.54E-06	0.9252109671	0.402	0.291	0.005075050874	7
GINS2	2.93E-06	0.3291127033	0.511	0.491	0.005862929945	7
TPX2	4.09E-06	0.3039302061	0.354	0.409	0.008177554464	7
MCM10	9.35E-06	0.2797837682	0.323	0.395	0.01869876571	7
SPC24	1.00E-05	0.256357397	0.395	0.344	0.02005898342	7
NHLH1	1.26E-306	0.6934349295	0.957	0.261	2.52E-303	8
HES5	5.43E-289	2.153964876	0.986	0.567	1.09E-285	8
ST8SIA5	1.34E-246	0.4241758758	0.978	0.646	2.68E-243	8
MFNG	5.46E-232	0.2541784838	0.864	0.142	1.09E-228	8
TESC	3.09E-212	0.4365467345	0.99	0.687	6.19E-209	8
HES6	1.56E-192	2.021645952	0.951	0.426	3.13E-189	8
RYR3	1.19E-185	0.2682948596	0.927	0.477	2.38E-182	8
PCDHB14	6.04E-166	0.2998589626	0.925	0.502	1.21E-162	8
VIM	1.91E-163	-0.5370881227	1	1	3.83E-160	8
ATP1A3	5.93E-157	0.3537363747	0.842	0.387	1.19E-153	8
RCAN1	2.19E-140	-0.4109882724	0.339	0.753	4.37E-137	8
PAX6	2.54E-138	0.3005890282	0.909	0.402	5.09E-135	8
CITED4	7.56E-134	0.3724951109	0.941	0.491	1.51E-130	8
SOX4	3.57E-131	1.296301698	0.968	0.855	7.13E-128	8
PMP22	3.24E-128	-0.9328545882	0.74	0.956	6.47E-125	8
RETREG1	1.08E-126	-0.3547751675	0.375	0.746	2.17E-123	8
BHLHE41	5.02E-125	-0.2763370761	0.312	0.678	1.00E-121	8
CHST2	5.86E-121	-0.3302590921	0.438	0.735	1.17E-117	8
PLS3	2.69E-120	-0.7455610221	0.811	0.892	5.37E-117	8
MCM4	2.33E-118	-0.2751618798	0.146	0.42	4.67E-115	8
DLL3	3.47E-118	0.6993239268	0.801	0.298	6.95E-115	8
SOX11	9.74E-118	1.253243193	0.941	0.778	1.95E-114	8
CD24	8.29E-117	1.278369888	0.777	0.24	1.66E-113	8
CD9	1.50E-116	-0.3583499492	0.146	0.431	2.99E-113	8
ANXA2	1.17E-115	-0.6742503013	0.972	0.975	2.34E-112	8
SEZ6L2	1.28E-115	0.5219882797	0.88	0.38	2.56E-112	8
IGFBP2	2.28E-112	-0.6314521872	1	1	4.56E-109	8
MOXD1	2.56E-109	-0.2658875746	0.491	0.74	5.13E-106	8
SLIT2	2.93E-109	-0.300120305	0.29	0.638	5.85E-106	8
ELMOD1	3.76E-106	-0.5065598248	0.527	0.838	7.52E-103	8
PGPEP1	3.82E-106	-0.3801838603	0.296	0.642	7.64E-103	8
COL4A1	2.62E-102	-0.8320815595	0.842	0.938	5.23E-99	8

MIAT	1.01E-101	1.270873028	0.87	0.656	2.03E-98	8
MLC1	1.04E-101	-0.7375679525	0.706	0.875	2.08E-98	8
APLP2	3.11E-101	-0.7309585469	0.897	0.963	6.23E-98	8
KCTD12	6.95E-100	-0.2833271206	0.438	0.734	1.39E-96	8
ADGRL2	3.15E-99	-0.281384872	0.353	0.672	6.31E-96	8
CDH11	3.14E-98	-0.2712366267	0.26	0.539	6.28E-95	8
CHODL	9.52E-98	-0.4567230344	0.235	0.48	1.90E-94	8
HTRA1	1.29E-97	-0.781441116	0.769	0.925	2.58E-94	8
MYOF	2.34E-97	-0.5051495842	0.414	0.706	4.68E-94	8
NES	6.15E-97	-0.7075464574	0.751	0.941	1.23E-93	8
SPRY1	1.77E-94	-0.6053230691	0.594	0.842	3.55E-91	8
TENT5A	1.04E-93	-0.355529513	0.503	0.714	2.08E-90	8
GRN	7.86E-93	-0.6892645672	0.604	0.887	1.57E-89	8
TMEM200C	1.08E-92	-0.2749277363	0.57	0.755	2.16E-89	8
ITGB4	5.34E-92	-0.5776447434	0.609	0.822	1.07E-88	8
C21orf62	2.67E-91	-0.2613344821	0.493	0.731	5.34E-88	8
SYNM	6.88E-91	-0.6530785014	0.97	0.889	1.38E-87	8
SYNJ2	2.62E-90	-0.4398857467	0.387	0.64	5.25E-87	8
CNTFR	4.92E-90	0.2988451266	0.911	0.616	9.85E-87	8
CDO1	7.10E-90	-0.2870744934	0.247	0.491	1.42E-86	8
SPARCL1	7.11E-89	-0.7859467698	0.978	0.931	1.42E-85	8
CACNA1A	2.07E-87	0.6148264467	0.726	0.371	4.13E-84	8
HEG1	9.99E-87	-0.4441267486	0.422	0.739	2.00E-83	8
ARHGAP29	1.65E-86	-0.7651529353	0.71	0.893	3.30E-83	8
ITGA6	1.42E-85	-0.3179586076	0.41	0.645	2.83E-82	8
NETO2	2.75E-85	-0.5176237465	0.602	0.841	5.50E-82	8
STMN1	6.39E-85	0.6937695984	0.976	0.914	1.28E-81	8
CD44	1.55E-84	-0.6585681757	0.706	0.927	3.10E-81	8
RAB31	4.95E-84	-0.5058959001	0.645	0.827	9.91E-81	8
CSPG5	5.24E-83	-0.2501706885	0.43	0.711	1.05E-79	8
PLTP	8.06E-83	-0.699881232	0.909	0.919	1.61E-79	8
CTGF	1.11E-82	-0.8520520451	0.986	0.989	2.22E-79	8
TNIK	4.61E-82	-0.3034621215	0.408	0.671	9.23E-79	8
ACTN1	1.51E-80	-0.6881107197	0.68	0.852	3.02E-77	8
SPARC	4.99E-80	-0.4551276515	0.994	0.995	9.98E-77	8
GRIA1	7.14E-80	-0.5990836111	0.982	0.912	1.43E-76	8
CDH6	1.42E-78	-0.6976655664	0.961	0.862	2.85E-75	8
MYO1B	1.76E-78	0.2875777668	0.842	0.425	3.53E-75	8
NTRK2	2.24E-78	-0.7488905662	0.976	0.927	4.48E-75	8

ADAMTS16	7.25E-78	-0.3653387155	0.373	0.576	1.45E-74	8
PDPN	2.25E-77	-0.4981547414	0.657	0.893	4.49E-74	8
PLAT	2.71E-77	-0.5096584999	0.649	0.812	5.42E-74	8
PI15	4.83E-77	-0.7973542149	0.854	0.818	9.66E-74	8
EEA1	1.24E-76	-0.3986714292	0.485	0.768	2.47E-73	8
CA14	6.16E-76	0.2889487873	0.842	0.562	1.23E-72	8
WLS	2.66E-75	-0.5804000482	0.982	0.979	5.31E-72	8
DCC	4.57E-75	0.9090048653	0.74	0.44	9.14E-72	8
VASN	7.53E-75	-0.3452231907	0.361	0.607	1.51E-71	8
GPC4	8.62E-75	-0.6423813213	0.957	0.913	1.72E-71	8
OLFML2A	4.80E-74	-0.466682762	0.367	0.591	9.60E-71	8
LPP	4.90E-74	-0.4843445036	0.359	0.674	9.81E-71	8
FBN2	1.55E-73	-0.4046829205	0.442	0.667	3.10E-70	8
NPTX2	3.91E-73	0.4238501623	0.917	0.642	7.82E-70	8
COL12A1	1.80E-72	-0.5546548088	0.84	0.84	3.60E-69	8
GJA1	8.60E-72	-0.5450199965	0.475	0.73	1.72E-68	8
UPP1	2.68E-71	-0.3761608929	0.606	0.803	5.35E-68	8
C1QL1	4.28E-71	-0.570877582	0.992	0.954	8.57E-68	8
NRP2	8.20E-71	-0.2955416027	0.323	0.621	1.64E-67	8
SOCS3	2.61E-70	-0.3790240851	0.477	0.749	5.23E-67	8
MAP1A	9.05E-70	-0.4924153252	0.503	0.796	1.81E-66	8
CRISPLD1	3.85E-69	-0.5952696682	0.734	0.823	7.69E-66	8
SLIT1	7.61E-69	-0.4297766912	0.452	0.738	1.52E-65	8
COL4A2	1.57E-68	-0.5928356808	0.819	0.919	3.13E-65	8
TMEM47	2.59E-68	-0.4882652415	0.74	0.834	5.18E-65	8
ELAVL2	1.24E-67	0.7097296531	0.744	0.377	2.49E-64	8
LPL	3.19E-67	-0.3585947971	0.27	0.525	6.37E-64	8
GPM6B	5.46E-67	-0.6103860964	1	0.999	1.09E-63	8
NTRK3	7.70E-67	-0.5603301245	0.734	0.851	1.54E-63	8
CCDC85B	7.74E-67	-0.4432369019	0.424	0.755	1.55E-63	8
PRSS12	1.78E-66	0.2597210481	0.738	0.372	3.56E-63	8
CAST	2.06E-66	-0.4741413153	0.416	0.66	4.12E-63	8
IFI6	5.30E-66	-0.3908343842	0.481	0.784	1.06E-62	8
ENPP2	1.11E-64	-0.4285908751	0.966	0.799	2.21E-61	8
TOP2A	1.39E-64	-0.483421851	0.266	0.475	2.79E-61	8
COL5A2	1.55E-64	-0.5847281702	0.665	0.844	3.10E-61	8
CRB2	2.23E-64	-0.6049341158	0.795	0.838	4.47E-61	8
COL3A1	2.79E-64	-0.6434455747	0.732	0.896	5.57E-61	8
ZNF106	6.53E-64	-0.4037161941	0.517	0.775	1.31E-60	8

LINC00599	1.35E-63	0.8999094749	0.641	0.236	2.69E-60	8
ITM2C	3.50E-63	-0.4830595743	0.523	0.838	6.99E-60	8
SEPT11	5.45E-63	-0.5589344627	0.759	0.877	1.09E-59	8
WSCD1	2.36E-62	0.3425901123	0.994	0.814	4.71E-59	8
FAM43A	2.45E-62	-0.2631216638	0.379	0.592	4.90E-59	8
NSG2	3.35E-62	0.4376501506	0.627	0.253	6.70E-59	8
IFITM1	3.43E-62	-0.3118598443	0.505	0.761	6.87E-59	8
HSPA5	3.84E-62	-0.4919609599	0.931	0.975	7.68E-59	8
AKAP12	1.06E-61	-0.6185717816	0.458	0.709	2.13E-58	8
SCG3	1.37E-60	0.4623428586	0.728	0.494	2.73E-57	8
FOSL2	1.63E-60	-0.3013042406	0.448	0.645	3.25E-57	8
LYPD1	1.84E-60	-0.5085825825	0.675	0.856	3.68E-57	8
LRP2	3.04E-60	-0.4099106208	0.974	0.826	6.09E-57	8
MYLK	9.57E-60	-0.3384119652	0.667	0.735	1.91E-56	8
NUAK1	3.19E-59	-0.2700752442	0.306	0.578	6.38E-56	8
PRSS23	7.90E-59	-0.5703117272	0.868	0.913	1.58E-55	8
CPD	2.63E-58	-0.3538280912	0.684	0.768	5.26E-55	8
COL11A1	5.05E-57	-0.6353753552	0.876	0.881	1.01E-53	8
PTPRZ1	6.85E-57	-0.4380097967	0.996	0.964	1.37E-53	8
PTMA	1.80E-55	0.5706640992	0.986	0.958	3.60E-52	8
ITSN1	7.74E-55	-0.4626018336	0.714	0.852	1.55E-51	8
GDF10	1.87E-54	-0.4673825033	0.976	0.829	3.75E-51	8
LRRIQ1	4.63E-54	-0.4139581672	0.813	0.808	9.26E-51	8
C1orf61	1.86E-53	0.3323011162	0.99	0.863	3.72E-50	8
BTG2	3.61E-53	0.6279133713	0.801	0.485	7.23E-50	8
NPAS3	1.18E-52	-0.5097915804	0.757	0.821	2.36E-49	8
TENM2	1.25E-52	-0.4197343969	0.895	0.861	2.49E-49	8
TMSB15A	3.51E-52	0.5136168408	0.712	0.274	7.02E-49	8
CALD1	6.31E-52	-0.6031400273	0.994	0.995	1.26E-48	8
LMNA	2.46E-51	-0.4918048163	0.793	0.904	4.92E-48	8
CCDC80	3.14E-51	-0.5824026098	0.856	0.901	6.28E-48	8
CAVIN1	3.69E-51	-0.4586968937	0.479	0.701	7.37E-48	8
TTYH1	8.89E-51	-0.4908448426	0.994	0.961	1.78E-47	8
LBH	9.62E-51	-0.2886626696	0.316	0.477	1.92E-47	8
LIPA	9.74E-51	-0.2614666222	0.671	0.743	1.95E-47	8
ABCA1	1.21E-50	-0.3102963072	0.677	0.807	2.43E-47	8
FAM89A	1.64E-50	-0.3614508981	0.913	0.843	3.27E-47	8
PON2	1.71E-50	-0.4691956124	0.85	0.96	3.42E-47	8
SPOCK2	1.75E-49	-0.5772152246	0.984	0.875	3.50E-46	8

RAI14	3.54E-49	-0.3313771462	0.46	0.657	7.08E-46	8
STMN2	9.66E-49	1.401236069	0.688	0.344	1.93E-45	8
UBALD2	1.72E-48	0.2702265025	0.819	0.397	3.44E-45	8
SDC3	2.76E-48	-0.3418472018	0.929	0.812	5.51E-45	8
LAMA4	1.17E-47	-0.3003635961	0.45	0.698	2.34E-44	8
PBX3	1.68E-47	0.7189936034	0.882	0.607	3.35E-44	8
CAV2	2.15E-47	-0.2909172521	0.391	0.672	4.30E-44	8
ROBO3	2.25E-47	1.034282516	0.728	0.546	4.50E-44	8
TM7SF2	2.35E-47	-0.315805666	0.523	0.761	4.71E-44	8
MXRA5	2.43E-47	-0.2951731567	0.789	0.75	4.87E-44	8
A2M	3.05E-47	-0.4478119159	1	1	6.11E-44	8
ITGAV	4.45E-47	-0.2558192226	0.483	0.695	8.89E-44	8
NEFL	8.53E-47	-0.2763656516	0.972	0.839	1.71E-43	8
FBN1	9.72E-47	-0.2679110886	0.363	0.514	1.94E-43	8
DACH1	1.22E-46	0.3397618611	0.917	0.644	2.45E-43	8
CFLAR	2.34E-45	0.2557736982	0.852	0.503	4.69E-42	8
PPP1R14C	1.11E-44	0.2705901047	0.966	0.745	2.22E-41	8
YWHAH	4.11E-44	-0.3165297643	0.448	0.637	8.22E-41	8
LRP1	5.35E-44	-0.3768690475	0.789	0.894	1.07E-40	8
ROBO2	1.30E-43	0.4054227236	0.728	0.573	2.60E-40	8
PTK7	2.15E-43	-0.3571802372	0.452	0.678	4.31E-40	8
COL18A1	2.25E-43	-0.3404282767	0.44	0.65	4.50E-40	8
THY1	2.89E-43	-0.4093252345	0.531	0.709	5.78E-40	8
P4HB	5.57E-43	-0.323009746	0.824	0.904	1.11E-39	8
SORBS2	8.31E-43	-0.4835628405	0.515	0.741	1.66E-39	8
SRGAP3	1.13E-42	0.7962442964	0.947	0.843	2.25E-39	8
GPC1	1.19E-42	-0.3687772422	0.696	0.831	2.38E-39	8
PHGDH	1.22E-42	-0.3991411276	0.448	0.654	2.45E-39	8
STK38L	1.86E-42	0.3271947742	0.834	0.472	3.71E-39	8
EPB41L3	3.88E-42	-0.2981218513	0.59	0.775	7.76E-39	8
LY6H	4.56E-42	-0.3441019229	0.994	0.975	9.11E-39	8
ADGRG1	7.14E-42	0.4221387933	0.933	0.732	1.43E-38	8
PCDH10	7.75E-42	-0.31059047	0.886	0.784	1.55E-38	8
THSD7A	1.05E-41	1.384332293	0.673	0.457	2.11E-38	8
FIBIN	1.86E-41	-0.352406435	0.968	0.794	3.73E-38	8
PTPRO	3.69E-41	0.2543424286	0.805	0.546	7.37E-38	8
MARCKSL1	4.29E-41	0.4737107375	0.955	0.912	8.59E-38	8
HLA-C	6.05E-41	-0.4798715209	0.718	0.861	1.21E-37	8
RANGAP1	3.48E-40	0.3131852941	0.803	0.435	6.95E-37	8

ASCL1	6.41E-40	0.457930553	0.325	0.415	1.28E-36	8
SARAF	3.11E-39	-0.3473032567	0.949	0.974	6.23E-36	8
MMP2	3.47E-39	-0.4717873373	0.801	0.885	6.93E-36	8
PEA15	1.41E-38	-0.3812215268	0.621	0.815	2.81E-35	8
LAPTM4B	2.91E-38	-0.3176163218	0.598	0.825	5.82E-35	8
CALU	3.29E-38	-0.3741681251	0.74	0.866	6.58E-35	8
KLHL24	3.78E-38	0.3128796992	0.846	0.576	7.56E-35	8
IQGAP2	6.16E-38	-0.384371153	0.864	0.776	1.23E-34	8
EDNRB	2.21E-37	-0.3393716828	0.937	0.778	4.42E-34	8
NAV1	2.96E-37	0.3385935143	0.819	0.486	5.91E-34	8
TMEFF2	3.90E-37	0.2813999888	0.665	0.298	7.81E-34	8
PALLD	6.06E-37	-0.4179122447	0.726	0.853	1.21E-33	8
NTM	2.99E-36	0.6630241281	0.779	0.478	5.98E-33	8
CYR61	1.41E-34	-0.4916897107	0.961	0.97	2.82E-31	8
LIMCH1	1.06E-33	-0.3778796743	0.791	0.783	2.12E-30	8
PAM	1.10E-33	-0.2885500076	0.919	0.878	2.20E-30	8
TMEM158	3.62E-33	-0.361459459	0.629	0.812	7.25E-30	8
PLA2G16	5.71E-33	-0.2992804423	0.866	0.816	1.14E-29	8
ATP2B1	6.03E-33	-0.4225257162	0.868	0.821	1.21E-29	8
CXCR4	7.55E-33	0.4164156856	0.813	0.484	1.51E-29	8
NT5E	1.53E-32	-0.2558378635	0.469	0.598	3.06E-29	8
MSMO1	4.76E-32	-0.2692793905	0.566	0.777	9.52E-29	8
LINC00461	1.78E-31	0.5687012904	0.992	0.898	3.56E-28	8
SFRP1	4.15E-31	-0.502238088	0.913	0.812	8.30E-28	8
DCX	6.62E-31	0.6405745986	0.615	0.235	1.32E-27	8
CHST7	2.08E-30	-0.2736321804	0.868	0.739	4.15E-27	8
TGFB2	2.57E-30	-0.2773229214	0.422	0.613	5.14E-27	8
RAD21	3.30E-30	0.4891938052	0.963	0.745	6.61E-27	8
MKI67	4.76E-30	-0.3010255337	0.872	0.472	9.52E-27	8
CDKN1A	1.52E-29	0.2895113877	0.773	0.412	3.04E-26	8
CRABP1	1.54E-29	0.3214196225	0.428	0.568	3.08E-26	8
CD47	1.54E-29	-0.269042444	0.775	0.902	3.09E-26	8
SMOC1	1.78E-29	0.4490467697	0.992	0.802	3.55E-26	8
GSN	2.20E-29	-0.3740486524	0.966	0.863	4.40E-26	8
HLA-A	4.03E-29	-0.3832757733	0.801	0.875	8.06E-26	8
KCNJ6	5.41E-29	0.2741429157	0.86	0.634	1.08E-25	8
SDC2	2.11E-28	-0.3080333883	0.787	0.866	4.22E-25	8
DDR1	4.17E-28	-0.3218816164	0.832	0.93	8.35E-25	8
FBLN5	4.37E-28	-0.4400216341	0.949	0.839	8.73E-25	8

PTX3	5.41E-28	-0.4151948405	0.988	0.936	1.08E-24	8
PLD3	8.30E-28	-0.2966360233	0.937	0.962	1.66E-24	8
TIMP2	1.89E-27	-0.2856981407	0.986	0.953	3.78E-24	8
ARL6IP1	2.63E-27	-0.2695556275	0.639	0.819	5.25E-24	8
FBXO32	3.03E-27	-0.4393594783	0.653	0.778	6.06E-24	8
GADD45B	3.06E-27	-0.2583099257	0.558	0.738	6.12E-24	8
ABLIM1	3.22E-27	-0.262043417	0.41	0.481	6.43E-24	8
COL1A2	3.37E-27	-0.5622523275	0.748	0.821	6.75E-24	8
ATP1B1	4.12E-27	-0.30359647	0.807	0.836	8.24E-24	8
PSAP	8.10E-27	-0.2758499593	0.935	0.949	1.62E-23	8
HLA-DRB5	1.68E-26	-0.2901708335	0.961	0.708	3.36E-23	8
IGFBP5	2.46E-26	-0.3917096543	0.704	0.766	4.93E-23	8
EFNB2	7.92E-26	-0.3907202693	0.848	0.833	1.58E-22	8
JPT1	9.63E-26	0.3942735175	0.824	0.771	1.93E-22	8
NEAT1	1.57E-25	-0.7944108114	0.98	0.9	3.15E-22	8
NTN1	7.32E-25	-0.3860620926	0.899	0.764	1.46E-21	8
TUBB2B	1.24E-24	0.2870953344	1	0.996	2.48E-21	8
TPM1	1.51E-24	-0.3578776413	0.968	0.967	3.02E-21	8
JUN	1.72E-24	-0.2878692296	0.915	0.928	3.44E-21	8
EZR	2.07E-24	0.5060914899	0.783	0.523	4.14E-21	8
ZFP36L2	3.01E-24	-0.3668379541	0.85	0.78	6.03E-21	8
PDE1C	5.99E-24	-0.3597906193	0.669	0.685	1.20E-20	8
MSH6	7.13E-24	0.3053788112	0.822	0.513	1.43E-20	8
DKK3	1.26E-23	-0.3153972118	0.913	0.889	2.52E-20	8
MYH9	2.35E-23	-0.3378569323	0.598	0.764	4.70E-20	8
CEBPD	4.73E-23	-0.3844695498	0.915	0.809	9.46E-20	8
NDFIP1	8.64E-23	-0.284474477	0.935	0.943	1.73E-19	8
ARID5B	8.81E-23	-0.4164521862	0.937	0.866	1.76E-19	8
BEX1	1.49E-22	0.4942798438	0.801	0.652	2.97E-19	8
BTG1	2.62E-22	0.6678093688	0.71	0.655	5.24E-19	8
IER2	1.59E-21	0.5022922072	0.899	0.716	3.18E-18	8
MT-CO3	2.34E-21	0.275805054	0.998	0.985	4.69E-18	8
CNTN2	7.65E-21	0.5299016704	0.357	0.273	1.53E-17	8
ANXA1	9.47E-21	-0.2930513653	0.736	0.812	1.89E-17	8
TUBB2A	9.57E-21	-0.262116347	0.966	0.974	1.91E-17	8
CTSC	6.08E-20	-0.2844514779	0.982	0.921	1.22E-16	8
HLA-DRA	1.07E-19	-0.6127343961	0.878	0.928	2.14E-16	8
TACC1	1.43E-19	-0.3457527454	0.917	0.805	2.85E-16	8
HLA-DPB1	1.66E-19	-0.3245675426	0.858	0.743	3.32E-16	8

RHOBTB3	8.91E-19	-0.2638927995	0.895	0.929	1.78E-15	8
AC092807.3	1.68E-18	-0.2608834867	0.582	0.552	3.37E-15	8
EMP2	1.94E-18	-0.3121278623	0.882	0.744	3.88E-15	8
CELF5	6.85E-18	0.5569379023	0.538	0.279	1.37E-14	8
IER3	7.03E-18	-0.3934317277	0.838	0.827	1.41E-14	8
LPCAT2	2.56E-17	-0.2806666923	0.89	0.751	5.11E-14	8
ZNF703	4.83E-17	0.2729687238	0.602	0.294	9.67E-14	8
KLF6	7.41E-17	-0.3284798843	0.968	0.87	1.48E-13	8
ELAVL3	6.89E-16	0.6245644431	0.621	0.443	1.38E-12	8
WEE1	1.24E-15	-0.303472527	0.903	0.783	2.49E-12	8
HMGN2	1.36E-15	0.3361621011	0.89	0.805	2.71E-12	8
SLC3A2	2.18E-15	-0.2607989934	0.878	0.903	4.36E-12	8
IER5L	5.30E-15	0.5890561302	0.661	0.488	1.06E-11	8
INSM1	1.84E-14	0.5747924398	0.402	0.48	3.68E-11	8
DLL1	9.39E-14	0.4237571308	0.647	0.394	1.88E-10	8
ZEB1	5.62E-13	0.4752191719	0.921	0.834	1.12E-09	8
CP	1.07E-12	-0.3005132283	0.972	0.887	2.14E-09	8
CELF4	1.18E-12	0.466515681	0.598	0.402	2.35E-09	8
PLAU	1.19E-12	-0.2596729377	0.621	0.666	2.38E-09	8
TAGLN	5.70E-12	-0.2544374141	0.99	0.978	1.14E-08	8
CFI	3.64E-11	-0.2552581817	0.915	0.733	7.28E-08	8
FBLN1	5.13E-11	0.3601429422	0.777	0.542	1.03E-07	8
CKB	1.14E-10	0.2805909123	0.953	0.933	2.27E-07	8
PMEPA1	2.31E-10	0.3092583326	0.803	0.76	4.63E-07	8
KIF5C	2.83E-10	0.3737193134	0.876	0.883	5.67E-07	8
RGS6	7.06E-10	-0.2654254407	0.957	0.786	1.41E-06	8
TGFBI	7.43E-10	-0.2959598	0.742	0.74	1.49E-06	8
GRIA2	1.72E-09	0.6206331312	0.606	0.55	3.44E-06	8
FN1	1.84E-09	-0.3644364188	0.988	0.948	3.67E-06	8
CENPF	2.01E-09	-0.3694412722	0.505	0.556	4.02E-06	8
LMO4	3.52E-09	0.3186542868	0.799	0.656	7.04E-06	8
TAC1	4.73E-09	0.3430284376	0.327	0.2	9.46E-06	8
MT-ATP6	6.83E-09	0.3510449755	0.939	0.906	1.37E-05	8
SAMD11	8.35E-09	0.3355998069	0.337	0.162	1.67E-05	8
CCDC102B	1.16E-07	-0.3267969033	0.862	0.796	0.0002318131657	8
MFAP2	3.32E-07	0.2566195372	0.572	0.297	0.0006630941091	8
CXADR	7.97E-07	0.4212315255	0.692	0.534	0.001594772748	8
MEST	8.37E-07	0.2899942171	0.793	0.733	0.001674721752	8
POU2F2	2.23E-06	0.2800356167	0.331	0.245	0.00445868576	8

APC2	2.39E-06	0.4376820024	0.868	0.782	0.004785964021	8
CYP26A1	2.00E-05	0.3151643689	0.515	0.609	0.03992226996	8
HMGB3	2.54E-05	0.3481927931	0.688	0.543	0.05080823373	8
COL27A1	4.63E-05	-0.4019197608	0.919	0.696	0.09253148272	8

Supplemental Table 4.7. HD iAstro IPA Canonical Pathway Enrichment Analysis Per Cluster

Ingenuity Canonical Pathways	-log(p-value)	Ratio	z-score	Molecules	Cluster
Kinetochore Metaphase Signaling Pathway	8.59	0.105	-3.162	BIRC5,CCNB1,CDK1,CENPE,CENPK,H2AX,H2AZ1,MXD3,NUF2,PTTG1,ZWINT	0
Hepatic Fibrosis / Hepatic Stellate Cell Activation	6.74	0.0619		A2M,CCN2,COL11A1,COL1A1,COL5A1,COL6A1,COL6A2,COL6A3,EDNRB,FN1,MYH9,TNFRSF11B	0
Antigen Presentation Pathway	4.62	0.128		CD74,HLA-DPA1,HLA-DPB1,HLA-DQA1,HLA-DRA	0
GP6 Signaling Pathway	3.84	0.0551	-1.89	COL11A1,COL1A1,COL5A1,COL6A1,COL6A2,COL6A3,LAMB1	0
IGF-1 Signaling	3.47	0.0577		CCN1,CCN2,IGFBP2,IGFBP7,JUN,SOCS3	0
B Cell Development	3.24	0.093		HLA-DPA1,HLA-DPB1,HLA-DQA1,HLA-DRA	0
MSP-RON Signaling In Macrophages Pathway	3.2	0.0513	2.449	HLA-DPA1,HLA-DPB1,HLA-DQA1,HLA-DRA,JUN,SOCS3	0
GADD45 Signaling	3.15	0.15		CCNB1,CCND2,CDK1	0
Cell Cycle: G2/M DNA Damage Checkpoint Regulation	2.99	0.08		CCNB1,CDK1,CKS2,TOP2A	0
Zymosterol Biosynthesis	2.94	0.333		MSMO1,TM7SF2	0
Th2 Pathway	2.84	0.0438		HLA-DPA1,HLA-DPB1,HLA-DQA1,HLA-DRA,JUN,SOCS3	0
ATM Signaling	2.75	0.0515	0.447	CCNB1,CDK1,H2AX,JUN,SMC2	0
Sertoli Cell-Sertoli Cell Junction Signaling	2.6	0.034		A2M,ITGA6,ITGB8,JAM2,JUN,TUBA1B,TUBB2B	0
PD-1, PD-L1 cancer immunotherapy pathway	2.58	0.0472		HLA-DPA1,HLA-DPB1,HLA-DQA1,HLA-DRA,TNFRSF11B	0
Aryl Hydrocarbon Receptor Signaling	2.51	0.0377	0.447	CCND2,CYP1B1,JUN,MCM7,NFIA,NR2F1	0
Role of Osteoblasts, Osteoclasts and Chondrocytes in Rheumatoid Arthritis	2.39	0.0312		APC2,COL1A1,DKK3,GSN,JUN,SFRP1,TNFRSF11B	0
Hypoxia Signaling in the Cardiovascular System	2.37	0.0541		JUN,UBE2C,UBE2S,UBE2T	0
Th1 and Th2 Activation Pathway	2.35	0.0349		HLA-DPA1,HLA-DPB1,HLA-DQA1,HLA-DRA,JUN,SOCS3	0
WNT/β-catenin Signaling	2.34	0.0347	-1.633	APC2,DKK3,JUN,SFRP1,SOX2,SOX9	0
Th1 Pathway	2.32	0.041		HLA-DPA1,HLA-DPB1,HLA-DQA1,HLA-DRA,SOCS3	0

Inhibition of Matrix Metalloproteases	2.3	0.0769		A2M,MMP15,SDC2	0
Cholesterol Biosynthesis I	2.24	0.154		MSMO1,TM7SF2	0
Cholesterol Biosynthesis II (via 24,25-dihydrolanosterol)	2.24	0.154		MSMO1,TM7SF2	0
Cholesterol Biosynthesis III (via Desmosterol)	2.24	0.154		MSMO1,TM7SF2	0
IL-6 Signaling	2.24	0.0391	0.447	A2M,COL1A1,JUN,SOCS3,TNFRSF11B	0
Axonal Guidance Signaling	2.23	0.0217		ADAM9,EFNB2,ITGA6,ITGB8,MMP15,NTN1,NTRK2,SDC2,SLIT1,TUBA1B,TUBB2B	0
Acute Phase Response Signaling	2.2	0.0324	0.816	A2M,CP,FN1,JUN,SOCS3,TNFRSF11B	0
Actin Cytoskeleton Signaling	2.19	0.0286	-1.342	APC2,FN1,GSN,IQGAP2,ITGA6,ITGB8,MYH9	0
Neuroinflammation Signaling Pathway	2.13	0.0254	0	APP,BIRC5,GRIA1,HLA-DPA1,HLA-DPB1,HLA-DQA1,HLA-DRA,JUN	0
Regulation of Cellular Mechanics by Calpain Protease	2.08	0.0449		CCND2,CDK1,ITGA6,ITGB8	0
Role of Macrophages, Fibroblasts and Endothelial Cells in Rheumatoid Arthritis	2.05	0.0246		APC2,CEBPD,DKK3,FN1,JUN,SFRP1,SOCS3,TNFRSF11B	0
IL-4 Signaling	2.02	0.043		HLA-DPA1,HLA-DPB1,HLA-DQA1,HLA-DRA	0
p53 Signaling	1.94	0.0408		BIRC5,CCND2,JUN,SERPINE2	0
DNA damage-induced 14-3-3σ Signaling	1.91	0.105		CCNB1,CDK1	0
Cell Cycle Control of Chromosomal Replication	1.87	0.0536		CDK1,MCM7,TOP2A	0
Pyrimidine Deoxyribonucleotides De Novo Biosynthesis I	1.79	0.0909		RRM2,TYMS	0
Osteoarthritis Pathway	1.73	0.0256	0	FN1,GREM1,HTRA1,ITGA6,ITGB8,SOX9	0
Germ Cell-Sertoli Cell Junction Signaling	1.73	0.0292		A2M,GSN,ITGA6,TUBA1B,TUBB2B	0
Mitotic Roles of Polo-Like Kinase	1.68	0.0455		CCNB1,CDK1,PTTG1	0
14-3-3-mediated Signaling	1.57	0.0315		GFAP,JUN,TUBA1B,TUBB2B	0
Superpathway of Cholesterol Biosynthesis	1.56	0.069		MSMO1,TM7SF2	0
Sonic Hedgehog Signaling	1.56	0.069		CCNB1,CDK1	0
Neurotrophin/TRK Signaling	1.52	0.0395		JUN,NTRK2,SPRY1	0
Signaling by Rho Family GTPases	1.48	0.0224	2	CDH6,GFAP,ITGA6,ITGB8,JUN,STMN1	0
RAC Signaling	1.45	0.029		IQGAP2,ITGA6,ITGB8,JUN	0

BEX2 Signaling Pathway	1.45	0.037		JUN,LGALS1,MAP2	0
Inhibition of Angiogenesis by TSP1	1.44	0.0588		JUN,SDC2	0
Hereditary Breast Cancer Signaling	1.42	0.0282		CCNB1,CCND2,CDK1,H2AX	0
Coagulation System	1.41	0.0571		A2M,TFPI	0
Cyclins and Cell Cycle Regulation	1.41	0.0357		CCNB1,CCND2,CDK1	0
Agranulocyte Adhesion and Diapedesis	1.37	0.0234		FN1,ITGA6,MMP15,MYH9,PODXL2	0
Serine Biosynthesis	1.36	0.2		PHGDH	0
dTMP De Novo Biosynthesis	1.36	0.2		TYMS	0
Calcium Signaling	1.35	0.0231		ATP2B1,GRIA1,MYH9,TPM1,TPM4	0
IL-17A Signaling in Fibroblasts	1.35	0.0526		CEBPD,JUN	0
Hepatic Fibrosis / Hepatic Stellate Cell Activation	9.06	0.067		CCN2,COL11A1,COL12A1,COL27A1,COL3A1,COL4A1,COL4A2,COL5A2,MMP2,MYH10,MYH9,SERPINE1,TGFB2	1
Antigen Presentation Pathway	6.6	0.154		B2M,HLA-A,HLA-C,HLA-DPA1,HLA-DRB5,HLA-E	1
Neuroinflammation Signaling Pathway	5.74	0.0381	-1.897	APP,B2M,FOS,GRIA1,HLA-A,HLA-C,HLA-DPA1,HLA-DRB5,HLA-E,JUN,S100B,TGFB2	1
Tumor Microenvironment Pathway	5.39	0.0503	-0.707	COL3A1,FOS,HLA-A,HLA-C,HLA-E,JUN,MMP15,MMP2,TGFB2	1
PD-1, PD-L1 cancer immunotherapy pathway	5.08	0.066	1.342	B2M,HLA-A,HLA-C,HLA-DPA1,HLA-DRB5,HLA-E,TGFB2	1
GP6 Signaling Pathway	4.57	0.0551	-1.89	COL11A1,COL12A1,COL27A1,COL3A1,COL4A1,COL4A2,COL5A2	1
IGF-1 Signaling	4.1	0.0577		CCN1,CCN2,FOS,IGFBP7,JUN,SOCS3	1
Aryl Hydrocarbon Receptor Signaling	3.95	0.044	-0.378	CCND2,FOS,HSP90AB1,JUN,NFIA,NR2F1,TGFB2	1
Caveolar-mediated Endocytosis Signaling	3.79	0.0667		B2M,HLA-A,HLA-C,HLA-E,ITGB1	1
Neurotrophin/TRK Signaling	3.76	0.0658	0	FOS,JUN,NTRK2,SPRY1,SPRY2	1
Glucocorticoid Receptor Signaling	3.74	0.0224		B2M,FOS,HLA-A,HLA-C,HLA-DPA1,HLA-DRB5,HLA-E,HSP90AB1,HSPA5,JUN,MMP2,SERPINE1,TGFB2	1
WNT/β-catenin Signaling	3.72	0.0405	1.89	APC2,DKK3,JUN,SFRP1,SOX2,SOX4,TGFB2	1
Role of OCT4 in Mammalian Embryonic Stem Cell Pluripotency	3.56	0.087		NR2F1,NR2F2,PARP1,SOX2	1
Natural Killer Cell Signaling	3.35	0.0352	0.378	B2M,COL3A1,HLA-A,HLA-C,HLA-E,HSPA5,ITGB1	1
Apelin Cardiac Fibroblast Signaling Pathway	3.3	0.13		CCN2,SERPINE1,TGFB2	1

TGF-β Signaling	3.29	0.0521	-1.342	FOS,JUN,PMEPA1,SERPINE1,TGFB2	1
HIF1α Signaling	3.24	0.0337	-1.89	HSPA5,JUN,MMP15,MMP2,PKM,SERPINE1,TGFB2	1
Axonal Guidance Signaling	3.13	0.0217		DPYSL5,EFNB2,ITGB1,MMP15,MMP2,NTN1,NTRK2, SDC2,SLIT1,SLIT2,TUBB	1
Virus Entry via Endocytic Pathways	3.13	0.0481		B2M,HLA-A,HLA-C,HLA-E,ITGB1	1
Phagosome Maturation	3.1	0.0377		B2M,HLA-A,HLA-C,HLA-DRB5,HLA-E,TUBB	1
Role of Tissue Factor in Cancer	2.92	0.0431		CCN1,CCN2,EGR1,ITGB1,P4HB	1
MSP-RON Signaling In Macrophages Pathway	2.9	0.0427	-0.447	FOS,HLA-DPA1,HLA-DRB5,JUN,SOCS3	1
Tight Junction Signaling	2.85	0.0337		FOS,JAM2,JUN,MYH10,MYH9,TGFB2	1
CDC42 Signaling	2.69	0.0191	-2.236	APC2,B2M,FOS,HLA-A,HLA-C,HLA-DPA1,HLA-DRB5,HLA-E,IQGAP2,ITGB1,JUN	1
Regulation Of The Epithelial Mesenchymal Transition By Growth Factors Pathway	2.68	0.0312	-2.449	EGR1,FOS,JUN,MEST,MMP2,TGFB2	1
PPARα/RXRα Activation	2.67	0.0311	0.816	ABCA1,HSP90AB1,JUN,LPL,NR2F1,TGFB2	1
IL-17A Signaling in Fibroblasts	2.66	0.0789		CEBPD,FOS,JUN	1
RAR Activation	2.64	0.0306		FOS,JUN,NR2F1,NR2F2,PARP1,TGFB2	1
Inhibition of Matrix Metalloproteases	2.62	0.0769		MMP15,MMP2,SDC2	1
Th2 Pathway	2.6	0.0365		HLA-A,HLA-DPA1,HLA-DRB5,JUN,SOCS3	1
B Cell Development	2.5	0.0698		HLA-A,HLA-DPA1,HLA-DRB5	1
Crosstalk between Dendritic Cells and Natural Killer Cells	2.45	0.044		HLA-A,HLA-C,HLA-DRB5,HLA-E	1
DNA Double-Strand Break Repair by Non-Homologous End Joining	2.4	0.143		PARP1,PRKDC	1
Role of Osteoblasts, Osteoclasts and Chondrocytes in Rheumatoid Arthritis	2.35	0.0268		APC2,DKK3,FOS,GSN,JUN,SFRP1	1
p53 Signaling	2.34	0.0408		CCND2,JUN,PRKDC,SERPINE2	1
Granzyme B Signaling	2.28	0.125		PARP1,PRKDC	1
HOTAIR Regulatory Pathway	2.28	0.0307	0	COL3A1,JAM2,MMP15,MMP2,PCDH10	1
NRF2-mediated Oxidative Stress Response	2.23	0.0253	-1	ENC1,FOS,HERPUD1,HSP90AB1,JUN,JUNB	1
PPAR Signaling	2.2	0.0374		FOS,HSP90AB1,JUN,NR2F1	1
Th1 and Th2 Activation Pathway	2.18	0.0291		HLA-A,HLA-DPA1,HLA-DRB5,JUN,SOCS3	1

Actin Cytoskeleton Signaling	2.17	0.0245	-0.816	APC2,GSN,IQGAP2,ITGB1,MYH10,MYH9	1
Role of Macrophages, Fibroblasts and Endothelial Cells in Rheumatoid Arthritis	2.15	0.0215		APC2,CEBPD,DKK3,FOS,JUN,SFRP1,SOCS3	1
CDK5 Signaling	2.13	0.0357		EGR1,ITGB1,NTRK2,PPP1R14C	1
Hepatic Fibrosis Signaling Pathway	2.08	0.0191	-2.646	APC2,CCN2,COL3A1,FOS,ITGB1,JUN,SERPINE1,TGFB2	1
Neuroprotective Role of THOP1 in Alzheimer's Disease	2.06	0.0339		APP,HLA-A,HLA-C,HLA-E	1
IL-17 Signaling	2.03	0.0267	-2.236	FOS,HSP90AB1,JUN,MMP2,TGFB2	1
Th1 Pathway	2.01	0.0328		HLA-A,HLA-DPA1,HLA-DRB5,SOCS3	1
ILK Signaling	1.93	0.0253	-2.236	FOS,ITGB1,JUN,MYH10,MYH9	1
Protein Ubiquitination Pathway	1.93	0.0218		B2M,HLA-A,HLA-C,HLA-E,HSP90AB1,HSPA5	1
IL-10 Signaling	1.88	0.0417		FOS,JUN,SOCS3	1
IL-17A Signaling in Gastric Cells	1.87	0.0769		FOS,JUN	1
Role of PKR in Interferon Induction and Antiviral Response	1.85	0.0294	0	FOS,HSP90AB1,HSPA5,JUN	1
Hypoxia Signaling in the Cardiovascular System	1.85	0.0405		HSP90AB1,JUN,P4HB	1
Agranulocyte Adhesion and Diapedesis	1.8	0.0234		ITGB1,MMP15,MMP2,MYH10,MYH9	1
Calcium Signaling	1.78	0.0231		ATP2B1,GRIA1,MYH10,MYH9,TPM2	1
Thyroid Cancer Signaling	1.77	0.038		FOS,JUN,NTRK2	1
JAK/STAT Signaling	1.73	0.0366		FOS,JUN,SOCS3	1
HER-2 Signaling in Breast Cancer	1.7	0.022	-1.342	FOS,ITGB1,JUN,MMP2,MT-CO1	1
TNFR2 Signaling	1.7	0.0625		FOS,JUN	1
Synaptogenesis Signaling Pathway	1.69	0.0192	-2.449	CDH6,EFNB2,GRIA1,MAP1B,NTRK2,SYT11	1
Prolactin Signaling	1.68	0.0349		FOS,JUN,SOCS3	1
Inhibition of Angiogenesis by TSP1	1.65	0.0588		JUN,SDC2	1
Coagulation System	1.62	0.0571		SERPINE1,TFPI	1
Unfolded protein response	1.62	0.0333		CEBPD,HSPA5,P4HB	1
RANK Signaling in Osteoclasts	1.61	0.033		FOS,GSN,JUN	1
T Cell Receptor Signaling	1.6	0.0147	-2.333	B2M,FOS,HLA-A,HLA-C,HLA-DPA1,HLA-DRB5,HLA-E,ITGB1,JUN	1
IL-4 Signaling	1.59	0.0323		HLA-A,HLA-DPA1,HLA-DRB5	1
Human Embryonic Stem Cell Pluripotency	1.57	0.0241		APC2,NTRK2,SOX2,TGFB2	1

HMGB1 Signaling	1.56	0.024		FOS,JUN,SERPINE1,TGFB2	1
UVA-Induced MAPK Signaling	1.53	0.0306		FOS,JUN,PARP1	1
Germ Cell-Sertoli Cell Junction Signaling	1.52	0.0234		GSN,ITGB1,TGFB2,TUBB	1
Neuropathic Pain Signaling In Dorsal Horn Neurons	1.49	0.0297		FOS,GRIA1,NTRK2	1
Erythropoietin Signaling Pathway	1.48	0.0226	-1	CCND2,FOS,JUN,TGFB2	1
April Mediated Signaling	1.48	0.0476		FOS,JUN	1
Molecular Mechanisms of Cancer	1.48	0.0157		APC2,CCND2,FOS,ITGB1,JUN,PRKDC,TGFB2	1
Mouse Embryonic Stem Cell Pluripotency	1.46	0.0288		APC2,ID4,SOX2	1
B Cell Activating Factor Signaling	1.46	0.0465		FOS,JUN	1
MIF Regulation of Innate Immunity	1.44	0.0455		FOS,JUN	1
Signaling by Rho Family GTPases	1.43	0.0187	-2.236	CDH6,FOS,ITGB1,JUN,SEPTIN11	1
Colorectal Cancer Metastasis Signaling	1.43	0.0186	-2	FOS,JUN,MMP15,MMP2,TGFB2	1
Coronavirus Replication Pathway	1.42	0.0444		IFITM3,TUBB	1
Acute Phase Response Signaling	1.42	0.0216	-1	FOS,JUN,SERPINE1,SOCS3	1
GNRH Signaling	1.4	0.0213	-2	EGR1,FOS,JUN,MMP2	1
Granulocyte Adhesion and Diapedesis	1.39	0.0212		ITGB1,MMP15,MMP2,SDC2	1
iNOS Signaling	1.39	0.0426		FOS,JUN	1
Leukocyte Extravasation Signaling	1.36	0.0207		ITGB1,JAM2,MMP15,MMP2	1
Cell Cycle: G2/M DNA Damage Checkpoint Regulation	1.34	0.04		PRKDC,TOP2A	1
OX40 Signaling Pathway	1.33	0.0146		B2M,HLA-A,HLA-C,HLA-DPA1,HLA-DRB5,HLA-E,JUN	1
Ceramide Degradation	1.33	0.143		ASAH1	1
UVC-Induced MAPK Signaling	1.32	0.0392		FOS,JUN	1
TNFR1 Signaling	1.31	0.0385		FOS,JUN	1
UVB-Induced MAPK Signaling	1.31	0.0385		FOS,JUN	1
Hepatic Fibrosis / Hepatic Stellate Cell Activation	11.8	0.067		A2M,COL11A1,COL18A1,COL1A2,COL27A1,COL3A1,COL4A1,COL4A2,COL6A2,FN1,IGFBP5,MYH9,SERPINE1	2
GP6 Signaling Pathway	7.19	0.063	0	COL11A1,COL18A1,COL1A2,COL27A1,COL3A1,COL4A1,COL4A2,COL6A2	2
Caveolar-mediated Endocytosis Signaling	4.79	0.0667		ACTG2,CAV1,CAVIN1,ITGA3,ITGB1	2

Osteoarthritis Pathway	4.23	0.0299	0.816	ANXA2,CEBPB,FN1,GREM1,HTRA1,ITGA3,ITGB1	2
Actin Cytoskeleton Signaling	4.1	0.0286	1.633	ACTG2,ACTN1,FN1,ITGA3,ITGB1,MYH9,MYLK	2
Germ Cell-Sertoli Cell Junction Signaling	4.07	0.0351		A2M,ACTG2,ACTN1,ITGA3,ITGB1,TUBB2B	2
Apelin Liver Signaling Pathway	3.76	0.115		COL18A1,COL1A2,COL3A1	2
Ferroptosis Signaling Pathway	3.72	0.0397	0.447	H2AX,H2AZ1,SLC1A5,SLC3A2,SQSTM1	2
Sertoli Cell-Sertoli Cell Junction Signaling	3.63	0.0291		A2M,ACTG2,ACTN1,ITGA3,ITGB1,TUBB2B	2
Integrin Signaling	3.55	0.0282	2.449	ACTG2,ACTN1,CAV1,ITGA3,ITGB1,MYLK	2
Hepatic Fibrosis Signaling Pathway	3.41	0.0191	1.414	CEBPB,COL18A1,COL1A2,COL3A1,ITGA3,ITGB1,MYLK,SERPINE1	2
Coagulation System	3.37	0.0857		A2M,PLAU,SERPINE1	2
Antigen Presentation Pathway	3.23	0.0769		CD74,HLA-DPB1,HLA-DRA	2
Intrinsic Prothrombin Activation Pathway	3.14	0.0714		COL18A1,COL1A2,COL3A1	2
Kinetochore Metaphase Signaling Pathway	3	0.0381	-2	CCNB1,CENPE,H2AX,H2AZ1	2
Acute Phase Response Signaling	2.95	0.027	-0.447	A2M,CEBPB,CP,FN1,SERPINE1	2
Paxillin Signaling	2.95	0.037	2	ACTG2,ACTN1,ITGA3,ITGB1	2
Regulation of Actin-based Motility by Rho	2.84	0.0345	1	ACTG2,ITGA3,ITGB1,MYLK	2
ILK Signaling	2.83	0.0253	1.342	ACTG2,ACTN1,FN1,ITGB1,MYH9	2
Agranulocyte Adhesion and Diapedesis	2.68	0.0234		ACTG2,FN1,ITGA3,ITGB1,MYH9	2
Atherosclerosis Signaling	2.66	0.0308		CLU,COL18A1,COL1A2,COL3A1	2
Mitotic Roles of Polo-Like Kinase	2.57	0.0455		CCNB1,HSP90AB1,PLK2	2
Remodeling of Epithelial Adherens Junctions	2.53	0.0441		ACTG2,ACTN1,TUBB2B	2
NRF2-mediated Oxidative Stress Response	2.49	0.0211		ACTG2,HERPUD1,HSP90AB1,JUNB,SQSTM1	2
Signaling by Rho Family GTPases	2.26	0.0187	0.447	ACTG2,GFAP,ITGA3,ITGB1,MYLK	2
Regulation of Cellular Mechanics by Calpain Protease	2.2	0.0337		ACTN1,ITGA3,ITGB1	2
Tumor Microenvironment Pathway	2.16	0.0223		COL1A2,COL3A1,FN1,PLAU	2
Leukocyte Extravasation Signaling	2.05	0.0207	2	ACTG2,ACTN1,ITGA3,ITGB1	2
Clathrin-mediated Endocytosis Signaling	2.05	0.0207		ACTG2,CLU,ITGB1,SH3BP4	2

Virus Entry via Endocytic Pathways	2.02	0.0288		ACTG2,CAV1,ITGB1	2
Natural Killer Cell Signaling	2	0.0201	1	COL18A1,COL1A2,COL3A1,ITGB1	2
Glucocorticoid Receptor Signaling	1.95	0.012		A2M,CAV1,HLA-DPB1,HLA-DRA,HSP90AB1,PLAU,SERPINE1	2
Autophagy	1.9	0.0188	-1	SLC1A5,SLC3A2,SLC7A5,SQSTM1	2
RHOGDI Signaling	1.89	0.0186		ACTG2,ITGA3,ITGB1,MYH9	2
Neuregulin Signaling	1.88	0.0256		HSP90AB1,ITGA3,ITGB1	2
FAK Signaling	1.88	0.0256		ACTG2,ITGA3,ITGB1	2
PAK Signaling	1.87	0.0254		ITGA3,ITGB1,MYLK	2
B Cell Development	1.85	0.0465		HLA-DPB1,HLA-DRA	2
RHOA Signaling	1.81	0.0242		ACTG2,MYLK,NRP2	2
Cell Cycle: G2/M DNA Damage Checkpoint Regulation	1.73	0.04		CCNB1,TOP2A	2
Axonal Guidance Signaling	1.7	0.0119		ITGA3,ITGB1,NRP2,SLIT1,SRGAP3,TUBB2B	2
CSDE1 Signaling Pathway	1.63	0.0357		FABP7,FN1	2
Dilated Cardiomyopathy Signaling Pathway	1.63	0.0205		ACTG2,MYH9,TPM1	2
Cellular Effects of Sildenafil (Viagra)	1.6	0.0201		ACTG2,MYH9,MYLK	2
Semaphorin Neuronal Repulsive Signaling Pathway	1.59	0.0199		ITGA3,ITGB1,NRP2	2
Agrin Interactions at Neuromuscular Junction	1.46	0.0286		ACTG2,ITGB1	2
Senescence Pathway	1.44	0.0135	1	CCNB1,CEBPB,SERPINE1,SQSTM1	2
Hypoxia Signaling in the Cardiovascular System	1.41	0.027		HSP90AB1,UBE2C	2
Tight Junction Signaling	1.41	0.0169		ACTG2,MYH9,MYLK	2
VDR/RXR Activation	1.37	0.0256		CEBPB,IGFBP5	2
NF-κB Activation by Viruses	1.37	0.0256		ITGA3,ITGB1	2
Neuroinflammation Signaling Pathway	1.36	0.0127		HLA-DPB1,HLA-DRA,S100B,SLC1A2	2
Kinetochore Metaphase Signaling Pathway	42.7	0.333	4.642	AURKB,BIRC5,BUB1,BUB1B,BUB3,CCNB1,CDC20,CDCA8,CDK1,CENPA,CENPE,CENPH,CENPK,CENPN,CENPU,CENPW,DSN1,H2AX,H2AZ1,KIF2C,KNL1,MAD2L1,MXD3,NDC80,NEK2,NUF2,PLK1,PTTG1,RAD21,SMC1A,SPC24,SPC25,SPDL1,TTK,ZWINT	3

Cell Cycle Control of Chromosomal Replication	18.4	0.286	4	CDC45,CDC6,CDK1,CDT1,DBF4,LIG1,MCM2,MCM3,MCM4,MCM5,MCM6,MCM7,ORC6,PCNA,POLA2,TOP2A	3
Cell Cycle: G2/M DNA Damage Checkpoint Regulation	12.9	0.24	-1.667	AURKA,BRCA1,CCNB1,CCNB2,CDK1,CHEK1,CKS1B,CKS2,PLK1,PRKDC,TOP2A,YWHAH	3
Mitotic Roles of Polo-Like Kinase	12.8	0.197	1.667	CCNB1,CCNB2,CDC20,CDK1,FBXO5,HSP90AA1,KIF11,KIF23,PLK1,PRC1,PTTG1,RAD21,SMC1A	3
Role of BRCA1 in DNA Damage Response	9.12	0.138	1.414	BARD1,BRCA1,BRCA2,CHEK1,E2F1,FANCA,FANCD2,MSH6,PLK1,RFC3,RFC4	3
Hereditary Breast Cancer Signaling	8.44	0.0915		BARD1,BRCA1,BRCA2,CCNB1,CDK1,CHEK1,E2F1,FANCA,FANCD2,H2AX,MSH6,RFC3,RFC4	3
Role of CHK Proteins in Cell Cycle Checkpoint Control	8.11	0.158	-0.447	BRCA1,CDK1,CHEK1,CLSPN,E2F1,PCNA,PLK1,RFC3,RFC4	3
BER (Base Excision Repair) Pathway	7.77	0.182	2.828	E2F1,FEN1,HMGB1,LIG1,PARP1,PCNA,RFC3,RFC4	3
Mismatch Repair in Eukaryotes	6.31	0.312		FEN1,MSH6,PCNA,RFC3,RFC4	3
ATM Signaling	6.06	0.0928	1	BRCA1,CCNB1,CCNB2,CDK1,CHEK1,FANCD2,H2AX,SMC1A,SMC2	3
NER (Nucleotide Excision Repair, Enhanced Pathway)	5.84	0.0874	1.89	CHAF1A,H4C3,LIG1,PCNA,POLA2,POLD3,RFC3,RFC4,TOP2A	3
Pyrimidine Deoxyribonucleotides De Novo Biosynthesis I	5.55	0.227	2.236	DTYMK,DUT,RRM1,RRM2,TYMS	3
DNA damage-induced 14-3-3σ Signaling	4.39	0.211		BRCA1,CCNB1,CCNB2,CDK1	3
GADD45 Signaling	4.3	0.2		BRCA1,CCNB1,CDK1,PCNA	3
Hepatic Fibrosis / Hepatic Stellate Cell Activation	3.65	0.0464		COL1A1,COL1A2,COL3A1,COL6A1,COL6A2,COL6A3,FN1,IGFBP5,MYH10	3
Cyclins and Cell Cycle Regulation	3.59	0.0714	1.633	CCNA2,CCNB1,CCNB2,CDK1,CDKN2C,E2F1	3
DNA Double-Strand Break Repair by Homologous Recombination	3.42	0.214		BRCA1,BRCA2,LIG1	3
Granzyme B Signaling	3.24	0.188		LMNB1,PARP1,PRKDC	3
p53 Signaling	3.22	0.0612	-0.447	BIRC5,BRCA1,CHEK1,E2F1,PCNA,PRKDC	3
dTMP De Novo Biosynthesis	2.97	0.4		DHFR,TYMS	3
Coronavirus Replication Pathway	2.9	0.0889	2	TUBA1B,TUBB,TUBB4B,TUBB6	3
Aryl Hydrocarbon Receptor Signaling	2.82	0.044	1.633	CCNA2,CHEK1,CYP1B1,DHFR,E2F1,HSP90AA1,MCM7	3
GP6 Signaling Pathway	2.64	0.0472	-2.449	COL1A1,COL1A2,COL3A1,COL6A1,COL6A2,COL6A3	3
Estrogen-mediated S-phase Entry	2.6	0.115		CCNA2,CDK1,E2F1	3

Apelin Liver Signaling Pathway	2.6	0.115		COL1A1,COL1A2,COL3A1	3
Senescence Pathway	2.36	0.0303	-1	CCNB1,CCNB2,CDK1,CHEK1,DHCR24,E2F1,EZH2,PARP1,PHF19	3
Pyridoxal 5'-phosphate Salvage Pathway	2.29	0.0606	2	CDK1,NEK2,PLK1,TTK	3
Remodeling of Epithelial Adherens Junctions	2.24	0.0588		TUBA1B,TUBB,TUBB4B,TUBB6	3
Hypoxia Signaling in the Cardiovascular System	2.11	0.0541		HSP90AA1,UBE2C,UBE2S,UBE2T	3
Protein Ubiquitination Pathway	2.05	0.0291		BRCA1,CDC20,DNAJC9,HSP90AA1,UBE2C,UBE2S,UBE2T,USP1	3
DNA Double-Strand Break Repair by Non-Homologous End Joining	2.04	0.143		PARP1,PRKDC	3
Intrinsic Prothrombin Activation Pathway	2.01	0.0714		COL1A1,COL1A2,COL3A1	3
14-3-3-mediated Signaling	1.95	0.0394		TUBA1B,TUBB,TUBB4B,TUBB6,YWHAH	3
Role of OCT4 in Mammalian Embryonic Stem Cell Pluripotency	1.9	0.0652		BRCA1,PARP1,SOX2	3
RAN Signaling	1.87	0.118		KPNA2,RANGAP1	3
Granzyme A Signaling	1.78	0.105		H1-10,HMGB2	3
Salvage Pathways of Pyrimidine Ribonucleotides	1.7	0.0408	2	CDK1,NEK2,PLK1,TTK	3
Asparagine Degradation I	1.68	0.5		ASRGL1	3
Spermine Biosynthesis	1.68	0.5		SMS	3
Sumoylation Pathway	1.63	0.0388		PCNA,RANGAP1,RFC3,RFC4	3
Epithelial Adherens Junction Signaling	1.6	0.0318	2.236	ECT2,KIF23,MYH10,RACGAP1,YWHAH	3
Phagosome Maturation	1.58	0.0314		HLA-DRA,TUBA1B,TUBB,TUBB4B,TUBB6	3
Glycolysis I	1.55	0.08		ENO1,PKM	3
HOTAIR Regulatory Pathway	1.53	0.0307	0	COL1A1,COL1A2,COL3A1,EZH2,FOXM1	3
Superpathway of Cholesterol Biosynthesis	1.43	0.069		DHCR24,FDPS	3
Sonic Hedgehog Signaling	1.43	0.069		CCNB1,CDK1	3
Spermine and Spermidine Degradation I	1.38	0.25		SAT1	3
Ferroptosis Signaling Pathway	1.35	0.0317	-2	FANCD2,H2AX,H2AZ1,SAT1	3
Atherosclerosis Signaling	1.31	0.0308		CLU,COL1A1,COL1A2,COL3A1	3

Hepatic Fibrosis / Hepatic Stellate Cell Activation	4.84	0.0309		COL1A1,COL27A1,COL4A1,COL4A2,IGFBP5,MMP2	4
GP6 Signaling Pathway	4.61	0.0394	-1.342	COL1A1,COL27A1,COL4A1,COL4A2,TLN1	4
Mitochondrial Dysfunction	2.92	0.0234		APP,MT-CO1,MT-CYB,MT-ND4	4
WNT/β-catenin Signaling	2.9	0.0231	1	DKK3,SFRP1,SOX2,SOX6	4
Oxidative Phosphorylation	2.48	0.0273		MT-CO1,MT-CYB,MT-ND4	4
Estrogen Receptor Signaling	2.32	0.0124		HSP90AA1,HSP90AB1,MMP2,MT-CYB,MT-ND4	4
Glucocorticoid Receptor Signaling	2.31	0.0103		HSP90AA1,HSP90AB1,HSPA5,MMP2,MT-CYB,MT-ND4	4
Reelin Signaling in Neurons	2.31	0.0238		APP,GRIN2B,MAP1B	4
Role of PKR in Interferon Induction and Antiviral Response	2.22	0.0221		HSP90AA1,HSP90AB1,HSPA5	4
eNOS Signaling	2.03	0.0189		HSP90AA1,HSP90AB1,HSPA5	4
Aldosterone Signaling in Epithelial Cells	2	0.0183		HSP90AA1,HSP90AB1,HSPA5	4
Synaptogenesis Signaling Pathway	1.99	0.0128	-1	GRIN2B,MAP1B,NTRK2,TLN1	4
Mitotic Roles of Polo-Like Kinase	1.86	0.0303		HSP90AA1,HSP90AB1	4
Glutamate Receptor Signaling	1.86	0.0303		GRID2,GRIN2B	4
IL-17 Signaling	1.84	0.016		HSP90AA1,HSP90AB1,MMP2	4
Hypoxia Signaling in the Cardiovascular System	1.76	0.027		HSP90AA1,HSP90AB1	4
HIF1α Signaling	1.72	0.0144		HSP90AA1,HSPA5,MMP2	4
BEX2 Signaling Pathway	1.69	0.0247		LGALS1,MMP2	4
BAG2 Signaling Pathway	1.66	0.0238		HSP90AA1,HSPA5	4
Role of Osteoblasts, Osteoclasts and Chondrocytes in Rheumatoid Arthritis	1.64	0.0134		COL1A1,DKK3,SFRP1	4
Xenobiotic Metabolism AHR Signaling Pathway	1.63	0.023		HSP90AA1,HSP90AB1	4
Embryonic Stem Cell Differentiation into Cardiac Lineages	1.57	0.1		SOX2	4
Neuropathic Pain Signaling In Dorsal Horn Neurons	1.51	0.0198		GRIN2B,NTRK2	4
Sperm Motility	1.5	0.0118		DDR1,NTRK2,PDE4B	4
IGF-1 Signaling	1.49	0.0192		IGFBP2,IGFBP5	4
Telomerase Signaling	1.47	0.0187		HSP90AA1,HSP90AB1	4

PPAR Signaling	1.47	0.0187		HSP90AA1,HSP90AB1	4
Prostate Cancer Signaling	1.43	0.0179		HSP90AA1,HSP90AB1	4
Protein Ubiquitination Pathway	1.41	0.0109		HSP90AA1,HSP90AB1,HSPA5	4
Amyotrophic Lateral Sclerosis Signaling	1.41	0.0174		GRID2,GRIN2B	4
Neuregulin Signaling	1.39	0.0171		HSP90AA1,HSP90AB1	4
Neuroprotective Role of THOP1 in Alzheimer's Disease	1.39	0.0169		APP,HTRA1	4
Nitric Oxide Signaling in the Cardiovascular System	1.38	0.0168		HSP90AA1,HSP90AB1	4
LXR/RXR Activation	1.36	0.0163		CLU,PLTP	4
IL-15 Production	1.36	0.0163		DDR1,NTRK2	4
Sirtuin Signaling Pathway	1.35	0.0103		APP,MT-CYB,MT-ND4	4
FXR/RXR Activation	1.34	0.0159		CLU,PLTP	4
Axonal Guidance Signaling	1.31	0.00791		LRRC4C,MMP2,NTRK2,SRGAP3	4
Atherosclerosis Signaling	1.31	0.0154		CLU,COL1A1	4
Hepatic Fibrosis / Hepatic Stellate Cell Activation	17.4	0.155		A2M,CCL2,CCN2,COL10A1,COL11A1,COL1A1,COL1A2,COL25A1,COL26A1,COL27A1,COL3A1,COL5A1,COL5A2,COL5A3,COL6A1,COL6A2,COL6A3,COL8A1,EDNRB,FN1,IGFBP3,IGFBP4,KLF6,MYH9,MYL9,PDGFRB,SERPINE1,TGFB2,TNFRSF11B,VEGFA	5
Axonal Guidance Signaling	15.5	0.087		ABLIM1,ADAM12,ADAM9,ADAMTS1,ADAMTS12,ADAMTS14,ADAMTS6,BMP2,BMP7,DPYSL2,DPYSL5,EFNB2,EPHA4,FZD1,HHIP,ITGA11,ITGA6,ITGB1,ITGB4,ITGB8,ITSN1,LRRC4C,MMP14,MMP15,MMP17,MYL9,NTN1,NTN4,NTRK2,NTRK3,PAPPA,SDC2,SEMA6D,SLIT1,SRGAP3,TUBA1A,TUBA1C,TUBB2A,TUBB2B,TUBB6,UNC5B,VEGFA,WNT11,WNT5A	5
GP6 Signaling Pathway	8.24	0.126	3	COL10A1,COL11A1,COL1A1,COL1A2,COL25A1,COL26A1,COL27A1,COL3A1,COL5A1,COL5A2,COL5A3,COL6A1,COL6A2,COL6A3,COL8A1,LAMB1	5
Inhibition of Matrix Metalloproteases	7.21	0.231	0	A2M,ADAM12,HSPG2,MMP14,MMP15,MMP17,SDC1,SDC2,TIMP3	5
Antigen Presentation Pathway	7.21	0.231		B2M,CD74,HLA-A,HLA-B,HLA-C,HLA-DMA,HLA-DPA1,HLA-DRA,HLA-DRB5	5

Osteoarthritis Pathway	7.2	0.0855	1.387	ANXA2,BMP2,CEBPB,COL10A1,DCN,DDR2,FN1,FZD1,GREM1,HES1,HTRA1,ITGA11,ITGA6,ITGB1,ITGB4,ITGB8,S1PR3,SOX9,TIMP3,VEGFA	5
Hepatic Fibrosis Signaling Pathway	6.9	0.0644	1.342	APC2,CACNA2D3,CCL2,CCN2,CEBPB,CNR1,COL10A1,COL1A1,COL1A2,COL3A1,COL5A3,FTH1,FZD1,ITGA11,ITGA6,ITGB1,ITGB4,ITGB8,JUN,MYL9,PDGFRB,SERPINE1,TGFB2,TNFRSF11B,VEGFA,WNT11,WNT5A	5
Tumor Microenvironment Pathway	6.86	0.095	1	CCL2,CD44,COL1A1,COL1A2,COL3A1,FN1,HLA-A,HLA-B,HLA-C,JUN,MMP14,MMP15,MMP17,SLC2A1,SLC2A3,TGFB2,VEGFA	5
Caveolar-mediated Endocytosis Signaling	6.53	0.147		B2M,CAVIN1,HLA-A,HLA-B,HLA-C,ITGA11,ITGA6,ITGB1,ITGB4,ITGB8,ITSN1	5
Semaphorin Neuronal Repulsive Signaling Pathway	5.64	0.0927	1.155	CD44,DPYSL2,DPYSL3,DPYSL5,ITGA11,ITGA6,ITGB1,ITGB4,ITGB8,MYL9,PDE4B,PPP1CB,SEMA6D,VCAN	5
Coronavirus Replication Pathway	5.55	0.178	0.707	IFITM1,IFITM2,IFITM3,TUBA1A,TUBA1C,TUBB2A,TUBB2B,TUBB6	5
Inhibition of Angiogenesis by TSP1	5.37	0.206	0	CD47,HSPG2,JUN,SDC1,SDC2,THBS1,VEGFA	5
HOTAIR Regulatory Pathway	5.24	0.0859	1.941	CD44,COL1A1,COL1A2,COL3A1,JAM2,MMP14,MMP15,MMP17,PCDH10,SNAI2,TWIST1,TWIST2,WNT11,WNT5A	5
Apelin Liver Signaling Pathway	4.98	0.231	2.449	COL10A1,COL1A1,COL1A2,COL3A1,COL5A3,PDGFRB	5
WNT/β-catenin Signaling	4.95	0.0809	1.604	APC2,CD44,DKK3,FZD1,GJA1,JUN,SFRP1,SFRP2,SOX2,SOX6,SOX9,TGFB2,WNT11,WNT5A	5
Sertoli Cell-Sertoli Cell Junction Signaling	4.71	0.0728		A2M,ACTN1,DLG1,ITGA11,ITGA6,ITGB1,ITGB4,ITGB8,JAM2,JUN,TUBA1A,TUBA1C,TUBB2A,TUBB2B,TUBB6	5
Human Embryonic Stem Cell Pluripotency	4.49	0.0783		APC2,BMP2,BMP7,FZD1,INHBA,NTRK2,NTRK3,PDGFRB,S1PR3,SOX2,TGFB2,WNT11,WNT5A	5
PD-1, PD-L1 cancer immunotherapy pathway	4.26	0.0943	2.121	B2M,HLA-A,HLA-B,HLA-C,HLA-DMA,HLA-DPA1,HLA-DRA,HLA-DRB5,TGFB2,TNFRSF11B	5
Neuroinflammation Signaling Pathway	4.12	0.0571	-3	APP,B2M,CALB2,CCL2,FZD1,GRIA1,GRIN2B,HLA-A,HLA-B,HLA-C,HLA-DMA,HLA-DPA1,HLA-DRA,HLA-DRB5,JUN,S100B,SLC1A2,TGFB2	5
Phagosome Maturation	4.03	0.0755		B2M,CTSC,HLA-A,HLA-B,HLA-C,HLA-DRA,HLA-DRB5,TUBA1A,TUBA1C,TUBB2A,TUBB2B,TUBB6	5

B Cell Development	3.68	0.14		HLA-A,HLA-B,HLA-DMA,HLA-DPA1,HLA-DRA,HLA-DRB5	5
Virus Entry via Endocytic Pathways	3.6	0.0865		B2M,CXADR,HLA-A,HLA-B,HLA-C,ITGB1,ITGB4,ITGB8,ITSN1	5
Adipogenesis pathway	3.39	0.0741		BMP2,BMP7,CEBPB,CEBPD,FZD1,LPL,RBP1,SOX9,TXNIP,WNT5A	5
Basal Cell Carcinoma Signaling	3.22	0.0972		APC2,BMP2,BMP7,FZD1,HHIP,WNT11,WNT5A	5
Role of Osteoblasts, Osteoclasts and Chondrocytes in Rheumatoid Arthritis	3.19	0.058		APC2,BMP2,BMP7,COL1A1,DKK3,FZD1,JUN,MMP14,SFRP1,SFRP2,TNFRSF11B,WNT11,WNT5A	5
PTEN Signaling	3.03	0.0667	0.816	ITGA11,ITGA6,ITGB1,ITGB4,ITGB8,NTRK2,NTRK3,PDGFRB,PREX2,SYNJ2	5
Atherosclerosis Signaling	2.9	0.0692		CCL2,CLU,COL10A1,COL1A1,COL1A2,COL3A1,COL5A3,LPL,PLAAT3	5
RHOGDI Signaling	2.84	0.0558	-0.378	CD44,CDH11,CDH13,CDH6,DLC1,ITGA11,ITGA6,ITGB1,ITGB4,ITGB8,MYH9,MYL9	5
Intrinsic Prothrombin Activation Pathway	2.83	0.119	2.236	COL10A1,COL1A1,COL1A2,COL3A1,COL5A3	5
Granulocyte Adhesion and Diapedesis	2.8	0.0582		CCL2,CD99,ITGB1,MMP14,MMP15,MMP17,SDC1,SDC2,SDC3,THY1,TNFRSF11B	5
Leukocyte Extravasation Signaling	2.72	0.057	-0.333	ACTN1,CD44,CD99,DLC1,ITGB1,JAM2,MMP14,MMP15,MMP17,THY1,TIMP3	5
Regulation of Cellular Mechanics by Calpain Protease	2.68	0.0787		ACTN1,CCND2,ITGA11,ITGA6,ITGB1,ITGB4,ITGB8	5
Amyotrophic Lateral Sclerosis Signaling	2.64	0.0696	-0.816	CACNA2D3,GRIA1,GRID2,GRIN2B,NEFL,RNF19A,SLC1A2,VEGFA	5
ILK Signaling	2.64	0.0556	1.265	ACTN1,BMP2,FN1,ITGB1,ITGB4,ITGB8,JUN,MYH9,MYL9,SNAI2,VEGFA	5
Natural Killer Cell Signaling	2.62	0.0553	-0.302	B2M,COL10A1,COL1A1,COL1A2,COL3A1,COL5A3,HLA-A,HLA-B,HLA-C,HSPA5,ITGB1	5
Remodeling of Epithelial Adherens Junctions	2.61	0.0882		ACTN1,TUBA1A,TUBA1C,TUBB2A,TUBB2B,TUBB6	5
Germ Cell-Sertoli Cell Junction Signaling	2.61	0.0585		A2M,ACTN1,ITGA6,ITGB1,TGFB2,TUBA1A,TUBA1C,TUBB2A,TUBB2B,TUBB6	5
Ephrin Receptor Signaling	2.59	0.0547	-1	EFNB2,EPHA4,GRIN2B,ITGA11,ITGA6,ITGB1,ITGB4,ITGB8,ITSN1,SDC2,VEGFA	5
IL-4 Signaling	2.57	0.0753		HLA-A,HLA-B,HLA-DMA,HLA-DPA1,HLA-DRA,HLA-DRB5,SYNJ2	5
TGF-β Signaling	2.49	0.0729	-0.447	BMP2,BMP7,INHBA,JUN,SERPINE1,SMURF2,TGFB2	5

HIF1α Signaling	2.47	0.0529	0.302	HSP90AA1,HSPA5,JUN,MMP14,MMP15,MMP17,SERPINE1,SLC2A1,SLC2A3,TGFB2,VEGFA	5
p53 Signaling	2.44	0.0714	0.816	CCND2,JUN,PERP,PMAIP1,SERPINE2,SNAI2,THBS1	5
Serine Biosynthesis	2.41	0.4		PHGDH,PSAT1	5
Actin Cytoskeleton Signaling	2.38	0.049	2.121	ACTN1,APC2,FN1,IQGAP2,ITGA11,ITGA6,ITGB1,ITGB4,ITGB8,MYH9,MYL9,PPP1CB	5
Agranulocyte Adhesion and Diapedesis	2.38	0.0514		CCL2,CD99,FN1,ITGA6,ITGB1,MMP14,MMP15,MMP17,MYH9,MYL9,PODXL	5
Acute Phase Response Signaling	2.36	0.0541	-0.378	A2M,CEBPB,CP,CRABP2,FN1,JUN,RBP1,SERPINE1,SERPINF1,TNFRSF11B	5
IGF-1 Signaling	2.3	0.0673		CCN1,CCN2,IGFBP2,IGFBP3,IGFBP4,IGFBP7,JUN	5
Interferon Signaling	2.24	0.111	-2	IFI6,IFITM1,IFITM2,IFITM3	5
Regulation of the Epithelial-Mesenchymal Transition Pathway	2.2	0.0513		FZD1,HMGA2,LOX,PDGFRB,SNAI2,TGFB2,TWIST1,TWIST2,WNT11,WNT5A	5
Role of Macrophages, Fibroblasts and Endothelial Cells in Rheumatoid Arthritis	2.19	0.0431		APC2,CCL2,CEBPB,CEBPD,DKK3,FN1,FZD1,JUN,SFRP1,SFRP2,TNFRSF11B,VEGFA,WNT11,WNT5A	5
RAC Signaling	2.16	0.058	-1	CD44,IQGAP2,ITGA11,ITGA6,ITGB1,ITGB4,ITGB8,JUN	5
IL-17A Signaling in Fibroblasts	2.16	0.105		CCL2,CEBPB,CEBPD,JUN	5
HIPPO signaling	2.14	0.0706		CD44,DLG1,FRMD6,PPP1CB,PPP1R14C,WWC1	5
CDK5 Signaling	2.12	0.0625	1.342	FOSB,ITGA6,ITGB1,LAMB1,NTRK2,PPP1CB,PPP1R14C	5
Superpathway of Serine and Glycine Biosynthesis I	2.1	0.286		PHGDH,PSAT1	5
Regulation Of The Epithelial Mesenchymal Transition In Development Pathway	2.09	0.069	2.449	FZD1,LOX,SNAI2,TWIST1,WNT11,WNT5A	5
Signaling by Rho Family GTPases	2.08	0.0448	0	CDH11,CDH13,CDH6,GFAP,ITGA11,ITGA6,ITGB1,ITGB4,ITGB8,JUN,MYL9,SEPTIN11	5
Endocannabinoid Cancer Inhibition Pathway	2.07	0.0559	-0.707	CCND2,CNR1,NUPR1,SNAI2,TRIB3,TWIST1,TWIST2,VEGFA	5
Regulation of Actin-based Motility by Rho	2.04	0.0603		ITGA11,ITGA6,ITGB1,ITGB4,ITGB8,MYL9,PPP1CB	5
Neuregulin Signaling	2.03	0.0598		DCN,HSP90AA1,ITGA11,ITGA6,ITGB1,ITGB4,ITGB8	5
PAK Signaling	2.01	0.0593		ITGA11,ITGA6,ITGB1,ITGB4,ITGB8,MYL9,PDGFRB	5
Neuroprotective Role of THOP1 in Alzheimer's Disease	2.01	0.0593	0	APP,FAP,HLA-A,HLA-B,HLA-C,HTRA1,PRSS23	5

Glutamate Receptor Signaling	1.98	0.0758		GRIA1,GRID2,GRIN2B,SLC1A2,SLC38A1	5
Apelin Cardiac Fibroblast Signaling Pathway	1.97	0.13		CCN2,SERPINE1,TGFB2	5
Role of NANOG in Mammalian Embryonic Stem Cell Pluripotency	1.97	0.0583		APC2,BMP2,BMP7,FZD1,SOX2,WNT11,WNT5A	5
Synaptogenesis Signaling Pathway	1.96	0.0417	-2.496	CADM1,CDH11,CDH13,CDH6,EFNB2,EPHA4,GRIA1,GRIN2B,ITSN1,MAP1B,NTRK2,SYT11,THBS1	5
LXR/RXR Activation	1.91	0.0569	0.447	CCL2,CLU,LPL,PLTP,SCD,SERPINF1,TNFRSF11B	5
IL-15 Production	1.91	0.0569	-0.378	DDR1,DDR2,EPHA4,NTRK2,NTRK3,PDGFRB,PTK7	5
14-3-3-mediated Signaling	1.84	0.0551		GFAP,JUN,TUBA1A,TUBA1C,TUBB2A,TUBB2B,TUBB6	5
Netrin Signaling	1.83	0.0694	-0.447	ABLIM1,CACNA2D3,ENAH,NTN1,UNC5B	5
Aryl Hydrocarbon Receptor Signaling	1.82	0.0503	0.378	AHR,CCND2,CYP1B1,HSP90AA1,JUN,NFIA,NR2F1,TGFB2	5
RAR Activation	1.74	0.0459		BMP2,CRABP2,DUSP1,IGFBP3,JUN,NR2F1,RBP1,TGFB2,VEGFA	5
Neurotrophin/TRK Signaling	1.74	0.0658		JUN,NTRK2,NTRK3,SPRY1,SPRY2	5
Asparagine Biosynthesis I	1.7	1		ASNS	5
Th2 Pathway	1.68	0.0511		HLA-A,HLA-B,HLA-DMA,HLA-DPA1,HLA-DRA,HLA-DRB5,JUN	5
Paxillin Signaling	1.66	0.0556		ACTN1,ITGA11,ITGA6,ITGB1,ITGB4,ITGB8	5
CSDE1 Signaling Pathway	1.59	0.0714	0	CCL2,FABP7,FN1,SNAI2	5
Glucocorticoid Receptor Signaling	1.57	0.0327		A2M,B2M,CCL2,DUSP1,GJA1,HLA-A,HLA-B,HLA-C,HLA-DMA,HLA-DPA1,HLA-DRA,HLA-DRB5,HSP90AA1,HSPA5,IL13RA2,JUN,MT-CYB,SERPINE1,TGFB2	5
Calcium Signaling	1.51	0.0417	-1	ATP2B1,CACNA2D3,GRIA1,GRIN2B,MYH9,MYL9,TPM1,TPM2,TPM4	5
Breast Cancer Regulation by Stathmin1	1.5	0.0321	-1.886	ADGRG1,ADGRV1,CALCRL,CCND2,CNR1,EDNRB,FZD1,GPRC5B,JUN,PPP1CB,PPP1R14C,S1PR3,TGFB2,TUBA1A,TUBA1C,TUBB2A,TUBB2B,TUBB6,VEGFA	5
PCP (Planar Cell Polarity) Pathway	1.49	0.0667	1	FZD1,JUN,WNT11,WNT5A	5
Coagulation System	1.48	0.0857		A2M,SERPINE1,TFPI	5
Factors Promoting Cardiogenesis in Vertebrates	1.48	0.0464	0.816	APC2,BMP2,BMP7,FZD1,TGFB2,WNT11,WNT5A	5
Semaphorin Signaling in Neurons	1.44	0.0645		DPYSL2,DPYSL3,DPYSL5,ITGB1	5

Molecular Mechanisms of Cancer	1.44	0.0337		APC2,BMP2,BMP7,CCND2,FZD1,ITGA11,ITGA6,ITGB1,ITGB4,ITGB8,JUN,PMAIP1,TGFB2,WNT11,WNT5A	5
Crosstalk between Dendritic Cells and Natural Killer Cells	1.44	0.0549		HLA-A,HLA-B,HLA-C,HLA-DRA,HLA-DRB5	5
Th1 Pathway	1.43	0.0492	-2.236	HLA-A,HLA-B,HLA-DMA,HLA-DPA1,HLA-DRA,HLA-DRB5	5
Actin Nucleation by ARP-WASP Complex	1.4	0.0538		ITGA11,ITGA6,ITGB1,ITGB4,ITGB8	5
β-alanine Degradation I	1.4	0.5		ABAT	5
Regulation Of The Epithelial Mesenchymal Transition By Growth Factors Pathway	1.39	0.0417	0.707	HMGA2,JUN,MEST,PDGFRB,SNAI2,TGFB2,TNFRSF11B,TWIST1	5
CDC42 Signaling	1.36	0.0313	0	APC2,B2M,HLA-A,HLA-B,HLA-C,HLA-DMA,HLA-DPA1,HLA-DRA,HLA-DRB5,IQGAP2,ITGA11,ITGA6,ITGB1,ITGB4,ITGB8,JUN,MYL9,PPP1CB	5
IL-6 Signaling	1.35	0.0469	0	A2M,CEBPB,COL1A1,JUN,TNFRSF11B,VEGFA	5
Gap Junction Signaling	1.33	0.0404		GJA1,GRIA1,NPR3,TUBA1A,TUBA1C,TUBB2A,TUBB2B,TUBB6	5
PI3K/AKT Signaling	1.32	0.0402		HSP90AA1,IL13RA2,ITGA11,ITGA6,ITGB1,ITGB4,ITGB8,SYNJ2	5
Antigen Presentation Pathway	28.6	0.436		B2M,CD74,CIITA,HLA-A,HLA-B,HLA-C,HLA-DMA,HLA-DMB,HLA-DOA,HLA-DPA1,HLA-DPB1,HLA-DQA1,HLA-DQB1,HLA-DRA,HLA-DRB1,HLA-DRB5,HLA-E	6
B Cell Development	17.5	0.279		HLA-A,HLA-B,HLA-DMA,HLA-DMB,HLA-DOA,HLA-DPA1,HLA-DPB1,HLA-DQA1,HLA-DQB1,HLA-DRA,HLA-DRB1,HLA-DRB5	6
PD-1, PD-L1 cancer immunotherapy pathway	16.9	0.142	-3.606	B2M,HLA-A,HLA-B,HLA-C,HLA-DMA,HLA-DMB,HLA-DOA,HLA-DPA1,HLA-DPB1,HLA-DQA1,HLA-DQB1,HLA-DRA,HLA-DRB1,HLA-DRB5,HLA-E	6
Neuroinflammation Signaling Pathway	13.2	0.0571	3.742	APP,B2M,HLA-A,HLA-B,HLA-C,HLA-DMA,HLA-DMB,HLA-DOA,HLA-DPA1,HLA-DPB1,HLA-DQA1,HLA-DQB1,HLA-DRA,HLA-DRB1,HLA-DRB5,HLA-E,S100B,SLC1A2	6
IL-4 Signaling	13.1	0.129		HLA-A,HLA-B,HLA-DMA,HLA-DMB,HLA-DOA,HLA-DPA1,HLA-DPB1,HLA-DQA1,HLA-DQB1,HLA-DRA,HLA-DRB1,HLA-DRB5	6

Th1 Pathway	11.7	0.0984	3.162	HLA-A,HLA-B,HLA-DMA,HLA-DMB,HLA-DOA,HLA-DPA1,HLA-DPB1,HLA-DQA1,HLA-DQB1,HLA-DRA,HLA-DRB1,HLA-DRB5	6
Th2 Pathway	11.1	0.0876		HLA-A,HLA-B,HLA-DMA,HLA-DMB,HLA-DOA,HLA-DPA1,HLA-DPB1,HLA-DQA1,HLA-DQB1,HLA-DRA,HLA-DRB1,HLA-DRB5	6
MSP-RON Signaling In Macrophages Pathway	10.5	0.094	-3.317	CIITA,HLA-DMA,HLA-DMB,HLA-DOA,HLA-DPA1,HLA-DPB1,HLA-DQA1,HLA-DQB1,HLA-DRA,HLA-DRB1,HLA-DRB5	6
Th1 and Th2 Activation Pathway	9.92	0.0698		HLA-A,HLA-B,HLA-DMA,HLA-DMB,HLA-DOA,HLA-DPA1,HLA-DPB1,HLA-DQA1,HLA-DQB1,HLA-DRA,HLA-DRB1,HLA-DRB5	6
Glucocorticoid Receptor Signaling	7.97	0.0293		B2M,CAV1,HLA-A,HLA-B,HLA-C,HLA-DMA,HLA-DMB,HLA-DOA,HLA-DPA1,HLA-DPB1,HLA-DQA1,HLA-DQB1,HLA-DRA,HLA-DRB1,HLA-DRB5,HLA-E,MMP2	6
Dendritic Cell Maturation	7.88	0.0289	3.153	B2M,COL1A1,COL1A2,HLA-A,HLA-B,HLA-C,HLA-DMA,HLA-DMB,HLA-DOA,HLA-DPA1,HLA-DPB1,HLA-DQA1,HLA-DQB1,HLA-DRA,HLA-DRB1,HLA-DRB5,HLA-E	6
Crosstalk between Dendritic Cells and Natural Killer Cells	7.56	0.0879	2	ACTG2,HLA-A,HLA-B,HLA-C,HLA-DRA,HLA-DRB1,HLA-DRB5,HLA-E	6
OX40 Signaling Pathway	7.46	0.0313		B2M,HLA-A,HLA-B,HLA-C,HLA-DMA,HLA-DMB,HLA-DOA,HLA-DPA1,HLA-DPB1,HLA-DQA1,HLA-DQB1,HLA-DRA,HLA-DRB1,HLA-DRB5,HLA-E	6
Tumor Microenvironment Pathway	7.42	0.0559	-1.265	CD44,COL1A1,COL1A2,FN1,HLA-A,HLA-B,HLA-C,HLA-E,MMP17,MMP2	6
Allograft Rejection Signaling	7.41	0.0311		B2M,HLA-A,HLA-B,HLA-C,HLA-DMA,HLA-DMB,HLA-DOA,HLA-DPA1,HLA-DPB1,HLA-DQA1,HLA-DQB1,HLA-DRA,HLA-DRB1,HLA-DRB5,HLA-E	6
Systemic Lupus Erythematosus In T Cell Signaling Pathway	7.37	0.0266	4.123	B2M,CD44,HLA-A,HLA-B,HLA-C,HLA-DMA,HLA-DMB,HLA-DOA,HLA-DPA1,HLA-DPB1,HLA-DQA1,HLA-DQB1,HLA-DRA,HLA-DRB1,HLA-DRB5,HLA-E,RND3	6
Type I Diabetes Mellitus Signaling	7.12	0.0295		CPE,HLA-A,HLA-B,HLA-C,HLA-DMA,HLA-DMB,HLA-DOA,HLA-DPA1,HLA-DPB1,HLA-DQA1,HLA-DQB1,HLA-DRA,HLA-DRB1,HLA-DRB5,HLA-E	6
NUR77 Signaling in T Lymphocytes	7.08	0.0293		B2M,HLA-A,HLA-B,HLA-C,HLA-DMA,HLA-DMB,HLA-DOA,HLA-DPA1,HLA-DPB1,HLA-DQA1,HLA-DQB1,HLA-DRA,HLA-DRB1,HLA-DRB5,HLA-E	6

Graft-versus-Host Disease Signaling	7	0.0314		HLA-A,HLA-B,HLA-C,HLA-DMA,HLA-DMB,HLA-DOA,HLA-DPA1,HLA-DPB1,HLA-DQA1,HLA-DQB1,HLA-DRA,HLA-DRB1,HLA-DRB5,HLA-E	6
Autoimmune Thyroid Disease Signaling	6.92	0.0309		HLA-A,HLA-B,HLA-C,HLA-DMA,HLA-DMB,HLA-DOA,HLA-DPA1,HLA-DPB1,HLA-DQA1,HLA-DQB1,HLA-DRA,HLA-DRB1,HLA-DRB5,HLA-E	6
Caveolar-mediated Endocytosis Signaling	6.86	0.0933		ACTG2,B2M,CAV1,HLA-A,HLA-B,HLA-C,HLA-E	6
Phagosome Maturation	6.78	0.0566		B2M,CTSC,HLA-A,HLA-B,HLA-C,HLA-DRA,HLA-DRB1,HLA-DRB5,HLA-E	6
CDC42 Signaling	6.44	0.0261		B2M,HLA-A,HLA-B,HLA-C,HLA-DMA,HLA-DMB,HLA-DOA,HLA-DPA1,HLA-DPB1,HLA-DQA1,HLA-DQB1,HLA-DRA,HLA-DRB1,HLA-DRB5,HLA-E	6
T Cell Receptor Signaling	6.08	0.0244	3.873	B2M,HLA-A,HLA-B,HLA-C,HLA-DMA,HLA-DMB,HLA-DOA,HLA-DPA1,HLA-DPB1,HLA-DQA1,HLA-DQB1,HLA-DRA,HLA-DRB1,HLA-DRB5,HLA-E	6
Virus Entry via Endocytic Pathways	5.89	0.0673		ACTG2,B2M,CAV1,HLA-A,HLA-B,HLA-C,HLA-E	6
T Cell Exhaustion Signaling Pathway	5.76	0.0247		HLA-A,HLA-B,HLA-C,HLA-DMA,HLA-DMB,HLA-DOA,HLA-DPA1,HLA-DPB1,HLA-DQA1,HLA-DQB1,HLA-DRA,HLA-DRB1,HLA-DRB5,HLA-E	6
Calcium-induced T Lymphocyte Apoptosis	5.24	0.0261	3.162	HLA-A,HLA-B,HLA-DMA,HLA-DMB,HLA-DOA,HLA-DPA1,HLA-DPB1,HLA-DQA1,HLA-DQB1,HLA-DRA,HLA-DRB1,HLA-DRB5	6
T Helper Cell Differentiation	5.13	0.0255		HLA-A,HLA-B,HLA-DMA,HLA-DMB,HLA-DOA,HLA-DPA1,HLA-DPB1,HLA-DQA1,HLA-DQB1,HLA-DRA,HLA-DRB1,HLA-DRB5	6
Altered T Cell and B Cell Signaling in Rheumatoid Arthritis	4.94	0.0244		HLA-A,HLA-B,HLA-DMA,HLA-DMB,HLA-DOA,HLA-DPA1,HLA-DPB1,HLA-DQA1,HLA-DQB1,HLA-DRA,HLA-DRB1,HLA-DRB5	6
ICOS-ICOSL Signaling in T Helper Cells	4.82	0.0237	3.162	HLA-A,HLA-B,HLA-DMA,HLA-DMB,HLA-DOA,HLA-DPA1,HLA-DPB1,HLA-DQA1,HLA-DQB1,HLA-DRA,HLA-DRB1,HLA-DRB5	6
CD28 Signaling in T Helper Cells	4.73	0.0232		HLA-A,HLA-B,HLA-DMA,HLA-DMB,HLA-DOA,HLA-DPA1,HLA-DPB1,HLA-DQA1,HLA-DQB1,HLA-DRA,HLA-DRB1,HLA-DRB5	6
Neuroprotective Role of THOP1 in Alzheimer's Disease	4.42	0.0508		APP,C1R,HLA-A,HLA-B,HLA-C,HLA-E	6

PKCθ Signaling in T Lymphocytes	4.41	0.0215	3.162	HLA-A,HLA-B,HLA-DMA,HLA-DMB,HLA-DOA,HLA-DPA1,HLA-DPB1,HLA-DQA1,HLA-DQB1,HLA-DRA,HLA-DRB1,HLA-DRB5	6
Role of NFAT in Regulation of the Immune Response	4.18	0.0204	3.162	HLA-A,HLA-B,HLA-DMA,HLA-DMB,HLA-DOA,HLA-DPA1,HLA-DPB1,HLA-DQA1,HLA-DQB1,HLA-DRA,HLA-DRB1,HLA-DRB5	6
Hepatic Fibrosis / Hepatic Stellate Cell Activation	4.12	0.0361		COL1A1,COL1A2,COL6A1,COL6A3,FN1,IGFBP5,MMP2	6
Natural Killer Cell Signaling	4.05	0.0352	-1.134	B2M,COL1A1,COL1A2,HLA-A,HLA-B,HLA-C,HLA-E	6
HOTAIR Regulatory Pathway	3.65	0.0368	0	CD44,COL1A1,COL1A2,JAM2,MMP17,MMP2	6
Interferon Signaling	3.05	0.0833		IFITM1,IFITM2,IFITM3	6
Inhibition of Matrix Metalloproteases	2.95	0.0769		MMP17,MMP2,THBS2	6
Coronavirus Replication Pathway	2.77	0.0667		IFITM1,IFITM2,IFITM3	6
Protein Ubiquitination Pathway	2.47	0.0218		B2M,HLA-A,HLA-B,HLA-C,HLA-E,UBE2S	6
Leukocyte Extravasation Signaling	2.45	0.0259	1	ACTG2,CD44,JAM2,MMP17,MMP2	6
GP6 Signaling Pathway	2.34	0.0315	-2	COL1A1,COL1A2,COL6A1,COL6A3	6
Glioma Invasiveness Signaling	2.17	0.0411		CD44,MMP2,RND3	6
Apelin Liver Signaling Pathway	2.09	0.0769		COL1A1,COL1A2	6
L-DOPA Degradation	1.98	0.5		COMT	6
Complement System	1.79	0.0541		C1R,CFI	6
Acute Phase Response Signaling	1.78	0.0216		C1R,CP,FN1,FTL	6
Intrinsic Prothrombin Activation Pathway	1.69	0.0476		COL1A1,COL1A2	6
Role of OCT4 in Mammalian Embryonic Stem Cell Pluripotency	1.61	0.0435		NR2F1,NR2F2	6
Serine Biosynthesis	1.59	0.2		PHGDH	6
dTMP De Novo Biosynthesis	1.59	0.2		TYMS	6
Agranulocyte Adhesion and Diapedesis	1.58	0.0187		ACTG2,FN1,MMP17,MMP2	6
RHOGDI Signaling	1.57	0.0186	-1	ACTG2,CD44,CDH6,RND3	6
LXR/RXR Activation	1.57	0.0244		LPL,PLTP,SCD	6
RHOA Signaling	1.56	0.0242		ACTG2,NRP2,RND3	6
Lactose Degradation III	1.51	0.167		PSAP	6
Atherosclerosis Signaling	1.5	0.0231		COL1A1,COL1A2,LPL	6
Adipogenesis pathway	1.46	0.0222		CEBPD,LPL,NR2F2	6

Superpathway of Serine and Glycine Biosynthesis I	1.44	0.143		PHGDH	6
Hepatic Fibrosis / Hepatic Stellate Cell Activation	6.69	0.0619		A2M,CCN2,COL11A1,COL1A1,COL27A1,COL3A1,COL4A1,COL5A2,COL6A1,IGFBP5,MMP2,TIMP2	7
Caveolar-mediated Endocytosis Signaling	6.43	0.107		ACTB,CAVIN1,HLA-A,HLA-B,HLA-C,HLA-E,ITGB1,ITGB4	7
Virus Entry via Endocytic Pathways	4.36	0.0673		ACTB,HLA-A,HLA-B,HLA-C,HLA-E,ITGB1,ITGB4	7
Kinetochore Metaphase Signaling Pathway	4.34	0.0667	2.236	AURKB,BUB1B,CENPK,CENPU,MXD3,NDC80,SPC24	7
Natural Killer Cell Signaling	4.08	0.0452	1	COL1A1,COL3A1,HLA-A,HLA-B,HLA-C,HLA-E,HSPA5,HSPA8,ITGB1	7
Role of BRCA1 in DNA Damage Response	4.07	0.075	1.342	ACTB,BRCA2,BRIP1,E2F8,FANCA,FANCD2	7
Neuroprotective Role of THOP1 in Alzheimer's Disease	4.01	0.0593		APP,HLA-A,HLA-B,HLA-C,HLA-E,HTRA1,PRSS23	7
Phagosome Maturation	4.01	0.0503		CTSC,HLA-A,HLA-B,HLA-C,HLA-E,TUBA1A,TUBB2A,TUBB2B	7
GP6 Signaling Pathway	3.81	0.0551	-1.89	COL11A1,COL1A1,COL27A1,COL3A1,COL4A1,COL5A2,COL6A1	7
IGF-1 Signaling	3.45	0.0577		CCN1,CCN2,IGFBP2,IGFBP5,IGFBP7,SOCS3	7
Inhibition of Matrix Metalloproteases	3.39	0.103		A2M,MMP2,SDC2,TIMP2	7
Antigen Presentation Pathway	3.39	0.103		HLA-A,HLA-B,HLA-C,HLA-E	7
Sertoli Cell-Sertoli Cell Junction Signaling	3.24	0.0388		A2M,ACTB,ITGB1,ITGB4,JAM2,TUBA1A,TUBB2A,TUBB2B	7
Germ Cell-Sertoli Cell Junction Signaling	3.03	0.0409		A2M,ACTB,GSN,ITGB1,TUBA1A,TUBB2A,TUBB2B	7
Tumor Microenvironment Pathway	2.92	0.0391	0.816	COL1A1,COL3A1,HLA-A,HLA-B,HLA-C,HLA-E,MMP2	7
Crosstalk between Dendritic Cells and Natural Killer Cells	2.86	0.0549		ACTB,HLA-A,HLA-B,HLA-C,HLA-E	7
Cell Cycle Control of Chromosomal Replication	2.79	0.0714	2	LIG1,MCM8,ORC6,TOP2A	7
Hereditary Breast Cancer Signaling	2.74	0.0423		ACTB,BRCA2,CCND2,FANCA,FANCD2,WEE1	7
Axonal Guidance Signaling	2.66	0.0237		ADAM9,BMP7,DPYSL2,ITGB1,ITGB4,LRRC4C,MMP2,NTRK2,SDC2,TUBA1A,TUBB2A,TUBB2B	7
Glucocorticoid Receptor Signaling	2.62	0.0224		A2M,ACTB,GJA1,HLA-A,HLA-B,HLA-C,HLA-E,HSP90AA1,HSP90AB1,HSPA5,HSPA8,MMP2,MT-CYB	7

Mitotic Roles of Polo-Like Kinase	2.53	0.0606		HSP90AA1,HSP90AB1,KIF23,WEE1	7
Remodeling of Epithelial Adherens Junctions	2.48	0.0588		ACTB,TUBA1A,TUBB2A,TUBB2B	7
Protein Ubiquitination Pathway	2.45	0.0291		HLA-A,HLA-B,HLA-C,HLA-E,HSP90AA1,HSP90AB1,HSPA5,HSPA8	7
HOTAIR Regulatory Pathway	2.44	0.0368	-0.447	COL1A1,COL3A1,EZH2,JAM2,MMP2,VIM	7
Coagulation System	2.42	0.0857		A2M,F2R,TFPI	7
DNA Double-Strand Break Repair by Homologous Recombination	2.17	0.143		BRCA2,LIG1	7
Actin Cytoskeleton Signaling	2.16	0.0286	-0.816	ACTB,DIAPH3,F2R,GSN,IQGAP3,ITGB1,ITGB4	7
Coronavirus Replication Pathway	2.11	0.0667		TUBA1A,TUBB2A,TUBB2B	7
Role of PKR in Interferon Induction and Antiviral Response	2.11	0.0368	2	HSP90AA1,HSP90AB1,HSPA5,HSPA8,NLRP1	7
Clathrin-mediated Endocytosis Signaling	2.09	0.0311		ACTB,CLU,F2R,HSPA8,ITGB1,ITGB4	7
Unfolded protein response	2.05	0.0444	-2	CEBPD,HSPA5,HSPA8,P4HB	7
HIF1α Signaling	1.94	0.0288	-0.816	HSP90AA1,HSPA5,HSPA8,MMP2,PKM,VIM	7
PD-1, PD-L1 cancer immunotherapy pathway	1.81	0.0377	2	HLA-A,HLA-B,HLA-C,HLA-E	7
WNT/β-catenin Signaling	1.69	0.0289	1.342	DKK3,GJA1,SFRP1,SOX2,SOX4	7
Regulation of Actin-based Motility by Rho	1.68	0.0345		ACTB,GSN,ITGB1,ITGB4	7
Role of Tissue Factor in Cancer	1.68	0.0345		CCN1,CCN2,ITGB1,P4HB	7
Glycolysis I	1.68	0.08		ENO1,PKM	7
Neuregulin Signaling	1.67	0.0342		HSP90AA1,HSP90AB1,ITGB1,ITGB4	7
Apelin Liver Signaling Pathway	1.64	0.0769		COL1A1,COL3A1	7
14-3-3-mediated Signaling	1.56	0.0315		TUBA1A,TUBB2A,TUBB2B,VIM	7
Glioma Invasiveness Signaling	1.55	0.0411		F2R,MMP2,TIMP2	7
Hypoxia Signaling in the Cardiovascular System	1.54	0.0405		HSP90AA1,HSP90AB1,P4HB	7
Leukocyte Extravasation Signaling	1.52	0.0259	-1	ACTB,ITGB1,JAM2,MMP2,TIMP2	7
Gap Junction Signaling	1.47	0.0253		ACTB,GJA1,TUBA1A,TUBB2A,TUBB2B	7
Signaling by Rho Family GTPases	1.46	0.0224	-1.342	ACTB,CDH6,DIAPH3,ITGB1,ITGB4,VIM	7
Cyclins and Cell Cycle Regulation	1.4	0.0357		CCND2,E2F8,WEE1	7
BAG2 Signaling Pathway	1.4	0.0357		HSP90AA1,HSPA5,HSPA8	7
Regulation of Cellular Mechanics by Calpain Protease	1.33	0.0337		CCND2,ITGB1,ITGB4	7

Hepatic Fibrosis / Hepatic Stellate Cell Activation	10.9	0.0979		A2M,CCN2,COL11A1,COL12A1,COL18A1,COL1A2,COL27A1,COL3A1,COL4A1,COL4A2,COL5A2,EDNRB,FN1,IGFBP5,KLF6,MMP2,MYH9,TGFB2,TIMP2	8
Axonal Guidance Signaling	6.01	0.0435		ABLIM1,ADAMTS16,CXCR4,DCC,EFNB2,ITGA6,ITGAV,ITGB4,ITSN1,MMP2,NRP2,NTN1,NTRK2,NTRK3,ROBO2,ROBO3,SDC2,SLIT1,SLIT2,SRGAP3,TUBB2A,TUBB2B	8
Tumor Microenvironment Pathway	5.36	0.067	-0.905	CD44,CFLAR,COL1A2,COL3A1,CXCR4,FN1,HLA-A,HLA-C,JUN,MMP2,PLAU,TGFB2	8
GP6 Signaling Pathway	5.17	0.0787	-3.162	COL11A1,COL12A1,COL18A1,COL1A2,COL27A1,COL3A1,COL4A1,COL4A2,COL5A2,LAMA4	8
Caveolar-mediated Endocytosis Signaling	4.25	0.0933		CAVIN1,HLA-A,HLA-C,ITGA6,ITGAV,ITGB4,ITSN1	8
Th2 Pathway	4.09	0.0657	0	BHLHE41,CXCR4,DLL1,HLA-A,HLA-DPB1,HLA-DRA,HLA-DRB5,JUN,SOCS3	8
WNT/β-catenin Signaling	4.01	0.0578	-1.265	APC2,CD44,DKK3,GJA1,JUN,LRP1,SFRP1,SOX11,SOX4,TGFB2	8
Inhibition of Matrix Metalloproteases	3.83	0.128		A2M,LRP1,MMP2,SDC2,TIMP2	8
Antigen Presentation Pathway	3.83	0.128		HLA-A,HLA-C,HLA-DPB1,HLA-DRA,HLA-DRB5	8
Actin Cytoskeleton Signaling	3.4	0.0449	0.378	ACTN1,APC2,EZR,FN1,GSN,IQGAP2,ITGA6,ITGAV,ITGB4,MYH9,MYLK	8
IGF-1 Signaling	3.36	0.0673		CCN1,CCN2,IGFBP2,IGFBP5,JUN,SOCS3,YWHAH	8
Th1 and Th2 Activation Pathway	3.35	0.0523		BHLHE41,CXCR4,DLL1,HLA-A,HLA-DPB1,HLA-DRA,HLA-DRB5,JUN,SOCS3	8
PTEN Signaling	3.09	0.0533	1.342	CDKN1A,ITGA6,ITGAV,ITGB4,NTRK2,NTRK3,SYNJ2,YWHAH	8
Signaling by Rho Family GTPases	3.07	0.041	-1.414	CDH11,CDH6,EZR,ITGA6,ITGAV,ITGB4,JUN,MYLK,SEPTIN11,STMN1,VIM	8
Regulation of Cellular Mechanics by Calpain Protease	2.96	0.0674		ACTN1,CAST,EZR,ITGA6,ITGAV,ITGB4	8
Phagosome Maturation	2.92	0.0503		CTSC,EEA1,HLA-A,HLA-C,HLA-DRA,HLA-DRB5,TUBB2A,TUBB2B	8
Notch Signaling	2.83	0.105		DLL1,DLL3,HES5,MFNG	8
B Cell Development	2.63	0.093		HLA-A,HLA-DPB1,HLA-DRA,HLA-DRB5	8
Zymosterol Biosynthesis	2.61	0.333		MSMO1,TM7SF2	8
Netrin Signaling	2.6	0.0694	0.447	ABLIM1,CACNA1A,DCC,NTN1,RYR3	8
Glioma Invasiveness Signaling	2.57	0.0685	-1.342	CD44,ITGAV,MMP2,PLAU,TIMP2	8

PD-1, PD-L1 cancer immunotherapy pathway	2.57	0.0566	2	HLA-A,HLA-C,HLA-DPB1,HLA-DRA,HLA-DRB5,TGFB2	8
Hepatic Fibrosis Signaling Pathway	2.44	0.031	-2.121	APC2,CACNA1A,CCN2,COL18A1,COL1A2,COL3A1,ITGA6,ITGAV,ITGB4,JUN,LRP1,MYLK,TGFB2	8
Cell Cycle: G2/M DNA Damage Checkpoint Regulation	2.39	0.08		CDKN1A,TOP2A,WEE1,YWHAH	8
Glucocorticoid Receptor Signaling	2.37	0.0275		A2M,ANXA1,CDKN1A,GJA1,HLA-A,HLA-C,HLA-DPB1,HLA-DRA,HLA-DRB5,HSPA5,JUN,MMP2,MT-ATP6,PLAU,TGFB2,YWHAH	8
Neuroprotective Role of THOP1 in Alzheimer's Disease	2.34	0.0508		HLA-A,HLA-C,HTRA1,PRSS12,PRSS23,TAC1	8
Apelin Liver Signaling Pathway	2.34	0.115		COL18A1,COL1A2,COL3A1	8
Th1 Pathway	2.27	0.0492	-0.447	DLL1,HLA-A,HLA-DPB1,HLA-DRA,HLA-DRB5,SOCS3	8
HOTAIR Regulatory Pathway	2.24	0.0429	-1.633	CD44,CDKN1A,COL1A2,COL3A1,MMP2,PCDH10,VIM	8
Sertoli Cell-Sertoli Cell Junction Signaling	2.23	0.0388		A2M,ACTN1,ITGA6,ITGAV,ITGB4,JUN,TUBB2A,TUBB2B	8
Atherosclerosis Signaling	2.14	0.0462		COL18A1,COL1A2,COL3A1,CXCR4,LPL,PLAAT3	8
Germ Cell-Sertoli Cell Junction Signaling	2.13	0.0409		A2M,ACTN1,GSN,ITGA6,TGFB2,TUBB2A,TUBB2B	8
RHOGDI Signaling	2.13	0.0372	1	CD44,CDH11,CDH6,EZR,ITGA6,ITGAV,ITGB4,MYH9	8
IL-4 Signaling	2.13	0.0538		HLA-A,HLA-DPB1,HLA-DRA,HLA-DRB5,SYNJ2	8
Calcium Signaling	2.11	0.037	0.447	ATP2B1,CACNA1A,GRIA1,GRIA2,MYH9,RCAN1,RYR3,TPM1	8
Neuroinflammation Signaling Pathway	2.06	0.0317	-1.667	CFLAR,GRIA1,HLA-A,HLA-C,HLA-DPB1,HLA-DRA,HLA-DRB5,JUN,KCNJ6,TGFB2	8
RAC Signaling	2.02	0.0435		CD44,IQGAP2,ITGA6,ITGAV,ITGB4,JUN	8
Inhibition of Angiogenesis by TSP1	2.01	0.0882		CD47,JUN,SDC2	8
Coagulation System	1.97	0.0857		A2M,PLAT,PLAU	8
Virus Entry via Endocytic Pathways	1.93	0.0481		CXADR,HLA-A,HLA-C,ITGB4,ITSN1	8
Cholesterol Biosynthesis I	1.92	0.154		MSMO1,TM7SF2	8
Cholesterol Biosynthesis II (via 24,25-dihydrolanosterol)	1.92	0.154		MSMO1,TM7SF2	8
Cholesterol Biosynthesis III (via Desmosterol)	1.92	0.154		MSMO1,TM7SF2	8
Leukocyte Extravasation Signaling	1.86	0.0363	-0.378	ACTN1,CD44,CXCR4,EZR,MMP2,THY1,TIMP2	8
Semaphorin Neuronal Repulsive Signaling Pathway	1.84	0.0397	0	CD44,CSPG5,ITGA6,ITGAV,ITGB4,NRP2	8

Ephrin Receptor Signaling	1.77	0.0348		CXCR4,EFNB2,ITGA6,ITGAV,ITGB4,ITSN1,SDC2	8
Protein Kinase A Signaling	1.77	0.0274	-1	AKAP12,DCC,MYLK,NTN1,PDE1C,PPP1R14C,PTPRO,PTPRZ1,RYR3,TGFB2,YWHAH	8
Intrinsic Prothrombin Activation Pathway	1.76	0.0714		COL18A1,COL1A2,COL3A1	8
Neurotrophin/TRK Signaling	1.76	0.0526		JUN,NTRK2,NTRK3,SPRY1	8
Regulation of Actin-based Motility by Rho	1.74	0.0431		GSN,ITGA6,ITGAV,ITGB4,MYLK	8
Role of Tissue Factor in Cancer	1.74	0.0431		CCN1,CCN2,ITGA6,ITGAV,P4HB	8
MSP-RON Signaling In Macrophages Pathway	1.73	0.0427	0.447	HLA-DPB1,HLA-DRA,HLA-DRB5,JUN,SOCS3	8
Thyroid Cancer Signaling	1.7	0.0506	-1	CXCR4,JUN,NTRK2,NTRK3	8
Coronavirus Replication Pathway	1.68	0.0667		IFITM1,TUBB2A,TUBB2B	8
BEX2 Signaling Pathway	1.67	0.0494	-1	BEX1,CDKN1A,JUN,MMP2	8
14-3-3-mediated Signaling	1.59	0.0394		JUN,TUBB2A,TUBB2B,VIM,YWHAH	8
Taurine Biosynthesis	1.59	0.5		CDO1	8
GADD45 Signaling	1.56	0.1		CDKN1A,GADD45B	8
HGF Signaling	1.53	0.0379		CDKN1A,ITGA6,ITGAV,ITGB4,JUN	8
Crosstalk between Dendritic Cells and Natural Killer Cells	1.5	0.044		HLA-A,HLA-C,HLA-DRA,HLA-DRB5	8
STAT3 Pathway	1.49	0.037	-1	CDKN1A,NTRK2,NTRK3,SOCS3,TGFB2	8
Osteoarthritis Pathway	1.46	0.0299		ANXA2,FN1,HTRA1,ITGA6,ITGAV,ITGB4,LRP1	8
Acute Phase Response Signaling	1.46	0.0324	-1.342	A2M,CP,CRABP1,FN1,JUN,SOCS3	8
MSP-RON Signaling In Cancer Cells Pathway	1.46	0.0362	-0.447	ITGA6,ITGB4,JUN,VIM,YWHAH	8
Apelin Cardiac Fibroblast Signaling Pathway	1.44	0.087		CCN2,TGFB2	8
Granulocyte Adhesion and Diapedesis	1.42	0.0317		CXCR4,EZR,MMP2,SDC2,SDC3,THY1	8
ATM Signaling	1.42	0.0412		CDKN1A,GADD45B,JUN,ZEB1	8
Regulation Of The Epithelial Mesenchymal Transition By Growth Factors Pathway	1.39	0.0312	-0.816	JUN,MEST,MMP2,TGFB2,VIM,ZEB1	8
Dilated Cardiomyopathy Signaling Pathway	1.37	0.0342	0	CACNA1A,LAMA4,LMNA,MYH9,TPM1	8
Neuropathic Pain Signaling In Dorsal Horn Neurons	1.36	0.0396	0	GRIA1,GRIA2,NTRK2,TAC1	8

ILK Signaling	1.34	0.0303	-2.236	ACTN1,FN1,ITGB4,JUN,MYH9,VIM	8
Natural Killer Cell Signaling	1.33	0.0302	1.633	COL18A1,COL1A2,COL3A1,HLA-A,HLA-C,HSPA5	8
PI3K/AKT Signaling	1.33	0.0302		CDKN1A,ITGA6,ITGAV,ITGB4,SYNJ2,YWHAH	8